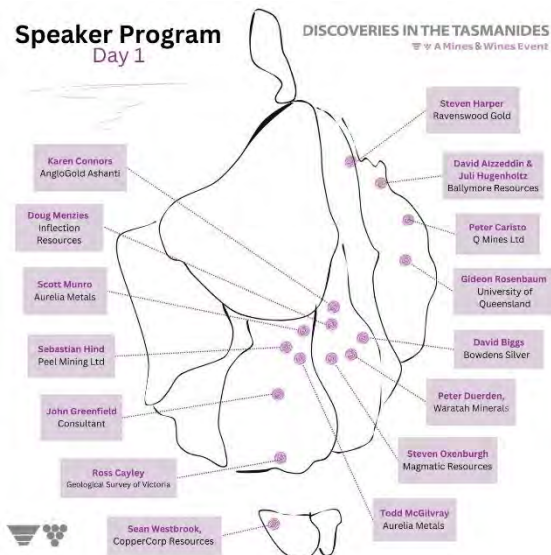




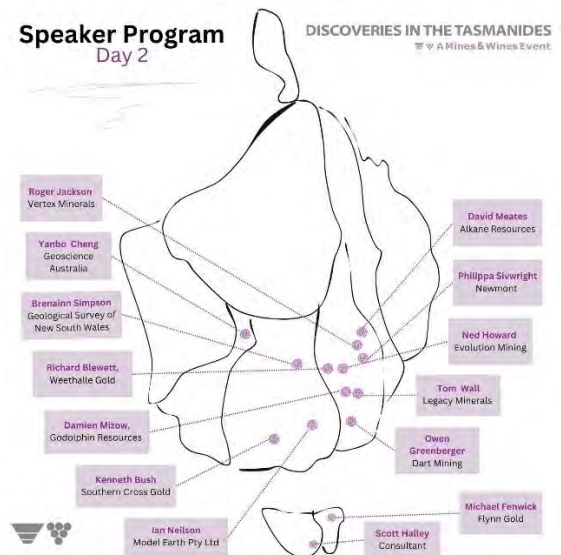
**AUSTRALIAN
INSTITUTE OF
GEOSCIENTISTS**



Speaker Program
Day 1



Speaker Program
Day 2



AIG BULLETIN 76

Publisher: Australian Institute of Geoscientists

ALBURY

September 2024

Australian Institute of Geoscientists
PO Box 576
CROWS NEST NSW 1585
Australia
Telephone: 08 9427 0820
Email aig@aig.org.au

ISBN: 978-1-876118-56-3
ISSN 0812 6089



**AUSTRALIAN
INSTITUTE OF
GEOLOGISTS**

This book is copyright. All rights reserved. No part of this publication may be reproduced, stored in a retrieval system, or transmitted in any form or by any means without the prior permission in writing of the copyright owners.

Bibliographic reference:

Greenfield, J.E. (compiler), 2024. Bulletin 76: Discoveries in Tasmanides 2024. Australian Institute of Geoscientists, PO Box 576 Crows Nest NSW 1585.

The Organising Committee sought to obtain a broad coverage of this topic. Every effort was made to minimise amendments in content of the resultant papers. The opinions and statements within the individual papers comprising this Bulletin reflect solely the viewpoint of their authors and are not necessarily shared by the Organising Committee or the Australian Institute of Geoscientists.

Short quotations from the text of this publication and copies of maps, figures, tables, etc. (excluding any subject to pre-existing copyright) may be used in scientific articles, exploration reports and similar works provided that the source is acknowledged and subject to the proviso that any excerpt used, must be strictly fair and balanced. Other than for the purposes of research or study the whole work must not be reproduced without the permission in writing of the Australian Institute of Geoscientists.

Organising Committee 2024

Kristyn	Adamczyk (Chairperson)
Melinda	Deacon (Chairperson)
Mark	Arundell
Jess	Askew
Richard	Blewett
Kenny	Bush
Kaylene	Camuti
Glenn	Coianiz
Fiona	Czuczman
Glen	Diemar
Toby	Erskine
Geoff	Fraser
Lindsay	Gilligan
John	Greenfield
Jaime	Livesey
Daniel	Logan
Doug	Menzies
Jeneta	Owens
Yamei	Wang

PREFACE

The 2024 Discoveries in the Tasmanides conference represents the culmination of two years of organisation by a dedicated volunteer committee from industry and government. Committee members generously donate their time to ensure that our community can meet on a biennial basis to network, exchange ideas and discuss exploration and project advances across the Tasmanides. Not only does this keep conference delivery costs down but it also makes it accessible to a wide variety of people including our pipeline of future geoscientists. We are extremely proud of the dedication and enthusiasm that this group has shown to make the 2024 conference a success.

The Tasmanides continues to be an exciting and bountiful place for mineral exploration. The tremendous industry support we have received once again is a direct reflection of this. On that note, we would like to extend a heartfelt thank you to our sponsors, booth holders and of course our speakers without which we wouldn't have a reason to meet nor a *raison d'etre*.

Discoveries in the Tasmanides conference was inaugurated in 2006 as a collaboration between SMEDG and the Geological Survey of NSW with the vision of providing exploration geoscientists the opportunity to present on their projects in the Palaeozoic Tasmanides of Eastern Australia. AIG subsequently joined the collaboration. To both complement and contextualise these projects Big Picture presentations are invited from recognised specialists in metallogenesis, tectonism and mineral exploration.

The foundation principles of the Discoveries in the Tasmanides conference are:

1. Conference speakers must recognise that all presentations are to be technical in nature and non-promotional. References to market capitalisation, share price, and the like, are strongly discouraged.
2. All committee members perform their roles on a volunteer, non-paid basis.
3. We encourage students to attend, contribute to the poster sessions and, where appropriate, apply for any financial assistance on offer.
4. Presentations are sought from across the Tasmanides with a diversity of commodities, deposit types, and locations represented.
5. We seek both mineral exploration practitioners to share their projects and specialists to inform us on relevant developments in minerals geoscience.
6. Conferences are held in areas that have a recognised wine industry.
7. Socialising over a good wine makes for effective networking in our profession which thrives on shared learnings.

This volume of extended abstracts will be made available through several website including:

- Discoveries in the Tasmanides: <https://discoveriesinthetasmanides.com.au/>
- The Sydney Mineral Economic Discussion Group (SMEDG): www.smedg.org.au
- The Australian Institute of Geoscientist (AIG) website: www.aig.org.au

Finally for the first time since its inauguration in 2006 we venture south to Albury, host to the famous Rutherglen wine region. We are thrilled to be sharing the spotlight with Australia's oldest wine region. Positioned on the plains of the Murray River, at an elevation of 150 metres, the region has garnered a well-deserved reputation, celebrated for its fortified wines, robust tannic reds and rich family heritage. We hope you find some time to sample and enjoy the delights that this fantastic part of the world has to offer.

We would like to once again, extend our appreciation to the volunteer committee members, speakers and sponsors whose support and collaboration have been instrumental in the organisation of this conference. We hope this volume serves as a useful reference and inspires further research and innovation in the important field of mineral exploration and discovery.

Kristyn Adamczyk & Melinda Deacon
Co-Chairs

CONTENTS

(titles abridged)

Author	Title	Page
David A-Izzeddin	Dittmer – A Cretaceous intrusive-related gold-copper System	1
David Biggs	The Evolution of the Bowdens Silver Ore Body	10
Richard Blewett	Gold around granite margins: Weethalle Gold project, central NSW	20
Kenneth Bush	Sunday Creek: High-grade Au-Sb discovery Clonbinane, Victoria	37
Peter Caristo	Mt Chalmers VHMS – New life for a forgotten gem	42
Ross Cayley	The giant Lachlan Orocline of eastern Australia	43
Yanbo Cheng	Mineral systems and metallogeny of the Delamerian Orogen margin	55
Karen Connors	Crustal nature and architecture of the Eastern Lachlan Orogen	66
Peter Duerden	Wallrock-hosted epithermal-porphyry system at the Spur Project, Cargo district NSW	84
Michael Fenwick	Discovering Golden Ridge and NE Tasmania's untapped potential	93
Owen Greenberger	Dorchap Lithium Project update, northeast Victoria	95
John Greenfield	State of Play for Mineral Exploration in the Tasmanides	102
Scott Halley	Pathfinder element footprints: Eastern Australian Mineral Deposits	110
Sebastian Hind	Wirlong Cu-Ag Deposit, Cobar Basin, New South Wales	113
Ned Howard	New insights from the Cowal gold deposit	127
Roger Jackson	The unique, high-grade, Hill End Reward Gold Mine	131
Todd McGilvray	The Nymagee Cu-Zn-Pb-Ag-Au deposit, Nymagee NSW	148
David Meates	Northern Molong Porphyry Project- Boda-Kaiser Au-Cu Porphyry	159
Doug Menzies	Alkalic porphyry exploration in the northern Macquarie Arc	172
Damien Mizow	Geology and deposit model of the Narraburra REE Deposit	185
Scott Munro	Peak Gold Mine – 31 years of continuous production	195
Ian Neilson	The Haunted Stream goldfield – in Victoria's east Gippsland	196
Steven Oxenburgh	Myall Project: persistence under cover in the East Lachlan	204
Gideon Rosenbaum	Plate tectonics of the New England Orogen and its mineral deposits	214
Hugo Serra	Genesis of the Ravenswood Gold Deposit	220
Brenainn Simpson	Exploration potential for peralkaline REE deposits in central-west NSW	233
Tom Wall	The Bauloora Project, NSW: an Early Devonian epithermal system	236
Sean Westbrook	Pursuit of IOCG systems in Western Tasmania	245

Thank you to our 2024 conference sponsors, partners, and booth holders

Platinum Sponsor



Regis Resources
regisresources.com.au

Gold Sponsor



Newmont Australia
www.newmont.com

Gold Sponsor



AngloGold Ashanti
anglogoldashanti.com

Gold Sponsor



Evolution Mining
evolutionmining.com.au

Silver Sponsor



Alkane
alkane.com.au

Silver Sponsor



Bowdens Silver
bowdensilver.com.au

Bronze Sponsor



ALS Global
alsglobal.com

Bronze Sponsor



Max Geo
www.maxgeo.com

Bronze Sponsor



Fleet Space
fleetspace.com

Bronze Sponsor



Inflection Resources
inflectionresources.com

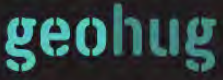
Bronze Sponsor



RME Geological Services

Thank you to our 2024 conference sponsors, partners, and booth holders

Media Partner



Geohug
geohug.rocks

Conference Dinner



Durock Drilling
durockdrilling.com.au

Ice Breaker Sponsor



Ophir Drilling
ophirdrilling.com.au

Rutherglen Wine Degustation Event



NSW Minerals Council
nswmining.com.au

Conference Lunches



Chief Drilling
chiefdrilling.com.au

Student Posters Sponsor



SMEDG
smedg.org.au

Name Tags



OREAS
oreas.com

Field Trip



Geological Society of Victoria
gsv.vic.gov.au

Coreshack Sponsor

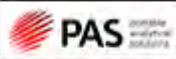
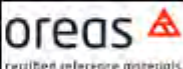
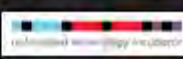


Southern Cross Gold
southerncrossgold.com.au

Notebook Sponsor



Geos Mining
geosmining.com

<p>Booth Holder</p>  <p>Fender Geophysics fendergeophysics.com.au</p>	<p>Booth Holder</p>  <p>Gap GeoPhysics gapgeo.com</p>	<p>Booth Holder</p>  <p>ALS https://www.alsglobal.com</p>	<p>Booth Holder</p>  <p>Gnomic www.gnomic.com.au</p>
<p>Booth Holder</p>  <p>AMETS https://amets.com.au</p>	<p>Booth Holder</p>  <p>SciAps sciap.com</p>	<p>Booth Holder</p>  <p>Prospectors prospectors.com.au</p>	<p>Booth Holder</p>  <p>Portable Analytical Solutions paslabs.com</p>
<p>Booth Holder</p>  <p>Dynamics G-Ex dynamicsgex.com.au</p>	<p>Booth Holder</p>  <p>MIME</p>	<p>Booth Holder</p>  <p>SRK srk.com</p>	<p>Booth Holder</p>  <p>Evident Australia evident.com.au</p>
<p>Booth Holder</p>  <p>SGS sgs.com</p>	<p>Booth Holder</p>  <p>Oreas www.oreas.com</p>	<p>Booth Holder</p>  <p>Max Geo www.maxgeo.com</p>	<p>Booth Holder</p>  <p>GSNSW Geological Survey</p>
<p>Booth Holder</p>  <p>Community Engagement communityengagement.com.au</p>	<p>Booth Holder</p>  <p>Geoscience Australia www.ga.gov.au</p>	<p>Booth Holder</p>  <p>GSQ gsq.gov.au</p>	<p>Booth Holder</p>  <p>EarthSQL EarthSQL</p>
<p>Booth Holder</p>  <p>Fleet Space fleet-space.com</p>	<p>Booth Holder</p>  <p>automated mineralogy incubator automatedmineralogy.com.au</p>	<p>Booth Holder</p>  <p>Mining One miningone.com.au</p>	

DITTMER – A CRETACEOUS INTRUSIVE-RELATED GOLD-COPPER SYSTEM

D. A-Izzeddin

Ballymore Resources Limited, Suite 606, Level 6, 10 Market Street, Brisbane, QLD, 4000

Key Words: Dittmer, Intrusive-Related Gold System (IRGS), gold, copper, Connors-Auburn Province, New England Fold Belt, Cretaceous

INTRODUCTION

North Queensland is a prolific gold-producing region, hosting over 40Moz of gold, with nearly half the deposits being recognised as Intrusive-Related Gold Systems (“IRGS”) (Morrison, 2017). The Proserpine area hosts many gold deposits and remains poorly explored. The Proserpine area is considered to have similarities with the Ravenswood intrusive-related gold system, hosting a range of vein-, breccia- and porphyry-hosted deposits.

Ballymore Resources Limited commenced exploring in the Proserpine district in 2019 to assess the potential of the area for IRG deposits. The Dittmer Project is located approximately 20km west of Proserpine and 30km south of Bowen in Northeast Queensland.

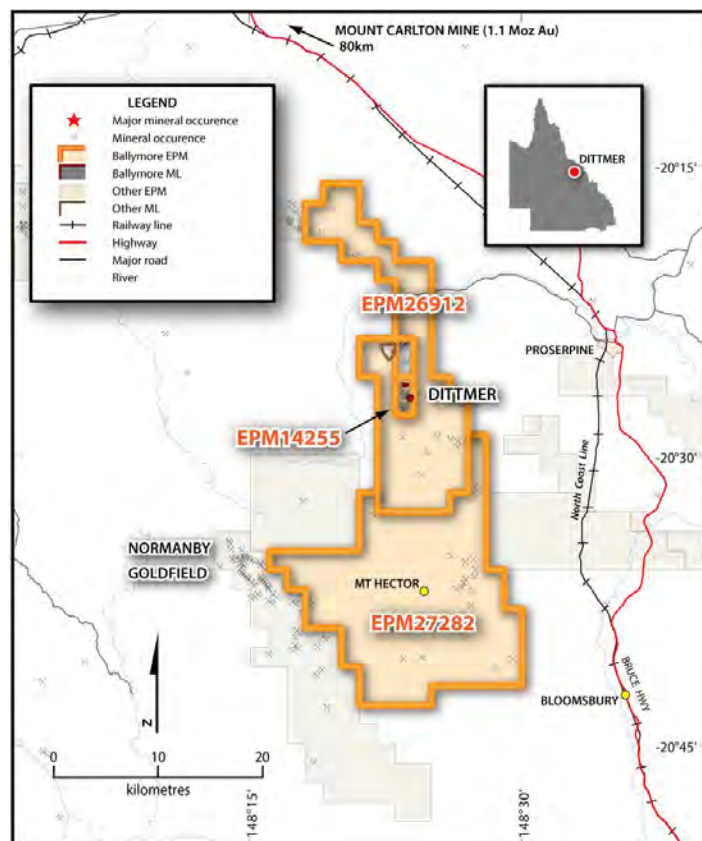


Figure 1: Dittmer Project

Intrusion-Related Gold Deposits (IRGD) form a major class of ore deposits, including various deposit styles as diverse as skarns, mineralised breccias, sheeted veins and disseminations within or peripheral to the causative intrusion. Most North Queensland IRGD are closely associated with Permo-Carboniferous intrusives and occur at porphyry

level (i.e. 2-5 km depth), with most deposits displaying a Bi +/- Te chemical association. While the Dittmer deposits occur within the thermal aureole adjacent to the main intrusive body and have a similar geochemical signature, the causative intrusive for the local gold deposits appears to be spatially related with younger, Cretaceous intrusive units of the Hecate Granite.

HISTORY

Gold was first discovered in the southern Dittmer Project area in 1872 and were operated in the late 1800's and early 1900's. A number of shallow, historic mines operated in the Dittmer area, and produced at extremely high gold grades, including Loch Neigh (567 g/t Au), Scorpion (355 g/t Au), Golden Gem (278 g/t Au) and Young Crusader (120 g/t Au).

The Dittmer Mine is historically the largest mine in the region and exploited the Duffer Reef. After its discovery in 1934, it was cited as one of the highest-grade gold mines in Australia¹. From 1935 to 1951 it produced over 54,500 oz of gold, 23,400 oz of silver and 295 long tons of copper (300 t) from 17,100 long tons of ore. Production figures are incomplete after 1947, but between 1935 and 1947 reported production figures indicate that the mine operated at an average mined grade of 151.1g/t Au 66.8g/t Ag and 2.8% Cu. Mining also occurred in the 1980's, reclaiming stopes in the upper levels of the mine.

The area was the focus of exploration for porphyry-style base metal occurrences in the 1960's-70's. MIM and CRA recognised two porphyry copper deposits at Julivon Creek and Andromache. Mineral Resource Development Pty Ltd established a crushing and cyanide treatment plant at Andromache to treat the oxide gold cap between 1979 and 1986.

Only limited modern exploration has been undertaken in the Dittmer Project area.

REGIONAL GEOLOGY

The Dittmer Project licences are located within the Connors-Auburn Province in the northern New England Fold Belt. The Connors-Auburn Province is a linear belt of predominantly subaerial, terrestrial felsic volcanics and granitoids of the Auburn Subprovince in the south and the Connors Subprovince in the north (Withnall et al, 2009). The northern part of the Connors Subprovince, which hosts the Dittmer Project, is dominated by plutonic rocks. Most of the magmatic belt is late Carboniferous – early Permian, but some volcanics and granitoids are early Carboniferous and considered to represent an Andean-style, continental volcanic arc associated with the Yarrol Province forearc assemblage and the accretionary wedge of the Wandilla Province (Withnall & Cranfield, 2013).

PROJECT GEOLOGY

The Dittmer Project area is dominated by volcanic and sedimentary units of the early Permian Carmila Beds which have been intruded by various Permo-Carboniferous and Cretaceous granitoids, including intrusive units of the Urannah Igneous Complex as well as the Cretaceous Hecate Granite. Reduced to Pole (RTP) magnetics data shows a strong northwest-trending magnetic high corridor on the margin of the Cretaceous Hecate Granite. This magnetic anomaly represents hornfelsing associated with the contact aureole.

¹ The Bowen Independent, Friday October 23, 1942

Mineral deposits often form in structurally active areas where large, steep crustal faults are intersected by other structures to produce active dilatant sites and deep plumbing systems during periods of intrusion and hydrothermal activity. Locally, there is a close spatial association of gold (and some copper) mineralisation with the structurally deformed margins of the Hecate Granite intrusion within the Dittmer Project area. A number of major northwest, northeast and north-south trending structures transect this area. The area has also been intruded by various stocks and dykes, considered to be comagmatic with the Hecate Granite, and have often exploited the pre-existing or active structures. In addition, many of the mineral occurrences in the region sit within this aureole and are often spatially associated with these later dykes and stocks.

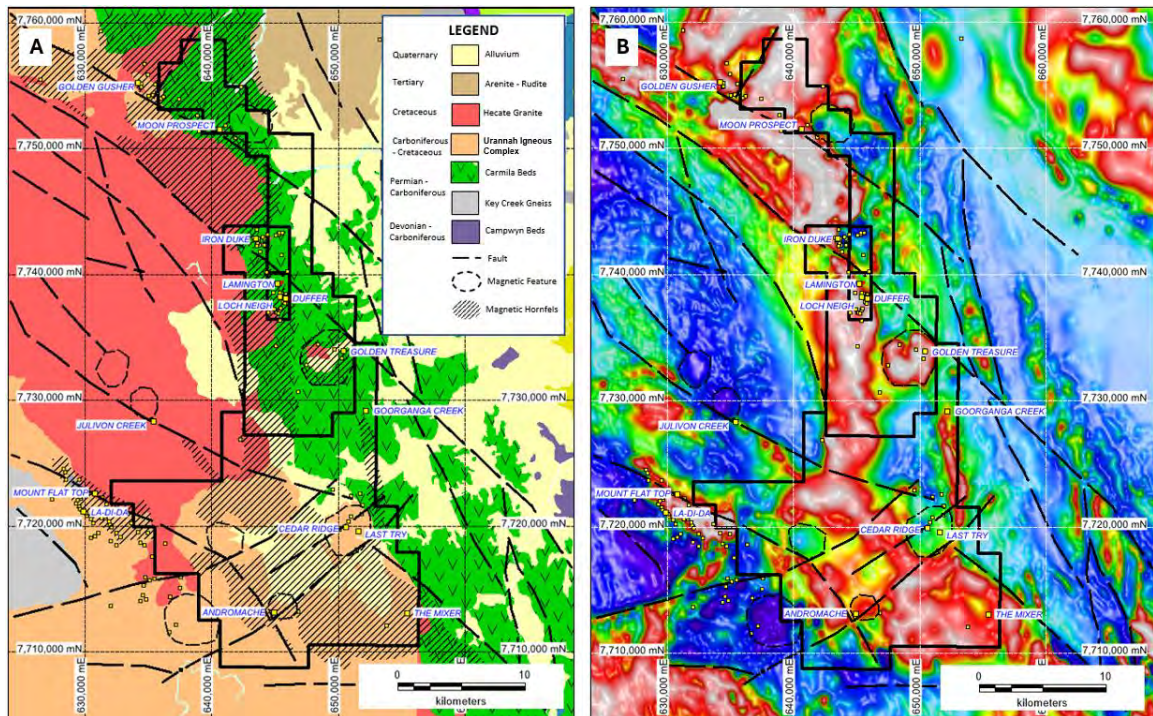


Figure 3: (A) Dittmer Project geological setting; (B) Dittmer Project Reduced to Pole Magnetics.

MINERALISATION

Many of the deposits recognised in the Dittmer Project show characteristics typical of IRGD. Deposit styles recognised in the Dittmer district include:

- Epithermal vein / silica cap (e.g. Mt Quandong)
- Mesothermal, discrete quartz-sulphide gold bearing veins (e.g. Dittmer, Lamington)
- Stockwork quartz-sulphide gold bearing veins (e.g. Cedar Ridge)
- Massive sulphide lead-zinc-copper (e.g. The Mixer)
- Gold-bearing breccia pipes / rhyolite flow dome (e.g. Mount Flat Top, Moon)
- Porphyry copper-gold deposits (e.g. Julivon Creek, Andromache)
- Iron-bearing skarns (e.g. Iron Duke, Iron Knob).

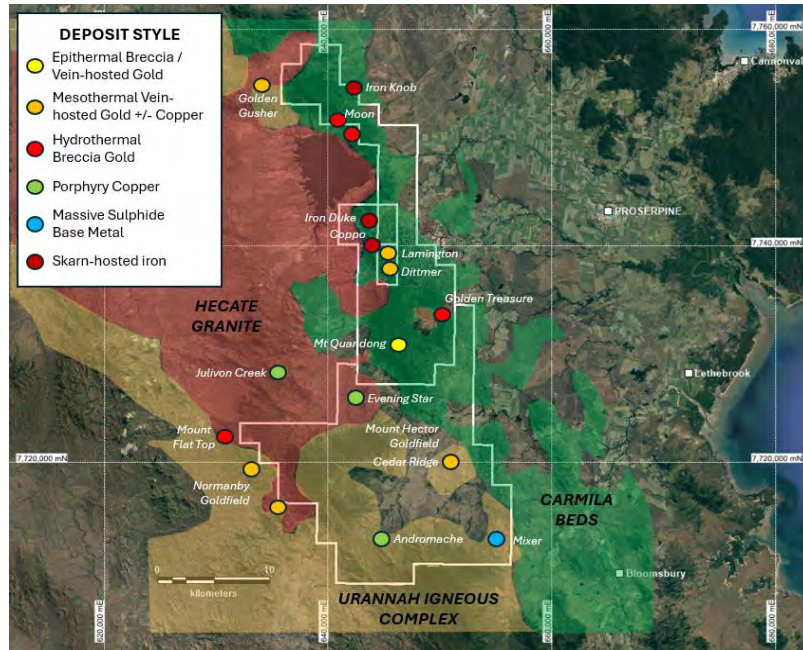


Figure 4: Deposit styles in Dittmer Project Area

Vein systems in the Dittmer Project area generally comprise quartz veins with associated pyrite, chalcopyrite, galena and sphalerite. Alteration associated with the veining includes fine-grained hematite and clay in felsic rocks; and sericite, epidote and disseminated ultrafine grained pyrite in mafic rocks.

In addition, a number of porphyry style copper-gold-silver-molybdenum deposits have been recognised in the local area. The Julivon Creek prospect is a porphyry Cu-Mo deposit which occurs over an area of 3.0 km x 1.5 km in altered granodiorite belonging to the Hecate Granite. The Andromache prospect hosts an intrusion (interpreted to be Cretaceous) of variably altered quartz feldspar porphyry and andesite dykes intruding a granodiorite with associated Cu-Au-Mo mineralisation.

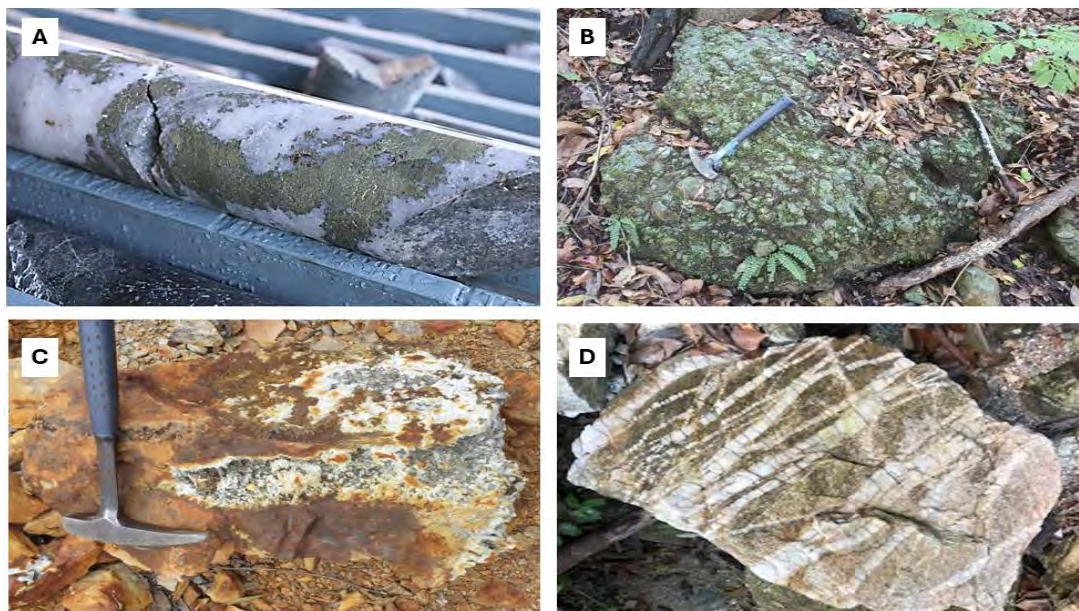


Figure 5: Dittmer Project mineralisation styles: (A) Duffer Lode mesothermal quartz-pyrite-chalcopyrite lode; (B) Golden Treasure hydrothermal breccia; (C) Cedar Ridge stockwork quartz-pyrite veining; (D) Julivon Creek stockwork quartz-chalcopyrite-molybdenite veining.

The age of gold mineralisation is postulated to be Cretaceous, based on the overprinting relationships of many veins identified through mapping and drilling in the Dittmer Project area. These commonly occur on the margins of Cretaceous dykes and within the contact aureole of the Hecate Granite. Mineralisation occurs as quartz and quartz-sulphide veins and breccia-fill in fault zones. Vein systems have been mapped for up to 1km and vary in thickness from several centimetres up to 1 to 2 metres thick. Mapped porphyry deposits also are associated with these later intrusions.



Figure 6: (A) Example of a quartz lode sitting on the contact between Camila Beds volcanic breccias and later dolerite dyke at Lamington (LMDD001); (B) Example of a flat-lying quartz lode sitting at contact between Urannah Igneous Complex granite and a later dolerite dyke at Cedar Ridge.

GEOCHEMISTRY

Metal associations in North Queensland IRG deposits also exhibit broadly similar chemical zonation patterns from core to periphery as follows:

- Cu +/- Te +/- Mo +/- W +/- Sn → Zn-Pb-Ag → As-Sb → Ca +/- F +/- Ba +/- Hg
Core → Margin

The Dittmer area has only undergone minor modern exploration and limited multi-element geochemical analysis. In the data available there is clear Cu-Pb-Zn zonation apparent in the stream sediment data.

The Dittmer Project area is defined by a broad north-northwest trending zinc geochemical anomaly that corresponds with the hornfelsed aureole adjacent to the Hecate Granite and extends for approx. 50km with the most elevated zone (i.e. >100ppm Zn) occurring in the Dittmer – Golden Treasure area, extending for over 15km, with the majority of the major historic gold deposits being located within this anomaly. The same area is also highlighted by moderately elevated lead with a few discrete targets highlighted by stronger anomalies (i.e. >100ppm Pb), including the Golden Treasure and The Mixer prospects.

Porphyry copper style mineralisation occurs on major northwest fault corridors with the Julivon Creek porphyry copper deposit (located adjacent to Ballymore Resource's Dittmer Project) and the Andromache deposit sitting on the same fault corridor. The Dittmer mine area sits on a similar northwest fault corridor and is also characterised by an elevated copper anomaly, which may be suggestive of an underlying porphyry copper system.

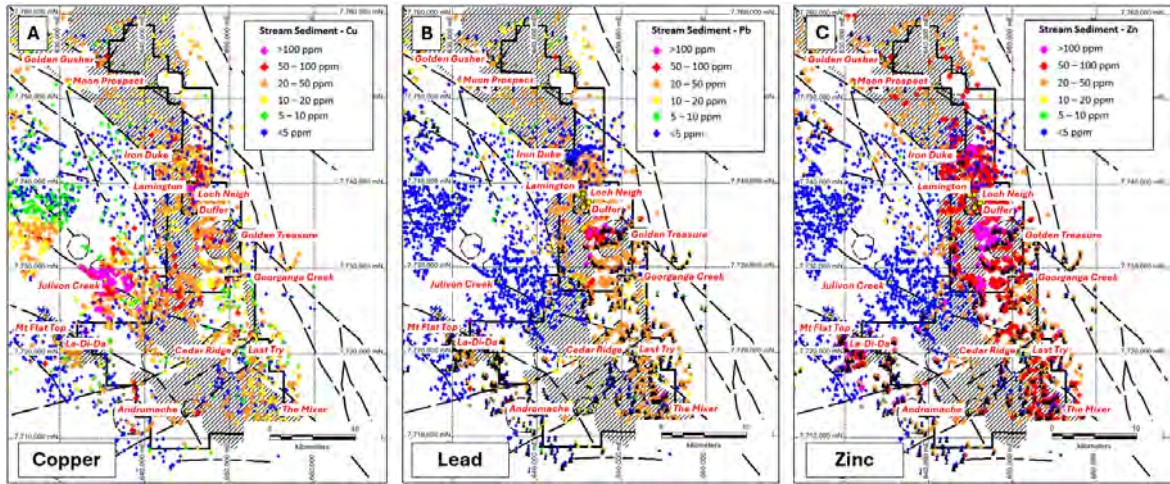


Figure 6: Dittmer Project stream sediment geochemistry (A) Copper; (B) Lead; (C) Zinc.

Maximum multi-element rock chip results collected within the project area include:

- Gold 544 g/t Au
- Silver 6530 g/t Ag
- Copper 28.2% Cu
- Antimony 254 ppm Sb
- Arsenic 849 ppm As
- Bismuth 2.42% Bi
- Lead 0.14% Pb
- Molybdenum 137 ppm Mo
- Tellurium 254 ppm Te
- Tungsten 2273 ppm W
- Zinc 0.36% Zn

Multi-element data collected by Ballymore has highlighted a classic IRGS geochemical signature of Au-Ag-Cu-Bi-Te-As-W-Se in the Dittmer Project area.

INTRUSIVE-RELATED GOLD SYSTEM GEOLOGICAL MODEL

Northeast Queensland is a prolific mineral province with over 40Moz of identified gold endowment, and nearly half of the deposits are recognised as IRG deposits. Our understanding of IRG systems has made great advances in the past 30 years with improved understanding of the magmatic sources, mineralisation styles, tectonic setting and geochemical zonation (Baker, 2002; Hart, 2007; Sillitoe & Thompson, 1998; Morrison, 2017).

The eastern coast of Queensland has a history of discovery and mining IRGS mineralisation. Morrison (2017) presented a mineralisation model for IRGS showing North Queensland examples (Figure 7). He reported that 130 IRG systems had been identified to date in North Queensland, with only 30 of these systems being well explored.

Many well-known gold deposits in Northeast Queensland have been assigned to the IRGS model, including Kidston (5 Moz Au), Ravenswood / Mount Wright (5.8 Moz Au), Mount Leyshon (3.5 Moz Au), Pajingo (3.5 Moz), Red Dome / Mungana (3.2 Moz Au), Mount Carlton (1.4 Moz Au) and Mount Morgan (17 Moz Au and 239 Kt Cu). A collation of data by Morrison (2017) suggests that the dominant causative intrusions for North Queensland IRG systems are Permo-Carboniferous age, slightly oxidised to slightly

reduced and moderately fractionated. Mineralisation is commonly associated with rhyodacitic intrusive stocks belonging to the Kennedy Igneous Association and are interpreted to have formed in cauldron subsidence complexes. These deposits typically exhibit Au-Sn-W-Mo metallogeny.

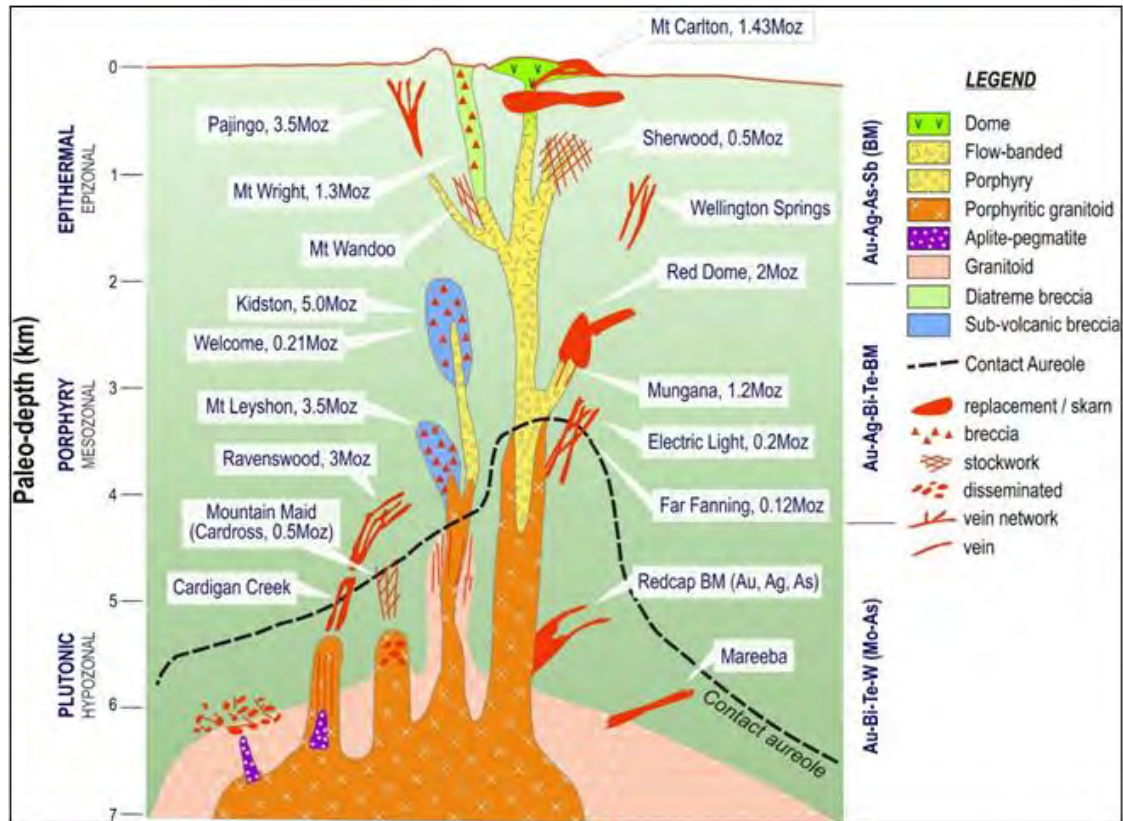


Figure 7: IRGS Mineral System Model with North Queensland Examples (Morrison, 2017).

The Dittmer Project hosts a range of vein-, breccia-, skarn- and porphyry-hosted deposits dominated with gold, silver, copper and other base and critical minerals. The Dittmer Project has many similarities with other IRG deposits in North Queensland. For example, mineralisation in the area exhibits a close spatial association with younger intrusions and generally occurs within the thermal aureole of the intrusion. In addition, the deposits exhibit a classic IRGS geochemical signature of Au-Ag-Cu-Bi-Te-As-W-Se.

While the Dittmer Project has many similarities with other North Queensland IRG deposits, the area has several inconsistencies and differences. The Dittmer deposits are interpreted to be Cretaceous in age, making them significantly younger than most IRG deposits in the region. Furthermore, the mineralisation is often more oxidised than is typically noted with Permo-Carboniferous age deposits. Massive specular hematite is commonly associated with copper-gold mineralisation within the Dittmer Project area. This suggests that mineralised fluids (at least one phase) emanating from the Hecate Granite was strongly oxidised and within the hematite stability field, representing a significant departure from the current IRGS model for North Queensland.

The mineralisation in the northern and central part of the project area (e.g. Dittmer / Lamington) are vein-style and typically hosted in volcanics and sediments of the Permian Carmila Beds, while the southern part of the project area, where the Andromache and Cedar Ridge prospects occur, is dominated by Carboniferous intrusive units of the Urannah Batholith. The southern project area, where the granitic rocks are exposed, likely represents a deeper erosional level where porphyry styles of mineralisation are exposed and dominate. In contrast, the northern and central part of the project area is

preserved to a higher level and is dominated by vein-hosted mesothermal / epithermal style mineralisation in volcanics / sediments and may have larger porphyry-style deposits preserved at depth.

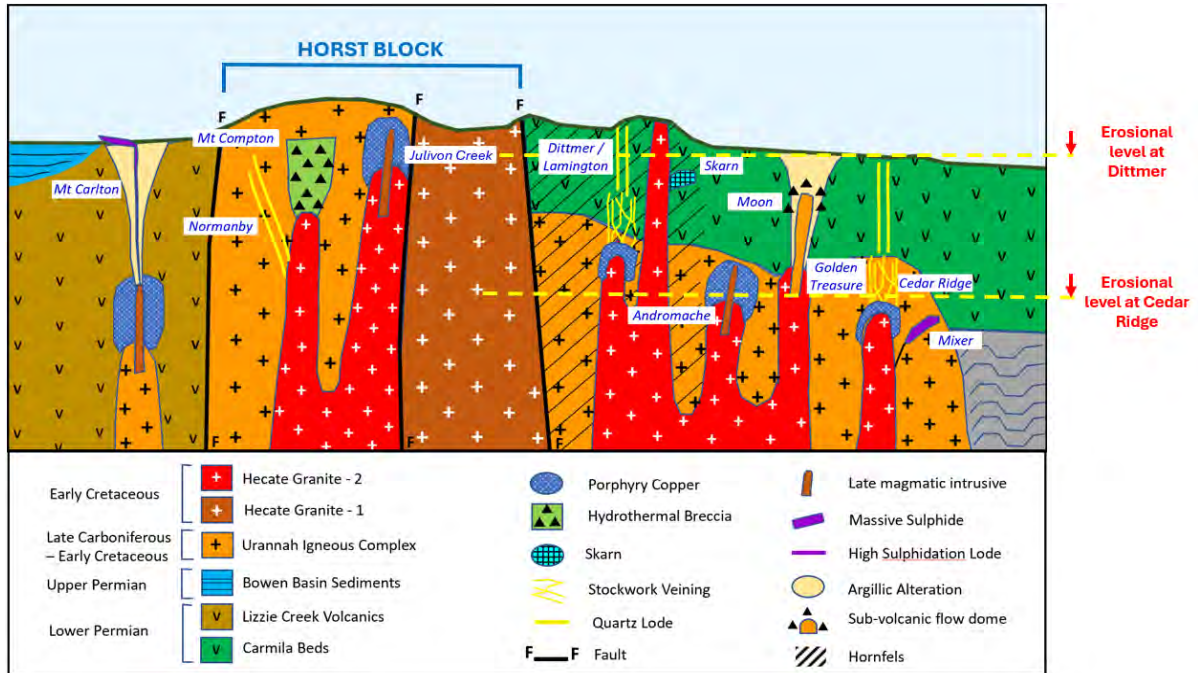


Figure 8: Conceptual model of depth of mineralisation in the Dittmer Project area.

CONCLUSIONS

The Dittmer area was historically mined for high-grade gold, and during operation, the Dittmer mine was one of the highest-grade gold mines in Australia. The area also hosts several porphyry copper deposits. Despite the presence of significant deposits, only limited modern exploration has been undertaken in the region.

Recent work by Ballymore has determined that the area hosts a range of deposit styles with characteristics typical of IRG deposits. Despite similarities to other North Queensland IRGS, the mineralisation is postulated to be Cretaceous in age and more oxidised. Further work is underway, including further mapping, multi-element geochemical surveys, detailed geophysical surveys and geochronology, to confirm the relationships between later intrusives and mineralisation observed in the area. Our better understanding has already yielded significant exploration results and ongoing work may lead to further exciting discoveries in this historic mining district.

ACKNOWLEDGEMENTS

Many people have contributed to the development of the understanding of the Dittmer deposits and models described, and special acknowledgement goes to David Webb, Deanna Houston, Shane Crees and Juli Hugenholtz.

REFERENCES

BAKER, T. 2002, Emplacement depth and CO₂-rich fluid inclusions in intrusion-related gold deposits. *Economic Geology* 97: 1109–1115.

HART, C.J.R., 2007, Reduced intrusion-related gold systems, in Goodfellow, W.D., ed., Mineral deposits of Canada: A Synthesis of Major Deposit Types, District Metallogeny, the Evolution of Geological Provinces, and Exploration Methods: Geological Association of Canada, Mineral Deposits Division, Special Publication No. 5, p. 95-112.

MORRISON, G, 2017. Intrusion-Related Gold Deposits in North Queensland. Presentation. GSQ Project final meeting, December 07, 2017

SILLITOE, R.H. & THOMPSON, F.H., 1998. Intrusion-Related Vein Gold Deposits: Types, Tectono-Magmatic Settings and Difficulties of Distinction from Orogenic Gold Deposits. *Resource Geology*, vol. 48, no. 2, 237–250, 1998.

WITHNALL, I.W. & CRANFIELD, L.C. 2013. *Geology of Queensland*. Geological Survey of Queensland online publication

WITHNALL, I.W., HUTTON, L.J., BULTITUDE, R.J., VON GNIELINSKI, F.E. & RIENKS, I.P., 2009: Geology of the Auburn Arch, southern Connors Arch and adjacent parts of the Bowen Basin and Yarrol Province, central Queensland. *Queensland Geology*, 12, 1–461.

THE EVOLUTION OF THE BOWDENS SILVER ORE BODY AND ITS EXPLORATION IMPLICATIONS

David Biggs¹, Emmanuel Madayag¹ Thomas Klein¹

¹Bowdens Silver Pty Limited, 68 Maloneys Road, Lue NSW, 2850

Key Words: Bowdens Silver, epithermal, rhyolite, caldera, seismic, wavelet, geological modelling, Bowdens Caldera Complex

INTRODUCTION

The Bowdens Ag-Zn-Pb-Au mineral system lies at the southern edge of an 11km wide Carboniferous felsic volcanic caldera within the Macquarie Arc of NSW, Australia. Its discovery was made in 1989 via stream sediment analysis (McConachy 2023). The mineral system is a well-preserved, textbook example of a zoned intermediate to low sulphidation epithermal system, possessing many distinct but recognisable features which are detailed in “Applied Structural Geology of Ore forming hydrothermal systems” (Rowland and Rhys, 2020). This extended abstract describes applied processes and workflows used by the Bowdens Silver technical team, to infer and characterise the mineral system geology. This workflow involves, integrating data and small-scale observations to identify and define causal features of the broader mineral and volcanic system. Equipped with this knowledge it has allowed the company to establish a framework to assess regional exploration prospects and define a geo-metallurgical framework for mining and process optimisation (Dominy *et al.*, 2018). The paper presents the results from the process of integration as a general geological model, a description of the kinematic drivers of the mineral system, a mineral system summary and the details of how recognized features were modelled. The Bowdens silver team is looking forward to rapidly deploying this integrated approach over its exploration prospects which display analogous geology and potential for mineral systems.

OVERVIEW

The Bowdens Silver Deposit (the Deposit) is located 240 kilometres west of Sydney near Lue in New South Wales. The current Ore Reserve, pending a 2024 update, comprises 29.9 million tonnes at 69g/t silver, 0.44% zinc and 0.32% lead which contains 66.32 million ounces of silver, 130.8 kilotonnes of zinc and 95.3 kilotonnes of lead.

The silver, zinc and lead mineralisation is hosted by the middle-Carboniferous aged Rylstone Volcanics (dated from U-Pb zircon and Ar-Ar muscovite, (Klein *et al.*, 2022)) and the underlying Ordovician aged Coomber Formation. Mineralisation outcrops on its southern part and dips shallowly to the north along the contact between the Rylstone volcanics and Coomber Formation. The volcanics unconformably overlie the eastern side of the northwest trending Northern Capertee Rise and are themselves unconformably overlain by the Permian to Triassic aged shallow marine to alluvial sedimentary rocks of the Sydney Basin. There is mounting evidence from deep drilling and seismic data, that the Deposit formed during the Carboniferous from volatile rich magmas that underplate the region. This has given rise to mineral occurrences and exploration prospects with similar metal compositions to the Deposit, both to the north and south, associated via a complex series of overlapping calderas, resurgent flow domes, cryptodomes, and regional, deep tapping structures, formed between the middle to late Carboniferous.

CONTINUED DEEP DRILLING, PETROLOGY, GEOCHEMISTRY SEISMIC SURVEYING AND 3D MODELLING

Since 2020, diamond drilling has continued both over the Deposit and at depth of the mineral system to the southwest, to a depth of 900m. 96.6km of seismic surveying has also been conducted across the Deposit and region, largely over the Rylstone Volcanics. Seismic surveying during 2023 built upon a previous seismic survey completed over the Deposit in 2022. This work has clearly identified the continuity of key mineral system features up to, and over, 1km depth across the region. This survey technique was well suited to the mostly flat lying geological contact of the Rylstone volcanics, resolving structure, and providing context for interpretation of near surface and drill observations. The interpretation of volcanic sequences is classically aided by facies analysis; however, these techniques are taxing to implement or impossible in RC chips where textural evidence of phenomena is destroyed or otherwise irreconcilable with diamond core.

EVOLUTION OF THE STRATIGRAPHY HOSTING THE BOWDENS MINERAL SYSTEM

The stratigraphy hosting the Deposit is principally more reactive volcanic breccia and ignimbrites of the Rylstone Volcanics which is a favorable setting for mineral deposition.

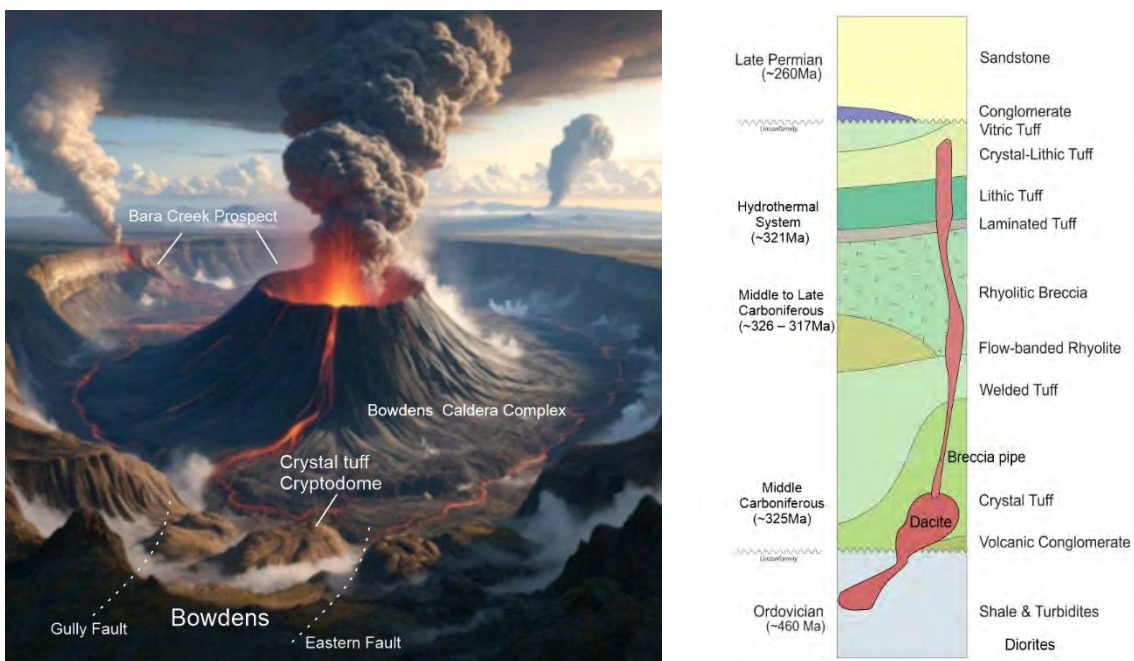


Figure 1 A rendition of the volcanic environment c.a. 326 Ma showing the early doming of the crystal tuff eastern and gully faults at the periphery of a caldera. The northern rim (in the distance on the left) depicts flows and eruptive centres akin to Bara creek. This caldera was later to form a crater lake and eventually be filled from ongoing volcanism.

The early setting for deposition of the main units is depicted in Figure 1. The stratigraphic package central to the mineral system is located at the periphery of the caldera and originates from two or more eruptive centres. The local eruptive centre is defined by a crystal tuff dome that is partially capped by variably welded tuffs. This crystal tuff dome could have resulted from the explosive disruption of a local magma chamber as a vulcanian eruption that deposited subaerially onto the paleo surface of the Coomber Formation. Alternatively, it may have formed via magma emplaced as a shallow dome beneath pre-existing welded tuffs which was then subject to a vulcanian eruption. It is suggested to be the latter, as uniform thermal alteration and crystal distribution of the ground mass would imply a constrained, non-expanded environment of emplacement, in

contrast to one of violent eruption and rapidly cooling. Later dacites continued to feed into this dome and have a similar texture as the crystal tuff (Figure 2).

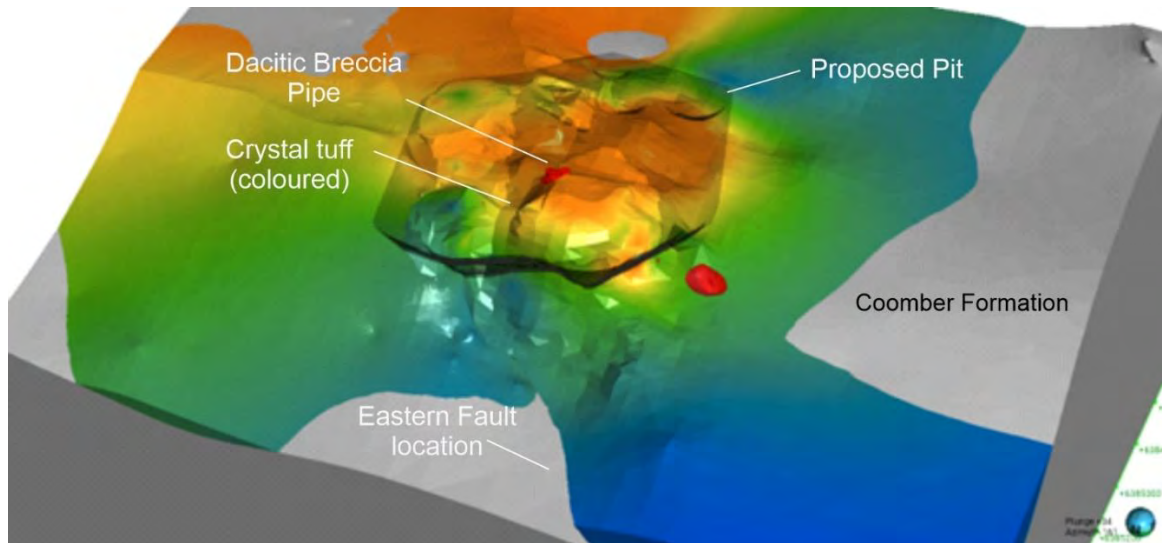


Figure 2 Crystal tuff at top basement colored by illite crystallinity (hot to cold), shows where the thermal zoning in the system is coincident with the Crystal tuffs doming center. Central to this dome is a small plug of volcanic breccia (red). This breccia comprises of entrained fragments of dacite.

The often-uniform nature of the crystal mass suggests the crystal tuff did not surface completely but was likely emplaced beneath the welded tuff and either domed or erupted through, brecciating and likely welding tuffs. Early magmatic brecciation of the welded and crystal tuff is linked to the emplacement of a dacitic magma that triggered eruption. Manganese rich carbonates (rhodochrosite and kutnohorite) pervade the dacite and are also present in the earliest colloform veins of the Northwest Zone (Carter, 2023), linking the mobilization of manganese in the deposit to the dacite. The source from which this crystal rich dome was fed is posited to be the same as the dacitic intrusive, which lies on a chemical continuum with the dacite (Figure 3).

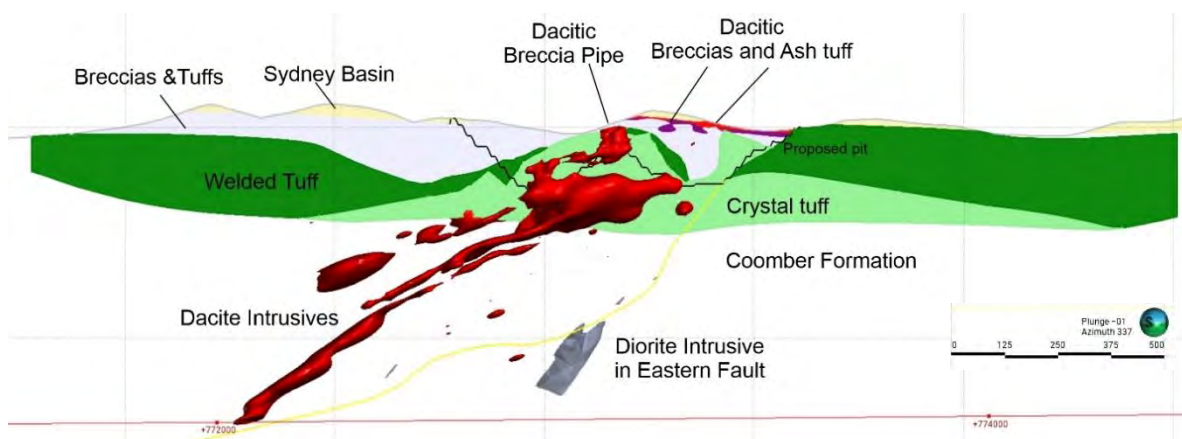


Figure 3 EW section showing the likely geometry of crystal tuff dome upwelling beneath the (green) welded tuff, emplaced synthetic to and in regionally active faults in the Coomber formation, evidently the melt evolved from rhyo-dacitic to dacitic in multiple pulses.

Welded tuffs fill an embayment within the crystal tuff and volumetrically it is unlikely to have erupted from the same vent. Later brecciation of this unit (including boulder clasts)

on the flanks of the dome implies the crystal tuff also domed beneath and up the eastern fault, brecciating the overlying welded tuff and deposited it on the flanks of the dome. Additional welded tuffs have been identified onlapping the crystal tuff on its northern and western sides, potentially related to a flow dome to the west (Figure 4).

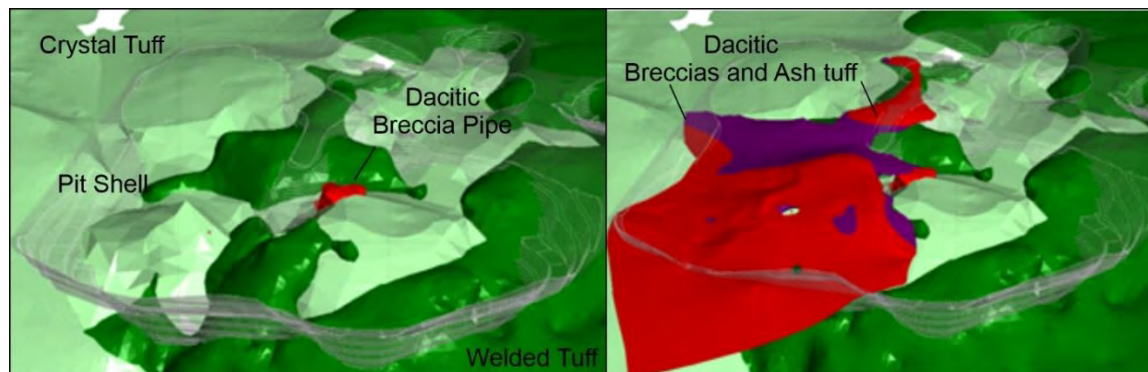


Figure 4 Looking southeast, the left panel shows the welded tuff (dark green) overlying the crystal tuff (light green) the dacitic breccia pipe central to the dome is in (red). The right panel shows the eruption of a dacitic breccia (purple) infilling the flank of the dome atop welded tuff, abutting the eastern fault. The final sequence depicted is a fine ash tuff (red) sharing a distinct chemical affinity with the underlying dacite and dacitic breccia. The Eastern block of welded tuff later rhyolitic breccias and lithic tuffs omitted for clarity.

The dacite was identified when it was discovered that it had been misclassified as crystal tuff in logging. This was then reclassified in other prior logged holes before being extended with further drilling. Notably anomalous intercepts were also identified using Data Mosaic, including a dacitic breccia pipe erupting to surface central to the deposit. This causal link established the mechanism of formation of the chemically similar units: narrow sills ascending into a breccia pipe and breccia flows of dacite underlying mixed ash flows at surface.

Following the identification of the pre-mineralisation eruptive events that connect the dacitic magma chamber to surface, also explains the zonation of alteration, and oxidation around the dacite. The elevated geothermal gradients likely proved sufficient as a conduit and catalyst for a convective hydrothermal cell and ground water interaction. The geometry of the dacite usefully defines the kinematics likely with melt crystallisation triggering a buildup of lithostatic overpressures allowing the propagation of sills, pipes and extensional fault networks.

Other key features of the Deposit that have been identified are minor paleo channels along the flanks of the resurgent dome into which cobbles of early pyrite mineralized material were deposited. Here exposed sulphides remain fresh in these clasts. This observation, along with mineral deportment, highlights the significant restite nature of the ore body where there is no gossan development. Typical epithermal system trace metal dispersion around the deposit is relatively constrained, but well explained by intense welding or fine ash material.

DEFINING HOW FLUID OVER PRESSURES ACTED ON MINERAL EMPLACEMENT.

The kinematics governing the mineral system are variably described in earlier work, which identified two major faults (Eastern and Gully faults) that have since been confirmed to be two of many listric faults. Locally, many east to west caldera collapse faults north of the Deposit may have focused crystal doming, intrusion and ore development, but there is limited evidence that they acted as the primary conduits to upwelling hydrothermal fluids.

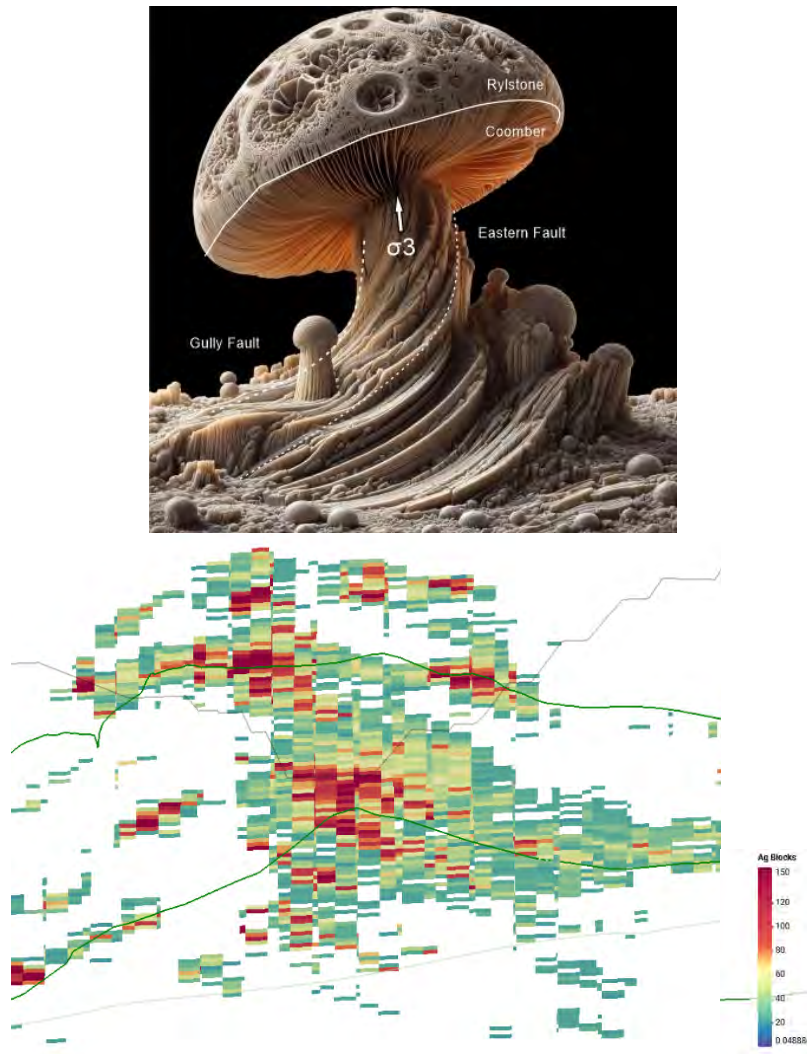


Figure 5 Left a depiction of how a natural system that propagates perpendicular to the earth's surface, the silver distribution in the Bowdens Mineral System on the right (Silver resource blocks > 30g/t) serves as an exploration model analogue.

The recognition that listric faults bound most of the mineralisation and form conduits to the site of emplacement is one of the key elements in a mineral system (McCuaig, Beresford and Hronsky, 2010). In this case, the active pathways lie within a brittle rhyolite that steepens near surface from near bedding parallel in the Ordovician Coomber Formation at depth. It is this feature of the system that jars against the bias and inbuilt intuition that most geological terrains have primed geologists with (Cowan, 2016).

Mineralisation throughout the Deposit is deposited at low temperatures, often emplaced within a halo of earlier silica - pyrite fluidised brecciation, which has clearly acted to impede porosity and create overpressures within a lower fluid pressure regime. This disequilibrium in fluid pressures has seemingly allowed a textbook rotation of the plane of detachment to be parallel to the land surface at depth (Yuan, Leroy and Maillot, 2020). The fineness of the silver minerals in the main zones tends to 80% with a deportment less than 20um. This is suggested to be due to fluids being injected (through micro seismic activity) into low porosity units, percolating upwards in a dendritic manner. This was followed by hydrothermal fracturing where fractures formed preferentially subparallel to bedding and volcanic stratigraphy with steep, randomly anastomosing veins, hindering typical kinematic analysis from oriented drill core.

Ample textural evidence suggests that failure was due to local low permeability and hydrothermal sealing permitting local overpressures (Carter, 2023). Flat lying faults with slicken fibres, and centimetre-scale black bands of cataclasite material, highlight the occurrence of repeated micro seismic events, characteristic of fluid injection stimulating brittle failure (Cox, 2020). Mineral systems are often formed by these repeated events to suitably concentrate ore. The initial RC drilling campaigns over the Bowdens Deposit provided a skewed representation of the silver mineralisation as being disseminated. Continued diamond drilling interpretation and study (Souvanan, 2018; Lay, 2019; Carter, 2023) have since better defined the paragenetic sequence of mineralisation across varying zones.

Texturally, the overprinting of brittle fractures and alteration of crystal-tuffs and ignimbrites (variously welded and brecciated), is a daunting level of complexity for any geologist to discern. Vein orientations provide minimal information as they originally propagated upwards in a random manner and mechanisms of alteration can be from in-situ fluid release or nearby volcanic sources. Additionally, volcanic erratics scattered throughout the sequence present further sources of confusion in drilling.

THE BOWDENS MINERAL SYSTEM SUMMARY

Source of Metals

Seismic surveying has highlighted a distinct contact at 1200m depth that is consistent throughout the region. Coincidentally, most exploration prospects lie at its periphery and have common epithermal metal associations. This is thought to be the top of a fractionated Carboniferous aged batholith, crystallising and exsolving metal bearing fluids into the country rock and an ultimate source of volcanism. It's emplacement into the Ordovician aged, Macquarie arc phase 4 volcanic basement may also have remobilised existing copper rich mineralisation (Ian Graham, 2023). Drilling to within 100m of this seismic feature encountered pegmatite veins and alteration assemblages, indicating an increase in temperature to muscovite – silica – epidote, which is indicative of being close to an intrusion. Mineralisation is also brought in with narrow pegmatite veins instead of typical quartz veins.

Transport Mechanism

Pre-existing crustal scale extensional faults in the Basement have been reactivated during the Carboniferous mineralisation events. These have served as conduits to magma and hydrothermal fluids regionally.

Trap and Deposition Sites

The deposition sites are within the chemically reactive rocks of both the Coomber Formation and the Rylstone Volcanics and described in detail in Klein *et al.*, (2022). As fluids encountered more carbonate and volcanoclastic rich units, they deposited mineralisation such as the Bundarra Zone as semi massive sulphides (Zn>Pb>Ag).

The next site of favourable deposition was at the unconformity between the Rylstone Volcanics and the paleo surface. This is host to most of the late gold mineralisation and is principally focused by the Gully Fault. Hydrothermal fluids were likely focused here late because earlier mineralisation built up in the Eastern Fault and hanging wall to act as an aquitard, preventing fluids from propagating further east and up.

As fluid pressures built and caused repeated hydraulic fracturing, metal bearing fluids were able to propagate in areas of rheological contrast and brittle hosts. Ascending fluids, when trapped by impermeable rocks, pooled beneath and permeated the groundmass as episodic fluid pulses, described in detail by Rory Carter (Carter, 2023).

The earliest sulphide bearing event of silica - pyrite fluidised brecciation, is noted to be within dacitic breccia; a highly permeable unit directly underlying a tight and impermeable dacitic ash tuff. This early silica - pyrite then served to make the dacitic breccia less permeable, allowing fluid pressure to build beneath. Early base metal fluids were overprinted by silver bearing fluids, highlighting a progression of system dynamics where energy and thermal gradient decreased over time and cool fluids deposited very fine silver.

Preservation Conditions

The high silica content of both the felsic volcanics and subsequent hydrothermal alteration, have helped preserve the Bowdens Silver mineral system. Notably, the oxidation profile is typically less than 8m and fresh sulphide remains at surface. No gossan development is present. Later burial by the Permian aged Sydney Basin has led to preservation from mechanical weathering over more than 265 million years.

Inference and modeling of the Mineral System

The process and techniques applied to model the volcanic facies are presented below. The processes and observations make inference about the geology without recourse to onerous facies analysis. It allows for simple falsification via specific facies checks, after which the model can be updated to reflect new knowledge from checks.

Geochemistry Aggregation

Several geochemical processes aided in distinguishing units to then be modelled at scale. Major elements for defining magma differentiation, such as V, Ti, and Cr, robustly

define the contacts of crystal tuff, dacite and dacitic breccia (Figure 6), however, they do not distinguish units that haven't been significantly fractionated, such as between the welded tuffs. Significant complexity within the welded tuffs and various volcanic breccias can be distinguished geochemically by examining the molar ratios of Al/Ti. Al serves as a proxy for silica which is present in feldspars and the degree of compaction of these in the pyroclastic events, relative to the degree of fractionation of the source magma. The base of the welded tuff is higher in Al relative to Ti, which is to be expected with eruptions from a magma chamber where the felsic fractionated parts erupt first, placing them at the bottom of the pile. This leaves a more evolved melt (dacitic) from which the crystal tuff could be sourced.

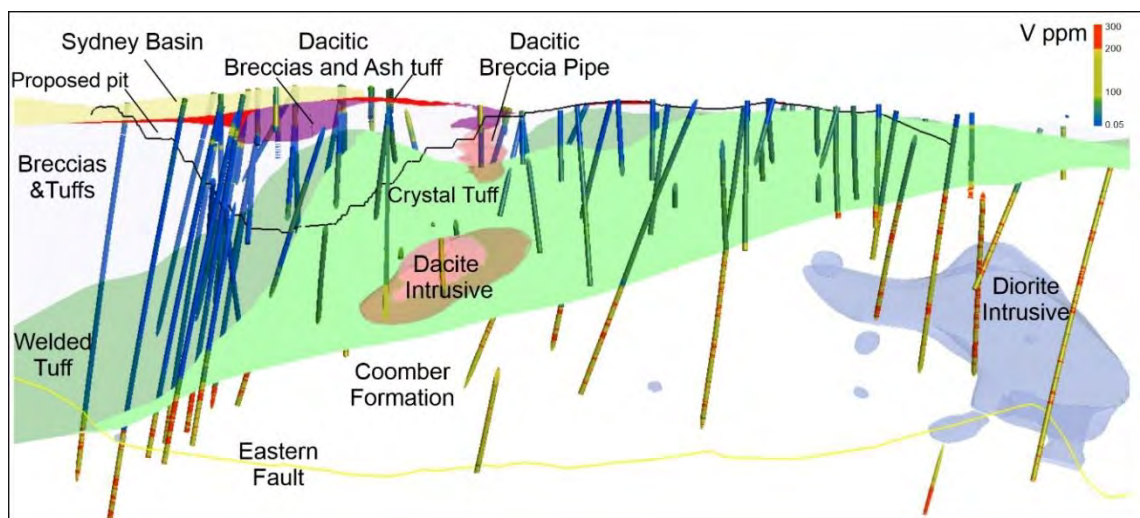


Figure 6 Long section of the pit and general stratigraphy highlighting to use of V clearly showing the distinction between the crystal tuff in green and the underlying Coomber Formation and the overlying volcanic sequences.

Figure 7 shows chemical stratification with oscillating Al/Ti ratios within units bounded by Al poor units (where Ti/V is relatively stable). This suggests differing flows and alteration at unit boundaries, possibly caused by potassium depletion and kaolinite/clay development from alteration. This metasomatism results from primary acidic fluids with mineralisation or in situ devitrification.

Mineral predictions, using downhole assays and with a linear solver constrained by an illite crystallinity model, aided the interpretation of facies and alteration. This was used to create a generalized 3D modelling, as fine resolution assay data is difficult to model consistently and must be aggregated to major or meaningful units. The scale of the interpretation was determined via experimentation using Data Mosaic (Hill, Pearce and Stromberg, 2021). Data Mosaic is a CSIRO product and implementation of wavelet tessellation provides useful graphical outputs that allow geologists to quickly evaluate drill hole data aggregation. This was done three times to refine different contacts within the volcanic pile. Using multiple, scaled interpretations that could be clustered gives consistent bounds to the interpretation for different facies and geological features. Following this prediction of the mineral assemblage over the entire drill hole assay database, the predictions were validated via qXRD, where K-S statistical tests checked ('Kolmogorov–Smirnov Test', 2008) if measured qXRD distributions were able to be derived from the predicted mineral distribution at 1m assay scale for each mineral

species. Finally, mineral species were predicted within the block model, and model interpretations placed in context of seismic data.

This process has highlighted the seismic response of various units and contacts relative to mineral species content allowing for geo-metallurgical factors, relevant to mine schedule planning to be constructed.

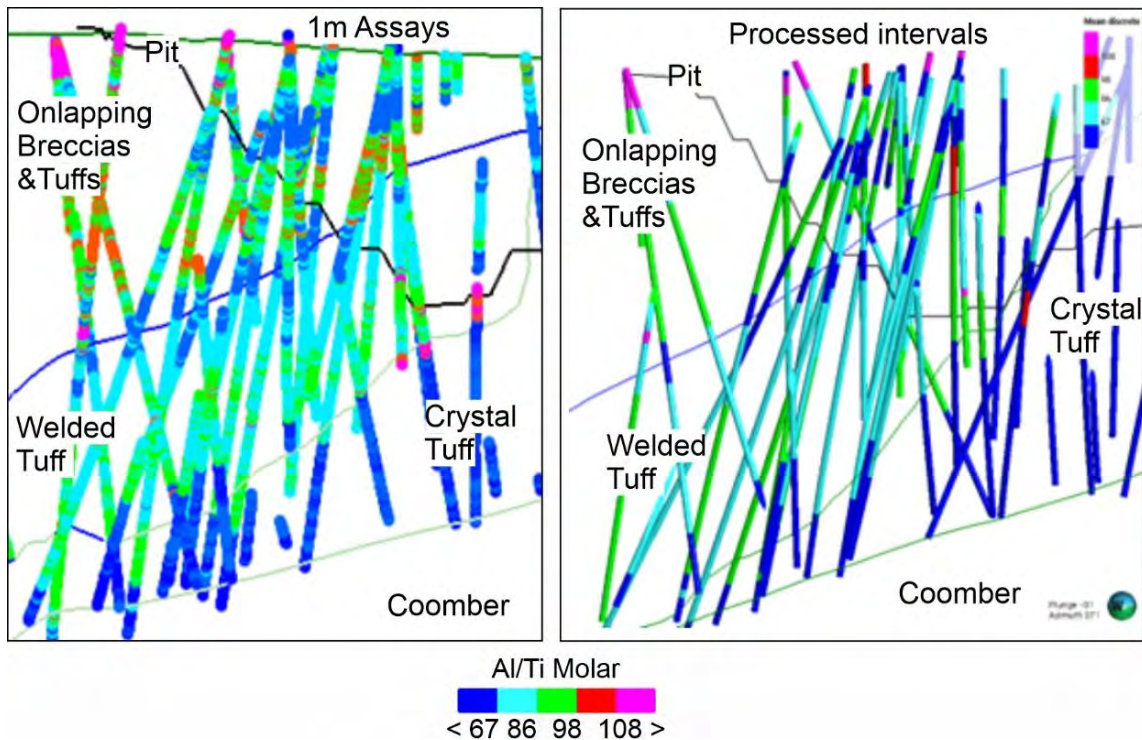


Figure 7 The left panel of a North South section (pit in black) with drill samples shows the variability within the volcanic pile, including likely alteration effects from overlapping flows and increased proportion of crystal packing in the lower half of the welded tuff (upper contact blue). Crystal tuff atop basement. (green lines). Right panel shows processed data for modelling.

CONCLUSION

The integration of exploration techniques including drilling geochemistry, hyperspectral models, seismic surveying, detailed petrology, mineral estimates, 3D geological modelling and facies observation in a falsifiable model, has helped define the geological setting effectively and identify key controls to the Bowdens Silver mineral system. With this knowledge, components of the mineral system can be quickly identified at the Bara Creek and Coomber prospects. By way of example Bara creek, at the northern rim of the Bowdens Caldera complex, possess a window of geochemical anomalism where ash tuffs are eroded. Bara Creek also has synthetic, or even the same crustal scale faults that fed the Bowdens system, identified by seismic surveying and confirmed via field mapping. Drilling planning to test the prospect is well underway.

REFERENCES

- CARTER, R. (2023) Comparison of the host rocks, alteration, and metal distribution between the Aegean and Northwest zones, Bowdens epithermal silver deposit.
- COWAN, J. (2016) 'How to Take Advantage of Geological Bias', How to Take Advantage of Geological Bias, 15 February. Available at: <https://www.linkedin.com/pulse/how-take-advantage-geological-bias-jun-cowan/>.
- COX, S.F. (2020) 'Chapter 2: The Dynamics of Permeability Enhancement and Fluid Flow in Overpressured, Fracture-Controlled Hydrothermal Systems', in Rowland, J. V. and Rhys, D. A., APPLIED STRUCTURAL GEOLOGY OF ORE-FORMING HYDROTHERMAL SYSTEMS. Society of Economic Geologists, pp. 25–82. Available at: <https://doi.org/10.5382/rev.21.02>.
- DOMINY, S.C. et al. (2018) 'Geometallurgy—A Route to More Resilient Mine Operations', Minerals, 8(12), p. 560. Available at: <https://doi.org/10.3390/min8120560>.
- HILL, E.J., PEARCE, M.A. AND STROMBERG, J.M. (2021) 'Improving Automated Geological Logging of Drill Holes by Incorporating Multiscale Spatial Methods', Mathematical Geosciences, 53(1), pp. 21–53. Available at: <https://doi.org/10.1007/s11004-020-09859-0>.
- GRAHAM, I., 2023. Petrographic analysis of intrusive intervals BD23003-267 AND BD23005-566. Internal REPORT ITG059. School of Biological, Earth and Environmental Sciences UNSW Australia.
- KLEIN, T. et al. (2022) 'Bowdens Epithermal Silver Deposit: Recent knowledge advancements and Machine Learning cogitations', in. Mines and Wines.
- 'Kolmogorov–Smirnov Test' (2008) in The Concise Encyclopedia of Statistics. New York, NY: Springer New York, pp. 283–287. Available at: https://doi.org/10.1007/978-0-387-32833-1_214.
- LAY, A. (2019) A comparative study of the mineralogy and geochemistry of the ore minerals from silver-rich polymetallic deposits of the Lachlan and New England Orogens, New South Wales, Australia. PhD Thesis (unpublished) University of New South Wales Sydney.
- MCCONACHY, T. (2023) 'A note on the discovery of Bowdens Silver Deposit'.
- MCCUAIG, T.C., BERESFORD, S. AND HRONSKY, J. (2010) 'Translating the mineral systems approach into an effective exploration targeting system', Ore Geology Reviews, 38(3), pp. 128–138. Available at: <https://doi.org/10.1016/j.oregeorev.2010.05.008>.
- ROWLAND, J.V. AND RHYS, D.A. (2020) Applied structural geology of ore-forming mineral systems. Society of Economic Geologists. Available at: <https://doi.org/10.5382/rev.21>.
- SOUVANAN, K. (2018) Origin and evolution of sediment-hosted mineralisation and alteration within the Coomber Formation underlying the volcanic-hosted Bowdens epithermal Ag deposit, Lue NSW. Honours Thesis (unpublished), School of Biological, Earth and Environmental Sciences, University of New South Wales Sydney.
- YUAN, X.P., LEROY, Y.M. AND MAILLOT, B. (2020) 'Control of fluid pressures on the formation of listric normal faults', Earth and Planetary Science Letters, 529, p. 115849. Available at: <https://doi.org/10.1016/j.epsl.2019.115849>.

GOLD AROUND GRANITE MARGINS: AN EXPLORATION WORKFLOW FOR THE WEETHALLE PROJECT, CENTRAL LACHLAN NSW.

Richard Blewett¹, David McInnes¹, Ben Goscombe², Ben Wade³

¹Weethalle Gold Pty Ltd, Royalla, NSW, 2620

²Integrated Terrane Analysis Research, Aldgate, SA, 5154

³University of Adelaide, Adelaide, SA, 5005

Key Words: Intrusion-related gold, orogenic gold, exploration workflow, Central Lachlan Orogen

INTRODUCTION

In deformed and metamorphosed terranes there is a common spatial or genetic association between certain felsic intrusions (granitoids) and mineralisation. Gold and base metal mineralisation can be directly or indirectly related to granites even if the mineralisation is distant from the intrusion both in space and/or time.

These contrasting direct or indirect associations are observed where:

- granites are direct sources of energy, fluid and metal in porphyry, epithermal and intrusion-related mineral Au-base metal systems,
- granites with contrasting rheology/competency compared to host country rocks control sites of brittle failure and thus potential dilation sites for mineralisation,
- intruding granites alter the physical or chemical properties of host country rocks, which can lead to mineralisation, and/or
- large granite intrusions alter regional stress trajectories, guiding strain into other areas where mineralisation may occur.

Gold deposits in the Central Lachlan Orogen have been interpreted as either intrusion (granite) related or as orogenic systems, both of which share features leading to misidentification and misinterpretation of some deposits (Wall, 2021; Hart, 2024). However, given the number of ways granites can be associated with mineralisation, and the vast volume of granite rocks in the region, it is imperative that the explorer understand the role these intrusions play and use this knowledge to guide their exploration strategies.

This Extended Abstract reports on recent mineral systems research conducted around the margins of an unusually circular-shaped Late Silurian granite pluton in the Central Lachlan Orogen. We show that high-grade gold and associated base metal mineralisation was multi-stage; with Stage 1 intimately linked to granite magmatism and contact metamorphism, and Stage 2 linked to regional orogenesis involving brittle failure of an older metamorphic aureole.

Based on the new research, a pragmatic exploration workflow has been developed and applied during recent exploration. This workflow aims to maximise the predictive power of integrated science with the goal of increasing the chance of an economic discovery in a cost-effective and environmentally sensitive manner. The workflow has broader applicability for others exploring for gold around granites and their margins in the Tasmanides.

REGIONAL GEOLOGICAL SETTING

The Central Lachlan Orogen developed in the back-arc to the Ordovician Macquarie Arc, which was active to the east. The orogen extends to the north-northwest from the

Victorian border to north of Cobar and is bound on the east by the crustal-scale Gilmore Fault Zone (Fig. 1). Between these major terrane-bounding structures are a series of faults that bound sub-basins, disrupt regional folds, and link into the major faults at depth (Carlton et al., 2019).

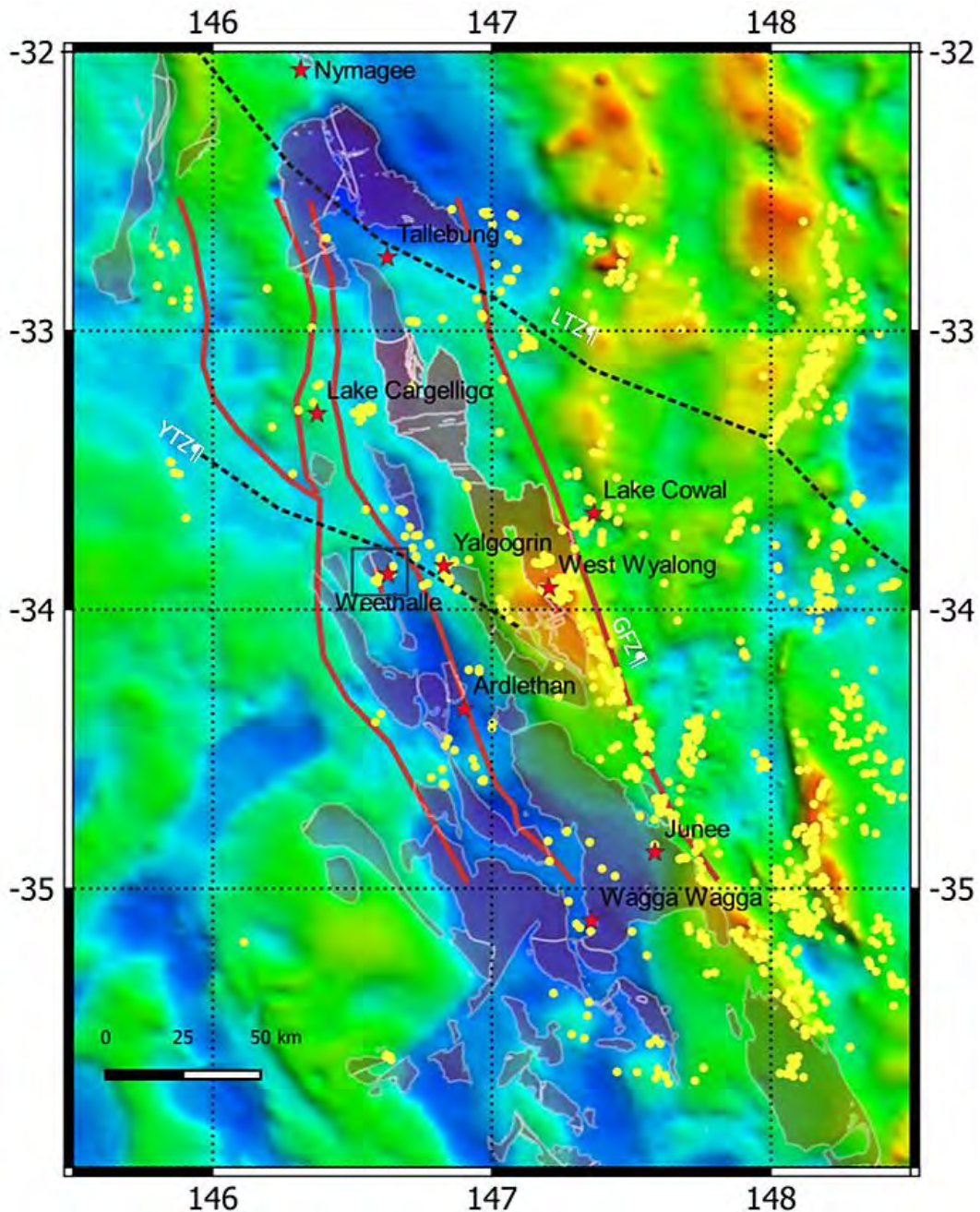


Figure 1: Bouguer gravity map with granites pale red (source: Geoscience Australia), gold occurrences and major structures. (LTZ – Lachlan Transfer Zone, YTZ – Yalgogrin Transfer Zone, GFZ- Gilmore Fault Zone), Box is Fig. 2 location.

There is a common spatial and genetic association between mineralisation and deep faults, cross structures and conductivity anomalies in the lower crust (Kirkby et al. 2022). This association is particularly important for the Weethalle area as it is located at the intersection of an array of big structures that trend north-northwest, northwest, northeast and east-northeast (Fig. 1). These big structures are mapped from the base of the crust (magnetotelluric data), mid to upper crust (gravity data), upper crust (magnetic data) and at the surface (LiDAR, DEM data and geological mapping) (Figs. 1, 2). For example, at the Weethalle area, there is a marked 'step-over jog' in the regional north-northwest

trending gravity low that extends from Wagga Wagga in south to just south of Nymagee in the north. This step-over strikes northeast and the circular Weethalle Granite fits neatly within (Fig. 1). Cross-cutting this northeast trend is a northwest-trending sharp gravity gradient that corresponds to the Yalgogrin Transfer Zone (Glenn & Walshe, 2002). The trace of Yalgogrin Transfer Zone (Fig. 2) is coincident with a northwest-trending conductivity anomaly mapped at 40 km depth in magnetotelluric data. Prominent northeast and east-northeast trending faults offset the regional strike of local stratigraphy and are easily mapped in magnetic data.

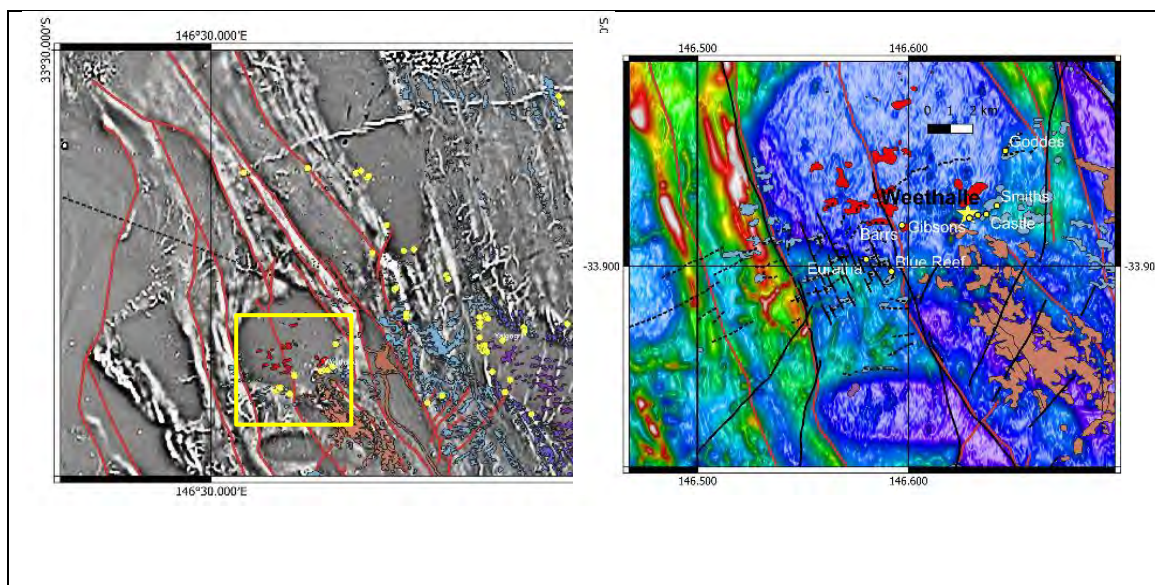


Figure 2: A) Greyscale magnetics (GSNSW) showing gold deposits surrounding granites (low magnetisation), major structures and outcrop (GSNSW), pecked line is trace of Yalgogrin Transfer Zone; B) Reprocessed TMI map (GSNSW) showing named gold deposits, major and minor structures. Outcrop polygons (GSNSW) Gurragong Group – brown, Adaminaby Group – blue and Weethalle Granite – red.

The regional stratigraphy (Colquhoun et al., 2005) comprises north-northwest trending belts of Ordovician marine metasedimentary rocks that were metamorphosed and deformed in the early Silurian. From the Late Silurian to early Mid Devonian a series of extensional events resulted in the intrusion of abundant S-type granitoids and deposition of sedimentary and volcanic rocks. Further extension in the Mid Devonian resulted in deposition of quartz-rich terrestrial sedimentary rocks. Unconformities and disconformities separate the main stratigraphic groups, which correspond to Lachlan-wide deformation and metamorphism event cycles, viz the Benambran, Kanimblan, and Tabberabberan events.

Mineralisation in the Central Lachlan Orogen is diverse, with large, and in places world-class, deposits of Au, Sn-W, and sediment-hosted Cu-Au and base metals (Cobar Basin). Most of the orogen's known gold mineralisation is clustered along the Gilmore Fault Zone, although numerous gold deposits are scattered throughout a range of settings to the west and are particularly closely associated with granites (Fig. 1). Of particular interest to this study are the gold deposits surrounding the Late Silurian S-type granites. These deposits have been variably interpreted as orogenic and/or as intrusion (granite) related.

GEOLOGICAL SETTING AROUND THE WEETHALLE GRANITE

The Weethalle region is dominated by flat plains with relict Quaternary systems containing aeolian, fluvial and lacustrine deposits. Overall outcrop is <5% of the area, so large parts of the region are poorly known. This lack of knowledge is amplified by the very limited amount of exploration drilling, most of which was 50 m or less in depth.

Within these extensive, flat aeolian sandplains there are low residual rises with sub-cropping deeply weathered basement rocks, some of which contain the only known mineral deposits (Fig. 2B). Dendritic palaeochannels transect the region. They contain maghemite and are highly magnetic, strongly influencing magnetic images and models.

Known gold deposits

There are seven known gold deposits in the Weethalle region. All but one are hosted within the contact aureole along the east and southern margins of the Weethalle Granite (Fig. 2B). The one known exception is the Barrs deposit, which is hosted within the pluton itself. Except for Smiths Mine, most gold-bearing veins in the six other deposits record ore that strikes consistently east-northeast (070°), crosscutting bedding at a high angle (Kenny, 1932). The deposits have generally been interpreted as late-stage orogenic (eg., Stuart et al., 2020), although there has been limited testing of this interpretation.

Stratigraphic relationships

The oldest rocks in the study area are steeply dipping to sub-vertical mid to late Ordovician Adaminaby Group and Bendoc Group sandstones, siltstones and shales. Regional metamorphism is low to sub-greenschist (Colquhoun et al., 2005). The rocks are mostly weakly magnetic although a marker bed of an unknown member is highly magnetic (Fig. 2). This magnetic marker bed defines the regional north-northwest strike, folds and associated faults, and allows structural interpretations and 3D magnetic models to be made, including identifying a gently south-dipping enveloping surface of the regional F1 folds.

The Weethalle Granite is a 12-km diameter circular-shaped body (Fig. 2) emplaced at ~427 Ma into Adaminaby Group metasedimentary rocks (Black, 2004). It is poorly exposed, and described as grey, coarse- to medium-grained porphyritic biotite granite with biotite-rich microgranular enclaves (Colquhoun et al., 2005). The pluton is larger than the contact outline at the surface, with roof carapaces extending ~6 km in the north and ~1-2 km in the east and south (Colquhoun et al., 2005).

Geochemistry indicates the Weethalle Granite is strongly felsic, reduced, highly fractionated, peraluminous and of a compositionally evolved S-type composition (Blevin, 2004). A 1-2 km-wide contact aureole envelopes the pluton margin and carapace of Adaminaby Group country rock. Contact metamorphism resulted in recrystallisation and growth of andalusite, cordierite, tourmaline, and mica. The system has the hall marks of a Sn-W granite and associated features expected of hosting reduced intrusion-related gold deposits (Hart, 2024).

To the southeast of the pluton, volcanic rocks of the ~418 Ma A-type Gurragong Group (Black, 2005) (Fig. 2B) erupted as rhyolites, ignimbrites and tuffs and were inferred by Colquhoun et al. (2005) to be intruded by the porphyritic Schillers Lane Granite. These early Devonian rocks are correlatives of the Ural Volcanics of the Rast Trough of the Cobar Basin. Their distribution is controlled by the Weethalle Fault on their western margin, an unconformably on Ordovician rocks to the east. The unconformity with the Weethalle Granite to the north implies significant exhumation and erosion of >7 km of crust in <10 Myr (between Weethalle Granite emplacement and Gurragong Group volcanic deposition).

Other than Cenozoic rocks, the youngest rocks preserved are the Mid Devonian Cocoparra Group sandstones, conglomerates and shales, which are preserved east of Weethalle in the F2 Narriah Syncline.

Structural relationships

The basement Adaminaby Group rocks were deformed during D1 into north-northwest trending tight to isoclinal upright folds with an axial planar cleavage. Fold amplitudes extend for 10s of kilometres. The result is a pronounced structural grain evident in the strike of the geology, most topography, and the trends of the magnetics. A series of north-northwest trending steep reverse faults formed on the limbs of major folds. These D1 Benambran structures developed in the earliest Silurian and were associated with low to sub-greenschist regional metamorphism.

During late Silurian east-northeast oriented extension, the Weethalle Granite was emplaced into a fault-bounded anticline between two regional-scale F1 synclines. This north-northwest trending fault – here called the Weethalle Fault – partitions the pluton into a shallower east and deeper west for the base of the body. The Weethalle Fault does not appear to have any strike-slip movement as the circular pluton shape is maintained despite the fault transecting the entire body and faulting out the F1 anticline between the two regional synclines. The fault is also parallel to other north-northwest trending faults, located along the east and west sides of the pluton (Fig. 2).

To the south and southeast of the pluton, the Weethalle Fault forms a basin-bounding fault that controlled the eruption and preservation of the Early Devonian Gurrangong Group (Fig. 3A). The fault is mapped as a west-dipping reverse fault on the Ungarie 1:100k map sheet (Colquhoun et al., 2005), although it is not clear this interpretation is correct.

South of the pluton, and west of the Weethalle Granite, are a series of subtle east-northeast trending ridges in the landscape, which are at a high angle to the prevailing lithological strike. Readily mapped on LiDAR data, these ridges extend to the west and define 'soft linkage' of the Weethalle Fault and an equivalent growth fault bounding the Rast Trough to the west.

These ridges are parallel to the veins and faults associated with the gold deposits. Their strike indicates local extension directions to the northwest and southeast, which is orthogonal to the Silurian and Devonian extension directions. Such apparent extension direction contradictions are reconciled by interpreting the Weethalle Granite behaving as a competent buttress that generated a relay-ramp accommodation zone between two major north-northwest trending growth faults. As a result, the southern margin of the pluton would have experienced localised extension to the north-northwest and east-southeast during the Late Silurian and Early Devonian (Fig. 3A).

Outcrop around the Blue Reef gold deposit (Fig. 2B) shows east-northeast trending quartz-sulphide veins associated with sinistral strike slip shearing. The timing of these fault movements is not known but they are likely D2 Tabberabberan in age (Fig. 3B). Wing tips on quartz-sulphide veins within stopes of the Euratha gold deposit (Fig. 2B) show sinistral-reverse movement directed to the northwest. These shears are cut by small offset north-northwest and north trending dextral faults that are common throughout the area. These are likely to be strike-slip movement guided along the regional north-northwest strike of steeply dipping bedding and related to northeast-southwest directed D2 contraction.

East of the pluton is the Narriah Syncline which is a southeast plunging fold of the Cocoparra Group. Limb dips of $>60^\circ$ means the regional unconformity has been folded into a steep attitude. The structure forms a footwall syncline to the regional D2 Tabberabberan-aged Narriah Fault, which thrusts Ordovician rocks to the east over Devonian rocks. Contraction to form these D2 structures was oriented northeast-southwest to east-northeast to west-southwest (Fig. 3B).

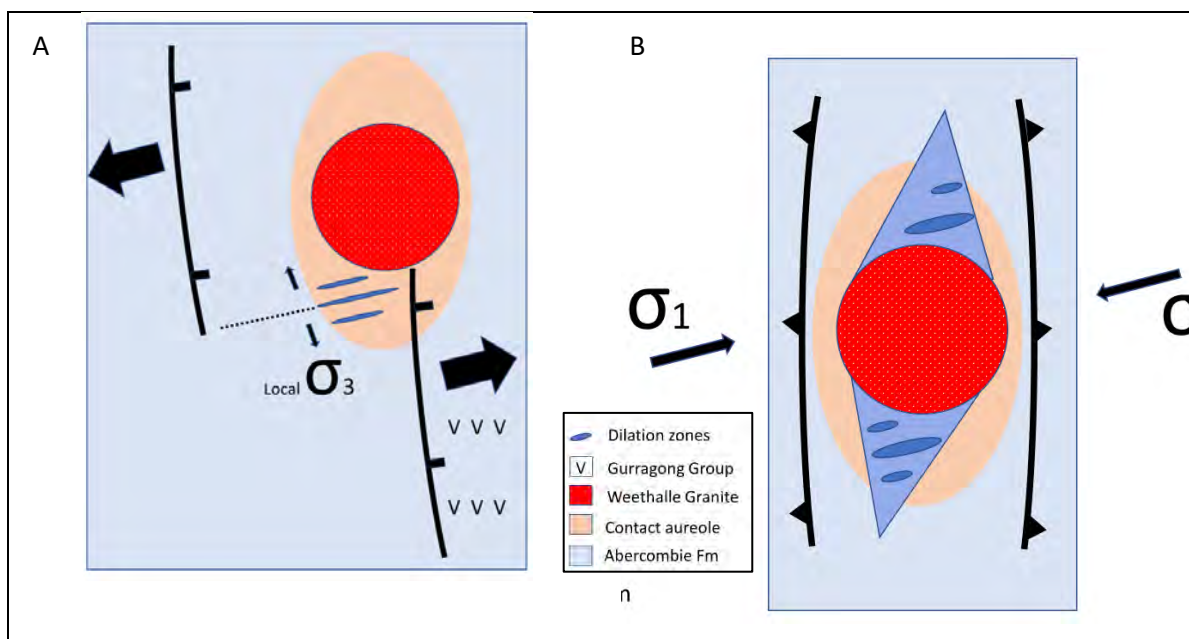


Figure 3: **A)** Camp-scale exploration hypothesis and cartoon for intrusion-related Stage 1 mineralisation where the pluton guides accommodation and localised extension during Early Devonian volcanism and magmatism; **B)** Stage 2 orogenic mineralisation controlled by regional far-field contraction associated with D2 Tabberabberan orogenesis.

EURATHA – A REDUCED INTRUSION-RELATED GOLD DEPOSIT WITH OROGENIC OVERPRINT

Overview and legacy studies

Gold was discovered around 1900 at what later became known as the Euratha mine. Workings extend for about 500 m on surface and to a depth of 85.5 m with gold mineralisation in quartz veins 40-60 cm wide. Consistent gold grades of 24 ppm Au and 60 ppm Ag along strike and down dip were recorded by Kenny (1932) and mine inspectors back in the 1910s. Other selected assays also returned more than 2 oz/t Au. Gold was described as very fine-grained and minor arsenopyrite, galena, sphalerite, and chalcopyrite were also recorded. Gold associated with 'gossan' and containing free Au in quartz assayed 0.54 oz/t (Kenny, 1932).

Sulphur isotopes $\delta^{34}\text{S}$ from pyrite and arsenopyrite at Euratha are 1.9 and 2.1 *per mil* respectively (Downes, 2004), which is consistent with a magmatic source of sulphur. Historical documents (Kenny, 1932 and earlier) record granitic and greisen rocks together with the host sedimentary rocks in the workings. These intrusive rocks are not mapped or suitably described by the GSNSW.

The main lode strikes between 050 and 090 and dip up to 85° south. The veins crosscut the host hornfels-altered sandstones and slates, which strike at around 340° and dip at 85° east. Some faulting, sub-parallel to bedding, and slickensides on lode walls, have also been described. These late strike-slip faults are likely D2 Tabberabberan in age.

In the 1980s Australia Pacific Resources identified zones of quartz veining up to 3 m wide, with the best drill intersection 2.31 ppm Au over 2 m (Smith, 1988). The company also undertook geological mapping, and a Rapid Reconnaissance Magnetic Induced Polarisation (RRMIP) survey, followed by soil sampling over some RRMIP anomalies. The soil geochemistry recorded elevated As anomalies coincident with the resistivity anomalies. The use of As-in-soil geochemistry and accompanying electrical geophysics as exploration tools was noted.

Tou Mining (2009) undertook an 8-hole diamond drilling programme across the Euratha workings, with assay results from DD08A returning - 1 m @13.5 ppm Au and 16.9 ppm Ag from 135-136 m, with associated element anomalism including 2.3% As, 1.43% Ca, 0.3% Pb, 14% Fe, 15% S, 0.26% Zn, and interestingly 47 ppm Cd and 15 ppm Sb. The DD08A logs show no core recovery between 137 m and 168 m, which may indicate drilling through the old workings and the samples analysed being the remaining wall material from the workings. Amongst the data there are Ag-rich intercepts with lower values of As, Fe and S (presumably pyrite and arsenopyrite) than the Au-rich intervals; with the former also accompanied by anomalous values of Pb, Zn, Cd, Sb, Cu, Bi, and B.

New Results: further building geological understanding and an exploration workflow

Building on a synthesis of existing legacy data, a number of new data types have been acquired and processed, modelled and integrated into the exploration workflow and a holistic understanding of the geological and minerals system of the region.

Geology: whole rock geochemistry of 'causative' granite – regional implications

Intrusion-related gold is obviously associated with granite magmatism (Hart, 2024). The general assumption has been that the granites found at Euratha were apophyses or sheets emanating from the larger Weethalle Granite, which is located only 160 m to the north.

The drill core from the Tou Mining exploration was located and selectively sampled for petrographic, paragenetic and geochemical studies. Unfortunately, the core tray labels were lost so no depth information was recovered. Nevertheless, the samples represent the range of lithologies, structures, alteration and mineralisation present at the deposit.

The drill core recovered a very distinctive coarse K feldspar porphyritic granite as dykes and sheets that is intimately associated with Stage 1 gold mineralisation. Magnetic susceptibility readings were taken and they are very low at $5-7 \times 10^{-5}$ SI units, consistent with the granite being a reduced (ilmenite-series) type, like the Weethalle Granite.

Unfortunately, there are no pre-competitive geochemistry or geochronology available to clearly match the causative granite at Euratha with the known plutons in the region. As such, samples of core were analysed for their majors & trace element whole-rock geochemistry for possible matching. Results indicate that the Euratha granites are likely A-type because they contain high Ga/Al₂O₃, Y/Nb and Rb/Nb ratios, and high Fe. The strong fractionation with high Th and very high U (for the SiO₂ levels) and very high Sn could also be interpreted as representing high-temperature S-type. Either way, the new geochemical data suggests that the causative granite is not the Weethalle Granite (as previously assumed).

Physically, the Euratha granites look remarkably similar to the outcropping Schillers Lane Granite (Bull & Fitzherbert, 2022) that is inferred to intrude the Gurragong Group volcanic rocks a few kilometres to the east (Colquhoun et al., 2005). Without geochemical data for the Schillers Lane Granite this comparative link is tentative.

If the causative granite at Euratha is a phase of the Schillers Lane Granite then main stage Au mineralisation is Early Devonian, which opens up the entire belt for Au potential. However, the PT conditions during Stage 1 are determined to be deep, which is not consistent with a sub-volcanic intrusion as inferred by the GSNSW mapping. Given the present understanding the Schillers Lane Granite – and by inference the Euratha granite – could be Late Silurian and be an anomalously high temperature variant of the S-type suites emplaced at that time?

Further tests on the contact relationships of the granites and volcanics in the Gurragong Group and further geochemical characterisation of all rock types is needed before the age and provenance of the causative Euratha granites can be resolved.

Hand specimens, thin section petrology and fluid interpretation

Core from beneath the Euratha workings was sampled in order to characterise and understand the range of lithology, vein, alteration, structures, PT conditions, and mineralisation present.

From this core, Goscombe (2024) identified a range of minerals in the hornfels and associated vein assemblages that indicate multiple fluids have been involved. For example, muscovite–tourmaline indicates reduced aqueous fluids, tourmaline is characteristic of magmatic fluids, biotite–carbonate indicates oxidized magmatic fluids, and pyrite–quartz–biotite–carbonate indicates reduced alkaline fluids. The characteristic hornfels and hornfels-related vein assemblage at Euratha is pyrite–biotite–tourmaline–Ca-Mg-Mn carbonate ± arsenopyrite indicating oxidized-alkaline fluids overall, which is characteristic of crustal magmatic fluids. Oxidised conditions during contact metamorphism are interpreted as magnetite is absent from all samples, and tourmaline (dravite) and rutile are both common.

The common muscovite and sericite indicate a second, reduced-acid hydrous fluid, typical of the shallow crust. Three stages of muscovite growth are identified: 1) hornfels metamorphism, 2) rare muscovite in vein assemblages, and 3) retrogressive fine-grained muscovite and sericite in hornfels and granite. The late-stage retrogressive muscovite-sericite probably indicates a reduced-acid hydrous fluid event subsequent to contact metamorphism. Retrograde ‘iddingsite’ in brittle fractures are probable hydrous Fe-oxides such as goethite (±Zn, Cu, Mn, Mg, As peaks in μ XRF) mixed with clays (K and Al peaks in μ XRF), also indicating oxidised fluids late in the history and related to the orogenic event (seen elsewhere).

Gold mineralisation – newly defined paragenetic sequence

The identification of a new comprehensive paragenetic sequence of events marks a vast improvement in the previous state of knowledge for the region (Table 1). The paragenetic work shows that Au mineralisation is not only late-stage orogenic as suggested by Stuart et al (2020). In contrast, Goscombe (2024) outlined 12 different events, including 3 separate Au events, with the main mineralising event intimately associated with magmatism which was later overprinted by orogenic fluids and Au.

Table 1. Newly defined paragenetic sequence for the Euratha workings.

Deposition of Adaminaby Gp turbidites, compositional layering/bedding (Ordovician).

- E1 – Granite intrusion: qz–mc–pl–bt–ms ± tur (Magmatic)
 E2 – Hornfels: qz–ms–bt–pl–tur–py±and±crd ±Au (Thermal)

Events related to the intrusion of biotite-muscovite granite (~427 Ma? Or 417 Ma?)

- E3 – Thin granite veins: qz–mic–pl–bt–ms (Magmatic)

E4 – Thick hydro-magmatic veins: qz–ms–tur–py–ap(?)	main Au	(Fluids)
E5 – Thin planar veinlets: qz–py–carb or tur		(Fluids)
Alteration halos: tourmaline common but not always present		(Fluids)
E6 – Thin planar veinlets: qz ± py		(Fluids)
E7 – Thin curvi-planar laminated veins: qz–py–tur ± ms		(Fluids)
Alteration halos: tourmaline distinct and characteristic		(Fluids)
E8 – Thick irregular shaped veins: qz–tur–py–apy ± carb–rt		(Fluids)
Alteration halos: disseminated py–carb ± tur common		(Fluids)
Thick laminated/banded veins: qz–tur–py ± carb ± ms		(Fluids)
Alteration halos: ser–bt–chl(?), disseminated py		(Fluids)
E9 – Curvi-planar veins: carbonate		(Fluids)
Alteration halos: disseminated carbonate		(Fluids)
E10 – Planar fracture veinlets: qz, py, tur, carb		(Fluids)
<i>E4 to E10 veins have similar quartz–pyrite–tourmaline–carbonate ± (muscovite) assemblages, interpreted as progressive veining associated with hydro-magmatic fluids in a cooling contact aureole.</i>		

Late-stage retrogressive alteration - hydrous fluids from non-magmatic source (<427 Ma)

- E11 – Retrogressive alteration: ser–ms ± chl growth (Non-magmatic fluids)

Post-granite deformation and hydrous fluids from non-magmatic source 380 Ma?

- E12 – Thick milky ‘dog-tooth’ qz veins: qz–py - **Au** (Orogenic fluids)

Gold assays, polished thin sections & μ XRF analysis

Fire-assay gold analyses were conducted on a range of mullock heap samples located adjacent to the old workings, with returns of up to 36 ppm gold obtained. These gold-bearing samples were cut into polished thin sections and scanned using a μ XRF to map major elements, including gold (Fig. 4). Most gold was smaller than the 100 μ m pixel size of the instrument, but where imaged, was present in association with pyrite, arsenopyrite and in places free in quartz (Fig. 4). By analogy, 5-20 μ m Au is closely associated with sulphides in the granite-hosted Au deposits at Yalgogrin some 10 km east (Dennis Walsh, written comm, 2023).

The E4 veins described by Goscombe (2024) are coarse-grained grey to milky polygonal granoblastic veins dominated by quartz, pyrite & arsenopyrite (Fig. 4). The μ XRF scans of ore samples also mapped an abundance of minerals with elevated P, Bi, Ti, W. The tourmaline is the Mg end-member dravite, which is a characteristic of intrusion-related systems.

Pressure-Temperature estimates

A series of P-T estimates were calculated for the contact metamorphism of the Adaminaby Group rocks. A temperature of ~500–540 °C at a depth of ~2.0–3.0 kbar is calculated from a range of geothermometers and geobarometers, including Si in white mica, Ms-Bt-Chl, and Fe-Mg exchange in Tur-Ms-Bt-Chl.

This depth estimate for contact metamorphism (and associated mineralisation) at Euratha is similar to the reported depth of mineralisation at Yalgogrin, where two-phase fluid inclusions show that no boiling had occurred (Dennis Walsh, written comm, 2023).

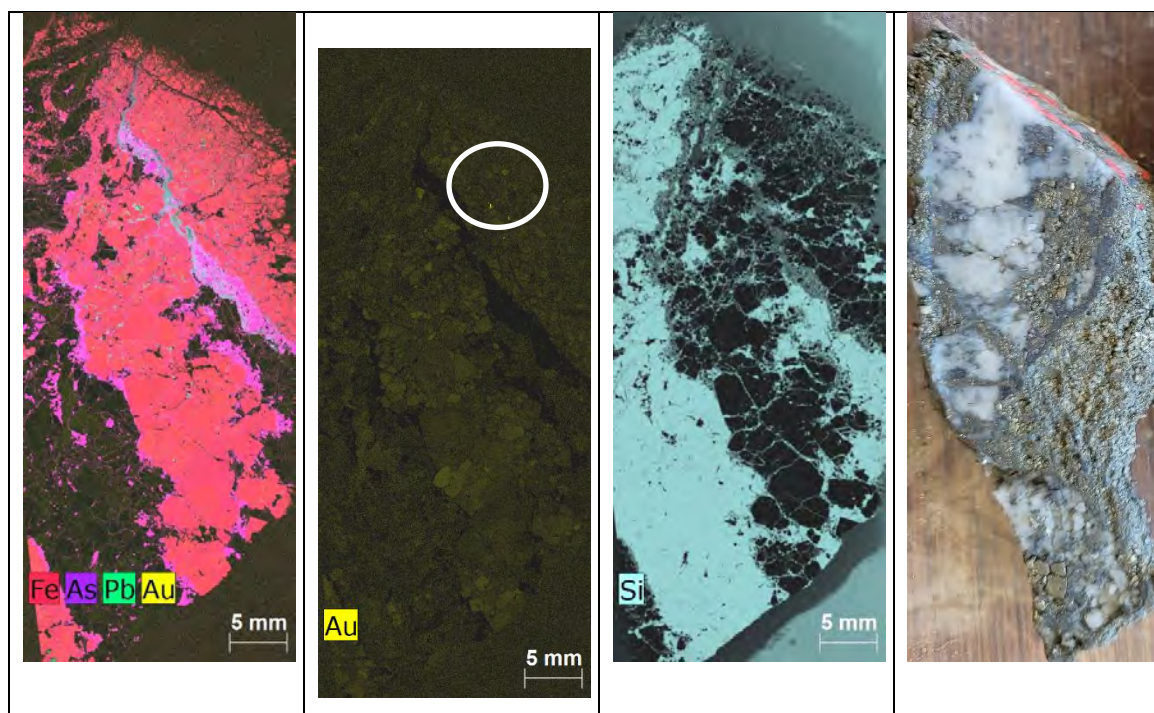


Figure 4 – μ XRF scans of E4 vein assaying 23.7 ppm Au. Scans show Fe-As-Pb-Au, Au and Si. To the right is photo of the slabbed sample. Note the >100 micron gold developed pyrite (in circle).

LiDAR – processing, modelling and interpretation of digital elevation model (DEM)

The explorer working in flat landscapes now has access to pre-competitive LiDAR data, which are freely available and are perfect for mapping subtle structures, identifying catchments, streams traces and understanding landscape evolution, regolith and soil.

The LiDAR data have been merged and processed into a new regional dataset at 1 m and 5 m resolution digital elevation models (DEM). The DEMs beautifully define the regional topography, but around the southwest margin of the Weethalle Granite a series of subtle *en échelon* 2-3 m high rises and ridges that strike east-northeast are also mapped.

The east-northeast strike of these ridges is anomalous with respect to the regional north-northwest lithological strike defined by the Ordovician basement, making the region one of significant geomorphological interest. In places, the east-northeast ridges step sharply north or south across north-northwest linear features interpreted as late D2 strike-slip faults.

The subtle east-northeast ridges also coincide with enhanced electrical resistivity and their relative physical resistance to erosion is interpreted to be related to silicification associated with mineralisation and alteration. Both physical and electrical resistance share the same strike as known mineralisation. Not surprisingly, LiDAR-mapped ridges also coincide with the outcrop shapes of Ordovician rocks and their associated Th anomalies in radiometrics.

Surface studies: stream & soil geochemistry, regolith

Geochemistry is a common exploration technique and forms a key element of the workflow. Using an image-enhanced DEM of LiDAR data to locate best sample sites, a regional stream sediment geochemistry study was conducted around the Weethalle Granite. Gold and many base metals were found to be anomalous throughout the region, which is encouraging given the reported very fine nature of gold and the deep weathering present in the region. The best Au value of 0.011 ppm was obtained from the streams draining the Gurragong Group.

Given the known association of gold with sulphides, especially arsenopyrite, a correlation matrix analysis was done on legacy multi-element assays to determine which elements could be best used as a geochemical proxy for gold. A very strong relationship between Au and As was found, and a lesser one with Pb and Zn. This finding provides a useful proxy for gold in values of As, Pb and Zn, which are readily measurable with a pXRF machine and relatively stable to weathering and leaching.

Using radiometrics, Sentinel 2 satellite band ratios, and field observations it was determined that the 'cover' in and around Euratha was residual and the surface comprised the products of deep weathering of insitu basement materials. As such a series of orientation tests were conducted in the field to determine how best to sample the soil geochemistry in terms of sample depth, sample material, sample spacing. Tests involved varying the traverse spacing (100-200 m), sample spacing (10-30 m), and sample depth (10-80 cm). As a result of these experiments an efficient workflow protocol was developed and around 1000 soil samples collected.

Both direct insitu soil and bagged soil sample analyses were made using an Olympus Vanta pXRF. The results were plotted for As, which for typical background was around 6 ppm, and at highest levels more than 500 ppm. Anomalous Pb and Zn also follow the As patterns.

Airborne magnetics – processing, modelling and interpretation

Pre-competitive aeromagnetic data are freely available enabling mapping of structure, lithology, and alteration, in order to place the known mineralisation into a local and regional context. Using these data, a 200 m mesh 3D magnetic inversion model was run using a clip from the GSNSW regional magnetic total magnetic intensity grid (2023 release). The 3D model resulted a number of new findings and interpretations (Fig. 5A), including:

- high magnetisation anomalies dominantly hosted within the Adaminaby Group rocks,
- the Weethalle Granite is divided in two halves by the Weethalle Fault, with a shallow east (2 km thick) and deeper west,
- the Weethalle Granite intrudes the axis of a regional-scale anticline with complementary syncline to the east and west and transected by the intrusion,
- the regional folds close to the north and plunge 10-15° south towards the granite,
- due to resolution, the 3D model cannot adequately define shallow features, however it does identify regular east-northeast oriented magnetic trends,
- the magnetic sources in the southeast over the Gurragong Group are far less prominent compared to other areas, suggesting an absence of Adaminaby Group or that basement is deep.

To better define the local structure and the shallow geology along the southern margin of the Weethalle Granite, a high-resolution aeromagnetic survey was flown using 25 m-spaced flight lines oriented north-northwest to cross the granite-basement contact and the strike of the known mineralisation at Euratha and Blue Reef at a high angle (Fig. 2). The data have been prepared using a series of meshes at 50 m and 20 m, together with complex multi-stage overlapping tile meshes at 5 m. These high-resolution 3D models allow shallow and deeper structure to be more precisely defined, the known mineralisation to be understood in 3D magnetic space and for potential extensions of mineralisation to be targeted.

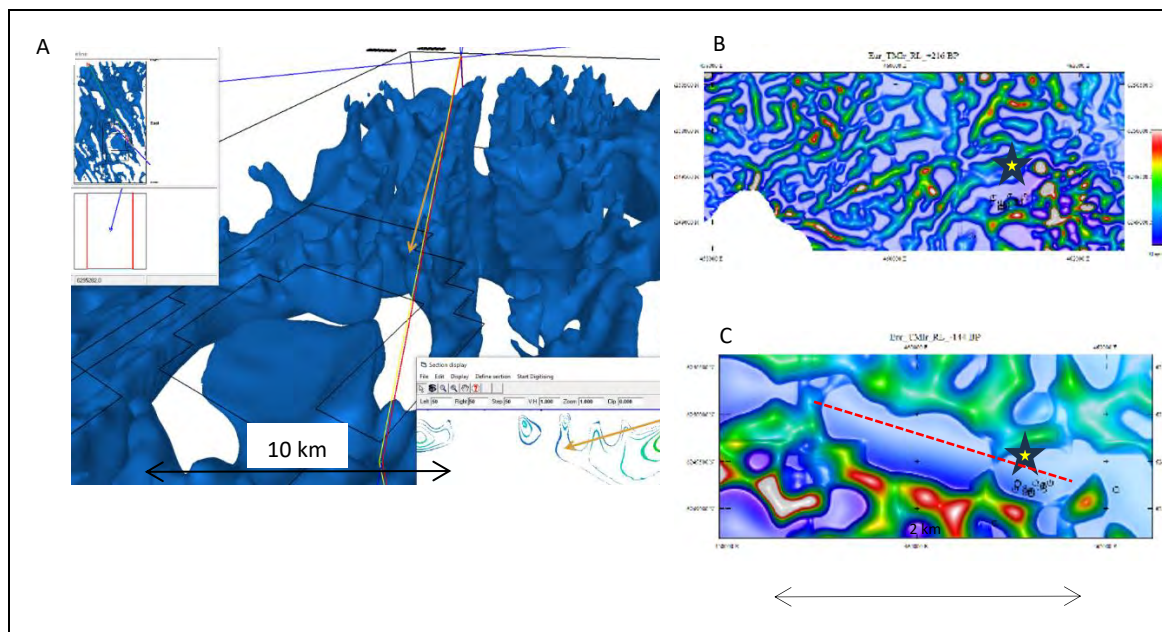


Figure 5: A) 3D isosurface of magnetic model view NW showing F1 folds and major faults, with inset long section showing gentle south-southeast plunge, black lines are outline of EL9134 **B)** Band pass filtered magnetic image of 25 m-flight line data at 35 m depth showing dendritic palaeochannels. Euratha mine = yellow star; **C)** Band pass filtered magnetic image of 25 m-flight line data at 200 m depth showing deeper west-northwest trending contact (red pecked line) between magnetic and non-magnetic basement that is not evident in Fig. 3B, Euratha mine = yellow star.

The high-resolution data ‘suffers’ from swamping by high frequency near-surface anomalies. These anomalies have a dendritic pattern and are interpreted as Miocene-aged palaeochannels containing maghemite (Fig. 5B). The palaeochannels lie between the LiDAR-mapped ridges, which suggests that these present-day ridges have persisted as more resistant landscape features since at least the Miocene.

The magnetic response of the palaeochannel is a relatively high amplitude and high frequency. Problems arise because channel-like anomalies such as these create a broad spatial wavelength. Only using standard image filtering techniques will fail to remove these broad wavelengths and will falsely display them as deeper-sourced features.

As part of the workflow, 3D magnetic modelling has been used to ‘capture’ these shallow anomalies in the top part of the model leaving a clearer definition of the basement magnetic response below. As a result, a well-defined west-northwest trending, south-dipping, magnetic contact is thus revealed in the 200 m+ RL40 m slice, with Euratha located on the eastern end of this contact (Fig. 5C). This detailed contact and fault definition enables optimal planning of the exploration workflow for subsequent geochemical and electrical geophysical programmes.

Induced polarisation – gradient array

Australia Pacific Resources (Smith, 1988) successfully used ground geophysical exploration methods around Euratha to show that the mineralisation had an electrical response. With this knowledge, a new suite of induced polarisation data were acquired, processed, modelled and integrated as part of the workflow.

A total of 17 traverses 1 km-long 100 m- and 200 m-spaced Gradient Array IP (GAIP) were collected over Euratha and its western strike extension using three transmitter spreads for around 3 km² coverage. All data were collected using 25 m receiver dipoles. Image processing of the observed gradient array data mapped the known mineralisation within a chargeable resistor, that is open and untested as extensions to the east, west and northwest (Fig. 6). GAIP is a method with a low impact on the environment and it quickly identifies target areas.

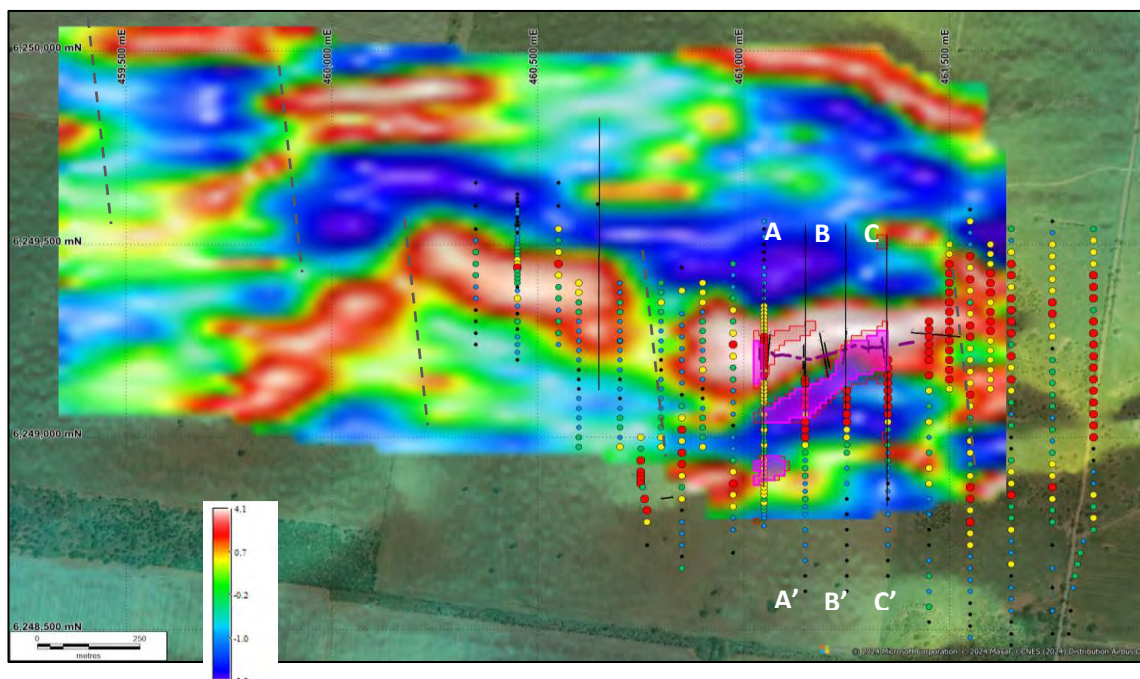


Figure 6: 100 m Band-pass filtered chargeability interpretation on Gradient Array IP. The anomalies extend for at least 2 km along strike and are all untested by drilling. Projected drill traces with lode/workings located on the southern contact of the chargeable resistor (Purple dashed trace); interpreted north-northwest dextral faults = grey dashed lines. Coloured points = some of the soil geochemistry data classified by As (ppm). A-A', B-B', C-C' are dipole-dipole sections (Fig. 7).

The electrical response to the known mineralisation is complex and significantly broader than the actual mineralisation, which appears on the southern contact margin of the chargeable resistor (Fig. 6). These chargeable resistors are 'offset' by a series of spaced, mostly dextral faults, which coincide with offsets in the LiDAR-defined ridges, faults inferred from the high-resolution magnetic models and faults described in the old workings (Kenny, 1932).

Induced polarisation – dipole-dipole

To characterise the mineralised system in 2D and 3D and investigate for strike/depth extensions of mineralisation, five traverses of Dipole-Dipole IP (DDIP) were collected over the Euratha deposit and along strike to the west. All traverses were collected using a 25 m and/or 50 m receiver dipole with a 50 m transmitter dipole. Three lines were collected using a 'roll-along' collection of 12 simultaneous dipoles. The other two were collected using a static 'shoot through' with the collection of 16 simultaneous dipoles.

The model for the chargeability data over the Euratha mine defines a chargeable body that terminates at about 100 m depth, a level that was confirmed in the diamond drilling by Tou Mining (red circle in Fig. 7).

Around 150 m south of the mine there is a strong chargeable body that is open at depth and increasing in intensity to the southwest (R1 and R2 in Fig. 7). This chargeable body is coincident with an elevated chargeability response detected in the southern stations of the gradient array survey data (Fig. 6). The Dipole-Dipole chargeability data and models also show that the system is open to the east (Fig. 7) and is coincident in gradient array IP with As-in-soil anomalies that extend even further east (Fig. 6).

Changes in the oxidation (weathering) depths are well mapped by the modelling of the resistivity component. Over the exposed Euratha mineralisation the weathering zone thins and it is difficult to discern an isolated high resistivity anomaly associated with the mineralisation. Line 61550e has a mild low resistivity but this could well be due to contamination and the difficult data collection conditions over/through the actual historic workings due to the difficulties in establishing stable electrodes.

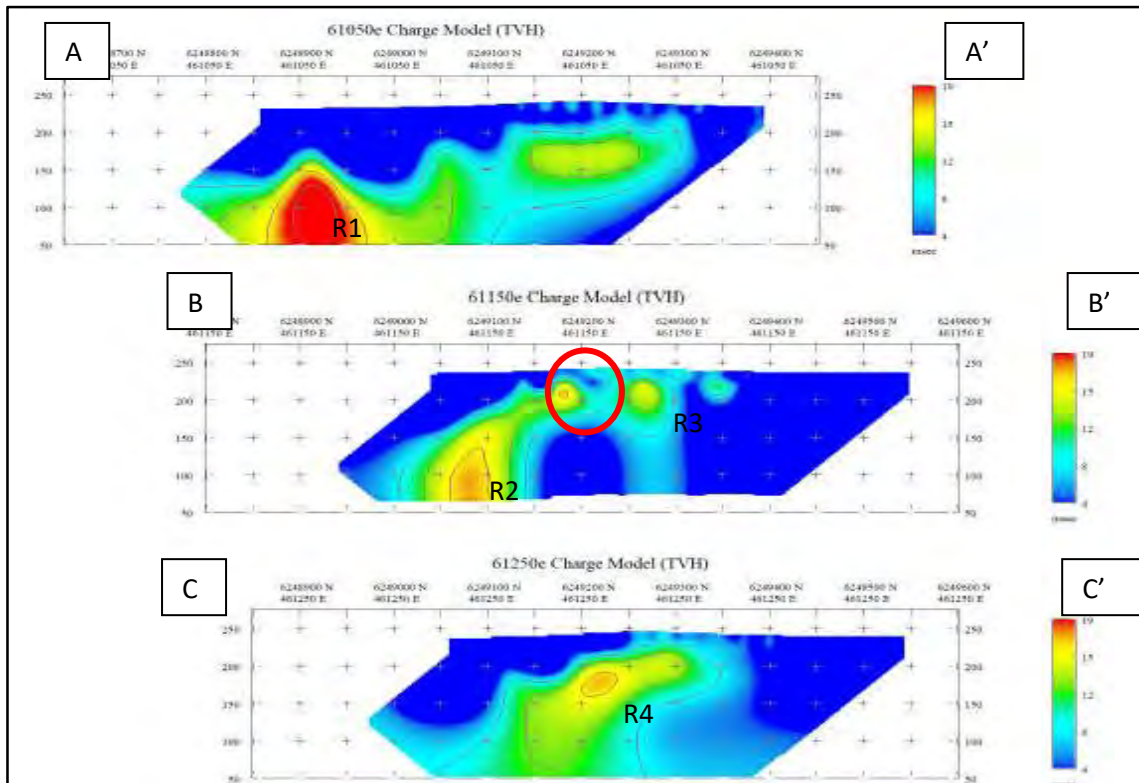


Figure 7: A-A', B-B', C-C' are north south oriented dipole-dipole sections through the main line of lode. The Euratha mineralisation is a chargeable resistor (red circle) that terminates at around 100 m depth (confirmed by drilling). The presence of deeper and open-at-depth chargeable anomalies (R1, R2, R3, R4) shows that there is significant untested potential.

On the southern ends of the traverses, to the south of the chargeable body, a deeper conductive horizon is defined, although it is not fully covered/constrained by the data. To the northwest of the Euratha mine the weathering depth varies from 35 m to 80 m. The deeper portion (80 m) being in the non-magnetic altered zone south of the Weethalle Granite and north of the modelled basement magnetic contact. At the modelled contact position weathering shallows and a deep chargeable body is defined. This body is coincident with the chargeable anomaly identified as the northern offset western extension of the known mineralisation as defined in the gradient array data (Fig. 6).

SUMMARY

Granites are intimately involved in the mineralisation process. They reuse deep structures during emplacement, alter host rocks (make more brittle and change minerals), provide contrasting fluids and elements into the system, deliver heat, and influence the behaviour of later deformation events by guiding both extensional and contractional stresses oblique to regional fields. The role of granites is therefore a key element to understanding mineral systems and for mineral exploration targeting (Wall, 2021).

The improved knowledge of the mineral potential of the Weethalle area suggests these systems share many features with the better understood world-class systems in the Yukon and Alaska (Wall, 2021; Hart, 2024). Given the number of granites in the region, there is therefore excellent potential for the new discovery of significant reduced intrusion-related gold deposits locally around the Weethalle Granite, and within the Central Lachlan Orogen more generally.

Around the southern contact aureole of the Weethalle Granite, gold and base metal mineralisation was multi-stage with several contrasting fluids identified. In detail, the

mineral system is complicated by telescoping of the original thermal event and overprinting of element/mineral zonation into the one space at different times.

A pragmatic workflow has been developed and applied to the southern margin of the Weethalle Granite. A series of new targets have been identified near known mineralisation. These now require drill testing.

NEXT STEPS

The age of the main (Stage 1) mineralisation event has not been directly measured. Also, the intrusive relationships between the mineralising intrusion and the surrounding stratigraphy need to be determined, although the A-type chemistry of the intrusive may suggest an early Devonian age. Both these questions remain to be answered with confidence.

In terms of further local exploration work, the encouraging combination of IP and soil geochemical targets identified at Euratha require drill testing.

In terms of further regional exploration work, there remains the entire metamorphic carapace of the Weethalle Granite to explore for other reduced intrusion-related gold deposits. In the north there is a prominent apophysis 500 m wide extends 3.5 km in a finger-like projection from the Weethalle Granite pluton into the surrounding hornfels. There is a large area around the northwest margin of the pluton that has never seen a drill hole. Here, the top of the granite is modelled to extend 6 km to the north beneath the hornfels carapace. Such areas create new exploration opportunities although the exploration workflow may need to be adjusted as this region has tens of metres of transported Cenozoic cover.

ACKNOWLEDGEMENTS

Weethalle Gold wishes to acknowledge the cooperation and access to land by the landowners of the tenements. We also acknowledge the Traditional Owners – the Wiradjuri people – and pay our respects to their elders.

We are grateful to Glenn Diemar from Australian Gold & Copper for access to his pXRF. John Wilford advised on landscape evolution and regolith of the region and generated Sentinel 2 images. David Champion advised on all ‘things’ granites and geochemistry in general. Yanbo Cheng advised on intrusion-related gold deposits and their characteristics.

The pre-competitive tools and data delivered for free by the Geological Survey of NSW and Geoscience Australia are gratefully acknowledged and immensely appreciated and valued.

REFERENCES

BLACK, L.P. 2005. SHRIMP U-Pb zircon ages obtained during 2004/05 for the NSW Geological Survey, Geological Survey of New South Wales.

BLEVIN, P.L. 2004. Chemistry of igneous units of the Cargelligo 1:250 000 map sheet area, New South Wales (updated and revised). Geological Survey of New South Wales, File GS2004/451 (unpublished).

BONNAY, M. 2005. Report on 30 thin sections from the Cargelligo 1:250 000 map sheet area. Geological Survey of New South Wales, File GS2005/192 (unpublished).

BULL K.F., & FITZHERBERT J.A., 2022. Early Devonian volcanic facies, central Lachlan Orogen, New South Wales: implications for tectonic and metallogenic models. Australian Journal of Earth Sciences. Vol 69, 953-982.

- CARLTON, A., SPAMPINATO G., & MORIARTY, T. 2019. Geological Survey of New South Wales: New products and data. In: ASEG Preview, 201.
- COLQUHOUN, G.P., MEAKIN, N.S. & CAMERON, R.G., 2005. CARGELLIGO 1:250 000 GEOLOGICAL SHEET 3rd edition SI/55-6 (compilers). Geological Survey NSW.
- DOWNES, P.M., 2004. Sulphur and lead isotope studies for the Cargelligo 1:250,000 sheet area. GSNSW Quarterly Notes 117.
- GLEN, R.A., & WALSHE J.L., 2002. Cross-structures in the Lachlan Orogen: the Lachlan Transverse Zone example. AJES. 46(4):641–658.
- GOSCOMBE, B. 2024. Weethalle Au-prospect, Summary Structural–Petrology Report to Weethalle Gold (unpublished).
- HART, C.J.R., 2024. Craig Hart - Expanding opportunities within Intrusion-related Gold Models. GeoHug, <https://www.youtube.com/watch?v=jNcTUXiSK-E>
- KENNY, E.J., 1932. Geology and Mineral Prospects of the Weethalle district and Weethalle District: Some recent Developments, NSW report R00025756.
- KIRKBY, A., CZARNOTA, K., HUSTON, D.L., AND HEINSON, G, 2022. Lithospheric conductors reveal source regions of convergent margin mineral systems. Nature Scientific Reports: 12(1):8190
- SMITH, M. 1988. Exploration Licence 2139, Euratha, NSW, Six-Monthly Report, Period Ending 11th December 1987, Australia Pacific Resources Limited. Unpublished Report GS1987/172, Dept. Min. Resources NSW
- STUART, C.A., RICKETTS, M., & GILMORE, P.J., 2020. Structurally controlled low sulfide gold mineralisation in the East Riverina region of NSW. GS2019/1091, 61 pp.
- TOU MINING, 2009. Exploration Licence 6914 Weethalle Annual Report, 18 Oct. 2008 to 17 Oct. 2009. R00036103 (GS2010/0391). 15 p.
- WALL, V., 2021. TAG: Thermal Aureole (pluton-related) Gold Vic Wall's Original Presentation to CERCAMS Workshop In Bishkek Kyrgyzstan 2003. Presented to SMEDG on 24 June 2021 Greg Hall. [Greg-Hall-Vic-Wall-Thermal-Aureole-Gold.pdf \(smedg.org.au\)](#)

SUNDAY CREEK: HIGH-GRADE GOLD-ANTIMONY DISCOVERY IN CLONBINANE, VICTORIA

Kenneth Bush⁽¹⁾ & Michael Hudson⁽²⁾

⁽¹⁾ Exploration Manager; ⁽²⁾ Managing Director, Southern Cross Gold.

Key Words: Gold, Antimony, Orogenic, Epizonal, Melbourne Zone.

INTRODUCTION

The Sunday Creek project occurs within the Melbourne Zone of the Palaeozoic Lachlan Fold Belt, 60 km north of Melbourne. Historic small-scale mining has been undertaken in the project area since the 1880s continuing through to the early 1900s. Historical production occurred with multiple small shafts and alluvial workings across the Clonbinane goldfield. Production of note occurred at the Clonbinane area with total production being reported as 41,000 oz gold at a grade of 33 g/t gold (Leggo and Holdsworth, 2013). Larger historic workings along the trend from west to east include Christina, Golden Dyke, Rising Sun and Apollo in the main Sunday Creek area and historic workings are present to the east-northeast for 11 kilometres until intersecting the Reedy Creek gold trend. The historic Reedy Creek gold trend on the eastern side of the Sunday Creek project area is a dominantly NW striking set of quartz veins with hundreds of small workings that extend over a four-kilometre strike length.

LOCAL GEOLOGY

The Melbourne Formation (Silurian) and the Humevale Siltstone (early Devonian) are the major stratigraphic units with mapped exposures folded and thrust-faulted by the Late Devonian Tabberabberan Orogeny into dominantly SE-striking open to tight folds (Figure 8). The Mount Disappointment granite (late Devonian age 375.3 ± 2.5 Ma and 376.9 ± 2.6 Ma for early crystallisation (Clemens et al., 2022)) is emplaced into this sequence 8 kilometres south-east of the project tenements. Contact metamorphic effects are not obvious within the project, but dykes apparently related to the granite are significant in the project.

Dark grey turbiditic siltstone is the dominant host lithology at Sunday Creek with subordinate fine- to medium-grained laminated sandstone (Figure 9). Corals and fossiliferous bands have been intersected in Southern Cross diamond drilling. Graded beds in the siltstone are rare and where present indicate the sequence is not overturned. The metamorphic grade of the host sequence is low (sub-greenschist facies). The sequence is described as conformable and monotonous, with a number of marker units (informal members) and subtle gradational changes.

Folds are open to tight, with correlation of individual strata across the Southern Cross Gold's Sunday Creek diamond drill holes confirming this in areas of non-destructive alteration. Emplacement of a multi-phase dyke swarm caused marginal brecciation of the host rocks producing two distinct breccia types. The first breccia type has a quartz-carbonate matrix with angular dyke clasts and the second type has the host sediments as the breccia matrix. Both breccia types are mapped adjacent or within dykes and contain common pale cream to yellow alteration (carbonate and sericite) although adjacent altered and unaltered sediment breccia clasts are common.

The Sunday Creek dyke swarm is a series of intermediate monzodiorite – diorite dykes and breccias that trend near east-west on 080° and dip steeply north and have highly variable textures and compositions. The earliest emplaced aphanitic varieties occur along thin fracture sets. These fine-grained dykes locally grade into porphyritic to massive varieties as the thickness of the dykes increases. Typically, multiple dykes, ranging from centimetre scale to ten metres wide, also sills; occur within a sericite-

ALTERATION

Alteration surrounding the mineralisation is zoned from distal to proximal (Figure 10);

- Regional chlorite alteration weakly pervades the sediments
- Change in mica composition from phengitic to muscovitic mica approaching mineralisation
- Increasing carbonate spotting and cementation of groundmass
- Proximal to the dyke swarm a very intense, texturally destructive alteration of sericite-carbonate-silica “bleaching” of the sediments and dyke swarm. This alteration begins as patchy selective replacement of sediments and increases in intensity until no discernible protolith can be determined.

Pale green fuchsite and albite are common accessory minerals of the alteration assemblage within the dyke.

MINERALISATION

The mineralisation at Sunday Creek is structurally controlled and has a clear spatial relationship with the dyke rocks and the enclosing altered sediments. Distally, mineralisation is represented by disseminated pyrite in the visually unaltered sediments, with increasing frequency and small pyritic veinlets following the dyke swarm trend proximal to veining and visual “bleached” sediments (Figure 10).

Mineralisation is dominantly hosted within zones of sub-vertical, brittle, semi-brittle to ductile shear veins and associated extension veins, containing visible gold, quartz, stibnite, uncommon fibrous sulfosalts and minor ferroan carbonate infill. The veins are typically striking north-north-westerly with a sub-vertical to steep east/west dip (Stereonet: Figure 10), Subordinate vein sets in other orientations are recorded in Southern Cross drilling and are interpreted to be linkage features between the steep dipping trends. An associated selvage of disseminated sulphides in the form of arsenian pyrite, pyrite and arsenopyrite are observed within the proximal mineralised zones. The mineralised zones orthogonally crosscut the east-west trending bleached sediments and altered dyke and the zones are typically between 5-30m wide, 20-100m in strike and currently defined vertically down to 1km depth. Each of these zones repeats every 10-20m within the Apollo and Rising Sun areas with 45 vein sets currently defined to date.

The strong presence of stibnite (> percent levels), and a general transition of brittle, semi-brittle and ductile veins with depth is consistent with classic orogenic gold belts around the world showing a continuum of mineralisation genesis and potential for focus at depth and presence of higher tenor mineralisation. The features observed at Sunday Creek would place it within the classification of Epizonal, or shallow orogenic deposits. Mineralisation has been estimated to have occurred in the late Devonian associated with the Tabberabberan Orogeny, consistent with surrounding epizonal deposits of similar characteristics (e.g. Fosterville and Costerfield).

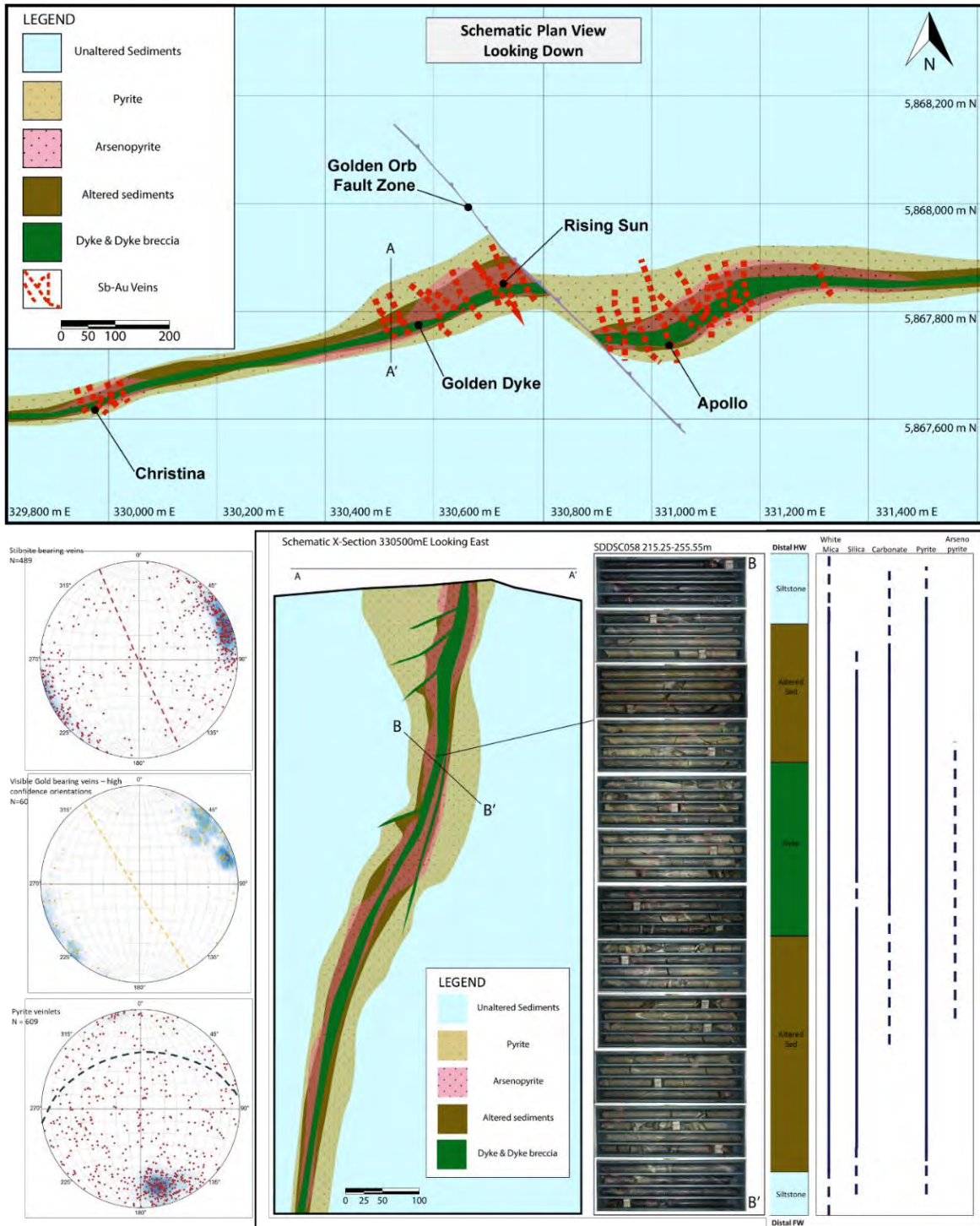


Figure 10: Schematic Plan view and section view of the geology and alteration within the Sunday Creek project area, with high confidence structural measurements of the mineralisation.

Structure and Controls on Mineralisation

The primary control on mineralisation at Sunday Creek is the competency contrast of the dyke swarm and altered sediments relative to the unaltered sediments. The alteration has strengthened the rock mass and increased the competency of the units promoting an increase and focus in fracturing and fluid pathways within the altered sediments and dyke material.

Structural analysis of mineralised veins and faults within the project area suggest whilst a regional NNE-SSW compression was occurring during mineralisation, a local extensional

regime was occurring around the dyke host with a small component of strike-slip movement. This caused a high propensity for steep plunging oreshoots within the mineralised package associated with several geological features;

- The intersection of conjugate extension veins
- The intersection of extension veins with shear veins
- Intersection lineation of the dyke swarm and vein sets
- Slickenlines and slickenfibres.

Cataclastic fault zones are common within the mineralised rocks at Sunday Creek. These fault zones both contain and transect the mineralisation and are interpreted by Southern Cross to be approximately synchronous with the deposition of gold and antimony with a component of post-mineralisation movement. Significant dextral strike-slip faults are interpreted along the ENE Clonbinane dyke swarm trend, in particular at Sunday Creek, the Golden Orb fault zone (Plan View: Figure 10) where bedding trends appear to steepen into this fault from both north and south.

HIGH TENOR MINERALISATION

The culmination of structural controls on the epizonal mineralisation and competency contrasts by host rocks and alteration, allows for very high tenor gold and antimony mineralisation to be present at Sunday Creek (7330 g/t Au in SDDSC107 and 55.8 % Sb in SDDSC077b are the maximum observed results to date). For example, SDDSC107 (drilled in February 2024 at Rising Sun) intercepted the highest-grade gold and best intersection drilled to date at Sunday Creek of 0.3 m @ 7,330 g/t Au within 1.0 m @ 2,318 g/t Au (estimated true width 0.7 m) from 684.3 m, within a broader interval traversing 12 high-grade vein sets of 455.3 m @ 7.2 g/t Au (uncut) from 335.0 m.

REFERENCES

CLEMENS, J. D., STEVENS, G. AND COETZEE, L., 2022. Dating initial crystallisation of some Devonian plutons in central Victoria and geological implications; *AJES*, 70 (12), 1-13.

LEGGO, N. AND HOLDSWORTH, K.H. 2013: Independent Geologist's Report on the Reedy Creek Mineral Property in Australia for Auminco Mines Limited 5 February 2013. Corvidae Pty Ltd as Trustee for Ravensgate Unit Trust Trading as Ravensgate.

MT CHALMERS VHMS – NEW LIFE FOR A FORGOTTEN GEM

Peter Caristo & Glenn Whalan

QMines Limited

QMines Limited's (ASX:QML) Mt Chalmers project is located 17 km east of Rockhampton, Queensland. Gold was first discovered in the area in 1860 with production beginning in 1869 with the establishment of the first battery by Mr Chalmers. After a few years mining, copper was discovered at Mt Chalmers with mining starting in 1899. Organised mining took place between 1907-1914 with the establishment of Great Fitzroy Mines. The mine reopened during World War Two for a brief period, operated by Mt Morgan Limited (1941-1943). After a long hiatus, modern open-pit mining was undertaken by Geopeko (owner and operator of the Mt Morgan mine) between 1979-1982, with the ore carted to and treated at Mt Morgan, providing the Mt Morgan processing plant with its last few years of ore.

Sporadic exploration took place from its closure through to QMines taking over the project and listing on the ASX in March 2021. Since listing, QMines has established, expanded and upgraded the mineral resource at Mt Chalmers, and during April 2024 completed a pre-feasibility study supporting a 10.4 year mine-life, to produce 65 kt Cu, 160 koz Au, and 1.8 Moz Ag. Regional exploration driven by an airborne VTEM geophysical survey culminated in the discovery of the Artillery Road skarn deposit.

Mt Chalmers is a Kuroko-style VHMS deposit, formed in the Berserker sub-province on the eastern margin of the Yarrol Province of the New England Orogen. The Berserker sub-province is a 100 km by 5-15 km wide fault-bounded rift basin formed during the Permian (volcanics dated 268.2-277 Ma). There is some contention as to whether the Yarrol Province formed in a back-arc or fore-arc setting.

The deposit is hosted within a sequence of volcanoclastics, tuffs, sandstones and mudstones, intruded by rhyolite, and later intrusive andesite and quartz-feldspar porphyry. Sulphides are predominantly pyrite-chalcopyrite-sphalerite-galena. The metal zonation and fluid inclusion work completed by Zaw et.al (2003) suggests that the metal source is magmatic, with possibly two distinct pulses (Cu-Au and Zn-Pb-Ag). This is supported by observation of the metal distribution and zonation which is somewhat structurally controlled. The Zn-Pb-Ag mineralisation is confined to the massive/semi-massive-exhalite zone, while Cu-Au is more extensive and extends into the stringer zone.

Alteration is similarly zoned and somewhat structurally controlled, with silica alteration extensive through the stringer and footwall, kaolinite confined to exhalite-massive zone and along structure, and sericite more confined to the better Cu-Au zones. Chlorite is extensive, with sudoite (dioctahedral chlorite) associated with sericite-dolomite (more closely related to Cu-Au) and trioctahedral chlorite throughout extending into the cover rocks.

REFERENCES

ZAW, K., HUNNS, S.R., LARGE, R.R., GEMMELL, J.B., RYAN, C.G. AND MERNAGH, T.P., 2003. Microthermometry and chemical composition of fluid inclusions from the Mt Chalmers volcanic-hosted massive sulfide deposits, central Queensland, Australia: implications for ore genesis. *Chemical Geology*, 194: 225-244.

**THE GIANT LACHLAN OROCLINE OF EASTERN AUSTRALIA –
A rAdiCaL NEW WAY OF THINKING ABOUT THE ORDOVICIAN-DEVONIAN
TECTONICS AND MINERAL SYSTEMS OF EASTERN AUSTRALIA**

R. A. Cayley*, R. J. Musgrave

*Geological Survey of Victoria (Resources Victoria)

Key Words: Lachlan Orocline, Lachlan Orogen, geodynamics, accretionary orogen, mineral systems, Macquarie Arc, Selwyn Block, Vandieland.

INTRODUCTION

The Lachlan Orocline hypothesis (Cayley & Musgrave, in prep.) is a geodynamic model for the Early Palaeozoic evolution of the Australian Continent proposed by Cayley (2010, 2012) that advocates for the presence of a huge (hundreds of kilometre amplitude) Silurian-aged Z-shaped, vertically plunging megafold – the Lachlan Orocline – superimposed over a previously linear and relatively simple Ordovician Lachlan Fold Belt (LFB) suprasubduction-accretion system developed above a single, continent-dipping subduction zone that had formed parallel to the eastern edge of Gondwana. The Ordovician suprasubduction system included the Macquarie Arc (Crawford et al., 2007; Glen et al., 2007) built, in part at least, on a substrate of thin Early-Mid Cambrian MORB to intraoceanic arc/backarc crust that crops out widely in Victoria (Crawford, 1988; Squire et al, 2006), was largely not involved in Delamerian orogenesis (VandenBerg, 1991, VandenBerg et al., 2000) and instead lay undeformed in a deep marine proto-LFB Paleopacific setting into the Ordovician.

The origins of the Lachlan Orocline model lie in the quest for a single unifying geodynamic scenario able to rationally explain the plethora of apparently contradictory fundamental geological (and particularly paleogeographic) constraints long recognised and well documented in the Early Palaeozoic geology of Eastern Australia, and well documented in Victoria in particular.

THE LACHLAN OROCLINE HYPOTHESIS

The Lachlan Orocline model is a development – effectively a simplification – of the multiple, coeval divergent subduction zone hypothesis proposed by Gray & Foster (1998) for the same region for the southern LFB. Their model includes a central distinctly separate east-dipping subduction zone.

Rather than advocating for three separate but broadly coeval subduction zones in an oceanic environment to explain the observed distribution of Ordovician arc rocks and observed coeval accretionary wedge symmetries in Victoria in particular (and possibly Tasmania – e.g. Reed, 2001), the Lachlan Orocline model proposes that the westernmost west-dipping subduction zone of the Gray & Foster (1998) model was not active post-Cambrian (Cayley et al., 2011; 2018) with Ordovician-Devonian ‘western’ Lachlan Fold Belt deformation instead attributed to intraplate processes, and reinterprets the ‘central’ east-dipping subduction zone of Gray & Foster (1998) as the southernmost part of their easternmost west-dipping subduction zone, but reoriented in the central limb of the superimposed Lachlan Orocline megafold.

The near-contiguous limbs of the Lachlan Orocline occur in Ordovician deep marine siliciclastic rocks, including rocks in eastern Victoria that preserve characteristics of syn-sedimentary deformation in an accretionary wedge setting. The orocline limbs are

exposed near-continuously across the east-west trending portion of the southern Great Dividing Range, which extends from the easternmost Delamerian Orogen in western Victoria across the full width of the LFB to the east coast of Australia.

Behind (ie north-of) the near-contiguous orocline limbs, field relationships exposed in Victoria, which can be extended into NSW with confidence using geophysics, and paleomagnetic data, all show that Ordovician Macquarie Arc crust together with associated Wagga-Omeo Zone back-arc (and, in Queensland, parts of the adjacent continent – e.g. the Anakie Inlier; Offler et al., 2011; and Nebine Ridge; Finlayson & Collins, 1987; see Figure 3) became variously rifted, fragmented, translated and clockwise rotated during Silurian orocline growth, collectively chasing the oceanward-retreating eastern hinge of the Lachlan Orocline, in a persistently extensional/dextral transtensional setting (Collins, 2002b) similar to that envisaged for the adjacent, younger New England Orogen (Rosenbaum, 2012). Due to the transtensional setting that precipitated and accompanied Silurian LFB modification, the Ordovician terrane fragments can preserve little internal evidence of their Silurian lateral translation, other than the presence of thin linear ‘rifts’ and ‘basins’ and syn-rift intrusions of this age that surround, bury and/or intrude the fragment margins and so typically obscure bounding relationships. Some fragments do, however, show clear structural evidence of significant internal extension at this time as, for example, Silurian flat-lying high-temperature metamorphic complexes imposed on Ordovician terranes.

By the end of the Silurian, different parts of the previously linear and simple Ordovician continent-fringing intra-oceanic suprasubduction zone system had been modified into a complex intermix of terrane fragments, including some parts rotated to such high strike-angles that they have long been considered entirely different orogenic systems (the Thomson Fold Belt; Spampinato et al., 2015; Doublier et al., 2018; Figure 1).

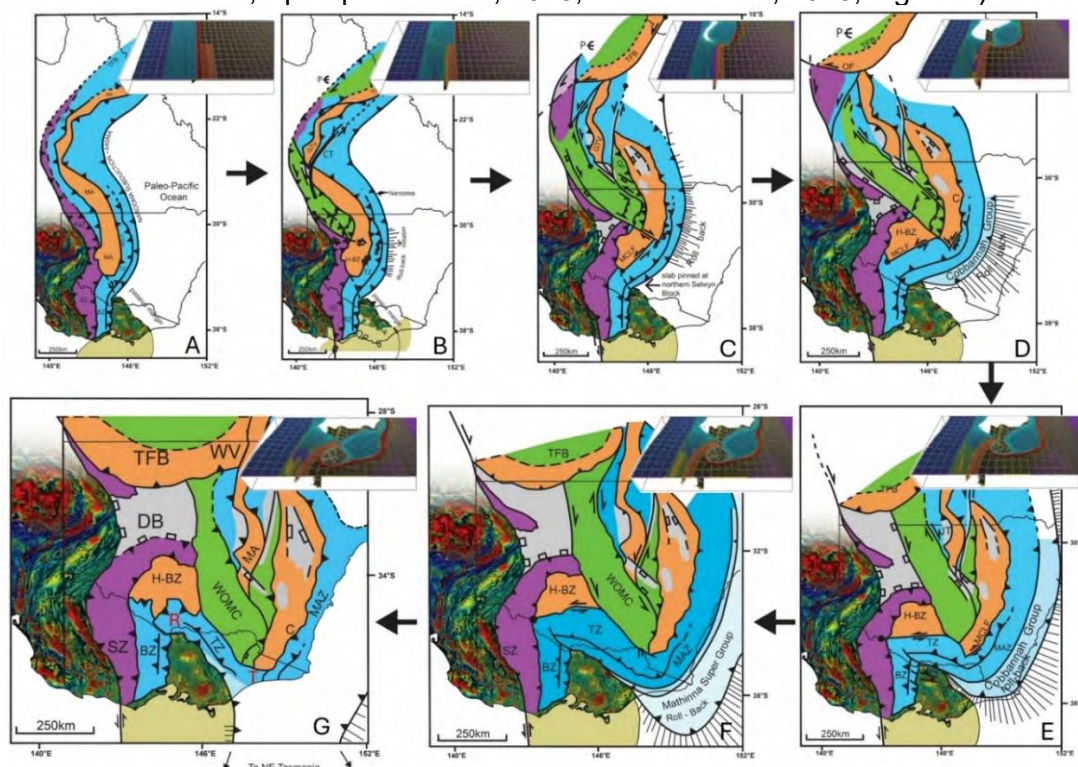


Figure 1: Time-sequence summary of the progressive evolution of the LFB and growth of the Lachlan Orocline on mainland Australia from ~445 Ma (A) - 405 Ma (G), with inset interval snap-shots of the numerical model 80s of Moresi et al. (2014) with an age of oceanic lithosphere (~80My), geographic scale and run-duration directly comparable to the Lachlan Orocline. BZ=Bendigo Zone; DB=Darling Basin; C=Cooma Complex; CB=Cobar Basin; GTV= Goonumbla-Trangie Volcanic Belt; H-BZ=Hay-Booligal Zone; KaZ=Kayrunnera Zone; MA=Macquarie Arc; MAZ=Mallacoota Zone; SZ=Stawell Zone; TFB = Thomson Fold Belt; TZ=Tabberabbera Zone; WOMC=Wagga-Omeo Metamorphic Complex. **R** = Riverina Hinge. **T** = Tambo Hinge

Our review of Victorian, NSW and Qld Cambrian-Ordovician geology in the light of modern convergent margin systematics and diagnostic attributes has identified clear Ordovician arc, back-arc, fore-arc, accretionary and intraplate components, spatially ordered in a way that demands continent-dipping subduction polarity throughout the Ordovician, particularly in NSW. Although atypical ordering exists in places (e.g.: multiple parallel belts of Macquarie Arc volcanics separated by atypical coeval rocks such as Kirribilli Formation in NSW, and the east-dipping and facing Ordovician accretionary rocks of the Tabberabbera Zone in Victoria), these can be explained by subsequent tectonism (e.g. Packham, 1987; Fergusson 2009; see Figure 1) without need to invoke additional complexity into the Ordovician convergent margin system.

Lachlan Orocline growth is attributed to Silurian-aged asymmetric slab 'rollback' of the NSW portion of a single, simple, west- (ie continent-) dipping subduction zone that had been active along the NSW- Queensland portion of the East-Gondwana margin throughout the Ordovician. Silurian asymmetric slab 'rollback' of the subduction zone portion that lay in NSW in the Ordovician is attributed to the collision of an exotic microcontinent Vandieland (Cayley, 2011) into the southern end of the Macquarie Arc subduction zone (Cayley, 2012; Moresi et al. 2014) beginning at the end of the Ordovician. Vandieland comprises Proterozoic western Tasmanian crust and its northern Selwyn Block extension into central Victoria (Cayley et al., 2002). Vandieland geology shares key Proterozoic geological characteristics with Antarctic Gondwana, was likely a legacy of Rodinia breakup (Moore et al, 2016) and was definitively involved in, and cratonised by, Cambrian Delamerian orogenesis. This is a key feature that sets it apart from the conformable Early Cambrian – Ordovician sea-floor successions that underpin the rest of the Lachlan Orogen, well exposed and long understood in central and eastern Victoria (VandenBerg, 1991) and in SE NSW (Stokes et al 2015; Packham et al 2016) and now being identified in central-west NSW (P. Blevin, pers. comm. May 2024).

Following Delamerian orogenesis, Vandieland became separated from Gondwana as part of the Paleopacific plate, which mostly comprised undeformed Cambrian MORB, intra-oceanic arc and back-arc sea-floor crust now exposed in adjacent parts of the LFB in Victoria. Post-Delamerian, the Paleopacific plate appears to have commenced sinistral-oblique subduction beneath the eastern edge of NSW and Qld Gondwana throughout the Ordovician, forming the Macquarie Arc in NSW and Qld in the process. Being embedded in the Paleopacific plate, Vandieland was drawn obliquely out from the east-Gondwana margin and northwards towards the Macquarie Arc trench (Cayley, 2011). Its eventual end-Ordovician collision into the southern end of the Macquarie Arc subduction zone (Figure 1A) was inevitable.

Continental crust is buoyant so that Vandieland resisted subduction after collision, instead locally congesting and stalling the lateral advance of the downgoing Paleopacific oceanic plate within which the microcontinent was embedded. With lateral Paleopacific plate-advance dramatically slowed, continued subsidence of mafic oceanic plate portions north of Vandieland under the influence of gravity caused rapid trench retreat or 'rollback' of the uncongested portions oceanward (Figure 1B). Slab 'rollback' collapsed the Ordovician LFB supra-subduction crust in NSW and Qld into persistent regional-scale dextral transtension, chasing the retreating plate boundary. This is a 'tectonic mode switch' (Collins, 2002a; Cayley, 2015) and is preceded by, and coincides with, introduction of a host of mineral systems, including a pulse of metalliferous magmatism into the Macquarie Arc. The Cadia, Parkes, Ridgeway, etc porphyry systems were formed by decompression anatexis at this time (Huston, et al., 2015; Figure 2).

The giant Lachlan Orocline of eastern Australia

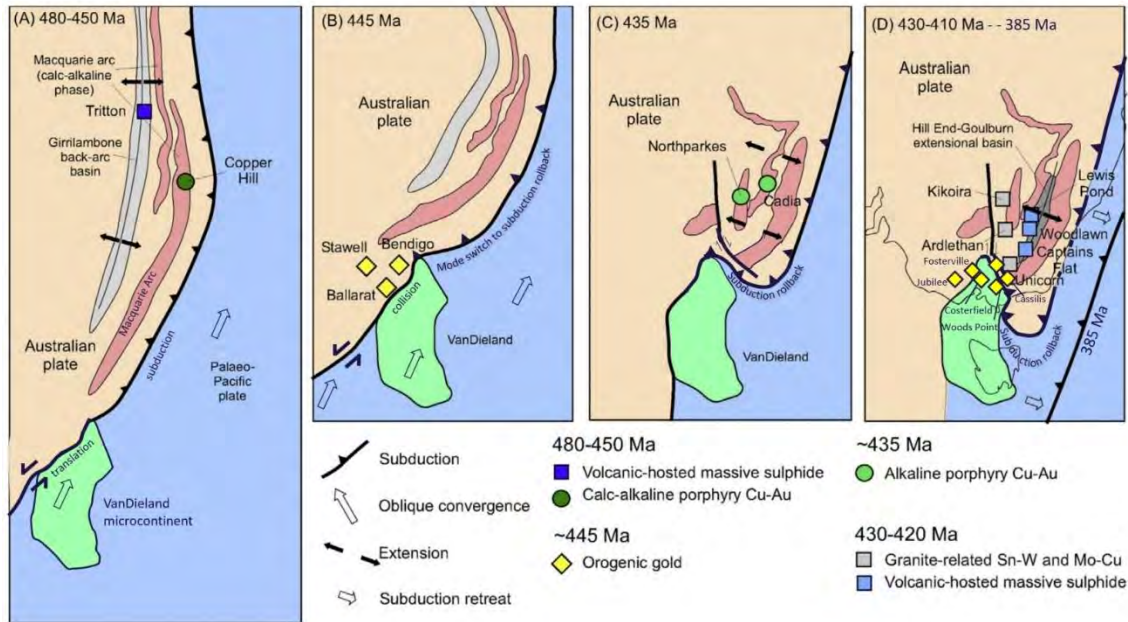


Figure 2: The Lachlan Orocline concept (Cayley, 2012; Cayley & Musgrave, in prep.) envisages the Ordovician proto-Lachlan Fold Belt as a simple linear subduction/accretion system (including the Macquarie Arc) developed along the east Gondwana margin (A). In the Late Ordovician the microcontinent VanDieland, embedded within the Paleopacific lower plate, was drawn into the southern end of the subduction zone, congesting it (B). Oblique collision with amagmatic parts of the Gondwana plate south of the arc across a sinistral transform fault at this time formed the Bendigo Zone (and Bendigo Zone orogenic gold). (C) With Paleopacific slab advance stalled by the buoyant microcontinent, the uncongested parts of the down-going slab fell into asymmetric roll-back, pivoting around the apex of the collider, dismembering, and translating the Macquarie Arc, which was intruded by phases of porphyry mineralisation, and forming a highly curved oroclinal trench (Moresi et al., 2014; Silurian LFB dismemberment described in the text is not unpacked in this summary figure – see Figure 1 for details). (D) As the northern and then eastern parts of Vandieland were drawn progressively into the trench, the collider was enveloped entirely by LFB suprasubduction zone crust, with widespread crustal thickening upon the collider. Eventually the trench reorganised to become linear once more, with final phases of orogenic gold introduced (~385 Ma). Figure adapted from: Huston et al., 2015; Moresi et al., 2014, Cayley & Musgrave, in prep.

With the southern part of the Macquarie Arc subduction zone (and downgoing Paleopacific slab) pinned at the point of Vandieland collision, roll-back of the adjacent uncongested slab was forced into asymmetry, wrapping clockwise around, and therefore being progressively further congested by, the northeastern and then eastern flank of the Vandieland microcontinent (e.g. Cayley, 2012; Moresi et al, 2014; Figure 1C-F).

Plan-view clockwise rotation and progressive congestion of the parts of the formerly linear and uniformly continentally-dipping subduction zone closest to the region of microcontinental collision continued throughout the Silurian, progressively wrapping this part of the subduction zone, together with the accretionary wedge that had developed above it in the Ordovician, around the eastern margin of Vandieland, rotating the former continental dip of this portion of the subduction system into a local oceanward dip-direction in the process, thus forming the accretionary Tabberabbera Zone (Collins & Vernon, 1992; VandenBerg et al., 2000) in its presently observed orientation as the Lachlan Orocline middle limb.

The Tabberabbera Zone is the key feature that inspired interpretation of the central east-dipping subduction zone in the Gray & Foster (1998) hypothesis. The congested subduction zone segment that underlies the Tabberabbera Zone accretionary wedge is still preserved today as the Governor Fault Zone, a major, kilometres-thick, east-dipping mega-thrust that separates the Selwyn Block footwall to the west from the overthrust Tabberabbera Zone accretionary crust hangingwall to the east, now definitively imaged in the SLaCT deep seismic reflection data (Cayley et al., 2019; 2022; in prep).

Ongoing southeastwards trench retreat at typical modern ~5-8 cm/year plate-tectonic rates for ~30 million years progressively grew the length this rotated portion into the middle, east-dipping limb of a large, vertically plunging Z-shaped oroclinal fold that progressively wrapped the entire eastern margin of Vandieland, eventually extending down into northeastern Tasmania (Figure 1G). This scenario supports, and provides regional context for, interpretations of northeast Tasmania that note similarities – including structural similarities such as recumbent folds – between the Ordovician Tippoogoree Group in northeast Tasmania and the coeval Pinnak Sandstone of the Tabberabbera Zone (Reed, 2001). In this style of interpretation, the Governor Fault extension south into Tasmania was positioned near the present-day Tyers Fault System (Direen & Leaman, 1997) which is a younger, subsequent structure.

Two broad, rounded, subvertically-plunging oroclinal hinges separate the Tabberabbera Zone from coeval but west-dipping and north-trending Ordovician-aged thrust-systems that are preserved to the west (Bendigo Zone; Cayley et al., 2011) and east (Kuark/Mallacoota zone / Narooma Terrane; e.g. Powell, 1983; Miller & Gray 1997) in Victoria and SE NSW.

The Riverina Hinge marks the transition from the northern Tabberabbera Zone westwards into the Bendigo Zone. It marks the point of initial Vandieland collision into the Macquarie Arc subduction zone system ('R' in Figure 1G). It is exposed only intermittently due to Murray Basin cover, but modern potential geophysics allows scattered outcrops to be linked together with confidence to define its overall form. Its geometry at crustal scale, including the northerly dip of the Governor Fault Zone that marks the initial point of continental collision, has been imaged in deep seismic data (Cayley et al., 2011).

The Tambo Hinge transition from the southeastern Tabberabbera Zone eastwards into the Kuark and Mallacoota Zones is well exposed in the southern Victorian Alps and has been mapped in great detail ('T' in Figure 1G). The core of this hinge subsequently became the locus of transtensional rifting in the Early Devonian to form the Buchan Rift, however inversion of this rift in the Middle Devonian Tabberabberan Orogeny (VandenBerg et al., 2000) evicted much of the Devonian rift fill (Ogden et al., 2016), particularly in the south, so that the gap between Ordovician outcrops that span the along-strike transition between the Tabberabbera and Kuark/Mallacoota zone transition is only a few km wide in places, inconsequential for interpretation of Ordovician-Silurian continuity across the Tambo Hinge.

Oroclinal folds formed by asymmetrically pinned slab rollback are characterised by a growth history that can involve simultaneously increasing amplitude and wavelength (e.g. Schellart & Lister, 2004). Which such characteristics, the folds can exhibit exponentially increasing amounts of extension within their cores. The Tambo Hinge exhibits these characteristics and provides a logical and area-balanced scenario that can accommodate the whole of the rest of the Lachlan Fold Belt, including the entirety of the Macquarie Arc and extensions in Australia, becoming progressively fragmented and drawn southeastwards by hundreds of kilometres throughout the Silurian. These rocks were migrating and collapsing laterally into the progressively growing and laterally migrating Tambo Hinge core (Figure 1C-1E).

Combined with eastwards rollback of the rest of the continental-dipping portions of the former Macquarie Arc subduction zone throughout the Silurian (Collins, 2002), also triggered by Vandieland collision (Moresi et al., 2014), the start of the Silurian marks an abrupt tectonic mode-shift to persistent dextral-dominated transtension that affected the

entire Australian portion of the east Gondwana convergent margin. Much of this system subsided back below sea-level to receive rejuvenated marine sedimentation throughout the Silurian and Early Devonian (Fergusson, 2010), while also rifting, extending, fragmenting and clockwise-rotating, locally juxtaposing and intermixing fault-slices of arc-crust with fault-slices of accretionary and back-arc crust in disordered ways not observed in modern unmodified subduction-accretion systems (e.g. Kirribilli Formation; Packham, 1987).

Southeastwards transtensional collapse of Lachlan Fold Belt suprasubduction zone crust related to Lachlan Orocline growth appears to have followed a classic tectonic progression (e.g. Buck, 2012): Early ‘core complex’ modes of extension reflect early fragmentation of the LFB and created the Early Silurian high-T Omeo Metamorphic Complex (Morand, 1990) and the Cooma and Kuark metamorphic complexes. As strain became increasingly partitioned into fractures between the fragments, LFB collapse transitioned into an intermediate ‘wide rift’ mode, involving the opening of large basins, including the large Middle-Silurian Darling Basin and the Hill End and Tumut troughs. As the regional stress-field stabilised into persistent dextral transtension, a more long-lived ‘narrow rift’ mode developed, whereby conjugate transtensional fault networks were able to link up and persistently feed crustal blocks – including Macquarie Arc segments – southwards into the retreating and growing Tambo Hinge core, continuing throughout the mid-late Silurian and into the Early Devonian. Such elongate fault networks are marked by features such as the lithospheric-scale dextral strike-slip Bootheragandra / Kancoona / Kiewa Fault, the Cowra Trough, and related Siluro-Devonian magmatic complexes.

Thus the entire LFB, all the pre-Silurian mineral deposits it contained, and eventually even the North Australian Craton and surrounding regions were drawn southwards into and/or towards the Lachlan Orocline core (Figure 3).

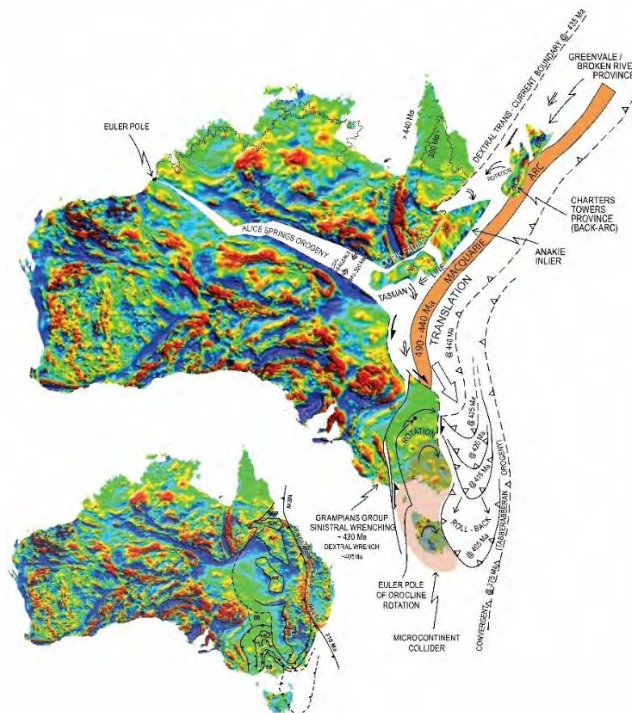


Figure 3: TMI image of Australia (GDA94 transverse Mercator to exaggerate relative scale of southern Australia), depicting Vandieland (orange shading; SB=Selwyn Block), interpreted pre-Silurian positions of the Nebine Ridge (NR), Anakie Inlier (AI), Macquarie Arc (MA; HBZ), Mossman Orogen (CTP=Charters Towers Province; BRP=Broken River Province), and Lachlan Orocline evolution, depicting successive positions of the East-Gondwanaland subduction trench as it evolved and migrated east and south from 440 to 375Ma. Inset: Post- 360 Ma geology (including the New England Orogen).

By the Early Devonian, the entire eastern flank of Vandieland had become drawn against rotated Macquarie Arc accretionary wedge material that now formed the middle limb of the Lachlan Orocline. At this point the subduction zone underlying southeastern Australia and northeastern Tasmania was highly folded, the folded middle-limb component highly congested and stalled by the eastern flank of Vandieland but evidently remaining intact at depth to continue acting as the plate-boundary barrier that had, throughout the Silurian, separated the rampant upper-plate dextral transtension within the Tambo Hinge core from the lower plate that contained Vandieland and the Bendigo Zone and which preserves no evidence of Silurian tectonism.

The common expression of the sinistral-transpressional Middle Devonian Tabberabberan Orogeny in the rock-record across the width of Eastern Australia, across the width of Tasmania, in the Robertson Bay Terrane in North Victoria Land, Antarctica and even in New Zealand indicates that, by the Middle Devonian, the highly folded and congested east-dipping portion of the Gondwana-Paleopacific plate boundary that had partitioned tectonism within the LFB throughout the Silurian was no more. The entire system had reunited in a simple, linear, suprasubduction zone system above a reestablished uniformly continent-dipping subduction zone aligned along the eastern Gondwana margin, but now further outboard. The Tabberabberan Orogeny shows that by the Middle Devonian this simplified slab was undergoing uniform Andean-style trench advance along its length.

The change from a highly curved, partly congested subduction zone in the Silurian to a simple west-dipping subduction zone located farther outboard in the Middle Devonian necessitates detachment of east-dipping, congested portion of the subducted Paleopacific slab from beneath the middle limb of the Lachlan Orocline. Slab detachments involve either 'tearing' or the opening of 'slab windows' that then grow laterally. Each process is expected to leave a number of characteristic legacies in the directly overlying rock-record.

The search for such characteristic legacies ended up in Bass Strait and in western Tasmania, where a second-order isoclinal orocline – the Early Devonian Dundas-Fossey Orocline – and associated lithospheric-scale rifting and magmatism, were identified from the distribution of Cambrian calc-alkaline rocks and associated sequences, including in legacy drillholes (Cayley & Musgrave, in prep.). Initiation of this second-order orocline is interpreted to involve lithospheric tearing in response to the opening of a 'slab window' beneath the Bass Strait portion of the central Lachlan Orocline limb. This slab window grew laterally north and south away from the point of initiation beneath the middle Lachlan Orocline limb to facilitate total separation of the congested east-dipping slab component from its Vandieland margin.

Slab windows cause initially tightly focussed and therefore rapid asthenospheric flows, and it is the focussed southeastwards flow of asthenosphere beneath Bass Strait that is considered to be the geodynamic driver of long-term rift-related lithospheric thinning that is expressed directly above, and to this day, as the Bass Strait topographic depression. Localised asthenospheric flow rafted the overlying lithosphere, producing lithospheric tearing and localised clockwise rotation of lithosphere that eventually formed the promontory-like eastern limb of the Dundas-Fossey Orocline. The Dundas-Fossey Orocline eastern limb was apparently tightened to isoclinal in the Middle Devonian at the culmination of the compressional Tabberabberan Orogeny, with the Tiers Fault System formed from inversion of extensional faults along the flank of the lithospheric promontory.

Modern geological and geophysical tools are able to constrain and test (ie falsify) such hypotheses. Paleomagnetic studies can test for evidence of rotations of the appropriate

magnitude and at the appropriate times (Musgrave, 2015; Musgrave & Job, 2020). Seismic reflection and passive seismic data image geometries at depth, and at lithospheric scale, constrain and test geometric predictions of Lachlan Orocline concept (Drummond et al., 2000; Rawling et al., 2011; Cayley, 2016; Rawlinson et al., 2011, 2014; Pilia et al., 2015; Cayley et al., 2019, in prep.). Magnetotellurics can identify crustal scale conductivity trends (Kirkby et al., 2020). Geochronology and geochemistry and good old targeted field mapping and reinterpretation of legacy datasets constrains and tests other critical predictions of the model (Cayley & Musgrave, in prep).

Understanding and constraining the origins and geodynamics and nature of the resolution of this process has enabled constrained, area-balanced plan-view fold-belt-scale retro-deformations to be constructed, based on regional potential field (mainly aeromagnetic) datasets. Such reconstructions reveal a possible pre-orocline configuration for the LFB, together with the original context and inter-relationships of contained pre-orocline mineral systems (Figure 1). We have undertaken higher resolution retrodeformations of key parts of this event where data allows (e.g. Cayley et al., 2018). This style of constrained reconstruction has potential to unlock vast areas of concealed Eastern Australian geology to effective predictive exploration for repeats of mineral systems in terranes already understood and known to be economic elsewhere. This is the ultimate aim of the UNCOVER initiative.

In a region of relatively poor exposure (Australia has low topographic relief, and much of the LFB lies buried beneath post-Early Palaeozoic cover rocks), a robust geodynamic understanding of the evolution of the LFB is critical in order to improve understanding of the possible causes for, and context of, its known contained world class mineral endowment (Huston et al., 2015), including the current quest to understand Australia's Critical and Strategic minerals endowments. An additional opportunity exists for other endowment types so-far unknown in eastern Australia, by comparison with modern systems of similar configuration.

REFERENCES

- BUCK, R.W., 2012. Modes of continental lithospheric extension. *Journal of Geophysical Research: Solid Earth* 96, 20161 – 20178.
- CAYLEY, R.A., 2010. South-directed oroclinal folding in the Lachlan Fold Belt: unravelling mid-late Silurian fold belt assembly to solve apparent Ordovician–early Silurian complexity. Geological Society of Australia, 2010 Australian Earth Sciences Convention (AESC) 2010, Earth systems: change, sustainability, vulnerability. Abstract No 98 of the 20th Australian Geological Convention, National Convention Centre, Canberra, Australian Capital Territory. July 4-8 July, 59-60.
- CAYLEY, R.A., 2011. Exotic crustal block accretion to the eastern Gondwanaland margin in the Late Cambrian – Tasmania, the Selwyn Block, and implications for the Cambrian-Silurian evolution of the Ross, Delamerian and Lachlan Orogens. *Gondwana Research* 19, 628 – 649.
- CAYLEY, R. 2012. Oroclinal folding in the Lachlan Fold Belt: Consequence of SE-directed Siluro-Devonian subduction rollback superimposed on an accreted arc assemblage in eastern Australia. *In: Selwyn Symposium 2012. Geol. Soc. Aust. Abst.*, 103, 34-43.
- CAYLEY, R.A., 2015. The giant Lachlan Orocline - a powerful new predictive tool for mineral exploration under cover across *eastern Australia*. *Australian Institute of Geoscientists Bulletin*, 62, 29-38.

CAYLEY, R.A., 2016. Revised project proposal: the Eastern Victorian / Central-East Lachlan Deep Seismic Reflection Transect. Geological Survey of Victoria Unpublished Report 2016/1. Earth resources Policy and Programs, 19 pp.

CAYLEY R. A., KORSCH R. J., MOORE D. H., COSTELLOE R. D., NAKAMURA A., WILLMAN C. E., RAWLING T. J., MORAND V. J., SKLADZIEN P. B. & O'SHEA P. J., 2011. Crustal architecture of central Victoria. results from the 2006 deep crustal reflection seismic survey. *Australian Journal of Earth Sciences* 58, 123–156.

CAYLEY, R.A., MCLEAN M.A., SKLADZIEN, P.B., & CAIRNS, C.P., 2018. Stavely Project - Regional 3D Geological Model. Stavely Project Report 3. Geological Survey of Victoria. Department of Economic Development, Jobs, Transport and Resources.

CAYLEY, R.A. & MUSGRAVE, R.J., in prep. The giant Lachlan Orocline – a new geodynamic model for the Ordovician-Devonian evolution of Eastern Australia. Currently being re-scoped for submission to *Australian Journal of Earth Science*.

CAYLEY R. A., SKLADZIEN P.B., CAIRNS C.P., HAYDON S., MCLEAN M.A., TAYLOR D.H., FOMIN T., COSTELLOE R.D., KIRKBY A., JINGMING D., DOUBLIER M., MUSGRAVE R., STOLZ N., SPAMPINATO G., GILMORE P., GREENFIELD J. & RAWLING T.J., 2019. The Southeast Lachlan Crustal Transect – planning, acquisition and some preliminary results from a 629 km long deep seismic reflection profile across the Australian Alps, *Mineral Exploration in the Tasmanides 2019*, AIG Bulletin 69, Australian Institute of Geoscientists.

CAYLEY, R.A., SKLADZIEN, P.B., CAIRNS, C.P., HAYDON, S., MCLEAN, M.A., TAYLOR, D.H., FOMIN, T., COSTELLOE, R.D., KIRKBY, A., JINGMING, D., DOUBLIER, M.P., MUSGRAVE, R.J., STOLZ, N., SPAMPINATO, G., GILMORE, P., GREENFIELD, J., CARLTON, A.A., & RAWLING, T.J. 2022. Profiles across a fossil congested subduction zone – is the Governor Fault in Victoria a ~5 km thick megathrust progressively superimposed on a probable Rodinian-age passive margin, and a control on the distribution of subsequent mantle-derived dykes and orogenic gold mineralisation? In: Armistead, S. E. (ed.). Specialist Group in Tectonics and Structural Geology conference. Geological Society of Australia Abstracts Number AB 134, pp. 11.

CAYLEY, R.A., SKLADZIEN, P.B., CAIRNS, C.P., HAYDON, S.J., MCLEAN, M.A., TAYLOR, D.H., FOMIN, T., COSTELLOE, R.D., KIRKBY, A.L., DUAN, J., DOUBLIER, M.P., MUSGRAVE, R.J., STOLZ, E.M., SPAMPINATO G., GILMORE, P.G., CARLTON, A.A., GREENFIELD, J.E., RAWLING, T.J., in prep, Geological interpretation of deep 2D seismic reflection survey lines 18GA-SL1, 18GA-SL2 and 18GA-SL3 undertaken as part of the Southeast Lachlan Crustal Transect. Geological Survey of Victoria. Department of Jobs, Precincts and Regions.

CAYLEY, R. A., TAYLOR, D. H., VANDENBERG, A. H. M & MOORE, D. H., 2002. Proterozoic–Early Palaeozoic rocks and the Tyennan Orogeny in central Victoria: the Selwyn Block and its tectonic implications. *Australian Journal of Earth Science* 49, 225–254.

COLLINS, W.J., 2002a. Hot Orogens, tectonic switching and creation of continental crust. *Geology* 30, 535-538

COLLINS W.J. 2002b. Nature of extensional accretionary orogens. *Tectonics* 21 (4);1258-1272 (10.1029/2000TC001272).

COLLINS, W.J. & VERNON, R.H., 1992. Palaeozoic arc growth, deformation and migration across the Lachlan Fold Belt, southeastern Australia. *Tectonophysics*, 214, 381-400.

- CRAWFORD, A.J., 1988. Cambrian. In: Douglas, J.G. & Fergusson, J.A. (eds.) *Geology of Victoria*, edition 2, Victorian Division of the Geological Society of Australia, Melbourne, 37-62.
- CRAWFORD, A.J., MEFFRE, S., SQUIRE, R.J., BARRON, L.M. & FALLOON, T., 2007. Middle and Late Ordovician magmatic evolution of the Macquarie Arc, Lachlan Orogen, New South Wales. *Australian Journal of Earth Sciences* 54, 181-214.
- DIREEN, N. G. & LEAMAN, D. E. 1997. Geophysical modelling of structure and tectonostratigraphic history of the Longford Basin, Northern Tasmania. *Exploration Geophysics* 28, 29–33.
- DOUBLIER, M. P., PURDY, D. J., HEGARTY, R., NICOLL, M. G., & ZWINGMANN, H. (2018). Structural elements of the southern Thomson Orogen (Australian Tasmanides): a tale of megafolds. *Australian Journal of Earth Sciences*, 65(7–8), 943–966. <https://doi.org/10.1080/08120099.2018.1526213>
- FERGUSSON, C.L., 2009. Tectonic evolution of the Ordovician Macquarie Arc, central New South Wales: arguments for subduction polarity and anticlockwise rotation. *Australian Journal of Earth Sciences* 56, 179–194.
- FERGUSSON, C. L., 2010. Plate-driven extension and convergence along the East Gondwana active margin: Late Silurian-Middle Devonian tectonics of the Lachlan Fold Belt, southeastern Australia. *Australian Journal of Earth Sciences* 57, 627 – 649.
- FERGUSSON, C. L., GRAY, D. R. & CAS, R. A. F., 1986. Overthrust terranes in the Lachlan Fold Belt, southeastern Australia. *Geology* 14, 519–522.
- FINLAYSON, D. M., & COLLINS, C. D. N. (1987). Crustal differences between the Nebine Ridge and the central Eromanga Basin from seismic data. *Australian Journal of Earth Sciences*, 34(2), 251–259. <https://doi.org/10.1080/08120098708729408>
- GLEN, R.A., CRAWFORD, A.J., PERCIVAL, I.G & BARRON, L.M., 2007. Early Ordovician development of the Macquarie Arc, Lachlan Orogen of southeastern Australia. *Australian Journal of Earth Sciences* 54, 167 – 179.
- GRAY D.R. & FOSTER D.A. 1998. Character and kinematics of faults within the turbidite-dominated Lachlan Orogen: implications for tectonic evolution of eastern Australia. *Journal of Structural Geology* 12, 1691–1720.
- HUSTON, D.L., MERNAGH, T.P., HAGEMANN, S.G., DOUBLIER, M.P., FIORENTINI, C., CHAMPION, D.S., LYNTON, J.A., CZARNOTA, K., CAYLEY, R.A., SKIRROW, R., & BASTRAKOV, E., 2015. Tectono-metallogenic systems – the place of mineral systems within tectonic evolution, with an emphasis on Australian examples. *Ore Geology Reviews* 76, 168-210 doi:10.1016/j.oregeorev.2105.09.005
- KIRKBY, A.L., MUSGRAVE, R.J., CZARNOTA, K., DOUBLIER, M.P., DUAN, J., CAYLEY, R.A. & KYI, D., 2020. Lithospheric architecture of a Phanerozoic orogen from magnetotellurics: AusLAMP in the Tasmanides, southeast Australia, *Tectonophysics* 793, <https://doi.org/10.1016/j.tecto.2020.228560>.
- MORESI, L., BETTS, P.G., MILLER, M.S. & CAYLEY, R.A., 2014. Dynamics of continental accretion. *Nature* 508, 245-248. doi:10.1038/nature13033
- MILLER, J. MC. L. & GRAY, D.R., 1997. Subduction related deformation and the Narooma anticlinorium, eastern Lachlan Fold Belt. *Australian Journal of Earth Sciences* 44, 237-251.
- MOORE, D.H., BETTS, P.G., & HALL, M., 2016. Constraining the VanDieland microcontinent at the edge of East Gondwana, Australia, *Tectonophysics*, 687, pp 158-179. <https://doi.org/10.1016/j.tecto.2016.09.009>.

- MORAND, V.J., 1990. Low-pressure regional metamorphism in the Omeo Metamorphic Complex, Victoria. Australia. *Journal of Metamorphic Geology* 8, 1 – 12.
- MUSGRAVE, R.J., 2015. Oroclines in the Tasmanides. *Journal of Structural Geology* 80, 72-98.
- PACKHAM, G.H., 1987. The eastern Lachlan fold belt of southeast Australia. A possible Late Ordovician to Early Devonian sinistral strike slip regime. IN: Leitch E.C. & Scheibner, E. eds. *Terrane Accretion & Orogenic Belts*, 67 – 82, AGU Geodynamic Series 19.
- MUSGRAVE, R. J. & JOB, K., 2020. Palaeomagnetism of the Dundas–Fossey Trough, Tasmania: Oroclinal rotation and Late Cretaceous overprinting. *Tectonophysics* 786. <https://doi.org/10.1016/j.tecto.2020.228453>.
- OGDEN, T., MCLEAN, M., RAWLING, T. & CAYLEY, R., 2016. Redefined crustal structure of the Buchan Rift, northeast Victoria: evidence from potential field modelling of newly acquired land-based gravity data. *Australian Journal of Earth Sciences*, 63(5), pp. 551-570. doi:10.1080/08120099.2016.1229692
- OFFLER, R., PHILLIPS, G., FERGUSON, C. & GREEN, T., 2011. Tectonic Implications of Early Palaeozoic Metamorphism in the Anakie Inlier, Central Queensland, Australia. *Journal of Geology*. 119. 10.1086/661191.
- PACKHAM, G.H., 1987. The eastern Lachlan fold belt of southeast Australia. A possible Late Ordovician to Early Devonian sinistral strike slip regime. IN: Leitch E.C. & Scheibner, E. eds. *Terrane Accretion & Orogenic Belts*, 67 – 82, AGU Geodynamic Series 19.
- PACKHAM, G. H., & HUBBLE, T. C. T. (2016). The Narooma Terrane offshore: a new model for the southeastern Lachlan Orogen using data from rocks dredged from the New South Wales continental slope. *Australian Journal of Earth Sciences*, 63(1), 23–61. <https://doi.org/10.1080/08120099.2016.1150346>
- PILIA, S., RAWLINSON, N., CAYLEY, R.A., BODIN, T., MUSGRAVE, R., READING, A.M., DIREEN, N.G. & YOUNG, M.K., 2015. Evidence of micro-continent entrainment during crustal accretion. *Scientific Reports* 5. Doi: 10.1038/srep08218
- POWELL, C. McA., 1983. Tectonic relationship between the Late Ordovician and Late Silurian palaeogeographies of southeastern Australia. *Journal of the Geological Society of Australia* 30, 353 – 373.
- RAWLING, T.J., OSBORNE, C.R., MCLEAN, M.A., SKLADZIEN, P.B., CAYLEY, R.A. & WILLIAMS, B., 2011. 3D Victoria Final Report. *GeoScience Victoria 3D Victoria Report* 14. Department of Primary Industries.
- RAWLINSON, N., ARROUCAU, P., MUSGRAVE, R. CAYLEY, R., YOUNG, M & SALMON, M., 2014. Complex continental growth along the proto-Pacific margin of East Gondwana. *Geology* 42, 783-786.
- RAWLINSON, N., KENNETT, B.L.N., VANACORE, E., GLEN, R.A., & FISHWICH, S., 2011. The structure of the upper mantle beneath the Delamerian and Lachlan orogens from simultaneous inversion of multiple teleseismic datasets. *Gondwana Research* 21, 302-304.
- REED, A. R., 2001. Pre-Tabberabberan deformation in eastern Tasmania: a southern extension of the Benambran Orogeny. *Australian Journal of Earth Sciences* 48, 785 – 796
- ROSENBAUM, G. (2012), Oroclines of the southern New England Orogen, eastern Australia, *Episodes*, 35(1), 187–194.

SCHELLART, W., & LISTER, G. S. (2004). Tectonic models for the formation of arc-shaped convergent zones and backarc basins. *Geological Society of America Special Publication*, 383, 237 - 258.

SPAMPINATO, G.P.T., BETTS, P. G., AILLERES, L. & ARMIT, R. J., 2015. Early tectonic evolution of the Thomson Orogen in Queensland inferred from constrained magnetic and gravity data. *Tectonophysics*, 651–652, pp 99-120
<https://doi.org/10.1016/j.tecto.2015.03.016>.

SQUIRE, R., WILSON, C., DUGDALE, L., JUPP, B. & KAUFMAN, A., 2006. Cambrian backarc-basin basalt in western Victoria related to evolution of a continent-dipping subduction zone. *Australian Journal of Earth Sciences*. 53. 707-719.
10.1080/08120090600827405.

STOKES, N., FERGUSSON, C.L., & OFFLER, R. (2015). Backarc basin and ocean island basalts in the Narooma Accretionary Complex, Australia: setting, geochemistry and tectonics. *Australian Journal of Earth Sciences*, 62, 37 - 53.

VANDENBERG, A.H.M., 1991. Kilmore 1:50 000 map geological report. Geological Survey of Victoria Report 91.

VANDENBERG, A. H. M., WILLMAN, C. E., MAHER, S., SIMONS, B. A., CAYLEY, R. A., TAYLOR, D. H., MORAND, V. J., MOORE, D. H. & RADOJKOVIC, A., 2000. The Tasman Fold Belt System in Victoria. Geological Survey of Victoria Special Publication.

MINERAL SYSTEMS AND METALLOGENY OF THE DELAMERIAN OROGEN MARGIN

Yanbo Cheng¹, P. Gilmore¹, C. Lewis¹, I. Roach¹, A. Clark¹, D. Mole¹, L. Pitt¹, M. Doublie¹, G. Sanchez¹, A. Schofield¹, A. O'Rourke¹, A. Budd^{1,2}, D. Huston¹, K. Czarnota¹, S. Meffre³, S. Feig³, R. Maas⁴, A. Brotodewo⁵, S. Gilbert⁵, C. Cairns⁶, R. Cayley⁶, T. Wise⁷, C. Wade⁷, M. Werner⁷, C. Folkes⁸, K. Hughes⁸

- 1 Geoscience Australia
- 2 MinEx CRC
- 3 University of Tasmania
- 4 University of Melbourne
- 5 Adelaide University
- 6 Geological Survey of Victoria
- 7 Geological Survey of South Australia
- 8 Geological Survey of New South Wales

Mineral deposits are formed through the interactions of multiple geological processes, which in turn are controlled by their tectonic setting and lithospheric architecture (Huston et al., 2016). Using the mineral system concept, individual mineral systems can be viewed as an expression of the combination of critical elements in time and space (McCuaig and Hronsky, 2014). Robust knowledge of the metallogenic characteristics of mineral systems and deposits and their ore formation mechanisms permits unravelling the characteristic geological features and their respective processes operating across a region, enabling an assessment of which mineral systems could have formed in space and time. This approach can substantially narrow the search space, thereby 'de-risking' mineral exploration.

The Delamerian Orogen is defined as the spatial extent of rocks first deformed by the Delamerian Orogeny (Glen 2005), with later impact from younger geodynamic events (Gilmore et al. 2023). On mainland southeastern Australia, the Orogen (which is one of the largest and most under-explored provinces in Australia) is mostly covered by younger rocks and sediments. However, in some areas where the rocks of the Delamerian Orogen have been exposed or intersected by drilling, mineralisation has been encountered.

This study presents the first systematic integration of mineral systems and metallogeny, including coincident critical mineral resources, in the Delamerian Orogen on mainland Australia. We seek to unite the fragmented knowledge on the mineral prospects and deposits of the Delamerian Orogen into cohesive mineral system classifications and regional metallogenic events, to further uncover the regional exploration potential, in the context of tectonic evolution.

MINERAL SYSTEMS OF THE DELAMERIAN OROGEN

The Delamerian Orogen marks the transition from Precambrian Australia to the Phanerozoic Tasmanides of eastern Australia, including a Cambrian convergent margin setting along the East Gondwana Margin (Foden et al., 2006; Greenfield et al., 2011; Cayley et al., 2018; Gilmore et al., 2023; Clark et al., 2024). The Delamerian Orogen is superimposed in part over a Neoproterozoic passive margin succession – the Adelaide Superbasin (Lloyd et al., 2020), which formed during Rodinia breakup (Powell et al., 1994), and has itself been overprinted by the effects of Ordovician-Devonian orogenesis during development of the outboard East Australian Tasmanides. Therefore, the Delamerian Orogen and its contained mineral systems now present a complex amalgam

of overlapping passive margin, convergent margin, intraplate and distal back-arc settings that span the Neoproterozoic to Devonian (Huston et al., 2018; Hong et al., 2023; Gilmore et al., 2023).

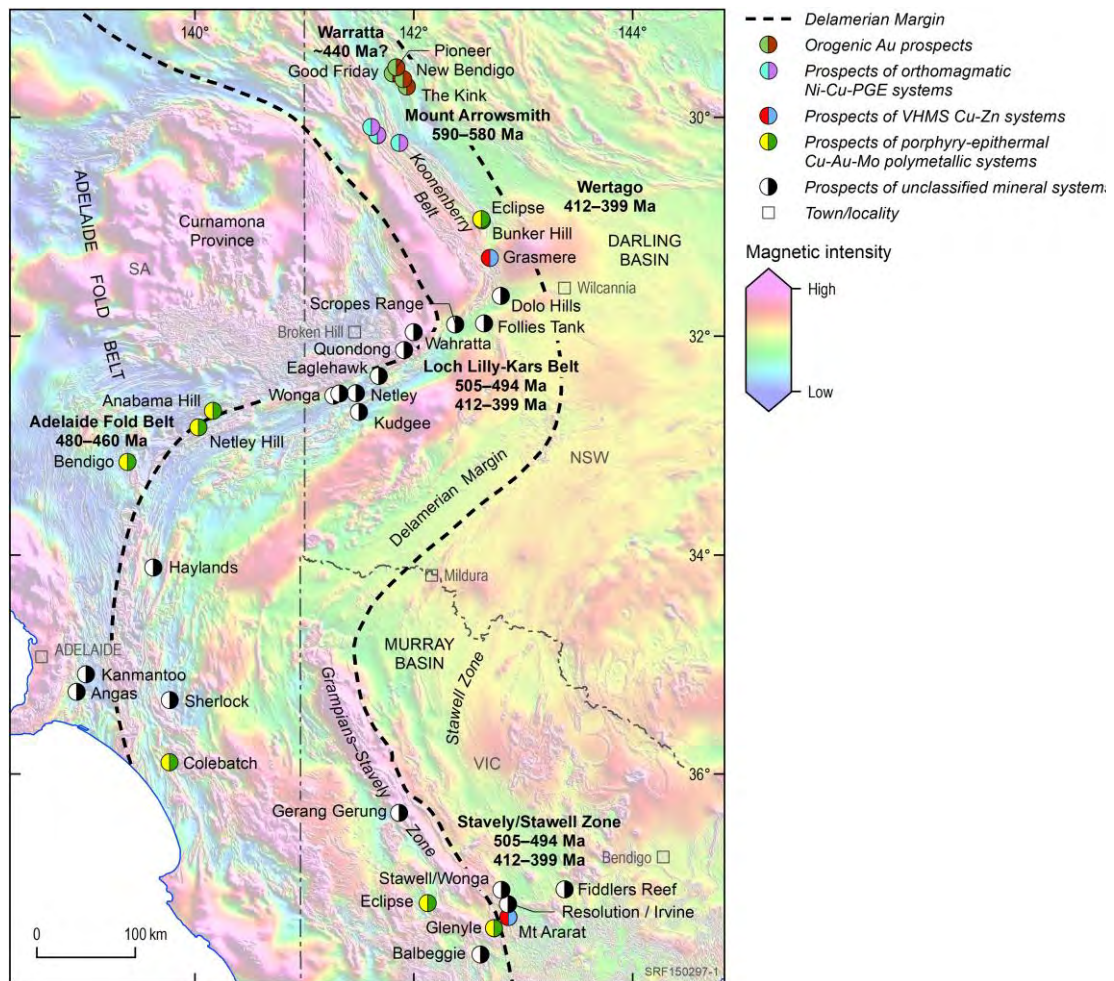


Figure 4 Key mineral prospects and deposits by metallogenetic type in the Delamerian Orogen margin (outline from Raymond et al., 2018), with the time-sliced geochronological results of the key metallogenetic belts/clusters marked. The background imagery shows the total magnetic intensity (TMI; Minty and Poudjom Djomani, 2019). The TMI data is available from the Geoscience Australia Portal: <https://portal.ga.gov.au/>. SA = South Australia; NSW = New South Wales; VIC = Victoria.

Cheng et al. (2024a) investigated mineral assemblages, textures and paragenetic relationships in mineralised rocks from key prospects and deposits throughout the Delamerian Orogen in mainland Australia, in order to determine the characteristics of its key mineral systems (Figure 1). Four key mineral systems are identified based on their petrological evidence, details see Cheng et al. (2024a).

Porphyry-epithermal mineral systems

As well as the proven porphyry-style copper (Cu)-gold (Au) mineralisation in the Grampians–Stavely Zone (Victoria), there is petrological characteristics of porphyry and epithermal mineralisation in multiple regions of the Delamerian Orogen, including the Wertago Au region of the Koonenberry Belt (NSW), Loch Lilly-Kars Belt Cu-Au (NSW), Adelaide Fold Belt molybdenum (Mo) (SA); Glenelg Zone and Delamerian margin Cu-Mo in southeastern SA, and the Stawell Zone copper-gold-zinc mineralisation (Victoria).

Volcanic hosted massive sulphide (VHMS) mineral systems

Petrologic features and ore textures of VHMS systems observed in the Delamerian Orogen were described by Cheng et al. (2024a), including the Mt Ararat Cu-Zn (Victoria) and Grasmere Cu-Zn (NSW) prospects and deposits. These systems are associated with Cambrian rocks in a convergent margin setting.

Orogenic gold mineral systems

Orogenic Au mineralisation appears to be associated with major fault systems on the eastern margin of the Delamerian Orogen, linked to regional metamorphism and deformation, e.g. the Warratta Inlier in the north of the Koonenberry Belt (Gilmore, 2010).

Orthomagmatic copper-nickel-platinum group element (Cu-Ni-PGE) mineral systems

Petrological, mineralogical and mineral chemistry data demonstrated in Cheng et al. (2024a) confirmed that orthomagmatic copper-nickel-platinum group element (Cu-Ni-PGE) mineralisation formed in the Koonenberry Belt (NSW), which is associated with the mafic-ultramafic magmatism related to the breakup of the Rodina supercontinent in the Ediacaran Period.

Other magmatic-hydrothermal systems

Due to a paucity of information, or robust interpretations across the literature, many of the mineral deposits and prospects in the Delamerian Orogen margin have ambiguous classifications. Cheng et al. (2024a) suggests that many of these prospects are magmatic-hydrothermal systems based on their mineral assemblages and textures, which are best interpreted to be formed by the hydrothermal fluids of magmatic origin.

TIMING OF MINERALISATION IN THE DELAMERIAN OROGEN

New advances in understanding mineral systems have been facilitated by the recent development of in-situ dating of minerals associated with hydrothermal fluids, such as titanite and apatite (U-Pb), carbonate minerals (Lu-Hf) and micas (Rb-Sr) (e.g., Simpson et al., 2024). Detailed petrology by Cheng et al. (2024a) identified key samples that display clear genetic connections between hydrothermal alteration and deposition of sulphide minerals, enabling the dating of mineralisation in deposits and prospects across the Delamerian Orogen (Figure 1).

New titanite U-Pb, apatite U-Pb and fluorite Sm-Nd dates from 11 mineral deposits and prospects have been plotted in Figure 2. Details of these geochronological results can be found in Cheng et al. (2024b). For comparison, the six molybdenite Re-Os ages reported by Hong et al. (2023) from four porphyry Cu-Mo prospects in SA are included in the plot.

Four temporally distinct metallogenic events are identified in the Delamerian Orogen, including:

- 590–580 Ma, reflected by apatite U-Pb dates obtained from mafic-ultramafic rocks associated with orthomagmatic Ni-PGE-Cu systems in the northern Koonenberry Belt.
- 505–494 Ma, the Cambrian metallogenic event, including the porphyry–epithermal mineral systems in both the Loch Lilly–Kars Belt and the Grampians–Stavely Zone, is defined by the titanite and apatite U-Pb and fluorite Sm-Nd dates.

- 480–460 Ma, largely confined to porphyry style Cu-Mo mineralisation based on the results by Hong et al. (2023) using Re-Os in molybdenite (e.g. Anabama Hill, Netley Hill, and Bendigo prospects in SA).
- 412–399 Ma, apatite and titanite U-Pb dates revealed a widespread magmatic-hydrothermal mineralisation event across the Delamerian Orogen resulted in porphyry Au–Cu prospects in the Wertago area in the Koonenberry Belt and intrusion-related gold systems in the Grampians-Stavely and Stawell zones of western Victoria.

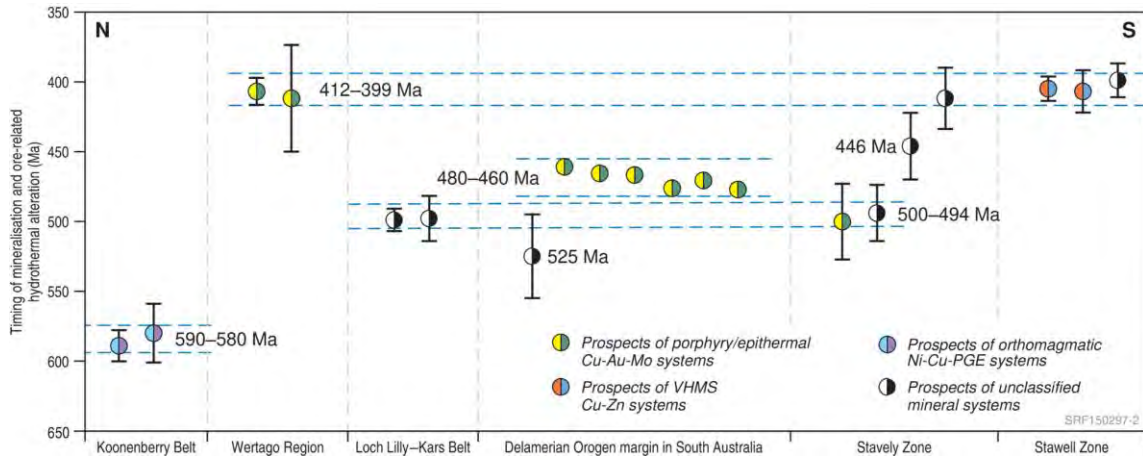


Figure 2 Time-space diagram (from north to south) comparing dates of ore-related hydrothermal alteration minerals (titanite and apatite U-Pb, and fluorite Sm-Nd) and ore mineral (molybdenite Re-Os) from mineral prospects and deposits in the Delamerian margin. Note the molybdenite Re-Os ages (the 6 ages with invisible error bars) of the porphyry Cu-Mo deposits and prospects of the Delamerian Orogen margin in South Australia are from Hong et al. (2023). Error bars shown for individual dates are 2 sigma.

However, care must be taken when interpreting the dating results. Geological evidence presented by Cayley et al. (2018) indicates that instead of representing the timing of VHMS Cu-Zn mineralisation at Mt Ararat, the 407–405 Ma apatite U-Pb ages acquired by this study likely record resetting by magmatic thermal perturbation associated with emplacement of the nearby Ararat Granite at c.405 Ma (Cayley and Taylor, 2001).

Note also that there are two outliers in the plots shown in Figure 2: the c. 525 Ma age from the Sherlock Cu-Zn prospect of the Kanmantoo-Glenelg Zone in SA, and the c. 446 Ma age of the Eclipse prospect (Grampians–Stavely Zone). Neither lies within the four metallogenic events identified above, and it is possible that they relate to different, poorly understood geological processes in the Delamerian Orogen margin which require further study.

FERTILITY OF THE DELAMERIAN OROGEN

Evolution of the continental crust imposes a crucial control on the endowment of a region, which ultimately affects the time–space fertility for the formation of specific mineral systems. Regional scale zircon Hf-O isotope and trace element mapping have demonstrated potential for unravelling regional crustal architecture and inferences on crustal metal fertility. Mole et al. (2023) outlined the overall crustal architecture, evolution,

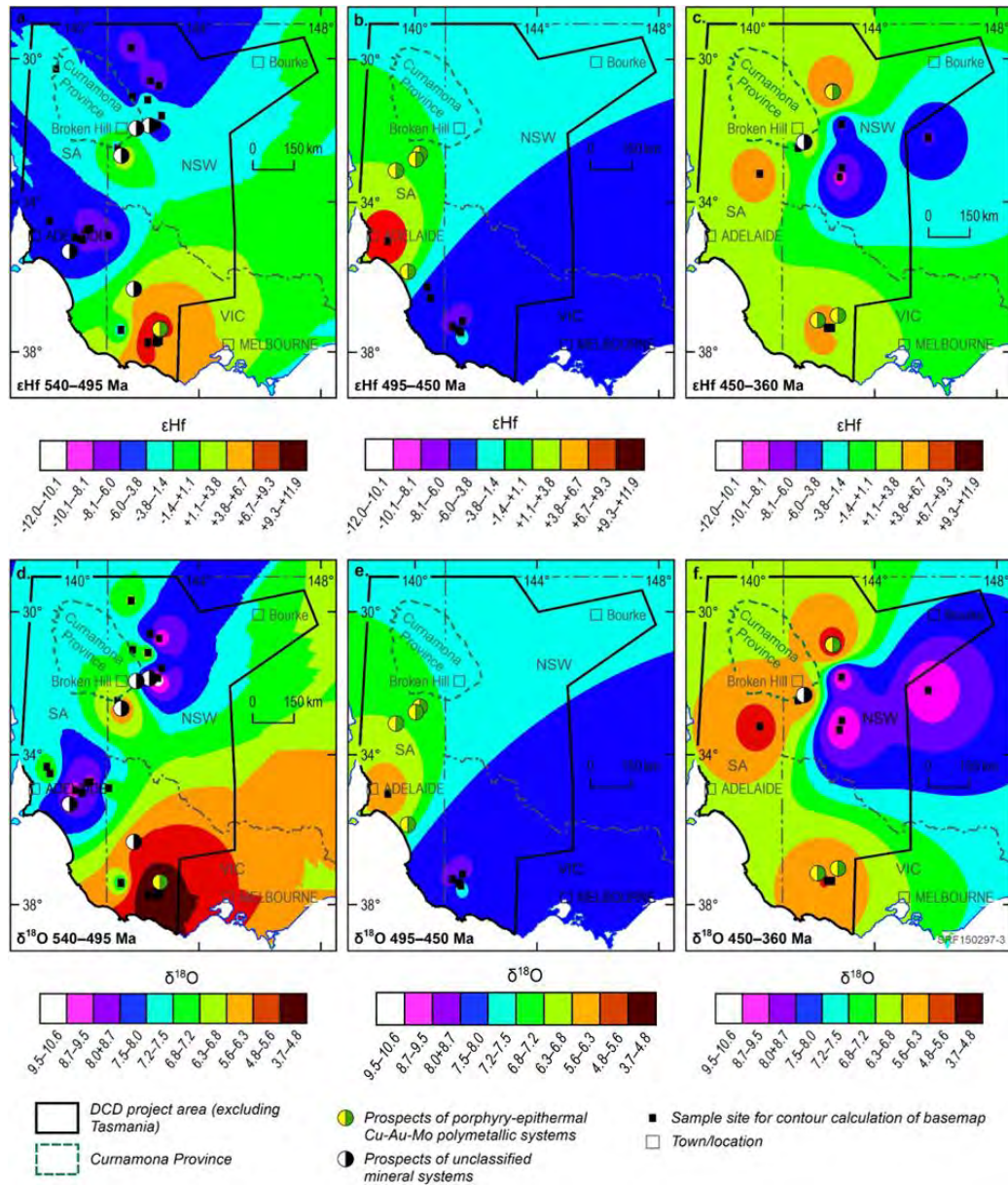


Figure 3 Time-sliced zircon Hf-O isotopic colour contour maps showing the spatial variation of zircon $\epsilon\text{Hf}(t)$ and $\delta^{18}\text{O}$ values for felsic magmatic rocks and their relationship to significant mineral prospects and deposits in the Delamerian Orogen at (a) and (d) 540–495 Ma (Delamerian arc period), (b) and (e) 495–450 Ma (the post orogenic period), and (c) and (f) 450–360 Ma (the Tabberabberan Cycle extension period; Gilmore et al., 2023). ϵHf represents the deviation of the $^{176}\text{Hf}/^{177}\text{Hf}$ ratio in a sample relative to a standard, and $\epsilon\text{Hf}(t)$ in this study refers to the ϵHf isotopic composition at the time of zircon crystallization. $\delta^{18}\text{O}$ is a measure of the deviation in the (stable) isotopic ratio $^{18}\text{O}/^{16}\text{O}$ in a sample, relative to an established standard.

and fertility of the Delamerian Orogen through analyses of zircon Hf-O isotope and trace element values. Since this initial assessment, updated versions of the zircon Hf-O isotope maps with 16 new samples have been developed and are shown in Figure 3.

The time-sliced zircon Hf-O isotopic colour contour maps show the spatial variation of zircon $\epsilon\text{Hf}(t)$ and $\delta^{18}\text{O}$ values (for explanations of $\epsilon\text{Hf}(t)$ and $\delta^{18}\text{O}$ see Figure 3 caption) for felsic magmatic rocks and their relationship to significant mineral prospects and deposits in the Delamerian Orogen. These maps show events at (a) 540–495 Ma (including the period of Cambrian convergent margin/arc magmatism and the Delamerian Orogeny), (b) 495–450 Ma (the post-Delamerian Orogeny and extension related to the Benambra cycle), and (c) 450–360 Ma (a period including the Benambra Orogeny

followed by widespread extension across the Tasmanides as part of the Tabberabberan cycle; Gilmore et al., 2023).

Figure 3 reveals a heterogeneous crustal architecture, comprising spatially juxtaposed ancient/reworked (high $\delta^{18}\text{O}$ and low $\epsilon\text{Hf}(t)$) and juvenile (low $\delta^{18}\text{O}$ and high $\epsilon\text{Hf}(t)$) crustal domains over a 180-million-year history. These time-sliced zircon Hf-O isotope maps further identify spatial relationships between crustal sources and mineral system types in the Delamerian Orogen. For example, porphyry Cu-Au deposits occur predominantly in juvenile crustal domains. The $\epsilon\text{Hf}(t)$ and $\delta^{18}\text{O}$ spatial patterns show juvenile materials in the Stavely Arc (540 Ma to 495 Ma), and the porphyry Cu-Au prospects of the Wertago region between 450 Ma and 360 Ma. These results demonstrate a crustal architectural control on the location and formation of mineral systems in the Delamerian Orogen. The new dataset suggests that mineral endowment varies as a function of crustal sources, and possibly metal availability, and could be effective in delineating prospective areas for mineral exploration and discovery.

MINERAL SYSTEMS AND METALLOGENY OF THE DELAMERIAN OROGEN

The geological and tectonic settings of different mineral systems in the Delamerian Orogen have been developed using the fundamental geological framework of Sanchez et al. (2024) and Clark et al. (2024). Integration of data from this study with the distribution of different packages of magmatic rocks in the Delamerian Orogen demonstrate regional metallogenic potential for a variety of mineral systems that formed between 600 and 400 Ma (Figure 4).

- Mafic-ultramafic rocks, formed between 590 Ma and 580 Ma in the Mount Arrowsmith region, and extend southeast over 200 km towards Wilcannia, are likely associated with the development of orthomagmatic Ni-Cu-PGE systems.
- The Middle to Late Cambrian was a key interval for the development of a magmatic arc system (515–495 Ma) within a convergent margin setting (Schofield et al., 2018; Clark et al., 2024). This marks a major regional metallogenic event, facilitating the formation of a range of mineral systems, including porphyry, epithermal, skarn and VHMS, which are intimately associated with the 515–495 Ma arc rocks in the Delamerian Orogen.
- Widespread 490–460 Ma granite magmatism, particularly in SA, postdated the Delamerian Orogeny. Porphyry Cu-Mo mineralisation at this time is interpreted to have developed in an extensional setting associated with slab roll-back during eastward shifting of the plate boundary (Glen, 2005; Kemp et al., 2009; Foden et al., 2020). This coincides with the metallogenic evolution of porphyry Cu-Mo systems in South Australia by Hong et al. (2023).
- The metallogeny of orogenic Au systems is associated with the distribution of greenschist to amphibolite facies metamorphism of turbidite sequences and activation of regional-scale fault systems of the Late Ordovician to Early Silurian Benambran Orogeny (Gilmore, 2010). These systems have been found in the east of the Cambrian volcanic arc and north of the Koonenberry Belt.
- Silurian to Devonian (420–400 Ma) magmatic rocks distributed along the eastern margin of the Delamerian Orogen are likely responsible for the formation of a series of magmatic-hydrothermal mineral systems, including porphyry, epithermal and intrusion-related Au mineralisation.

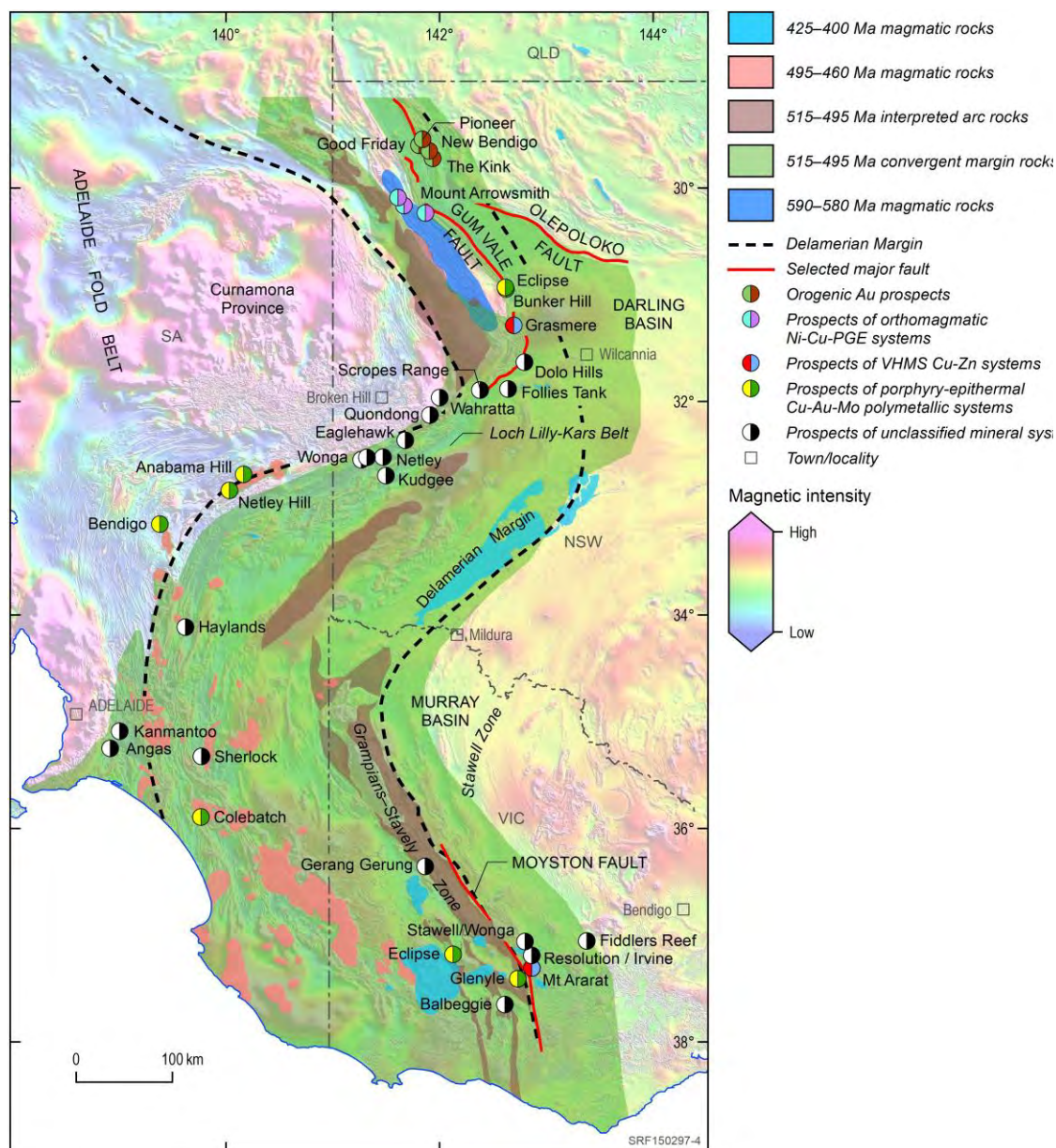


Figure 4 Mineral potential indicative map highlighting areas of interest for multiple types of mineral systems formed during different events between c. 600Ma and c. 400Ma in the Delamerian Orogen margin based on the distributions of their geological, geophysical, and metallogenic controls. Solid geology interpretation by Sanchez et al. (2024) and Clark et al. (2024). The background imagery shows the total magnetic intensity (TMI; Minty and Poudjom Djomani, 2019). The TMI data is available from the Geoscience Australia Portal: <https://portal.ga.gov.au/>.

Figure 4 illustrates the spatial extent of magmatic rocks from different time intervals in the history of the Delamerian Orogen. Although outcrop and basement-intersecting drilling is limited throughout the Orogen, particularly along the eastern margin, Figure 4 shows the potential for magmatic-hydrothermal and other mineral systems identified in this study to exist elsewhere within the relevant geological sequences under cover. This mineral potential indicative map can aid explorers to identify mineral systems along the Delamerian Orogen margin.

The thickness of cover sequences in the Delamerian Orogen has been estimated at <200 m in the Loch Lilly-Kars Belt from airborne electromagnetic (AEM) surveys (Wong et al., 2023) and depth to magnetic source estimations (Foss, 2020), and confirmed by the recent Delamerian Margins NSW National Drilling Initiative campaign (Pitt et al.,

2023). These thickness values have been integrated into the Estimates of Geological and Geophysical Surfaces database (Hope, 2023) to aid exploration targeting across the Delamerian Orogen.

Kirkby et al. (2022) showed correlations between orogenic gold and lithospheric electrical conductors at mid- to lower crustal level (25–30 km) imaged in magnetotelluric (MT) inversions, which can be useful in mapping fertile regions for orogenic gold deposits. The latest MT models reveal conductive anomalies on both the northern and southern sides of the Koonenberry Belt (Duan and Huston, 2024), which may also shed light on the potential of orogenic gold systems of the region.

Initial results of a deep crustal seismic survey conducted as part of Geoscience Australia's Darling-Curnamona-Delamerian project provide an understanding of the crustal architecture, timing and geometries of major structures and fluid pathways, and the distribution prospective rock units in the concealed, central part of the Delamerian Orogen, further improving the understanding of mineral potential (Doublier et al., 2024).

Furthermore, new S-isotope data on sulphide minerals from the Eaglehawk, Scropes Range and Wahratta prospects identified hydrothermal fluids with multiple origins, including fluids with a sedimentary origin, and fluids with different magmatic origins of different nature (Cheng et al., 2024b), that were likely involved in the processes of sulphide deposition in the Loch Lilly-Kars Belt, NSW.

Findings of this study complement the regional geological framework (Clark et al., 2024) and underpin mineral potential of several types of mineral systems in the Delamerian Orogen. These new interpretations open new opportunities for a greater understanding of the Orogen and future mineral discovery for resources such as Au, Cu, Ag, Pb, Zn, and critical minerals like Co in a range of mineral systems. This study also further informs national-scale mineral prospectivity maps, which indicate REE potential in the Neoproterozoic rift-related systems in northwestern NSW (Ford et al., 2023), and potential for iron oxide copper-gold (IOCG) systems in the Kanmantoo-Glenelg River Zone, SA (Cloutier et al., 2024).

SUMMARY

The basement rocks of the Delamerian Orogen are largely hidden by overlying cover sequences, making mineral exploration challenging. This study presents new geological, geochemical, geochronological, and isotopic evidence that fills knowledge gaps that presented barriers in identifying mineral systems and evaluating the regional mineral potential in the Delamerian Orogen of mainland Australia. We present the first systematic assessment of multiple mineral systems in the region, including their metallogenic characteristics, temporal-spatial framework, regional-scale metallogenic fertility, and integrated mineral potential indications. The major findings include:

- confirmation of four mineral system types hosted by the Delamerian Orogen, in addition to several unclassified magmatic-hydrothermal mineral prospects.
- four metallogenic events in the Delamerian Orogen are identified, at 590–580 Ma, 505–494 Ma, 480–460 Ma and 412–399 Ma.
- results that indicate prospectivity of several areas for a variety of mineral systems across the Delamerian Orogen.
- a mineral potential indicative map highlighting the areas of interest for multiple types of mineral systems formed between c. 600 Ma and c. 400 Ma in the Delamerian Orogen on mainland Australia.

This study provides new insights into the distribution, timing and characteristics of mineral systems that have the potential to host precious metals, base metals, and critical

mineral resources in the Delamerian Orogen on mainland Australia. In addition to supporting mineral exploration, the findings of this study can further improve the understanding of mineral systems and mineral potential for the under-explored and largely under-cover rocks of the Delamerian Orogen. Outcomes of this study demonstrate the potential to reinvigorate exploration activity and increase economic prosperity for the region, including meeting the growing demand for critical minerals in Australia and globally.

ACKNOWLEDGEMENTS

Geoscience Australia acknowledges the traditional custodians of the country where this work was undertaken. Published with permission of the CEO, Geoscience Australia. The authors thank Marina Costelloe for sponsoring the project, and Urszula Czarnota for her project management efforts. The project team also thank many others at Geoscience Australia as well as from the geological surveys, universities and mining companies of New South Wales, Victoria, South Australia, Australian Capital Territory and Tasmania, who contributed to data acquisition and interpretation. The authors thank Simon Bodorkos and Arianne Ford for their reviews on an earlier version, Chris Evenden for drafting the figures for this abstract.

REFERENCES

- CAYLEY, R., TAYLOR, D., SKLADZIEN, P., CAIRNS, C., DUNCAN, R., HUSTON, D., SCHOFIELD, A., LEWIS, C., 2018. Geodynamic synthesis and implications for the geological evolution of Stavely. In: Schofield, A. (ed.) Regional geology and mineral systems of the Stavely Arc, western Victoria. Record 2018/02, pp. 165–184. Geoscience Australia, Canberra. <https://doi.org/10.11636/Record.2018.002>
- CAYLEY, R.A., TAYLOR, D.H., 2001. Ararat 1:100 000 map area geological report. *Geological Survey of Victoria Report 115*. <http://earthresources.efirst.com.au/product.asp?pid=507&cld=39>
- CHENG, Y., GILMORE, P., LEWIS, C., ROACH, I., DOUBLIER, M., PITT, L., CLARK, A., MOLE, D., HUSTON, D., SCHOFIELD, A., O'ROURKE, A., MEFFRE, S., FEIG, S., DIETZ, C., MAAS, R., GILBERT, S., WILLIAMS, I., WANG, Y., CAIRNS, C., CAYLEY, R., BROTODEWO, A., WISE, T., WADE, C., WERNER, M., HUGHES, K., FOLKES, C., 2024b. Geochronology and geochemistry of legacy drill core samples from key mineral prospects of the Delamerian Orogen, Australia. Geoscience Australia, Canberra. In review.
- CHENG, Y., GILMORE, P., LEWIS, C., ROACH, I., DOUBLIER, M., PITT, L., CLARK, A., SCHRODER, I., TAYLOR, H., BUDD, A., THOMAS, M., WELLS, J., HUSTON, D., SCHOFIELD, A., O'ROURKE, A., MEFFRE, S., FEIG, S., CAIRNS, C., CAYLEY, R., WISE, T., WADE, C., WERNER, M., HUGHES, K., FOLKES, C., 2024a. Metallogenic characteristics of key mineral prospects in the Delamerian Orogen, Australia. Record 2024/01. Geoscience Australia, Canberra. <https://doi.org/10.26186/149025>
- CLARK, A.D., GILMORE, P.J., MOLE, D.R., CHENG, Y., JIANG, W., DOUBLIER, M.P., TAYLOR, H., PITT, L., LEWIS, C., ROACH, I., SANCHEZ, G., THOMAS, M., BUDD, A. 2024. Cambrian convergent margin configuration in the Delamerian Orogen of mainland Australia. Exploring for the Future Extended Abstract. Geoscience Australia, Canberra. In review.
- CLOUTIER, J., FORD, A., HUSTON, D., HAYNES, M., SCHOFIELD, A., DOUBLIER, M., SANCHEZ, G., DUAN, J., GOODWIN, J., RICHARDS, S., BEYER, E., CHAMPION, D., MORFIADAKIS, A., FRASER, G., CHENG, Y., WALTENBERG, K., BURNHAM, A., CZARNOTA, K. 2024. First national mineral system assessment of Australia's iron oxide copper-gold potential. Exploring for the Future Extended Abstract. Geoscience Australia, Canberra. In review.

- DUAN, J., HUSTON, D., 2024. AusLAMP – mapping lithospheric architecture and reducing exploration search space in central and eastern Australia. Exploring for the Future Extended Abstract. Geoscience Australia, Canberra. In review.
- DOUBLIER, M.P., et al. 2024. Crustal architecture along seismic line 22GA-CD2: new insights from the Delamerian-Curnamona-Darling deep seismic reflection survey. Exploring for the Future Extended Abstract. Geoscience Australia, Canberra. In review.
- FODEN, J., ELBURG, M., TURNER, S., CLARK, C., BLADES, M.L., COX, G., COLLINS, A.S., WOLFF, K., GEORGE, C., 2020. Cambro-Ordovician magmatism in the Delamerian orogeny: Implications for tectonic development of the southern Gondwanan margin. *Gondwana Research* 81, 490–521. <https://doi.org/10.1016/j.gr.2019.12.006>
- FODEN, J., ELBURG, M.A., DOUGHERTY-PAGE, J., BURTT, A., 2006. The timing and duration of the Delamerian Orogeny: correlation with the Ross Orogen and implications for Gondwana assembly. *The Journal of Geology* 114(2), 189–210. <https://doi.org/10.1086/499570>
- FORD, A., HUSTON, D., CLOUTIER, J., DOUBLIER, M., SCHOFIELD, A., CHENG, Y., BEYER, E., 2023. A national-scale mineral potential assessment for carbonatite-related rare earth element mineral systems in Australia. *Ore Geology Reviews* 161, 105658. <https://doi.org/10.1016/j.oregeorev.2023.105658>
- FOSS, C., 2020. Magnetic data enhancements and depth estimation. In: Gupta, H. (ed.) *Encyclopedia of Solid Earth Geophysics*. Encyclopedia of Earth Sciences Series. Springer. https://doi.org/10.1007/978-3-030-10475-7_104-1
- GILMORE, P., ROACH, I., DOUBLIER, M., MOLE, D., CHENG, Y., CLARK, A., PITT, L., 2023. The Delamerian Orogen: exposing an undercover arc. Exploring for the Future Extended Abstract. Geoscience Australia, Canberra. <https://doi.org/10.26186/148679>
- GILMORE, P.J., 2010. Mineral Systems. In: Greenfield J.E., Gilmore, P.J., Mills, K.J. (eds.) Explanatory notes for the Koonenberry Belt geological maps. *Geological Survey of New South Wales Bulletin* 35, pp. 401–424. <https://nswdpe.intersearch.com.au/nswdpejspui/handle/1/1372>
- GLEN, R.A., 2005. The Tasmanides of eastern Australia. In: Vaughn, A.P.M., Leat, P.T., Pankhurst, R.J. (eds.) *Terrane Processes at the Margins of Gondwana*. *Geological Society, London, Special Publication* 246, pp. 23–96. <https://doi.org/10.1144/GSL.SP.2005.246.01.02>
- GREENFIELD, J.E., MUSGRAVE, R.J., BRUCE, M.C., GILMORE, P.J., MILLS, K.J., 2011. The Mount Wright Arc: A Cambrian subduction system developed on the continental margin of East Gondwana, Koonenberry Belt. *Gondwana Research* 19, 650–669. <https://doi.org/10.1016/j.gr.2010.11.017>
- HONG, W., FABRIS, A., WISE, T., COLLINS, A.S., GILBERT, S., SELBY, D., CURTIS, S., REID, A.J., 2023. Metallogenic setting and temporal evolution of porphyry Cu-Mo mineralization and alteration in the Delamerian Orogen, South Australia: insights from zircon U-Pb, molybdenite Re-Os, and in situ white mica Rb-Sr geochronology. *Economic Geology* 118(6), 1291–1318. <https://doi.org/10.5382/econgeo.5012>
- HOPE, J., 2023. Mapping the Chronostratigraphy of Australia with EGGs: New Data in the Eastern Resources Corridor. Geoscience Australia, Canberra. <https://pid.geoscience.gov.au/dataset/ga/146304>
- HUSTON, D.L., BASTRAKOV, E., DUNCAN, R., SCHOFIELD, A., CAYLEY, R., CAIRNS, C., 2018. Synthesis of mineral system styles and potential of Stavely. In: Schofield, A. (ed.) *Regional geology and mineral systems of the Stavely Arc, western Victoria*. Record 2018/02. Geoscience Australia, Canberra. <https://doi.org/10.11636/Record.2018.002>

HUSTON, D.L., MERNAGH, T.P., HAGEMANN, S.G., DOUBLIER, M.P., FIORENTINI, M., CHAMPION, D.C., JAQUES, A.L., CZARNOTA, K., CAYLEY, R., SKIRROW, R., BASTRAKOV, E., 2016. Tectono-metallogenic systems — The place of mineral systems within tectonic evolution, with an emphasis on Australian examples. *Ore Geology Reviews* 76, 168–210. <https://doi.org/10.1016/j.oregeorev.2015.09.005>.

KEMP, A.I.S., HAWKESWORTH, C.J., COLLINS, W.J., GRAY, C.M., BLEVIN, P.L. 2009. Isotopic evidence for rapid continental growth in an extensional accretionary orogen: The Tasmanides, eastern Australia. *Earth and Planetary Science Letters* 284, 455–466. <https://doi.org/10.1016/j.epsl.2009.05.011>

KIRKBY, A., CZARNOTA, K., HUSTON, D.L., CHAMPION, D.C., DOUBLIER, M.P., BEDROSIAN, P., DUAN, J., HEINSON, G. 2022. Lithospheric conductors reveal source regions of convergent margin mineral systems. *Scientific Reports* 12, 8190. <https://doi.org/10.1038/s41598-022-11921-2>

LLOYD, J.C., BLADES, M.L., COUNTS, J.W., COLLINS, A.S., AMOS, K.J., WADE, B.P., HALL, J.W., HORE, S., BALL, A.L., SHAHIN, S., DRABSCH, M., 2020. Neoproterozoic geochronology and provenance of the Adelaide Superbasin. *Precambrian Research* 350, 105849. <https://doi.org/10.1016/j.precamres.2020.105849>

MCCUAIG, T.C., HRONSKY, J.M.A., 2014. The mineral system concept: the key to exploration targeting. In: Kelley, K.D., Golden, H.C. (eds.) Building Exploration Capability for the 21st Century. *Society of Economic Geologists, Special Publication* 18. <https://doi.org/10.5382/SP.18.08>

MINTY, B.R.S., POUDJOM DJOMANI, Y., 2019. Total Magnetic Intensity (TMI) Grid of Australia 2019 - seventh edition - 40 m cell size. Geoscience Australia, Canberra. <https://doi.org/10.26186/5dd5fb557fffb>

MOLE, D., BODORKOS, S., GILMORE, P.J., FRASER, G., JAGODZINSKI, E.A., CHENG, Y., CLARK, A.D., DOUBLIER, M., WALTEBERG, K., STERN, R.A., EVANS, N.J., 2023. Architecture, evolution and fertility of the Delamerian Orogen: Insights from zircon. Exploring for the Future Extended Abstract. Geoscience Australia, Canberra. <https://doi.org/10.26186/148981>

PITT, L., ROACH, I., BUDD, A., CLARK, A., TAYLOR, H., LEWIS, C., GILMORE, P.J., SUTTI, M., THOMAS, M., WELLS, J., DOUBLIER, M., CHENG, Y., SCHRODER, I., SCHOFIELD, A., O'ROURKE, A., 2023. Delamerian Margins National Drilling Initiative - Summary of field data acquisition. Record 2023/46. Geoscience Australia, Canberra. <https://doi.org/10.26186/148645>

POWELL, C.M., PREISS, W.V., GATEHOUSE, C.G., KRAPEZ, B., LI, Z.X., 1994. South Australian record of a Rodinian epicontinental basin and its mid-Neoproterozoic breakup (approximately 700 Ma) to form the palaeo-Pacific Ocean. *Tectonophysics* 237, 113–140. [https://doi.org/10.1016/0040-1951\(94\)90250-X](https://doi.org/10.1016/0040-1951(94)90250-X)

RAYMOND, O.L., TOTTERDELL, J.M., WOODS, M.A., STEWART, A.J., 2018. Australian Geological Provinces 2018.01 edition. Geoscience Australia, Canberra. <https://doi.org/10.26186/116823>

SANCHEZ, G., et al., 2024. First continent-wide layered chrono-lithostratigraphic solid geology of Australia. Exploring for the Future Extended Abstract. Geoscience Australia, Canberra. In review.

IMPORTANCE OF CRUSTAL TYPE AND ARCHITECTURE TO EXPLORATION: A NEW LOOK AT THE EASTERN LACHLAN OROGEN

Karen Connors

AngloGold Ashanti

Key Words: Tasmanides, Lachlan Orogen, Macquarie Arc, crustal architecture, nature of the lower crust, tectonic evolution.

INTRODUCTION

Given the role of the lower crust and mantle as source regions for the melts, fluids, and metals involved in formation of various mineral deposits, a well-developed interpretation of the crustal architecture and the timing of juxtaposition of crustal blocks, are key to understanding the prospectivity of any region. In the Macquarie Arc, for example, porphyry style mineralisation formed at several stages during its evolution, with the highly prospective phase 4 porphyries forming *during* the collisional stage (Crawford et al., 2007; Glen et al., 2007). The more we can improve our understanding of this accretion event, the blocks involved, and the resulting crustal architecture, the better we can assess the prospectivity of the late stages of the Macquarie Arc as well as the subsequent mineralisation of the adjacent Silurian basins (VMS, epithermal, carbonate-hosted base metal deposits).

Interpretation of the mid to lower crust beneath the Tasmanides has been strongly influenced by paleogeographic and/or geodynamic models linked to the evolution of the margin and the geological units exposed at surface. Remnant ocean crust is preserved in narrow belts and locally underlies turbidite basins in the southwest Lachlan Orogen. These observations have led to interpretation of widespread preservation of oceanic crust beneath the turbidite basins of the Lachlan and Thomson orogens (Harrington, 1974; Glen, 2013; Glen et al., 2013; Fergusson and Colquhoun, 2018). Despite the growing evidence for continental crust from zircon isotopic studies (e.g. Siégel et al., 2018) and the well accepted recognition of at least two continental blocks, Selwyn / Vandieland in Victoria and Tasmania (Berry et al., 2008; Willman et al., 2010; Cayley, 2011; Cayley et al., 2011), and a smaller fragment beneath the New England Orogen (Powell and O'Reilly, 2007; Shaw et al., 2010; Champion, 2013), widespread oceanic crust remains the favoured interpretation in many Tasmanide models (e.g., Glen, 2013; Fergusson and Colquhoun, 2018).

In the absence of any direct observations, it is important to consider the full range of available data. The datasets investigated here (plate reconstructions, tomography, reflection seismic, isotopic datasets, and outcrop geology), indicate that the lower crust of the Eastern Lachlan Orogen comprises a significant component of continental crust. This crust is interpreted herein to represent fragments rifted from the Gondwanan margin and reaccreted, as suggested for the previously identified continental blocks (e.g., Li et al. 1997; Direen & Crawford 2003; Fergusson et al., 2009; Berry & Bull, 2012). The late Proterozoic to early Palaeozoic ocean basins may have been vast (e.g. Glen, 2013), but it is considered more likely that all that remains today are narrow belts of oceanic crust accreted / obducted onto continental blocks, as documented in the southwest (Willman et al., 2010; Cayley et al., 2011; in prep.).

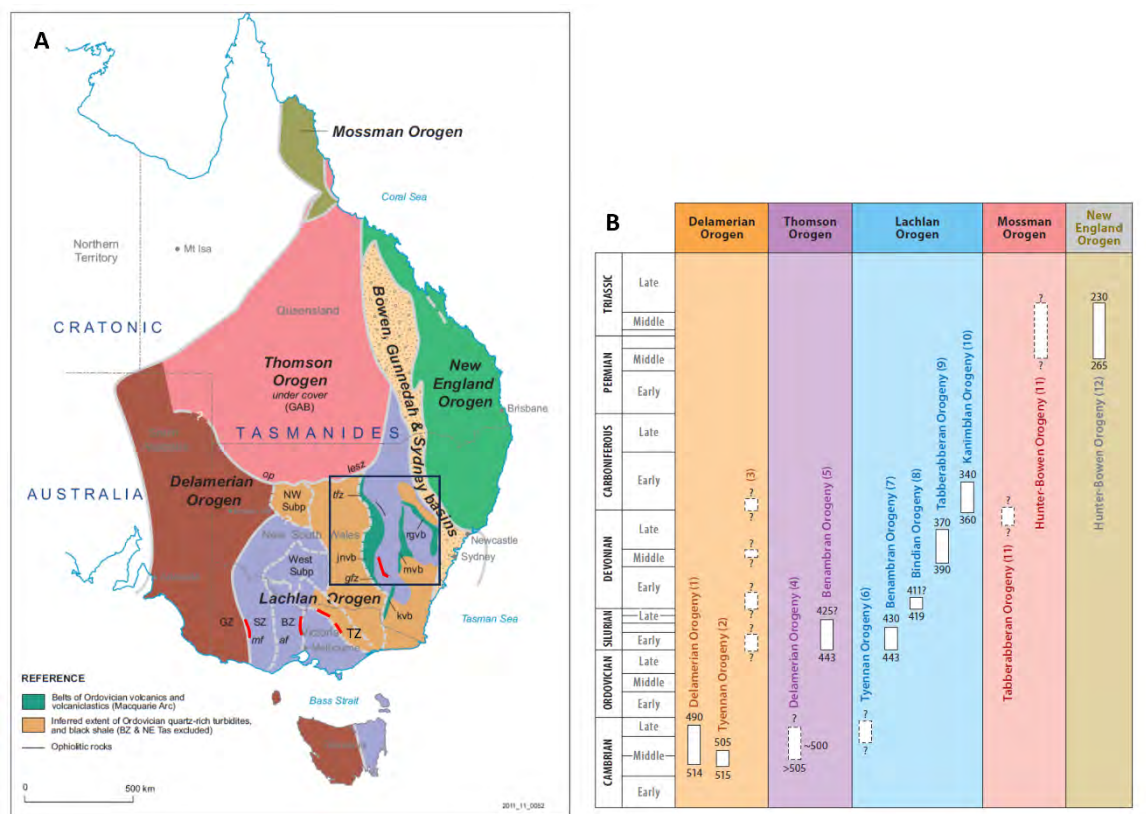


Figure 1A. Map showing the Lachlan, Thomson, Delamerian, New England and Mossman orogens of the Tasmanides (modified after Glen et al., 2012). The Lachlan Orogen is subdivided into zones and subprovinces. The major Ordovician sequences are shown in green (volcanic) and orange (quartz-rich turbidites). The main oceanic belts are highlighted in red (others are too small). The focus of this study is shown by the black box. Abbreviations: BZ = Bendigo Zone; GAB = Great Australian Basin; GZ= Grampians-Stavely Zone, western boundary omitted; SZ = Stawell Zone. Arc belts: jnvb=June-Narromine Volcanic Belt; mvb=Molong Volcanic Belt; rgvb=Rockley-Gulgong Volcanic Belt; kvb=Kiandra Volcanic Belt. Faults: af = Avoca Fault; mf = Moyston Fault; gfz=Gilmore Fault Zone; lesz = Louth- Eumarra Shear Zone; op = Olepoko Fault; TZ = Tabberabberan Zone; tfz=Tullamore Fault Zone. Figure 1B. Summary of orogenic events within the five orogens of the Tasmanides (from Rosenbaum, 2018). The highly prospective phase 4 porphyries Of the Macquarie Arc are broadly coeval with the Benambran Orogeny (Crawford et al., 2007; Glen et al., 2007).

REGIONAL GEOLOGY

The five orogenic belts of the Tasmanides include the Cambrian Delamerian Orogen, the Cambrian to Devonian Lachlan, Thomson and Mossman orogens, and the late Palaeozoic to Mesozoic New England Orogen (Figure 1a). The western limit of the Tasmanides varies between workers but is generally recognised as the rifted margin formed during Neoproterozoic breakup of Rodinia (e.g., Diren and Crawford, 2003). This study focuses on the region around the Macquarie Arc in the Eastern Lachlan Orogen (Figure 1a) but integrates data from throughout the Tasmanides.

The Tasmanides have had a long Palaeozoic and Mesozoic history as an active plate boundary (Figure 1b; Glen, 2013; Rosenbaum, 2018 and references therein). Evolution of this region, however, has been dominated by extensional tectonics (trench retreat), and compressional events have been short lived resulting from periods of trench advance / shallow subduction (e.g., Rosenbaum, 2018).

The thicker than average crust of the Lachlan Orogen implies a large volume of crust is present beneath the turbidite basins and volcanic belts exposed at surface. The Moho is relatively flat on a regional scale ranging from 37–45 km depth (Kennett et al., 2011) in

contrast to the global average of ca. 35 km. Typically, ocean crust is 7–10 km in thickness and has a higher density than continental crust (average 3.0 vs 2.7 g/cc).

DATASETS

The wide-ranging datasets used here provide insights on the nature of the underlying crust and its architecture. In the absence of direct observation of the lower crust, it is important to step out and look at the surrounding regions.

Outcrop geology

Outcrop across the Lachlan Orogen is dominated by upper crustal packages including vast turbidite basins and large volcanic belts (likely island arc) of broadly Ordovician age (Figure 1), which are overlain by Silurian-Devonian basins and intruded by Silurian to Carboniferous granitoids (e.g., Vandenberg et al., 2000; Glen, 2013; Champion, 2016; Rosenbaum, 2018 and references therein). The Ordovician to earliest Silurian volcanic belts of the Macquarie Arc include the Junee-Narromine (JNB), Molong (MB), Rockley (RB) and Kiandra belts (Figure 1a). Patchy outcrop of these volcanics extends for 200–250 km and the JNB and MB belts are interpreted to extend for another 150–200 km undercover based on gravity and magnetic data.

Oceanic crust occurs in several belts throughout the Lachlan Orogen (Figure 1a; Vandenberg et al., 2000; Meffre et al., 2007; Glen, 2013; Champion, 2016; Rosenbaum, 2018 and references therein).

- In the southwest, oceanic units are found along the western margin of the Stawell zone, eastern margin of the Bendigo zone (Heathcote Fault zone), and the western margin of the Tabberabberan zone (Figure 1a).
- Oceanic units in the Central Lachlan Orogen include mafic volcanics within the Girilambone Formation (including those at the Triton mine).
- Oceanic units in the Eastern Lachlan Orogen include the Jindalee belt (between the JNB and MB; Figure 1a) and smaller remnants in fault zones – Snowy Mountains (Coolac belt), Wyangala dam, east of Parkes and around Rockley.

Plate reconstructions and paleogeographic maps – importance of Zealandia

To fully understand the evolution of the Tasmanides, all the major crustal blocks must be included in any plate reconstruction or paleogeographic model. Zealandia represents a largely submerged continent (Figure 2a; Mortimer et al., 2017; Gallais et al., 2019), comprising: 1) the Western Province dominated by quartz-rich greywackes and schists with Cambrian to Ordovician protolith ages and strong 700–500 Ma detrital zircon population similar to the Lachlan Orogen (and distinct from the younger New England Orogen), 2) the 265–105 Ma Median Batholith, and 3) the Eastern Province forearc and accretionary wedge related to the Median Batholith Arc (Figure 2a; Mortimer et al., 2017; 2023). Well before official continent status, large tracts of thinned continental crust were recognised (e.g., Gaina et al., 1998). Regardless, Zealandia terranes are commonly absent in plate reconstructions prior to 100 Ma (e.g., Li et al., 2023; Meredith et al., 2021) or only small fragments are included (e.g., Turnbull et al., 2021). Even Palaeozoic reconstructions focused on the Tasmanides exclude the large continental blocks such as the Lord Howe Rise (Figure 2a and 2c).

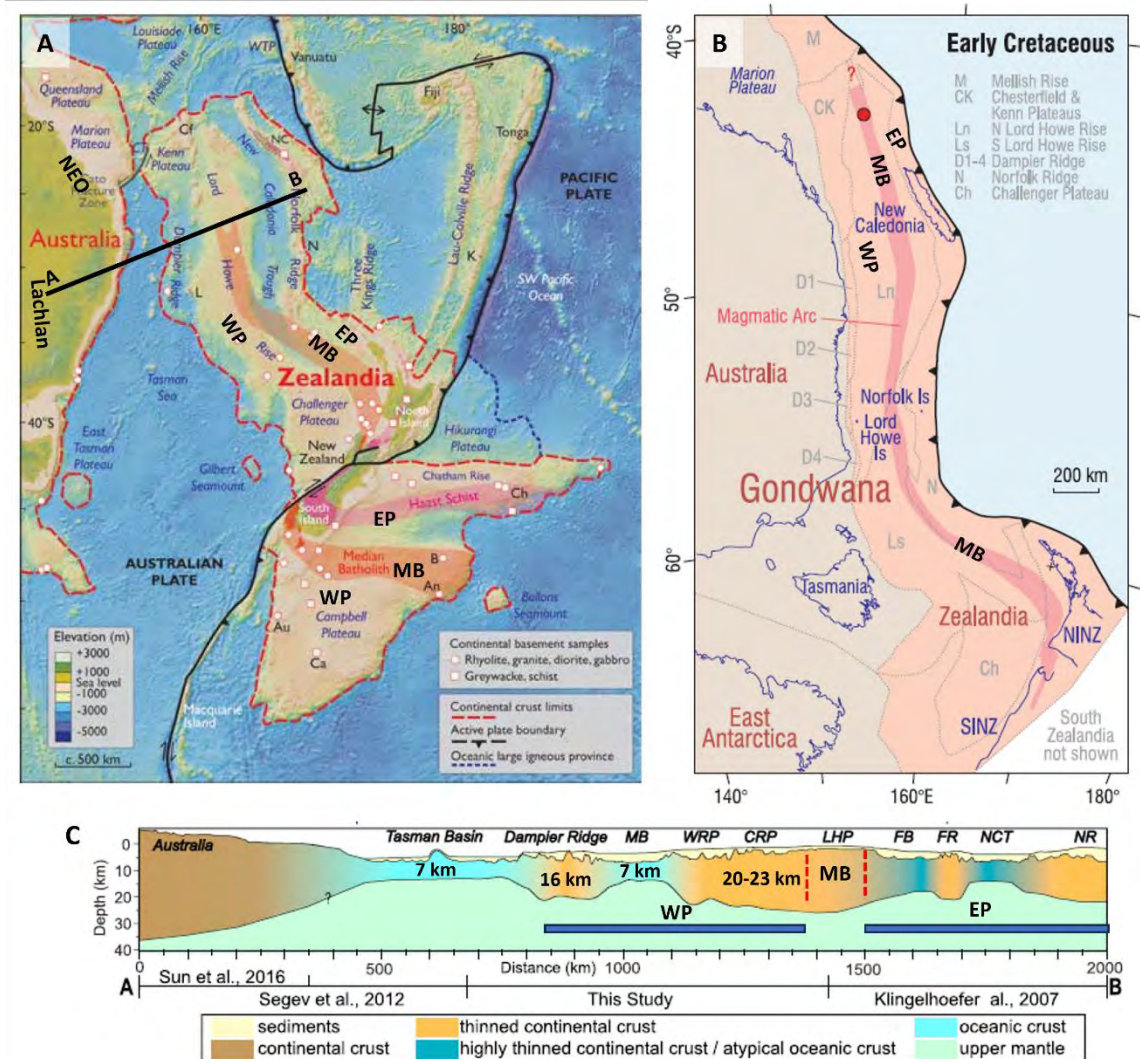


Figure 2. A) Map showing the extent of the continent of Zealandia from Mortimer et al. (2017) and B) an Early Cretaceous reconstruction showing the location of Zealandia on the eastern Gondwanan margin just as the 265 to 105 Ma Median Batholith Arc ceases due to trench roll back (Mortimer et al. (2023). EP = Eastern Province; MB = Median Batholith; WP = Western Province; NEO = New England Orogen. C) Crustal scale cross section across northern Zealandia based on refraction and reflection seismic from Gallais et al. (2019). The continental crust ranges from 16 to 23 km thick and the overlying sedimentary basins are 2-4 km. The approximate location of the Median Batholith is shown based on Mortimer et al. (2017). The ribbons of thinned continental crust of northern Zealandia, separated by ocean basins or transitional crust provide an excellent model for continental fragments rifted from Gondwana during Neoproterozoic Rodinia breakup.

Zealandia formed a continent in the late Cretaceous with the opening of the Tasman Sea (Figure 2a and 2c), however, detailed zircon isotope studies show that Zealandia was likely east of Australia in Rodinian time (Adams and Ramsay, 2022) and that it has a concealed “Rodinia” lithospheric keel (Turnbull et al., 2021). Rifting and late Neoproterozoic breakup of Rodinia resulted in calving of several continental ribbons (e.g., Direen and Crawford, 2003) similar to present day Zealandia (Figure 2c). Given Zealandia’s presence on the Australian margin in both Cretaceous Gondwana (Figure 2b) and Neoproterozoic Rodinia, as well as the similar protoliths and detrital zircon populations, it follows that Zealandia must have been present to the east of Australia as one or more continental ribbons throughout the Palaeozoic evolution of the Tasmanides (Begg et al., 2023).

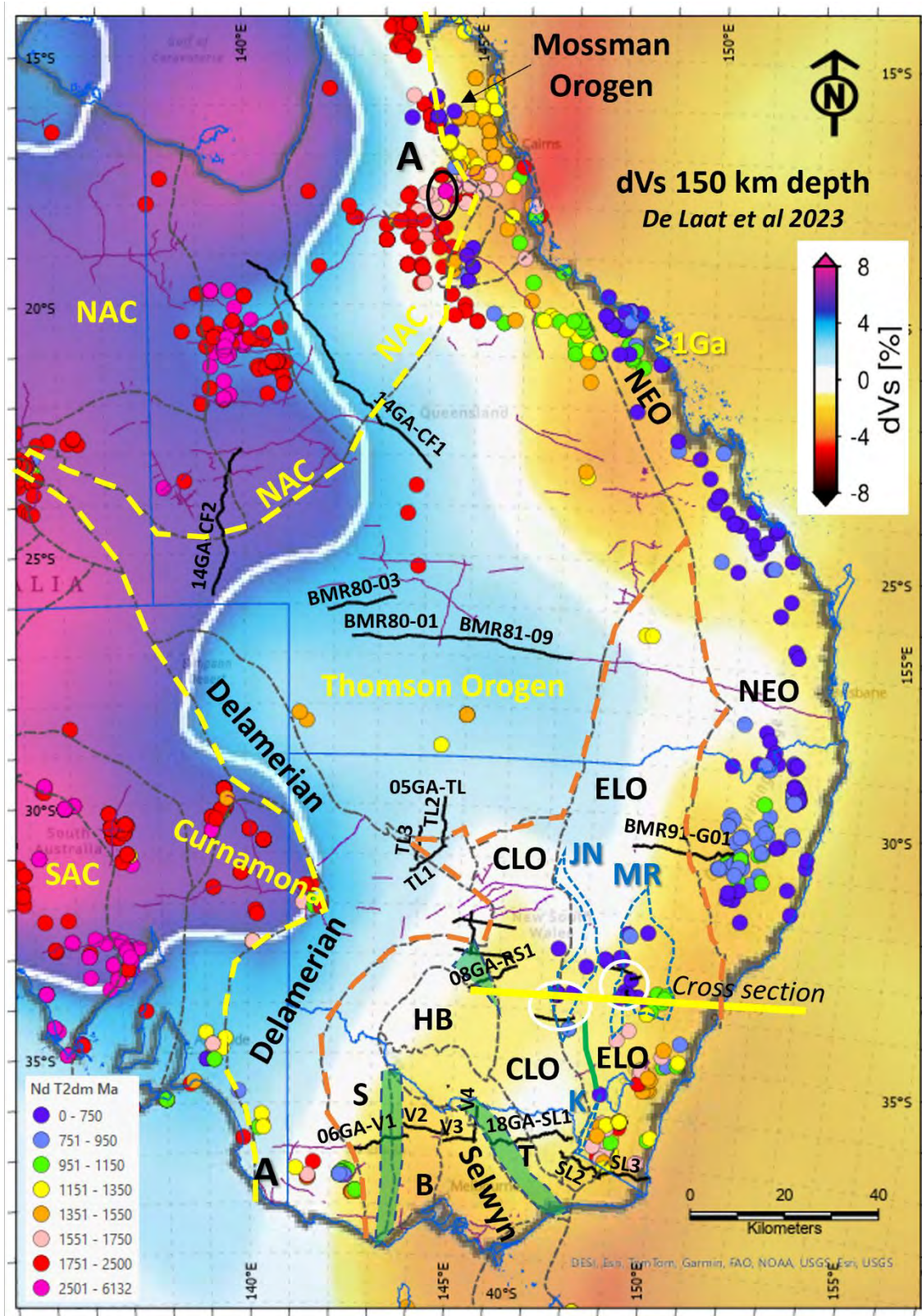


Figure 3. Map of eastern Australia showing the S-wave velocity tomographic model at 150 km depth (modified after De Laat et al., 2023). The image shows dVs, the change in velocity relative to a reference velocity of 4.39 km/s. The Lachlan Orogen (orange dashed outline) lies within the region overprinted by Cenozoic within-plate magmatism along the Eastern Highlands of Australia (e.g., De Laat et al., 2023; Figure 3). De Laat et al. (2023) highlight 3 main subdivisions from thick, cold cratonic lithosphere with a higher velocity (purple) to intermediate lithosphere (pale blue) to hotter lithosphere with a slower velocity (yellow). See text for further discussion. Grey dashed lines show the major tectonic boundaries modified after Geoscience Australia. Yellow dashed line highlights the limit of the Tasmanides. The location of the Junee-Narromine

and Molong-Rockley belts are outlined in blue. Dots show Nd model ages (T_{2dm}) from Champion (2013; including I-type, S-type, and A-type felsic and mafic intrusions). The location of Mt Gambier and the Archean mantle xenolith is indicated by “A” and the location of Archean Nd model ages in the eastern Etheridge Province is circled in black in the north. Seismic lines mentioned in the text are shown in black and are labelled. The location of the 99AGS-EL1-3 and 97AGS-L1-3 seismic surveys are indicated by the white circles. B = Bendigo zone; CLO = Central Lachlan Orogen (Wagga-Omeo zone); ELO = Eastern Lachlan Orogen; HB = Hay-Booligal domain; JN = Junee-Narromine belt; K = Kiandra belt; MR = Molong Rockley belt; NAC = North Australian Craton; NEO = New England Orogen; SAC = South Australian Craton; S = Stawell zone; T = Tabberabberan zone. The location of the crustal scale cross section in Figure 5 is shown by the thick yellow line. The narrow extent of mafic units *at the base of the crust* from the seismic lines is highlighted in green.

Passive seismic - Tomography

Several seismic velocity models have been produced for the Australian crust and lithosphere over several decades (De Laat et al., 2023 and references therein). These models are all consistent in their general definition of a large zone of faster velocity extending to 150 km, and deeper, representing thick, continental lithosphere of the North Australian (NAC), West Australian (WAC) and South Australian (SAC) cratons (e.g., S-wave velocity tomographic model of De Laat et al., 2023; Figure 3). This higher velocity lithosphere transitions eastward to slightly slower, but above average, velocity beneath much of the Tasmanides and then to slower than average velocities along the thinned continental margin and into the oceanic crust of the Tasman Sea (De Laat et al., 2023; Figure 3). These slower velocities indicate hotter lithosphere resulting from younger magmatism, thinning of the continental crust and lithosphere, and the presence of oceanic lithosphere of the Tasman Sea. The extent of the distinct zone of intermediate velocity lithosphere matches many of the interpretations of oceanic crust beneath the late Neoproterozoic to early Palaeozoic sequences of the Tasmanides, especially the Thomson and Lachlan orogens.

Isotopic data and mantle xenoliths

Compilation of Nd model ages by Champion (2013) provides regional insight into the age of the underlying crust. For example, Nd model ages provide additional data regarding the extent of Paleoproterozoic to Archean crust and match well with the faster velocity lithosphere (Figure 3).

Much of the intermediate velocity zone defined by De Laat et al. (2023) has widespread cover and limited outcrop (e.g., Thomson and northern Lachlan), however, this zone extends north and the south into areas with more outcrop and data (Figure 3). In the north, the Etheridge Province forms the eastern margin of the NAC (Jell, 2013) and corresponds well with the zone of intermediate velocity lithosphere (Figure 3). The Mesoproterozoic to late Palaeozoic intrusions of this region are dominated by Paleoproterozoic to late Archean Nd model ages (T_{2dm} 2600–1600 Ma; Champion, 2013). In fact, Archean model ages extend to within 30 km of the eastern boundary of the NAC where it is juxtaposed with the Mossman Orogen which has distinctly younger model ages (T_{2dm} 1700–1000 Ma; Champion, 2013; Figure 3). Similarly in the south, Archean mantle xenoliths at Mt Gambier (Alard et al., 2002) as well as numerous Proterozoic Nd model ages throughout the Delamerian terranes (Champion, 2013) confirm that the zone of intermediate velocity lithosphere comprises Archean to Proterozoic crust (Figure 3).

The Thomson Orogen coincides with the widest zone of intermediate velocity lithosphere (Figure 3). As highlighted by Siégel et al. (2018), a continental substrate with high heat

production is required, as Neoproterozoic oceanic can't account for the well-established, elevated geothermal gradients. Zircon Hf model ages for early Palaeozoic intrusions range from 2150 to 1050 Ma with juvenile input at ca. 1330–1200 Ma (Siégel et al., 2018), and Nd model ages are 1846–1813 Ma in the north and 1484–1329 Ma in the southwest (Champion, 2013). The continental substrate is therefore likely to be Paleoproterozoic to Mesoproterozoic (Siégel et al., 2018).

In the Eastern Lachlan Orogen, whole rock and zircon isotope data for the Ordovician to earliest Silurian Macquarie Arc volcanics show radiogenic ϵNd and ϵHf values (Champion, 2013; Kemp et al., 2020), and there is no evidence for involvement of continental crust in the generation of the Macquarie Arc (Crawford et al., 2007). The widespread and thick Ordovician turbidites through much of the Lachlan Orogen complicate isotopic data for Palaeozoic intrusions, resulting in wide ranging interpretations on the relative contribution of metasedimentary, crustal and mantle components, with some arguing for variations in isotopic and chemical composition of the source region rather than mixing of 2 or 3 components (Champion, 2013). Despite the need for caution, detailed studies can provide some clarity (Champion, 2013). One such study shows that the zircons of 437–420 Ma intrusions, within the easternmost Macquarie Arc, have ϵNd and ϵHf signatures suggesting the presence of lower crust of the Australian margin in their source area, including granites similar to those of the Delamerian Orogen (Zhang et al., 2020). The 1800–1100 Ma Nd model ages for I-type intrusions of the Eastern Lachlan, southeast of the Macquarie Arc (Champion, 2013), are consistent with the interpretation of Zhang et al. (2020) but more detailed work is required to assess the amount of inheritance.

In addition, two independent parameters of Pb-Pb isotopes show two distinct Pb sources beneath the Tasmanides: 1) Pacific plate and 2) Australian Plate (Huston et al., 2017; Huston and Champion, 2023). Within the Lachlan Orogen, the Pacific plate is recognised from the Macquarie Arc, whereas Pb-Pb isotopes to the east and west were sourced from the Australian Plate, with the crust lying beneath the Central Lachlan Orogen showing a more evolved signature than that of the Eastern Lachlan (southeast of Macquarie Arc; Huston et al., 2017; Huston and Champion, 2023).

Reflection seismic

Crustal architecture of accreted oceanic crust and island arcs

Reflection seismic (2006) and AusLAMP data show the geometry and extent of oceanic belts of the western Lachlan (Willman et al., 2010 and Cayley et al., 2011; Kirkby et al., 2020). The seismic data shows thrust-stacking of the turbidites and mafic units onto the Delamerian margin (Stawell zone), and onto the Selwyn block in the east (Bendigo zone; Willman et al., 2010; Figure 4a). The AusLAMP data shows a distinct change in resistivity from the Bendigo zone to the Selwyn block that matches well with the crustal scale boundary in seismic (Kirkby et al., 2020). The imbricated oceanic crust is preserved in a bivergent belt overlying continental crust to the west and east (Willman et al., 2010; Cayley et al., 2011), resulting in a narrow “footprint” at the base of the crust (Figure 3, 4a).

Despite the lower data quality / resolution of seismic across the Macquarie Arc, the dominant west-dipping reflections of the mid to lower crust are well imaged (Glen et al., 2002; Figure 4b), and this geometry is supported by gravity modelling and refraction data (Finlayson et al., 2002; Direen et al., 2001). The outcropping / subcropping JNB volcanic belt correlates with a ~30 km thick, ~60–80 km wide body interpreted as a relict island arc (Glen et al., 2002; Crawford et al., 2007). The accreted arc lies within a crustal scale thrust stack overlain by Ordovician turbidites to the west (Central Lachlan; Glen et al., 2002; Figure 4b). The underlying block to the east was originally interpreted to include oceanic crust (Glen et al., 2002) but preservation of deformed “layer” of oceanic crust is unlikely as shown by the intricately thrust mafic volcanics (and turbidites) at Stawell and Bendigo (e.g., Willman et al., 2010). Reflection seismic across the Molong Belt ~70 km to the northeast shows a similar geometry, although the island arc crust comprises a smaller volume (Glen et al., 2002; Direen et al., 2001). Refraction seismic in the Molong Belt indicates a velocity of 6.75 to 7 km/s for the lower crust (below the arc) consistent with a density of 2.8-2.85 g/cc (Finlayson et al., 2002).

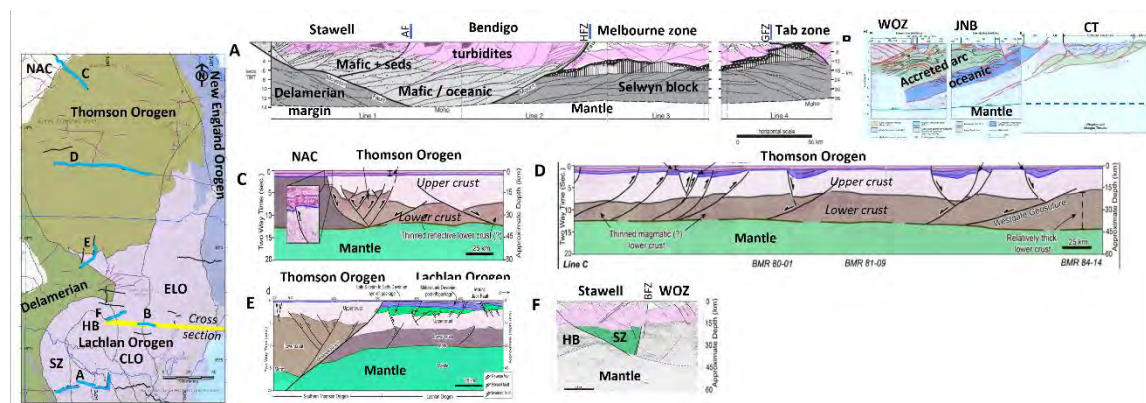


Figure 4. Interpretations of reflection seismic lines from throughout the Lachlan and Thomson orogens. These examples show the contrast between the thrusting / stacking of well-documented oceanic and island arc crust (A, B, F) in comparison to the widespread “two-layered” crust of the Thomson and northern Lachlan (C, D, E). A) Seismic lines 06GA-V1 to V4 showing interpretation by Willman et al. (2010). Quartz-rich turbidites are highlighted in pink. AF = Avoca Fault; GFZ = Governor Fault Zone; HFZ = Heathcote Fault Zone. B) Seismic lines 99AGS-L1 and L2 and a cross section through the Cowra Trough from Glen et al. (2002). C) Interpretation of part of seismic line 14GA-CF1 from the boundary of the NAC and Thomson Orogen (from Abdullah and Rosenbaum, 2018). D) Interpretation of composite seismic line in the central Thomson Orogen (from Abdullah and Rosenbaum, 2018). E) Seismic lines 05GA-TL1-2 showing the crustal architecture of the northern Lachlan Orogen and the thickened crust of the southern Thomson Orogen (from Abdullah and Rosenbaum, 2018). F) Simplified interpretation of 08GA-RS1 highlighting the two-layer crust and major structures. Inset map shows the location of the 6 seismic lines. See also Figure 3 for location of these and other seismic lines referred to in the text. BFZ – Bootheragandra fault zone; CLO = Central Lachlan Orogen; CT = Cowra Trough; ELO = Eastern Lachlan Orogen; HB = Hay-Boooligal block; JNB = Junee-Narromine Belt; NAC = North Australia Craton; SZ = Stawell zone; WOZ – Wagga Omeo zone of Central Lachlan.

Crustal architecture northern LO and TO

Several reflection seismic lines provide insights on the crustal architecture along the northern (14GA-CF1-2) and southern borders of the Thomson (05GA-TL01-03), through its centre (BMR80-01 and 03) and in the Central Lachlan (08GA-RS1, RS2; 13GA-TY1 and 2; Figure 3 and 4). These seismic lines all show a distinct two-layer crust, below the Devonian to Mesozoic basins (~4–9 km; Murray, 1990; Spampinato et al., 2015; Abdullah and Rosenbaum, 2018). The 14GA-CF1 (Figure 4c) and CF2 seismic lines show the northern faulted boundary of the Thomson Orogen with the NAC and the two-layer crust cut by normal faults (Abdullah and Rosenbaum, 2018; Connors et al., 2021).

The Thomson crustal architecture is remarkably similar in the central area (e.g., BMR80-03, BMR80-01, BMR80-09; Figure 4d) as well as the south (05GA-TL01-03; Figure 4e; Glen et al., 2013; Abdullah and Rosenbaum, 2018; Spampinato et al., 2015). The Thomson lower crust is 12–24 km thick (4–8 sec TWT; thickening to ~13 sec TWT at the southern boundary; Figure 4e) and comprises strong, high-amplitude reflections whereas the upper crust varies from packages of weak reflections to largely transparent (e.g., Abdullah and Rosenbaum, 2018). Gravity modelling suggests the average density of the upper and lower crust are ~2.80 and 2.90 g/cc, respectively, indicating additional mafic material in the lower crust (Spampinato et al., 2015). The entire crust is cut by listric faults that vary from high angle to moderate dips, some of which have been reactivated during Palaeozoic extension and later shortening (e.g., Abdullah and Rosenbaum, 2018).

The seismic of the northern Central Lachlan shows a remarkably similar crustal architecture to that of the central Thomson. Line 05GA-TL1 shows a distinct two-layer crust very similar to the Thomson seismic (Figure 4e; Glen et al., 2013; Abdullah and Rosenbaum, 2018). Three hundred kilometres further south in the Cobar Basin, 08GA-RS1 (Figure 4f) shows the same distinct two-layered crust (see also seismic lines 08GA-RS2 and 13GA-TY1-TY2 to the north, Figure 4 inset). The crust in this region has been more strongly faulted and varies more rapidly in thickness due to Palaeozoic extension in the region (Figure 4f). Seismic line 08GA-RS1 crosses two domain boundaries which are well defined with the lower crust. The central Stawell zone has an east-dipping boundary with the Selwyn-Hay Booligal continental block to the west and a steep fault (Bootheragandra fault zone; Figure 4f) to the east coinciding with a change in seismic velocity at 25 km depth, indicating a crustal scale structure (Pilia et al., 2015).

The upper crustal layer of the Thomson Orogen (below the basins) comprises a thick metasedimentary package (9–15 km; Figure 4) deposited during Neoproterozoic rifting and breakup, and subsequent Ordovician to Silurian rifting events (e.g., Jell, 2013; Spampinato et al., 2015; Abdullah and Rosenbaum, 2018; Purdy et al., 2018). In the northern Lachlan Orogen, the upper crustal layer is dominated by Ordovician turbidites (Glen, et al., 2013; Abdullah and Rosenbaum, 2018) ranging to Cambrian age in the Stawell zone (Vanderberg et al., 2000).

DISCUSSION

Nature and origin of the lower crust

Given that any oceanic crust that formed beneath the Thomson Orogen during Rodinia breakup would have been late Neoproterozoic in age, it is highly unlikely to have survived intact. Any ocean crust of this age will have been subducted, with only narrow ophiolite belts remaining. Globally, the oldest “intact” oceanic crust preserved today is Lower Jurassic (e.g., Central Atlantic), and crust of similar age is subducting in the west Pacific (Seton et al., 2020). Although a small fragment of oceanic crust in the eastern Mediterranean is interpreted as 340 Ma (Granot, 2016), Palaeozoic and older oceanic crust is found only as fragmented and accreted ophiolites in orogenic belts around the world.

The widespread extent of highly reflective lower crust in the Thomson and northern Lachlan is instead more consistent with highly thinned continental crust (12–24 km), as

indicated by the zircon isotope data and elevated geotherm (Siégel et al., 2018). This extensive lower crust likely represents a thinned block of the NAC (40–45 km; Spampinato et al., 2015; Connors et al., 2021). The widespread normal faults provide further support for an extensional history (Abdullah and Rosenbaum, 2018). The high amplitude seismic reflections likely result from a combination of low angle shear zones and intrusion of mafic bodies during extension, consistent with an average 2.9 g/cc density. It is unclear whether the thinned continental crust of the northern Central Lachlan represents a fragment with a similar origin to that of the Thomson Orogen (e.g., NAC) or a different continental block such as the Curnamona craton or surrounding Proterozoic orogenic belts. Regardless the Lachlan and Thomson orogens have had a different evolution during the Palaeozoic (e.g., distinct Hf signatures for Ordovician igneous units; Siégel et al., 2018).

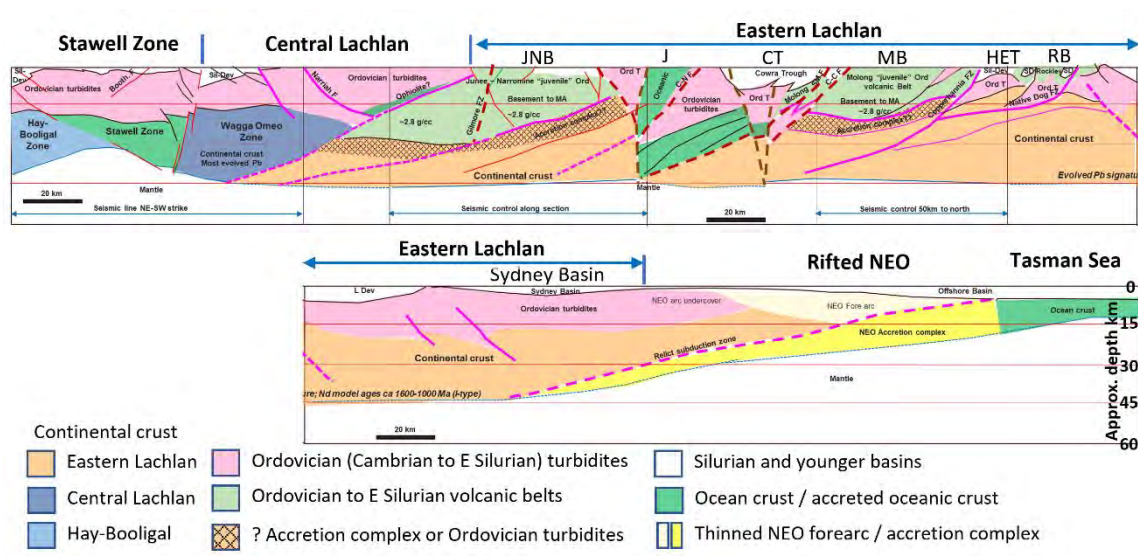


Figure 5. Crustal scale cross section extending ~750 km from the Central Lachlan through the Eastern Lachlan and to the Tasman Sea Basin. See Figure 3 for location. The segments that are more closely constrained by nearby seismic lines are indicated. The thickness of the Silurian and younger basins in the western half are based on seismic, but those to the east are poorly constrained. The Sydney Basin is estimated as 2-4 km deep (Geognostics, 2021). The highly thinned crust of the passive margin includes parts of the New England Orogen (NEO). The forearc and relict accretion complex are shown schematically, and are based potential field data, crustal thickness, and seismic to the north (BMR91-G01; Guo et al., 2007). Refer to the text for a discussion of key features. CT = Cowra Trough; HET = Hill End Trough; J = Jindalee belt oceanic units; JN = Junee-Narramine belt; MB = Molong belt; NAC = North Australian Craton; NEO = New England Orogen; RB = Rockley belt. Silurian and younger basins are blank, and the widespread intrusions are omitted for simplicity.

Crustal architecture – Regional cross section

In order to investigate the regional architecture and nature of the crust, and relationships between different belts, all the information has been integrated into a regional cross section extending ~750 km from the Central Lachlan through the Eastern Lachlan and to the Tasman Basin (Figure 5). The information summarised above highlights two key points. First, any preserved oceanic crust is likely to occur within a narrow ophiolite belt accreted to a crustal block (e.g., Stawell and Bendigo zones; Willman et al., 2010). Second, there is support for widespread presence of continental crust throughout the Thomson and Lachlan orogens from the integrated interpretation of reflection seismic, tomography and isotopic data. In addition, the involvement of Zealandia since the Neoproterozoic (or earlier) points to a significant volume of continental lithosphere along

the Australian margin that has been largely ignored in studies focused on the Lachlan Orogen and the Australian Tasmanides.

The regional cross section roughly coincides with seismic lines 99AGS-L2 and L1 (Figure 3 and 4 inset). Other seismic lines used to constrain the cross section include: 08GA-RS1 (southern Cobar Basin; 5–60 km north), 97AGS-EL3 and EL2 (Molong Belt; 40–70 km north), and BMR91-G01 (Sydney Basin; 300 km north). The seismic lines that are more distant were used to constrain the general architecture of the crust. The base of crust is based on reflection seismic data and the 2017 AusMoho model (Kennett et al., 2011).

Macquarie Arc

The limits and geometry of the JNB and MB-RB (Figure 5) are constrained by the 1997 and 1999 seismic (Figure 4). The interpretation depicted here is broadly similar to Glen et al. (2002) and Direen et al. (2001), the main difference being interpretation of the Jindalee oceanic units as a narrow “accreted” ophiolite rather than a 10 km layer of deformed oceanic crust extending from surface to lower crust. The Molong belt appears to have a more limited depth extent (Figure 5; Glen et al., 2002; Finlayson et al., 2002).

Unfortunately, the seismic does not extend across the Cowra Trough (Figure 4b). Given the dominance of S-type Silurian granites and volcanics within the Cowra Trough, a reasonably thick package of Ordovician turbidites is required and may extend east beneath part of the Molong Belt given the interpreted west dipping, listric faults along its western margin (e.g., Meakin and Morgan, 1999; Pogson and Watkins, 1998). The structures within the Hill End trough, ~80 km to the north, are dominated by low angle, listric thrust faults (Meakin and Morgan, 1999). The deep-seated structures controlling the Cowra Trough depocenter are unknown but could range from low angle listric structures (Figure 4b) to steep, strike slip faults as tentatively depicted in Figure 5.

Isotopic, geochemical and lithological data for the Macquarie volcanic belt favour its formation as an intra oceanic island arc with no influence from continental crust or detritus until the final stages (Crawford et al., 2007; Kemp et al., 2020) thus requiring a wide ocean basin during the Ordovician. Arc magmatism ended in the early Silurian when the Macquarie Arc was accreted to adjacent crustal blocks (e.g., Glen et al., 2007). The lower crust beneath the Macquarie Arc and turbidites comprises several west dipping crustal slices. The detailed work of Zhang et al. (2020) favour continental crust similar to the Australian margin beneath the eastern Molong and Rockley belts. In addition, the velocity of lower crust below Molong Belt is consistent with a density of 2.8 to 2.85 g/cc (Finlayson et al., 2002) similar to detailed gravity modelling to the south where the mid to lower crust of the Eastern Lachlan has an average density of 2.79 g/cc (lines 18GA-SL1-3; Skladzien et al., 2023). This density is typical of lower crustal values and matches that of the Selwyn block (Skladzien et al., 2023). Zones of higher density, to 2.84 g/cc, indicate some component of more mafic crust is present, but this value is distinctly lower than the 2.95 g/cc density of the lower crust of the Tabberabberan zone (Skladzien et al., 2023) which is recognised to comprise accreted oceanic crust (Vandenberg et al., 2000; Willman et al., 2002; Cayley et al., in prep).

Whilst thrusting of an island arc over continental crust is not the most likely geometry expected, there are scenarios in which this occurs. Options consistent with the known geology include: 1) negative buoyancy of the leading margin of continental crust resulting from hyperextension and mantle exhumation; or 2) negative buoyancy resulting from accretion of oceanic crust to the leading continental edge prior to island arc accretion.

East of Macquarie Arc

The crust of the Eastern Lachlan Orogen, to the east of the Macquarie Arc is ~40–45 km thick (AusMoho 2017) and thins to the east forming the rifted passive margin of eastern Australia (Figure 5). Seismic line BMR91-G01 and gravity modelling 300 km to the north (Guo et al., 2007) were used to constrain the general geometry of the easternmost Lachlan and New England orogens. NEO is interpreted to continue south to this region (Figure 5) and further south from offshore dredge samples (Packham and Hubble, 2016). The upper crust comprises Devonian and younger basins overlying Ordovician turbidites estimated here to average 15 km thickness based on the seismic elsewhere in the Lachlan (Figure 4; Abdullah and Rosenbaum, 2018). The crust underlying the turbidites is therefore estimated as 30 km thick beneath the Rockley Belt and to the east, *comprising two-thirds* of the total crustal thickness (and volume) east of the Molong Belt (Figure 5). The isotopic datasets summarised above favour the presence of continental crust in this region (Figure 3) consistent with the significant volume of crust (Figure 5).

West of Macquarie Arc

The quartz-rich turbidites of the Central Lachlan are thrust east over the JNB along a suture with a dip of ~20–30° (Figure 4b and 5; Glen et al., 2002). This fault is interpreted here to extend to the base of the crust like the boundary imaged on seismic lines 18GA-SL1-2 to the south (Cayley et al., in prep.). The turbidites extend to ~5 sec TWT / 15 km depth (99AGS-L2) but are likely to extend a bit deeper above the suture zone (Figure 5). Isotopic datasets show that the crust of the main segment of the Central Lachlan has a more evolved continental signature and is distinct from that of the eastern Central Lachlan (featuring Girilambone Group turbidites) which show a strong mantle influence interpreted to arise from the underlying Macquarie Arc (Huston et al., 2017; Waltenberg et al., 2018; Huston and Champion, 2023).

The Stawell zone wraps around the Selwyn-Hay Booligal block to intersect the regional cross section (Figure 5) and seismic lines of the southern Cobar Basin (Figure 3). A simplified interpretation of seismic line 08GA-RS1 (Figure 4f) highlights the major structures and crustal domains. The lower crust of the Stawell zone comprises a narrow belt of oceanic crust accreted onto the Selwyn-Hay Booligal continental block to the west similar to the Delamerian margin in western Victoria (Figure 4a; e.g., Willman et al., 2010; Cayley et al., 2011). The well-defined Moho indicates thinner crust around this suture zone likely resulting from Silurian-Devonian extension (Darling and Cobar basins). The steep Bootheragandra fault zone forming the eastern boundary of the Stawell zone is interpreted to correlate with the Kancoona - Keiwa – Barmouth fault system to the south which forms the eastern boundary to the Tabberabberan zone (Willman et al., 2002; Cayley et al., in prep).

The geometry of the Stawell zone depicted by seismic line 08GA-RS1 (Figure 4f and 5) is remarkably similar to that of the Tabberabberan on seismic line 18GA-SL1-2, 350 km to the south (Cayley et al., in prep). Plan view interpretations of geological domains / zones from gravity and magnetic data, show truncation of the Tabberabberan and Stawell zones (Figure 1 and 3), however, interpretation of deeper features in these datasets is obscured by younger intrusions. In contrast, the consistent geometry in seismic data suggest that a combined Stawell-Tabberabberan terrane may be better preserved between the Selwyn-Hay Booligal and Central Lachlan (Wagga-Omeo Zone) blocks than currently interpreted.

SUMMARY AND CONCLUSIONS

The work presented here is based largely on published data and interpretations, and it highlights the new (and rediscovered) ideas and interpretations that arise from integration of wide-ranging datasets. In this case, the focus has been on developing a model of the nature of the crust, the crustal architecture and its evolution, with the overall aim of supporting target generation and exploration.

This study highlights several lines of evidence pointing to the widespread presence of continental crust beneath the Lachlan Orogen. These crustal blocks originated on the east Gondwanan (Australian) margin, were calved off during late Neoproterozoic Rodinia breakup and reaccreted during various Palaeozoic events up to the ca. 250 Ma Hunter Bowen Orogeny. The ribbons of thinned continental crust of northern Zealandia, separated by ocean basins or transitional crust (Figure 2c) provide an excellent analogue for thinned continental fragments rifted from Gondwana during Neoproterozoic Rodinia breakup.

Our understanding of the evolution of the Macquarie Arc indicates that it formed within a wide ocean basin with no influence of continental crust (Crawford et al., 2007) and that the arc was accreted to adjacent blocks during the late Ordovician to early Silurian (Benambran Orogeny; Glen et al., 2007). The results of this study suggest that this accretion event involved thinned, continental ribbons to both the east and west of the arc, and that subsequent shortening eventually led to crustal scale stacking of the island arc segments and continental crust (Figure 5). Remnants of the Palaeozoic (or older) ocean basins are found as ophiolite slivers along major fault zones (e.g., Jindalee Group).

The presence of several continental blocks, all of which lay along the east Gondwanan margin in Rodinia time, provides a broadly similar source for the Ordovician quartz-rich turbidites (e.g., Adaminaby Group) across the orogen and removes the need for complex sediment pathways through a large ocean basin. Although some of the quartz-rich turbidites were deposited on ocean crust (e.g., Stawell and Bendigo zones, and Girilambone Group), other turbidite basins may have been deposited over thinned continental crust, or along the passive margins of the continental ribbons.

Most of the focus during exploration is typically at the camp to district scale. Although some explorers step out to a province or terrane scale, this work less commonly includes interpretation of the *3D crustal scale* architecture, which is required to better understand the project area. Development of cross sections (and long sections) are a key tool for understanding the geology and architecture at the terrane/province scale as well as

camp and deposit scale. This work will not only provide key insights into the exploration project, but it will also bring to light many of the unanswered questions.

REFERENCES

- ABDULLAH, R., & ROSENBAUM, G. 2018. Devonian crustal stretching in the northern Tasmanides (Australia) and implications for oroclinal bending. *Journal of Geophysical Research: Solid Earth*, 123, 7108–7125. <https://doi.org/10.1029/2018JB015724>
- ADAMS, C.J. & RAMSAY, W.R.H. 2022. Archean and Paleoproterozoic zircons in Palaeozoic sandstones in southern New Zealand: evidence for remnant Nuna supercontinent and Ur continent rocks within Zealandia. *Australian Journal of Earth Sciences*, 69:8, 1061-1081, DOI: 10.1080/08120099.2022.2091039
- ALARD, O., GRIFFIN, W.L., PEARSON, N.J., LORAND, J.P., O'REILLY, S.Y. 2002. New insights into the Re-Os systematics of sub-continental lithospheric mantle from in situ analysis of sulphides. *Earth and Planetary Science Letters* 203, 651-663.
- BEGG, G., ADAMS, C., GREAU, Y., GRIFFIN, W.L., O'REILLY, S.Y., & KORSCH, R. 2023. An Eastern Gondwanan ca 650-500 Ma magmatic arc built on Archean lithosphere hidden beneath Zealandia. *Australian Earth Sciences Conference*, Perth, June 2023.
- BERRY R. F., STEELE D. A. & MEFFRE S. 2008. Proterozoic metamorphism in Tasmania: implications for tectonic reconstructions. *Precambrian Research* 166, 387–396.
- BERRY, R.F. & BULL, S.W., 2012. The pre-Carboniferous geology of Tasmania. *Episodes* 35, 195–204.
- CAYLEY RA. 2011. Exotic crustal block accretion to the eastern Gondwanaland margin in the Late Cambrian–Tasmania, the Selwyn Block, and implications for the Cambrian–Silurian evolution of the Ross, Delamerian, and Lachlan orogens. *Gondwana Research* 19, 628–49.
- CAYLEY R. A., KORSCH R. J., MOORE D. H., COSTELLOE R. D., NAKAMURA A., WILLMAN C. E., RAWLING T. J., MORAND V. J., SKLADZIEN P. B. & O'SHEA P. J. 2011. Crustal architecture of central Victoria, results from the 2006 deep crustal reflection seismic survey. *Australian Journal of Earth Sciences* 58, 123–156.
- CAYLEY, R.A., SKLADZIEN, P.B., CAIRNS, C.P., HAYDON, S., MCLEAN, M.A., TAYLOR, D.H., FOMIN, T., COSTELLOE, R.D., KIRKBY, A., J. Duan, DOUBLIER, M.P., MUSGRAVE, R.J., STOLZ, N., SPAMPINATO, G., GILMORE, P., GREENFIELD, J., CARLTON, A.A., & RAWLING, T.J. in prep. Geological interpretation of deep 2D seismic reflection survey lines 18GA-SL1, 18GA-SL2 and 18GA-SL3 undertaken as part of the Southeast Lachlan Crustal Transect. Geological Survey of Victoria Technical Record.
- CHAMPION, D.C. 2013. Neodymium depleted mantle model age map of Australia: explanatory notes and user guide. Record 2013/044. Geoscience Australia, Canberra. <http://dx.doi.org/10.11636/Record.2013.044>.
- CHAMPION, D. C. 2016. Geodynamic Synthesis of the Phanerozoic of eastern Australia. Second Edition. Record 2016/07. Geoscience Australia, Canberra. <http://dx.doi.org/10.11636/Record.2016.007>
- CONNORS, K., SIMPSON, J. & BROWN, D. 2021: Mount Isa Province Seismic Interpretation. Queensland Minerals and Energy Review 27. Queensland Minerals and Energy Review Series, University of Queensland & Department of Resources. <https://geoscience.data.qld.gov.au/report/cr124986>

CRAWFORD A. J. & BERRY R. F. 1992. Tectonic implications of Late Proterozoic–early Palaeozoic igneous rock associations in western Tasmania. *Tectonophysics* 214, 37–56.

CRAWFORD, A. J., MEFFRE, S., SQUIRE, R. J., BARRON, L. M., & FALLOON, T. J. 2007. Middle and Late Ordovician magmatic evolution of the Macquarie Arc, Lachlan Orogen, New South Wales. *Australian Journal of Earth Sciences*, 54, 181–214.

DIREEN N. G., LYONS P., KORSCH R. J. & GLEN R. A. 2001. Integrated geophysical appraisal of crustal architecture in the eastern Lachlan Orogen. *Exploration Geophysics* 32, 252 – 262.

DIREEN N. G. & CRAWFORD A. J. 2003a. The Tasman Line. Where is it, what is it, and is it Australia's Rodinian breakup boundary? *Australian Journal of Earth Sciences* 50, 491–502.

FERGUSON C. L., OFFLER R. & GREEN T. J. 2009. Late Neoproterozoic passive margin of East Gondwana: Geochemical constraints from the Anakie Inlier, central Queensland, Australia. *Precambrian Research* 168, 301–312.

FERGUSON C. L. & COLQUHOUN G.P. 2018. Ordovician Macquarie Arc and turbidite fan relationships, Lachlan Orogen, southeastern Australia: stratigraphic and tectonic problems. *Australian Journal of Earth Sciences* 65:3, 303-333, DOI: 10.1080/08120099.2018.1425909

FINLAYSON, D., LEVEN, J., WAKE-DYSTER, K., & JOHNSTONE, D. 1990. A crustal image under the basins of southern Queensland along the Eromanga–Brisbane Geoscience Transect, The Eromanga–Brisbane Geoscience Transect: A guide to basin development across Phanerozoic Australia in southern Queensland. *Bureau of Mineral Resources Bulletin*, 232, 153–175.

FINLAYSON D. M., KORSCH R. J., GLEN R. A., LEVEN J. H. & JOHNSTONE D. W. 2002. Seismic imaging and crustal architecture across the Lachlan Transverse Zone, a cross-cutting feature of eastern Australia. *Australian Journal of Earth Sciences* 49, 311–321.

GAINA, C., MULLER, D.R., ROYER, J-Y., STOCK, J., HARDEBECK, J., & SYMONDS, P. 1998. The tectonic history of the Tasman Sea: A puzzle with 13 pieces *JOURNAL OF Geophysical Research*, 103, 12,413-12,433.

GALLAIS, F., FUJIE, G., BOSTON, B., HACKNEY, R., KODAIRA, S., MIURA, S., et al. 2019. Crustal structure across the Lord Howe Rise, northern Zealandia, and rifting of the eastern Gondwana margin. *Journal of Geophysical Research: Solid Earth*, 124, 3036–3056. <https://doi.org/10.1029/2018JB016798>

GLEN R. A., KORSCH R. J., DIREEN N. G., JONES L. E. A., JOHNSTONE D.W., LAWRIE J. C., FINLAYSON D. M. & SHAW R. D. 2002. Crustal structure of the Ordovician Macquarie Arc, Eastern Lachlan Orogen, based on seismic-reflection profiling. *Australian Journal of Earth Sciences* 49, 323 – 348.

GLEN R. A. 2005. The Tasmanides of eastern Australia. *In: Vaughan A. P. M., Leat P. T. & Pankhurst R. J. eds., Terrane Processes at the Margins of Gondwana. Special Publication of the Geological Society London* 246, 23–96.

GLEN R. A. 2013. Refining accretionary orogen models for the Tasmanides of eastern Australia: *Australian Journal of Earth Sciences* 60, 315–370.

GLEN, R.A., QUINN, C.D., & COOKE, D.R. 2012. The Macquarie Arc, Lachlan Orogen, New South Wales: its evolution, tectonic setting and mineral deposits. *Episodes* 35-1.

GLEN R. A., MEFFRE S. & SCOTT R. J. 2007b. Benambran Orogeny in the Eastern Lachlan Orogen, Australia. *Australian Journal of Earth Sciences* 54, 385 – 415.

- GLEN R. A., KORSCH R. J., HEGARTY R., SAEED A., POUDJOM DJOMANI Y., COSTELLO R. D. & GRIFFIN W. L. 2013. Geodynamic significance of the boundary between the Thomson Orogen and the Lachlan Orogen, northwestern New South Wales: implications for Tasmanide tectonics. *Australian Journal of Earth Sciences* 60, 371–412.
- GEOGNOSTICS. 2021. OZ SEEBASE® 2021 (March 2021). Geognostics Australia Pty Ltd, <https://www.geognostics.com/oz-seebase-2021>
- Granot, R. 2016. Palaeozoic oceanic crust preserved beneath the eastern Mediterranean. *Nature Geoscience*, 99, 701–705. <https://doi.org/10.1038/ngeo2784>
- GUO B., LACKIE M. A. & FLOOD R. H. 2007. Upper crustal structure of the Tamworth Belt, New South Wales: constraints from new gravity data, *Australian Journal of Earth Sciences*, 54:8, 1073-1087, DOI: 10.1080/08120090701615725
- HARRINGTON H. J. 1974. The Tasman Geosyncline in Australia. In: Denmead A. K., Tweedale G. W. & Wilson A. F. eds. *The Tasman geosyncline—a symposium in honour of Professor Dorothy Hill*, pp. 383–407. Geological Society of Australia, Queensland Division, Brisbane.
- HUSTON D. L., CHAMPION D. C., MORRISON G., MAAS R., THORNE J. P., CARR G., BEAMS S., BOTTRILL R., CHANG Z.-S., DHNARAM C., DOWNES P. M., FORSTER D. B., GEMMELL J. B., LISITSIN V., MCNEILL A. & VICARY M. 2017. Spatial variations in lead isotopes, Tasman Element, eastern Australia. *Record* 2017/09. Geoscience Australia, Canberra. <http://dx.doi.org/10.11636/Record.2017.009>
- HUSTON DL & CHAMPION DC (2023) Applications of lead isotopes to ore geology, metallogenesis and exploration. In: Huston DL, Gutzmer J (eds), *Isotopes in economic geology, metallogenesis and exploration*, Springer, Berlin, Mineral Resource Reviews, https://doi.org/10.1007/978-3-031-27897-6_6
- JELL PA. 2013. *Geology of Queensland*. Brisbane: Geological Survey of Queensland.
- JESSOP, K., DACZKO, N.R., & PIAZOLO, S. 2019. Tectonic cycles of the New England Orogen, eastern Australia: A Review. *Australian Journal Of Earth Sciences* <https://doi.org/10.1080/08120099.2018.154837>
- KEMP A.I.S., BLEVIN P.L., NORMAN M.D. & EDINBURGH ION MICROPROBE FACILITY. 2020. A SIMS U-Pb (zircon) and Re-Os (molybdenite) isotope study of the early Palaeozoic Macquarie Arc, southeastern Australia: Implications for the tectono-magmatic evolution of the paleo-Pacific Gondwana margin. *Gondwana Research*, 82, 73-96.
- KENNETT B. L. N., SALMON M., SAYGIN E. & AUSMOHO WORKING GROUP. 2011. AusMoho: the variation of Moho depth in Australia. *Geophysical Journal International* 187, 946–958. AusMoho 2017 was used for this study.
- KIRKBY A.L., MUSGRAVE R.J., CZARNOTA K., DOUBLIER M.P., DUAN J., CAYLEY R.A., & KYI D. 2020. Lithospheric architecture of a Phanerozoic orogen from magnetotellurics: AusLAMP in the Tasmanides, southeast Australia. *Tectonophysics*, <https://doi.org/10.1016/j.tecto.2020.228560>
- LI Z. X., BAILLIE P. A. & POWELL C. MCA. 1997. Relationship between northwestern Tasmania and East Gondwanaland in the Late Cambrian/Early Ordovician: palaeomagnetic evidence. *Tectonics* 16, 161–171.
- MEAKIN N.S. & MORGAN E.J. (compilers) 1999. *Dubbo 1:250 000 Geological Sheet 51/55-4, 2nd edition. Explanatory Notes*. Geological Survey of New South Wales, Sydney, xvi + 504 pp.

- MEFFRE S., SCOTT R. J., GLEN R. A. & SQUIRE R. J. 2007. Re-evaluation of contact relationships between Ordovician volcanic belts and the quartz-rich turbidites of the Lachlan Orogen. *Australian Journal of Earth Sciences* 54, 363 – 383.
- MERDITH, S.A., WILLIAMS, S.E., COLLINS, A.S., TETLEY, M.G., MULDER, J.A., BLADES, M.L., YOUNG, A., ARMISTEAD, S.E., CANNON, J., ZAHIROVIC, S., MÜLLER, R.D., 2021. Extending full-plate tectonic models into deep time: Linking the Neoproterozoic and the Phanerozoic, *Earth-Science Reviews*, Volume 214, 2021, 103477, ISSN 0012-8252, <https://doi.org/10.1016/j.earscirev.2020.103477>.
- MORTIMER, N., CAMPBELL, H.J., TULLOCH, A.J., KING, P.R., STAGPOOLE, V.M., WOOD, R.A., RATTENBURY, M.S., SUTHERLAND, R., ADAMS, C.J., COLLOT, J., SETON, M., 2017. Zealandia: Earth's Hidden Continent. *GSA Today* vol 27 pp27-35.
- MORTIMER N., WILLIAMS S., SETON M., CALVERT A., WAIGHT T., TURNBULL R., NELSON D., PALIN M., RAMEZANI J., SAGAR M.W., TULLOCH A., STRATFORD W., COLLOT J. & ETIENNE S. 2023. Reconnaissance Basement Geology and Tectonics of North Zealandia. *Tectonics*, 42, e2023TC007961. <https://doi.org/10.1029/2023TC007961>
- MURRAY C. G. 1990. Summary of geological developments along the Eromanga–Brisbane geoscience transect. In: Finlayson D. M. ed. *The Eromanga–Brisbane Geoscience Transect: a guide to basin development across Phanerozoic Australia in southern Queensland*. Bureau of Mineral Resources, Geology and Geophysics Bulletin 232, 11–20.
- MURRAY C., & FINLAYSON D. 1990. Summary of geological developments along the Eromanga–Brisbane Geoscience Transect, *The Eromanga–Brisbane Geoscience Transect: a guide to basin development across Phanerozoic Australia in southern Queensland*. Bureau of Mineral Resources Australia Bulletin, 232, 11–20.
- MUSGRAVE R. J. 2022. Structure of an accreted intra-oceanic arc: potential field model of a crustal cross-section through the Macquarie Arc, Lachlan Orogen, southeastern Australia, *Australian Journal of Earth Sciences*, 69:1, 47-60, DOI: 10.1080/08120099.2021.1939158
- PACKHAM G. H., & HUBBLE T. C. T. 2016. The Narooma Terrane offshore: A new model for the southeastern Lachlan Orogen using data from rocks dredged from the New South Wales continental slope. *Australian Journal of Earth Sciences*, 63, 23–61.
- PILIA S., RAWLINSON, N., CAYLEY, R. A. BODIN, T. MUSGRAVE, R. READING, A. M. DIREEN N. G. & YOUNG M. K. 2015 Evidence of micro-continent entrainment during crustal accretion. *SCIENTIFIC REPORTS* | 5 : 8218 | DOI: 10.1038/srep08218
- POGSON D. J. & WATKINS J. J. (Editors) 1998. Bathurst 1:250 000 Geological Sheet SI/55-8 Explanatory Notes. Geological Survey of New South Wales. Sydney.
- POWELL W. & O'REILLY S. 2007. Metasomatism and sulfide mobility in lithospheric mantle beneath eastern Australia: implications for mantle Re–Os chronology. *Lithos* 94, 132–147.
- PURDY D. J., ROSEMARY H., & MICHAEL D. 2018. Basement geology of the southern Thomson Orogen. *Australian Journal of Earth Sciences*. <https://doi.org/10.1080/08120099.2018.1453547>
- ROSENBAUM G. 2018. The Tasmanides: Phanerozoic tectonic evolution of eastern Australia. *Annual Review of Earth and Planetary Sciences*, 46(1), 291–325. <https://doi.org/10.1146/annurev-earth-082517-010146>
- SETON M., MÜLLER R. D., ZAHIROVIC S., WILLIAMS S., WRIGHT N. M., CANNON J., et al. 2020. A global data set of present-day oceanic crustal age and seafloor spreading

parameters. *Geochemistry, Geophysics, Geosystems*, 21, e2020GC009214.
<https://doi.org/10.1029/2020GC009214>

SHAW S. E., FLOOD R. H. & PEARSON N. J. 2010. The New England Batholith: interpretations from zircon Hf isotopic ratios. In: Buckman S. & Blevin P. L. eds. *New England Orogen 2010 Conference Proceedings*, pp. 307–312. University of New England, Armidale.

SHAW S. W., FLOOD R. H. & PEARSON N. J. 2011. The New England Batholith of eastern Australia: evidence of silicic magma mixing from $^{176}\text{Hf}/^{177}\text{Hf}$ ratios. *Lithos* 126, 115–126.

SIÉGEL C., BRYAN S. E. ALLEN C. M. PURDY D. J. CROSS A. J. UYSAL I. T. & GUST D. A. 2018. Crustal and thermal structure of the Thomson Orogen: constraints from the geochemistry, zircon U–Pb age, and Hf and O isotopes of subsurface granitic rocks. *Australian Journal Of Earth Sciences* 65, 967–986.

SKLADZIEN P.B., CAYLEY R.A., HAYDON S.J., CAIRNS C.P. 2023. Gravity modelling of crooked line traverses to constrain Southeast Lachlan Crustal Transect 2D seismic reflection interpretations in the Australian Alps. *Australasian Exploration Geoscience Conference*, Brisbane

SPAMPINATO G. P., AILLERES L., BETTS P. G., & ARMIT R. J. 2015. Crustal architecture of the Thomson Orogen in Queensland inferred from potential field forward modelling. *Australian Journal of Earth Sciences*, 62, 581–603.
<https://doi.org/10.1080/08120099.2015.1063546>

TURNBULL R.E., SCHWARTZ J.J., FIORENTINI M.L., JONGENS R., EVANS N.J., LUDWIG T., MCDONALD B.J., KLEPEIS K.A. 2021. A hidden Rodinian lithospheric keel beneath Zealandia, Earth's newly recognized continent. *Geology*.
<https://doi.org/10.1130/G48711.1>.

VANDENBERG A.H.M., WILLMAN C.E., MAHER S., SIMONS B.A., CAYLEY R.A., et al. 2000. *The Tasman Fold Belt System in Victoria: Geology and Mineralisation of Proterozoic to Carboniferous Rocks*. Melbourne: Geological Survey of Victoria.

WALTENBERG K., BODORKOS S., ARMSTRONG R., & FU B. 2018. Mid- to lower-crustal architecture of the northern Lachlan and southern Thomson orogens: evidence from O–Hf isotopes. *Australian Journal of Earth Sciences*, 65:7-8, 1009-1034, DOI: 10.1080/08120099.2018.1463928

WILLMAN C.E., VANDENBERG A.H.M. & MORAND V.J., 2002. Evolution of the southeastern Lachlan Fold Belt in Victoria. *Australian Journal of Earth Sciences* 49, 271–289.

WILLMAN C.E., KORSCH R.J., MOORE D.H., CAYLEY R.A., LISITSIN V.A., RAWLING T.J., MORAND V.J., & O'SHEA P.J. 2010. Crustal-Scale Fluid Pathways and Source Rocks in the Victorian Gold Province, Australia: Insights from Deep Seismic Reflection Profile. *Economic Geology*, 105, 895-915.

ZHANG Q., NUTMAN A., BUCKMAN S. & BENNETT V.C. 2020. What is underneath the juvenile Ordovician Macquarie Arc (eastern Australia): A question resolved using Silurian intrusions to sample the lower crust. *Gondwana Research*, 81, 362-377.

DEFINING A WALLROCK-HOSTED EPITHERMAL-PORPHYRY SYSTEM AT THE SPUR PROJECT, CARGO DISTRICT, EASTERN LACHLAN OROGEN, NEW SOUTH WALES

Peter Duerden

Waratah Minerals Ltd

Key Words: Eastern Lachlan, Macquarie Arc, Cargo, Epithermal, Porphyry, Alkalic

INTRODUCTION

The Spur Project in the Cargo district has been explored since the 1960's, with a focus on outcropping 'Intrusion-hosted' copper porphyry mineralisation within the main Cargo Intrusive Complex (CIC). Waratah Minerals (Waratah) acquired the project in early 2024 and is using an alternative exploration model, targeting a later stage alkalic epithermal-porphyry system positioned outside/at the margin of the main early-stage CIC.

The importance of wallrock-hosted settings at the margin of major Benambran-aged intrusive complexes is apparent at several major Macquarie Arc deposits e.g. Cadia (>50Moz Au, 9.5Mt Cu, Newmont 2023), Cowal (9.6Moz Au, Evolution 2023) and Boda (6.4Moz Au/1Mt Cu, Alkane 2023).

Strong evidence for the preservation of a significant wallrock epithermal-porphyry system at Spur comes from ongoing drilling results, including 89m @ 1.73g/t Au, 0.08% Cu from 115m associated with epithermal veins/stringers overprinting early stage (high-temperature) K-feldspar + albite + tourmaline, albite-silica-hematite (Inner-propylitic), skarn porphyry alteration (SPD007, ASX WTM 2 July 2024).

Elsewhere in the Macquarie Arc, the link between early-stage (high-temp) alkalic porphyry alteration (hematite – kspars – albite ± tourmaline) and epithermal mineralisation is evident (e.g. Cowal and Boda) with the setting of the E41 and E42/Dalwhinnie zones at Cowal considered particularly relevant to the emerging Spur discovery.

GEOLOGICAL SETTING

The Spur Project is situated within the north-south oriented Western Molong Volcanic Belt of the Lachlan Fold Belt (Figure 1), consisting of a thick succession of Middle to Late Ordovician aged andesitic volcanics to volcaniclastic rocks of the Cargo Volcanics- a part of the Middle to early Late Ordovician Kenilworth Group (Simpson et al., 2011). These volcanic units comprise dominantly massive sub-aqueous lavas, sills and dykes with less abundant monomictic andesite breccias with minor peperitic textures. Simpson et al. (2011) report that the Cargo Volcanics have been cut by four main suites of intrusions, namely: (1) dacitic domes; (2) monzonite suite; (3) medium to coarse grained dolerite dykes; and (4) fine-grained basalt dykes.

The oldest of these intrusions is developed as a series high-level plagioclase-quartz-hornblende phyric dacite domes termed the "Cargo dacite complex, Cargo Intrusive Complex, CIC".

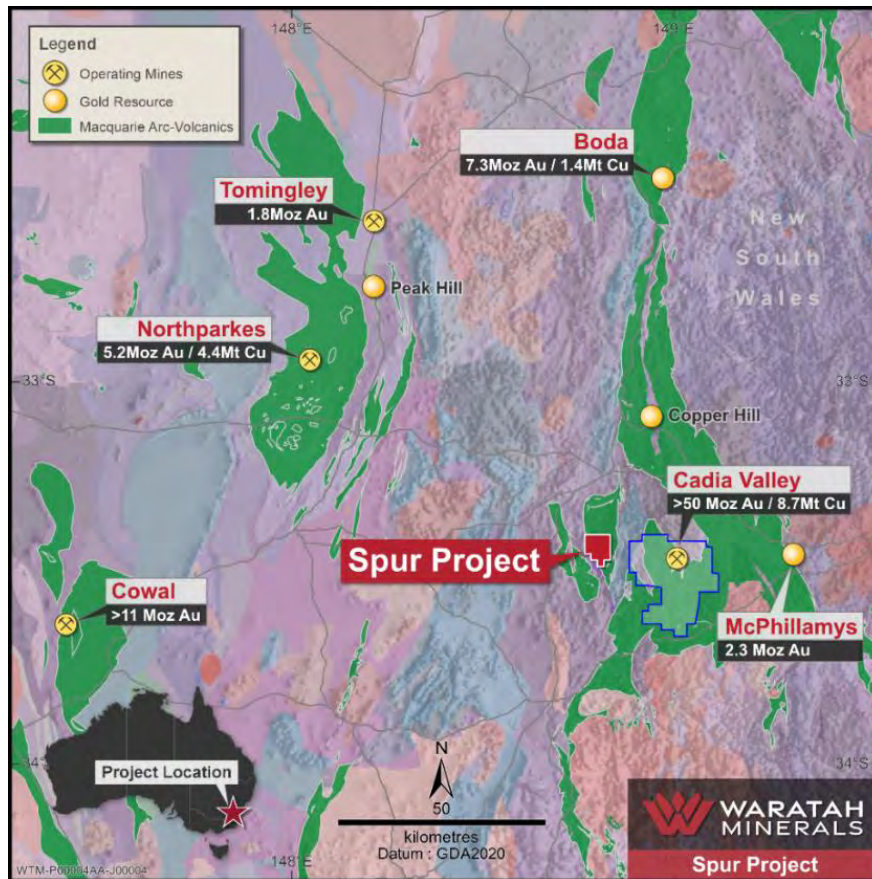


Figure 12: Spur Project, total metal endowment from Phillips 2017, Newmont 2023, CMOG 2023, Evolution 2023, Alkane 2023, Regis 2023

The second group of intrusions reported by Simpson et al. (2011) comprise younger monzonite dykes that cut the early-stage intrusions of the CIC and are concentrated in the Spur area.

DISTRICT GEOLOGY

The gold bearing lodes, which are often described as radial features emanating from the CIC (Figure 2), host massive white quartz with minor dark brown, Fe-rich high temperature sphalerite and minor amounts of chalcopyrite and molybdenite (Menzies 2015). Previous workers have interpreted these veins/lodes to represent a radial array of D-veins related to the main Cargo Intrusive Complex. Waratah interprets these as an array of deep level epithermal veins, with current geometries reflecting the influence of movement along a post-porphyry NW-trending dextral fault system which, when reconstructed, produces a broadly north-south oriented zone along the eastern margin of the CIC.

Ptygmatic quartz-K-feldspar bearing A veins, occur in drill holes proximal to the magmatic-hydrothermal breccia within the CIC and within the >0.2% Cu and >40 ppm Mo in down holes assay shell. These veins locally contain minor amounts of chalcopyrite-bornite mineralisation, but generally report low Cu contents and moderate Mo. Quartz-chalcopyrite bearing B veins, characterised by centrally terminating quartz crystals and K-feldspar selvages, occur in drill holes proximal to the magmatic-hydrothermal breccia and associated with dacitic intrusions (Menzies 2015; Figure 3).

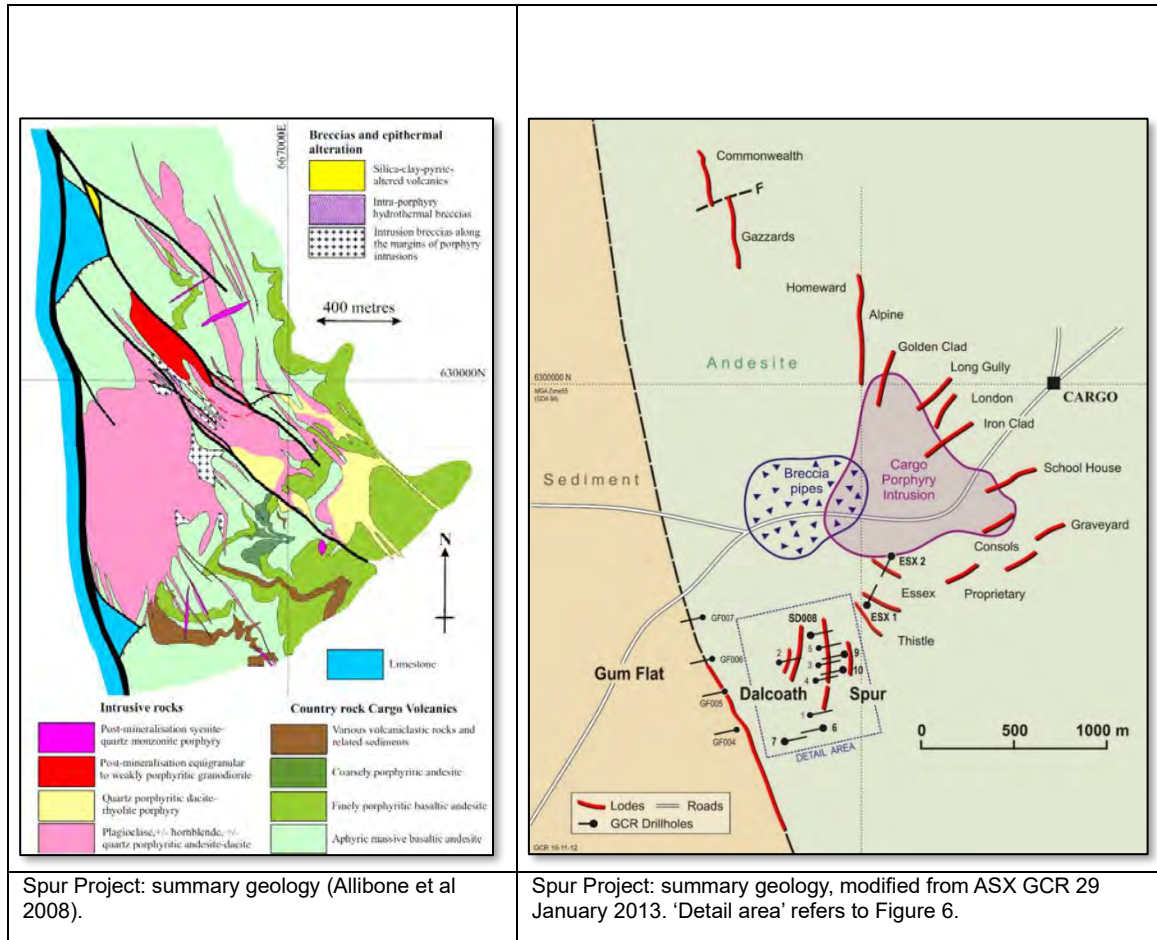


Figure 13: Geology summary maps of the Spur Project, Cargo Intrusive Complex.

REGIONAL FRAMEWORK

Waratah's exploration model is targeting a younger 'progenitor' epithermal-porphyry intrusive suite outside the Cargo Intrusive Complex, which is not dated by current geochronology studies (Figure 4). Based on paragenetic observations and those reported by Simpson et al. (2011), there is an extensive younger multiphase alkalic intrusive suite that hasn't been dated and is the focus of current geochronology studies.

TARGETING RATIONALE

The Spur Project encompasses the wider Cargo gold-copper porphyry district, where much of the historical exploration focus has been within the main Cargo Intrusive Complex for 'intrusion-hosted' porphyry-style copper-gold mineralisation.

Most high-grade gold-copper porphyry-epithermal deposits in the East Lachlan are positioned outside/at the margins of major intrusive complexes (Wallrock-hosted). These systems include 1) 'Wallrock-hosted' porphyry gold-copper deposits (e.g. Ridgeway, 6Moz Au/1Mt Cu, Cadia East, 38Moz Au/7.5Mt Cu) and 2) Epithermal-porphyry gold-copper deposits (e.g. Cowal and Boda).

The equivalent position at the margin of and outside the main Cargo Intrusive Complex is therefore a key exploration criteria for Waratah in the Spur district, and marks a zone characterised by widespread epithermal sulphide stringer/lode mineralisation and alkalic porphyry alteration including 89m @ 1.73g/t Au, 0.08% Cu from 115m (SPD007, ASX WTM 2 July 2024).

Waratah's exploration model and targeting strategy is also guided by an interpretation that the epithermal sulphide stringers represent the upper levels of a porphyry system as

evident at several major East Lachlan deposits (e.g. Cowal and Boda). There appears to be increasing evidence for this link at the Spur Project, given the identification of K-feldspar + albite + tourmaline (alkalic lithocap), pervasive albite-silica-hematite (Inner-propylitic) and skarn porphyry alteration associated with gold-copper mineralisation (ASX WTM 10 April 2024, Figure 3).

Indeed the epithermal sulphide stringer/lode mineralisation can represent a compelling target in its own right, as demonstrated by the resources and mining operations at Cowal – 305Mt @ 0.98g/t Au (9.6Moz, Evolution 2023), Brucejack - 22.5Mt @ 10g/t Au, 67.5g/t Ag (7.2Moz Au, 48.8Moz Ag, Newcrest 2021) and Fruta del Norte – 18Mt @ 8.68g/t Au, 11.4g/t Ag (5Moz Au, 6.6Moz Ag, Lundin Gold 2022).

Within the Cargo Intrusive Complex: Mineralised veining post-dates the intrusions (Menzies 2015)			
			
Quartz-actinolite-K-feldspar-chalcocopyrite vein in sericite altered monzonite from 367.5m in CYC010 which reported 2 m at 36 ppm Cu, 0.004 g/t Au and 7 ppm Mo.	Quartz-K-feldspar-chalcocopyrite-bornite vein which cuts both clasts and matrix of the breccia from 76.2m in drill hole CN1 which reported 2m at 0.19% Cu, 0.06 g/t Au and 60 ppm Mo.	Quartz-K-feldspar-chalcocopyrite-bornite bearing A vein within K-feldspar-actinolite altered dacite from 255.9m in drill hole NCG003 which reported 0.1% Cu, 0.03 g/t Au and 102 ppm Mo.	Strong sericite-kaolinite-dickite altered dacite from 116.3m in drill hole NCG005 which reported 28 ppm Cu, <0.01 g/t Au, 5 ppm Mo.

Figure 14a: Summary of mineralisation and alteration within the Cargo Intrusive Complex (Menzies 2015).

<p>Outside the Cargo Intrusive Complex: Well-developed epithermal gold overprinting early stage alkalic porphyry event</p>			
			
<p>SD010 – 160m, massive hematite + silica (red-rock) alteration, pyrite-chalcopyrite stringers, 0.82g/t Au (Inner Propylitic Porphyry)</p>	<p>SD010 – 196m, massive kspars + albite + silica + tourmaline alteration + pyrite-chalcopyrite stringers, 2g/t Au, 0.14% Cu (Alkalic lithocap Porphyry)</p>	<p>SPD001 – 253m, strong k-feldspar alteration. (Inner Propylitic Porphyry Alteration)</p>	<p>SD010 – 137.5m, pyrite - chalcopyrite, sub vertical stringers, 124g/t Au, 1% Cu. (Int-Sulphidation Epithermal)</p>

Figure 15b: Summary of mineralisation and alteration outside the Cargo Intrusive Complex (Menzies 2015).

A LINK BETWEEN ALKALIC EPITHERMAL AND PORPHYRY

The Cowal/E41 and E42 Deposits provide a relevant analogue to the early-stage Spur discovery, showing similar evidence for a transition from early, high-temperature (hematite-albite) porphyry-style veins and alteration to lower-temperature epithermal-style gold mineralization (Figure 5). The paragenetic history of Endeavour 41 records a transition from deep-level to shallow-level magmatic hydrothermal activity. High-temperature assemblages (e.g., actinolite-magnetite, biotite, and K-feldspar-epidote) indicate that epithermal mineralization occurred proximal to a magmatic-hydrothermal centre and that there is potential for the discovery of alkalic porphyry copper-gold mineralization below the current level of diamond drilling (Zukowski 2010), as there is at Spur.

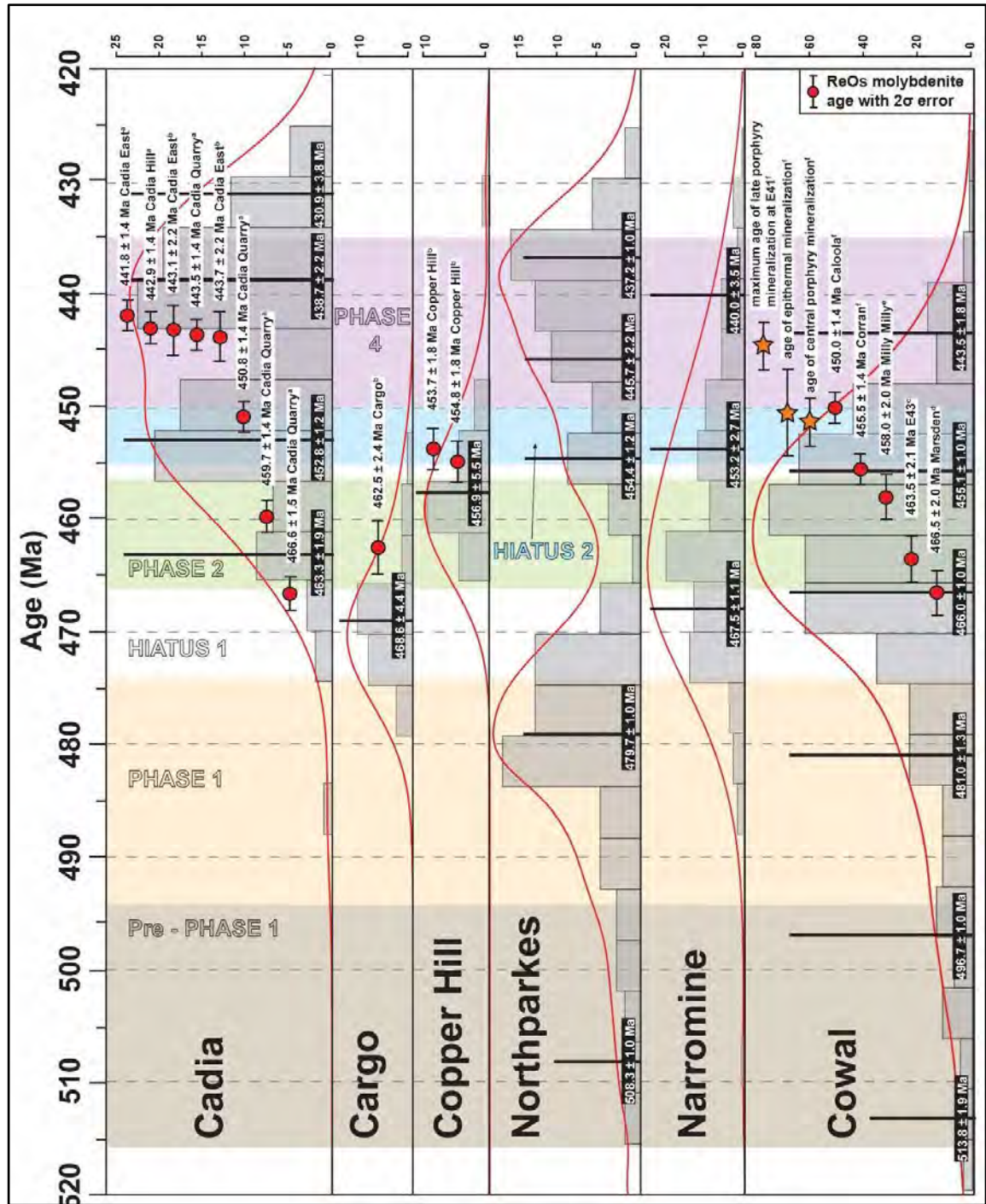


Figure 16: Pb/U zircon and Re-Os molybdenite geochronological data compiled from key intrusive complexes in the Macquarie Arc. Relative probability plots (red lines) and associated zircon age histograms highlight zircon age populations from each district and include both zircons interpreted as magmatic and zircons interpreted as inherited. Ages interpreted as being too young due to Pb-loss were removed from the Cowal Igneous Complex compilation. Population ages (black lines) are calculated using the Unmix function in Isoplot 4.15 (Ludwig, 2008). Zircon ages are sourced from Butera et al. (2001), Wilson et al. (2007), Lickfold et al (2007), Crawford et al. (2007), and Kemp et al. (2020). ReOs molybdenite ages are compiled from, (a) Wilson et al. (2007), (b) Kemp et al. (2020), (c) Zukowski (2010), (d) Rush (2013), (e) Forster et al. (2015), (f) current study. Macquarie Arc magmatic phases are from Percival and Glen (2007) and Glen et al. (2007a). Yellow stars in the Cowal compilation are interpreted mineralisation ages based on crosscutting relationships and U-Pb zircon magmatic ages (Leslie 2021).

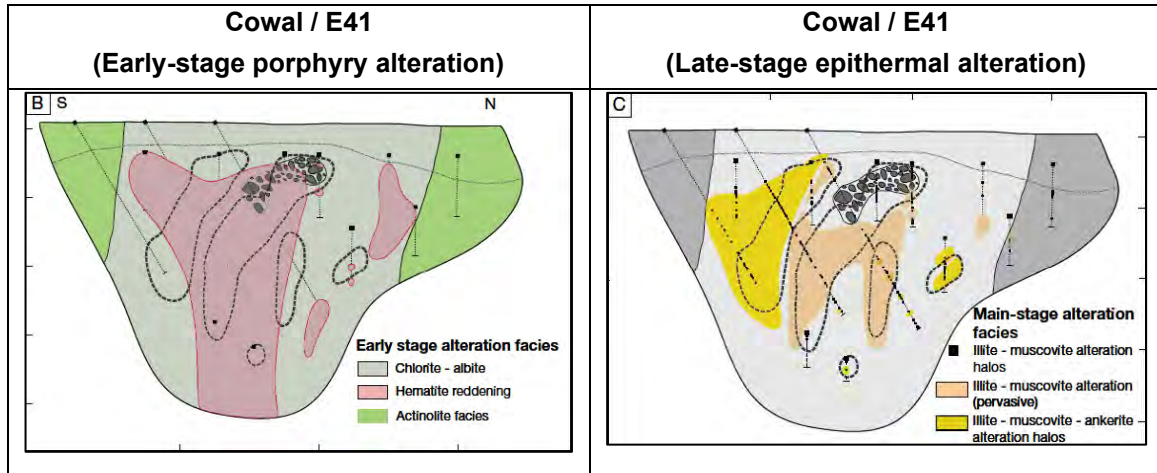


Figure 5: Alteration and gold distribution on cross section 86200E through west pod at Cowal/E41. B. Distribution of early-stage alteration facies. C. Distribution of main-stage illite-muscovite ± ankerite alteration facies. (Zukowski et al, 2014).

EXPLORATION ACTIVITY

Waratah’s ongoing exploration activity includes RC and core drilling supported by 4-acid multielement geochemistry, detailed ground magnetics, 3D Ambient Noise Tomography and geochronology studies, with drilling coverage and geology summary summarised in Figure 6.

Initial drilling activity is designed to test extensions of shallow epithermal gold mineralisation and investigate a potential link with an alkalic porphyry gold-copper system down plunge. Drilling is demonstrating a rapid increase in grades with depth within epithermal gold zones, and an important structural control at the margins of intrusive bodies, with selected drill results shown in Table 1.

Table 1. Selected recent Waratah Minerals drill results at Spur (see Figure 6 for drillhole locations).

SPRC002	11m @ 10.82g/t Au, 0.12% Cu from 154m	SPUR EAST
inc	7m @ 16.78g/t Au, 0.18% Cu from 154m	SPUR EAST
and	69m @ 0.49g/t Au from 28m	SPUR EAST
SPRC007	89m @ 1.73g/t Au, 0.08% Cu from 115m	SPUR
inc	57m @ 2.50g/t Au, 0.11% Cu from 115m	SPUR
also	16m @ 5.59g/t Au, 0.32% Cu from 156m	SPUR
also	9m @ 9.33 g/t Au, 0.38% Cu from 163m	SPUR

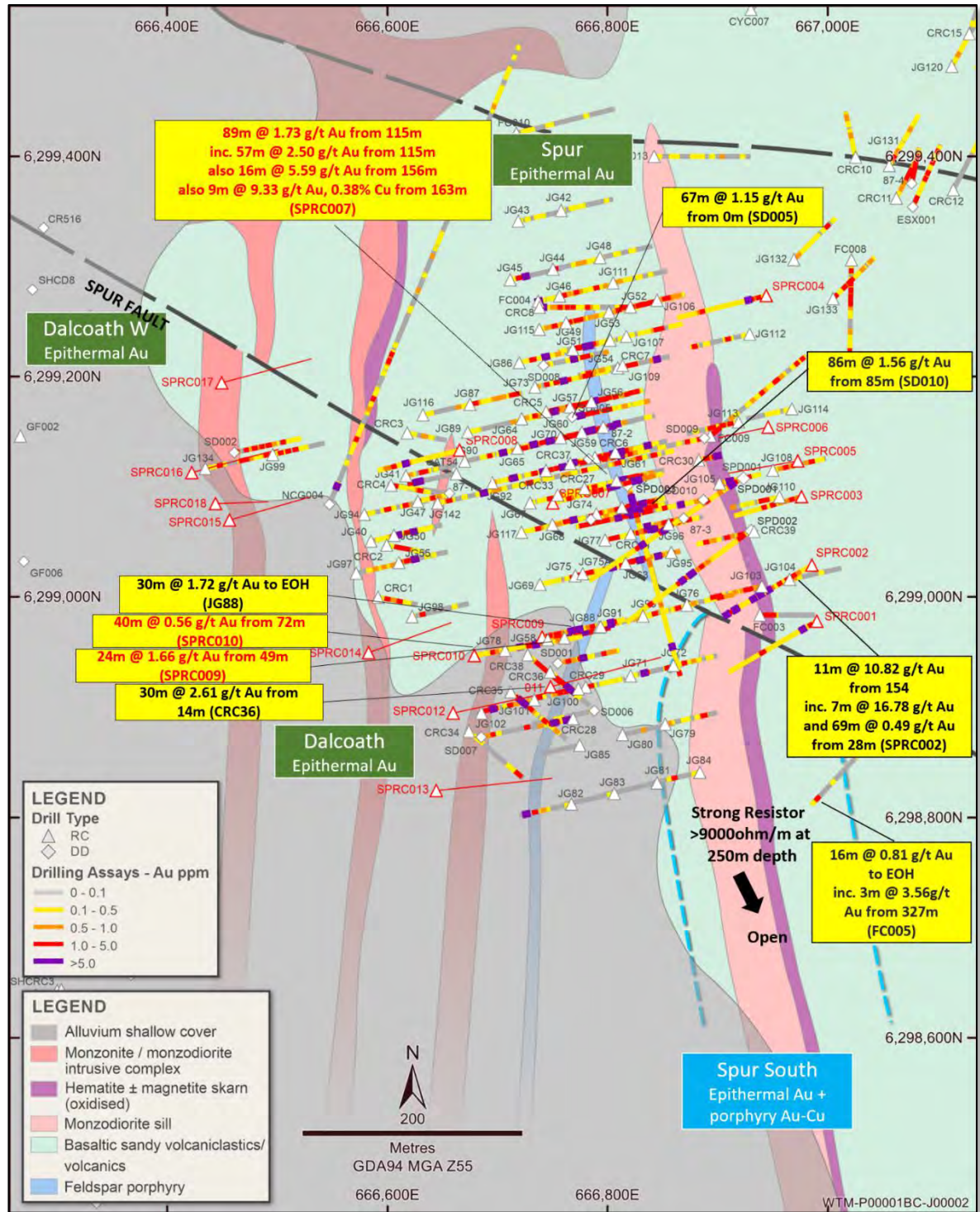


Figure 6: Spur drilling coverage and geology summary, showing RC completed and planned drillholes, recent results shown in red

ACKNOWLEDGEMENTS

Mineral exploration is an iterative process with the work of previous geologists and 'believers' in the potential of the Cargo District greatly appreciated and recognised. Bret Ferris, Andrew Allibone, Tully Richards, Doug Menzies, Brian Locke, David Timms, Glen Twomey, Robyn Hee, Chris Torrey, Peter Silversmith, Mike Erceg, Peter White, Murray Flitcroft, Bruce Mowatt, Andrew Allibone, Stuart Hayward, Matt Alderdice, Kim Boundy,

Ian Freeland, Bill Finlayson, John McCarron in particular are recognised for their contributions.

REFERENCES

- ALKANE, 2023. ASX Announcement, Boda Resource Update Increases Gold and Copper Grades, 14 December 2023.
- ALLIBONE, A., SMILLIE, HART, 2008. Cargo Project: Annual report for February 2007 – February 2008.
- CMOC, 2023. China Molybdenum Company Limited, 2022 Annual Report, <http://www.cmocinternational.com/>
- EVOLUTION, 2023. Mining Annual Mineral Resources and Ore Reserves Statement.
- EVOLUTION, 2024. Cowal Site Visit Presentation, 20 June 2024.
- HARRIS, COOKE, CUISON, GROOME, WILSON, FOX, HOLLIDAY, TOSDAL, 2020. Geologic Evolution of Late Ordovician to Early Silurian Alkalic Porphyry Au-Cu Deposits at Cadia, New South Wales, Australia, SEG Special Publication 23.
- HOLLIDAY AND COOKE, 2007. Advances in Geological Models and Exploration Methods for Copper + Gold Porphyry Deposits "Proceedings of Exploration 07: Fifth Decennial International Conference on Mineral Exploration".
- KEMP, A.I.S., BLEVIN, P.L., AND NORMAN, M.D., 2020. A SIMS U-Pb (zircon) and Re-Os (molybdenite) isotope study of the early Palaeozoic Macquarie Arc, southeastern Australia: Implications for the tectono-magmatic evolution of the paleo-Pacific Gondwana margin: *Gondwana Research*, v. 82, p. 73-96.
- LESLIE, 2021. Metallogeny of the Cowal district, New South Wales, Australia, PhD, University of Tasmania / CODES.
- MENZIES AND CORBETT, 2015. A Review of the Cargo Porphyry Cu-Au ± Mo Prospect, NSW for Golden Cross Resources NL. Technical Report.
- NEWMONT, 2023. Mining Annual Mineral Resources and Ore Reserves Statement, <https://operations.newmont.com/reserves-and-resources>.
- PHILLIPS, G N (Ed), 2017. *Australian Ore Deposits* (The Australasian Institute of Mining and Metallurgy: Melbourne).
- REGIS RESOURCES, 2023. Annual Mineral Resource and Ore Reserve Statement 8 June 2023.
- SIMPSON, C. J., et al., 2007. Volcanology, geochemistry and structure of the Ordovician Cargo Volcanics in the Cargo–Walli region, central New South Wales. *Australian Journal of Earth Sciences* 54.2-3 (2007): 315-352.
- ZUKOWSKI, 2010. Geology and Mineralisation of the Endeavour 41 Gold Deposit, Cowal District, NSW, Australia. Submitted in fulfilment of the requirements for the degree of Doctor of Philosophy. November, 2010. CODES, ARC Centre of Excellence in Ore Deposits at the University of Tasmania.
- ZUKOWSKI, COOKE, DEYELL, MCINNES, SIMPSON, 2014. Genesis and Exploration Implications of Epithermal Gold Mineralization and Porphyry-Style Alteration at the Endeavour 41 Prospect, Cowal District, New South Wales, Australia, *Economic Geology*, v. 109, pp. 1079–1115.

DISCOVERING GOLDEN RIDGE AND NORTHEAST TASMANIA'S UNTAPPED POTENTIAL

Michael Fenwick

Flynn Gold Limited

Flynn Gold is targeting gold mineralisation in Northeast Tasmania due to the geological similarities with the world class Victorian goldfields. It is regarded as the southernmost extent of the Lachlan Fold Belt, and shares similar types of gold mineralization, age and type of host rocks and age of felsic intrusions with the Central and Eastern Provinces of the Lachlan Fold Belt in Victoria (Bierlein et al. 2005).

There are around 600 gold occurrences in Northeast Tasmania. Total production in the historic period from ~1860 to 1914 is around 1.73 million ounces, with over 90% coming from 4 main areas:

Beaconsfield	1877-1914:	854,000 oz @ ~25g/t Au
	(1999-2012	923,000 oz @ 11g/t Au)
Lisle	~1880-1930	250,000 oz
Mathinna	1887-1926	253,000 oz @ ~26g/t
Lefroy	1872-1896	167,184 oz

The Tasmania Reef at Beaconsfield is the only mine to operate in Northeast Tasmania in modern times and is one of the richest single reef gold mines in southeast Australia. Mining ceased in 2012 due to reduced gold prices and high operating costs. There is currently no active gold production in northeast Tasmania (Botrill et al. 1992; Hills 2017; Roach 1992).

Most of the 600 gold occurrences in Northeast Tasmania were not mined below 60m deep however the Tasmania Reef at Beaconsfield is around 1200m deep and the historic Golden Entrance mine in the Mathinna goldfield reached depths of 500m. The Mineral Resources Tasmania borehole database records only 40 drillholes exceeding 250m long that test greenfield or brownfields gold occurrences in Northeast Tasmania. Despite significant gold deposits and geological similarities to Victoria, most of the gold occurrences in Northeast Tasmania remain under-explored in modern times (Taheri et al. 1994).

Flynn Gold strives to resurrect the Northeast Tasmanian goldfields, with discoveries and re-discoveries at the Golden Ridge IRGS. The Trafalgar Prospect, along with Flynn's Brilliant and Link Zone prospects occur within a 2.5km corridor of gold mineralization that trends along the Golden Ridge Granodiorite and Mathinna Supergroup country-rock contact. The corridor is contained in a broader zone of gold anomalism defined by soil sampling that forms around the contact with a total length exceeding 9km. Diamond drilling at the Trafalgar prospect, on the eastern side of the granodiorite has returned spectacular grades, including:

TFDD005	12.3m @ 16.8 g/t Au, incl. 0.7m @ 152.5g/t Au from 120.3m
TFDD013	4.0m @ 23.7g/t Au, incl. 0.5m @ 169.8g/t Au from 25.9m.
TFDD015	1.1m @ 51.3g/t Au inc. 0.4m @ 137.8g/t Au from 353.9m

Mineralisation is contained in auriferous quartz veins with arsenopyrite, pyrite and galena, and hosted within the Golden Ridge Granodiorite and the contact-metamorphosed Mathinna Supergroup.

REFERENCES

BIERLEIN F.P., FOSTER D.A., GRAY D.R. & DAVIDSON G.J. 2005. Timing of orogenic gold mineralization in northeastern Tasmania: implications for the tectonic and metallogenetic evolution of Palaeozoic SE Australia. *Mineralium Deposita* 39, 890-903.

BOTRILL R.S., HUSTON D.L., TAHERI J. & ZAW K. 1992. Gold in Tasmania. *Bulletin of the Geological Survey of Tasmania*. 70, 24-56.

HILLS P.B., 2017. Tasmania gold deposit, Beaconsfield. *Australian Ore Deposits*. AusIMM Monograph 32, 6th edn: 851-854.

ROACH M.J. 1992. Geology and geophysics of the Lisle-Golconda goldfield, northeast Tasmania. *Bulletin of Geological Survey of Tasmania*. 70: 189-198.

TAHERI J., BOTRILL R.S., KEELE R.A. & GREEN G.R. 1994. A study of the nature and origin of gold mineralization, Mangana-Forester area northeast Tasmania. *Mineral Resources Tasmania Report*. 1994/05.

CRITICAL MINERALS IN THE TASMANIDES: A DORCHAP LITHIUM PROJECT UPDATE

Owen Greenberger, Dean Turnbull

Dart Mining NL

Key Words: Tasmanides, LCT Pegmatites, Exploration, Discovery

INTRODUCTION

Lithium-Caesium-Tantalum (LCT) pegmatites are derived from S-type granitic sources, formed by the melting of mica schists, and demonstrate a regional geochemical zonation trend in their mineralisation (Figure 1a). This zonation is broadly concentric around the source granite intrusion. The most proximal pegmatites are the least evolved, or least fractionated, with the greatest fractionation and greatest enrichment of Li, Cs, Ta, Nb, and Be occurring in the most distal pegmatite dykes (Figure 1a).

Because of this distinct fractionation trend with increasing distance, whole-rock geochemistry of pegmatites samples can be used as a pathfinder towards establishing the fractionation trends of a particular system and can continually guide ongoing exploration.

Dart Mining’s Dorchap Range pegmatite exploration program in northeast Victoria is an excellent example of this, where the fractionation trend outlined by diminished K/Rb and K/Cs ratios (Figure 1b) also highlighted areas of significant Li, Cs, Ta, Sn and Be enrichment, particularly in north-eastern areas of the Dorchap Range (Figure 2). The pegmatite sampling program identified a strong fractionation trend across the Dorchap Range, resolving a 20 x 12 km zone of strongly fractionated pegmatites bearing enriched Li, Cs, Ta, Be and Sn mineralisation (Figure 2).

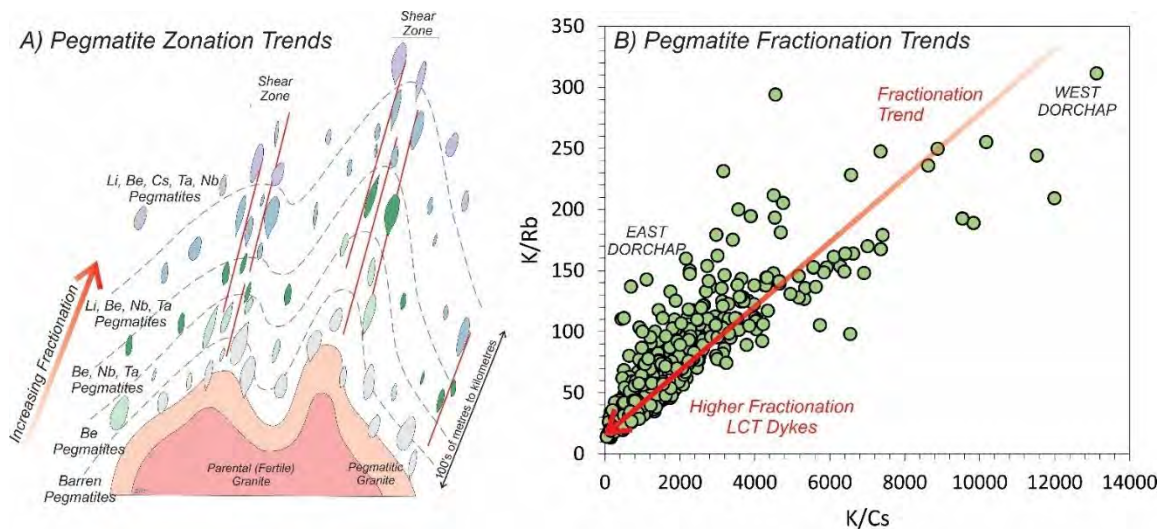


Figure 17: A) Model of mineralised pegmatite zonation in dykes surrounding and radiating from the host intrusive granite. B) Pegmatite fractionation trends from Dart Mining pegmatite samples across the Dorchap Range, demonstrating a distinct increase in fractionation towards the east. Figure 1a modified after Bradley et al. (2017).

Dorchap Lithium Project update, northeast Victoria

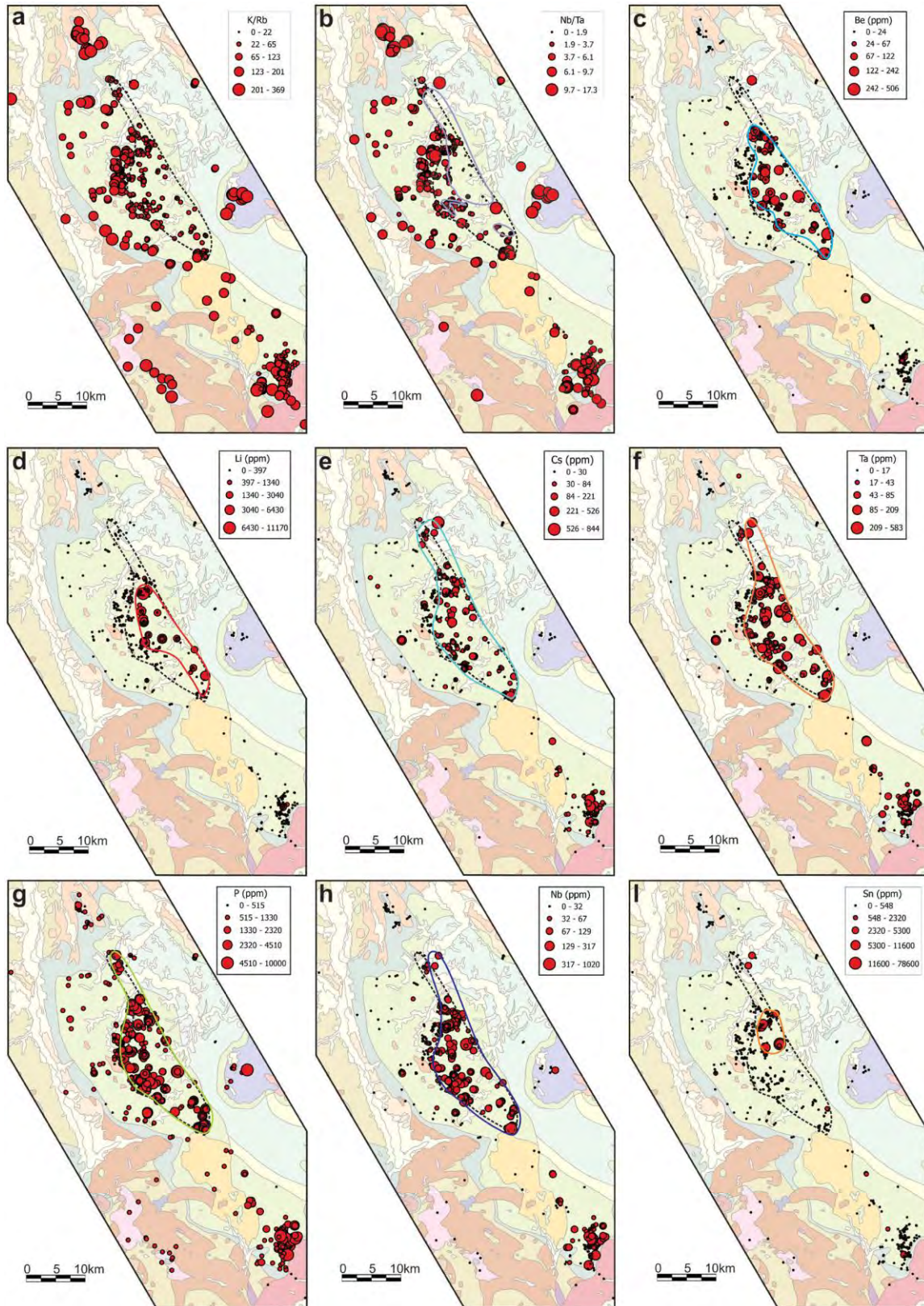


Figure 18: Spatial trends in elemental enrichment across the Dorchap Dyke Swam, Plotted over regional geology. Taken from Hines et al. 2023.

DISCOVERY

Dart Mining geologists first identified the lithium prospectivity of pegmatite dykes in the Dorchap Range in 2016 and set about acquiring exploration leases across the region ([Dart ASX May 2016](#); [Dart ASX August 2016](#)). These were the first recorded lithium pegmatites identified in eastern Australia. The Dorchap Range and Glen Wills pegmatite dykes have intruded as shallowly plunging, lenticular dykes, primarily along a steeply dipping, northeast-trending shear zone. The pegmatites were believed to have been sourced from the Mt Wills Granite.

The discovery sampling program consisted of 826 samples across the Dorchap Range and Glen Wills work areas, representing a cumulative total of over 800 pegmatite dykes visited and assessed across the course of the work program.

Extensive aerial surveys were undertaken by Dart Mining to identify pegmatite outcrops across the Dorchap Range and Glen Wills project areas ([Dart ASX June 2019](#)). With an airborne LiDAR mapping program commencing in early 2021 ([Dart ASX March 2021](#)), which allowed additional detailed mapping of pegmatite dykes that were previously overlooked in pockets of dense bush across the Dorchap Range.

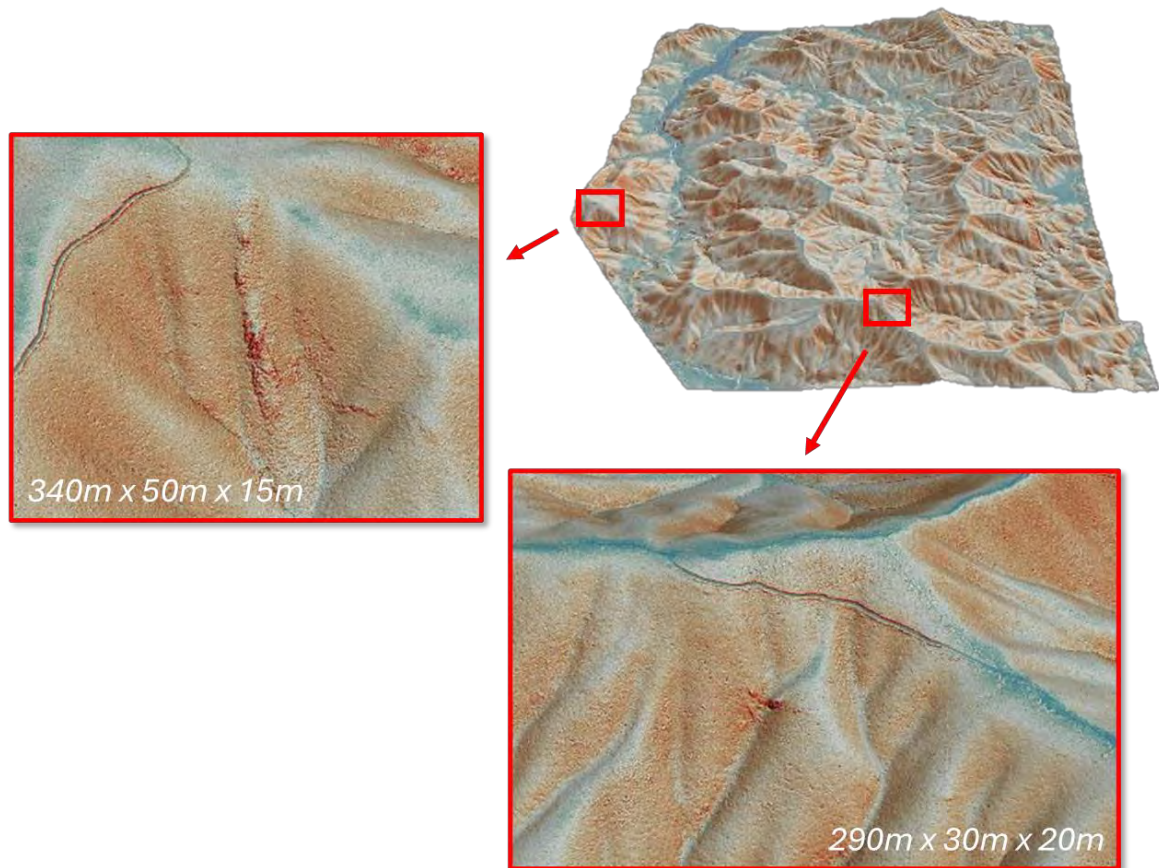


Figure 19: LiDAR survey results from the Dorchap Lithium project highlighting outcropping pegmatites.

Exploration for Lithium in the Dorchap Range and Glen Wills areas has identified several pegmatite dykes that demonstrate significant Ta, Cs and Sn mineralisation that require follow-up investigation.

DRILLING

In 2019 a small, low impact, roadside reverse circulation (RC) drilling program was undertaken by Dart Mining, targeting two prospects: The Holloway Road and Eagle dykes in the Dorchap Range ([Dart ASX March 2019](#); [Dart ASX June 2019](#)). Due to the low impact nature of the workplan and difficulties in accessing some of the pegmatites, positioning of drill holes was significantly restricted. The drilling results confirmed the Lithium prospectivity of the Eagle Dyke returning reasonable widths but low grade results. MIEDRC003 returned 20m @ 0.33% Li₂O which included 2m @ 1.158% Li₂O as the highlight of the program.

2023 saw the first diamond drilling on the project, with ~3,000m of drilling completed from existing tracks under the low impact exploration guidelines. 5 regions of dyke outcrops were tested with drilling again confirming the lithium potential of the region. Drilling overall returned low grade results on all except the Boons Target in the north of the project with both holes drilled returning positive results ([Dart ASX October 2023](#)). MIDDH009 (10.0m @ 1.08% Li₂O including 7m @ 1.38% Li₂O) and MIDDH010 (2.0m @ 1.07% Li₂O) both intersected the Boons Dyke at depth returning the first positive results from drilling at the project.

The current interpretation of the geological evolution and structural emplacement of the Dorchap Dyke Swarm pegmatites involves variable syn-emplacement to post-emplacement shearing of the dykes (extensive at the Eagle Dyke) that has generated mylonitic (sheared) textures that likely caused partial recrystallisation within some pegmatite bodies and re-mobilised a portion of the contained lithium from the dyke into the surrounding sediments as an exomorphic halo. Broadly, higher drilled Li grade appears to correlate with larger primary pegmatite crystal size (preserved megacrystic texture). This important textural characteristic appears indicative of undeformed or weakly deformed portions of the pegmatites tested to date. The deformation and hydrothermal alteration noted in portions of the pegmatites may be responsible for the broader, but overall lower grade lithium intersections at Eagle dyke (34.67m @ 0.11% Li₂O) and similar recrystallised intersections, in contrast, the dominant megacrystic pegmatite intersected at Boones (MIDDH009 and MIDDH010) show higher grades with up to 10m @ 1.08% Li₂O (Dart Mining ASX September 2023).

The understanding of the structural evolution of the region is critical to exploration success due to the controls on the emplacement, alteration and preservation of primary lithium grades in the Dorchap pegmatite dykes.

RECENT FIELD WORK

2023-2024 summer field season saw the continuation of field testing and sampling of LiDAR targets. An additional 357 sites were inspected for pegmatite outcrop, with 105 samples submitted for analysis. Results continued to confirm the fractionation zone and highlighted a corridor of elevated Lithium grades from the Eagle dyke in the south to Boones in the north of the project. ([Dart ASX 10th April 2024](#)).

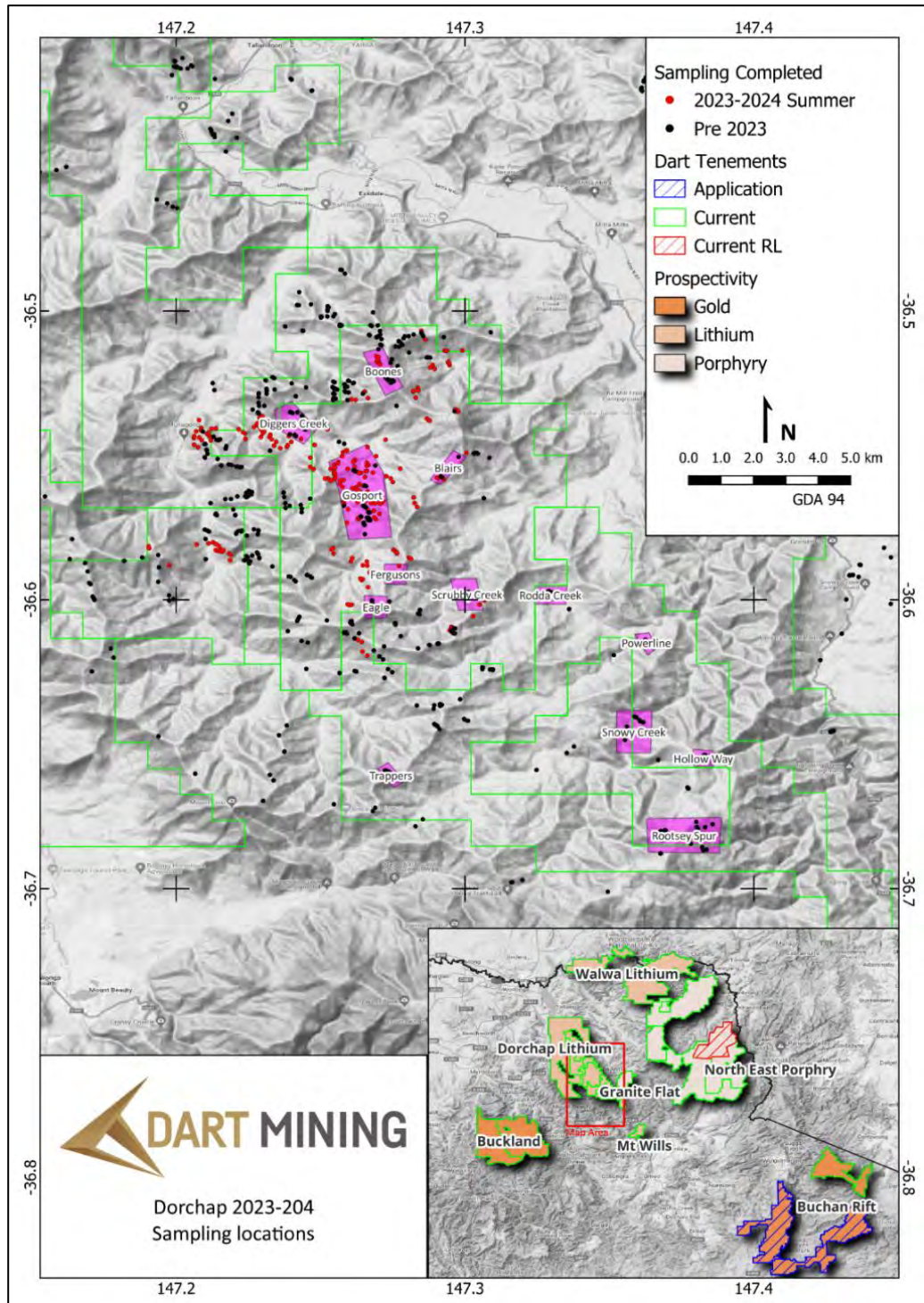


Figure 4. 2023-2024 field sampling locations.

After the drilling success at Boones Dyke, the LiDAR imagery was reviewed, with additional zones of possible outcrop sites identified along strike to the North. Inspection and sampling identified the continuation of the Boons Dyke along strike extending the mapped outcrop to approximately 1.2km in length. Sampling of the dyke returned the highest Li₂O grades of the project with samples returning 5m at 2.0% Li₂O and 2m @ 2.35% Li₂O from channel samples across the outcrop ([Dart ASX 10th April 2024](#)).

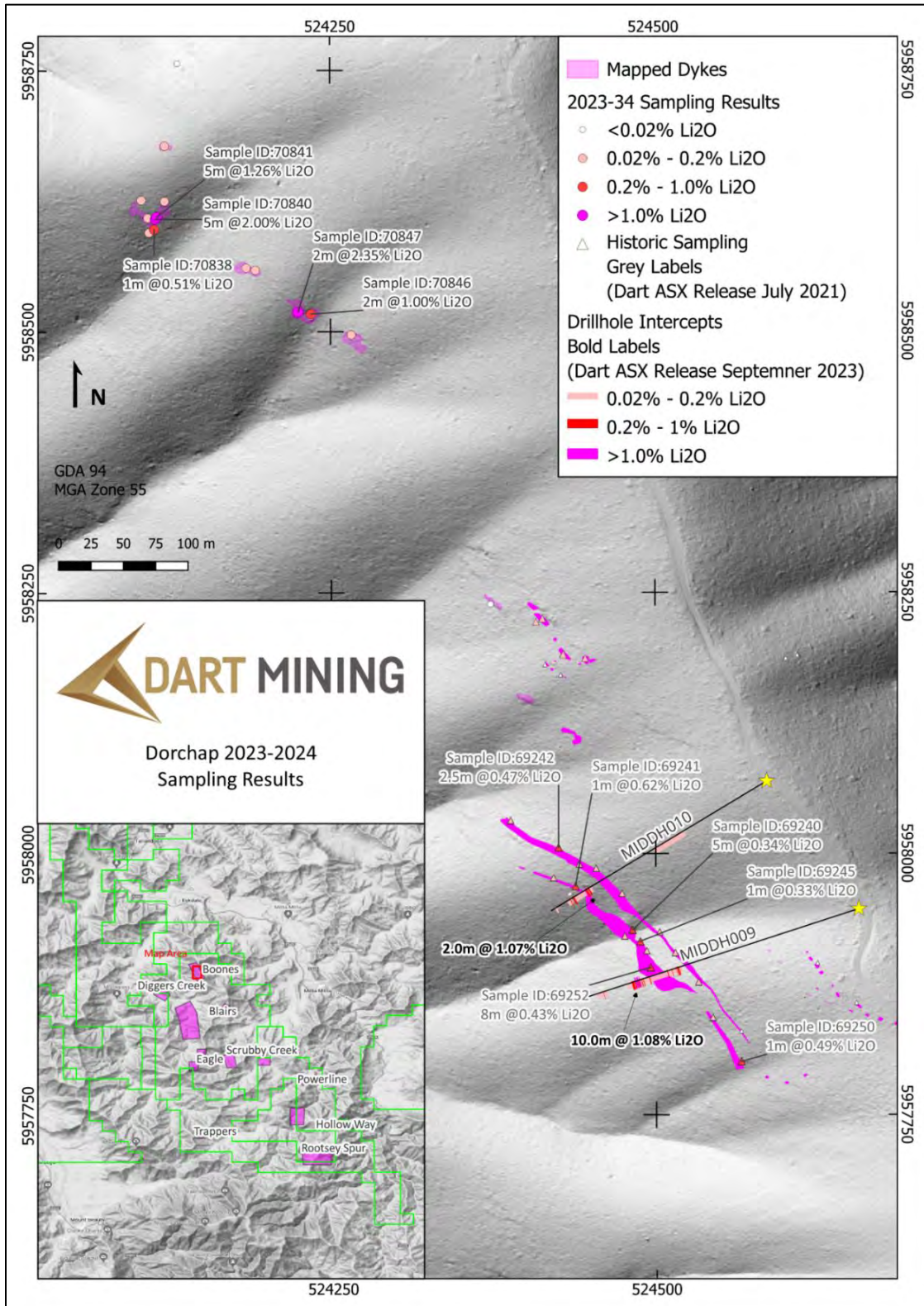


Figure 5. Dorchap 2023-2024 sampling results, including drillhole traces.

FUTURE WORK

Unfortunately, after the success of the drilling and sampling across the project during 2023 and 2024 the lithium price crashed early in 2024. Upon the improvement of sentiment around lithium exploration projects the company plans to continue with our exploration efforts at the project.

The company is currently progressing a work plan application for accessing the Gosport region of the project. The Gosport region is situated in the middle of the prospective corridor and fractionation zone. Gosport provides one of the more compelling targets with some of the projects highest rock chip sample grades returned from multiple dykes in close proximity providing both grade and tonnage prospectivity. Approximately 3,000m of diamond drilling is planned from several sites along a 2km planned access track.

Further low impact drilling is also planned, following up on the successful 2023 drilling campaign as well as testing the northern extension of the Boons Dyke. Drill access is planned from Dorchap Track, under low impact guidance to drill test the northern extension of the dyke.

SUMMARY

The Dorchap Range is host to a LCT prospective pegmatite dykes which show significant potential to host economic grades of Lithium. Since the discovery of lithium potential by Dart Mining in 2016 the company has taken over 950 samples across the project and defined a critical geochemical fractionation zone and corridor of pegmatite outcrop showing elevated lithium grades.

Drilling has confirmed the continuation of lithium prospectivity at depth below outcropping pegmatites. The diamond drilling has identified some key mineralogical and structural components of Pegmatite emplacement, and each drill hole shines new light on what is a compelling region.

REFERENCES

BRADLEY, D. C., MCCAULEY, A. D. & STILLINGS, L. M., 2017. Mineral-deposit model for lithium-cesium-tantalum pegmatites. *U.S. Geological Survey Scientific Investigations Report 2010–5070–O*, 48 p., <https://doi.org/10.3133/sir20105070O>.

DART MINING NL, 2016. ASX Announcement May 2016 – Exploration Tenement Update.

DART MINING NL, 2016. ASX Announcement August 2016 – Company Update – Lithium.

HINES, B.R., TURNBULL, D., ASHWORTH, L., MCKNIGHT, S., 2023. Geochemical characteristics and structural setting of lithium-caesium-tantalum pegmatites of the Dorchap Dyke Swarm, northeast Victoria, Australia.

STATE OF PLAY FOR MINERAL EXPLORATION IN THE TASMANIDES 2022-2024

John Greenfield

Consultant Geologist

Key Words: Tasmanides, mineral exploration, mineral deposit discovery, exploration drilling.

INTRODUCTION

The aim of this study is to provide a snapshot of mineral exploration progress in the Tasmanides of eastern Australia dating from the last 'Discoveries in the Tasmanides' Conference in May 2022.

The Tasmanides refers to the geological province in the eastern third of Australia comprising north-south trending, Neoproterozoic to Mesozoic arc to back-arc volcano-sedimentary sequences, affected by five overlapping orogens plus a Permian-Triassic rift to foreland basin system (Fig. 1). The Tasmanides underlie five Australian state jurisdictions with a long and successful history of exploration and mining activity (Queensland, New South Wales, Victoria, Tasmania and a narrow belt of South Australia).

In the review period May 2022-2024, despite weak global financing, particularly for junior explorers, exploration expenditure in the Tasmanides was still at historic highs although coming down slightly from a post-pandemic peak in March 2022. This contrasted with national drilling data which has been in steady decline in drilling activity since March 2021.

The top 30 publicly reported precious/base metal drilling intersections (May 2022-May 2024) have been highlighted from the Tasmanides, with AuEq gram*metre values over 200 (Appendix 1). The standout intercept for the two-year period was Southern Cross Gold's Sunday Creek project, with 455 m @ 7.2 g/t Au, 0.3 % Sb from 335 m reported in March 2024. This was just one of ten 200+ AuEq gm*m intercepts reported at Sunday Creek between May 2022 and May 2024.

Notes on data used

The Australian Bureau of Statistics (ABS) and S&P Global exploration expenditure and drilling data for Queensland, NSW, Victoria and Tasmania in this study have been used as a proxy to Tasmanides data, since ABS and S&P Global sub-divide jurisdiction data for Australia into state and territory subsets. Thus, there are slightly inflated state expenditures due mainly to the inclusion of Broken Hill and Mt Isa exploration data, but on balance, it is missing South Australian data from the narrow belt of Delamerian Orogen ground that lies along the eastern South Australian border (Fig. 1).

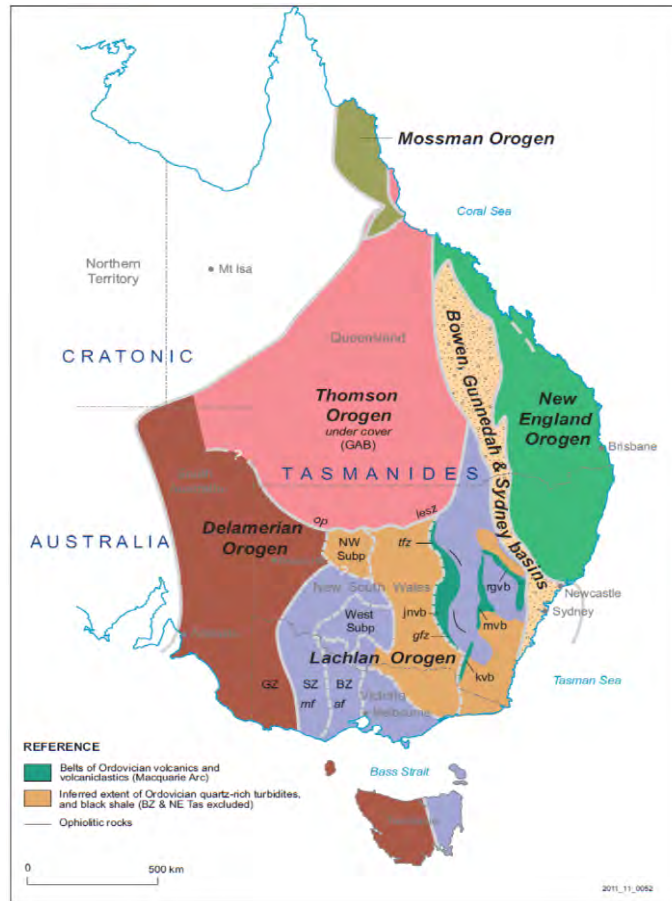


Figure 1. Tasmanides of eastern Australia (source: Glen et al. 2012). (BZ = Bendigo Zone; GAB = Great Australian Basin; GZ = Grampians-Stavely Zone; SZ = Stawell Zone. Macquarie Arc belts: jnvb = June-Narromine Volcanic Belt; mvb = Molong Volcanic Belt; rgvb = Rockley-Gulgong Volcanic Belt; kvb = Kiandra Volcanic Belt. Faults: af = Avoca Fault; mf = Moyston Fault; ggz = Gilmore Fault Zone; lesz = Louth-Eumarra Shear Zone; op = Olepoloko Fault; tfz = Tullamore Fault Zone).

GLOBAL TRENDS 2022-2024

In May 2022, at the eighth edition of Discoveries in the Tasmanides, the mood at the conference was upbeat; exploration budgets and metal prices were at a nine-year high, supported by renewed industrial activity and bullish post-pandemic investment. Recent iconic Tasmanides discoveries were presented at the conference – Alkane Resources’ Boda and Tomingley extensions, Stavely Minerals’ Cayley Lode, Aurelia Metals’ Federation, Aeris Resources’ Constellation, and Peel Mining’s Southern Cobar Basin deposits.

Two years later, the mood has dampened, with military conflicts and rising inflation resulting in lower metal prices (except gold and silver) and patchy investment. Capital raisings for ASX explorers have been on the decline since January 2022 (source MinEx consulting, BDO). Miners have seen their operational costs rise, curbing profits despite record gold and strong silver prices. The global average all-in-sustaining-cost for gold production has been rising since 2016 and reached a record high in Q1 2024 at US\$1425/oz (source: World Gold Council). In the case of nickel and zinc, the dramatic increase in supply has compounded bear market conditions and resulted in many Australian operations coming under pressure.

To sum up the mood, the global mining aggregate market cap slipped from \$2.58 trillion in March 2022 to \$1.89 trillion in October 2023 (source: S&P Global Market Intelligence). At home in Australia, resource stocks on the ASX200 fell 11.1% between January and July 2024, and for all ASX resource stocks, micro-cap Juniors have suffered the most, dropping 70% in value since April 2022 (Lion Selection Group 2024).

TASMANIDES EXPLORATION 2022-2024

Despite the state of the global market and local investment, exploration and mining activity in Australia and the Tasmanides has continued apace between 2022-2024. Mining development approvals in the Tasmanides, particularly in NSW, have increased, while 18 maiden inferred/indicated resources have been announced (plus several mineral resource estimates [MRE], e.g. in January 2024 Sky Metals released updated MRE for Tallebung NSW estimating 15.6 Mt @ 0.15% tin for 23kt of contained tin).

Gold majors Newmont and AngloGold Ashanti resumed generative exploration in the Macquarie Arc of NSW, including a range of joint ventures, and Newmont’s acquisition of Newcrest in November 2023, signalled a new era for eastern Australia’s most productive and profitable metal mine, Cadia Valley Operations. Evolution Mining also increased its presence in the Macquarie Arc with the December 2023 purchase of China Molybdenum’s 80% stake in Northparkes Mine.

National exploration expenditure has been on an upward trajectory to record levels from a peak in the first half of 2016 on the back of strong West Australian performance (Fig. 2). According to BDO, recent national expenditure was dominated by junior and mid-tier explorers, with a 23% increase in small- to mid-cap companies that spent between \$100,000-300,000 in 2023.

Expenditure in Tasmanide states (Qld, NSW, Vic, Tas) has followed the rise in expenditure since 2016, albeit at a shallower trajectory. Expenditure has flatlined in the last two years (Fig. 2). However, it is still at a healthy \$287m average spend per quarter.

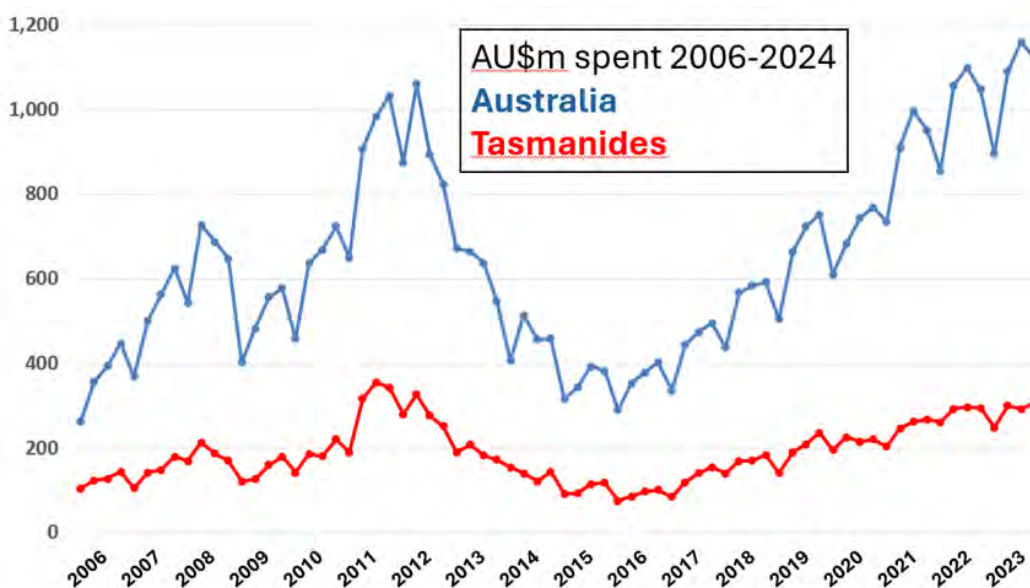


Figure 2. Australian Mineral exploration expenditure from March 2006 to March 2024. Australian Bureau of Statistics data. Tasmanides data comprises combined Tasmania, Victoria, NSW and Queensland data.

DRILLING SUCCESS

With healthy exploration expenditure in Australia and the Tasmanides in the last two years, you would expect drilling activity to follow suit, however drilled metres in Australia have steadily declined from a quarterly peak of 3,644m in June 2021 to 1,999.3m in March 2024 (Fig. 3). This may reflect increased administrative costs imposed on exploration companies which have reached unprecedented levels (BDO Dec 2023 Quarterly Cash Update), resulting in less budget available for drilling.

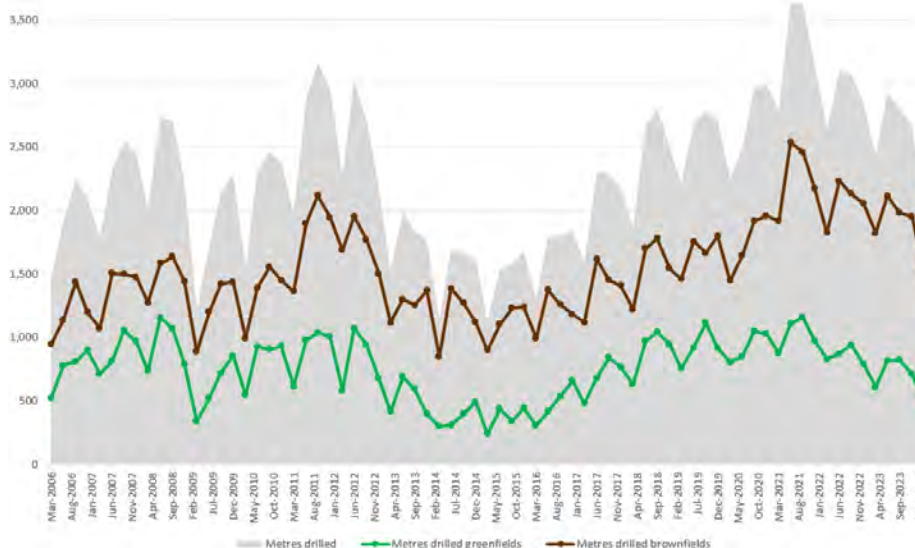


Figure 3. Mineral exploration drilling metres March 2006 to March 2024. Australian Bureau of Statistics data. Greenfields data are ABS-defined “new deposits” and brownfields data are “existing deposits”.

According to Opaxe, in 2023, Australia had 431 ASX-listed mining companies releasing 1,366 drilling results announcements, the majority for gold. Drilling results in the Tasmanides were encouraging. S&P Global recorded 516 precious and/or base metal drill intercepts at 169 projects from listed stock markets between May 2022 and April 2024 (Table 1). 60% of these intercepts were considered significant by S&P Global, and 84 achieved >200 AuEq gram*m.

Of the states, Victoria’s orogenic/epizonal deposits provided the best bang for buck, with the greatest proportion of quality intercepts recorded compared to the expenditure and number of projects with drilling results available.

Table 1. Summary of exploration performance in the Tasmanides from May 2022 to May 2024. Exploration data are from ABS, while project and intercept data are from S&P Global. *ABS exploration expenditure data are jurisdiction-wide, which has the effect of slightly inflating data for Queensland and NSW via exploration of Proterozoic deposits.

Jurisdiction	Expenditure 1/4/22>1/4/24	# Projects	# intercepts	# >200 AuEq g*m
Queensland	\$1,156m*	51	145	18
NSW	\$716m*	68	213	32
Victoria	\$327m	34	116	29
Tasmania	\$81m	16	42	5

THE TOP 30 DRILL RESULTS SINCE MAY 2022

The top 30 publicly reported precious/base metal drilling intersections (May 2022-July 2024) have been highlighted from the Tasmanides, with AuEq gram*metre values over 200 (Figure 4, Appendix 1). Only the best intercept from each project has been chosen to improve the spread of deposits.

The quality of the intercepts is impressive given the market conditions of the last two years, although only nine of the projects could be considered modern Greenfields targets (Fig. 4). The standout intercept for the two-year period was Southern Cross Gold’s (spun out of Mawson Gold) Sunday Creek project, with 455 m @ 7.2 g/t AuEq (7.2 g/t Au, 0.3 % Sb) from 335 m reported in March 2024. This was just one of ten 200+ AuEq gm*m intercepts reported at Sunday Creek in the study period. A key feature of the Sunday Creek drill results is the substantial true width of mineralisation in many holes. This contrasts with other orogenic gold projects where the high-grade mineralised intervals are less than 10m in true width.

Gold is the dominant metal sought after in the Tasmanides, and therefore, it’s not surprising it features strongly in these results. In contrast, copper-mineralised intervals were over 500m wide at Bottletree, Mt Cannindah and Boda, plus an outstanding 8.9% Cu over 50.4m at CSA in Cobar. Silver-rich base-metal hits in NSW were drilled at Cobar and southern New England, with the Greenfields Achilles discovery hole in the Ural Volcanics continuing to extend modern exploration potential further south in the Cobar Basin. The resurgence of tin as a critical mineral was reflected in substantial hits at Doradilla, North Scamander (with silver) and a standout 26.9m @ 4.57% Sn at Renison tin mine.

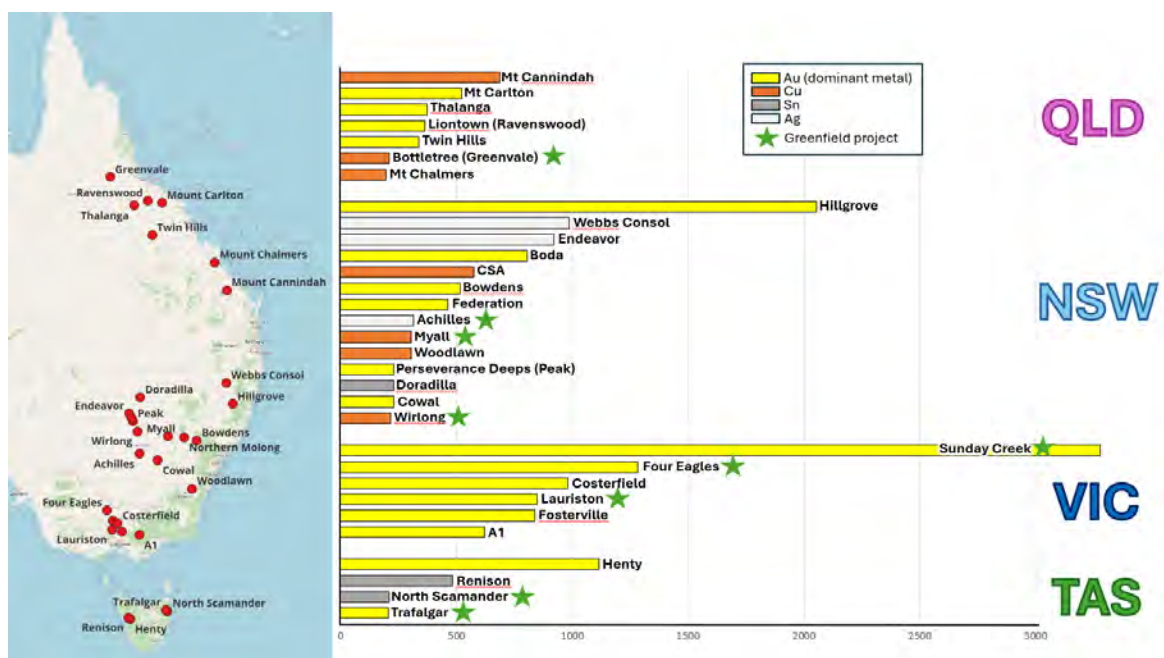


Figure 4. Standout drilling intercepts recorded between May 2022 and July 2024. Refer to Appendix 1 for more drilling intercept details.

CONCLUSIONS

Despite strong progress for mining in the Tasmanides based on resource definitions and mine approvals, this has been a very tough two years for mineral exploration. Very solid exploration expenditure in the Tasmanides was at odds with systemic decline in drilling activity. Microcaps have been particularly hard hit, and funding has dried up for explorers on the ASX and TSX in particular. The good news is that there was a decent success rate with the drilling that was recorded, with exceptional hits for gold (e.g. Sunday Creek), silver (e.g. Webbs Consol), copper (e.g. Mt Cannindah) and tin (e.g. Renison).

REFERENCES

LION SELECTION GROUP, 2024. Lion Selection Update July 2024. From website: <https://lionselection.com.au/>

APPENDIX 1

Table 2. Thirty-one highlighted drilling intercepts from projects in the Tasmanides.

AuEq gm*m	Project name	Reported by	Date reported	Main Metal	Interval	Hole ID
3278	Sunday Creek	Southern Cross Gold Ltd.	5/03/2024	Gold	455.3m @ 7.2 g/t Au from 335m	SDDSC107
2053	Bakers Creek (Hillgrove)	Larvotto Resources Ltd.	8/04/2024	Gold	31m @ 65.8g/t Au from 244m	BKC015
1282	Four Eagles	Catalyst Metals Ltd.	1/06/2023	Gold	6.5m @ 197.2 g/t Au from 293.8m	FEDD150
1116	Henty	Catalyst Metals Ltd.	5/09/2022	Gold	8.7m @ 129 g/t Au from 45.6m	Z22563
986	Webbs Consol	Lode Resources Ltd.	1/02/2023	Silver	116.1m @ 254g/t Ag, 0.02 g/t Au, 0.24% Cu, 8.35% Zn, 6.35% Pb from 90.9m	WCS045
979	Costerfield	Mandalay Resources Corp.	13/09/2022	Gold	1.5m @ 129 g/t Au from 60.8m	BC262
921	Endeavor	Polymetals Resources Ltd.	17/04/2023	Silver	81m @ 1.15 g/t Au, 473 g/t Ag, 5.5% Pb, 7.4% Zn, 0.11% Cu from 77m	MET_1LS_1
848	Lauriston	Great Pacific Gold Corp.	11/01/2024	Gold	8m @ 129 g/t Au from 95m	CRC007
838	Fosterville	Agnico Eagle Mines Limited	15/02/2024	Gold	5.6m @ 129 g/t Au from 89.1m	UDH4834
806	Northern Molong (Boda)	Alkane Resources Ltd.	4/08/2023	Gold	1,601.9m @ 0.30g/t Au,	BOD121

State of Play for Mineral Exploration in the Tasmanides

					0.15% Cu from 256m	
687	Mount Cannindah	Cannindah Resources Ltd.	15/08/2022	Copper	1022m @ 0.31% Cu, 0.2 g/t Au, 5.5 g/t Ag from 64m	22CAEDD011
621	A1	Kaiser Reef Ltd.	2/05/2022	Gold	4.6m @ 129 g/t Au from 36m	A1UDH-472
575	CSA	Metals Acquisition Ltd.	11/09/2023	Copper	50.4m @ 8.9% Cu, 36 g/t Ag from 170.6m	UDD20134
523	Mount Carlton	Navarre Minerals Ltd.	15/09/2022	Gold	22.7m @ 22.7 g/t Au, 28.5 g/t Ag from 96m	BV1DD005
515	Bowdens	Silver Mines Ltd.	12/09/2022	Gold	131m @ 0.49 g/t Au, 16 g/t Ag, 0.25% Zn from 65m	BD22029
482	Renison	Metals X Ltd.	26/09/2022	Tin	26.9m @ 4.57% Sn, 0.14% Cu from 225.1m	S1671
463	Federation	Aurelia Metals Ltd.	15/08/2022	Gold	20m @ 12.5 g/t Au, 13.2% Pb, 13.6% Zn, 19 g/t Ag, 0.8% Cu from 499m	FDD184W5
375	Thalanga	Sunshine Metals Ltd.	5/02/2024	Gold	17m @ 22.05 g/t Au from 67m	23LTRC002
364	Liontown (Ravenswood)	Sunshine Gold Ltd.	13/03/2024	Gold	20m @ 18.2 g/t Au from 114m	24LTRC005
337	Twin Hills	GBM Resources Ltd.	23/05/2022	Gold	186m @ 1.77g/t Au, 3.43g/t Ag from 47m	309DD22006
316	Achilles (South Cobar)	Australian Gold & Copper	4/06/2024	Silver	43m @ 2.20 g/t Au, 219 g/t Ag, 0.1% Cu, 1.1% Pb, 2.5% Zn from 99m	A3RC030
305	Myall	Magmatic Resources Ltd.	20/03/2023	Copper	875.2m @ 0.21% Cu, 0.04g/t Au, 0.50g/t Ag from 146.8m	23MYDD422
304	Woodlawn	Develop Global Ltd.	15/05/2023	Copper	75m @ 2.10% Cu, 3.10% Zn, 8.90g/t Ag from 351m	23WNUD00011
229	Doradilla	Sky Metals Ltd.	1/05/2024	Tin	81m @ 0.48% Sn from 5m	3KDD018

State of Play for Mineral Exploration in the Tasmanides

229	Perseverance Deeps (Peak)	Aurelia Metals Ltd.	20/10/2023	Gold	13m @ 17.6 g/t Au	UD23PD0526
228	Cowal	Evolution Mining Ltd.	17/01/2024	Gold	63.7m @ 2.49% Au from 91m	RDU0062
217	Wirlong	Peel Mining Ltd.	10/11/2022	Copper	82m @ 2.07% Cu, 5 g/t Ag from 425m	WLDD077
210	North Scamander	Stellar Resources Ltd	19/09/2023	Tin	32m @ 141 g/t Ag, 0.34% Sn, 3.8% Zn, 2.0% Pb, 77 g/t In & 19 g/t Ga from 130m	NSD005
210	Bottletree (Greenvale)	Superior Resources	2/06/2022	Copper	632m @ 0.21% Cu	BTDD004
207	Trafalgar	Flynn Gold	14/02/2023	Gold	12.3m @ 16.8 g/t Au from 108.7m	TFDD005
197	Mt Chalmers	QMines Ltd	13/06/2022	Copper	69m @ 0.55g/t Au, 2.50g/t Ag, 1.62% Cu from 137m	MCRC012

PATHFINDER ELEMENT FOOTPRINTS OF EASTERN AUSTRALIAN MINERAL DEPOSITS

Scott Halley,

Mineral Mapping Pty Ltd

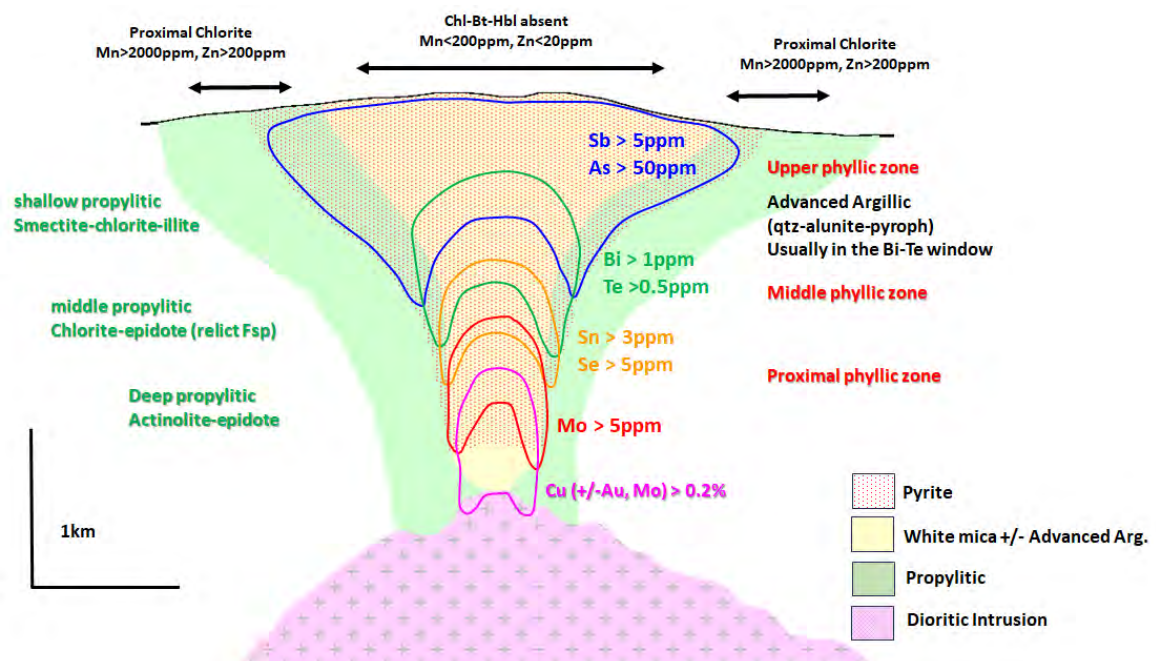
Key words: pathfinder elements, mineral deposits, eastern Australia.

INTRODUCTION

Pathfinder elements increase the detectable footprints of mineral deposits because they have a wider spatial distribution than the commodity metals being sought. The most useful elements are those that are hosted in common alteration minerals such as pyrite, white mica or chlorite. Since those minerals have a wide distribution, every sample within the anomalous footprint of a particular element returns an anomalous value, i.e. every sample is likely to contain pyrite or muscovite or chlorite, thus give an anomalous result for the pathfinders contained in that mineral. That increases the likelihood that any one sample will be representative of a larger volume of rock, and it reduces the number of samples needed in order to detect the footprint of a hydrothermal system.

Porphyry Cu deposits, for example, have the same metal zoning patterns and relative abundance of elements regardless of their geographic location. This indicates the patterns are controlled by the same chemical and physical processes, more so than local factors.

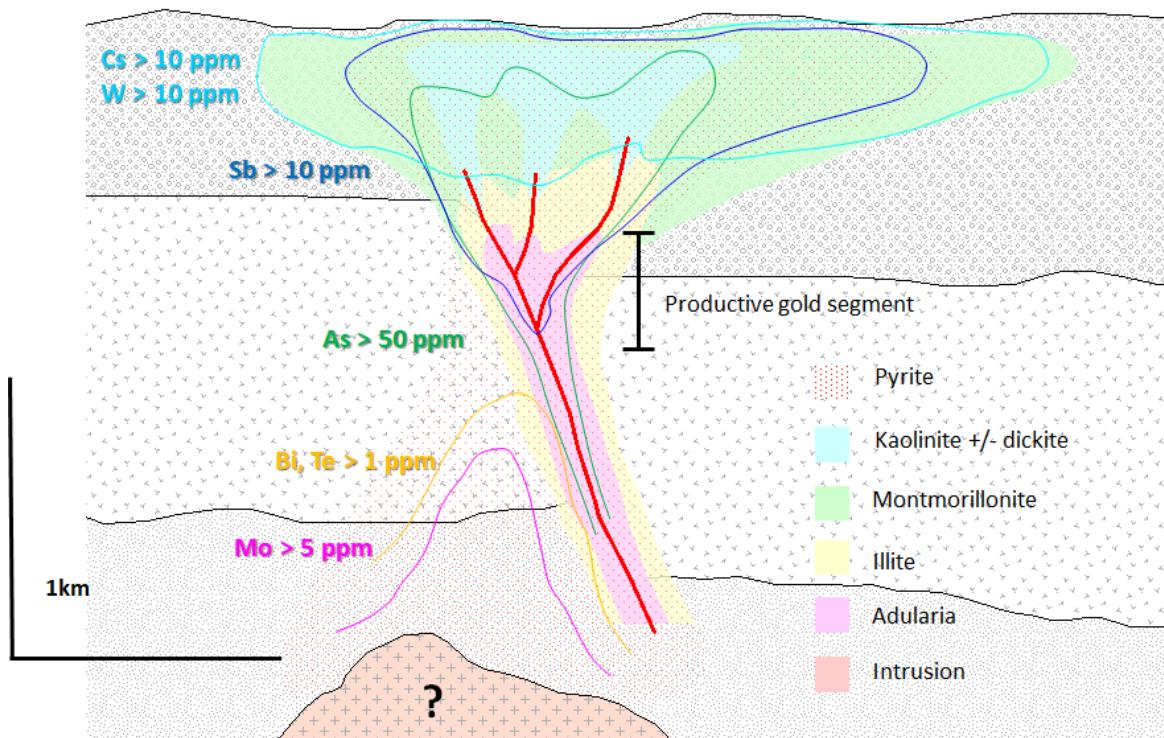
PORPHYRY COPPER PATHFINDERS



In the outflow zone above and laterally from porphyry centers there is a metal zoning; Mo - Se - Sn - Te - Bi - As - Sb. Sn occurs in the most proximal white mica. Mo, Se, Te, Bi, As, Sb are hosted in pyrite and are accommodated sequentially in the pyrite lattice as temperature declines (Halley et al., 2015). The pathfinder element zoning pattern around

a porphyry system is a proxy for temperature, regardless of whether the pyrite is associated with phyllic or advanced argillic alteration. In acid alteration zones, ie phyllic and advanced argillic, where Fe-Mg silicates are replaced, Mn and Zn in particular are stripped from the rock. These metals tend to be enriched on the margins of the acid alteration where there is enough relict feldspar to neutralise the acid. Mn is enriched in chlorite and/or carbonates and Zn is enriched in chlorite and/or sulfides in propylitic alteration on the margins of the phyllic zones.

LOW SULFIDATION EPITHERMAL PATHFINDERS

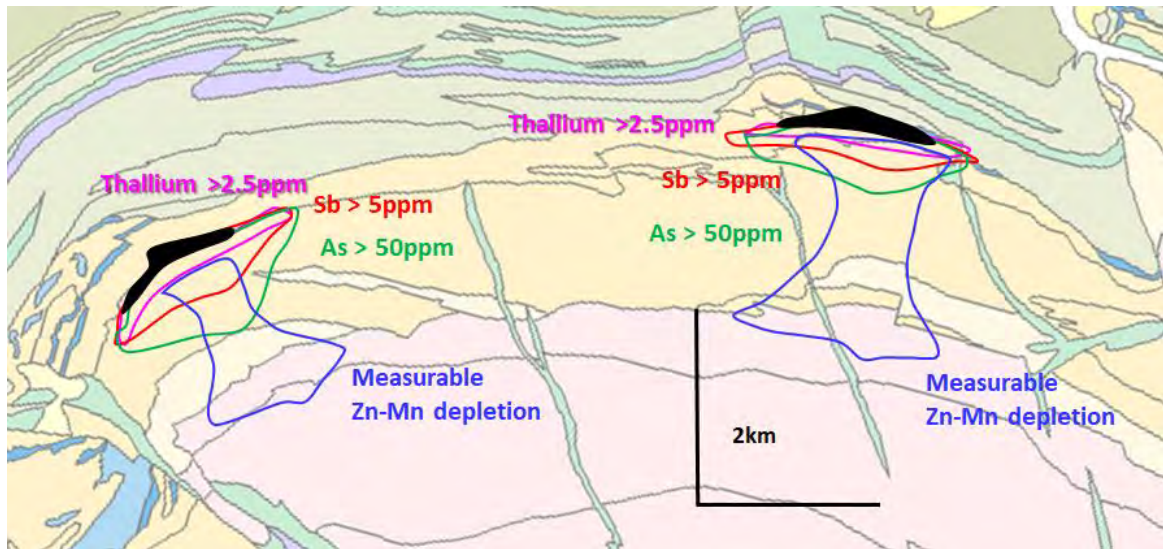


Epithermal systems are dominated by low temperature fluids. In active geothermal systems, antimony values above 2ppm and cesium above 10ppm are mostly limited to within 1km of the surface and are precipitated at temperatures less than 200 degrees (Chambefort and Dilles, 2023). In the near surface environment, it is common to see lateral fluid flow producing extensive clay blankets. Sb is a proxy for low temperature pyrite. Cs, Li and W are proxies for low temperature phyllosilicates. In LSE systems eroded to deeper levels, it is common to see anomalous Mo-Bi-Te zones that are likely fed by upwelling magmatic fluids. At a prospect scale, the association of elements should make it possible to determine the level within the system, and the outflow from blind LSE ore shoots should be evident (Thompson et al., 2023).

VMS PATHFINDERS

In VMS systems, hydrothermal fluids quench directly into cold seawater. A characteristic of this is pyrite containing high levels of thallium. Pyrite in the massive sulfide and in the footwall quartz-sericite-pyrite +/- chlorite alteration contains high levels of As-Sb-Tl. Systems that have a direct magmatic contribution also have high levels of Bi and Te deeper in the stringer zones. In the acid footwall alteration zones there is a measurable

depletion in zinc and manganese especially. Where the host sequence has been sufficiently tilted but not dissected by faulting, the depletion zones might be traceable back to an underlying granite pluton (Brauhart et.al, 2001).



SAMPLING STRATEGIES

ICP-MS analysis is required to achieve suitable detection limits for elements such as Sb, Bi, Te, Se, Sn and W. A 4-acid digestion is required to liberate elements contained within silicate minerals and refractory oxide phases. Sampling in-situ bedrock material is strongly preferred rather than partial leach or ultra-fine fraction methods in transported overburden, ie a pattern of aircore drilling to obtain bedrock samples. For any system of a substantial size, a sampling pattern of 400m by 400m should be sufficient. This pattern is certainly adequate in first-pass exploration of porphyry Cu deposits. The big advantage of using pathfinder signatures in deeply weathered regolith profiles is that elements such as Mo, Bi, Te, As, Sb etc form oxy-anion complexes which are relatively immobile in the regolith, even where Cu, Zn, Au and Ag are strongly leached and depleted.

REFERENCES

BRAUHART, C.W., HUSTON, D.L., GROVES, D.I., MIKUCKI, E.J. AND GARDOLL, S.J., 2001. Geochemical mass-transfer patterns as indicators of the architecture of a complete volcanic-hosted massive sulfide hydrothermal alteration system, Panorama district, Pilbara, Western Australia. *Economic Geology*, 96(5), pp.1263-1278.

CHAMBEFORT, I. AND DILLES, J.H., 2023. Chemical vectoring in continental geothermal systems: Composition of altered rocks and illite as guides to magmatic degassing. *Geothermics*, 110, p.102682.

HALLEY, S., DILLES, J.H. AND TOSDAL, R.M., 2015. Footprints: Hydrothermal alteration and geochemical dispersion around porphyry copper deposits. *SEG newsletter*, (100), pp.1-17.

THOMSON, B., PRATT, W.T., RHYS, D.A., OLIVER, N.H., HALLEY, S.W., FISCHL, P., AKININ, V.V. AND DOTZOV, D., 2023. The Kupol Epithermal Au-Ag Vein District, Chukotka, Far Eastern Russia. *Economic Geology*, 118(1), pp.93-122.

THE GEOLOGICAL HISTORY OF THE WIRLONG CU-AG DEPOSIT, COBAR BASIN, NEW SOUTH WALES

Sebastian Hind¹ and Carol Simpson²

¹ Peel Mining Limited, ² Consultant Geologist

Key words: Woorara Fault, John Owen Fault, Shuttle Fault, Wirlong, Shume Formation, Shuttleton Rhyolite Member, Basin inversion

INTRODUCTION

Wirlong is a high-grade Cu-Ag deposit located ~80km SSE of Cobar and ~35km N of Peel Mining's flagship Mallee Bull Cu-Ag-Au-Pb-Zn deposit. Copper was initially discovered on the 'Wirlong Run' in November 1900 by the legendary prospector John "Jacky" Owen and co-discoverer Thomas Shuttle. Following the discovery, several small shafts and shallow pits were sunk to exploit it, with the deepest, Star of the West, reaching 200ft (Polkinghorn, 1906). However, upon the sinking of these shafts, the presence of copper mineralisation was attributed to the secondary enrichment of narrow zones of near-surface chalcopyrite, leading to the abandonment of the area (Voisey, 1949).

Over a century later, in late 2015, Peel Mining drilled WLRCD015 and WLDD001 to test Bouguer gravity and conductive DHEM anomalies beneath a multi-element surface geochemical anomaly located approximately 1.5km north of the historic Star of the West mine. WLRCD015 yielded 4.9m @ 4.3% Cu, 13 g/t Ag from 402.1m, while WLDD001 returned 9m @ 8.0% Cu, 17 g/t Ag & 0.21 g/t Au from 616m (Peel Mining ASX release 19th January 2016), marking the discovery of high-grade copper at the prospect. In early 2020, WLDD003, WLDD004 & WLDD005 confirmed the discovery and orientation of the chalcopyrite-dominant ore body, which has since been proven to host a JORC 2012 indicated and inferred resource of 4.3 million tonnes at 1.75% copper and 6 g/t silver (Peel Mining ASX release 9th January 2023).

ACKNOWLEDGEMENTS

This study builds on previous and ongoing work by Peel geologists without whom the generation of the current model would not have been possible. We particularly acknowledge contributions made by Sunao Mochizuki (JOGMEC), Martin Scott, Jun Cowan, Steve Garwin, Bob Brown and Mel Quigley. We thank Dave Edgecombe for his input and passion, Rob Tyson for his constant backing of the field team, Angus Hornabrook for his extensive knowledge and teachings and Mick Oates for enabling the generation of the current model and being the glue that held the field team together during a resource drill out that took place in winter during a COVID-19 lockdown.

REGIONAL GEOLOGY

The Wirlong deposit occurs in the central southern part of the Cobar Basin at the boundary between a deep water turbidite sequence (Shume Formation) and coherent rhyolite (Shuttleton Rhyolite Member) (Fig. 1). The eastern margin of the deposit is proximal to (<2km), and west of, the NNW-trending Woorara Fault, a major Cobar Basin structure that extends to the Lake Cargelligo area in the south. The sedimentary succession at Wirlong is proposed to sit between the informally defined lower and upper parts of the Amphitheatre Group. The lower Amphitheatre Group has been interpreted as belonging to the rift phase of the Cobar Basin (Glen, 1994 & Fitzherbert & Downes,

2021) and the upper Amphitheatre Group to the sag phase with the Shume Formation thereby marking the transition.

The Shuttleton Rhyolite Member is wholly enclosed within the lower part of the Shume Formation and occurs as a series of four north-striking lenses within the sedimentary package (MacRae, 1987). The Wirlong deposit occurs at the northern end of the best exposed, eastern-most lens, which outcrops relatively well over a strike length of ~6km south to the Red Shaft prospect. The Shume Formation contains minimal fossils (Zhen et al., 2023) and its age is poorly constrained. Available fossil ages and correlation with other Cobar Basin units to the north has led various authors to propose an age spanning Lochkovian to Pragian (~412-408 Ma; MacRae, 1987, Jones et al., 2020). A sample of Shuttleton Rhyolite Member from the western part of the unit on the Shuttleton property has been SHRIMP U-Pb dated at 421.9 ± 2.7 Ma (Waltenberg et al., 2016), and a second sample from a drill hole into the Wirlong deposit has been SHRIMP U-Pb dated at 420.8 ± 1.9 Ma (Jones et al., 2020). Both dates are within error of each other and with dates from many other crystal-rich rhyolitic bodies in the Cobar Basin, including those at the Mallee Bull deposit.

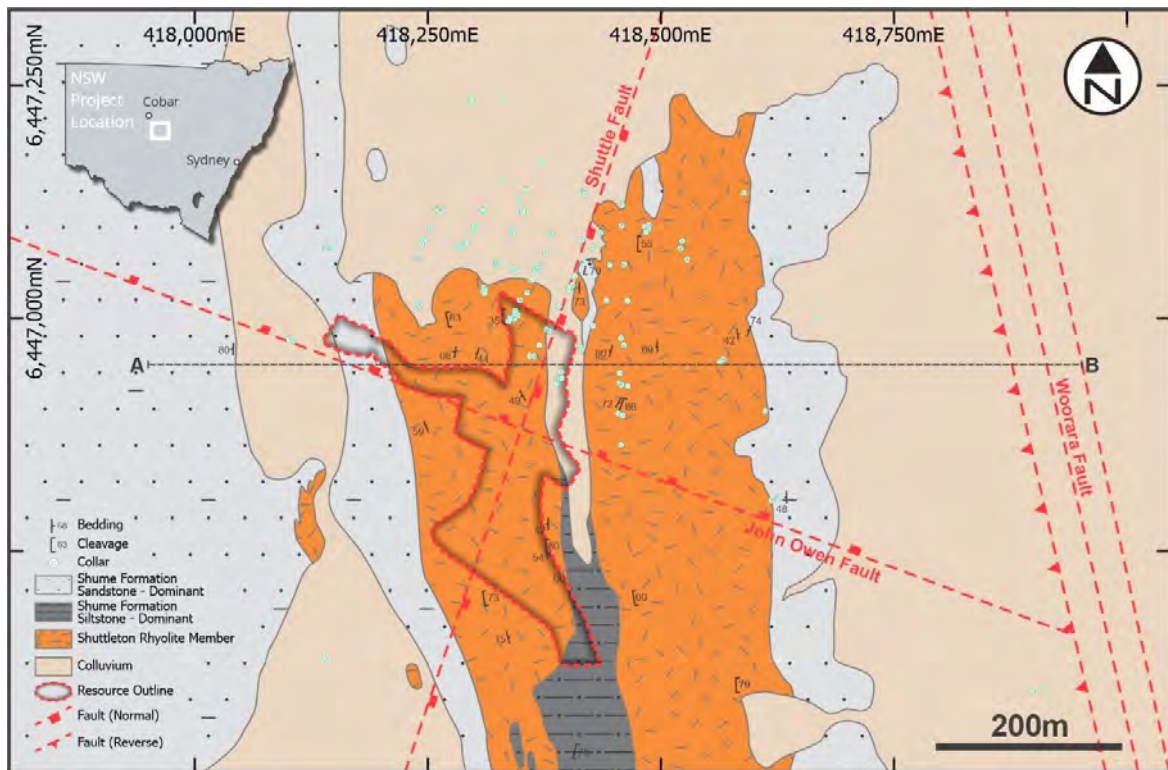


Figure 1. Geological map of the Wirlong deposit showing drillhole collars, location of major faults, outline of resource and section-line 6446900N (A-B). Modified from Brown (2016).

DEPOSIT GEOLOGY

Shume Formation

The Shume Formation at Wirlong is dominated by fine- to medium-grained sandstone (Fig. 2a), particularly below the level of the Shuttleton Rhyolite Member. Individual sandstone beds with variably sharp to loaded bed bases, range up to >10m thick. They are massive or planar laminated and ungraded or graded only in the upper few cm. Some sandstone beds are amalgamated into intervals up to >40m thick. Less abundant intervals of thinly bedded, very fine-grained sandstone occur, and these vary from massive to ripple cross-laminated and include mm- and cm-scale dark siltstone. There are also rare intervals of massive or planar laminated siltstone up to ~20m thick.

Evidence of soft sediment deformation is widespread within thinly bedded parts of the sequence, especially near rhyolite contacts and includes bedding distortion/truncation, cm-scale folds and microfaulting (Fig. 2b). Shume Formation sandstone beds are well sorted and texturally mature and composed of sub-rounded and sub-angular detrital quartz grains and up to ~20-25% lithic grains of micaceous siltstone and subordinate chert and trace amounts of detrital feldspar, muscovite and zircon (sublitharenite). Siltstone layers are composed predominantly of very fine-grained sericite and chlorite and subordinate quartz.

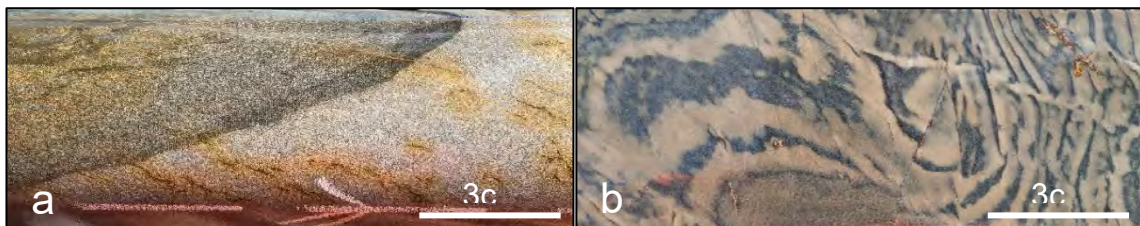


Figure 2. Drill core photographs (a) Fine-grained sandstone in sharp contact with medium-grained sandstone in WLDD012, 124.7m. (b) Soft sediment deformation of thinly bedded turbidites, including convolution of layering about disrupted sandstone layers and microfaults in WLDD012, 329.1m

Shuttleton Rhyolite

Drilling indicates the presence of an eastern, steeply west-dipping rhyolite (Eastern Rhyolite), up to approximately 150m wide, which is offset by the John Owen & Shuttle faults and a smaller, shallower rhyolite to the west of the eastern body (Western Rhyolite). A narrow, irregular screen of sedimentary rocks separates these two rhyolites. A third rhyolite occurrence at depth in the west of the deposit is inferred from only two drill intersections (Fig. 3) and is not described further.

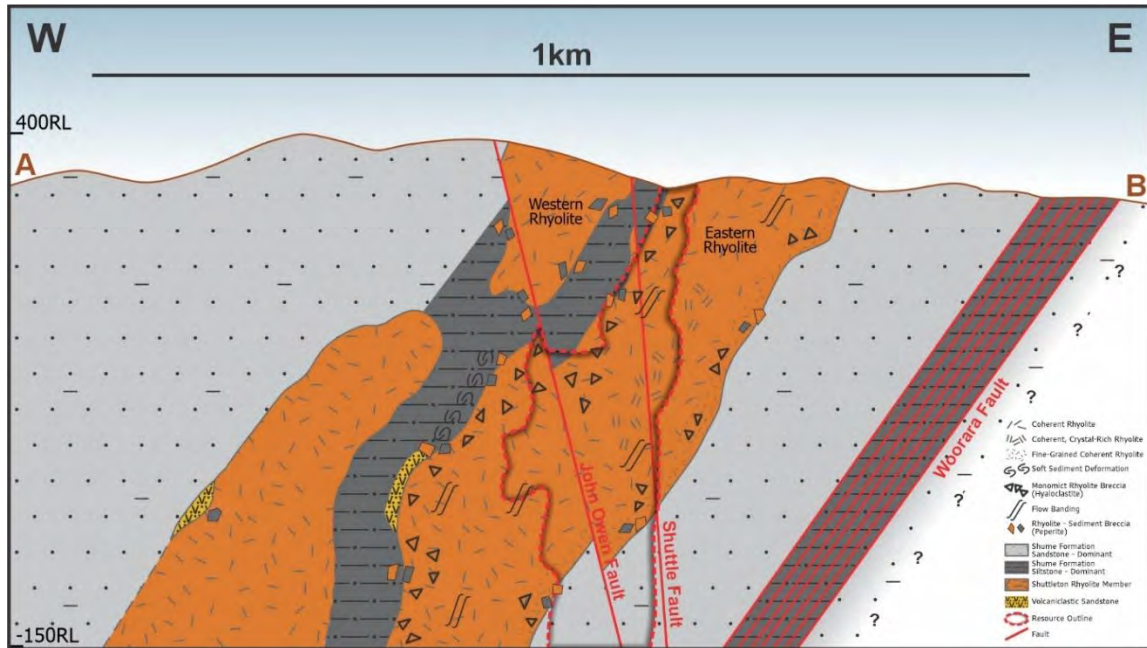


Figure 3. Schematic cross-section of the Wirlong deposit centered on line 6446900N displaying facies distribution, major faults and resource outline.

The Shuttleton Rhyolite Member exhibits six distinct facies. The most voluminous is the massive coherent rhyolite, predominant in both the Eastern and Western Rhyolite. This facies contains approximately 30-35% evenly distributed and non-fragmented phenocrysts of embayed quartz and euhedral feldspar (Fig. 4a), the latter including alkali feldspar and variably sericite, albite or alkali feldspar-replaced plagioclase. There are minor chlorite-replaced probable ex-hornblende phenocrysts and chlorite-sericite-replaced ex-biotite phenocrysts. The groundmass displays varying degrees of chlorite \pm sericite alteration that partly obscures a finely microcrystalline quartz-feldspathic aggregate, which in places retains perlitic, micropoikilitic or spherulitic textures, indicative of an originally glassy groundmass.

The second-most common facies is the monomict rhyolite breccia, predominantly found in the upper part of the Eastern rhyolite where intervals can range in thickness from tens of cm to >50m. The monomict breccia is matrix-supported and composed of dark, angular clasts of coherent rhyolite, which range from sub-mm size to >10-15cm, hosted within a pale, fine-grained and less crystal-rich matrix (Fig. 4b). They are interpreted as hyaloclastite, formed by quench fragmentation of originally glassy coherent rhyolite. This has produced a permeable, finely granulated matrix that supports residual clasts of intact rhyolite that have undergone considerably more intense chlorite-sericite alteration than adjacent coherent massive rhyolite. Clast-supported, unaltered primary autobreccia formed due to viscosity increase during cooling is present but much less common.

Distinctive rhyolite-sediment breccia is common although volumetrically minor and occurs at contacts between rhyolite and sedimentary rocks, mainly at upper rhyolite contacts. Ranging from a few cm to ~5m thick, it contains irregular clasts of fine-grained sediment within rhyolite and blocky clasts of rhyolite within disturbed sediment (Fig. 4c). Locally, individual fragmented phenocrysts from rhyolite occur within a matrix of siltstone. This breccia is interpreted as peperite, formed by non-explosive mixing

between rhyolite and unconsolidated wet sediment facilitated by quench fragmentation at rhyolite margins. Many breccia intervals exhibit intense sericite ± silica alteration and are strongly foliated.

Minor facies include finer-grained coherent rhyolite, likely representing chilled rhyolite against the cold, wet underlying sediment, and flow-banded rhyolite, characterised by alternating bands reflecting variable devitrification fabrics subsequently enhanced by domianial alteration (Fig. 4d) and reflects intervals of preserved higher viscosity within massive rhyolite. Rare volcanoclastic sandstone facies, occurs immediately above the rhyolite and consists of massive to diffusely planar laminated, texturally immature angular fragments of volcanic quartz, minor feldspar, and clasts of rhyolite groundmass.

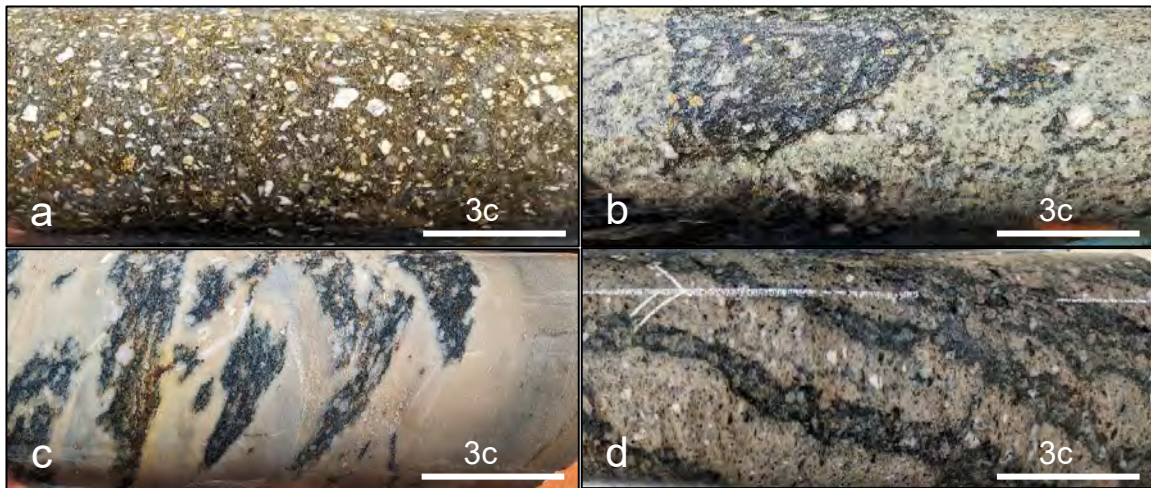


Figure 4. Drill core photographs (a) Massive, crystal-rich rhyolite in WLDD031, 91.7m. (b) Monomict breccia composed of dark chloritised rhyolite clasts within finely fragmented pale matrix in WLDD013, 212.2m. (c) Rhyolite-sediment breccia in which the sediment is silica-sericite altered in WLDD010, 219m. Note faint relict bedding on right of image (d) Flow banding enhanced by domianial alteration in rhyolite in WLDD012, 55.6m.

Depositional Setting and Mode of Rhyolite Emplacement

Our observations of the Shume Formation at Wirlong align with MacRae's (1987) interpretation as a sand-dominated proximal turbidite succession in a low-energy deep-water setting. The turbidites show a provenance of quartz-sedimentary lithics, likely sourced from uplifted Ordovician turbidites or the unroofed Erimeran Granite. Besides rare volcanoclastic sandstone beds, the Shume Formation lacks significant volcanic input.

The Shuttleton Rhyolite Member consists of medium- to coarse-grained crystal-rich rhyolite, varying from massive to strongly brecciated. Mostly intrusive, it forms sills within the Shume Formation near the basin floor, evidenced by widespread peperite at upper and lower contacts. Extensive quench fragmentation below upper peperitic contacts has produced hyaloclastite and together with abundant soft sediment deformation suggests contemporaneous sedimentation and rhyolite emplacement. Small amounts of the rhyolite appear to have locally breached the basin floor and been fragmented and slightly resedimented.

STRUCTURAL GEOLOGY

Bedding

Bedding (S_0) within the Wirlong deposit predominantly dips moderately to steeply westward but is locally overturned to steep easterly dips adjacent to the margins of the Shuttleton Rhyolite Member. Here, its emplacement into coeval, unconsolidated sediments has induced soft sediment deformation (Fig. 2b). Rare, graded bedding, load casts, and flame structures indicate a broadly upright, westward younging sequence. Primary flow-banding in the Shuttleton Rhyolite Member aligns parallel to S_1 cleavage (discussed below), however its orientation may vary significantly over short distances, suggesting that it represents a primary feature that has been transposed during regional deformation (D_1).

Cleavage

The dominant cleavage in the Wirlong deposit (S_1) typically dips moderately to steeply ENE, with an average dip/dip direction of 62/073, and is interpreted to have formed as a result of regional deformation (D_1) associated with basin inversion. The bulk of the strain from D_1 has been concentrated in thinly bedded sediments around the peripheries of the Shuttleton Rhyolite Member, giving rise to a distinct penetrative cleavage marked by intense chlorite. Within the Shuttleton Rhyolite Member, aligned white mica and ex-ferromagnesian minerals delineates a weak foliation parallel to S_1 that locally intensifies proximal to faults and shears. In the massive quartz-rich sandstones, very fine-grained pyritic stylolites faintly align to define S_1 (Fig. 2a).

A secondary, steeply west-dipping cleavage (S_2), averaging 78/259, becomes prominent at depth within the deposit, where 'drag' along the adjacent Woorara Fault has led to the rotation of S_1 . S_2 has primarily been identified in fine-grained sediments adjacent to the Woorara fault, where a strong penetrative cleavage defined by the alignment of chlorite is commonly exploited by narrow quartz veining and sulphides.

Slickenlines

The slickenlines observed at Wirlong mainly consist of quartz and chlorite, with pyrite, chalcopyrite, pyrrhotite, and arsenopyrite being less common. The planes on which slickenlines occur have an average dip/dip direction of 59/083, which is sub-parallel to S_1 (71/077), indicating that movement has taken place predominantly along cleavage planes. Furthermore, 87% of measured slickenlines have a reverse sense of movement with an average plunge/trend of 50/079, suggesting that they formed during reverse dip-slip movement along S_1 cleavage planes.

Folding

Bedding measurements and younging data collected from sedimentary features in diamond core have highlighted the presence of folds that range in style from open to isoclinal. Folding primarily occurs in sediments around the margin of the Shuttleton Rhyolite Member where the differing rheological properties of the two units has sponsored both brittle and ductile deformation during D_1 .

Faults

There are three major faults recognised at the Wirlong deposit: the John Owen fault, the Shuttle fault, and the regional-scale Woorara fault (Fig. 1). All three faults play a critical role in the localisation of ore-forming fluids and fault geometry and characteristics are key to understanding the distribution of mineralisation.

John Owen Fault

The John Owen fault is a WNW-ESE striking, steeply NNE dipping fault (Fig. 1 & 3) that has a damage zone approximately 40 meters wide. Geology (Fig. 3), geomorphology (discussed in Structural Architecture) and drilling (Fig. 5) indicate an oblique-slip fault with a sinistral shear sense that created local zones of dilation (extension) particularly within more brittle lithologies. This enabled the movement of mineralising fluids into pre-prepared structures and fabrics such as cleavages, fractures, breccias, and veins. Consequently, the orientation of mineralisation within the John Owen fault exhibits significant variability but generally manifests as a series of WNW-ESE striking, stacked en-echelon style lenses that exhibit an increase in grade and thickness towards the ESE. These stacked lenses collectively comprise the high-grade MBX domain, which contains 1.85Mt at 2.15% Cu & 7 g/t Ag (Peel Mining ASX release 9th January 2023).

The fault is most notably observed in drill core as an abrupt change in lithology, often marked by either brittle deformation or, more commonly, by mineralisation. At the surface, the fault has offset a prominent N-S striking ridge and manifests as narrow gossanous veins/breccias and a series of isolated, massive quartz veins ranging in thickness from <1m to >10m. While the fault has been mapped on the surface for over 1.3 kilometres, magnetic imagery (TMI, RTP & 1VD) reveals its continuation through the Cobar-Lyell Cu-Pb mine over ~5 kilometres to the northwest.

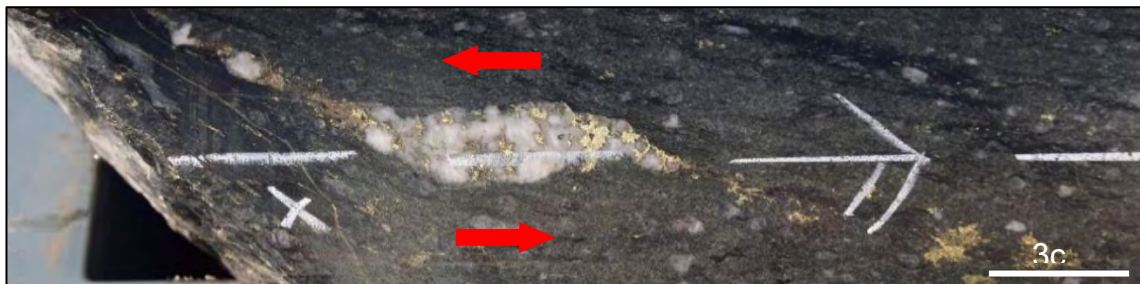


Figure 5. Quartz-chalcopyrite-pyrrhotite apparent sinistral dilatant jog hosted in Shuttleton Rhyolite Member from within the John Owen fault in WLDD024, 259.4m.

The Shuttle Fault

The Shuttle fault is a mineralising NNE-SSW striking, steeply ESE dipping fault (Fig. 1 & 3) that forms a conjugate structure to the John Owen fault. Compared to the John Owen fault, the Shuttle fault remains poorly understood, primarily because most of drilling conducted to date has been sub-parallel to its strike. However, geology (Fig. 3) and drilling tentatively suggests that the Shuttle fault is an oblique-slip fault that may have exhibited a dextral shear sense (Fig. 6). Mineralisation is presumed to have occurred syn-extension (discussed further in Geological History) during movement along the fault. Evidence for the presence of the Shuttle fault at surface is lacking due a thin layer of transported cover overlying the fault.

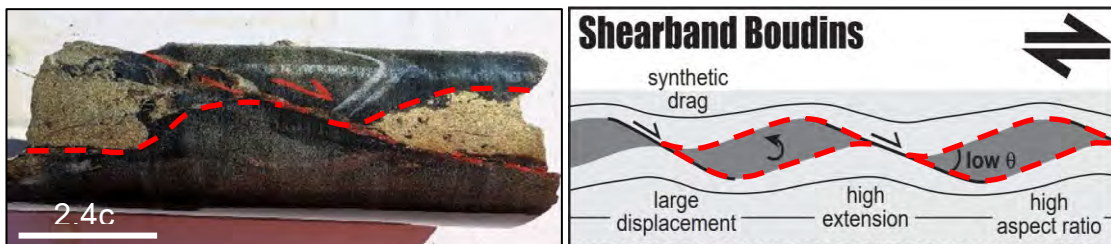


Figure 6. Chalcopyrite shearband boudins from within the Shuttle fault in WLRCD043, 739m with accompanying schematic diagram illustrating an apparent dextral sense of shear. From Goscombe & Passchier (2002).

Intersection Zone

The intersection of the Shuttle fault with the John Owen fault is accompanied by an increase in brittle deformation and created a zone of low stress (minimum σ_3) that drew in hydrothermal fluids to produce a thick, steeply SE plunging high-grade shoot (Fig. 7b). The best drill intercepts at the deposit such as 205m @ 1.4% Cu & 3 g/t Ag from 434m in WLDD040 (Peel Mining ASX release 27th October 2021) and 82m @ 2.07% Cu, 5g/t Ag from 425m in WLDD077 (Peel Mining ASX release 10th November 2022) have been returned from this intersection zone. Targeting the intersection zone down-plunge will be a key rationale for future, near mine exploration at the deposit.

The Woorara Fault

The Woorara fault is a regional-scale NNW-trending fault that dips ~55° west beneath the Wirlong deposit (Fig. 1 & 3) that appears to have exploited the contact between massive fine- to medium-grained sandstone and finer-grained, siltstone dominant units. The fault is interpreted by McRae (1987) as a listric growth fault that controlled the deposition of the Shume Formation and was subsequently reactivated as a reverse thrust fault during basin inversion in the Tabberabberan Contraction event (390-380 Ma) (Folkes & Stuart, 2020).

The fault is evidenced in drill core by thick intersections of intense silica-sericite alteration and intense fracturing and cataclastites that hosts sub-economic quantities of sulphides within narrow fractures and veins. Although the Woorara fault does not directly influence deposition of economic sulphides, it exerts an indirect influence through the development of a steeply west-dipping cleavage, S_2 which is proximal to the fault and has been exploited by Cu-rich fluids.

Structural Architecture

The current study proposes a conjugate fault system that formed during basin inversion (D_1), with a far-field direction of maximum shortening oriented NE-SW, as initially proposed by Glen (1990). Geomorphology supports this hypothesis, as topographic disruptions observed in satellite-derived imagery form conjugate lineament sets and indicate sinistral offset associated with the John Owen fault (Fig. 7a). Lithospheric shortening in the Wirlong area was accommodated through the formation of the conjugate John Owen and Shuttle faults and the reactivation of the Woorara fault, the latter resulting in the development of S_2 .

Transtension was present locally, evidenced by oblique normal movement along the John Owen and Shuttle faults. This created zones of dilation within more brittle lithologies that were exploited by Cu-rich fluids, resulting in the observed conjugate distribution of Cu mineralisation at the deposit (Fig. 7b). The intersection of these two structures created a zone of increased permeability that fluids exploited to produce a steeply SE-plunging high-grade shoot.

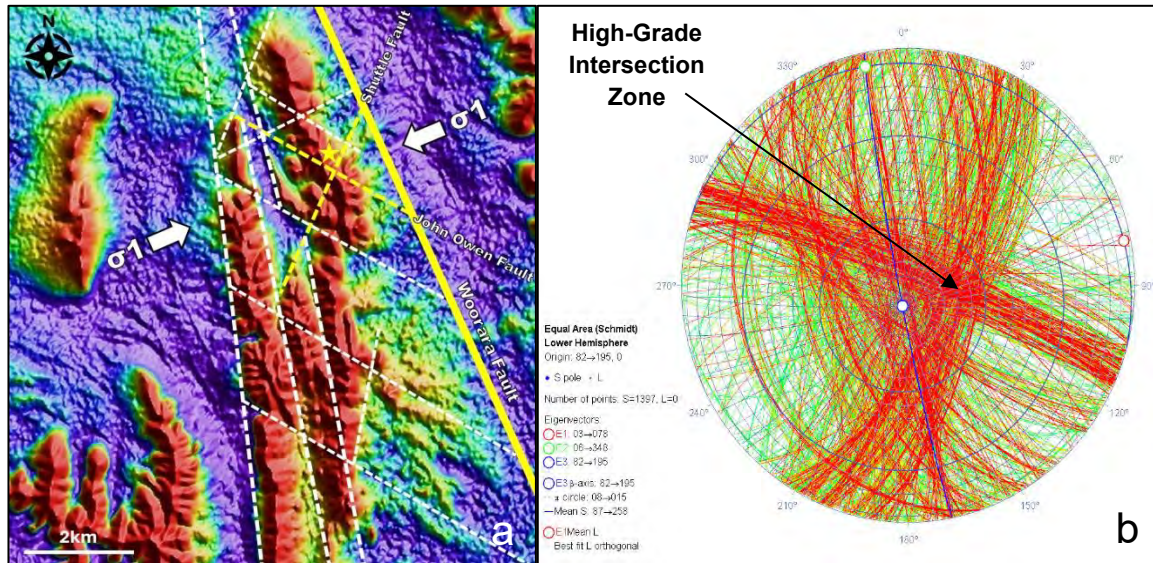


Figure 7. (a) Lineaments interpreted from 30m resolution topographic data delineating conjugate structures implying NE-SW transpression at Wirlong (yellow star). **(b)** Medium-range (100m) Cu continuity patterns at Wirlong demonstrating the conjugate geometry of Cu mineralisation. Great circles coloured by Cu assays (red = high). From Cowan (2022).

MINERALISATION & HYDROTHERMAL ALTERATION

Mineralisation at Wirlong is vein-hosted and comprises chalcopyrite-pyrrhotite-pyrite +/- arsenopyrite, sphalerite, galena locally oxidising to azurite, malachite, chalcocite, smithsonite above the base of oxidation. These veins display a variety of different styles with associated alteration assemblages that exhibit complex overprinting relationships with other veins that can be unravelled to establish a paragenesis for the deposit.

Dating of Cu mineralisation remains a challenge as datable minerals such as titanite and rutile have not been observed as intergrowths within the chalcopyrite. However, Pb-Zn mineralisation has been dated at 380.2Ma using high-precision Pb-Pb dating (Downes, pers. comm., 2022) and limited petrography suggests Cu, Pb & Zn are part of the same mineralising event.

Deformed Quartz Veins (V_1)

Early extensional quartz veins (V_1) have typically been deformed and folded parallel to S_1 (Fig. 8a) and represent the earliest vein set in the deposit and their formation pre-dates the regional D_1 event. These veins occur throughout the deposit and are usually barren but may locally contain minor sulphides.

Extensional Quartz Veins (V_2)

Barren extensional quartz (V_2) veins commonly exhibit characteristic quartz, chlorite and/or carbonate growth fibres at orthogonal angles to the vein margin. These veins overprint paragenetically earlier V_1 (Fig. 8b) and measurements show a dominant orientation parallel to S_1 . This vein type is distributed throughout the deposit and is locally overprinted by paragenetically later sulphides proximal to the two host faults.

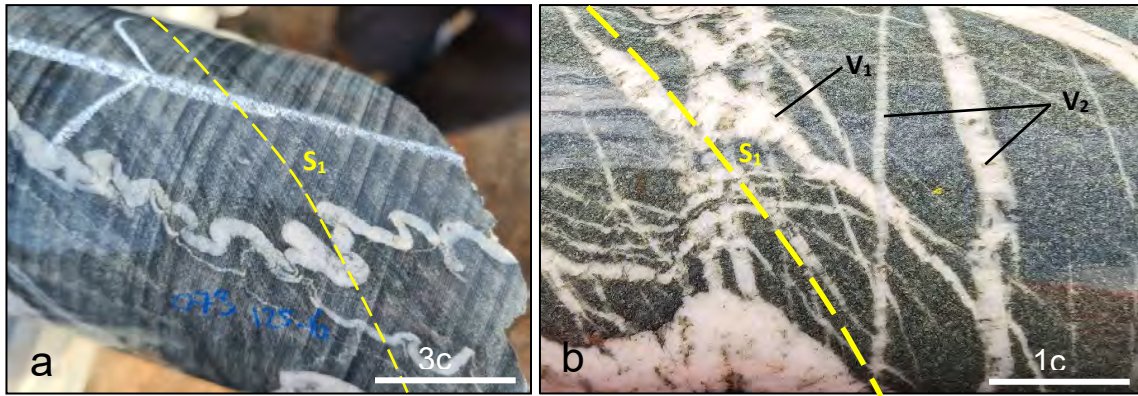


Figure 8. (a) V_1 quartz vein folded parallel to S_1 in WLDD073, 125.6m. (b) Narrow, fibrous extensional quartz-chlorite V_2 veins overprinting early deformed V_1 quartz veins in WLDD040, 463.7m.

Chalcopyrite Bearing Veins (V_3)

Milled Breccia Style

High-grade, massive to semi-massive breccia-fill chalcopyrite - pyrrhotite (+/- pyrite, sphalerite, galena) veins that typically host rounded to semi-rounded clasts of quartz and chlorite altered wall rock (Fig. 9a). These clasts have been milled through the repeated action of hydrothermal fluid-flow during sulphide deposition. Milled breccia veins overprint V_1 & V_2 and are both vertically and laterally extensive and are the dominant style that forms the high-grade core to the MBX domain (1.85Mt @ 2.15% Cu & 7 g/t Ag) which is hosted in the John Owen fault.

Composite Chlorite-Sulphide Style

Composite veins of Fe chlorite and chalcopyrite (+/- pyrite & pyrrhotite) exhibit a complex range of habits including stringer, breccia-fill and fracture-fill. Fe chlorite forms the matrix in breccia-fill veins or the selvage in stringer and fracture-fill veins. Locally, composite chlorite-sulphide veins exhibit a unique and distinctive chalcopyrite-chlorite selvage that often forms extension spurs (Fig. 9b). These are multi-phase veins that have formed during periodic pulses of Fe-Cu-rich hydrothermal fluids during incremental extension perpendicular to the vein axis.

Generally, the composite chlorite-sulphide veins overprint V_1 & V_2 and occur within all lithologies and together with composite quartz-sulphide veins form a stockwork halo around the high-grade MBX domain. However, veins exhibiting the unique chalcopyrite-chlorite selvage are lithologically controlled and only occur within massive quartz-rich sandstones and siltstones below -50RL.

Composite Quartz-Sulphide Style

Composite veins consisting of quartz and chalcopyrite (+/- pyrrhotite, pyrite, arsenopyrite, galena and sphalerite). Although sulphides always occur with quartz in these composite veins, the reverse is not always true, with massive, brecciated, fracture-fill and stringer quartz veins occurring without sulphides. Figure 9c demonstrates this relationship well and infers the sulphides have overprinted paragenetically earlier V_2 . These veins form part of the stockwork halo around the high-grade MBX domain.

Other Styles

Other less common styles of mineralisation at Wirlong comprise massive to semi-massive, high-grade chalcopyrite +/- pyrite and pyrrhotite stringer veins, which are usually sinuous in habit and typically do not have a distinctive chlorite selvage. Multiple styles can also combine to produce a complex network of veins that are hard to characterise. The distribution of these styles is highly variable and forms part of the high-grade MBX domain in addition to the stockwork halo that surrounds it.

Siderite Veins (V_4)

Siderite veins (V_4) are typically very narrow (widths of <1mm to ~1cm), commonly vuggy and usually occur with very fine-grained pyrite. They are paragenetically late and overprint all other vein types in the deposit and are thought to represent late-stage deformation within the deposit. This is evidenced by cataclastic and ductile shearing along siderite vein margins and by offset associated with the veins they are overprinting (Fig. 9d). Siderite veins have two dominant orientations, one parallel to S_1 and one parallel to the strike of the John Owen fault.

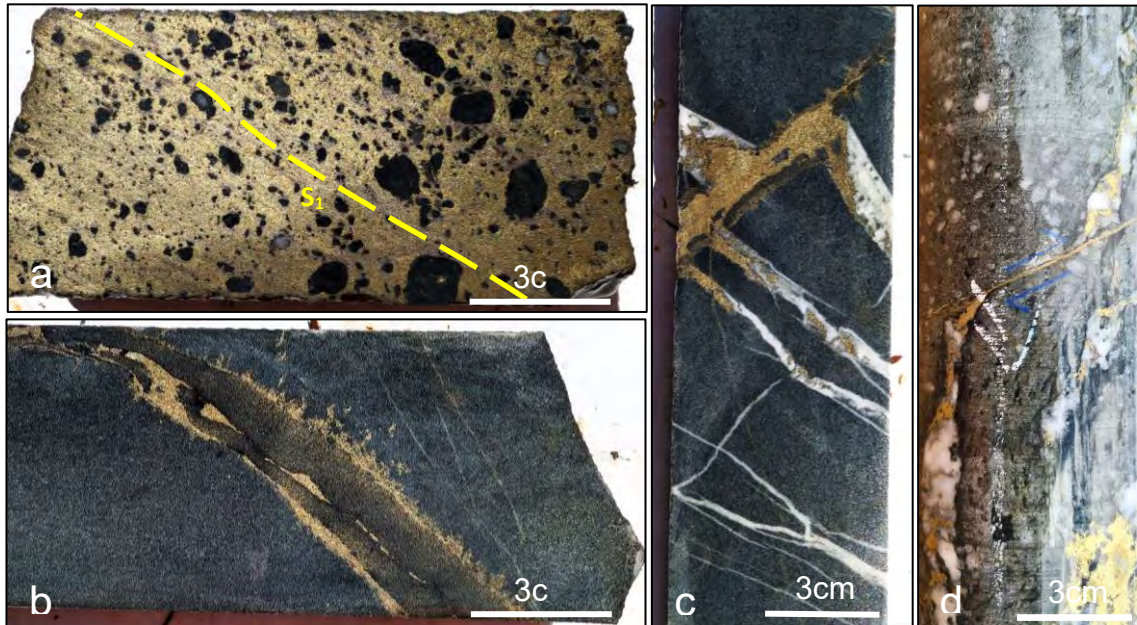


Figure 9. (a) Milled breccia style chalcopyrite-pyrrhotite vein (V_3) containing rounded clasts of chlorite altered wall rock and lesser quartz in WLDD006, 292.5m. S_1 is defined by the alignment of pyrrhotite. (b) multi-phase composite chlorite-chalcopyrite-pyrrhotite vein (V_3) exhibiting chalcopyrite extension spurs along the distinctive chalcopyrite-chlorite selvage in WLDD040, 558.8m. (c) Progressive overprinting of barren extensional quartz-chlorite veins (V_2) by a chalcopyrite-bearing fault in WLDD040, 622m. (d) Very narrow siderite vein (V_4) displacing a boudinaged quartz-chalcopyrite vein (V_3) in WLDD040, 273.9m.

Hydrothermal Alteration

Fe-Mg Chlorite

Spectral analysis of shortwave infrared (SWIR) measurements has identified the presence of intermediate Fe-Mg chlorite (~2252nm). It is observed in drill core as a weak pervasive background overprint that is typically pale green in colour and preferentially alters the groundmass of the Shuttleton Rhyolite Member peripheral to mineralisation. It is paragenetically the earliest of all alteration types and is overprinted by silica, sericite

and Fe chlorite. It is postulated to have formed during hydration of rhyolite ferromagnesian phenocrysts and glassy groundmass soon after its emplacement.

Silica

Pale grey, patchy to pervasive, weak texture retentive to locally intense texture destructive silica alteration predominantly overprints earlier Fe-Mg chlorite in the groundmass of the Shuttleton Rhyolite Member. Historically, silica alteration has been implied for the hard, brittle Shume Formation quartz-rich sandstones however, this is likely a function of the quartz-rich composition of the sandstone as opposed to hydrothermal silica alteration. Silica alteration forms a halo that flanks the orebody at Wirlong and is the most distal hydrothermal alteration assemblage.

Sericite

Typically, sericite is pale to dark green, patchy to pervasive and ranges in strength from weak texture retentive to locally intense texture destructive alteration and overprints earlier pervasive Fe-Mg chlorite in all lithologies. Hylogger data reveals the sericite has a composition that varies from muscovite to phengite. It is more proximal than silica alteration but commonly combines to comprise a flanking alteration assemblage around the Cu-rich orebody at Wirlong. This is evidenced by increasing K/Al values outwards from the Cu-rich ore zone (Garwin, 2022). Sericite is not observed overprinting silica alteration and the reverse is also not observed which indicates the two assemblages are most likely contemporaneous.

Fe Chlorite

SWIR analysis has confirmed the presence of Fe chlorite (~2258nm) alteration that occurs as a late overprinting phase that is spatially associated with Cu and Zn mineralisation. It ranges in colour from dark green to black and is commonly localised within faults, fractures, and veins and as selvages bounding composite chlorite-sulphide veins. Fe chlorite is paragenetically the latest alteration assemblage and overprints earlier silica, sericite and Fe-Mg chlorite.

GEOLOGICAL HISTORY

Phase 1. Deposition of the Shume Formation and emplacement of the Shuttleton Rhyolite Member (420.8 ± 1.9Mya)

A thick sequence of proximal turbidites was intruded by sills of crystal-rich rhyolite causing extensive soft sediment deformation in the unconsolidated wet sediments and peperitic margins, quench fragmentation and Fe-Mg chlorite alteration of the rhyolite. This occurred during the rift stage of the Cobar Basin (Fitzherbert & Downes, 2021), synchronous with extensive volcanism in the Cobar Basin and adjacent shelves.

Phase 2. Onset of basin inversion

The initiation of basin-wide inversion (D_1) with a far-field direction of maximum shortening oriented NE-SW. This resulted in the reactivation of the Woorara fault, folding of the Wirlong stratigraphy and the deformation of V_1 parallel to and during the development of S_1 (Fig. 8a).

Phase 3. Preparation of the Wirlong Cu-Ag deposit

As deformation intensified, crustal shortening was accommodated through reverse dip-slip movement along cleavage planes and the activation of the conjugate John Owen and Shuttle fault system. Oblique sinistral and dextral movements along the John Owen and Shuttle faults (Fig. 5 & Fig. 6, respectively) created zones of dilation, drawing in hydrothermal fluids that overprinted early Fe-Mg chlorite alteration with an assemblage of silica and sericite. V₂ were deposited primarily within S₁, overprinting V₁ in the process (Fig. 8b). Continued thrusting along the Woorara Fault led to the development of S₂.

Phase 4. Deposition of the Wirlong Cu-Ag deposit (380.2Mya)

Ongoing deformation continued to facilitate extension along the John Owen and Shuttle faults, which was subsequently exploited by one or more phases of Cu-rich hydrothermal fluids, leading to the deposition of V₃ (Fig. 9a, 9b & 9c). Deposition was syn-extension, as evidenced by chalcopyrite forming extension spurs along vein margins (Fig. 9b) and occupying the necks of boudinaged veins (Fig. 9d) and slickenline steps.

Phase 5. Concluding stages of deformation

The final stages of D₁ involve the closure of dilation zones and late-stage movement, primarily along cleavage planes and parallel to the strike of the John Owen fault. This late-stage movement is associated with the deposition of V₄ that overprint and offset all other vein types and sulphides (Fig. 9d).



Figure 10. Paragenesis of structural features developed during D₁ at Wirlong.

REFERENCES

BROWN R.E., 2016. Report on structural mapping and drill core examination for Peel Mining Ltd, Wirlong and Wirlong North Prospect areas, EL8307 and EL8126 Cobar Basin, New South Wales, pp.25

COWAN, E.J., 2022. Deposit-scale Structural Analysis of the Wirlong Massive Sulfide Deposit. Internal report to Peel Mining Ltd by Jun Cowan, unpublished.

FITZHERBERT J.A. & DOWNES P.M., 2021. A mineral system model for Cu-Au-Pb-Zn-Ag systems of the Cobar Basin, central Lachlan Orogen, New South Wales. Geological Survey of New South Wales report GS 2021/0042, Maitland.

FOLKES, C & STUART, C., 2020. Fault attribution for the western Lachlan Orogen of NSW.

GARWIN, S., 2022. Deposit Geometry, Mapping and Logging Training and Exploration Discussion. Internal report to Peel Mining Ltd by Steve Garwin, unpublished.

GLEN, R. A., 1990. Formation and inversion of transtensional basins in the western part of the Lachlan Fold Belt, Australia, with emphasis on the Cobar Basin. *Journal of Structural Geology*. Vol. 12, pp. 601–620.

GLEN, R. A., 1994. Geology of Cobar 1:100 000 Sheet 8035 (2nd edition). Geological Survey of New South Wales, Sydney.

GOSCOMBE, B & PASSCHIER, C., 2003. Asymmetric boudins as shear sense indicators—An assessment from field data. *Journal of Structural Geology*. Vol. 25, pp. 575-589.

JONES S.J., FITZHERBERT J.A., WALTENBERG K. & BODORKOS, S., 2020. New SHRIMP U-Pb zircon ages from the Cobar Basin, New South Wales: Mineral Systems Projects July 2018–June 2019. Geological Survey of New South Wales report GS 2020/0729, Maitland.

MACRAE, G. P., 1987. Geology of the Nymagee 1:100,000 Sheet 8133. Geological Survey of New South Wales, Sydney.

POLKINGHORNE, J., 1906. Particulars for Mine Records of Smaller Mines. *DIGS Geological Survey of NSW Search*.

VOISEY, A. H., 1949. Geology of the Wirlong Area. Report on an Investigation carried out on behalf of North Broken Hill Ltd., February 1949. *DIGS Geological Survey of NSW Search*.

WALTENBERG, K., BLEVIN, P. L., BULL, K. F., CRONIN, D. E., & ARMISTEAD, S. E., 2016. New SHRIMP U-Pb zircon ages from the Lachlan Orogen and the New England Orogen, New South Wales: Mineral Systems Projects, July 2015–June 2016. Geological Survey of New South Wales report GS2016/0810, Maitland.

ZHEN Y.Y., SMITH P.M., ZHANG Y.D., STRUSZ D.L., PERCIVAL I.G., BURROW C.J., RUTLEDGE J.M. & TRIGG S.J., 2023. Field Guide and catalogue of Ordovician-Devonian fossils from the Cargelligo and Nymagee 1:250,000 mapping areas, central New South Wales. *Quarterly Notes of the Geological Survey of New South Wales* 157, 83pp.

NEW INSIGHTS FROM THE COWAL GOLD DEPOSIT

Ned Howard^{1,2}, Ben Reid¹, Matthew Green¹ and Chris Leslie³

¹ Evolution Mining Limited, Sydney, NSW

² Corresponding author: ned.howard@evolutionmining.com

³ Principal Consultant, CDL Geological Consulting

Key Words: Cowal Gold Operations, Cowal Intrusive Complex, Macquarie arc, GRE46, Dalwhinnie, research, volcanology, igneous petrology.

INTRODUCTION

The Cowal Gold Operations are developed on gold deposits hosted within Ordovician rocks of the Junee-Narromine Belt, one of four slivers of the Cambro-Silurian Macquarie Arc now preserved in the Eastern Lachlan Orogen of New South Wales. Gold occurs in association with quartz-carbonate-sulfide veins, pyritic veinlets and disseminated pyrite in several ore zones spread out over the N-trending, ~6 km x ~2 km Gold Corridor. Major ore zones exploited thus far include E42 and the Cowal underground (GRE46), the latter including the recently discovered Dalwhinnie zone. There are additional resources contained in the E41E, E41W, E46, Galway and Regal open pit mining zones. With a total resource of 285.1 Mt @ 0.98 g/t Au for 8.998 Moz as at December 2023 (Evolution Mining Ltd, 2024a), past production under Barrick Gold of 2.4 Moz (2006-2015; S&P Capital IQ Pro, 2024) and 2.3 Moz under Evolution Mining Ltd (2015-2024; Evolution Mining Ltd, 2024b; Evolution Mining Ltd, 2024c) and considering gold recoveries, the Cowal gold system has a total pre-mining endowment of ~14 Moz.

Gold mineralisation at Cowal can be classified as intrusion-related low sulfidation epithermal of sub-types 'quartz-sulfide' to 'carbonate-base metal' in accordance with Corbett & Leach (1998); alternatively, gold mineralisation can be considered low to intermediate sulfidation epithermal (Hedenquist et al., 2000). Previous authors have suggested an alkalic low sulfidation epithermal classification (e.g. Zukowski et al., 2014), inferring a genetic relationship to alkalic intrusions, primarily on the basis of negative $\delta^{34}\text{S}$ values from ore-related sulphide minerals at E41 indicating oxidised (sulfate-stable) fluid conditions (Zukowski et al., 2014), a common feature of other alkalic intrusion related epithermal deposits.

Over the last nine years of Evolution Mining Ltd ownership, successful near-mine exploration has led to a significant increase in the Cowal gold corridor deposit resources and a significant improvement in the understanding of controls on these deposits, the host volcanic architecture and the petrogenesis of related intrusive phases.

ADVANCES IN GEOLOGICAL UNDERSTANDING

Key advances in the understanding of the Cowal underground, previously referred to as GRE46, in the last two years since the 2022 Discovery in the Tasmanides (Ila'ava et al., 2022) include:

- Continued expansion of the GRE46 underground resource to 34.8 Mt at 2.45 g/t Au for 2,738 koz as of December 2023 (Evolution Mining Ltd, 2024a).
- Infill drilling has led to improved definition of gold domains, resulting in decreasing tonnes at higher grade for slightly higher ounces in a given ore zone (Evolution Mining, 2023).
- Demonstration of greater continuity of mineralisation through the Edradour zone and to the east of existing ore zones with increased drill density in these areas (Evolution Mining Ltd, 2024d).
- Improved modelling of large veins (QSBs – quartz sulfide breccias) and understanding of their influence on grade distribution within the GRE46 deposit.
- Persistence of economic grades of gold mineralisation over a vertical interval of >1 km and through temperature-pH related geochemical zonation.

Key geological insights relevant to exploration and the genesis of the Cowal gold deposits that have been informed by ongoing collaborative research, principally PhD and post-doctoral researchers at the University of Tasmania - Centre for Ore Deposit and Exploration Studies (CODES), include:

- Igneous fertility signatures associated with intrusive phases in porphyry prospects of use for recognising potentially Cu-Au fertile districts, including:
 - Zircons displaying complex and varying textures, dissolution surfaces and rims or mantles with high Eu/Eu* (>0.35) and low Gd/Yb (<0.07) (Leslie et al., 2021).
 - Whole rock geochemical trends indicating high and increasing Sr/Y over time in younger intrusive phases associated with fractionation of hornblende, titanite, apatite and other accessory phases.
 - Recognition of a suite of Nb-enriched magmas with OIB-like Nb/Yb (Dewars Suite, Nb >20ppm) dated at 459.1 ± 1.9 Ma (Leslie, 2021).
- Testa and Cooke (2021), in part utilising data from Leslie (2021), analysed epidote from multiple prospects in the Cowal district containing highly elevated Sb (>10 ppm) and As (>100 ppm), consistent with the signature for 'distal' positions around giant porphyry systems.
- The interpreted roots to a lithocap environment, including acidic alteration mineral assemblages more typically associated with calc-alkalic porphyry systems than alkalic porphyry systems, are preserved to the NW and E of the gold corridor.
- Dating undertaken by Leslie (2021) demonstrated that almost all dated intrusive phases are >450 Ma, and that the ~440-435 Ma Phase 4 intrusive events are not confirmed and probably rare in the Cowal Intrusive Complex but associated with an interpreted lead-loss event.
- Three-dimensional reconstruction of the volcanic facies architecture by Malai Ila'ava at CODES (Ila'ava, et al., 2024) is helping to better understand the current

structural architecture and infer the earlier syn-volcanic architecture of the Gold Corridor.

- Current research through CODES and GSNSW is providing insights into the mineralogical and hyperspectral characteristics of Cowal underground, and the ages of host volcanics and intrusive phases.

The timing of the ~14 Moz Au endowed gold corridor is not precisely constrained but is likely to be ~450-455 Ma, younger than at the Marsden deposit (467 ± 2 Ma molybdenite Re-Os (Rush, 2013) to the SE and other porphyry prospects to the south, and significantly older than the earliest Silurian alkalic porphyry-style mineralisation at Cadia and Northparkes. The resource at Marsden (123 Mt at 0.46% Cu and 0.25g/t Au for 0.56 Mt Cu and 1.05 Moz Au; Evolution Mining Ltd 2024a) likely represents a small remnant of a much larger calc-alkalic porphyry Cu-Au deposit subjected to significant post-mineral faulting and erosion.

This protracted ~465-450 Ma porphyry-epithermal metallogenic episode was an important yet under-recognized contributor to the copper and gold endowment of Eastern Australia, offering a notable counterpoint to the persistent focus of the exploration community on the ~440 Ma alkalic porphyry systems.

REFERENCES

CORBETT, G. J., & LEACH, T. M. (1998). Southwest Pacific Rim gold-copper systems: Structure, alteration, and mineralization. Society of Economic Geologists, Special Publication, No. 6, 1, 236. <https://doi.org/10.5382/SP.06>

EVOLUTION MINING LTD. 2023. 2023 Investor Day Session 2 Presentation. Company presentation released to the ASX on 5 June 2023: <https://cdn-api.markitdigital.com/apiman-gateway/ASX/asx-research/1.0/file/2924-02672698-2A1452950&v=4015c7b87631faf94ecd96975272ff9ad5cb14c3>. p. 30-31.

EVOLUTION MINING LTD. 2024a. Annual Mineral Resource and Ore Reserve Statement as at 31 December 2023. Company Announcement released to the ASX on 14 February 2024: <https://cdn-api.markitdigital.com/apiman-gateway/ASX/asx-research/1.0/file/2924-02772317-2A1504726&v=4015c7b87631faf94ecd96975272ff9ad5cb14c3>.

EVOLUTION MINING LTD. 2024b. Interactive Analyst Centre TM by Virtua using data from ASX announcements by Evolution Mining Ltd. <https://apps.indigotools.com/IR/IAC/?Ticker=EVN&Exchange=ASX>. Accessed on 18th July 2024.

EVOLUTION MINING LTD. 2024c. Quarterly Report June 2024. Company Announcement released to the ASX on 18 July 2024: <https://cdn-api.markitdigital.com/apiman-gateway/ASX/asx-research/1.0/file/2924-02829044-2A1536296&v=4015c7b87631faf94ecd96975272ff9ad5cb14c3>.

EVOLUTION MINING LTD. 2024d. Cowal site visit presentation. Company presentation released to the ASX on 20 June 2024: <https://cdn-api.markitdigital.com/apiman->

gateway/ASX/asx-research/1.0/file/2924-02819118-2A1529985&v=4015c7b87631faf94ecd96975272ff9ad5cb14c3.

HEDENQUIST, J.W., ARRIBAS, A., Jr., and GONZALEZ-URIEN, E., 2000, Exploration for epithermal gold deposits: Reviews in Economic Geology, v.13, p. 245–277.

ILAAVA, M., GREENE, M., REID, B., MILOJKOVIC, T., CLIFFORD, M., BROWNE, C., BIGGAM, J., LESLIE, C., BARKER, A., HOWARD, N. & JUTZLER, M. 2022. Cowal gold mine: new insights and research update. AIG Bulletin 70: Discovery in the Tasmanides 2022 Conference Volume, p. 225-228.

ILAAVA, M., JUTZELER, M., CAS, R., & CAREY, R. 2024. 3D modelling of subsurface ancient volcanic successions: a workflow developed during regional reconstructions of the Cowal Igneous Complex in the Ordovician Macquarie Arc of NSW, Australia. Australian Journal of Earth Sciences, 71(5), 699–720.
<https://doi.org/10.1080/08120099.2024.2356134>.

LESLIE, C., MEFFRE, S., COOKE, D.R., THOMPSON, J., HOWARD, N. & BARKER, A. 2021. Chapter 10: Complex Petrogenesis of Porphyry-related Magmas in the Cowal District, Australia: Insights from LA ICP-MS Zircon Imaging. *In*: Sholeh, A. & Wang, R. eds., Tectonomagmatic Influences on Metallogeny and Hydrothermal Ore Deposits: A Tribute to Jeremy P. Richards (Volume II), Society of Economic Geologists Special Publications, no. 24, v.2, pp. 159-180.

LESLIE, C.D. 2021. Metallogeny of the Cowal district, New South Wales, Australia. Unpublished PhD Thesis. University of Tasmania. Hobart. pp. 161.

RUSH, J.A. 2013. Geology of the Marsden Cu-Au Porphyry, NSW. Unpublished Honours Thesis. University of Tasmania. Hobart. pp. 110.

S&P CAPITAL IQ. 2024. Cowal:Production. S&P Global Market Intelligence. New York: <https://www.capitaliq.spglobal.com/web/client#metalsAndMiningProperty/annualProduction?ID=28521>. Accessed 29th June 2024.

TESTA, F. & COOKE, D.R. 2021. Epidote and chlorite mineral chemistry as a tool for vectoring and fertility assessments in the Cowal district, NSW, Australia. Unpublished report to Evolution Mining Ltd. pp. 12.

ZUKOWSKI, W., COOKE, D. R., DEYELL, C. L., MCINNES, P., & SIMPSON, K. 2014. Genesis and exploration implications of epithermal gold mineralization and porphyry-style alteration at the Endeavour 41 prospect, Cowal district, New South Wales, Australia: Economic Geology, v. 109, p. 1079-1115.

THE HILL END REWARD GOLD MINE: A RENEWAL – THE UNIQUE HIGH-GRADE GOLD MINE

Roger Jackson

Vertex Minerals Limited 6 Bowen Street Hill End 2850

Key words: Hill End Mine, Reward Mine, Hargraves Mine, Hawkins Mine, Holtermann Nugget, orogenic gold, ore sorting, gravity separation.

INTRODUCTION

Geographically, the Reward gold mine sits just below the Hawkins Hill Gold mine at Hill End NSW - arguably Australia's highest-grade gold mine, which produced 435 Koz Au at 309 g/t (Figure 1). The Reward gold mine is located just few kilometres south of the Hill End township down in the Nuggety Valley Gorge. Hill End hosts one of the most famous high grade gold mines in Australia and it's also a well-preserved gold mining ghost town which is now an important historic site and a major tourist attraction. Hill End can be accessed either via Mudgee from the north (66 km) or Bathurst from the south (71 km). The Reward Project (Figure 2) is 100% owned by Vertex Minerals Limited (VTX) and is the flagship project for the larger Hill End and Hargraves tenements which covers approximately 30km in strike over the Hill End Anticline. The Reward mine sits on a set of Mining Leases that run along the line of lode for around 5kms. (Figure 2).

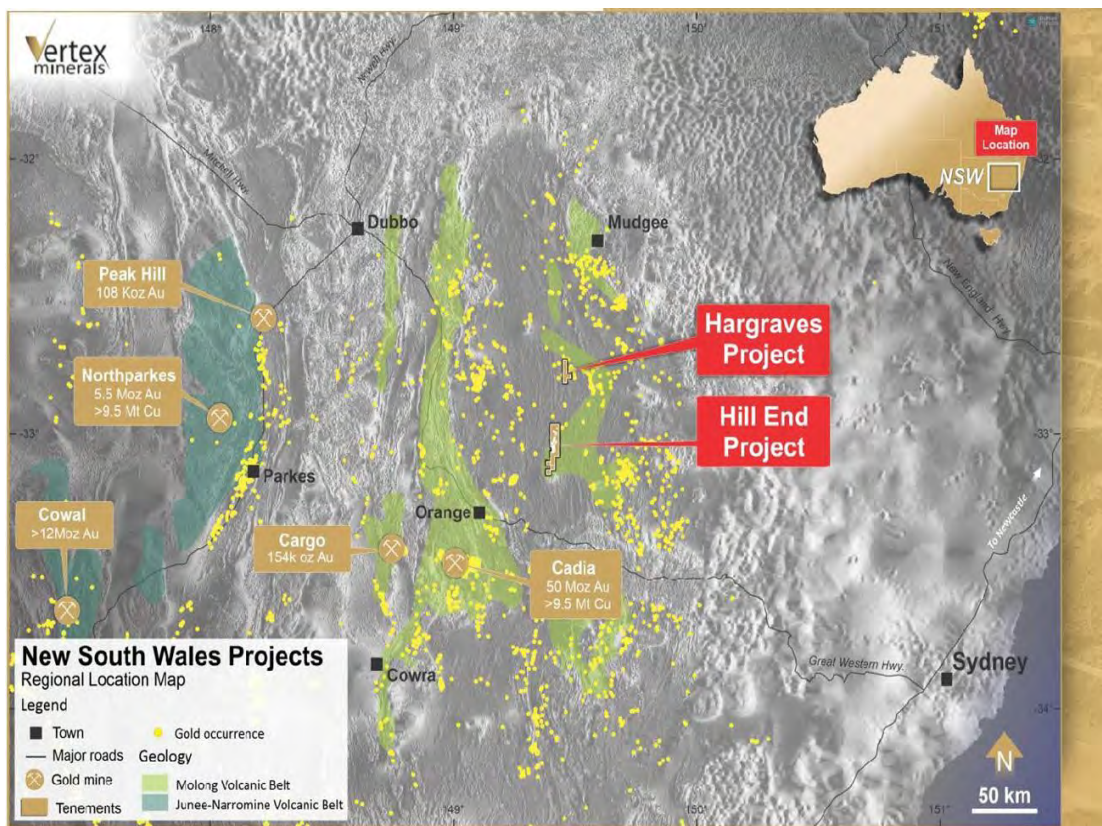


Figure 20. Location of Hill End Project in context with other mines in the region.

The unique high-grade Hill End Reward Gold Mine

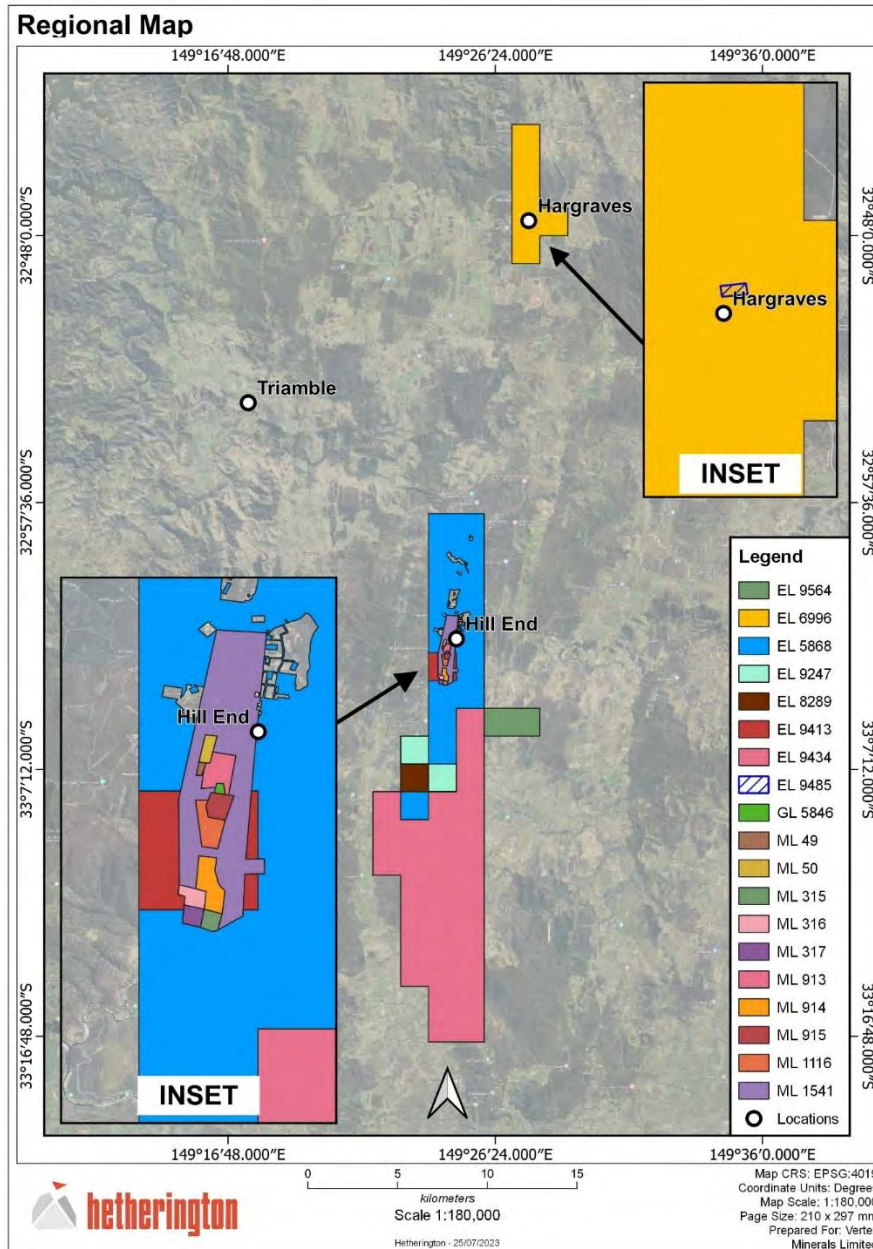


Figure 21 Vertex tenements at Hill End and Hargraves projects.

The Reward Gold mine has many unique features that makes it a standout gold mining operation – particularly with the increasing focus on mining operations with valid ESG credentials. The Reward resource is 419,000 tonnes for 225,200oz at a grade of 16.7 g/t Au and the ore is quartz carrying coarse 23-fine gold, above which is where the Holtermann Beyer nugget was found which is the world’s largest nugget (Figure 3). The Holtermann Beyer nugget was also 23 fine (95.83% Au), which is nearly as pure as gold will occur naturally. The Reward gold can be recovered by gravity concentrators to a Dore at a recovery rate greater than 92%. This means there are no chemicals involved in the process, no cyanide and no reagents. It also has a unique comminution, where the first pass gravity only requires a 650-micron crush. Therefore, there is no primary grind required in the processing of the Reward Mine ore and there is a very low energy/power consumption. Further, the ore can be sorted with an upgrade in gold grade by 320% between 15mm and 60mm. Given these qualities the tails that are produced from the gravity project are benign, and carry no metals, cyanide or chemicals and therefore are amenable to simple dry stacking. Because of the exceptional sorting characteristics, the

tails material can potentially be reduced by up to 70%, with the rejected sorted material going back into the mine as stope fill. With low metal content in the water, process water can be fully recycled and if necessary, released to the environment.



Figure 22. Reward Gold in quartz - 23 fine in purity in a natural state.

HISTORY

The Hill End Goldfield was one of the richest gold mining areas in NSW and the location of the first reef mining operation in Australia. Alluvial gold was first discovered in the area in 1851 and by the 1860's reef exploitation had emerged as the most popular and profitable method of mining. The first stamper battery in Australia was introduced in 1857 to crush ore from the mines, with reef underground mining, commencing at Hargraves in 1851.

The most successful mining was carried out immediately to the south of Hill End at Hawkins Hill from 1870 to 1872. In October 1872 the famous Beyers and Holtermann nugget was discovered – the largest single specimen of reef gold ever discovered in the world. It was found in the Star of Hope mine and weighed about 286kg. Hawkins Hill ultimately yielded 435,000oz of gold at a grade of 309 g/t. Major mining operations ceased after 1874.

From 1908 to 1920 there was a revival of activity at Hawkins Hill. The Hill End Reward Company took over the Emmett and Hughes and Reward shafts. In 1910 the Amalgamated Hill End Company began operations to work the central belt of Hawkins Hill below the ground from which the veins were worked in the 1880's. An aerial cableway was installed to supply the mine and the stamp battery with timber and other necessities. The Amalgamated mine was sold in 1917 to the Marshall's Hill End Company due to a lack of capital.

For the next 60 years from 1920 to 1980, only sporadic small-scale operations were undertaken on the field, but systematic exploration was not possible because the area was held under numerous small, independently owned leases. Two exploration licences were taken over the Hill End Anticline in the early 1970's but no significant exploration was carried out in either area.

In 1980 Silver Orchid Pty Ltd consolidated many of the titles and acquired three exploration licences. The combined titles covered an area of 420km², extending over a strike length of 32km of the Hill End Anticline. Between 1980 and 1983, Silver Orchid carried out an extensive literature search along with surveying, mapping, and sampling programmes. Maps of old workings were constructed from the records and through mapping and surveying some 1,000 shafts and workings were identified over a strike length of 18km. The company also processed 1,200m³ of alluvial gravels through a gravity separation plant.

In 1983 the Silver Orchid entered two joint ventures for the exploration of separate parts of the EL, with Flanagan McAdam to explore Red Hill Area and with Northern Gold NL to explore Hawkins Hill.

Over the period 1983 to 1986 Northern Gold carried out a comprehensive program of surface mapping, geophysical investigations, adit and shaft rehabilitation, underground and surface sampling and drilling. An initial program of seven diamond holes were drilled in the Reward area in 1984 (DDH R1 – DDH R7) for a total of 1,781m including three wedges. A further five holes for a total of 1,492m including three wedges were drilled in 1986 (DDH R8 - DDH R12). Four of these holes drilled beneath the Exhibition shaft reported several good grades.

BHP Exploration entered into a joint venture with Silver Orchid in 1989 to carry out a regional geochemical and rock chip sampling programme. Bulk Leach Extractable Gold (BLEG) samples were collected over the entire area at 200m intervals on traverses 1.5km apart. Rock chip samples were collected from outcrops and mullock heaps. No significant anomalous areas were identified, and BHP withdrew from the joint venture in 1991. Silver Orchid relinquished the EL the same year.

Following the withdrawal of BHP, no significant exploration of the area was undertaken until 1993 when Nugget Resources acquired an option on the Silver Orchid areas. An initial program consisting of four diamond holes were drilled in 1995 to test the structure and continuity of quartz veins on the crest of the Hill End Anticline at the southern end of Hawkins Hill. Quartz veins were intersected as predicted but did not contain significant gold grades.

Nugget Resources changed its name to Hill End Gold Ltd (HEGL) and was listed on the ASX in 2003 with mining lease 1541 granted the same year. The initial focus for Hill End Gold exploration was the historically very rich Hawkins Hill – Reward deposit, where diamond drilling beneath old workings delineated resources in a number of high-grade zones. Between 2003 and 2010 an extensive trial mining and processing project was undertaken. Approximately \$40m was spent by HEGL on exploration, development and facilities in the area.

HEGL conducted reverse circulation (RC) percussion drilling during 2004 which was subsequently followed by RC and diamond drilling between 2006 to 2008. During the Reward Gold Mine bulk sampling stage up to May 2010, there were 5,650m of underground development completed and a gravity plant at an Amalgamated portal processed 35,390 tonnes at an average grade of 10.6g/t Au with a metallurgical recovery of 91.4% at a coarse grind of ~P800.5mm for 11,029 ounces of payable refined gold.

Hill End Gold was later renamed Peak Minerals Ltd. The Hill End Project and associated tenements were acquired by a subsidiary of Peak Minerals, Vertex Minerals Limited (VTX), which was spun out of the parent company and listed on the ASX in January 2022.

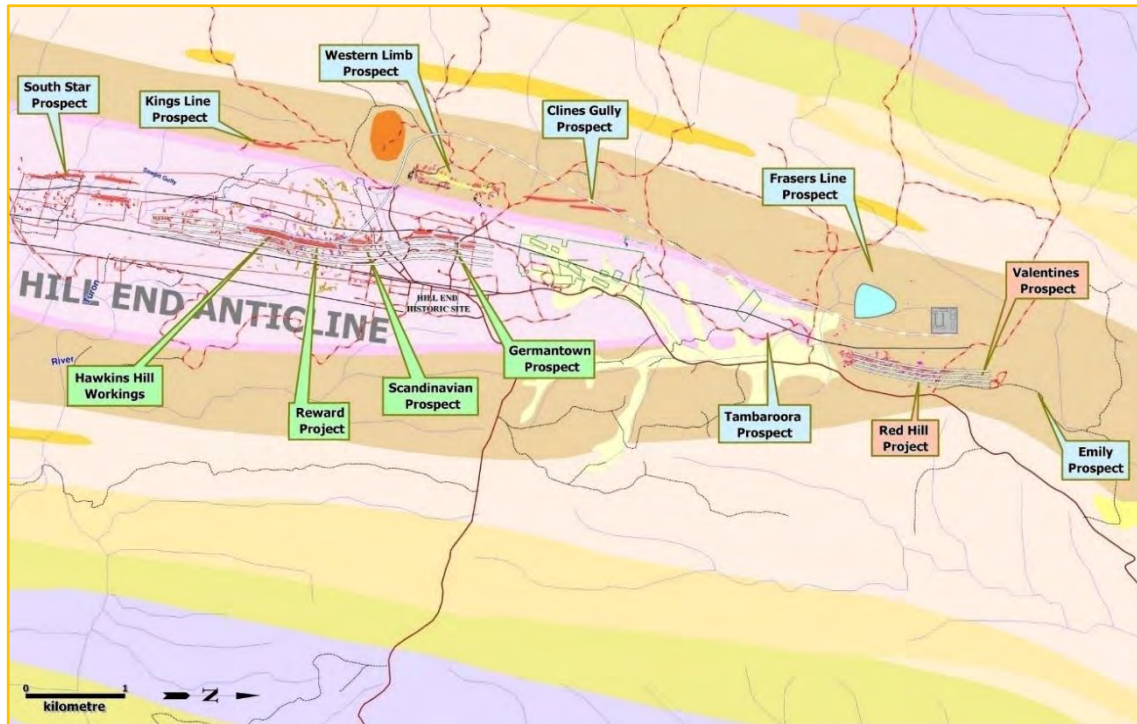


Figure 23. Locations of the main prospects on the Hill End tenements.

REGIONAL GEOLOGY

The Hill End Goldfield of central-western New South Wales (**Error! Reference source not found.**) lies within the Hill End Trough, a 7km thick succession of late middle Silurian to Middle Devonian (~425–385 Ma), deep-water, epiclastic and volcanoclastic sedimentary rocks. Wilkins and Quayle (2021) provide an excellent summary of the regional and project-scale geological settings:

The Hill End Trough is deep marine basin 70km-wide and more than 200km long, that is underlain by Ordovician volcanic rocks which lie between the Molong Volcanic Belt to the west and the Rockley-Gulgong Volcanic Belt to the east. Both these volcanic belts belong to the Ordovician Macquarie Arc in the Lachlan Fold Belt of eastern Australia (Fergusson, 2009).

The Late Silurian Chesleigh Formation (mineralisation host sequence) consists of interbedded fine-medium and coarse-grained, quartz-rich or quartzo-feldspathic, lithic sandstones (greywackes), siltstones and slates - including minor radiolarian chert and rhyolitic air-fall tuffs in the upper Chesleigh Formation. Bed thickness is generally 10cm to 50cm, with finer-grained units bedded at a centimetre scale and coarse units at a 1m to 2m scale. Graded bedding, soft-sediment deformation, and Bouma A to E sequences indicate deposition from deep-water turbidity currents in a submarine fan environment (Pogson and Watkins, 1998).

Furthermore, the Chesleigh Formation is conformably overlain by the Early Devonian Cookman, Turondale, Waterbeach, and Guroba formations that consist of rhythmically

bedded, turbiditic mass flow deposits. These are overlain conformably by the Merrions Formation, containing subaqueously emplaced lavas and volcanoclastics deposited as mass flows of explosive eruptive material into a deep marine environment, and the Cunningham Formation, the final major fill of the Hill End trough, consisting of thin bedded (1cm to 5 cm), fine-grained non-volcanic turbidites (Pogson and Watkins, 1998).

The Hill End trough has a prominent north-south structural trend caused by a major east-west shortening event. It has been deformed into prominent regional, tight to isoclinal, upright N-S trending, gently doubly plunging folds, with an associated penetrative slaty cleavage (Pogson and Watkins, 1998; Meakin and Morgan, 1999; Figure 5). Greenschist facies metamorphism to chlorite and biotite grade is recorded in the Hill End Trough (Smith, 1969; Lu, 1993) with some biotite porphyroblasts crosscutting the regional slaty cleavage, implying peak metamorphism outlasted the period of east-west shortening (Vernon and Flood, 1979). The unfoliated, coarse-grained Bruinbun Granite (part of the Bathurst Batholith) intrudes the core of the Hill End Anticline 14 km south of Hill End and has a 330 to 325 Ma mid-Carboniferous Rb/Sr age (Shaw and Flood, 1993; Pogson and Watkins, 1998), postdating both Middle Devonian (Tabberabberan) and early Carboniferous (Kanimblan) deformations (Glen, 2005).

After erosion accompanying deformation, sedimentation resumed on the flanks of the trough with the deposition of the Late Devonian siliceous sedimentary rocks of the Catombal Group (Molong High), Lambie Group, and Mt. Knowles Group (Capertee High), starting in the late Frasnian (367–363 Ma) and ending in the late Famennian or early Carboniferous (354–345 Ma). These Late Devonian sediments were also deformed and incorporated into folds and thrusts at the margins of the Hill End Trough.

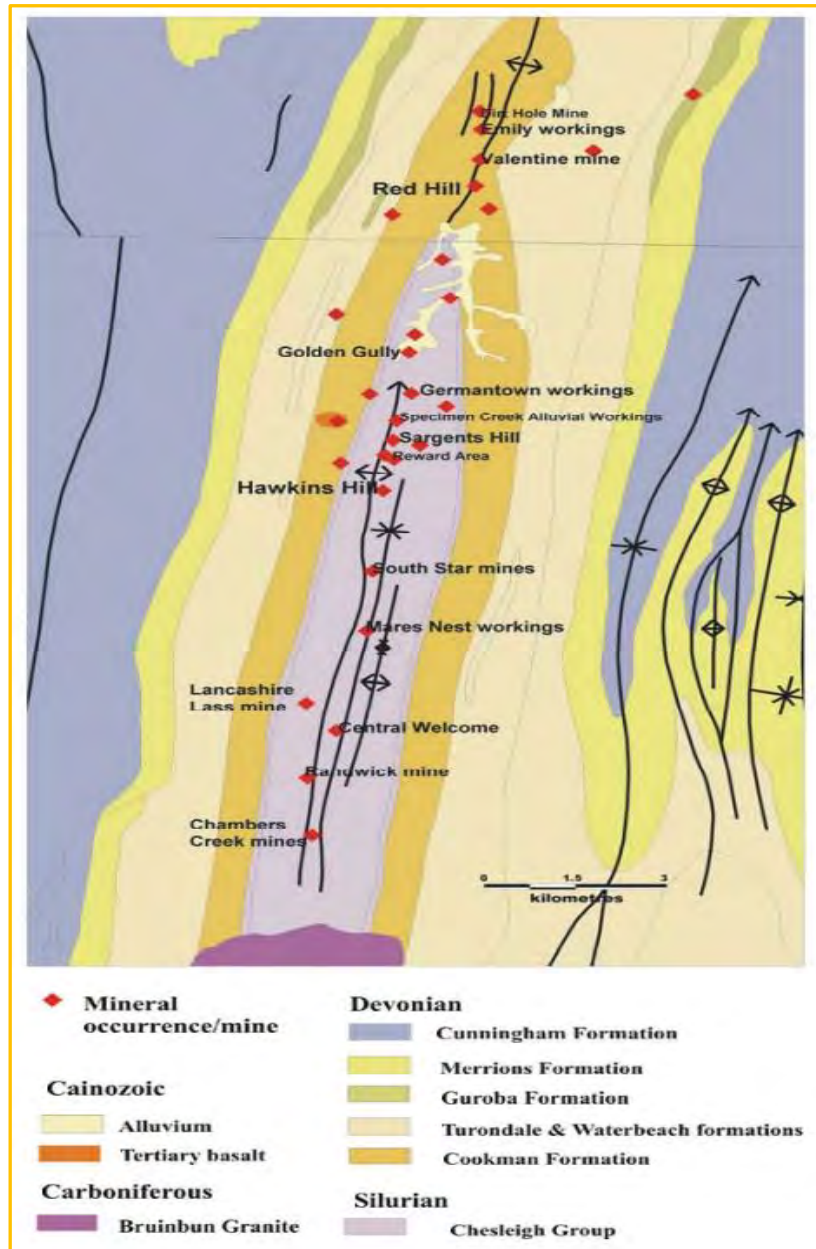


Figure 24. Geology of the Hill End system showing from Chambers Creek Mines in the south to Dirt Hole Mine in the north (Adapted from Raymond et al 1998 and Morgan et al 1999).

LOCAL GEOLOGY

Gold occurs along the 25km strike length of the Hill End Anticline (Harper, 1918; Joplin 1949; Seccombe and Hicks, 1989; Windh, 1995), including the historically important Hawkins Hill Mines at Hill End, where the late Silurian Chesleigh Formation hosts gold-bearing, bedding-parallel, laminated quartz veins and associated structures on the east limb of the Hill End Anticline. At Hill End, the anticlinal hinge consists of two closely spaced anticlines and an intervening syncline.

Previous mining at Hawkins Hill Mine worked a series of rich, gold-bearing veins over a strike length of 1km and to a depth of 200m from the surface in places.

Surface drilling identified potentially minable veins in the untested ground to the north and below previously stoped areas. Surface diamond drill holes are shown that

encountered mineralised bedding-parallel veins in a subvertical, north-striking mineralised corridor.

Exploration north from Hawkins Hill to Reward and Germantown mines indicated that bedding-parallel veins only showed significant gold mineralization (>10 g/t) in a subvertical and N-striking mineralized corridor (Figure 4) on the east limb of the westernmost anticline in the core of the Hill End Anticline.

From 2007 to 2010, the Amalgamated Adit (640 Level) was extended to intersect a new 286m shaft, known as Reward Shaft. The shaft also provides access to the Paxton's vein set above the 640 Level. The Consolidated 695 Level (35m above Amalgamated) was widened (from 1.5m to 2.3m) and heightened (to 2.5m) from the adit to the Phillipsons Vein.

The Reward Shaft contains east-dipping metasandstones and shales with associated mineralized bedding-parallel quartz veins. Both are crosscut by late W-dipping faults (e.g., the Reward Fault). High-grade gold shoots, mined from the Paxton's vein system, were concentrated between levels 671 and 695.

Level development and drilling in the Reward Mine have intersected 14 bedding-parallel vein sets within a 360m thick sequence of metaturbidites on the steeply E dipping anticline limb. Vein names date from the 1870s; on 640 access level. The most westerly vein (Lady Belmore) is followed by a 90m thick metasandstone unit. Then, from west to east, named veins are spaced stratigraphically at 5m to 25m apart and are sequentially encountered in higher levels in the mine. The principal veins are (Figure 6):

- Brand and Fletcher's,
- Amalgamated,
- Phillipson's,
- Mica,
- Star of Peace,
- Middle,
- Paxton's,
- Steven's (Moustaka's),
- Calcite (Herman's),
- Frenchman's (Star of Hope),
- Far East,
- Rowley's, and
- Mountain Maid

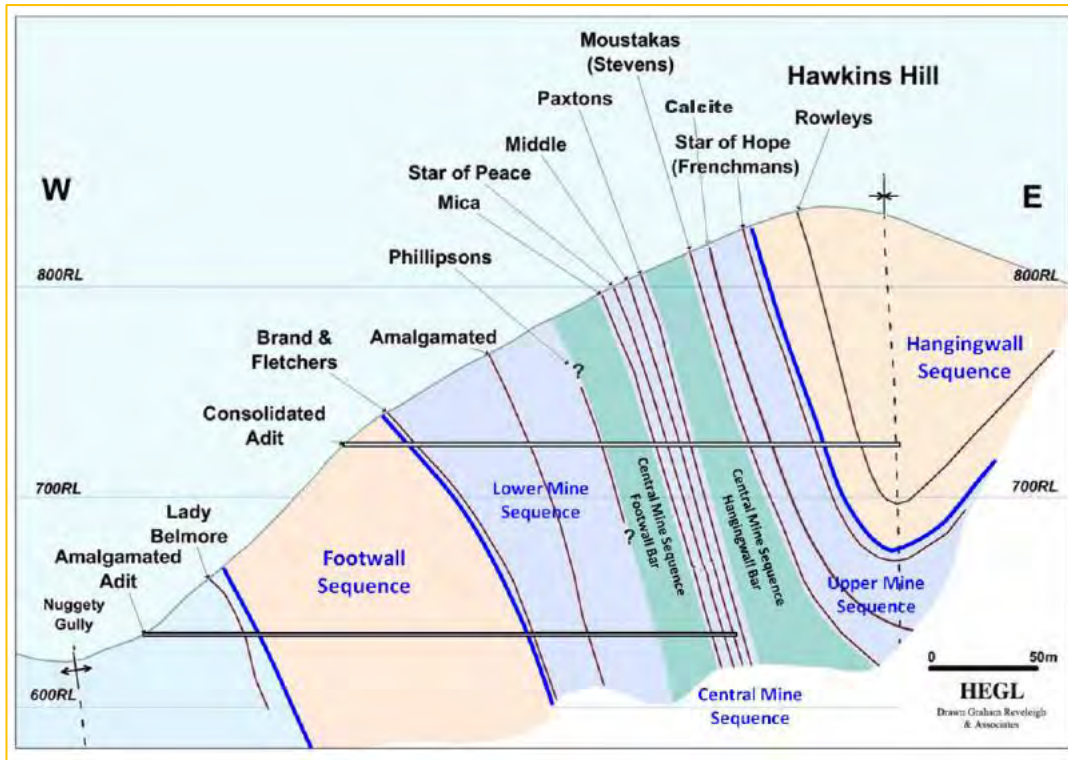


Figure 25. Stratigraphic framework and major bedding parallel quartz reefs on the east limb of the Hill End Anticline in the Reward - Hawkins Hill area, Hill End NSW (Source: Modified from HEGL).

In the Reward mine, metaturbidites young to the east and contain fining upward cycles. Diagenetic and syndeformational low-grade alteration (chlorite, calcite, muscovite, sericite, epidote, pyrite, and arsenopyrite) of sandstone-dominated metaturbidites is common throughout the mine sequence. However, bedding-parallel laminated quartz veins are restricted to shale beds (now represented by cleaved black slates) in either sandstone or shale dominated turbidites.

The principal bedding-parallel veins in the Reward Mine have a maximum thickness of ~75 cm. In narrow slate beds they may be represented by individual veins or sets of two to four veins (e.g., Mica and Paxton's). They initially appear to be constant features over 100s of meters; however, in detail along the strike and downdip they tend to have variable persistence, thickness, character, and grade distribution (1,000 g/t).

Other gold occurrences in the project area include the former alluvial gold workings at Golden Gully and Tambaroora.

MINERALISATION

Historically the Hill End deposit has been described as a slate-belt gold system. However, it is better modelled as a competency controlled low sulphide orogenic gold system associated with a series of imbricated high-angle reverse faults that developed post-ductile deformation. The Hill End mineral system is hosted by the Late Silurian Chesleigh Formation and overlying Early Devonian Cookman, Turondale, Waterbeach, and Guroba Formations that consist of rhythmically bedded, turbiditic mass flow deposits.

The system extends along strike for over 17 km from the Chambers Creek Mines in the south to the Dirt Hole Mine in the north. Within this area there is an 8km long zone that

contains the majority of significant hard-rock gold mines at Hill End. These include the Hawkins Hill, Sergeants Hill, Golden Gully, Red Hill and Valentine areas.

Gold production at Hill End exceeds 21.46t of gold, of which 12t of gold was recovered from Hawkins Hill Mine. The bedding parallel veins at Hawkins Hill Mine are laminated and consist of quartz with lesser carbonate, muscovite, chlorite, minor pyrite and gold, as well as pyrrhotite, marcasite, chalcopyrite, galena, arsenopyrite and sphalerite. At Hawkins Hill, bedding-parallel veins are located on the eastern limb of a parasitic fold in the Hill End Anticline.

These veins are narrow (typically 0.05 to 0.3 m wide) strike 190° and dip $\sim 60^{\circ}$. On some cross sections Hill End Gold, up to 8 mineralised veins have been recorded within a 125 m wide zone (HEGL). At least 13 mineralised bedding-parallel veins have been recorded at Hawkins Hill zone. Harper (1918) noted the presence of near horizontal "leader" veins intersecting the bedding-parallel veins. These "leader" veins are crack-seal and the intersection of the two vein-sets forms near-horizontal high-grade ore shoots (plunging at 10 to 20° north — Reveleigh pers comm 2002) similar to that found in other mineralised thrust systems. Seccombe et al (1993) noted that gold shoots also developed at the steep north-plunging intersections of bedding-parallel veins with narrow (4 to 50 mm) steeply north-dipping "leaders" in the hanging wall of the productive Star of Hope and Mica veins. Also present at Hawkins Hill are minor steeply dipping, crosscutting veins ("spurs") and "cross-courses" (faults) which kinematic analysis suggests resulted from minor dextral strike-slip movement.

Significant gold mineralisation was also found in intersection shoots formed by the intersection of these crosscutting structures and bedding parallel veins (Harper 1918). Minor normal faulting has subsequently offset units. Most of the high-grade mineralisation mined at Hawkins Hill was hosted in the bedding parallel veins located on the eastern limb of the Hill End Anticline. Windh (1995) noted that some auriferous veins were mined on the western limb of the anticline and on adjacent structures. Both Seccombe and Hicks (1989) and Windh (1995) noted that the saddle reefs in the core of the anticline are either barren or contain only minor gold. Significant near-surface remobilisation of gold has also occurred within the weathering environment at Hill End.

This has resulted in the development of supergene enriched zones within the veins, particularly those of the Hawkins Hill area. These zones are evident on the composite long sections showing stoping, by records relating to very rich zones mined between 40 to 50 m below surface (Harper 1918) and by the presence of the Beyers and Holtermann nugget (Figure 8).

The majority of auriferous veins at Hawkins Hill are laminated (crack-seal texture) which Seccombe and Hicks (1989) considered to have developed from metamorphically derived fluids. Lu and Seccombe (1993) identified a five-stage paragenesis of mineral deposition with gold and the majority of sulphides being deposited in Stages III-V, from low salinity, $H_2O-CO_2-CH_4$ fluids (Table 1).

The unique high-grade Hill End Reward Gold Mine

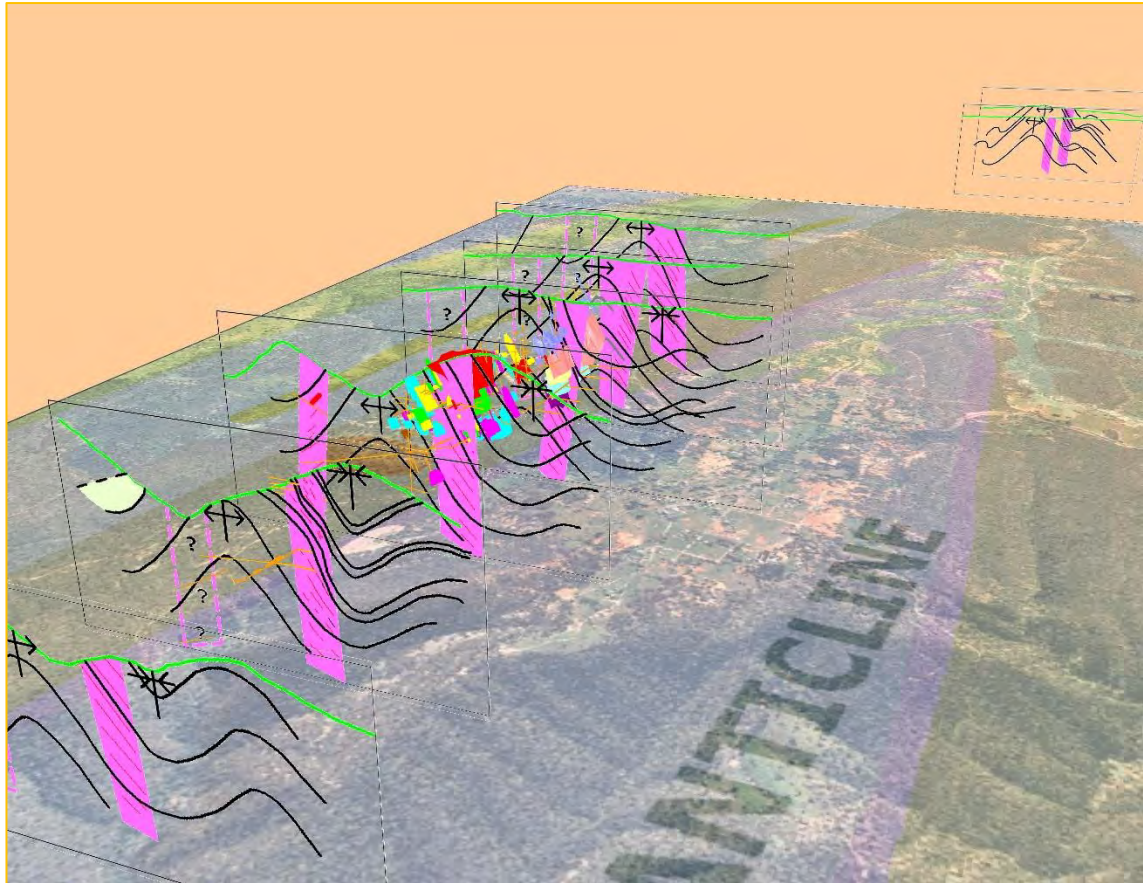


Figure 26. Mineralised zones (pink) on the eastern limb of the Hill End Anticline. Coloured areas have been previously mined in 2009 and 2010 and old workings from the 1800s. (Source HEGL).

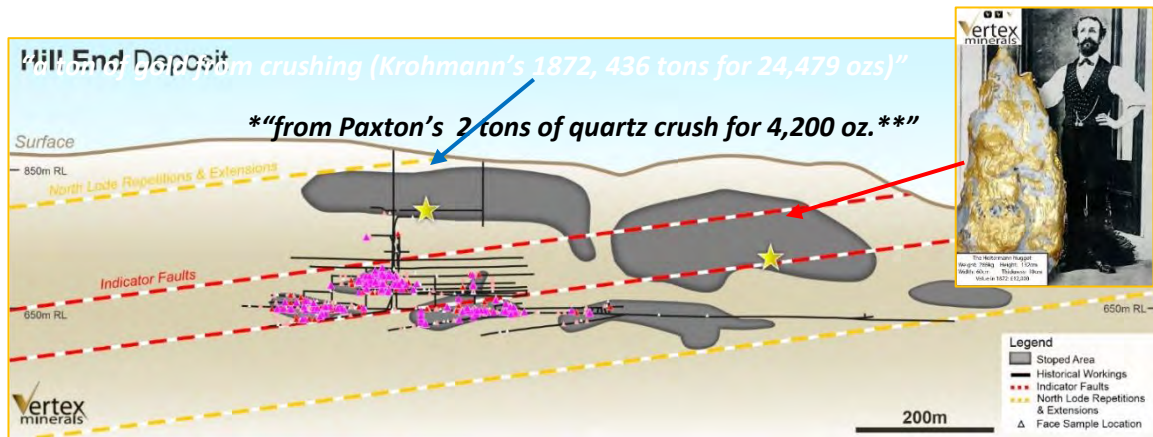


Figure 27. Long section through the Reward and Hawkins Hill Mining zones. Red arrow shows the location of the Holtermann Beyer Nugget discovery. In the Hawkins Hill area, the blue arrow shows the location of very high-grade zones of gold as recorded in the crushings quoted by Paxton and Krohmanns (Source M Drinkwater).

The unique high-grade Hill End Reward Gold Mine

Table 1. Paragenesis and conditions of Mineralisation – Hill End, adapted from Lu et al (1996A). Data summarised from Lu and Seccombe (1993).

^A Temperature after pressure correction during Stages III- V. Au precipitation lies in the range 293 – 340 °C (Lu,1993)

^B Gas – phase compositions determined by Ramen microprobe.

Paragenesis Stage	Mineral Assemblage	T _h of relevant fluid inclusions (C°)	Dominant gas phase in fluid inclusions	Ar ³⁹ Ar ⁴⁰ dating (Ma) Lu et al (1996b)	Summary of Events (Based on Windh,1995 and Lu et al 1996b)
Stage I	quartz	280- 350	N ₂	370 - 380	Development of bedding parallel veins
Stage II	quartz, muscovite, pyrrhotite	230 - 280	CH ₄	359 - 363	Principal Deformation: main phase of bedding parallel vein development with veins being folded due to continued deformation
Stage III	quartz, muscovite, chlorite, pyrrhotite, calcite, sphalerite, galena, chalcopyrite, gold	190 -250	CH ₄	356	Minor discordant cross cutting veins
Stage IV	muscovite, chlorite, pyrrhotite, pyrite, calcite, sphalerite, galena, chalcopyrite, gold	150 -250	CH ₄	340 - 345	Gold mineralisation in bedding parallel veins, breccias and leaders. Continued deformation results in folding existing veins and development of new veins.
Stage V	quartz, chlorite, pyrrhotite, pyrite, gold		CH ₄ CO ₂	No data	Minor discordant veins and dilatational veins in saddles

SUMMARY OF REWARD MINERALISATION

- High-grade mineralisation controlled by late stage, high-angle reverse faults. Similar to model to Bendigo-Ballarat/Fosterville.
- 5 unique mineralisation events identified.
- High-grade repetitions are likely to occur where the high-angle reverse faults controlling mineralisation intersect additional bedding parallel lodes on stratigraphic positions above and below the defined mineralisation.
- Multiple positions already defined are consistent with this model, forming a northerly plunge to the mineralisation.
- Stacked, bedding parallel, reverse-fault controlled mineralisation confirmed in backs mapping and extensive face sampling program completed during 2008 trial mining and underground mapping and sampling program.

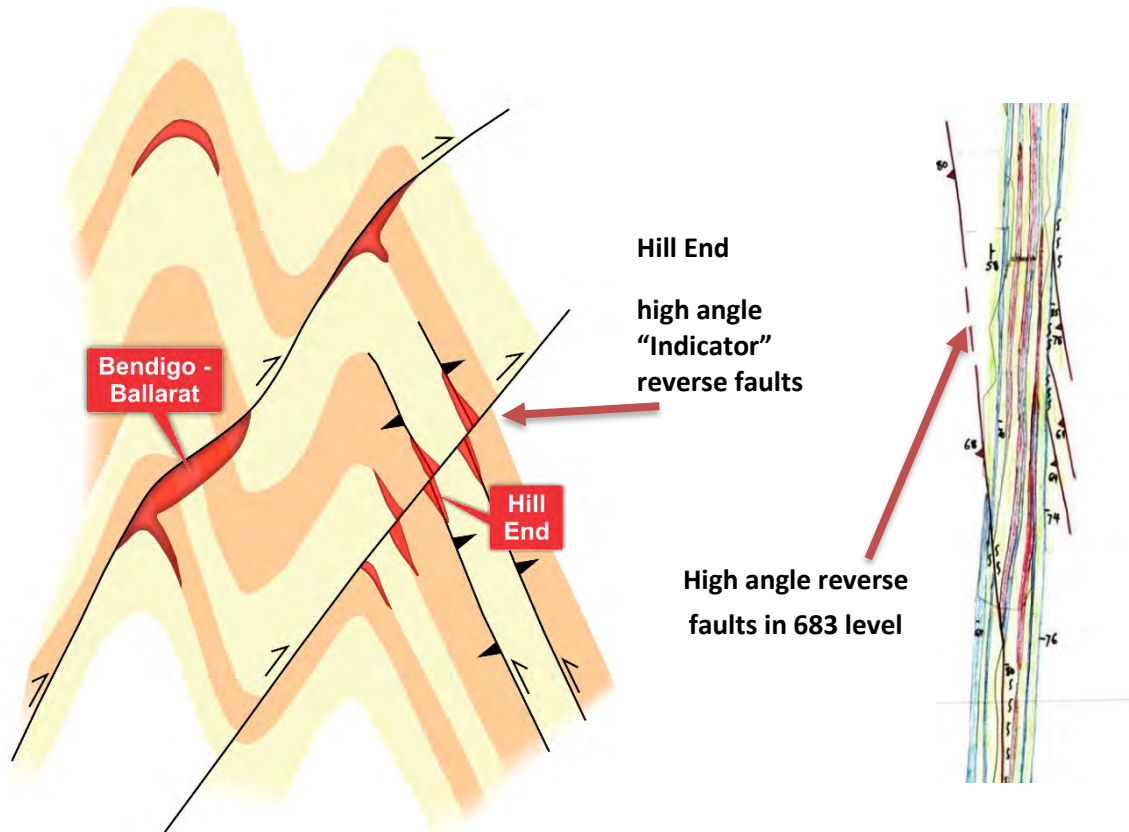


Figure 28 Cross section through Bendigo Gold Mine and the Reward showing the Reverse angle faulting relating to Au mineralisation (Modified after Dominy et al., 2003) Revised diagram R. Jackson Vertex presentation 2022 Australian Gold Conference.

The Reward mineralisation has distinct similarities to Fosterville including:

- Host turbidite sequence of sandstones, siltstone and shales/ black shales
- E-W compression faults produced early upright fold sets and late brittle faults
- Laminated quartz veins preferentially developed in shales. Usually bedding parallel and close, or on, sandstone contact
- Generally steeply west dipping reverse faults with a series of west dipping splay faults (figure 10.)

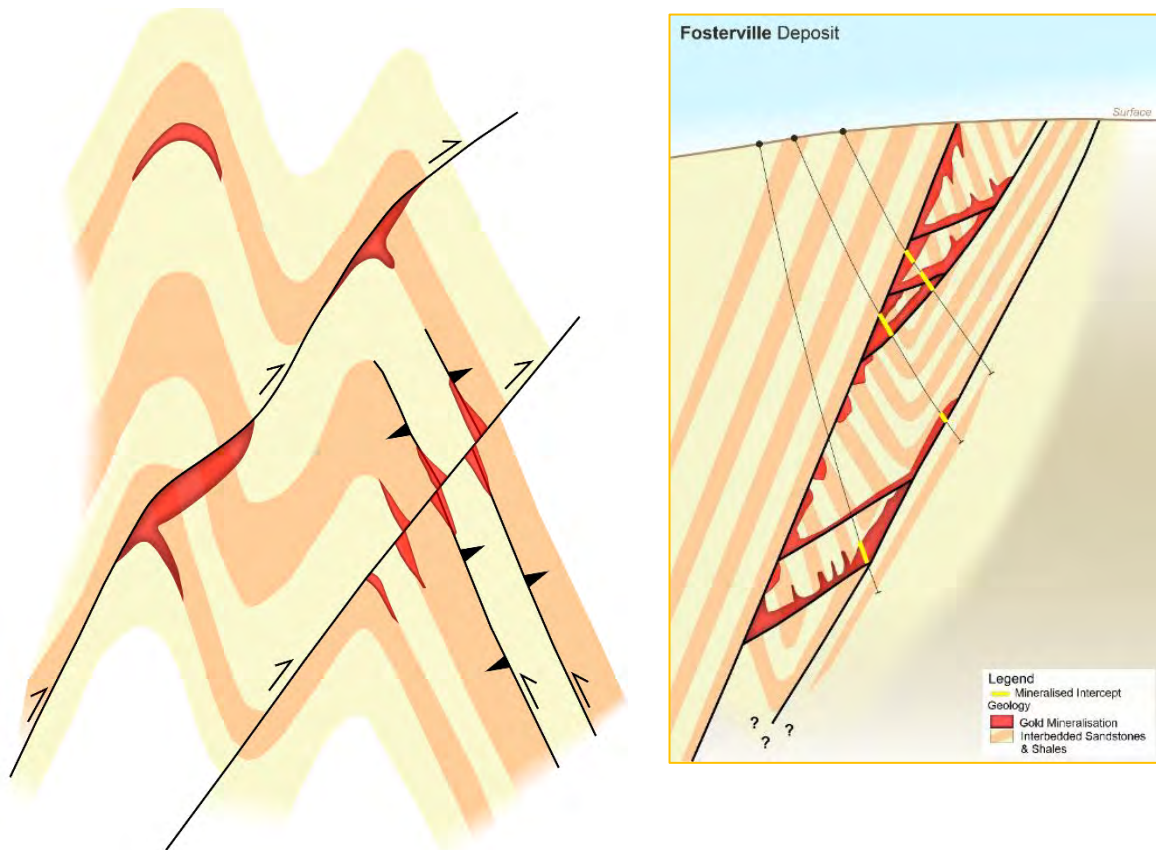


Figure 29. Bendigo cross-section (left; as per Fig. 9) compared to Fosterville Cross section (right) showing reverse angle faulting relative to mineralisation (After Fuller and Hann 2019) and Hitchman et al. (2017). Revised diagram R Jackson 2022 Australian Gold Conference).

STRUCTURE

The Reward mine at Hill End hosts structurally controlled orogenic gold mineralization in moderately S plunging, high-grade gold shoots located at the intersection between a late, steeply W dipping reverse fault zone and E-dipping, bedding-parallel, laminated quartz veins (the Paxton's vein system). The mineralized bedding-parallel veins are contained within the middle Silurian to Middle Devonian age, turbidite-dominated Hill End trough forming part of the Lachlan orogen in New South Wales. The Hill End trough was deformed in the Middle Devonian (Tabberabberan Orogeny), forming tight, N-S-trending, macroscopic D₂ folds (Hill End Anticline) with S₂ slaty cleavage and associated bedding-parallel veins.

Structural analysis indicates that the D₂ flexural-slip folding mechanism formed bedding-parallel movement zones that contained flexural-slip duplexes, bedding-parallel veins, and saddle reefs in the fold hinges. Bedding-parallel veins are concentrated in weak, narrow shale beds between competent sandstones with dip angles up to 70° indicating that the flexural slip along bedding occurred on unfavourably oriented planes until fold lockup. Gold was precipitated during folding, with fluid-flow concentrated along bedding, as fold limbs rotated, and hosted by bedding-parallel veins and associated structures. However, the gold is sporadically

developed, often with subeconomic grades, and is associated with quartz, muscovite, chlorite, carbonates, pyrrhotite, and pyrite.

East-west shortening of the Hill End Trough resumed during the Late Devonian to early Carboniferous (Kanimblan Orogeny), producing a series of steeply W dipping reverse faults that crosscut the eastern limb of the Hill End Anticline. Where W-dipping reverse faults intersected major E-dipping bedding-parallel veins, gold (now associated with galena and sphalerite) was precipitated in a network of brittle fractures contained within the veins, forming moderately S plunging, high-grade gold shoots. Only where major bedding-parallel veins were intersected, displaced, and fractured by late W-dipping reverse faults is there a potential for localization of high-grade gold shoots (>10 g/t). A revised structural history for the Hill End area not only explains the location of gold shoots in the Reward Mine but allows previous geochemical, dating, and isotope studies to be better understood, with the discordant W-dipping reverse faults likely acting as feeder structures introducing gold-bearing fluids sourced within deeply buried Ordovician volcanic units below the Hill End Trough.

A comparison is made between gold mineralisation, structural style, and timing at Hill End in the eastern Lachlan orogen with the gold deposits of Victoria, in the western Lachlan orogen. Structural styles are similar where gold mineralization is formed during folding and reverse faulting during periods of regional east-west shortening. However, at Hill End, flexural-slip folding-related weakly mineralized bedding-parallel veins are reactivated to a lesser degree once folds lock up (cf. the Bendigo zone deposits in Victoria) due to the earlier effects of fold-related flattening and boudinage. The second stage of gold mineralization was formed by an array of crosscutting, steeply W dipping reverse faults fracturing preexisting bedding-parallel veins that developed high-grade gold shoots. Deformation and gold mineralization in the western Lachlan orogen started in the Late Ordovician to middle Silurian Benambran Orogeny and continued with more deposits forming in the Bindian (Early Devonian) and Tabberabberan (late Early-Middle Devonian) orogenies.

This differs from the Hill End Trough in the eastern Lachlan orogen, where deformation and mineralization started in the Tabberabberan Orogeny and culminated with the formation of high-grade gold shoots at Hill End during renewed compression in the early Carboniferous Kanimblan Orogeny.

REWARD MINERAL RESOURCE ESTIMATE

The Minerals Resource Estimate for the Reward Gold Project was completed by HGS Australia (HGS) in June 2023, to meet the JORC 2012 code.

Table 2. JORC Mineral Resource estimate for Reward Gold deposit.

	Cut-off g/t	Tonnes	Au (g/t)	Ounces
Indicated	4.0	141,000	15.54	70,500
Inferred	4.0	278,000	17.28	154,700
Total	4.0	419,000	16.72	225,200

CONCLUSION

The unique Features of Reward Gold Mine are:

- The Reward Gold Mine sits just below the Hawkins Hill Gold mine- arguably Australia's highest-grade gold mine at 435koz at 309 g/t.
- High-Grade Resource: The Reward resource is 419,000 tonnes for 225,200 ounces at a grade of 16.7 g/t, with quartz ore carrying coarse and fine gold.
- The high-grade mineralisation controlled by late stage, high-angle reverse faults. Similar to the structural model for Bendigo-Ballararat and Fosterville.
- 5 unique mineralisation events identified.
- High-grade repetitions are likely to occur where the high-angle reverse faults controlling mineralisation intersect additional bedding parallel lodes on stratigraphic positions above and below the defined mineralisation.
- Multiple positions already defined consistent with this model, forming a northerly plunge to the mineralisation.
- Stacked, bedding parallel, reverse fault-controlled mineralisation confirmed in backs mapping and extensive face sampling program completed during 2008 trial mining
- Eco-Friendly Recovery: Gold can be recovered by gravity concentrators to a Dore at a recovery rate greater than 92%, requiring no chemicals, cyanide, or reagents.
- Efficient Processing: Unique comminution process needing only a 650-micron crush, with no primary grind required, thus low energy consumption.
- Effective Ore Sorting: Ore sorting can upgrade gold grade by 320% between 15 mm and 60 mm.
- Benign Tailings: Resulting tailings are benign, free from metals, cyanide, or chemicals, and can be dry-stacked. Tails material can be reduced by 70%, with sorted material used as stope fill.
- Recyclable Process Water: Low metal content in water allows complete recycling or safe environmental release.

REFERENCES

- DOWNES, P. M. & SECCOMBE, P. K., 2003. A review of the Hill End Mineral System, NSW, Australia. In VASSALLO J. J. & GLEN R. A. (EDS). Evolution of the Hill End Trough: Hill End Trough CD Geoscience Data package, pp 54-62. Open File GS Report 2003/291. Geological Survey of New South Wales, Sydney, Australia.
- DOMINEY, S., 2003. Grade and geological continuity in high-nugget effect gold-quartz reefs: Implications for resource estimation and reporting. December 2003 Applied Earth Science IMM Transactions section B 112(3):239-259.
- DRINKWATER M., 1982. Hill End Gold 3rd Edition, 30-33.
- FERGUSON, C. L., 2009. Tectonic evolution of the Ordovician Macquarie Arc, central New South Wales: arguments for subduction polarity and anticlockwise rotation. Australian Journal of Earth Sciences, 56(2), 2009, pp 179-193.
- HITCHMAN, S.P., PHILLIPS, N.J. AND GREENBERGER, O.J., 2017. Fosterville gold deposit: in Phillips, G.N., (Ed.), 2017 Australian Ore Deposits, *The Australasian Institute of Mining and Metallurgy*, Mono 32, pp. 791-796.

FULLER, HANN, 2019, after Hitchman et al. 2017. Updated NI 43-101 technical report, Fosterville gold mine In the State of Victoria, Australia Prepared for Kirkland Lake Gold LTD.

GLEN R.A. & WATKINS J.J. 1994. The Orange 1:100000 sheet: A preliminary account of stratigraphy, structure and tectonics, and implications for mineralisation. Geological Survey of New South Wales – Quarterly Notes 95, 1-17.

HARPER L.F. 1918. The Hill End-Tamboora Gold-Field, Geological Survey of New South Wales, Mineral Resources 27.

LU J. 1993. Geochemical studies of a turbidite-hosted auriferous vein system, Hill End Goldfield, NSW Australia. PhD Thesis University of Newcastle, Newcastle (unpublished).

LU J. & SECCOMBE P.K. 1992. A fluid inclusion study of auriferous quartz veins — Hill End Goldfield, NSW Australia. Geological Society of Australia Abstracts 32, 82-84.

LU J. & SECCOMBE P.K. 1993. Fluid evolution in a slate- belt gold deposit. A fluid inclusion study of the Hill End goldfield, NSW, Australia. Mineralium Deposita 28, 310-323.

LU J., SECCOMBE P.K. & ELDRIDGE C.S. 1996A. SHRIMP S-isotope evidence for fluid mixing during gold mineralisation in a slate-belt gold deposit (Hill End, New South Wales, Australia. Chemical Geology (Isotope Geoscience Section) 127, 229-240.

LU J., SECCOMBE P.K., FOSTER D. & ANDREW A.S. 1996B. Timing of mineralization and source of fluids in a slate-belt auriferous vein system, Hill End goldfield, NSW, Australia: Evidence from $^{40}\text{Ar}/\text{Ar}^{39}$ dating and O- and H- isotopes. Lithos 38, 147-165.

MORGAN E.J., CAMERON R.G., COLQUHOUN G.P., RAYMOND O.L., SCOTT M.M., WATKINS J.J., BARRON L.M., HENDERSON G.A.M., KRYNEN J.P., POGSON D.J., WARREN A.Y.E., WYBORN D., YOO E.K., GLEN R.A., JAGODZINSKI E.A. 1999. Dubbo 1:250 000 geological sheet SI/55-4 (second edition). Geological Survey of New South Wales, Sydney and Australian Geological Survey Organisation, Canberra.

PACKHAM G.H. 1999. Radiometric evidence for Middle Devonian inversion of the Hill End Trough, northeastern Lachlan Fold Belt. Australian Journal of Earth Sciences 46, 23-33.

RAYMOND O.L., WYBORN D., STUART-SMITH P., WALLACE D.A., HENDERSON G.A.M., POGSON D.J., KRYNEN J.P., SCOTT M.M., WATKINS J.J., MEAKIN S., MORGAN E.J., WARREN A.Y.E., GLEN R.A. 1998. Bathurst 1:250 000 geological map SI/55-08, Second Edition. Australian Geological Survey Organisation, Canberra and Geological Survey of New South Wales, Sydney.

SECCOMBE P.K. & HICKS M.N. 1989. The Hill End Goldfield, NSW, Australia - early metamorphic deposition of auriferous quartz veins. Mineralogy and Petrography 40, 257-273.

SECCOMBE P.K., LU J., ANDREW A.S., GULSON B.L. & MIZON K.J. 1993. Nature and evolution of metamorphic fluids associated with turbidite-hosted gold deposits: Hill End goldfield, Australia. Mineralogical Magazine 57, 423-436.

WINDH, J. 1995. Saddle reef and related gold mineralisation, Hill End Gold Field, Australia: Evolution of an auriferous vein system during progressive deformation. Economic Geology 90, pp 1764-1775.

WILKINS, C., AND QUAYLE, M., 2021, Structural Control of High-Grade Gold Shoots at the Reward Mine, Hill End, New South Wales, Australia, Economic Geology Volume 116, Number 4 June 2021.

THE NYMAGEE CU-ZN-PB-AG-AU DEPOSIT, NYMAGEE NSW

Todd McGilvray, Owen Thomas & Katrina Virgoe

Aurelia Metals Limited, Brisbane, QLD 4000.

Keywords: Nymagee, copper, mineral resource estimate,

OVERVIEW

The Nymagee Deposit is located within the historic copper mining town of Nymagee, NSW, and is 200m west of the town centre with historic mine workings marking the western extent of the township (Figure 1). The deposit is 1.2km long striking 330° (NNW) and up to 220m wide with a sub-vertical dip westward and consists of a series of fault-bounded massive sulphide lenses with inter-fault stockwork mineralisation. The current tenure is held in Joint Venture between Aurelia Metals Limited (95%) and Ausminindex Pty. Ltd. (5%).

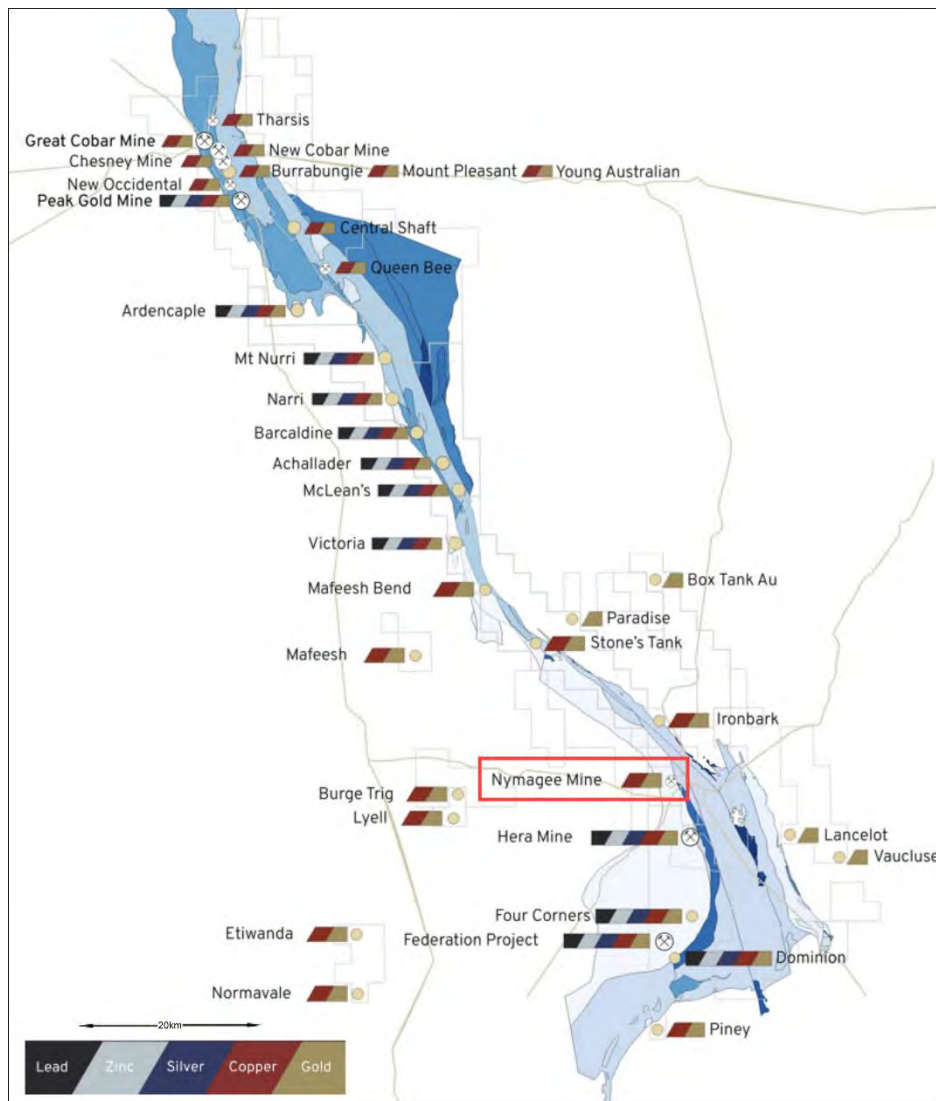


Figure 1: Illustrative plan view of the Nymagee/Cobar Districts with mines and prospect area locations and metal prospectivity (McGilvray 2024).

DEPOSIT HISTORY (FROM MCQUEEN 2017)

Copper carbonate minerals azurite and malachite were discovered on a hill near the boundary of the Nymagee and Hartwood Stations by two shepherds, Henry (Harry) Manly and 'Bryson' in September 1876. Harry Manly applied for a Mineral Conditional Purchase claim in November 1876 and was granted the claim in January 1880. Russell Barton purchased the claim from Manly in early 1880 and the Nymagee Copper Mining Company Ltd was formed in March 1880.

By the end of the year three shafts had been commenced on the Main Zone, Barton's Shaft, Pope's Shaft and Threlkeld's Shaft. Early development produced copper ores of malachite and chalcocite to a depth of around 160 feet (50m) and up to 40 feet (12m) in width. Primary chalcopyrite ore was first encountered in Pope's Shaft in October 1880 below the supergene zone.

Smelting commenced in early December 1880 via two reverberatory furnaces and at the height of production eleven reverberatory furnaces were utilised by 1884. Innovations to smelting technology resulted in reduction in the number of reverberatory furnaces to four and construction of three blast furnaces by 1906.

By the year 1883, 500 people were employed at the Nymagee Mine consisting of 109 miners, 200 woodcutters and carters and the remainder employed in the smelting and mine support areas. The mine was plagued by numerous issues including availability of timber, availability of coal, a fluctuating copper price, transportation constraints and severe drought limiting stock feed and water availability. The Nymagee Mine eventually closed permanently in 1917.

Total copper production for the Nymagee Mine between 1881 and 1917 was approximately 24,800 tons grading consistently above 10% copper until 1896 with the copper grade progressively declining to between 4% and 2% by 1917 averaging approximately 5.8% copper during the life of mining.

REGIONAL GEOLOGY

The Nymagee Deposit is located within the Nymagee 1:100 000 Geological Sheet and is described in detail by MacRae (1987). The deposit is located adjacent to the eastern margin of the Cobar Basin (Figure 2).

The oldest rocks in the region are the Ordovician turbiditic sediments of the Girilambone Group. These sediments are interpreted to have been deposited within a back-arc marginal sea (MacRae, 1987), with a dominant continental input. Deformation and metamorphism of the Girilambone Group was followed by emplacement of the Erimera Granite and Nymagee Igneous Complex during the Mid- to Late-Silurian. Subsequent uplift and erosion unroofed these igneous rocks prior to the Early Devonian (MacRae, 1987). A period of extension in the Cobar region in the Early Devonian resulted in the formation of the Cobar Basin. The bounding margins of the Cobar Basin were north to north-north westerly trending basement structures (e.g.: Rookery fault system). Initial shallow water facies deposition (e.g.: Mouramba and Kopyje Groups) was followed by a deep-water, syn-rift facies (Lower Amphitheatre Group, Shume Formation) and a subsequent post-rift facies (Upper Amphitheatre Group).

The Cobar Basin was deformed in the Early Devonian with basin forming structures such as the Rookery Fault inverted to near vertical thrust faults with high strain zones in the western, hanging wall side on the eastern margin of the Cobar Basin. The setting, structure and mineralisation of the Cobar Basin Region has been summarised by Geological Survey of NSW publications such as Glen (1991 and 1994), Glen et al. (1996), Suppel & Gilligan (1993), Gilligan & Byrnes (1995) and Fitzherbert et al. 2022.

The Nymagee Cu-Zn-Pb-Ag-Au deposit, Nymagee NSW

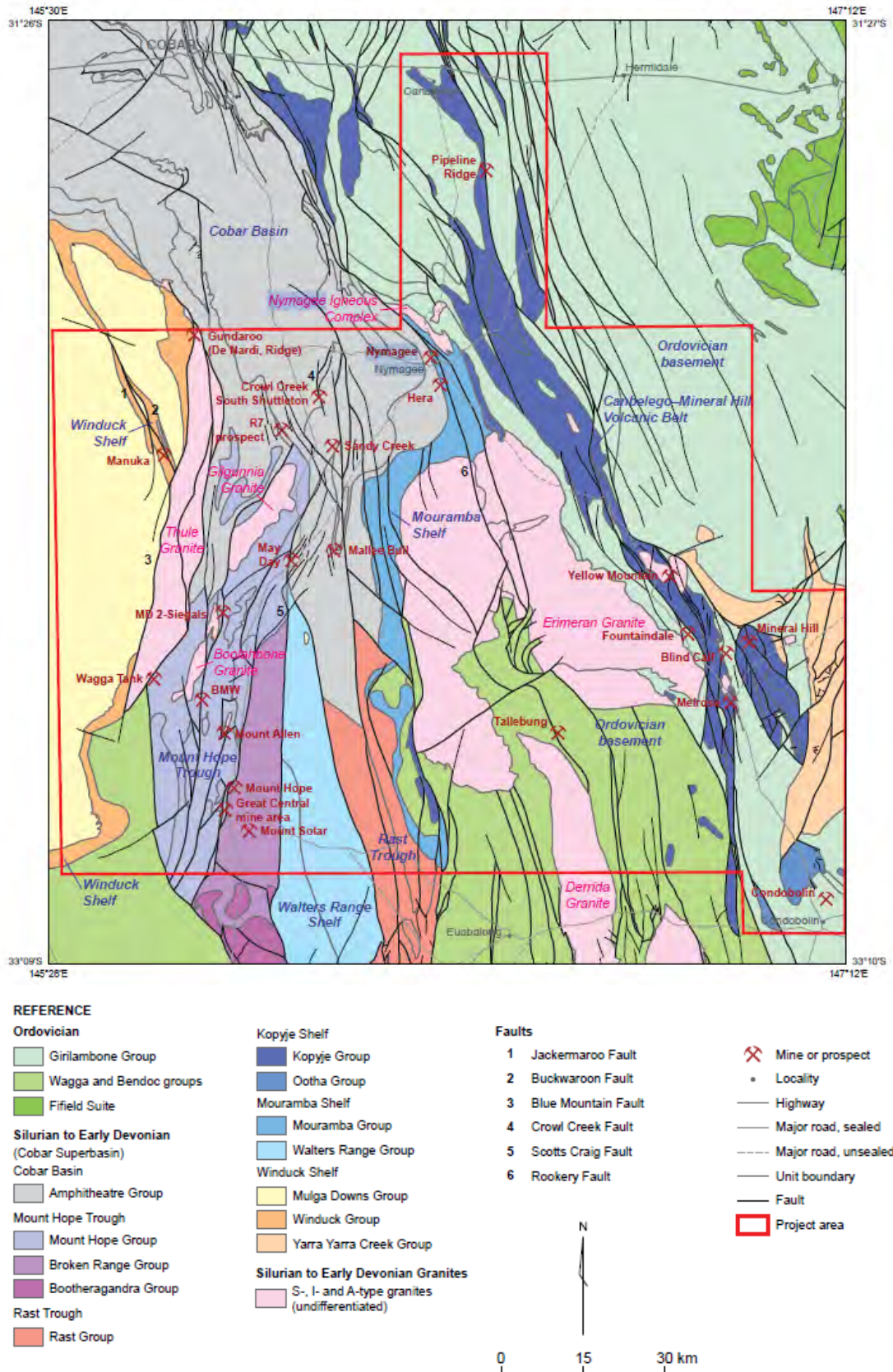


Figure 2: Generalised Geology and major tectonic units in the Nymagee District with major mineralised zones and geological groups (Downes et al. 2016).

LOCAL GEOLOGY

The Nymagee Mine is located near the eastern margin of the Cobar Basin, within a sequence of siltstone and fine-grained sandstone to greywacke units of the Mouramba Group. Sediments of the Mouramba Group are believed to have been deposited in an unstable slope environment due to the presence of intraformational breccias and soft sediment slump folding. The presence of heavy minerals observed in beds of the Mouramba Group, such as tourmaline, zircon, apatite and magnetite, suggests a granitic provenance. MacRae (1987) assigned the exposed rocks in the Nymagee Mine area to the Lower Amphitheatre Group based on the lack of ripple cross laminations within the siltstone beds which typifies the Mouramba Group. However, other sedimentary structures (soft sediment slumping and intraformational breccias) and petrographic descriptions (Paterson, 1974) suggest that the rocks within the Nymagee Mine area were deposited in an unstable slope environment more consistent with the Mouramba Group. Sediments of the Shume Formation are located west of the Nymagee Mine area.

The local mine geology sequence was subdivided by Paterson (1974) into eight units which includes a thin marker bed. The sequence is west facing, strikes approximately 330° (magnetic) and dips steeply west (>80° to vertical). There has been no major folding noted within the immediate vicinity of the mine. Cleavage within the sediment sequence typically strikes at 320° (magnetic) and has a vertical to very steep easterly dip. Several shear orientations have been delineated. The main shear direction strikes 300-310° (magnetic). A less prominent shear direction strikes 340° (magnetic). A more detailed account of the local geology at the Nymagee Mine is given by Paterson (1974).

Paterson's stratigraphy has been modified by review of additional drilling and mapping to produce the stratigraphic column presented below (Figure 3). The bulk of the mine sequence is considered to be part of the Mouramba Group with a major ductile shear on the western margin apparently separating the overlying Amphitheatre Group. Stratigraphy is largely steeply west dipping and west facing with minor "S" folds and shearing parallel to bedding.

The southern margin of the deposit stops abruptly in an area of anomalous folding leading to the interpretation of a significant east-west fault truncating mineralisation. Gravity and magnetic data suggest that this fault has displaced the alteration system 1 km eastwards to the Town Tank Prospect.

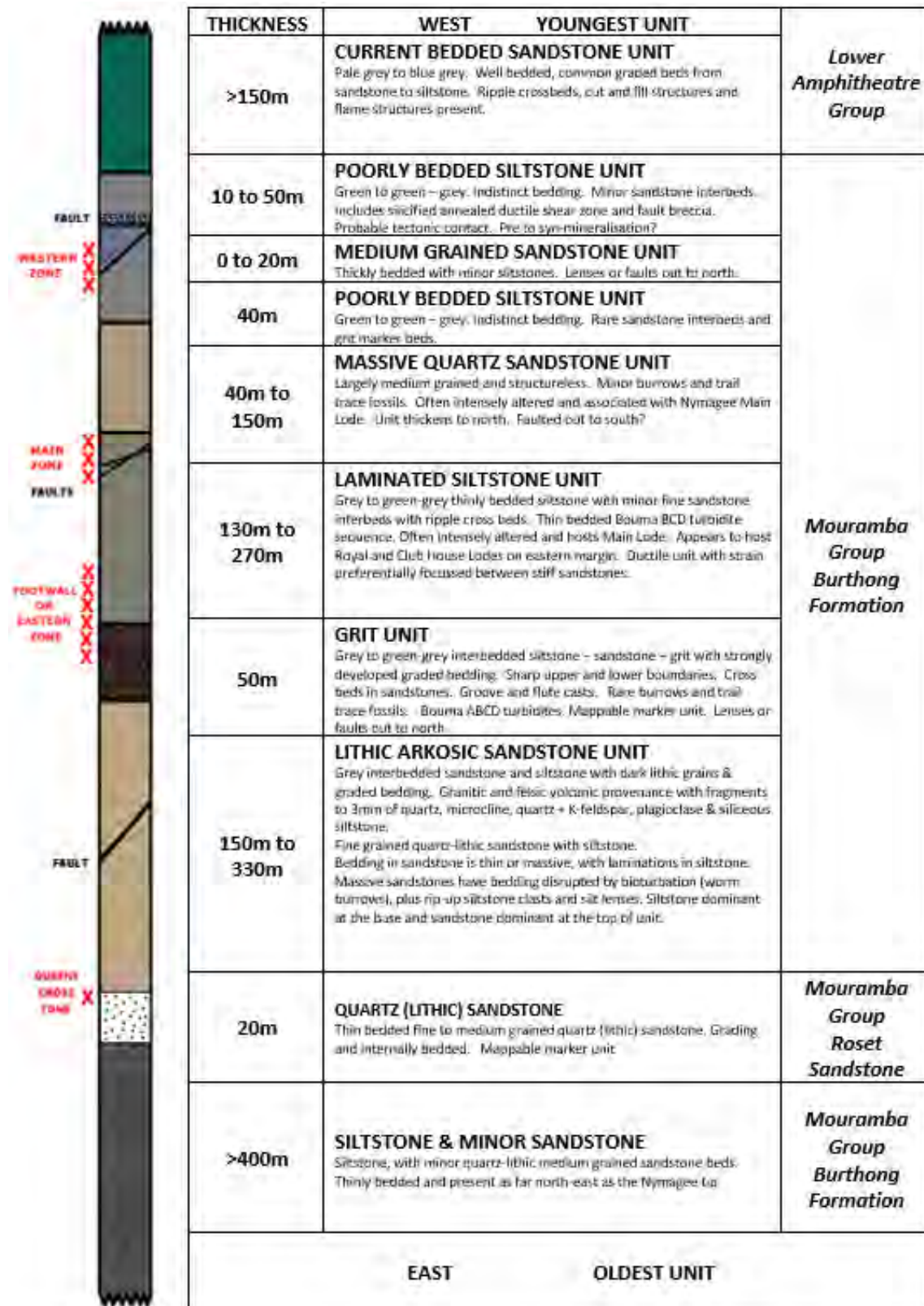


Figure 3: Nymagee Mine Stratigraphy (from McGilvray and Virgoe 2023, after Paterson 1974).

MINERALISATION

Nymagee Deposit mineralisation occurs as a series of parallel, structurally controlled zones with quartz + sulphide matrix breccias and multiple massive sulphide lenses in

each zone. Stockwork to stringer sulphide vein mineralisation occurs between the zones and have been identified as interzone mineralisation. Mineralisation has been previously subdivided into three main mineralised zones by Paterson (1974) (Figure 4).

The Western Zone comprises massive to multiple veins and lenses of sphalerite/galena + chalcopyrite with sporadic pyrrhotite/chalcopyrite veins. The mineralised zone is believed to extend approximately 900m along strike and is approximately 30m wide with a steep westerly dip. Narrow zones of significant Zn-Pb-Ag mineralisation have been intersected in this zone (e.g. CDDH3: 2.67m @ 33.0% Zn, 17.5% Pb and 275ppm Ag from 146.53m and NMD068: 7m @ 6.8% Zn, 3.4% Pb, 47ppm Ag from 207m).

The Main Zone consists of a series of overlapping Zn-Pb+/-Cu and Cu-rich ore horizons. The individual ore horizons typically pitch steeply to the south and occur within a broad halo of disseminated pyrrhotite and quartz veining. The complete zone extends approximately 500m along strike and is up to 30m wide. The mineralised zone typically exhibits a sharp western contact with a diffuse eastern contact into the Eastern Zone mineralisation. The western horizons are generally more Zn-Pb rich, and the Cu rich horizons occur in the east.

The Eastern Zone comprises stringers and veins of chalcopyrite/pyrrhotite, associated with narrow quartz veins. The mineralised veins are typically aligned within cleavage and fracture planes. The zone extends approximately 400m along strike and is up to 100m wide and subvertical. Primary mineralisation intersected to date within the mineralised zone is generally lower in grade (<2.5% Cu). Recent drilling has identified some new higher-grade areas in this footwall zone at depth, (e.g. Royal Lode and Club House Lode).

Additionally, the interzone stockwork and (Mine) hangingwall stockwork areas have shown significant grade potential from recent drilling with copper grades up to 5.7% copper encountered (Figure 5).

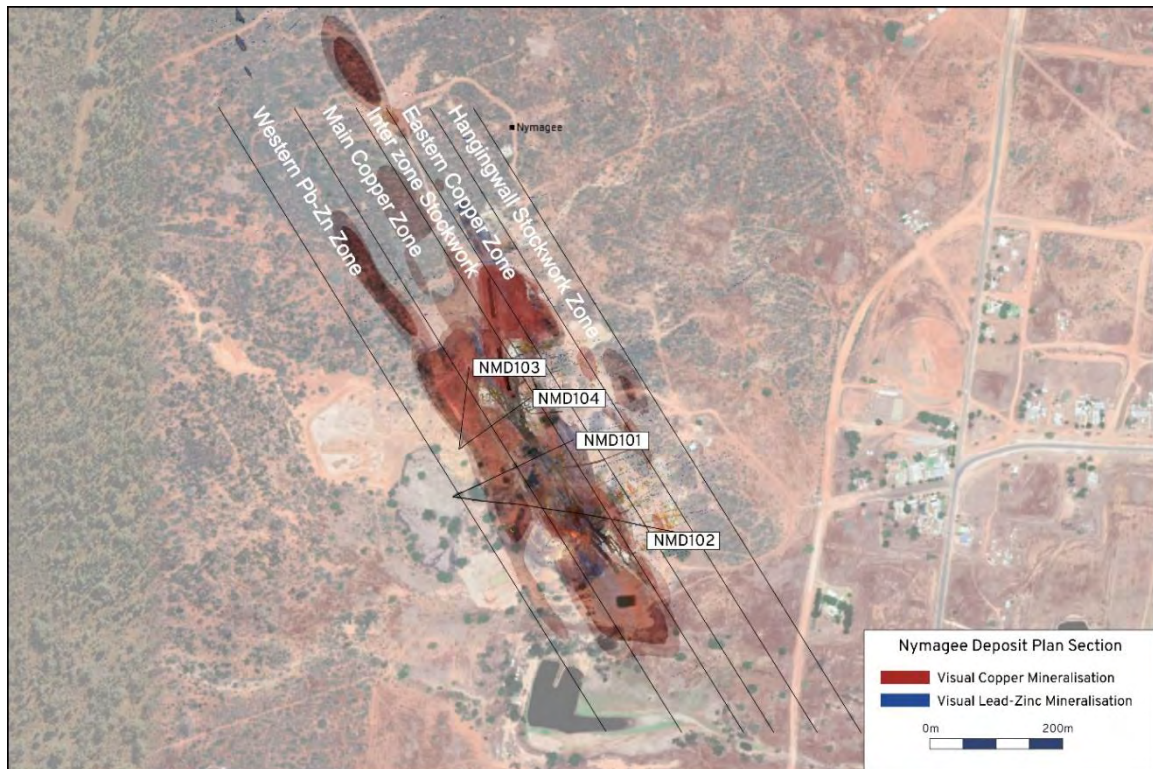


Figure 4: Plan view of the Nymagee Deposit with visual sulphide envelopes, zones of mineralisation and FY24 Aurelia Metals diamond drillholes (McGilvray 2024).

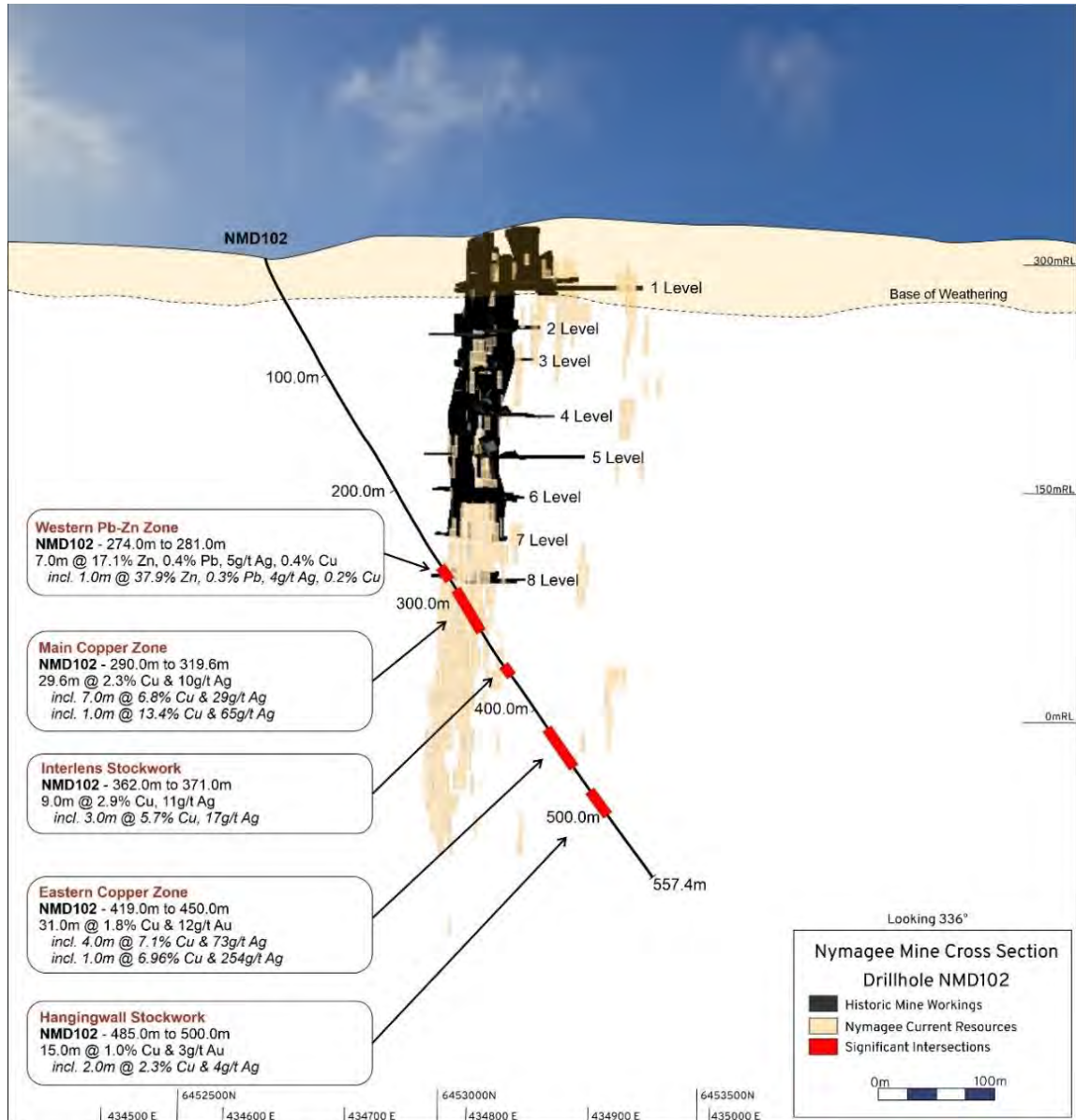


Figure 5: Cross Section of the Nymagee Deposit with historic mine development, block model outline of the FY23 resource estimate and FY24 Aurelia Metals diamond drillhole NMD102 (McGilvray 2024).

ALTERATION

Petrographic studies were collated and undertaken by Paterson (1974) on key diamond drillcore samples focussed on the Main Zone and unaltered rocks considered distal to the main mineral system. Regional alteration assemblages are consistent with Greenschist facies metamorphic assemblages. Deposit specific alteration assemblages vary between horizons and include biotite, chlorite, quartz, talc, stilpnomelane, pyrrhotite, and magnetite with minor sporadic garnet, pyroxene and tremolite.

Downes et al. (2016) conducted a hyperspectral study on deposits across the Nymagee Region including the Nymagee Deposit (Figure 6). It was noted there were significant changes in abundance, species and presence of minerals identified within the spectral data for zones proximal to mineralisation across the wider dataset. At Nymagee, systematic changes in chlorite composition from Fe- and/or Fe-Mg chlorites to more Mg-rich varieties were observed. Downes et al. (2016) suggested the change in chlorite composition may be due to either scavenging of Fe to form predominant Fe-bearing

sulphides such as pyrrhotite, pyrite, chalcopyrite or sphalerite, and/or there was an abundance of magnesium in the ore-forming fluids. If the fluids were undersaturated in Fe this would support an interpretation that many of the ore-forming fluids are of basinal or sea-water origin.

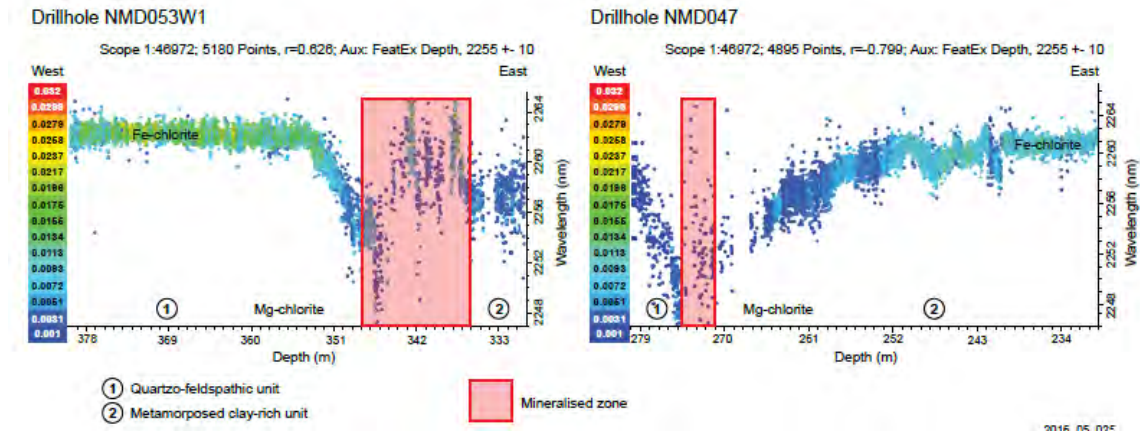


Figure 6: Changes in chlorite composition in response to alteration associated with mineralisation – Nymagee Copper Mine drillholes NMD053W1 (drilled from west to east), and NMD047 (drilled from east to west) (from Downes et al. 2016).

RESOURCE ESTIMATE

The FY23 Mineral Resource Estimate (MRE) for the Nymagee Deposit is reported with Indicated and Inferred classifications at an A\$120/t NSR cut-off value (Table 1). The MRE includes all blocks within the volumes produced by Deswick’s SO software and the reported estimates include an internal dilution component. All details can be found with Aurelia Metals Limited (2023).

Table 1: Nymagee Project MRE as at 30 June 2023 (Aurelia Metals Limited 2023).

Class	Tonnes (kt)	Cu (%)	Au (g/t)	Zn (%)	Pb (%)	Ag (g/t)
Indicated	1,900	2.2	0.1	1.1	0.6	16
Inferred	50	2.2	0.1	0.5	0.2	11
Total	1,900	2.2	0.1	1.1	0.6	16

Note: The Nymagee Project MRE utilises A\$120/t NSR cut-off mineable shapes that include internal dilution. Values are reported to two significant figures which may result in rounding discrepancies in the totals.

The diamond drilling campaign conducted in FY24 was aimed at assessing the spatial integrity of existing information, extending mineralisation to an inferred category, and testing the extent and grade tenor of the Eastern Copper Zone (Figure 7). The Eastern Copper Zone has significant potential for extension and will be targeted further in FY25.

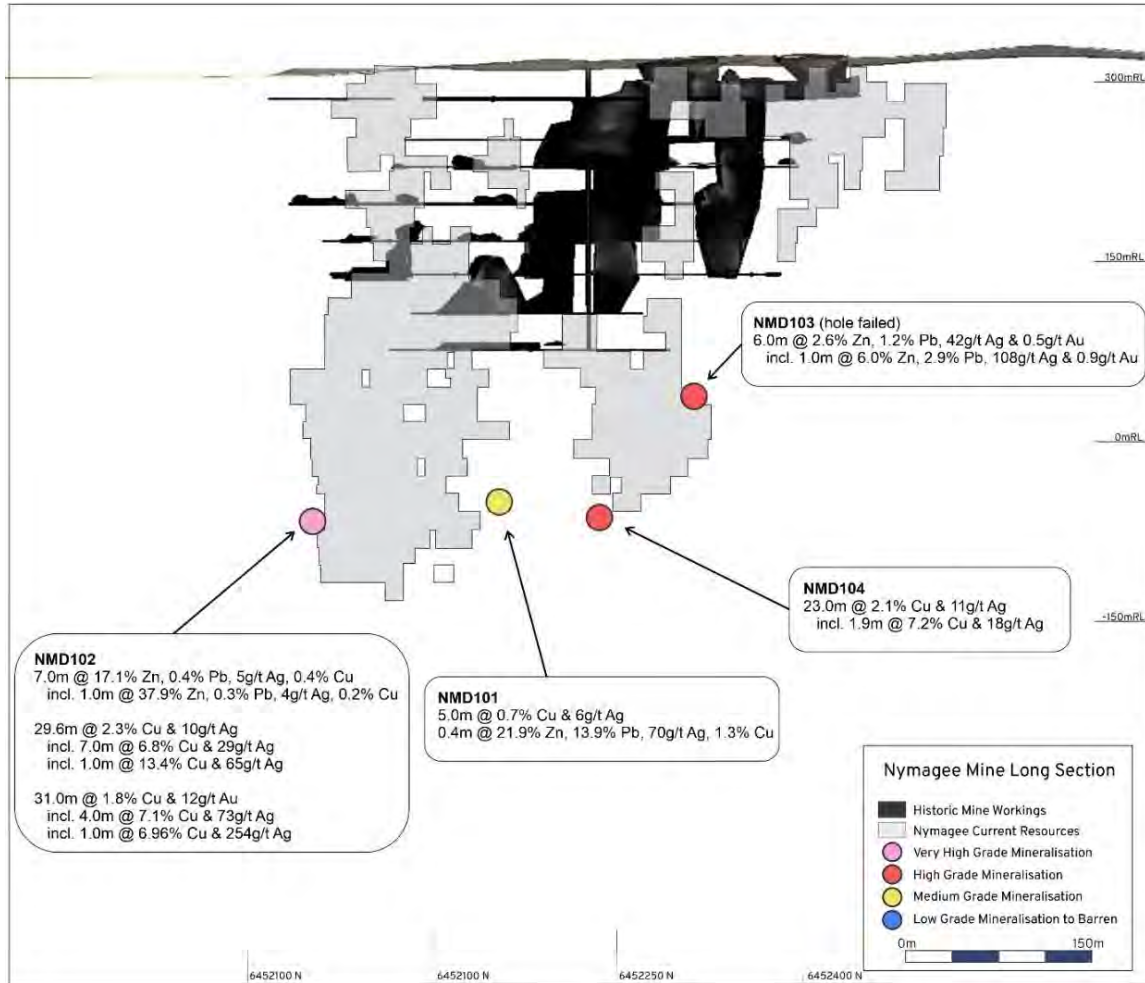


Figure 7: Long Section of the Nymagee Deposit with historic mine development, block model outline of the FY23 resource estimate and FY24 Aurelia Metals diamond drillholes (McGilvray 2024).

STRUCTURE (FROM PATERSON 1974)

Sediments at the Nymagee Deposit have an average strike of 330° magnetic north and a dip ranging from 80° west to vertical in the central mine area. Zones of drag folding and shearing occur locally ranging from isoclinal to open. Mineralisation appears to be conformable in the wider zones however interzone mineralisation appears to be localised in fractures, shear planes and quartz filled cleavages.

Bedding planes appear to have been utilised as slip planes during deformation however the magnitude and extent of this process has not been adequately quantified.

The most prominent cleavage in the mine area strikes 320° magnetic north and dips range from vertical to 80° east. The cleavage is often quartz filled and contains ore minerals as blebs and stringers in the eastern and main zones. The main cleavage has undergone several reactivations and is typically sheared. A second, less prominent, cleavage strikes at 340°-345° and dips east at generally flatter angles.

The main shear or fault direction strikes toward 300° to 310° magnetic north with a second shear or fault direction towards 340° magnetic north and is conjugate to the main shear. A large cataclastic zone occurs to the west of the mine parallel to the main shear orientation and appears to disrupt the western Pb-Zn Zone, post-dating mineralisation.

A second fault direction was recorded striking 90° to 100° magnetic north and appears to offset bedding, cleavage, mineralisation and alteration, typically associated with crushing

and re-welding of quartz veins. This structure post-dates mineralisation and offsets are typically small.

Further structural assessments will be carried out in FY25 to assess the impact of, and/or importance of the various structures present with regards to mineralisation. Mineralisation is dramatically terminated in the south by an apparent fault trending 90° to 100° magnetic north however the effect of parallel faults in the mine area is minimal. Previous literature has highlighted a southern plunge to mineralisation as an important factor however a northern plunge is apparent north of the main mine in the Western Pb-Zn Zone. A detailed structural review is anticipated in FY25 to support further exploration drilling (Figure 8).



Figure 8: Massive chalcopyrite-pyrrhotite mineralisation in the Main Copper Zone at the Nymagee Deposit (NMD 102 – 299.0m depth) intersected during the FY24 diamond drilling campaign.

CONCLUSIONS AND RECOMMENDATIONS

The Nymagee Deposit has significant growth potential within the known zones of mineralisation and has potential for further discoveries in close proximity to the mine. Aurelia Metals will transition to copper dominant ore feed in H2 FY25 and the Nymagee Deposit has potential to contribute further to this ore feed in the future. Exploration drilling will recommence in H1FY25 aiming to extend known resources and test EM conductor plates north of the main Nymagee Deposit. Detailed structural analysis will be conducted in H1 FY25 and metallurgical testwork will be reinitiated during the latter half of FY25.

REFERENCES

- AURELIA METALS LIMITED, 2023. Group Mineral Resource and Ore Reserve Statement. Aurelia Metals Limited ASX Announcement 30/08/2023.
- DOWNES, P. & BLEVIN, P., ARMSTRONG, R., SIMPSON, C., SHERWIN, L., TILLEY, D., BURTON, G., 2017. Outcomes of the Nymagee mineral system study — an improved understanding of the timing of events and prospectivity of the central Lachlan Orogen. Quarterly Notes of the Geological Survey of New South Wales. 147. 1-38.
- FITZHERBERT, J. & DOWNES, P. & BLEVIN, P., 2022. District-scale characteristics of mineralisation in the Cobar Superbasin: attempting to understand timing and genesis. Extended abstract in Lewis, P., 2022. Bulletin 70: Discoveries in Tasmanides 2022. Australian Institute of Geoscientists, PO Box 576 Crows Nest NSW 1585.
- GILLIGAN, L. B. & BYRNES, J. G., 1995. Cobar 1: 250 000 Metallogenic Map SH/55-14: Metallogenic Study and Mineral Deposit Data Sheets. Geological Survey of NSW, Sydney.
- GLEN, R. A., 1991. Inverted Transtensional Basin Setting for Gold and Base Metal Deposits at Cobar, New South Wales, BMR Journal of Geology and Geophysics, 120, pp 13-24.
- GLEN, R. A., 1994. Geology of the Cobar 1:100 000 sheet 8035, Second Edition. Geological Survey of NSW, Sydney.
- MCQUEEN, K., 2017. Nymagee copper: Birth, death and resurrection? Journal of Australasian Mining History, Vol. 15, 2017.
- MCGILVRAY, C. T., & VIRGOE, K., 2023. Annual Exploration Report for EL4458. Unpublished.
- MCGILVRAY, C. T., 2024. Nymagee Exploration Update. Aurelia Metals Limited ASX Announcement 22/02/2024.
- MACRAE, G. P. 1987. Geology of the Nymagee 1:100,000 Sheet 8133. Geological Survey of NSW, Sydney.
- PATERSON, R. G., 1974. The Geology and Economic Potential of the Nymagee Mine, Nymagee, NSW. Cyprus Mines Corporation – Final Report (GS1973/431)
- SUPPEL, D. W. AND GILLIGAN, L. B., 1993. Nymagee 1:250 000 Metallogenic Map SI/55-2: Metallogenic Study and Mineral Deposit Data Sheets. Geological Survey of NSW, Sydney.

NORTHERN MOLONG PORPHYRY PROJECT – Boda-Kaiser Au-Cu Porphyry System

David Meates¹, Rodney Dean¹, Alexander Cherry¹, Andrew Carras¹, Ian Chalmers²

¹Alkane Resources Ltd, 22 Cameron Place, Orange, NSW 2800

²Alkane Resources Ltd, PO Box 768, West Perth, WA 6872

Keywords: gold, copper, Boda, Kaiser, porphyry, Macquarie Arc, Molong Volcanic Belt

ABSTRACT

Alkane Resources discovered significant alkalic porphyry Au-Cu mineralisation at the Boda-Kaiser prospect area within the Northern Molong Porphyry Project (NMPP) in the Central West region of NSW. The discoveries are in the Molong Volcanic Belt (MVB) of the Macquarie Arc, the geological terrane that is also host to the world class Cadia Au-Cu porphyry deposits.

The Boda-Kaiser deposits are considered to represent a new style of Au-Cu porphyry mineralisation associated with the Late Ordovician – Early Silurian alkalic porphyries of the Macquarie Arc. Transitional magmatic-hydrothermal to hydrothermal breccias are central to the silica-deficient Au-Cu mineralisation hosted by coherent volcanic and volcanoclastic country rocks.

Several major drilling campaigns that commenced after the discovery of Boda in September 2019 have culminated in the estimation of two large Au-Cu resources at Boda (including Boda 2-3) and Kaiser. Indicated and Inferred Resources have been defined at Boda and Kaiser with the total standing at 796 million tonnes grading 0.33g/t Au, 0.18% Cu for 8.3 Moz Au and 1.5 Mt Cu (29 April 2024).

Regional exploration has since recommenced including a FALCON Airborne Gravity Gradiometry (AGG) survey over the entire project area. The survey identified an approximately 35km² gravity low interpreted to be a significant deep-seated intrusive complex (Comobella Intrusive Complex) central to the extensive low-grade Au-Cu porphyry mineralisation found throughout the project area. Exploration has now identified seven discrete intrusive complexes - Boda, Kaiser, Boda South, Driell Creek, Murga, Windora and Tompkins, all situated outboard of the major Comobella Intrusive Complex and within or proximal to a northwest trending structural corridor.

Extensive alteration and widespread, low-grade, Au-Cu mineralisation define the corridor including the two significant Au-Cu resources at Boda-Kaiser. Exploration continues to improve the understanding of the Boda-Kaiser geological setting and to test new targets throughout the NMPP, supporting the possibility that a new large-tonnage alkalic porphyry district is being defined in the Macquarie Arc.

INTRODUCTION

The NMPP is located within the MVB of the Macquarie Arc in the Eastern Lachlan Orogen. The NMPP is positioned 20km north-east of Wellington and approximately 250km north-west of Sydney in the Central West of NSW. The MVB is highly prospective for large scale porphyry Au-Cu deposits, as demonstrated by the Cadia porphyry district located 120km to the south. Cadia is one of the world's largest known alkalic porphyry systems with a total endowment, including past production and current resources, of 50 Moz Au and 9.5 Mt Cu (Harris et al., 2020).

The Boda discovery was the result of several years of extensive geological mapping, geophysical surveys, small drilling programs and litho-geochemical characterisation. Boda was discovered in 2019, with diamond core drill hole KSDD003 intersecting 502m grading 0.48g/t Au & 0.20% Cu from 211m. The follow up drilling program returned the world-class intercept of 1,167m grading 0.55g/t Au & 0.25% Cu from 75m in KSDD007, including a sulphide-cemented breccia with a high-grade intercept of 96.8m grading 3.97g/t Au & 1.52% Cu from 768m.

REGIONAL GEOLOGICAL SETTING

The project area coincides with the northernmost extent of exposed MVB volcanosedimentary rocks (**Figure 1**). The stratigraphy in the area has been mapped as the Late Ordovician Cheeseman Creek Formation of the Cabonne Group and comprises mafic to intermediate lava flows, subvolcanic intrusives, volcanoclastics and minor occurrences of limestone. The Cheeseman Creek Formation is inferred to have been deposited in a submarine volcanic arc environment, given the abundance of hyaloclastite fragments in volcanoclastic units, and the presence of calcareous debris through the formation (Meakin & Morgan, 1999). Late Ordovician-Early Silurian diorites, monzodiorites and monzonites intrude the succession as stocks, dykes and sills.

Unconformably overlying the above-mentioned package are the Silurian Mumbil Group (Hill End Trough). These rocks are only present to very limited extent within the project area where the basal unit is the fossiliferous Narragal Limestone. This unit is overlain by siltstones, shales and tuffs of the Barnaby Hills Shale and the Gleneski Formation which is comprised of felsic volcanic and volcanoclastic rocks (Morgan et al., 1999). To the east of the project area, this Silurian succession is overlain by the latitic to andesitic volcanoclastics and limestones of the Cuga Burga Volcanics which form part of the Devonian Gregra Group. Numerous unassigned Devonian intrusions crosscut the entire Ordovician-Devonian sequence.

The Nindethana Fault is a major crustal scale listric thrust located along the eastern margin of the project area. It trends north-south and displaces the Silurian-Devonian succession to the east and forms the contact between the Ordovician and Silurian succession to the north. To the east of this structure the sequence of Ordovician-Devonian rocks is intruded by the Carboniferous Wuuluman Granite. This pluton is compositionally defined as a megacrystic quartz monzodiorite.

In the northwestern extents of the project area, the entire Ordovician-Devonian sequence is unconformably overlain by, or is in fault contact with, Permian and Triassic siliciclastic units of the Gunnedah Basin (which obscures the remainder of the MVB to the north). The western margin of the project area coincides with the Macquarie Fault, a north-south trending east-dipping thrust that juxtaposes Ordovician volcanics in the east with Silurian sediments of the Cowra trough to the west.

BODA-KAISER DEPOSITS

The Boda district is located within a NW-SE trending structural corridor characterised by extensive calc-potassic alteration and low-grade Au-Cu mineralisation over an area of approximately 3km x 0.7km. The Boda and Boda 2-3 deposits are located on the western margins of magnetic complexes of approximately 0.6km x 0.3km and 1.0km x 0.6km respectively and the Kaiser deposit is coincident with and on the southwestern margin of a magnetic complex of approximately 1.0km x 0.4km. The Boda district is defined in the gravity data as being within a zone of moderate response, between a gravity high to the west interpreted to be a dense part of the Ordovician volcanics, and a large gravity low to the east coincident with the Wuuluman Granite. Mineralisation is associated with laterally

restricted, but vertically extensive magmatic-hydrothermal breccias that have emanated from a fertile intrusion at depth.

Local Geology

Gold-copper porphyry mineralisation is largely hosted within country rocks of submarine basaltic to andesitic lavas and volcanoclastics with subordinate latite flows. The dominant volcanic suite consists of hornblende-augite-plagioclase phyric basaltic andesite lavas and narrow feeder dykes. These lavas also contain magmatic biotite, often accompanied by apatite microphenocrysts. These lavas are rare for the Macquarie Arc and likely correlate with the uppermost parts of the Fairbridge Volcanics (Crawford, 2020) which outcrops to the south near Bakers Swamp and Molong. Crawford (2021) suggests the lava and volcanic breccia-dominant stratigraphic package indicates Boda-Kaiser formed on the flanks of a major submarine stratovolcano from which sediments were transported into surrounding basinal settings.

The volcanosedimentary sequence was intruded by pulses of high-K calc-alkaline to shoshonitic magmas ranging from diorite to monzodiorite and monzonite in composition, generally as narrow stocks, dykes and sills. Late mafic to felsic dykes crosscut the altered volcanic sequence. Several of the late felsic dykes are weakly Cu-Mo-Ag mineralised and have been linked to the Carboniferous Wuuluman Granite that outcrops approximately 1km to the east.

Transitional magmatic-hydrothermal breccias control the widespread calc-potassic alteration and Au-Cu mineralisation at the Boda district. These breccias likely emanate from deep monzodiorite stocks, capable of generating large volumes of magmatic-hydrothermal fluid that escaped, likely through long-lived but small-scale brittle fracturing events (Wilson, 2023). The magmatic-hydrothermal breccias are generally monomict and crackle to mosaic in form. The breccia cement transitions vertically from a purely igneous cement at depth with the composition ranging from diorite to monzonite, through magmatic-hydrothermal cement where there is a component of igneous cement as well as exsolved hydrothermal minerals, through to purely hydrothermal cement with the highest Au-Cu grades attributed to rare sulphide-cemented breccias. Largely, the hydrothermal cement contains varying proportions of calcite, actinolite, magnetite, pyrite and chalcopyrite with minor biotite and quartz.

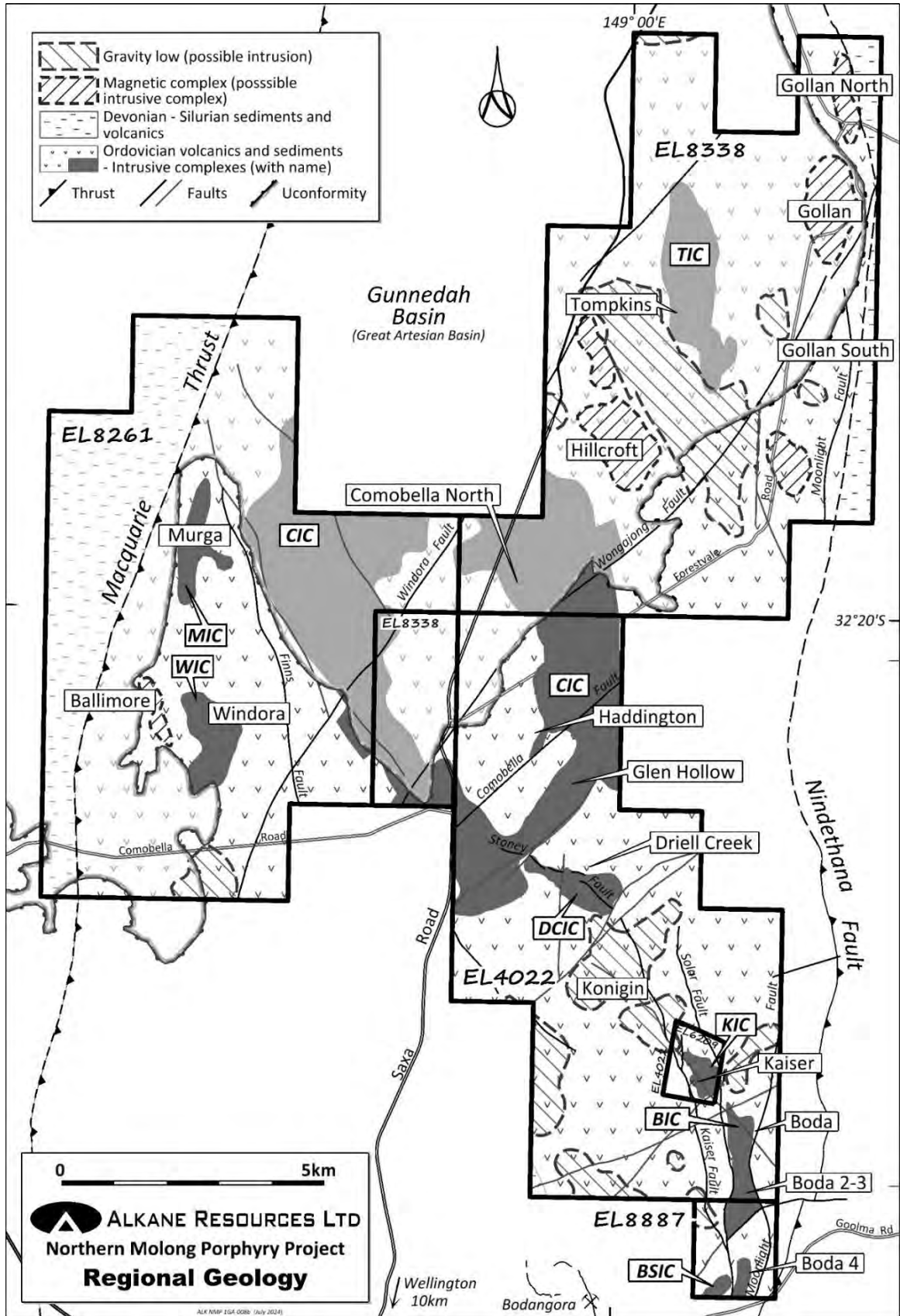


Figure 30: Regional geological setting.

The Boda district is situated within a northwest trending structural corridor, evident in the magnetic and gravity data. This structural corridor is host to mineralisation at Kaiser, Boda and Boda 2-3 and is dislocated by a post-mineral imbricate reverse fault system. Three significant north-south trending, west dipping reverse structures, the Solar, Moonlight and Reids Faults (**Figure 2**), have been intersected by drilling. A second order reverse fault, the Kaiser Fault, is moderate to steep east dipping and has only been intersected at the Kaiser deposit.

Modelling of the Solar Fault suggests that up to 500 metres of west-over-east reverse movement has displaced distal and barren propylitic alteration over the Boda and Boda 2-3 calc-potassic altered and Au-Cu mineralised rocks. Additionally, the Boda deposit is truncated by the Solar Fault resulting in an apparent northwest plunge to the mineralisation. At the Kaiser Deposit, the interplay of the Solar Fault and Kaiser Fault have created a “pop-up” block that hosts the Au-Cu mineralisation. As a result of this up-thrusting relative to the Boda deposit in the footwall of the fault, the Kaiser deposit is eroded to a much deeper level than at Boda where the top of the porphyry system is thought to be largely preserved. **Figure 2** displays a cross section through the Boda deposit from southwest to northeast (rotated 48°).

Alteration and Mineralisation

The local geology has undergone extensive and selectively pervasive calc-potassic to potassic alteration, often affecting both phenocrysts and the groundmass of the volcanic host rocks. This alteration is apparent over a strike length of greater than 4 km from Kaiser, southeast to Boda, then rotating and continuing south to Boda 2-3 and Boda 4, with more intense centres of hydrothermal alteration occurring at each of the prospects. Calc-potassic alteration comprises fine-grained biotite-actinolite ± epidote ± magnetite with minor zones of potassic alteration, generally in the northeast of the Boda and Kaiser deposits, comprising only biotite ± magnetite with up to 10% disseminated pyrite. This zone of alteration is Cu poor; however, Au grades can average from 0.2g/t to 0.6g/t over hundreds of metres, with occasional narrow intervals of >10g/t.

Calc-potassic alteration grades into propylitic alteration away from the breccia complexes and has a typical assemblage of actinolite-hematite-epidote-pyrite ± trace chalcopyrite proximal to the calc-potassic alteration zone. Moving further away from the mineralised centres the typical assemblage transitions to chlorite-calcite-albite-pyrite.

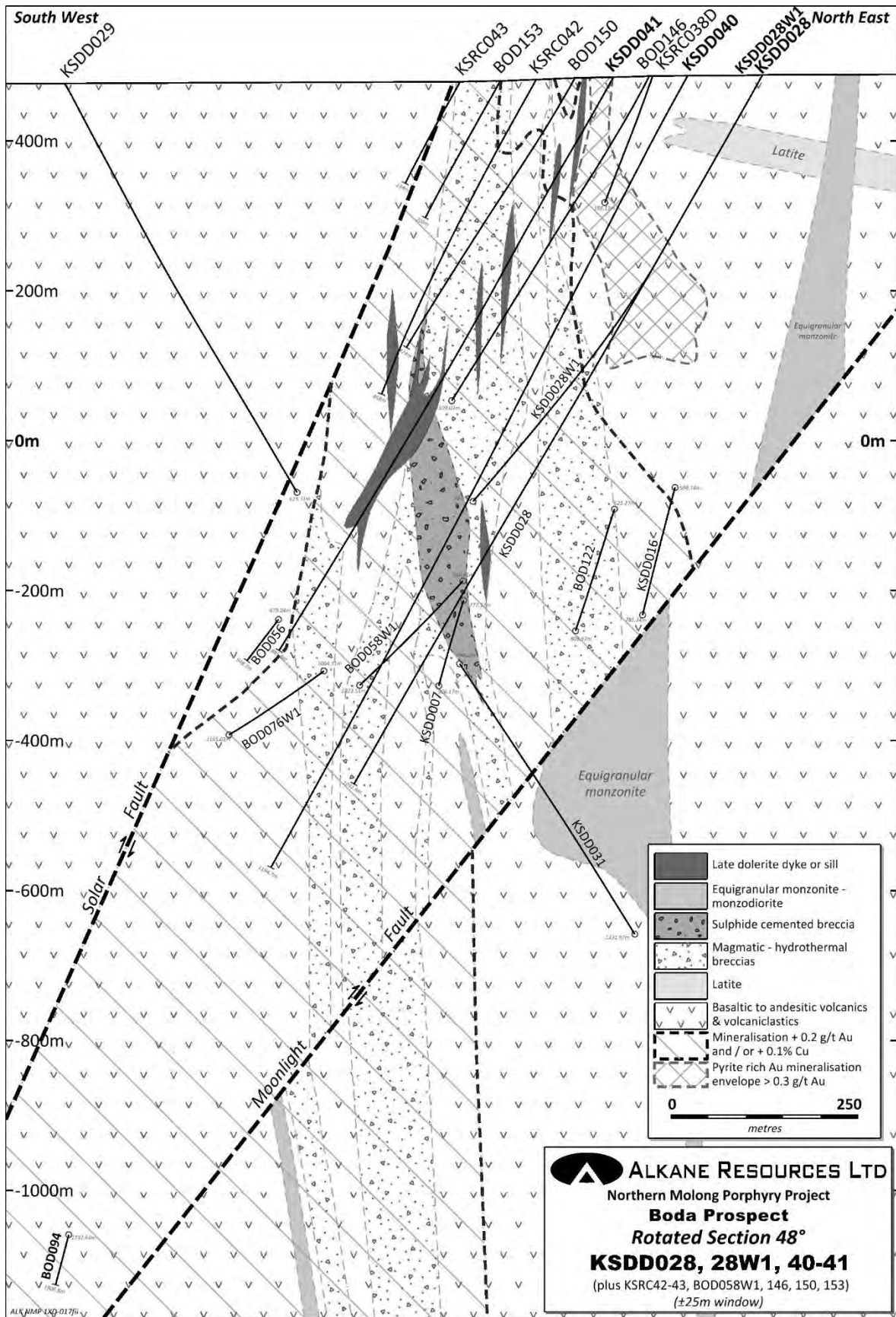


Figure 2: SW-NE cross section through the Boda deposit.

A late phyllic alteration event also overprints the northeastern shoulders of the deposits and within several major fault zones. This makes discerning any underlying hydrothermal alteration in those areas difficult. The phyllic alteration comprises sericite-quartz-calcite \pm albite with up to 10% pyrite by volume.

Copper mineralisation is observed throughout the prospect primarily as chalcopyrite with subordinate bornite and chalcocite, and rare covellite. Within the magmatic hydrothermal breccias, chalcopyrite and to a lesser extent bornite, occur predominantly as a cement mineral between the calc-potassic altered clasts. Disseminated sulphides are occasionally observed within the magmatic cement component of these breccias. Outside of the breccia bodies, Cu mineralisation is observed within epidote \pm calcite \pm quartz veins and as disseminations or patches, often intergrown with epidote. In the restricted oxide zone, secondary Cu minerals are dominated by malachite, azurite and cuprite.

At the Kaiser Deposit, an extensive zone of native Cu mineralisation is observed in oxidised zones that are spatially associated with the Kaiser Fault. This supergene mineralisation is interpreted to represent in-situ oxidation and replacement of Cu sulphide minerals, primarily chalcopyrite (Wilson, 2022). Gold distribution within this zone appears to be unaffected.

Alkane has calculated Mineral Resource Estimations for the Boda and Kaiser deposits with its last update occurring in early 2024. With a total combined resource for the Boda district of 796Mt at 0.33g/t Au, 0.18% Cu for 8.3 Moz Au and 1.5 Mt Cu (Alkane, 2024a).

Table 1: Mineral Resources Estimation at the Boda-Kaiser deposits.

DEPOSIT	INDICATED			INFERRED			METAL			TOTAL	
	Tonnes (Mt)	Au (g/t)	Cu (%)	Tonnes (Mt)	Au (g/t)	Cu (%)	Tonnes (Mt)	Au (g/t)	Cu (%)	Au (Moz)	Cu (Mt)
Open Pittable Resource (cut-off 0.3g/t AuEq)											
Boda	191	0.36	0.17	42	0.29	0.16	233	0.35	0.17	2.60	0.39
Kaiser	179	0.27	0.20	10	0.29	0.14	189	0.27	0.19	1.66	0.37
Subtotal	370	0.32	0.18	52	0.29	0.16	422	0.31	0.18	4.26	0.76
Underground Resource (cut-off 0.4g/t AuEq)											
Boda	151	0.34	0.20	198	0.34	0.18	350	0.34	0.18	3.78	0.65
Kaiser	16	0.30	0.22	8	0.36	0.20	24	0.32	0.21	0.24	0.05
Subtotal	167	0.34	0.20	206	0.34	0.18	374	0.34	0.18	4.02	0.70
TOTAL	537	0.32	0.19	258	0.33	0.18	796	0.33	0.18	8.28	1.46

SATELLITE PROSPECTS

Regional exploration recommenced in 2024 after the major resource drilling campaigns at Boda (including Boda 2-3) and Kaiser culminated in estimating the two updated mineral resources and a summary of this exploration can be found in Alkane (2024b). This work included a AGG survey using the FALCON system that was completed over the entire NMPP (**Figure 3**). The gravity data was integrated with Alkane's detailed

magnetic data to provide a project wide litho-structural interpretation as well as being used in an unconstrained 3D inversion.

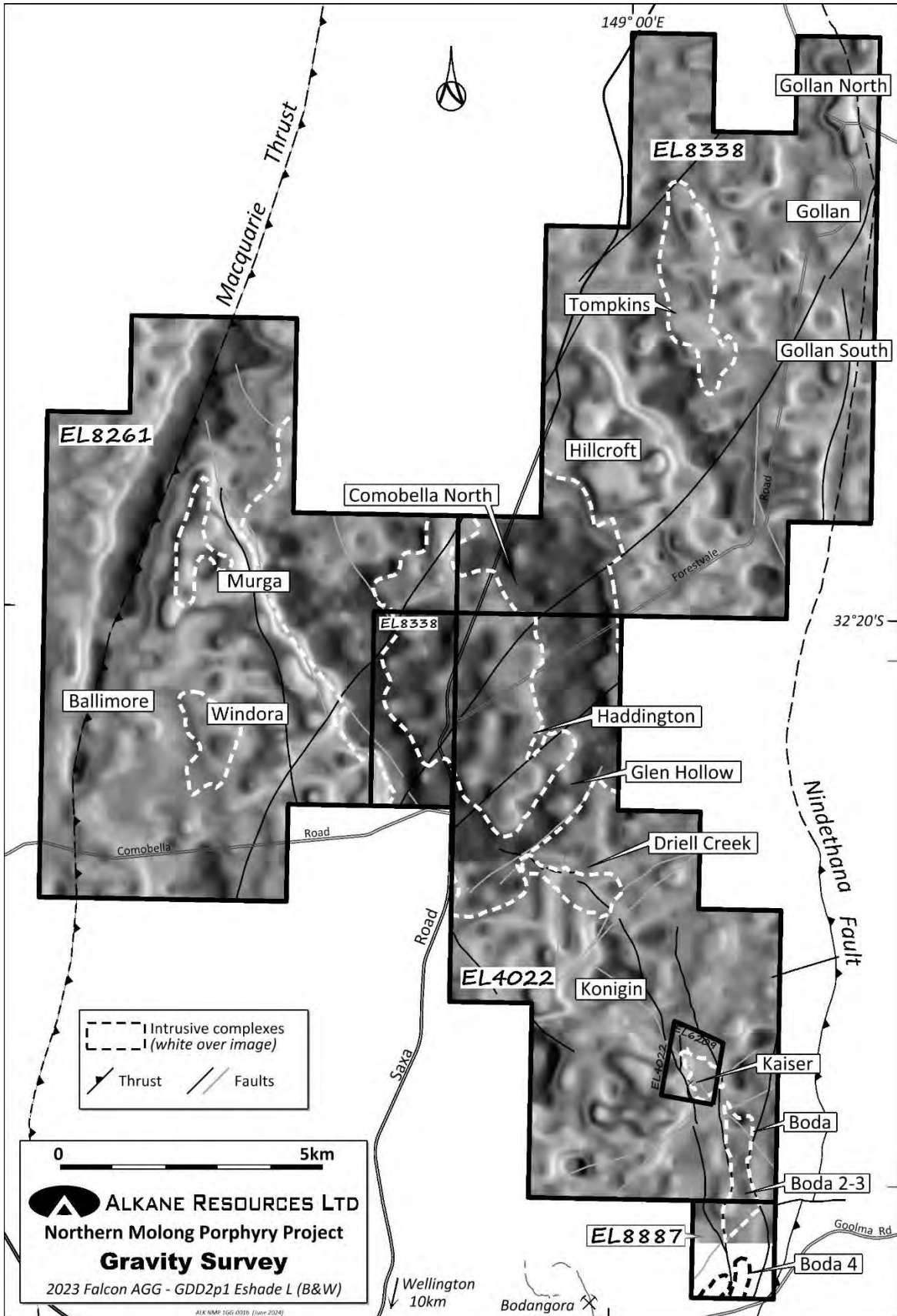


Figure 3: NMPP FALCON AGG Survey.

The AGG survey identified a significant (approximately 35km²) gravity low coincident with a magnetic high interpreted to be a major intrusive complex (Comobella Intrusive Complex – CIC) which is central to the extensive low-grade Au-Cu porphyry mineralisation in the central NMPP. The gravity low is inferred to represent a large, deep-seated monzonite intrusion or intrusive complex that may represent a major feeder to the porphyry systems in the NMPP. The subtly elevated gravity response in the middle of the CIC is interpreted to be a layer of preserved volcanics, surrounded by a ring of shallower monzonite intrusions.

Major intrusive complexes occur at all the significant Au-Cu porphyry-related deposits in the Macquarie Arc including Newmont's Cadia Operations and Evolution's Northparkes and Cowal Operations. These examples highlight the importance of a large intrusive centre such as the CIC to provide a significant source of metals and heat to the area. Porphyry apophyses can then further concentrate the Au-Cu bearing hydrothermal fluids into structures and the surrounding country rocks.

Also apparent in the integrated geophysical datasets is a significant west-northwest structural zone that may represent an arc-orthogonal transfer structure, like the Lachlan Transfer Zone that are inferred to control porphyry systems such as those in the Cadia district (Glen & Walshe, 1999). This structural corridor is likely the southeastern continuation of the Nyngan Transverse Zone - NTZ (Hilyard et al., 1996). This transverse zone is host to the 5km wide CIC and proximal to the Boda-Kaiser deposits. At a more detailed level, a northwest trending structural corridor is evident in both the magnetics and the recently acquired gravity data that coincides with the Boda, Kaiser, Driell Creek and Comobella prospects and may represent a splay structure associated with the larger transverse zone.

The merged high resolution magnetic surveys undertaken over the NMPP have identified seven major anomalies that drilling have confirmed to be intrusive complexes and they are the focus of recent and ongoing exploration. These are the Kaiser (KIC), Boda (BIC), Boda South (BSIC), Driell Creek (DCIC), Murga (MIC), Windora (WIC), and the Tompkins (TIC) intrusive complexes which are all located outboard of the major CIC. All these complexes have been tested by induced polarisation (IP) surveying apart from the TIC and most of the CIC. IP surveys aid in identifying the pyrite halo associated with porphyry mineralisation, which generally manifest as chargeability highs. Such chargeability highs have been identified along the northeastern margin of the Kaiser, Boda and Boda 2-3 deposits. Where the pyrite mineralisation has drill tested as anomalous in Au, it has provided an exploration vector to discovering underlying significant Au-Cu porphyry mineralisation.

Boda 4

The BSIC is located approximately 2km south and along strike from the BIC and comprises two linear magnetic highs approximately 800m in length and up to 200m wide separated by a north-south trending magnetic low interpreted to be the southern extension of the Solar Fault.

Drilling in the previous year intersected elevated levels of As and Zn, metals which are commonly detected in shallow and distal parts of a porphyry system. In addition, deeper drilling intersected low-grade Cu-Au mineralisation associated with calc-potassic alteration and fine disseminated chalcopyrite.

Recent assay results were received for one rock chip taken from an outcropping hydrothermal epidote-calcite breccia displaying a propylitic alteration assemblage with chalcocite and secondary malachite mineralisation. The sample returned grades of 1.2% Cu, 12.2g/t Ag & 0.1g/t Au (RK0000093).

Driell Creek

The DCIC covers an area of approximately 6km² within the northwest structural corridor. The complex includes numerous magnetic features aligned in a northwest to west-northwest orientation with a moderate to low gravity response.

The Driell Creek Prospect includes a coincident magnetic low and IP chargeability high with shallow level anomalous multi-element geochemistry (As-Bi-Zn) characterising a substantial phyllic alteration zone interpreted to be a potential lithocap to a porphyry system. A previous RC drill hole (COMRC040) was targeted 500m south of this feature and intersected 120m at 0.10% Cu & 0.10g/t Au from 168m to the end of hole.

Nine RC drill holes and one diamond core drill hole for a total of 3,393 metres were recently completed testing various targets within the DCIC. Three RC drill holes (DRC004, DRC008-9) and one diamond drill hole (DRC010) targeted the area 500m south of the Driell Creek lithocap, with two drill holes (DRC004 and DRC010) intersecting proximal inner propylitic and calc-potassic alteration. The presence of chalcopyrite centre-lined quartz veins (porphyry B veins) hosted in a diorite porphyry in DRC010, is evidence of a hydrothermal fluid sourced from a nearby hydrous, silica saturated magmatic source (causative porphyry).

Significant faulting dislocates the prospect area, including the major northwest trending Stoney Fault that appears similar in nature to the Solar Fault – a major syn-mineral structure that focused gold-copper mineralisation along its footwall at Boda. These structures have been reactivated during major deformation events, dislocating the volcanic packages in a reverse sense.

Significant Au-Cu intersections included 130m grading 0.25g/t Au & 0.11% Cu from 174m to the end of hole (DRC004), and 47.7m grading 0.12g/t Au & 0.15% Cu from 279.3m (DRC010).

Murga

Murga is a mineralised skarn target associated with a linear magnetic high in the Finns Crossing exploration licence (EL8261). The target was recently tested with five RC drill holes for a total of 1,250m. The drilling intersected propylitic (chlorite-epidote-magnetite ± hematite) with narrow zones of calc-potassic (biotite ± actinolite ± epidote ± magnetite) altered andesitic lavas, volcanoclastics, and intrusions ranging from diorites to monzonites. Disseminated pyrite occurred throughout the drilling (up to 3%), along with subordinate vein fill and stringers of pyrite. Trace chalcopyrite was logged sporadically within holes, often associated with magnetite. Gold-copper mineralisation was generally limited to narrow zones associated with the margins of the intrusives including 3m grading 0.09g/t Au & 0.10% Cu from 192 m (FCRC006) and 4m grading 0.15g/t Au & 0.09% Cu from 190m (FCRC007).

The outcropping Murga Diorite has been affected by weak potassic alteration with minor pyrite, trace chalcopyrite and quartz veins and is enclosed within a pyrite-rich sericite-quartz alteration zone in volcanic siltstone. Given the weak alteration and mineralisation it is likely that the Murga Diorite is a weakly developed and deeply eroded porphyry centre (Wilson, 2021). However, as illustrated by imbricated thrust faulting at Boda, shallower levels to a porphyry system may be preserved structurally.

Windora

Windora is a discrete magnetic high complex approximately 1.5km in diameter that is coincident with a moderate gravity signature. A historical IP survey completed by Newmont in 2010 mapped a resistivity high coincident with the magnetic complex rimmed by a chargeability high to the east and north. The interpretation of this geophysical response is the magnetic centre of a porphyry system with a peripheral pyrite halo. Drilling by Alkane in 2017 (FCRC002-4) tested the pyrite halo to north of the

Windora complex intersecting Au-Cu porphyry mineralisation associated with phyllic alteration with intercepts of 3m grading 0.05g/t Au & 0.12% Cu from 12m, 3m grading 0.17g/t Au & 0.06% Cu from 30m and 9m grading 0.07g/t Au & 0.05% Cu from 89m (FCRC004).

In 2011 Newmont completed six drill holes in the WIC and the surrounding areas, recording anomalous values of Au and Cu central to the system and pathfinder metals characteristic to upper levels of a porphyry system. The highest grades of Au and Cu occurred within the wall rock rather than in the propylitic altered monzonite porphyry, suggesting these porphyry dykes are late mineral and that a higher grade, causative porphyry may yet be discovered at depth.

Glen Hollow & Comobella North

The Glen Hollow prospect area coincides with the southeast margin of the large gravity low mapped as the CIC. The geology comprises a package of andesites and latites, intruded by monzonites with shoshonitic magmatic affinities. Hydrothermal breccias and skarns with anomalous Au and Cu mineralisation have been identified associated with the monzonite intrusions. Previous drill testing by Alkane has returned the significant result from COMRC009 of 45m grading 0.87g/t Au & 0.24% Cu from 60m including 21m grading 1.51g/t Au & 0.41% Cu from 84m.

The Comobella North prospect area coincides with the northern margin of the CIC. The geology comprises a package of andesites and latites, intruded by monzodiorites to quartz-monzonites. Historical work over this prospect included a 3.4 line-km MIMDAS survey by Mount Isa Mines Ltd in 2000 that generated two significant chargeability high anomalies. The weaker anomaly was tested by one diamond core drill hole intersecting 1m grading 0.33g/t Au & 0.01% Cu from 280m. The stronger chargeability high anomaly with a coincident multipoint geochemical anomaly from RAB drilling remains untested.

Haddington

The Haddington prospect is located to the north of the Glen Hollow prospect within the core of the CIC. The prospect area has several targets that include skarn mineralisation and extensive zones of porphyry related hydrothermal alteration.

Previous drilling has indicated broad Au-Cu intercepts, with narrower high-grade values. These include historical drilling by Newcrest in 2003 with intervals of 18 metres grading 0.95g/t Au & 0.15% Cu from 64 metres in NKRC003, including 2 metres grading 5.7g/t Au & 0.44% Cu.

Tompkins

The Tompkins prospect is defined by a magnetic complex positioned along the margin of a linear gravity low. The target area is 2.2km x 0.6km and is covered by Triassic sedimentary rocks and alluvium to a depth of approximately 40m. The prospect has been tested historically by seven shallow (<160m) RC drill holes. This broad spaced drilling intersected encouraging Au-Cu mineralisation, including HTRC037 with 12m grading 0.19g/t Au & 0.08% Cu from 34m and HTRC041 intercepting 8m grading 0.23g/t Au & 0.06% Cu from 130m.

GEOCHRONOLOGY

Three robust U-Pb zircon ages were determined from the NMPP as part of an ARC-Linkage project undertaken with CODES at the University of Tasmania. The first sample was selected from the Glen Hollow prospect in diamond core drill hole COMDD001 (449m) from a biotite-quartz-monzonite porphyry that was weakly hydrothermally altered with a distal propylitic assemblage (Crawford, 2012). An age of $459 \pm 3\text{Ma}$ was determined which is broadly contemporaneous with a single limestone sample obtained

nearby at Finns Crossing that was analysed for conodonts by Ian Percival of the GSNSW, delivering an age of $456-461 \pm 1.6\text{Ma}$ (per. comms., 2010). The limestone pods found in this area are believed to be generally allochthonous, having been shed from the flanks of the stratovolcano into the surrounding basin (Meakin & Morgan, 1999).

The second sample was also selected from the Glen Hollow prospect in diamond core drill hole COMDD002 (520m) from a quartz-hornblende-monzodiorite and returned an age of $449 \pm 3\text{Ma}$. The sample was noted as being relatively unaltered, displaying a weak lower greenschist facies assemblage (Crawford, 2012). A third sample of rock chips was selected from the outcropping Murga Diorite at Finns Crossing. It returned an age of $451 \pm 2\text{Ma}$. Samples selected from intrusions at Boda and Kaiser contained almost entirely metamict zircons and no robust ages were able to be determined.

Three Re-Os molybdenite dates have been determined at Kaiser. The first was analysed as part of the ARC-Linkage project with the sample being selected from the Newcrest diamond core drill hole NKD001 at 407m within a gold-copper mineralised, monzonite-cemented intrusive breccia. The sample returned an age of $436.8 \pm 1.4\text{Ma}$. All subsequent Re-Os molybdenite dating has been undertaken by Dr Robert Creaser of Specialist Analytical Services, 1365969 Alberta Ltd.

The remaining two Re-Os molybdenite samples were selected from recently drilled diamond core drill holes KAI073 and KAI119. The sample from KAI073 was collected from a large chalcopyrite-epidote-molybdenum vein in calc-potassic altered volcanics at a depth of 1046.5m and returned an age of $439.2 \pm 1.8\text{Ma}$. The sample from KAI119 was collected from a large chalcopyrite-epidote-molybdenum vein in calc-potassic altered volcanics at a depth of 609.8m and returned an age of $443.1 \pm 1.8\text{Ma}$.

Three Re-Os molybdenite ages have been determined at Boda. The first sample was collected from diamond core drill hole KSDD016 at 628.3m from a gold-copper mineralised, monzonite-cemented, magmatic-hydrothermal breccia. The sample returned repeated ages of $444.2 \pm 1.9\text{Ma}$ and $443.6 \pm 1.9\text{Ma}$. The second sample was collected from diamond core drill hole KSDD034W2 at 964.2m from a poorly mineralised, equigranular to weakly porphyritic, weakly phyllic altered monzonite dyke initially thought to be late mineral. The sample returned repeated ages of $337.2 \pm 1.4\text{Ma}$ and $336.6 \pm 1.4\text{Ma}$ indicating that this series of intrusions may be related to the Carboniferous Wuuluman Granite that outcrops to the east of the project area.

The final sample was collected from diamond core drill hole BOD106 at 835.6m from a narrow, Au-Cu mineralised, quartz-carbonate-sericite shear zone that had elevated Pb and Sb. The shear is hosted in a zone of calc-potassic, moderately mineralised volcanics and the sample returned repeated ages of $352.4 \pm 1.4\text{Ma}$ and $352.0 \pm 1.4\text{Ma}$ indicating that it is likely associated with an early Carboniferous, structurally focussed polymetallic event that may be related to the onset of felsic magmatism.

ACKNOWLEDGEMENTS

This paper is published with the permission of Alkane Resources Ltd. Acknowledgement is made to all past and present staff of Alkane, especially the 2023-2024 Boda-Kaiser exploration team of Lachlan Burrows, Jaygan Cannon, Karina Ramirez, Catherine Read, William Ryan, Matthew Schuler, Christopher Standard, James Trihey, Steven Wallis, and Ryan Williams whose contributions continue to formulate much of the understanding of the discoveries.

Further acknowledgment to Tony Crawford for his petrographic analysis and geological interpretation that continues to provide valuable insight into the mineralogy, alteration, and geological setting of the Boda-Kaiser deposits. Special acknowledgment to Alan Wilson, who has consulted with Alkane from the time of the Boda discovery and has

been instrumental in the developing story of the Boda district mineralisation. Finally, David Moyses is thanked for the figures in this publication.

REFERENCES

ALKANE, 2024a. ASX and Media Release: Revised Kaiser Resource Estimate Improves Confidence and Grade of Resource Base at Boda District. Alkane Resources Ltd. 29 April 2024.

ALKANE, 2024b. ASX and Media Release: NMPP Regional Exploration Update. Potential For New Au-Cu Porphyry Deposits Demonstrated. Alkane Resources Ltd. 21 June 2024.

CRAWFORD, A., 2012. Petrographic Report, 41 Rocks from the Comobella prospect on the Bodangora Porphyry Cu-Au Project, NSW: Unpublished.

CRAWFORD A., 2020. Petrographic report for 23 rocks from holes KSDD005 and KSDD007, Boda Prospect, Northern Molong Porphyry Project, NSW: Unpublished.

CRAWFORD A., 2021, Petrographic report for 41 rocks from the Boda and Boda Two Prospects, Northern Molong Porphyry Project, NSW: Unpublished.

GLEN, R.A. AND WALSHE, J. L., 1999. Cross-structures in the Lachlan Orogen: the Lachlan Transverse Zone example. Australian Journal of Earth Sciences, 46(4), p.641-658.

HARRIS, A. C., COOKE, D. R., CUISON, A. L. G., GROOME, M., WILSON, A. J., FOX, N., HOLLIDAY, J. AND TOSDAL, R., 2020. Geologic Evolution of Late Ordovician to Early Silurian Alkalic Porphyry Au-Cu Deposits at Cadia, New South Wales, Australia, in Sillitoe, R.H., Goldfarb, R.J., Robert, F., and Simmons, S.F., (Eds), Geology of the World's major gold deposits and provinces, Society of Economic Geologists Special Publication 23, p. 621-643.

HILYARD, D., DRUMMOND, M., CLARE, A., SANDERS, Y., AUNG, Z., GLEN, R., RUSZKOWSKI, P., FLEMING, G., LEWIS, P., ROBSON, D., 1996. Preliminary Palaeozoic bedrock interpretation of the Narromine & Nyngan 1:25 000 sheet areas Geological Survey of New South Wales, Quarterly Notes.

MEAKIN N. S., MORGAN, E. J., 1999. Dubbo 1:250 000 Geological Sheet SI55-4, 2nd edition. Explanatory Notes. Geological Survey of New South Wales, Sydney.

MORGAN E.J., CAMERON R.G., COLQUHOUN G.P., MEAKIN N.S., RAYMOND O.L., SCOTT M.M., WATKINS J.J., BARRON L.M., HENDERSON G.A.M., KRYNEN J.P., POGSON D.J., WARREN A.Y.E., WYBORN D., YOO E.K., GLEN R.A. & JAGODZINSKI E.A., 1999. Dubbo 1:250 000 Geological Sheet SI/55-4, (2nd edition). Geological Survey of New South Wales, Sydney and Australian Geological Survey Organisation, Canberra.

WILSON, A. J., 2021. A desktop Geological Assessment of the Exploration Potential of the Finns Crossing Project, North Molong Belt, New South Wales Australia: Unpublished.

WILSON, A. J., 2022. Geological Controls on Gold-Copper Mineralisation at the Kaiser Project, NSW, Australia, with Implications for Geological Modelling and Exploration: Unpublished.

WILSON, A. J., 2023. On the geology and exploration potential of certain aspects of the North Molong Porphyry Project, New South Wales, Australia: Unpublished.

EXPLORING FOR ALKALIC PORPHYRY-RELATED CU-AU MINERALISATION IN THE NORTHERN JUNEE-NARROMINE MACQUARIE ARC, A FOCUS ON MYALLMUNDI AND DUCK CREEK PROJECTS.

Doug Menzies*, Kristen Marris*, Tobias Erskine*, Alistair Waddell*

* Inflection Resources

Keywords: porphyry, copper, gold, Macquarie Arc, Junee-Narromine, Tasmanides, Ambient Noise Tomography (ANT)

INTRODUCTION

Inflection Resources' NSW tenement package covers the projected northerly extension of the Junee-Narromine Volcanic Belt of the Macquarie Arc, with a strategy to explore for porphyry Cu-Au mineralisation under significant thicknesses of sedimentary cover rocks (Figure 31). Recent exploration has led the company to focus on two project areas: Myallmundi 10 km north of Trangie, and Duck Creek 35 km northeast of Nyngan. Both projects are 100% owned by Inflection Resources (trading in NSW as Australian Consolidated Gold Holdings Pty Ltd) subject to a farm-in- agreement with AngloGold Ashanti Australia Limited.

EXPLORATION STRATEGY

Prior to the commencement of exploration, Inflection engaged consultant Douglas Haynes to identify targets prospective for porphyry Cu-Au mineralisation. This analysis applied Magnetic Vector Inversion (MVI) models of aeromagnetic data, and gravity data. Geophysical datasets from the Cadia, Northparkes and Boda-Kaiser porphyry Cu-Au and Cowal epithermal Au deposits were used as training datasets to refine the search spaces and identify targets.

Through this and further analyses of the regional geophysical data by Inflection, over 100 potential porphyry copper-gold targets were identified. Of particular interest was a large aeromagnetic-high complex coincident with an embayment in the Bouguer gravity data at Duck Creek, which is a similar scale to the large gravity low associated with Northparkes porphyry Cu-Au camp. Additionally, at Myallmundi a complex arcuate aeromagnetic response was identified.

Duck Creek, Myallmundi and other targets are being progressively drill tested with diamond core in basement, following mud-rotary drilling through sedimentary cover. All core is logged and analysed with pXRF and magnetic susceptibility recorded every metre. Two-metre composite half-core samples are submitted for 4-acid ICP-MS multi-element analysis, Au by fire-assay, and short-wave infrared (SWIR/spectral) analysis by ALS Global Laboratories.

Niche samples are submitted for petrographic, fusion whole-rock geochemistry, laser ablation green-rock mineral studies, and U/Pb dating of zircons where appropriate. These data have assisted Inflection to vector towards zones with the highest porphyry Cu-Au potential.

Induced polarisation and magnetotelluric surveys were ineffective due to conductive sedimentary cover. Ambient Noise Tomography (ANT) surveys have assisted in the geological interpretation at the prospect- and regional-scale.

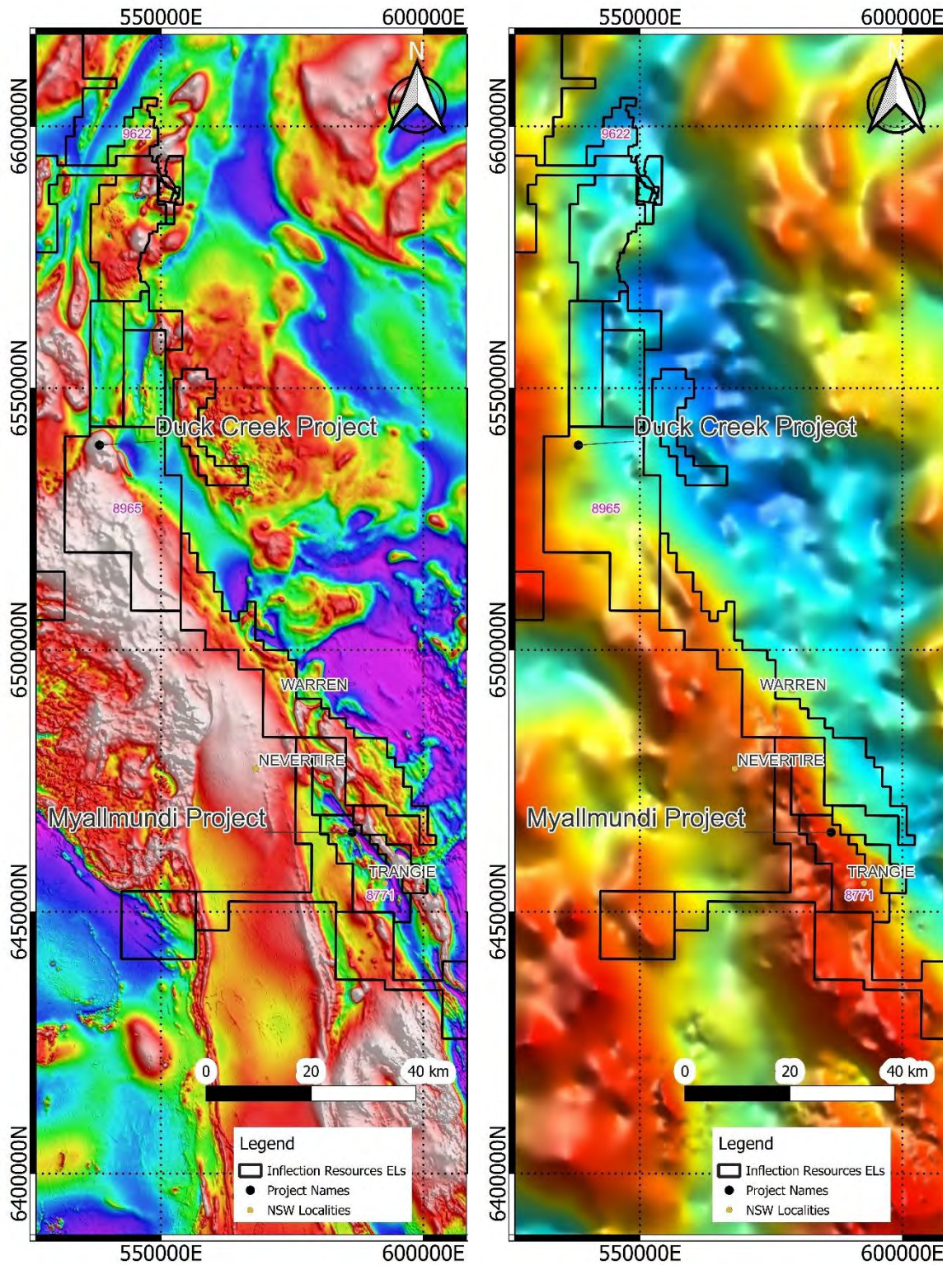


Figure 31. Regional geophysical images with Myallmundi and Duck Creek projects shown: left, reduced-to-pole total-magnetic-intensity aeromagnetic; right, Bouguer gravity image (data from the Geological Survey of NSW).

REGIONAL GEOLOGY

Inflection Resource's NSW project is almost entirely over the south-west of the Mesozoic Surat Basin, just north of where it onlaps the Junee-Narromine Volcanic Belt (JNVB). The JNVB is one of four dismembered belts of the Ordovician-Silurian Macquarie Arc and hosts the Northparkes Cu-Au deposit.

The extension of the JNVB northward beneath the basin cover is interpreted from regional aeromagnetic and gravity data. This is enveloped by Inflection tenements for over 300 km from south of Trangie north to Walgett. Before Inflection's exploration in the region, the nature of the basement was poorly understood, with only two drill holes penetrating Mesozoic cover into basement with the entire 7,500 km² of licences.

The cover sequence consists of poorly-lithified lacustrine, fluvial and shallow-marine sediments with thickness of between 70-500 m. Drill core through the Mesozoic unconformity does not exhibit a paleosol in the top of basement, and it is interpreted that any paleo-weathering profile was stripped prior to deposition of the basin sediments.

LOCAL GEOLOGY - MYALLMUNDI PROJECT

Rock types

At Myallmundi, the clastic sedimentary cover is approximately 180 m thick. Basement comprises an intercalated sequence of feldspar-phyric andesites and volcanoclastic-siltstones and -sandstones (Figure 32). The central area hosts intermediate to felsic intrusions including monzonite, monzodiorite and granite.



Plate 1. Sericite-pyrite-silica altered andesitic siltstone 0.215 g/t Au, 116 ppm Cu, 5.53 ppm Mo (MYLDH015, 236-238 m).



Plate 2. Quartz-actinolite-sphalerite vein in epidote-albite altered andesite (MYLDH015, 203.8 m).



Plate 3. K-feldspar-biotite-albite altered feldspar-phyric diorite (MYLDH004, 183.4 m).



Plate 4. Biotite-epidote altered quartz-monzonite with sericite-carbonate alteration overprint (MYLDH008, 192 m).

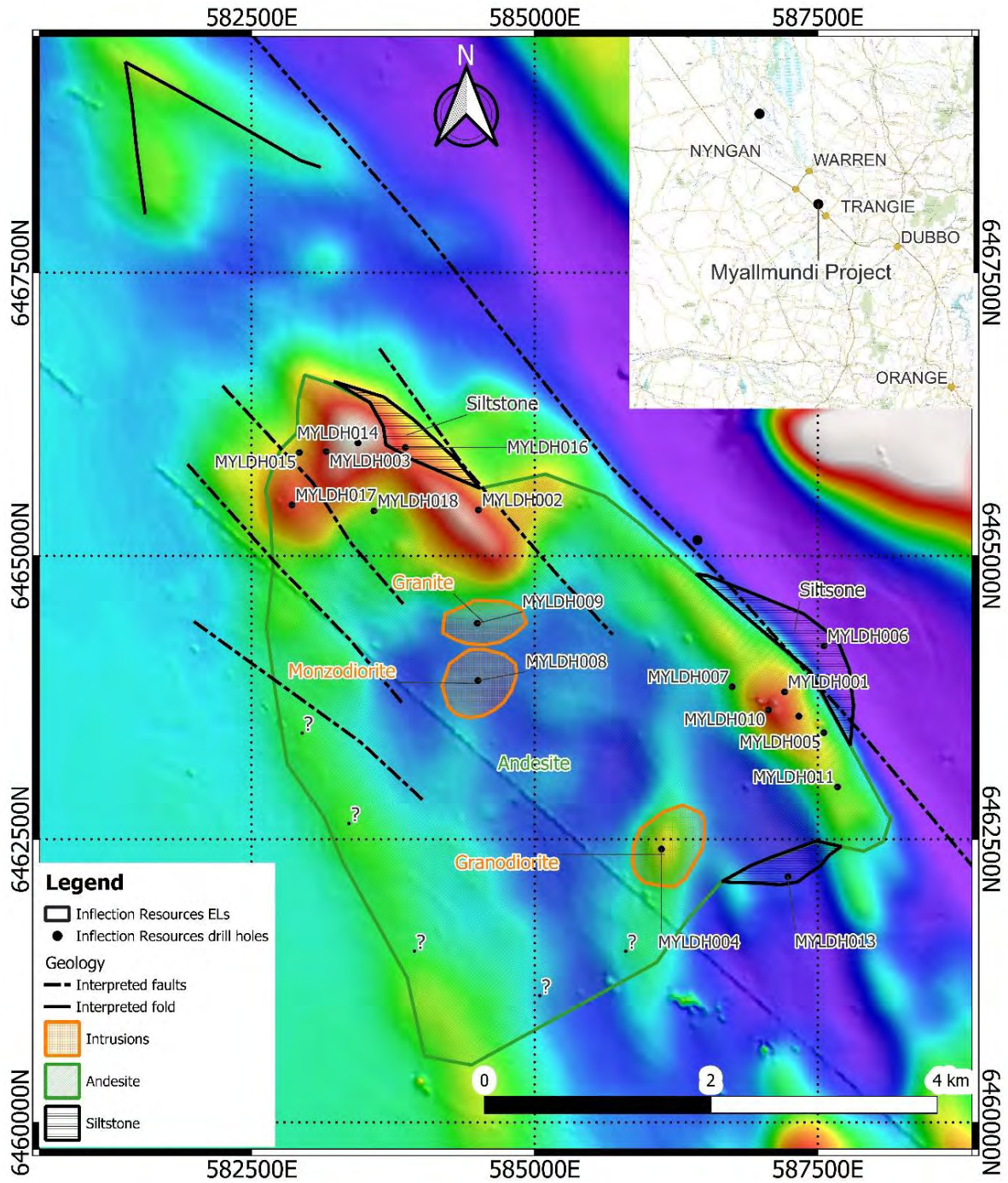


Figure 32. Aeromagnetic (TMI RTP) image of Myallmundi Project with drill holes and geological interpretation overlain.

Alteration

Volcanic rocks host intervals of epidote-chlorite-magnetite alteration, coincident with a zone of elevated aeromagnetic intensity (Figure 32, MYLDH014-17) in the NW of the drilled area, consistent with an inner propylitic porphyry style alteration (Plate 1, Plate 2, and Plate 6). Locally a magnetite-destructive sericite-carbonate alteration overprint is coincident with a zone of subdued aeromagnetic signature (Figure 32, MYLDH003).

Drill holes MYLDH004, MYLDH008 and MYLDH009 intersected biotite \pm K-feldspar altered monzonite and diorite (Plate 3 and Plate 4).

Mineralisation

Drill holes MYLDH003, MYLDH016 and MYLDH014 intersect minor disseminated and quartz-vein-hosted chalcopyrite-pyrite \pm molybdenite (Plate 5, Plate 6, and Plate 7); and hole MYLDH017 intersects molybdenite- \pm chalcopyrite bearing quartz veins (Plate 8, Plate 9, and Plate 10).



Plate 5. Fine-grained andesite with intense sericite alteration, cut by sheeted quartz-calcite \pm chalcopyrite veins and later chalcopyrite-pyrite stringers (MYLDH003, 223 m).



Plate 6. Quartz-chalcopyrite vein in magnetite-epidote altered feldspar-phyric andesite (MYLDH016, 384 m).

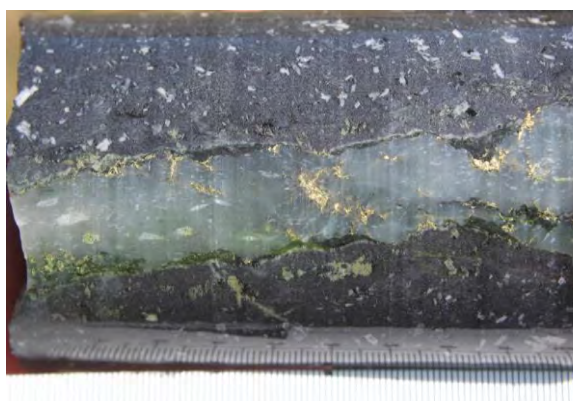


Plate 7. Quartz-chlorite-chalcopyrite-magnetite vein within plagioclase-phyric andesite (MYLDH016, 387.85 m).

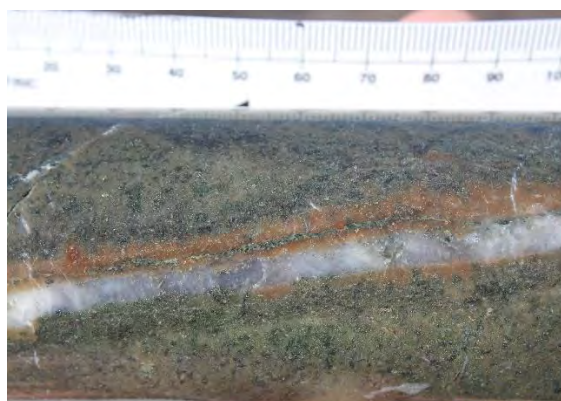


Plate 8. K-feldspar selvage around quartz-chalcopyrite-molybdenite vein in andesite, 2m at 10.5 ppm Mo, 279 ppm Cu (MYLDH017, 211 m).



Plate 9. Quartz-molybdenite vein in chlorite-epidote altered andesite, 2m at 219ppm Mo, 380ppm Cu (MYLDH017, 285.3 m).

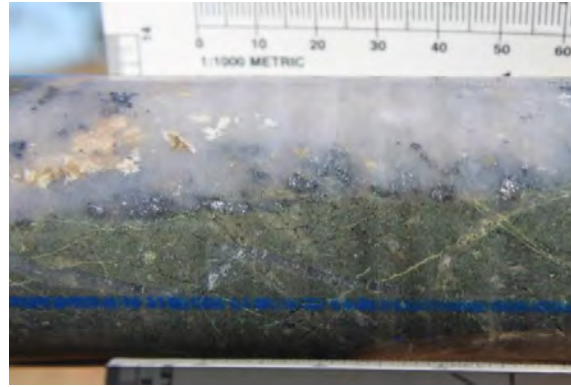


Plate 10. Quartz-molybdenite-K-feldspar vein in chlorite-magnetite-altered andesite (MYLDH0017, 287 m).

LOCAL GEOLOGY - DUCK CREEK PROJECT

Drilling at Duck Creek has focussed on a discrete magnetic high anomaly in the north of EL8965 with internal circular zones of lower magnetic intensity. Wide-spaced drilling has also targeted a regional-scale elevated-magnetic feature to the south (Duck Creek South).

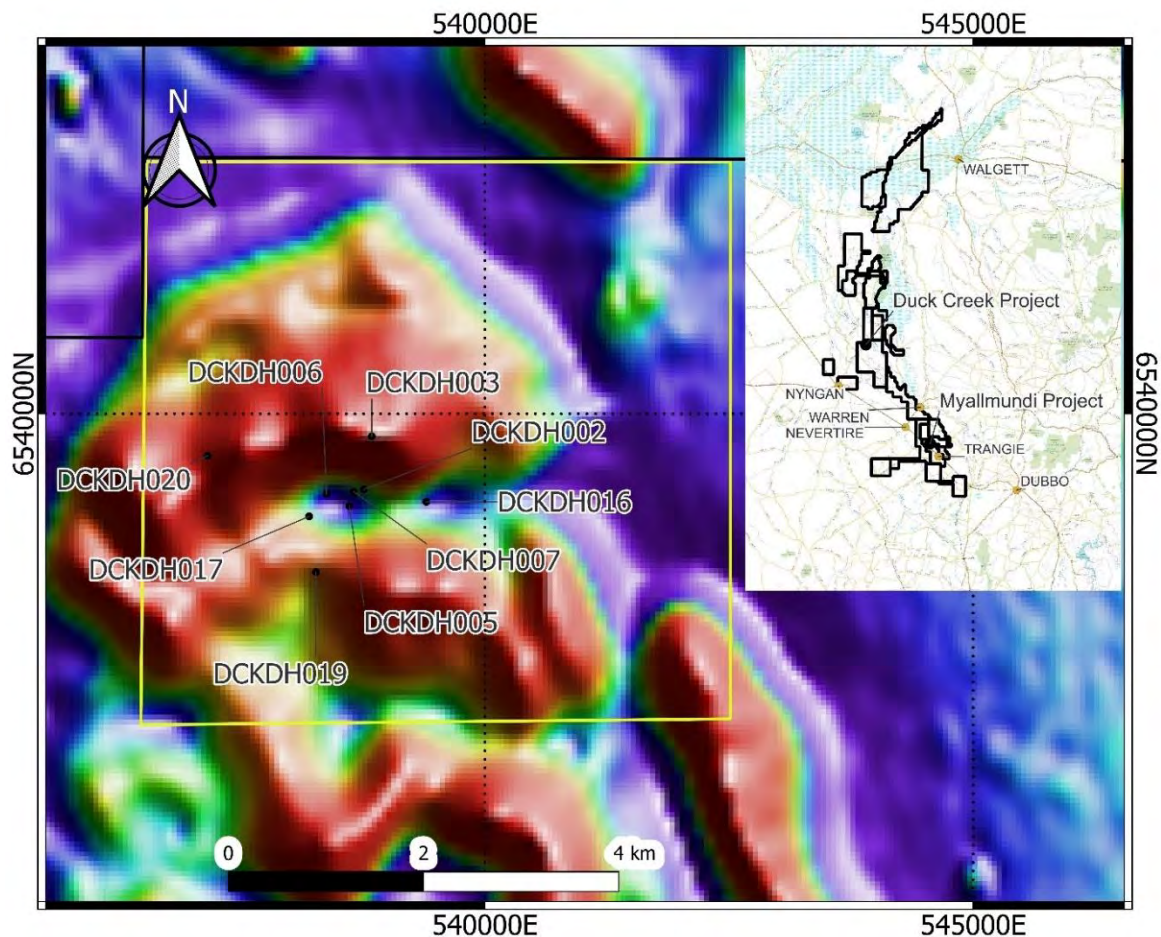


Figure 33. The location of holes drilled into the Duck Creek overlain on a reduced-to-pole, first vertical derivative aeromagnetic image with ANT survey boundary (yellow box).

Rock Types

Basement at Duck Creek, which is under approximately 350 m of clastic cover, consists of: andesites (Plate 11); andesitic volcaniclastic-breccias, conglomerates (Plate 12), sandstones and siltstones; and trachytes (Plate 13). These units are intruded by dolerite and monzonite (Plate 14).

Some andesite units are interpreted to exhibit peperitic textures, whereas a volcaniclastic-breccia in DCKDH004 hosts possible phreatomagmatic injection features.



Plate 11. Biotite altered andesite with mosaic breccia and carbonate-anhydrite veins, 2% pyrite (DCKDH002 409.8 m).



Plate 12. Hematite-sericite altered volcanic conglomerate (DCKDH006 380.9 m).



Plate 13. Volcaniclastic conglomerate and synchronous trachyte (DCKDH007 525.7 m).



Plate 14. Hematite altered monzonite cut by calcite veins (DCKDH020 657.4 m).

Alteration

At Duck Creek, drill holes intersect epidote—chlorite \pm pyrite alteration considered to be consistent with porphyry-associated propylitic alteration (Plate 15 - Plate 18). Localised reddening (dominantly hematite) overprints this association. Tourmaline-sericite-albite-pyrite alteration probably represents late, porphyry-style phyllic alteration (Plate 15 and Plate 18). This association has been reported above the Cadia East porphyry Cu-Au-Mo orebody (Wilson, 2003).



Plate 15. *Tourmaline-pyrite in albite-hematite altered andesite, (DCKDH002, 429.3 m).*



Plate 16. *K-feldspar-actinolite altered volcaniclastic conglomerate (DCKDH002, 378.2 m).*



Plate 17. *Epidote-pyrite-hematite altered volcaniclastic conglomerate (DCKDH006, 416.6 m).*



Plate 18. *Albite-tourmaline altered volcaniclastic conglomerate (DCKDH002, 426.9 m).*

Mineralisation

Duck Creek hosts minor vein occurrences that may be described with porphyry-style terminology (Gustafson and Hunt, 1975; Clarke; and Arancibia, 1995) including: minor wormy quartz veins as A-style (Plate 19); centreline quartz-pyrite veins as B-style (Plate 20, Plate 21); and massive quartz-magnetite veins as M--style. All are suggestive of a proximal porphyry environment. Additionally, drill holes DCKDH005 and DCKDH017 locally exhibit bornite-chalcopyrite-magnetite-epidote clots (Plate 23 and Plate 24), similar to those in the E22 deposit at Northparkes (hole E22D248 inspected at Londonderry core library), and suggestive of a fertile magmatic hydrothermal system and proximity to source.



Plate 19. Wormy 'A-style' quartz vein in K-feldspar altered volcanic conglomerate (DCKDH002, 400.8 m).



Plate 20. Quartz-pyrite 'B-style' vein in K-feldspar altered volcanic conglomerate (DCKDH002, 389.4 m).



Plate 21. Pyrite-chalcopyrite quartz 'B-style' vein, in monzonite (DCKDH016, 398.5 m).



Plate 22. Magnetite-quartz-epidote 'M' vein in K-feldspar altered breccia (DCKDH007, 714.8 m).

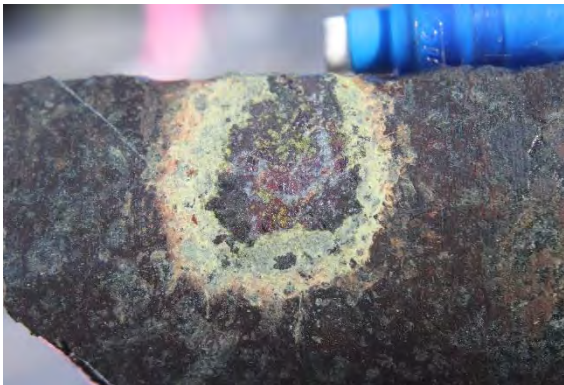


Plate 23. Bornite-epidote-chalcopyrite clot (DCKDH005, 395.5m).



Plate 24. Bornite clot (DCKDH017, 422.5 m).

LITHOGEOCHEMICAL DATA

Geochemical data from Duck Creek, Duck Creek South and Myallmundi can be broadly subdivided into two geochemical associations using the Hastie et al. (2007) Th-Co discrimination diagram, which utilises Th and Co as respective proxies for K_2O and SiO_2 to mitigate the effects of alteration and weathering. The diagram indicates that the Myallmundi, and Duck Creek South may have a calc-alkaline affinity, whereas Duck Creek is likely high-K / shoshonitic (or higher Th) (Figure 34). Additionally, Crawford (2023) noted apatite micro-phenocrysts suggest high-K calc-alkaline to dominantly shoshonitic affinity at Duck Creek.

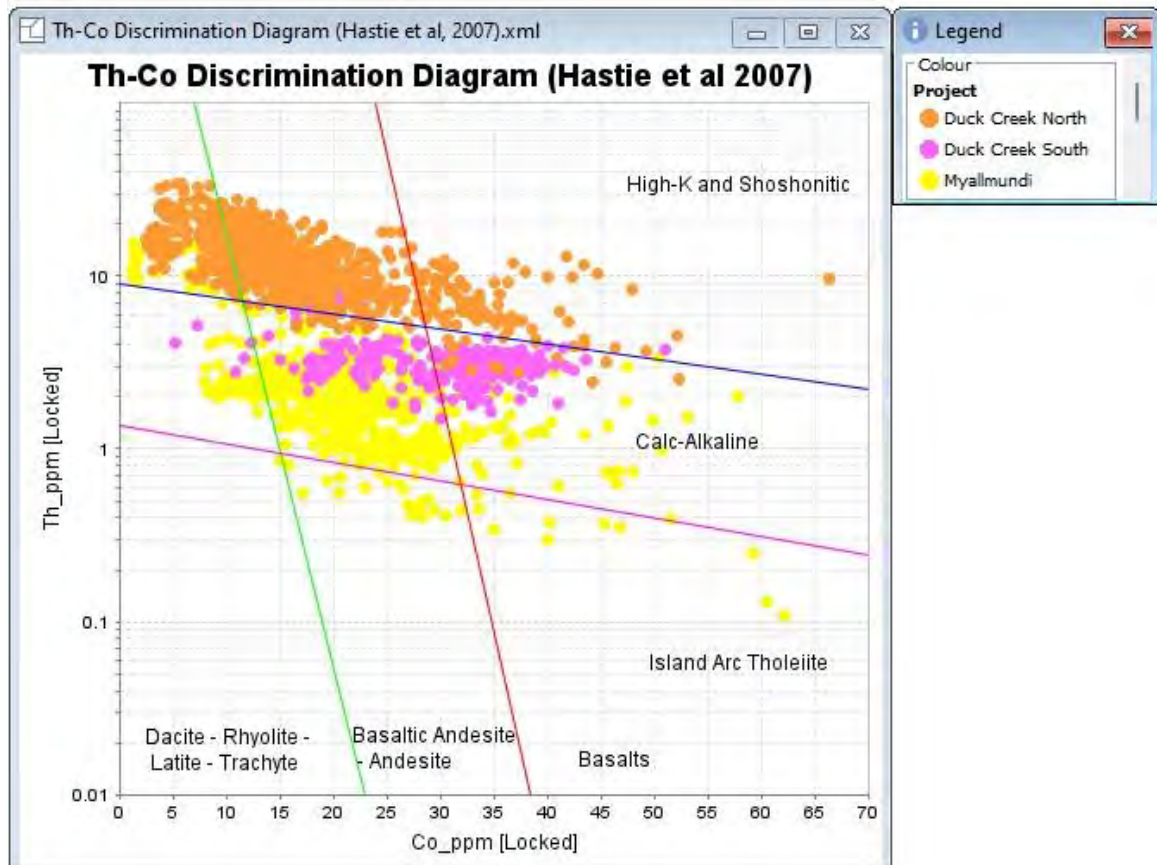


Figure 34. Th-Co plot of Myallmundi, Duck Creek South and Duck Creek volcanic and volcanoclastic rocks.

GEOPHYSICAL DATA

Ambient Noise Tomography

Inflection engaged Fleet Space to complete several ANT surveys, firstly a regional (800 m geod-spaced grid) survey covering $\sim 31 \text{ km}^2$, followed by a more detailed infill survey (400 m spaced-grid) over $\sim 7.8 \text{ km}^2$ centred over the magnetic-high anomaly at Duck Creek (Figure 35). Following this, a regional (5 km spaced grid) survey covering $\sim 1,800 \text{ km}^2$ was completed (Figure 36).

The detailed survey at Duck Creek identifies zones of higher and lower velocity that can be used in conjunction with other geophysical datasets to infer aspects of lithology and structure (Figure 35). Linear trends of decreased velocity and apparent breaks and offsets of higher velocity are interpreted as faults. Several zones of elevated velocity appear to be coincident with monzonite intersected in drilling (DCKDH016, DCKDH020).

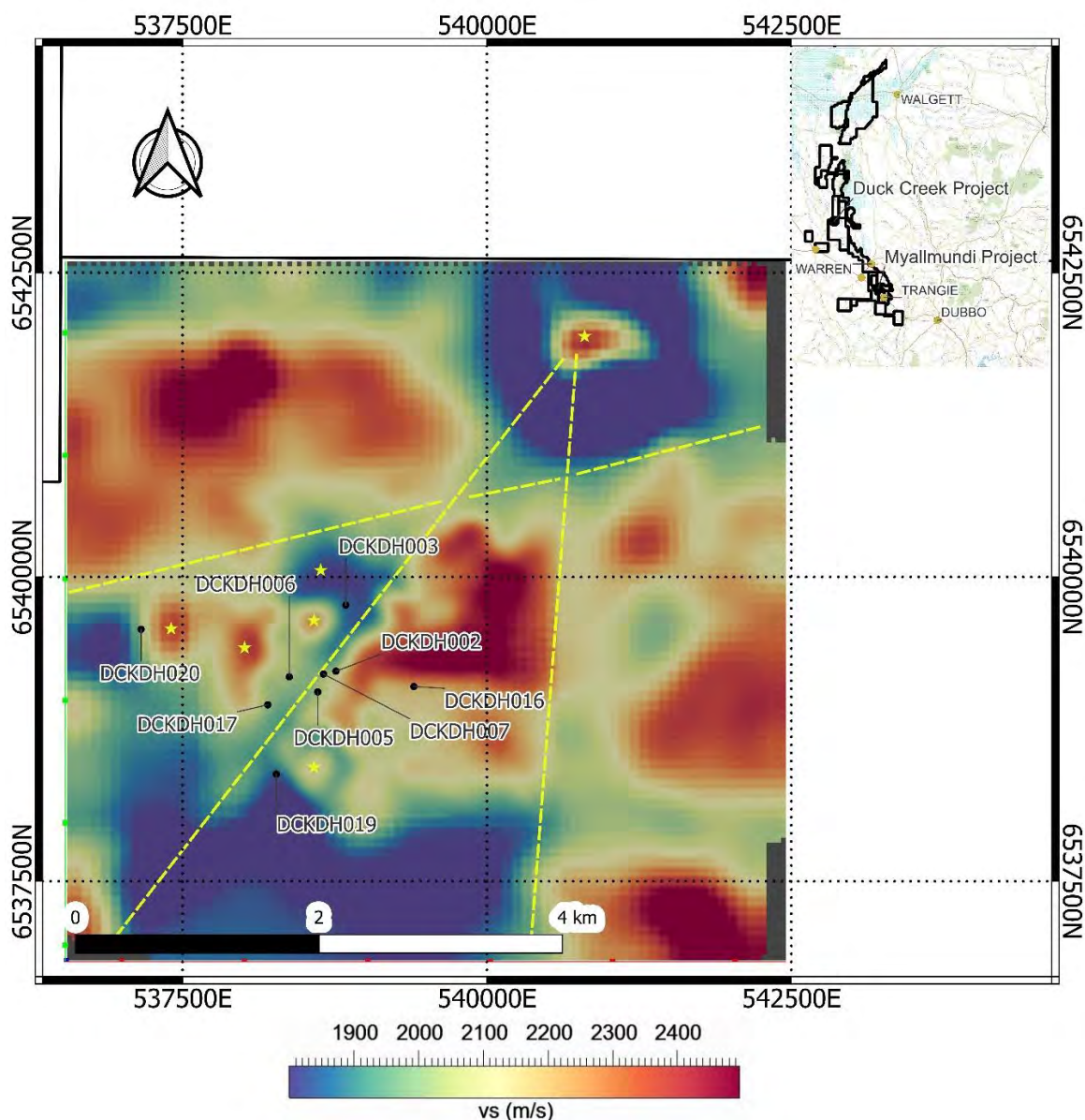


Figure 35. Duck Creek ANT survey plan view at -400 metre RL, or 570m below surface, showing zones of low (blue colours) and high (yellow to red colours) seismic velocity interpreted as new targets for hydrothermal alteration and intrusions respectively. Existing Inflection drill holes and inferred major structures are also shown (see Figure 3 for location).

The newly acquired regional ANT survey is currently being analysed in conjunction with aeromagnetic, gravity and drill data to assist in geological interpretation and structural targeting. Several possible regional structures have been identified (Figure 36).

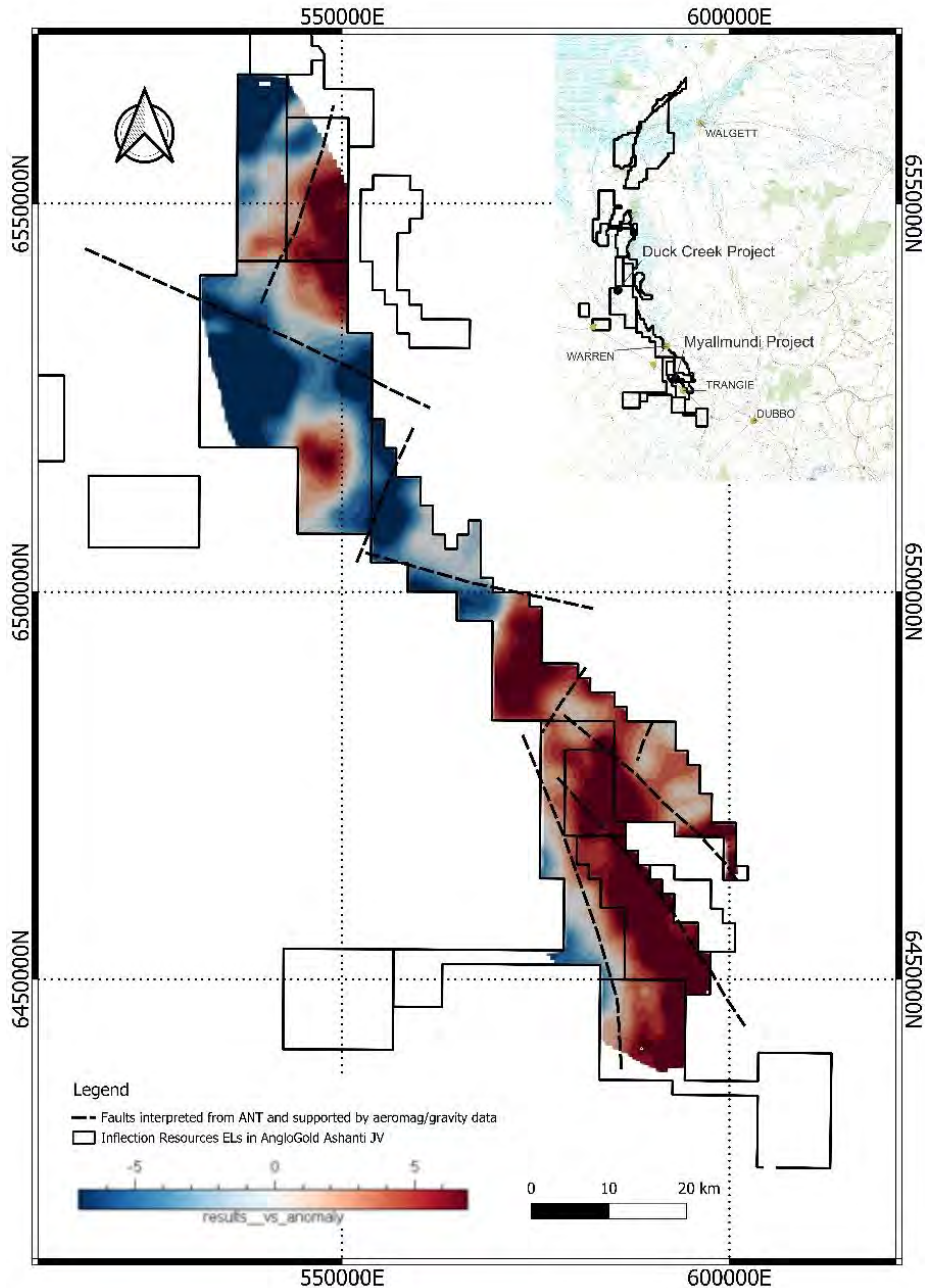


Figure 36. Regional ANT map at -450mRL which shows zones of relative elevated seismic velocity and interpreted faults (black dashed lines) which are supported by aeromagnetic and gravity data.

Down hole wireline data

Downhole wireline geophysical data was collected within drill hole DCKDH020, drilled to test a zone of elevated seismic velocity identified in the detailed ANT survey at Duck Creek.

This survey, completed by Ground Search Australia, delivered sonic velocity, magnetic susceptibility, induced polarization and inductive conductivity measurements on a 1 cm resolution downhole within basement to the bottom of the hole. Analysis of these data, together with the ANT survey, drilling, geological, geochemical and petrophysical data, suggests:

- There is a good correlation between the hand-held magnetic susceptibility data collected with a KT-10 instrument and the wireline magnetic susceptibility data, which confirms the validity of routine hand-held magnetic susceptibility measurements.
- There is a broad correlation between zone of elevated sonic velocity in the wireline data with monzonites and trachytes intersected in drill hole DKCHD020.
- The sonic velocity wireline data broadly validates the ANT model, however, is limited by the relatively coarse nature of the ANT model.

CONCLUSIONS

The Myallmundi Project exhibits quartz-chalcopyrite and quartz-molybdenite veins associated with epidote-albite alteration and overprinting sericite-carbonate alteration suggestive of a porphyry Cu-Au style mineralisation environment. Monzonite and diorite, which exhibit biotite-K-feldspar alteration, may suggest further potentially mineralised intrusions at depth.

The Duck Creek Project also has elements that suggest proximity to a porphyry related system. These include: epidote-chlorite- \pm K-feldspar- \pm pyrite and tourmaline-sericite-albite- \pm pyrite alteration; development of quartz-pyrite (A-style), quartz-pyrite \pm chalcopyrite (B-style), and quartz-magnetite (M-style) veins; and minor bornite-magnetite-epidote clots.

A prospect scale ANT survey indicates that monzonites may manifest as zones of elevated seismic velocity and major faults may be apparent as zones of lowered seismic velocity. This interpretation is supported by a downhole sonic velocity survey which recorded zones of elevated velocity associated with monzonite.

A regional ANT survey identifies elements that may aid in the structural interpretation when used in conjunction with other potential field datasets and drilling data.

REFERENCES

CLARK, A.H., AND ARANCIBIA, O.N., 1995. The occurrence, paragenesis, and implications of magnetite-rich alteration-mineralisation in calc-alkaline porphyry copper deposits in A.H. Clark Giant Ore Deposits II, Queens University at Kingston, Canada, p. 583-640.

COLGAN, J.P., DUMITRU, T.A., REINERS, P.W., WOODEN, J.L., AND MILLER, E.L., 2006, Cenozoic tectonic evolution of the basin and range province in northwestern Nevada, published in American Journal of Science, v 306, no. 8, pp. 616-654.

CRAWFORD, T., 2024. Petrographic report on 20 Rocks from Drilling on the Duck Creek Project, NE of Nyngan, NSW for Inflection Resources, unpublished report.

GUSTAFSON, L.B., AND HUNT, J.P., 1975, The porphyry copper deposit at El Salvador, Chile: Economic Geology, v. 70, p. 857- 912.

HASTIE, A., KERR, A., PEARCE, J., AND MITCHELL, S., 2007. Classification of Altered Volcanic Island Arc Rocks using Immobile Trace Elements: Development of the Th Co Discrimination Diagram. Journal of Petrology. 48. 2341-2357. 10.

WILSON, A. J., 2003. The geology, genesis and exploration context of the Cadia gold-copper porphyry deposits, New South Wales, Australia, an unpublished PhD thesis, University of Tasmania.

GEOLOGY AND DEPOSIT MODEL FOR THE NARRABURRA RARE EARTH DEPOSIT

Damien Mizow

Godolphin Resources Limited, Unit 13, 11 Williams Street, Orange, NSW 2800

Key Words: Rare Earths, A-type Granite, Peralkaline, Ionic Adsorption Clay Deposit

INTRODUCTION

The Narraburra Rare Earth Deposit is located 12km north of Temora in central western NSW, within the Palaeozoic Lachlan Orogen (Figure 1). The deposit contains an Inferred Mineral Resource of 94.9Mt @ 739ppm TREO(Y)* using a 300ppm TREO(Y)-Ce cutoff, *including 20Mt @ 1,079ppm TREO(Y) using a 600ppm TREO(Y)-Ce cutoff*. The Rare Earth Element (REE) mineralisation is hosted in saprolitic clays and sap-rock positioned directly above the peralkaline Narraburra Granite.

The grade and size of Narraburra is typical of other secondary type REE deposits and given diagnostic metallurgical leach test work has demonstrated extraction rates of between 80-95%, a Scoping Study has commenced to provide guidance on the economic significance of the deposit.

REGIONAL GEOLOGY

The deposit is located within the Western Central Zone of the Lachlan Orogen, between the Gilmore Fault Zone to the west and the Cootamundra Fault to the east (Warren et al, 1994).

Some of the oldest rocks in the project area are immediately west of the Gilmore Fault Zone and form part of the Lake Cowal Volcanic Complex, which records arc volcanism via westward subduction in the Ordovician (Lyons, 2000). This arc sequence is contemporaneous with porphyry/ epithermal gold and copper mineralisation in the region typified by the Lake Cowal Gold Deposit (Lyons, 2000) and the Gidginbung Gold Deposit.

As the arc migrated east and marginal basins developed, seafloor sedimentation occurred during the Siluro-Devonian and is mapped by a sequence of conglomerates, sandstones, siltstones and rare tuff. Younger Silurian intermediate volcanics are found near the township of Temora and host the historic Temora Gold Fields (Warren et al, 1994).

Intruding the Siluro-Devonian sedimentary package is the Narraburra Granitic Complex (Figure 1). This granitic complex is dated at 365 +/- 4 Ma and postdates arc magmatism by 75 Ma (Wormwald et al, 2004). It is positioned near the junction of the Gilmore Fault Zone, the Parkes Thrust, the Springvale Rift and the newly interpreted Narraburra Fault Zone and was likely emplaced during reactivation of these major faults in an extensional environment, during post-orogenic slab rollback of the subduction zone (Wormwald et al, 2004).

Wormald et al. (2004) describe three different suites within the Narraburra Granitic Complex. Suites 1 (Gilmore Hill) and 2 (Barmedman) are classified as I-type (formed during the melting of crustal igneous sources) while Suite 3 (Narraburra) represents an A-type peralkaline enriched magma.

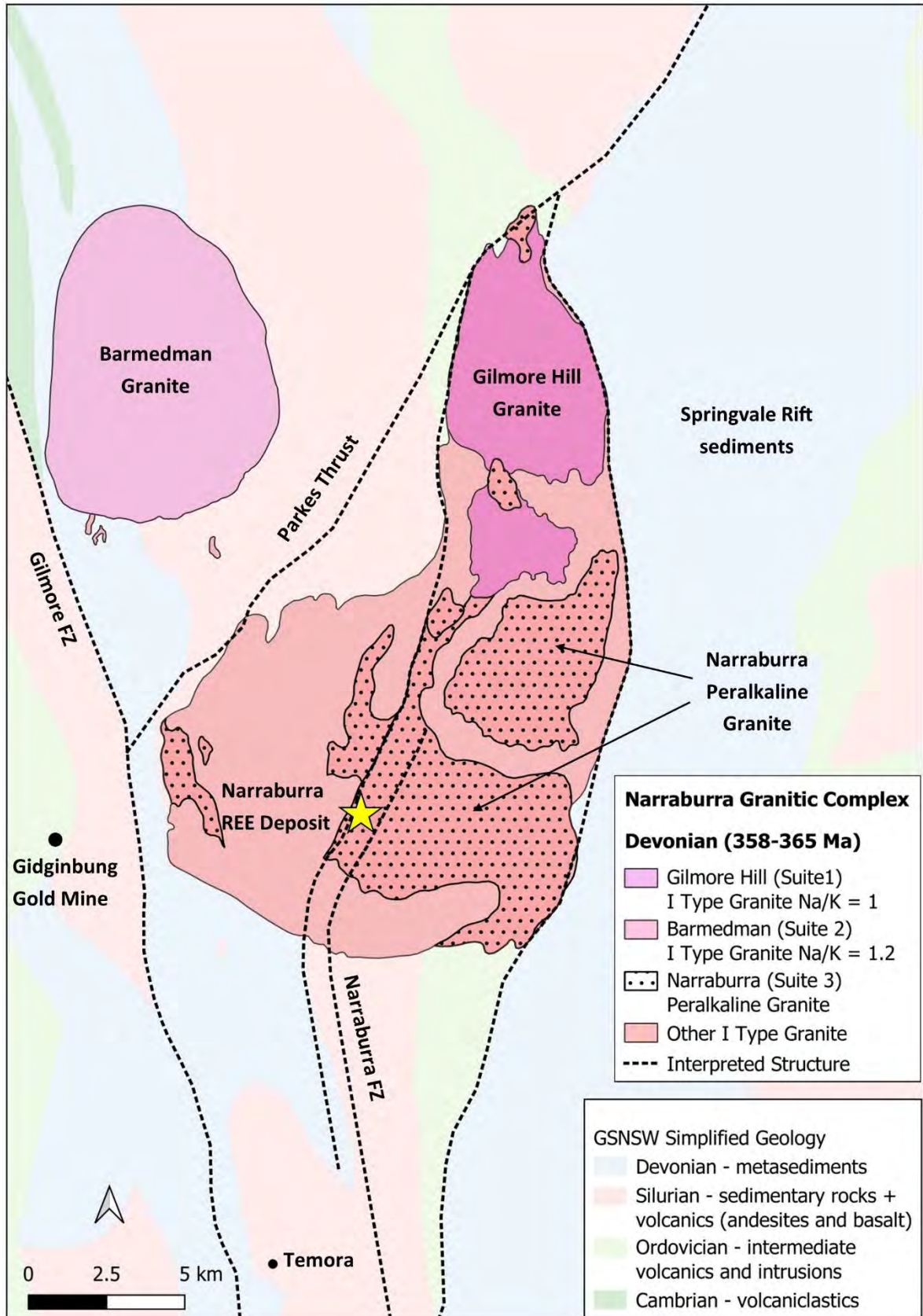


Figure 1: The Narraburra REE deposit is positioned within the Narraburra Granitic Complex, 12km north of the township of Temora, NSW.

PERALKALINE A-TYPE GRANITES

A-type granites range in composition from peraluminous ($Al > [Na + K]$) to peralkaline ($Al < [Na + K]$) – Figure 2. Of particular importance are the latter, which have been generated by fractional crystallisation of alkaline basaltic magmas and derived from the partial melting of the upper mantle (Dostal, 2017). Per-alkaline magmas are enriched in High Field Strength Elements (HFSE) such as zirconium, niobium and tantalum, enriched in REEs found in primary igneous minerals such as monazite and xenotime, and are also enriched in uranium and thorium (Dostal, 2017; Marquis, 2019).

Peralkaline rock types are therefore a critical exploration target vector when exploring for rare earth deposits.

The Narraburra peralkaline Suite 3 forms the source rock for the Narraburra Rare Earth Deposit and is mapped elsewhere across the project tenement portfolio, thereby providing future exploration targets.

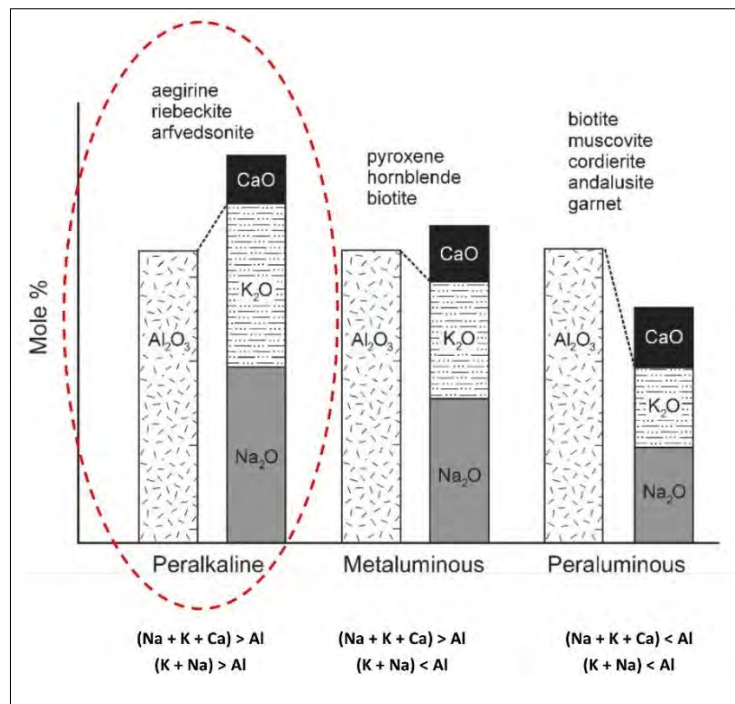


Figure 2: Classification of felsic rocks based upon mole % Aluminium (Al), Calcium (Ca), Sodium (Na) and Potassium (K) after Dostal (2017). Peralkaline granites have alkali content $(Na + K) > Al$.

CLASSIFICATION OF RARE EARTH DEPOSIT TYPES

Broadly speaking these deposits are categorised as either Primary or Secondary and vary in their genetic model, grade and REE mineralogy. The ore is extracted via different mining methods, meaning their CAPEX costs vary significantly as does the downstream processing cost. A summary of the key Primary and Secondary deposit types is discussed below and their characteristics captured in Table 1.

Primary deposits contain high concentrations of REEs and refer to high temperature magmatic/ hydrothermal processes, typified by carbonatites, alkaline igneous rocks, Iron-REEs (IOCG deposits) and hydrothermal veins (Marquis, 2019). Given their hard rock nature, traditional drill and blast and selective open pit mining is required. The associated CAPEX is high and removal of REEs from type minerals such as monazite and bastnäsite is energy intensive; whereby the REE concentrate must be decomposed

before leaching, which involves roasting or cracking the concentrate between 200-600°C with strong sulphuric acid (McNulty, 2022).

- **Carbonatites** are igneous rocks composed of >50 vol.% primary carbonate minerals and contain the highest concentration of REEs of any igneous rock (Verplanck, 2017). They are relatively rare with approximately 600 known carbonatites mapped globally and only a few that host economic REEs (Borst et al, 2020; Hellman, 2023). They are enriched in the Light Rare Earth Elements (LREEs) and overwhelming supply the LREE world market (Verplanck, 2017).
- The world's largest Carbonatite deposit is Bayan Obo in China: 57.4Mt @ 6% TREO (Fan et al, 2015). Mt Weld in Western Australia is another example with a similar resource of 54.7Mt @ 5.3% TREO (Hellman, 2023).
- **Alkaline to Peralkaline Igneous Complexes** consist of nepheline syenites and trachytes to peralkaline granites (Dostal, 2017). They are enriched in Na₂O and K₂O (alkalis) relative to silica and are generally lower grade (0.5 – 2% TREO) than carbonatites. They are Heavy Rare Earth Element (HREE) enriched but may also show LREE enrichment, with the main REE ore minerals being bastnäsite, eudialyte, loparite, gittinsite, xenotime, monazite, zircon and fergusonite (Dostal, 2017).
- Notable deposits include:
 - The LREE enriched Tardiff deposit in Canada: 213Mt @ 1.17% TREO (source: <https://vitalmetals.com/portfolio/nechalacho-project>)
 - The HREE enriched NorraKarr deposit in Sweden: 110Mt @ 0.5% TREO (source: <https://leadingedgematerials.com>)
 - Toongi deposit in Dubbo, Australia: 75.18Mt @ 1.89% ZrO₂, 0.74% TREO (source: <https://asm-au.com/dubbo-project/resources-and-reserves>)

Secondary Deposits refer to the lateritic weathering of an underlying fertile REE host rock (granite, felsic volcanics or syenite), which typically takes place in temperate to tropical climates (Marquis, 2019). **Ion Adsorption Deposits (IAD)** are currently the primary type of Secondary Deposits and are the world's primary source for HREEs (Borst et al, 2020).

In IADs, rare earth mineralisation is formed when the decomposing protolith is broken down by acidic soil water. This acidic soil water interacts with REE bearing minerals and releases REE³⁺ ions into ground water. The REE³⁺ ions move downward through the weathering profile at near neutral pH conditions, but as pH increases the REE cations are exchanged and physically adsorbed onto the surface of negatively charged clay minerals such as kaolinite and halloysite (Marquis, 2019; Sanematsu et al, 2016). This ion exchange capacity represents >50% of total REE mineralisation in IAD deposits (Sanematsu et al, 2016), however, the world's largest IAD deposit, Zudong, located in China, contains ~65% ion exchange capacity (Hellman, 2023). This observation dictates that a significant REE component is non ion-exchangeable and therefore either hosted within the regolith profile in primary minerals that have not been broken down (weathering resistant) or other secondary minerals.

While the majority of REE³⁺ ions migrate downward through the weathering profile, Ce³⁺ ions are oxidised to Ce⁴⁺ ions forming Cerianite (CeO₂). Thus, in the upper portion of the regolith profile of an IAD, a REE³⁺ leached zone exists and corresponds with Ce enrichment. Similarly, further down the regolith profile, where the REE³⁺ ions are adsorbed onto clay minerals, a REE Accumulation Zone is formed with relative Ce depletion. This key feature of IADs is observed in the Narraburra Rare Earth Deposit (Figure 5).

IAD deposits are low grade and average 800ppm TREO (Sanematsu et al, 2016) but are economic to extract due to 1) the absence of traditional mining techniques such as drill and blast, crushing and grinding and the ability to mine via shallow open pits; and

2) little mineral processing is required. This is because REE ions can be readily solubilized by displacing the REE ions adhered to the clay with an appropriate cation solution. Typical desorption conditions are achieved using 0.3-0.5 M ammonium sulphate at pH 4-5 for ~30 minutes at ambient temperatures. Under these conditions up to 70% extraction of TREO can be obtained, with very little dissolution of gangue elements, which makes for simple downstream processing to produce a mixed rare earth carbonate (MREC).

China controls 80% of the HREE market (Borst et al, 2020), however, emerging new IAD discoveries such as the Calderia Rare Earth Deposit in Brazil, the Makuutu Rare Earth Deposit in Uganda and Godolphin Resource’s Narraburra Rare Earth Deposit in NSW illustrate their global distribution.

Table 1: Summary characteristics of Primary and Secondary REE deposits

CLASS	DEPOSIT TYPE	REE	GRADE	REE HOSTED MINERALS	CAPEX COST	MINING METHOD	ACID (Processing)	LOCATIONS
Primary	Carbonatite	LREE	High > 5% TREO	bastnäsite, monazite, synchysite, paricite, ancyllite, and apatite	High	Open pit Drill and blast + crush and grind	High temperature, strong acid. Crack Monazite and use pH <1 to liberate REEs	Bayan Obo - China Mt Weld - WA Mountain Pass - California Tomtor - Russia
Primary	Alkaline- Peralkaline	HREE + LREE	Moderate > 0.5% TREO	Loparite, eudialyte, zircon, xenotime- (Y), fergusonite-Y, allanite and bastnäsite	High	Open pit and/ or underground	Strong Acid to liberate REEs	Nechalacho – Canada NorraKarr – Sweden Lovozero – Russia Toongij – NSW
Secondary	Ion Adsorption Clay (IAD)	HREE	Low >0.05% TREO	Kaolinite, halloysite (REE adsorbed onto clay minerals)	Low/ Medium	Open Pit. Strip mining / free digging	Weak Acid. Ambient temperature ammonium sulphate at pH 4-5. Tank leach or heap leach	Jiangxi / Guangdong Provinces in China <i>incl</i> Zudong Deposit Calderia - Brazil Makuutu - Uganda
Secondary	Hybrid - Ion Adsorption Clay (H-IAD)	LREE	Low >0.05% TREO	Kaolinite and smectite (REE adsorbed onto clay minerals) also in secondary minerals such as monazite and xenotime	Low/ Medium	Open Pit. Strip mining / free digging	Weak to moderate acid (pH 2 - 2.2), 50deg C, ammonium sulphate buffered with H2SO4. Tank leach or heap leach - TBD	Narraburra, NSW

*TREO(Y) = Trace Rare Earth Element Oxide + Yttrium ((La₂O₃ + CeO₂ + Pr₆O₁₁ + Nd₂O₃ + Sm₂O₃ + Eu₂O₃ + Gd₂O₃ + Tb₄O₇ + Dy₂O₃ + Ho₂O₃ + Er₂O₃ + Er₂O₃ + Tm₂O₃ + Yb₂O₃ + Lu₂O₃) + Y₂O₃)

*MREO (Pr₆O₁₁ + Nd₂O₃ + Tb₄O₇ + Dy₂O₃) is often quoted in Rare Earth Deposits. This is because ~74% of the current REE market value is contained within the MREOs and this is forecast to grow to 90% by 2033. Nd₂O₃-Pr₆O₁₁ represent the LREE magnets and have a spot price of \$51/kg. Dy₂O₃-Tb₄O₇ represent the HREE magnets; the spot price for Dy oxide = \$228/ kg and Tb oxide = \$676/ kg. Spot prices are in \$US and VAT inclusive. Prices quoted on 24/07/2024. Source <https://www.metal.com>

NARRABURRA RARE EARTH DEPOSIT

The Narraburra Rare Earth Deposit has an Inferred Mineral Resource of 94.9Mt @ 739ppm TREO(Y) using a 300ppm TREO(Y)-Ce cutoff, *including 20Mt @ 1,079ppm TREO(Y) using a 600ppm TREO(Y)-Ce cutoff – Figure 3A*. The reported resource does not include mineralisation in bedrock. The REE mineralisation reports to saprolitic clays and sap-rock positioned directly above a per-alkaline granite.

The deposit is weakly LREE enriched and contains a Magnet Rare Earth Oxide (*MREO) component of ~24%, calculated as *MREO/ (TREOY-Y₂O₃)*. The LREE magnet component (Nd₂O₃ + Pr₆O₁₁) = 99.7ppm, while the Heavy Rare Earth magnet component (Tb₄O₇ + Dy₂O₃) = 30.74ppm.

Deposit Dimensions

The deposit footprint is ~2.6km north-south and ~1.8km east-west and is open to the north, south and west. The Rare Earth Accumulation Zone is closest to the surface in the east (proximal to outcropping granite) and gently dips to the west, where it reaches a maximum

vertical distance of 48m below surface. The accumulation zone is 10-25m thick and thins as it approaches the Narraburra Hills.

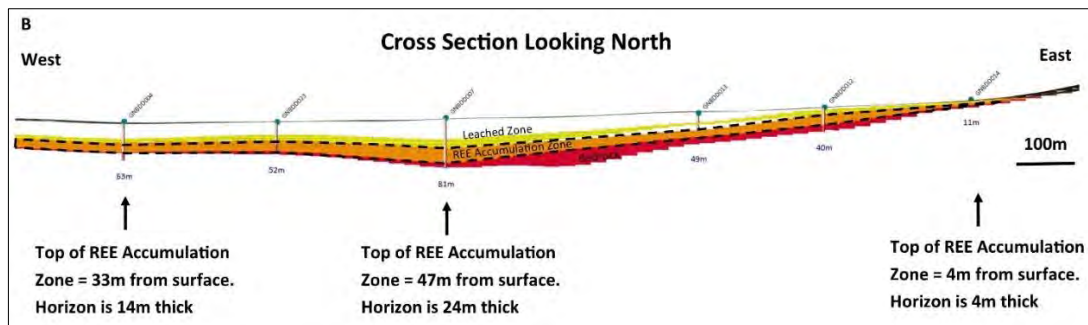
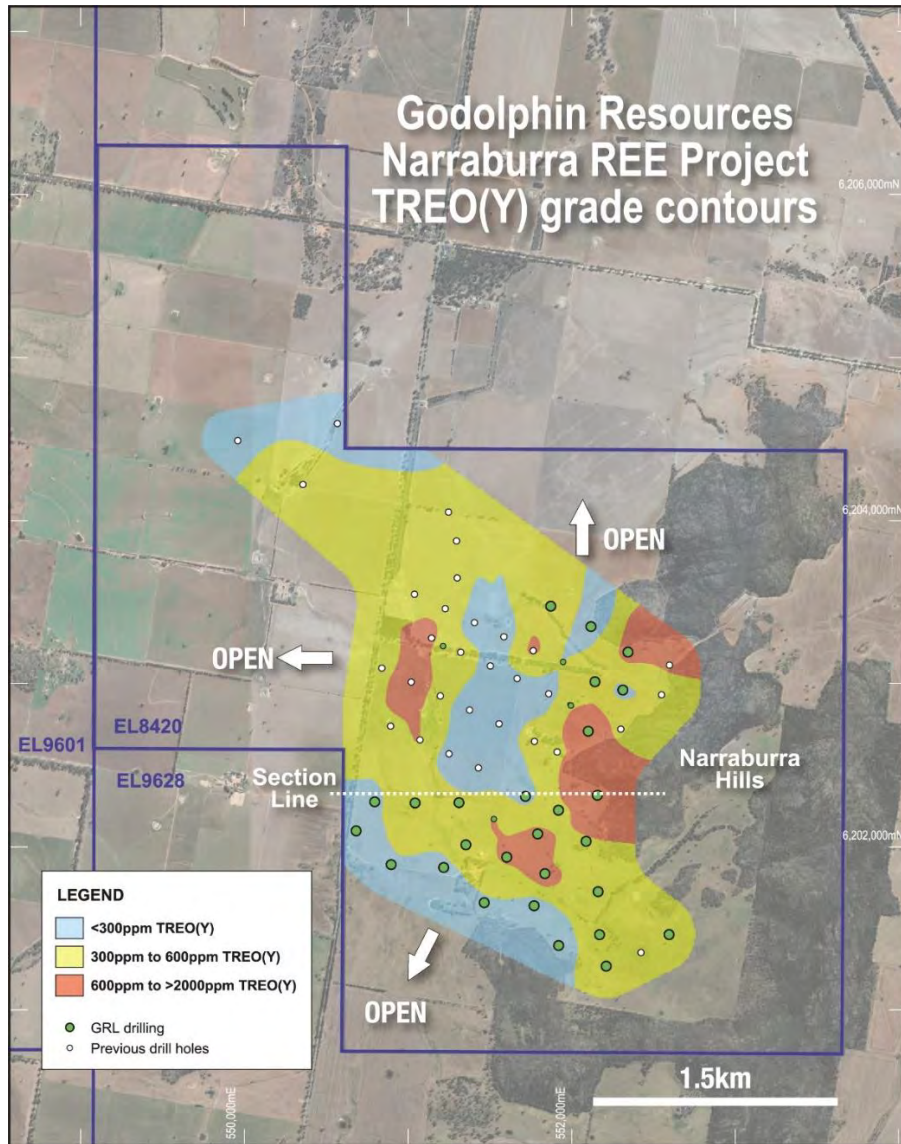


Figure 3: A) Plan view of the Narraburra Mineral Resource as a function of TREO(Y). B) Simplified cross section through the deposit model, showing the REE accumulation zone in orange dips gently to the west. Yellow = partially leached REE zone and Red = bedrock.

MINERALOGY

The dominant clay mineralogy is kaolinite > smectite with the REEs either adsorbed directly onto these clays, within secondary minerals or weathering resistant primary minerals. Two dominant secondary REE bearing minerals are mapped within the deposit and they are:

- Lanthanite-Nd: $(\text{Nd,La})_2(\text{CO}_3)_3 \cdot 8\text{H}_2\text{O}$ and
- Cerite-Ce: $(\text{Ce,La,Ca})_9(\text{Mg,Fe})(\text{SiO}_4)_3(\text{SiO}_3\text{OH})_4(\text{OH})_3$

Other REE minerals are also found in trace amounts:

- Monazite: $(\text{Ce,La,Nd,Th})\text{PO}_4\text{SiO}_4$
- Xenotime: YPO_4
- Britholite-Y: $(\text{Y,Ca})_5(\text{SiO}_4,\text{PO}_4)_3(\text{OH},\text{F})$
- Samarskite-Y: $(\text{Y,Fe,U})(\text{Nb,Ta})\text{O}_4$
- Titanian Samarskite-Y: $\text{YFe}(\text{Nb,Ti})_2\text{O}_8$ and
- Other unknown microcrystalline Rare Earth minerals

METALLURGY

Diagnostic metallurgical test work under typical desorption conditions (pH 4) shows extractions up to 17% TREO(Y) indicating a small percentage of the deposit is ionic in nature. In order to dissolve the remaining REEs a lower pH acid is required and involves using ammonium sulphate with additions of sulphuric acid to maintain a pH between 2 - 2.2. Given the moderate strength acid used, monazite and xenotime are not broken down, resulting in very low level uranium and thorium (<1ppm) in solution. This process achieves recoveries of up to 95% of the four high value magnet minerals (Nd-Pr-Tb-Dy).

The high recovery rate is attributed to the partial encapsulation of REE bearing secondary minerals which are found on the edges of kaolinite grains or other grains such as K-feldspar, albite or quartz (Figure 4), thereby facilitating their dissolution under moderately acidic conditions.

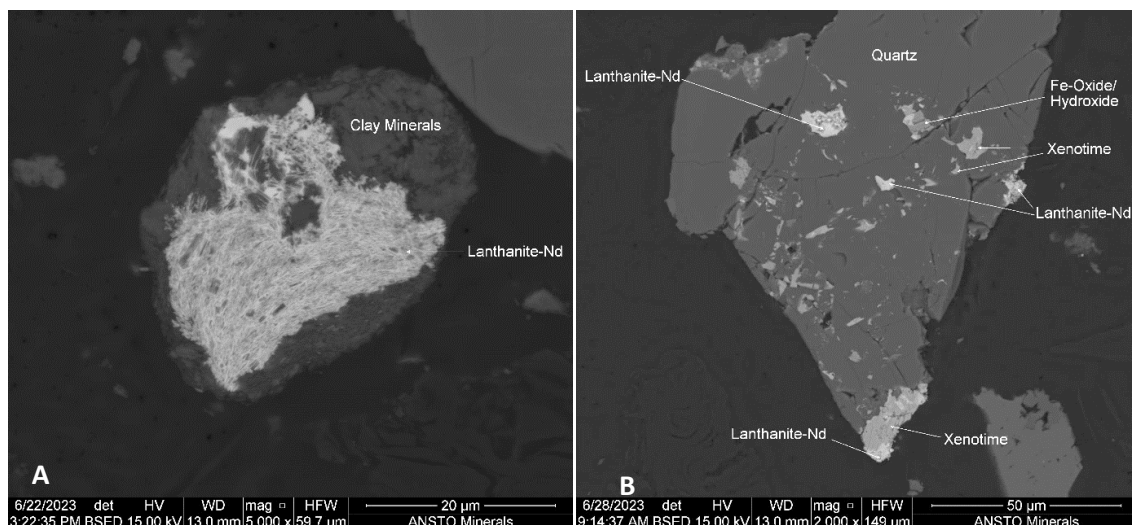


Figure 4. QEMSCAN images A) Near total encapsulation of REE mineral Lanthanide-Nd within clay. B) REE bearing minerals Lanthanide-Nd and Xenotime partially encapsulated by quartz.

PROFILE GEOLOGY

A typical profile through the deposit taken from hole GNBDD001 is presented below and shown in Figure 5.

- **0-9m: Pedogenic layer**
 - Upper 3m elevated in **TREO(Y) (300-500ppm)**

- **9 – 27m: Leached zone (188ppm TREOY)**
 - Completely weathered and mottled yellow-red-white-brown saprolitic clays (upper saprolite).
 - Leached zone corresponds with cerium enrichment, a typical signature of other IAD type deposits i.e.: Ce^{3+} oxidises to Ce^{4+} and forms CeO_2

- **27- 47m: Partial leach zone (537ppm TREOY)**
 - 27-42m: Thin upper ferruginous pisolitic zone grading into mottled white-yellow-brown saprolitic clay.
 - 42-47m: Lower saprolite. Purple-white-brown clay with recognisable granitic rock texture.

- **47- 56m: Rare Earth Accumulation Zone (1075ppm TREOY)**
 - Lower saprolite with purple-white-brown clays transitioning into moderate-weakly weathered granite (saprock).
 - Corresponds with Cerium depletion, a typical signature of IAD deposits in the Rare Earth Accumulation Zone.
 - Developed Neodymium anomaly at transition from sap-rock to fresh rock.

- **>56m: Peralkaline granite**
 - 56-70m: Enriched peralkaline granite (866ppm TREOY)
 - >70m: Fresh peralkaline granite (596ppm TREOY).
 - Granite composition is ~60% alkali feldspar, ~36% quartz, ~3-4% arfvedsonite (Na-amphibole), ~0-1% Aegirine (Na-clinopyroxene) with traces of zircon, monazite, fluorite and ilmenite.

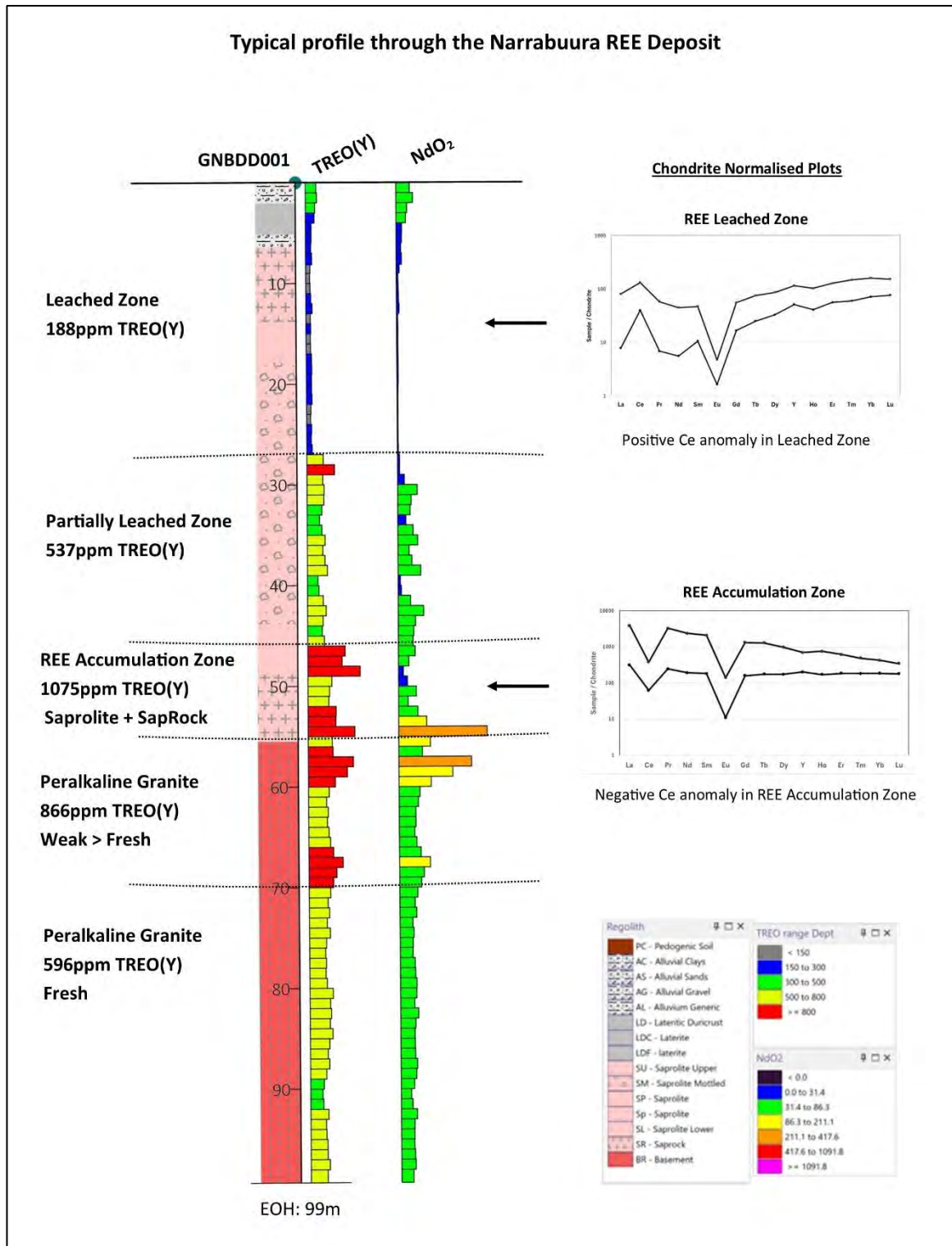


Figure 5: Typical profile through the Narraburra Rare Earth Deposit showing Cerium enrichment in the Leached Zone and corresponding Cerium depletion in the Rare Earth Accumulation Zone which are considered type features of IAD systems.

CLASSIFICATION SUMMARY

On the basis Narraburra has a similar regolith profile to other IAD deposits, exhibits cerium enrichment in the upper leached zone and cerium depletion in the Rare Earth Accumulation Zone, the deposit may be classified as an IAD style deposit. However, given a maximum extraction of 17% TREO(Y) under typical desorption conditions has

been achieved and a stronger acid is required at pH 2 -2.2 to leach REEs from secondary minerals, the deposit is more appropriately classified as a hybrid-IAD.

The overall profitability of extracting REEs at a pH of 2 -2.2 has not been formally assessed in such deposits located within Australia, which has led Godolphin to embark on a Scoping Study. It is envisaged that the greater revenue from higher recoveries using these pH levels and possibly higher temperatures, combined with the amount of high value heavy rare earth magnet minerals, will counteract the higher operating costs from this proposed process flowsheet. It is anticipated the results of this study will be made available in the final quarter of 2024.

REFERENCES

- BORST A, M., SMITH M.P., FINCH A.A., ESTRADE G., BENAVENT C., NASON P., MARQUIS E., HORSBURGH N, J. GOODENOUGH K, M., XU, C., KYNICKÝ J and GERAKI K. 2020. Adsorption of rare earth elements in regolith-hosted clay deposits. *Nature Communications*. <https://doi.org/10.1038/s41467-020-17801-5>
- DOSTAL J. 2017. Rare Earth Element Deposits of Alkaline Igneous Rocks. *Resources*, 6, 34.
- FAN, H.R., YANG K.F., HU F.F., LIU S. and WANG, K.Y. 2015. The giant Bayan Obo REE-Nb-Fe deposit, China: Controversy and ore genesis. *Geoscience Frontiers* 7 (2016) 335-344.
- HELLMAN P. 2023. Rare Earths. SMEDG.
- LYONS P. 2000. Geological History. In Lyons, P., Raymond, O.L. & Duggan, M.B. (compiling editors) *Forbes 1:250000 Geological Sheet S155-7*, 2nd edition, Explanatory Notes. AGSO Record 2000/20, pp 3-6.
- MARQUIS E. 2019. Rare Earth Element (REE) mobility in alkaline igneous rocks and the potential impact on the formation of ion adsorption type REE ores of the Ambohimirahavavy Alkaline Complex. Doctoral Thesis. University of Brighton
- MCNULTY T., HAZEN N and PARK S. 2022. Processing the ores of rare-earth Elements. *Mrs Bullentin*, V47. doi:10.1557/s43577-022-00288-4
- SANEMATSU K and WATANABE Y. 2016. Characteristics and Genesis of Ion Adsorption -Type Rare Earth Element Deposits. *Society of Economic Geologists, Inc Reviews in Economic Geology*, v. 18, pp. 55-79.
- VERPLANCK P. L. 2017. The role of fluids in the formation of rare earth element deposits. *Procedia Earth and Planetary Science*, 17, 758 – 761.
- WARREN A.Y.E., GILLIGAN L.B. and RAPHAEL N.M. 1995. *Geology of the Cootamundra 1:250000 map sheet*. viii + 160 pp. Geological Survey of New South Wales, Sydney.
- WORMALD R.J., PRICE R.C. and KEMP, I.S. 2004 Geochemistry and Rb–Sr geochronology of the alkaline-peralkaline Narraburra Complex, central southern New South Wales; tectonic significance of Late Devonian granitic magmatism in the Lachlan Fold Belt, *Australian Journal of Earth Sciences*, 51:3, 369-384, DOI: 10.1111/j.1400-0952.2004.01063.x

PEAK GOLD MINES – 31 YEARS OF CONTINUOUS PRODUCTION – TRANSITIONING FOR THE FUTURE

Scott Munro

Aurelia Metals Pty Ltd, Level 17, 144 Edward St Brisbane 4000

Keywords: Cobar, copper, gold, lead, zinc.

The polymetallic Peak Gold Mines is located within the Cobar Mineral Field, 8 km SE of Cobar in central western NSW. Since 2018, it has been owned and operated by Aurelia Metals Pty Ltd. The operation is currently within the 32nd year of continuous operation since commencement in late 1992. With an average annual throughput rate of approximately 600ktpa, production since commencement totals over 3.2M oz of gold, 140 kt of copper, 90 kt of lead and 63 kt of zinc.

The operation has experienced a notable shift in production output since 2018, due to the discovery of the Chronos lead/zinc/gold system in 2015. Prior to 2018, the operation, known predominantly as a gold/copper producer, nominally produced 100,000 oz of gold and 5,000 t of copper per annum. Since 2018, the operation has evolved to an increased base metal producer accompanied by a ramp down in gold production.

Current production is from two underground operations, Peak and New Cobar with the Federation Zinc-lead-gold mine set to become a third towards the end of 2024. Due to the nature of the polymetallic ore, feed through the Peak mill is split into two ore types;

1. Copper (gold) to produce a copper/gold concentrate and gold dore.
2. Lead/Zinc (gold) to produce separate lead/gold and zinc concentrates and gold dore.

Since Peak Gold Mines began production in 1992, it has had a remarkable record of exploration success that has continually extended its mine life. Significant brownfield discoveries within the past decade include the Chronos lead/zinc/gold lenses at Perseverance, the Anjea copper/gold lens at Great Cobar, the Kairos gold/lead/zinc and copper lenses below Peak and more recently, extensions to the Eastern gold/copper lens at Chesney.

Proved and Probable Ore Reserves for the Peak and New Cobar operations at 30 June 2023, total 0.7Mt @ 2.6g/t gold, 5.1% lead and 6.1% zinc in lead/zinc feed and 3.0Mt @ 1.7g/t gold and 1.8% copper in copper feed. In the coming years, the operation will once again transition with the majority of mill feed sourced from the New Cobar and Federation operations marking for the first time in the operations history where the majority of production has not been sourced via the original Peak infrastructure.

REFERENCES

AURELIA METALS, 2023. ASX release 30 August: Group Mineral Resource and Ore Reserve Statement.

A GOLD DISCOVERY IN A STRUCTURALLY COMPLEX TERRANE, THE HAUNTED STREAM GOLDFIELD, ELUCIATED VIA STRUCTURAL MAPPING, EAST GIPPSLAND, VICTORIA

Ian E Neilson

MSc Economic Structural Geologist Model Earth

Key Words: Auriferous, Benambran, Bindian, Tabberabberan, strain, Ordovician, discovery, tectonic, exploration, litho-structural, mapping, fold-interference, shear-zones, C-prime

INTRODUCTION

The north-west striking zone of Ordovician turbidites in east Gippsland is locus to the Haunted Stream goldfield, an ~8.5km stretch of tectonically complex and structurally highly evolved rocks containing many hundreds of historic gold workings active in the late 19th century, producing over 25k oz of gold spanning a narrow time period across 25 years of mining (Willman et al., 1999), the Haunted Stream goldfield has remained an enigmatic and elusive frontier for many exploration companies over the last 40 years. Exploration has been primarily driven by the high-grade nature of rock-chip and wall-rock sampling of historical workings regularly yielding >1oz Au/t to >14oz Au/t grades, with an aim to delineate an economic volume and representation of tenor for the mineral field as a whole. Previous explorers include Freeport, BHP, Barrick as well as Mantle Mining with the latter, one of the few companies to undertake a systematic approach to drill hole targeting within the Haunted Stream goldfield. Drilling was challenging, both logistically (access) and in-ground with only a few holes intersecting minor low-grade gold mineralisation with the source of the high-grade gold samples, continuing to remain elusive.

GEOLOGY

The Haunted Stream geological province is unique in its structural complexity with the preservation of up to three major deformation episodes across the project region. Historic workings display a variety of folding and shearing which impart a strong control on mineralisation.

The geology across the area surrounding the Ernestine is dominated by a major west-north-west to east-south-east trending, east-south-east gently plunging, upright F_1 fold axes. These earliest folds are attributed with the Benambran Orogeny (~440 Ma) and reflect a period of regional deformation. Coincidentally, the deformation across the Stawell and Bendigo regions during the Benambran Orogeny resulted in a similar series of structures comprising closely spaced tight to chevron style folds with near-vertical to inclined axial planes and high-angle thrusts. It is these early thrusts that are considered an important structure in the localisation of gold mineralisation via the rupture of the eastern limbs of upright to inclined F_1 folds. At Haunted Stream, these early thrust faults are present within the Ernestine area and are interpreted to have been reactivated during subsequent deformations.

The second major deformation event recognised at Haunted Stream is associated with the Bindian Orogeny ~420Ma to 410Ma. The Bindian Orogeny is associated with a regime dominated by strike-slip faulting/shearing, tight folding granite intrusions, gravitational collapse, reactivation of Benambran structures and importantly gold mineralisation.

The Bindian Orogeny is considered to reflect a progressive simple shear event as evidenced by the dominance of a series of protracted shear related structures across the district that are observed consuming local F_2 folds in divergent shear settings. During the Bindian, F_1 folds are superposed by subsequent F_2 shear folds and duplex systems which 'piggy-back' on the F_1 architecture, resulting in a corrugation effect on the stratigraphy.

It is postulated that the resulting sustained Bindian Deformation resulted in the dextral accommodation of the stratigraphic pile, which in part, further resulted in the back-rotation of the lithified sediments and accommodation of strain via sinistral north-east to south-west trending shearing. Observations from the surface and underground mapping supported the working structural model which was used for drill targeting.

In the Central Victorian goldfields, the Tarnagulla and Poverty Reefs are associated with gold mineralisation c.a. 416 – 401 Ma (Phillips et al, 2012). At Haunted Stream, the Ernestine ~ north-east to south-west trending sinistral shear-zones are Bindian structures and similarly are well mineralised with gold.

The third and final major deformation event recorded in structures at Haunted Stream is associated with the Tabberabberan Orogeny ~385 Ma to 375 Ma. The Tabberabberan event is associated with the development of tight to isoclinal, steeply plunging folds, faulting and reactivation of earlier structures.

A major gold mineralisation event is also associated with this event evident across the Melbourne Zone and eastern margins of Victoria. Numerous gold deposits including the Cohens Reef in Walhalla, the Morning Star, Woods Point Dyke Swarm, the Costerfield and Fosterville deposits are associated with significant gold mineralisation during this time. At Haunted Stream, numerous gold deposits are associated with the c.a. 385 Ma event including the Cassilis Mine (>100koz Au), Yahoo and Fizzle Creek with several other major historic workings hosted in Tabberabberan age structures including Rob Roy, Hibernia and the Ernestine.

STRUCTURAL GEOLOGY

Within the Ernestine area, a sinistral duplex hosting gold bearing structures is observed plunging moderately to the southwest with a well-defined, steeply west-dipping hanging wall mineralised shear. Footwall to this shear, a series of steep shears partition and define steep shear hosted mineralisation (Figure 1).

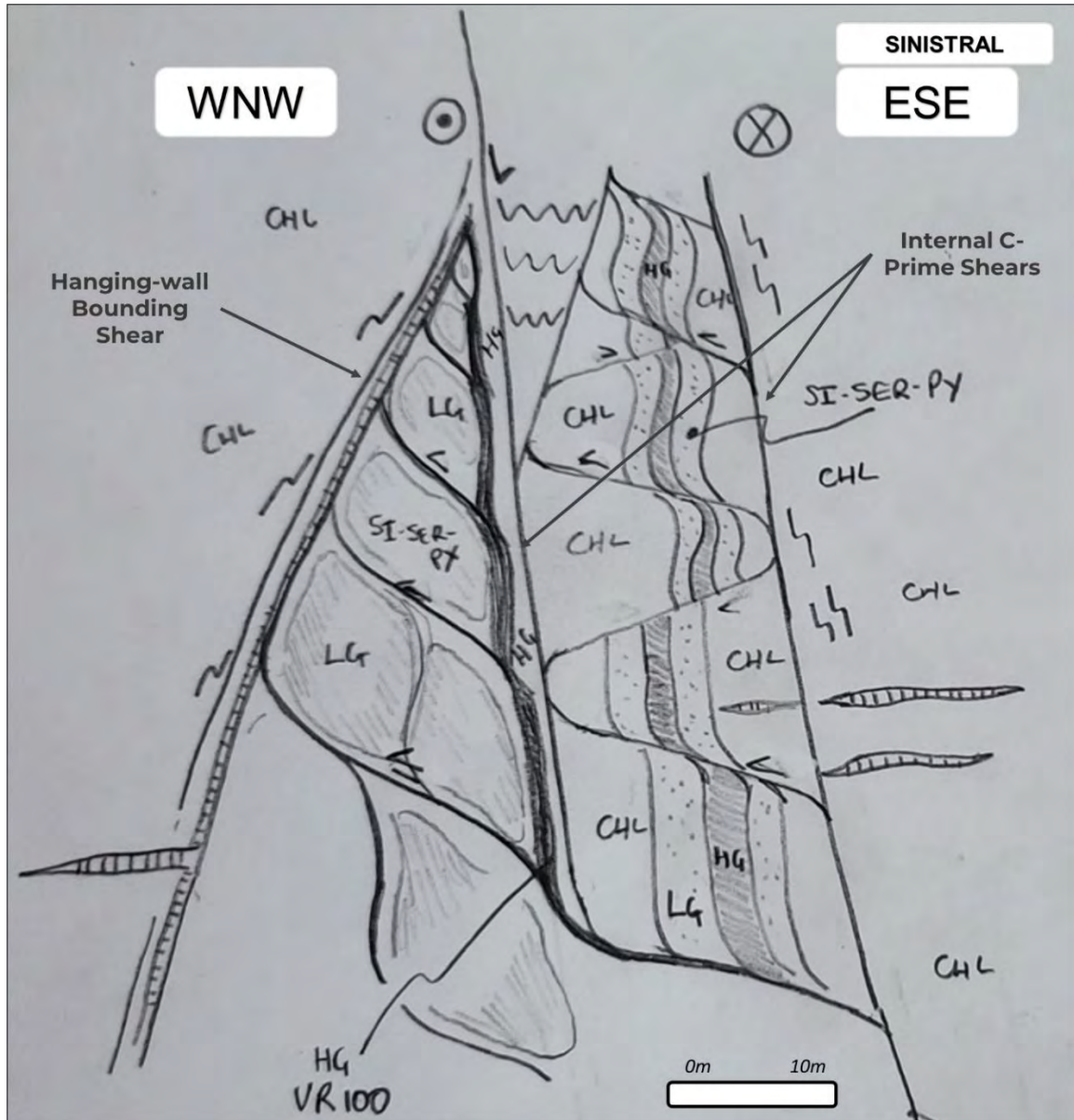


Figure 1: Sectional interpretation of the interpreted main fault controls on gold mineralisation identified from underground and surface mapping within the Ernestine – Hibernia area (see location for Figure 1 in Figure 3 Map). View to the north-east. (Note annotation codes: CHL = Chlorite alteration, LG = lower grade gold mineralisation, HG = high-grade gold mineralisation, SI-SER-PY = silica + sericite + pyrite alteration). The steep east dipping shears are sinistral C-Prime structures.

The mineralisation across the area is controlled by a series of sinistral duplex shear zones. In long section, the mineralisation occurs as shoots plunging back to the south-west (Figure 2).

The Haunted Stream goldfield – in Victoria's east Gippsland

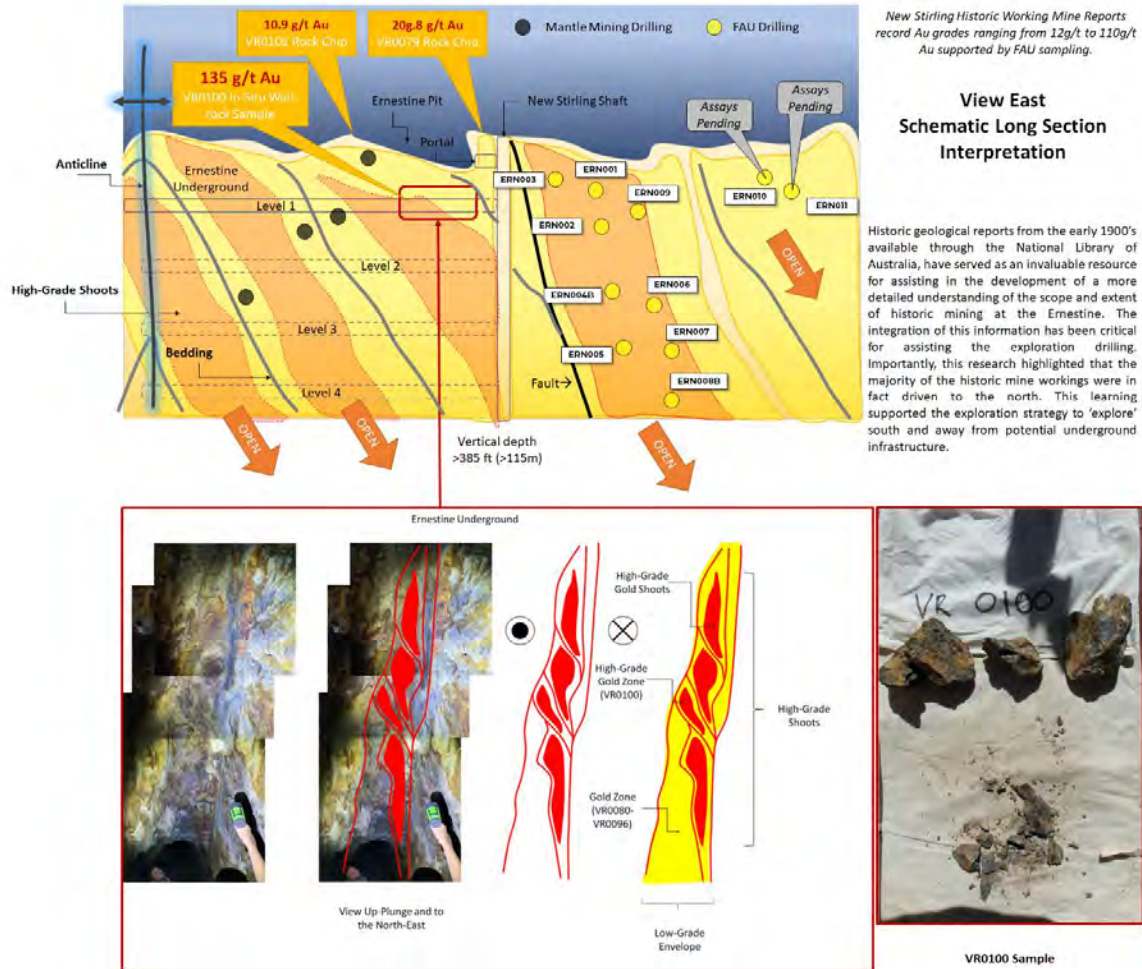


Figure 2: Within the Ernestine – Hibernia corridor, gold mineralisation is observed hosted in south-plunging shoots hosted within a duplex structure. The exploration drilling was designed to test this exploration model.

EXPLORATION

Initial field reconnaissance into the Haunted Stream goldfield in late 2020, highlighted several, if not many, complex structural inter-relationships and geometric curiosities. For example, the historic workings comprising stopes, open cut pits, costeans and underground drives, were excavated along north-east striking structures, yet the concentrations of old workings, including high-grade gold samples, followed the strike of the main layering and major fault of the belt, the Haunted Stream fault, along a north-west striking corridor. Further observations yielded from detailed litho-structural mapping, highlighted the presence of several generations of folding of varying intensity and scale, fold-interference patterns, shear-zones and strain partitioning.

Prior to exploration drilling, a detailed boots-on-ground approach focused on establishing key overprinting criteria in relation to the orientation of gold lodes mapped from surface and underground, across the Haunted Stream goldfield including examining what was happening to the rock-pile away from the mineralised settings in order to develop a comprehensive litho-structural map for the district. This geometric framework was assessed and evaluated against the regional geodynamic of the belt in order to develop a consistent understanding of the evolution of the region across all scales. The resulting

litho-structural maps, described '*compartments*' for targeting and when combined with a 3-dimensional model, were used to plan the drill holes for targeting.

While the aim of the exploration is to test for economic viability and scalability of gold mineralisation, the targeting is a function of the geological hypothesis and understanding of both mineralisation and structural paragenesis of the local setting. At Haunted Stream, the area of focus was narrowed to an accessible series of historic workings, at the eastern end of the goldfield known as the Ernestine – Hibernia corridor. At this location, a series of workings spanned across a zone ~500m long and 400m wide, north-east striking trend and provided sufficient surficial outcrop as well as underground exposure to facilitate both the litho-structural mapping of the hanging-wall and footwall positions of the lodes, but also to assess and observe the local structural controls on the ore-shoots reflected by relict ore-bodies and preserved margins of mineralised zones remanent from mining. It is from the on-ground observations, that the target locations were developed for testing.

TARGETING

The target stratigraphy comprises coarse to fine sandstones, silts and black shales that are folded about km-scale, F_1 folds. F_1 folds are chevron to tight, upright to moderately inclined north-east, striking north-west, with the northern overturned limb, often heavily disrupted by brittle faulting, resulting in a predominance of south dipping bedding along the length and breadth of the Haunted Stream district. A pervasive slaty to pressure solution cleavage, S_1 , occurs axial planar to F_1 folds.

F_1 fold limbs are buckled and warped by a series of north-east striking, shallow south-east plunging, open to close, moderately plunging, south-west plunging 100's metre-scale F_2 folds, defined by a well-developed, upright fracture spaced S_2 cleavage, axial planar to F_2 folds, offset along stratigraphic contacts by D_2 layer-parallel dextral dip-slip faults and further modified by a series of steep to sub-vertical sinistral shear-zones that strike ~north-east to south-west. The C-prime structures are oriented ~north-south and steeply to sub-vertical dipping. Steep tension veins are observed at the terminus of the ductile shear-zones. In addition to the existing complexity, a steep, ~north-south trending, steeply dipping to upright S_3 pressure solution cleavage axial planar to F_3 folds is observed folding the tectono-stratigraphy at the 10 to 100's of metre scale. Where observed, the F_3 folds are doubly plunging, however are generally observed plunging moderately south within the enveloping surfaces of the south-dipping, F_1 limbs.

The resulting superposition of structures resulted in the heterogenous distribution of strain across a series of compartmentalised blocks where mineralised was focused into low-mean stress sites. The juxtaposition of F_3 folds on D_2 shear-zones further results in F_3 axial planes developing sub-parallel to D_2 C-prime. Gold mineralisation is sited within D_2 shear-zones with high-grade zones (>1 oz/t Au) striking ~north-south and coincidentally, associated with hinges of F_3 folds.

The litho-structural mapping illustrated that mineralisation is constrained within and across a discrete series of compartments, where strain was accommodated by both ductile and brittle deformation, along a sinistral shear dominated, south-east trending corridor (Figure 3).

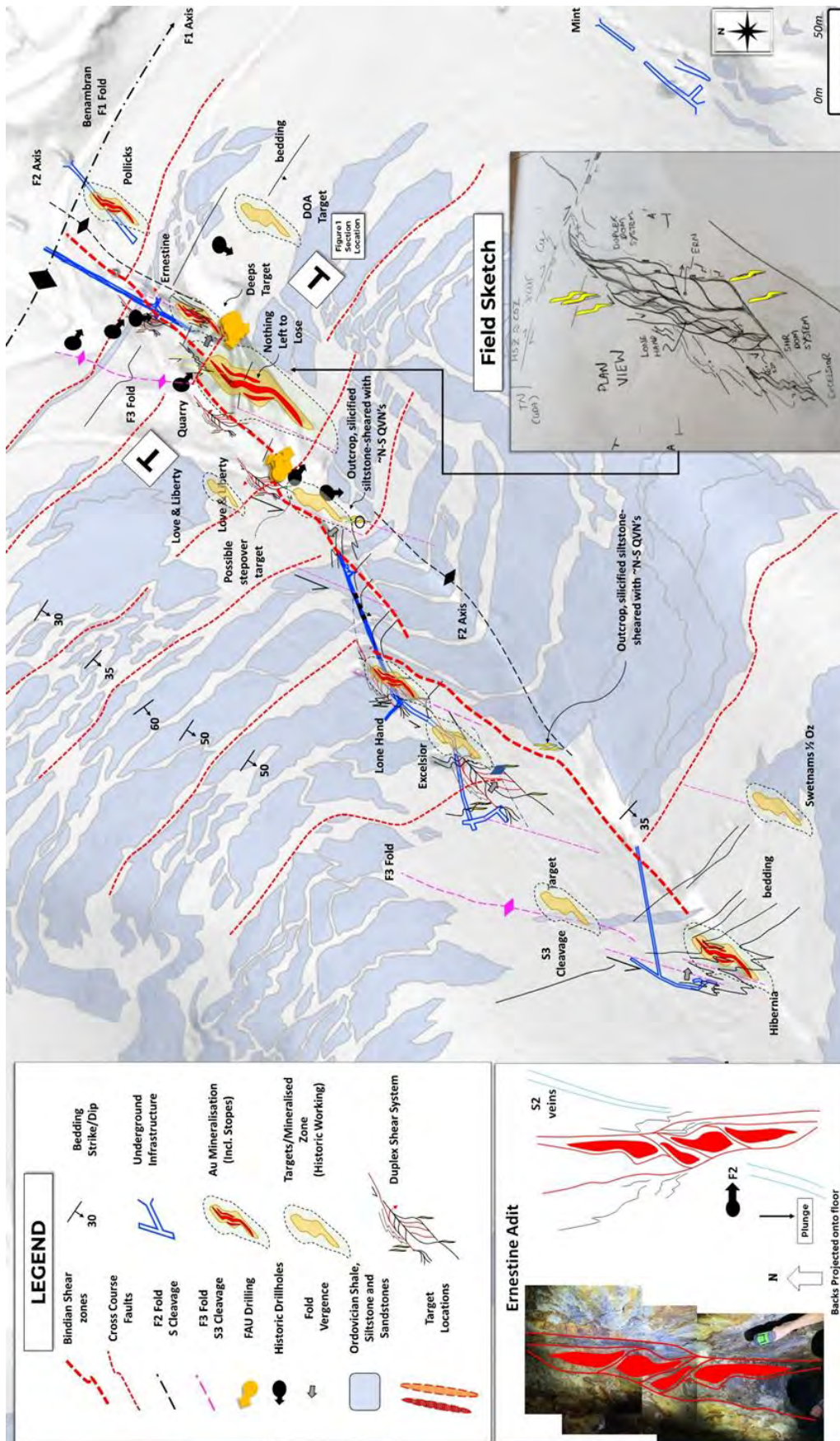


Figure 3: Litho-structural map for the Ernestine area with surface and underground mapping observations which assisted with defining drill targets.

SUMMARY OF DRILLING AND RESULTS

In May 2023, the first drillhole, ERN001, intersected the hanging-wall of a previously unknown lode from 37m resulting in 7.3m @ 5.11 g/t Au including 0.2m @36.88 g/t Au across a total interval of 12.9m @ 3.57 g/t Au. All subsequent drillholes intersected economic mineralisation down the plunge of the system resulting in the first newly identified economic zone in over 120 years (Figure 4).

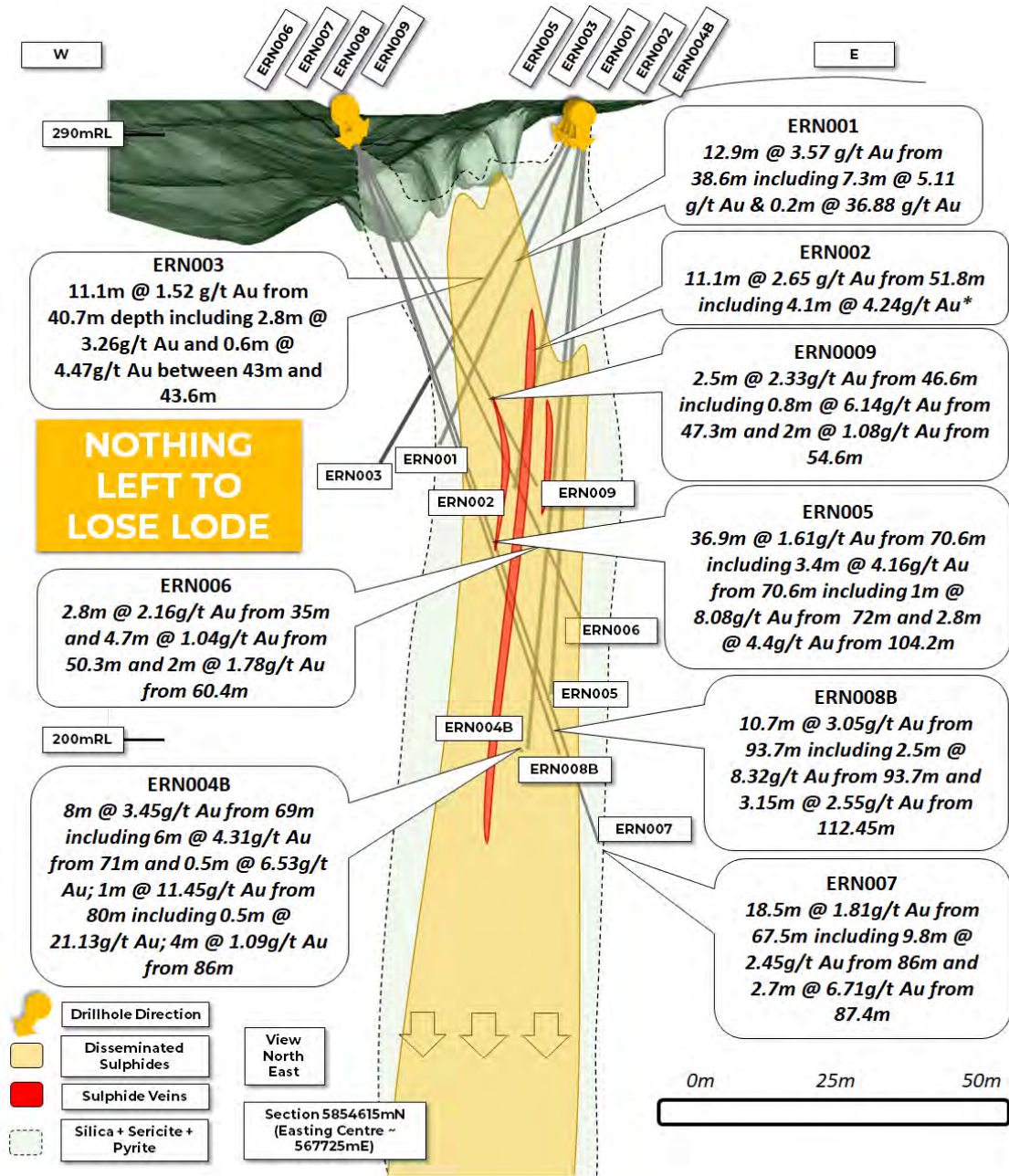


Figure 4: Section view North-East with assay results for all holes assayed. All coordinates in MGA94 Zone 55.

Targeting success is directly attributed to the development of a local lithological structural understanding of mineralisation controls prior to the commencement of drilling. The rehabilitation of the historic workings facilitated the safe passage and traverse of the vast network of underground drives, cross-cuts and adits providing access to the backs

and ribs along the workings enabling a detailed record of observations to be collected immediately adjacent and proximal to the mineralised lodes.

With the preservation of a structural record comprising all three major deformation episodes, evidence of gold mineralisation in multiple settings, the Haunted Stream mineral field presented a unique opportunity for further exploration. It is plausible that the critical controls on gold localisation and deposition were highly favourable and conducive for mineralisation during the Bindian Orogeny. Furthermore, these same settings contributed to the favourable ground conditions for subsequent gold mineralisation during the Tabberabberan resulting in the current distribution of mineralised settings observed across the Haunted Stream Project.

The culmination of the litho-structural mapping across the area underpinned the targeting strategy that assisted in developing a 3D model ultimately used for the drill targeting and testing.

REFERENCES

PHILLIPS, D., FU, B., WILSON, C. J. L., KENDRICK, M. A., FAIRMAID, A. M., & MILLER, J. (2012). Timing of gold mineralisation in the western Lachlan Orogen, SE Australia: A Critical Overview. *Australian Journal of Earth Sciences*, 59, 495-525. <https://doi.org/10.1080/08120099.2012.682738>.

WILLMAN, C.E., MORAND, V.J., HENDRICKX, M.A., VANDENBERG, A.H.M., HAYDON, S.J., CARNEY, C., 1999. Omeo 1:100 000 map area geological report. Geological Survey of Victoria Report 118.

MYALL PROJECT: THE VALUE OF PERSISTENCE UNDER COVER IN THE EAST LACHLAN

Steven Oxenburgh*, Adam McKinnon*, Peter Smith*, Vlad David*, Ilse Oxenburgh*

*Magmatic Resources Ltd,

Key Words: East Lachlan, Ordovician, copper, gold, breccia, porphyry mineralisation, monzonite, monzodiorite, intermediate volcanics

INTRODUCTION

The Myall Project, located in central western New South Wales (Figure 1), has an almost 30-year history of porphyry exploration beneath deep cover, using a combination of geophysical and geochemical techniques. The project was acquired by Magmatic Resources from Gold Fields Australasia in 2014, and in 2023 Magmatic Resources defined a Mineral Resource at the Corvette and Kingswood Deposits of 110 Mt at 0.27 % Cu, 0.07 g/t Au, 0.8 g/t Ag & 10 ppm Mo. The project has multiple additional porphyry and epithermal copper and gold targets, with recent efforts focussed on refining the geological understanding of the region and identifying future drilling targets. In March 2024, Magmatic entered into a Farm-in and Joint Venture Agreement over the Myall Project with FMG Resources Pty Ltd.

EXPLORATION AND DISCOVERY HISTORY

The Myall Copper-Gold Project covers the northern extension of the Junee – Narromine Volcanic Belt, located ~50 km north and along strike of the Northparkes copper-gold mining district. The project is centred over the Ordovician Narromine Igneous Complex (NIC) and is covered by 60-140 m of cover at the southern end of the Great Artesian Basin.

Geophysics

Samedan Oil completed a residual magnetic interpretation in 1980 while exploring for Pb-Zn-Ni-Co mineralisation along the Parkes Thrust in the eastern margin of the project area. Geopeko followed in 1981-83, targeting pipe-like features identified by the Samedan interpretation of the government acquired magnetic data. Geopeko also conducted a reconnaissance gravity survey and trialled dipole-dipole IP.

Renison Goldfields Consolidated (RGC) completed close space airborne magnetic and radiometric surveys in 1996 to support targeting for aircore drilling. In 2008, Clancy remodelled previous gravity data before forming a joint venture with Gold Fields. Gold Fields completed a ground gravity survey at 500m grid spacing over the majority of the tenement and a small infill survey at 250 m grid spacing over the Kingswood Prospect area in 2009.

In recent years Magmatic have completed remodelling and inversion of merged magnetic and gravity data in conjunction with completing a 100 m spaced infill gravity survey over the Corvette-Kingswood trend.

The regional aeromagnetic and gravity images (Figure 2) both identify coincident gravity lows and magnetic high over the NIC. These signatures are similar to those at Northparkes (4.4 Mt Cu / 5.2 Moz Au) and Cowal (13 Moz Au).

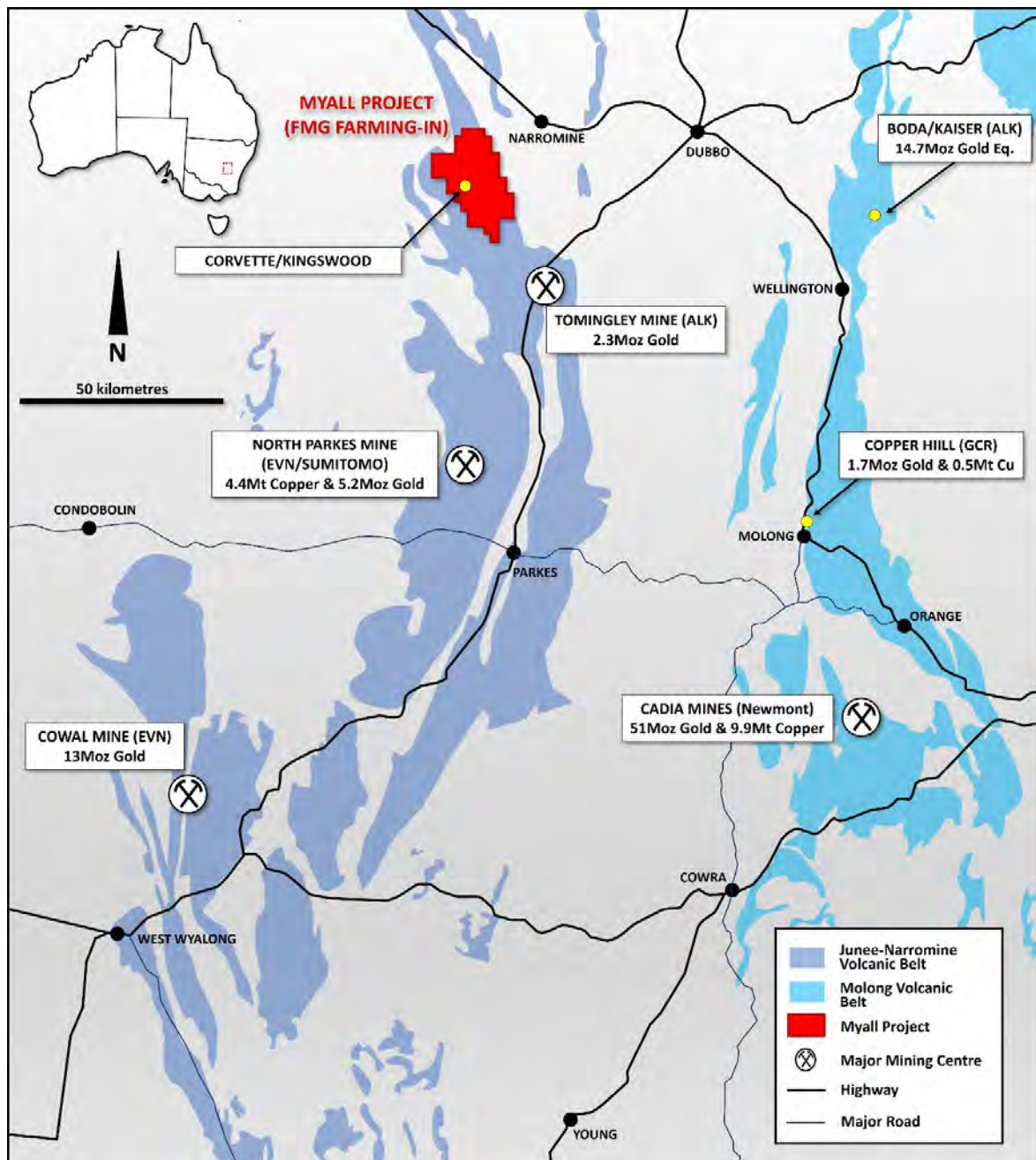


Figure 1. Myall Project location plan.

Initial Drilling and Geochemistry

Geopeko completed 31 auger-diamond drillholes in 1980 and 12 reverse circulation holes in 1981. Geopeko drilling focused on magnetic highs, defined as pipe-like features at Calais, Kingswood, Sandman and other targets along with completing a fence of vertical holes trending north-east through the centre of the current licence area.

RGC expanded on this work with systematic broad-spaced aircore drilling with selective short diamond tails. Initial spacing was 2 km by 1 km with incremental infill to 500 m by 500 m over anomalous zones. In total RGC completed 150 aircore holes with 40 diamond tails.

The first drilling with significant mineralisation in the region was RGC hole NACD008, intersecting a monzodiorite grading *10.3 m at 1,200 ppm Cu, 0.04 g/t Au (max. 2,480 ppm Cu)*. NACD008 is located 100 m east of the initial MRE later defined at Kingswood. Follow-up drilling by RGC consisted of eight aircore holes with diamond tails (NACD081-87, NACD91) drilled in a cross pattern away from NACD008 (see Figure 5). Four of those holes intersected >2,000 ppm Cu, with the northernmost of these holes (NACD91) within the Corvette Resource footprint. Early holes NACD091 and NACD085 are still amongst the best shallow aircore/diamond tail holes drilled at the project to date, with max assays of 8,383 ppm Cu and 8,140 ppm Cu respectively. These holes were the initial focus of follow up for RGCs joint ventures with both Resolute and then Newcrest.

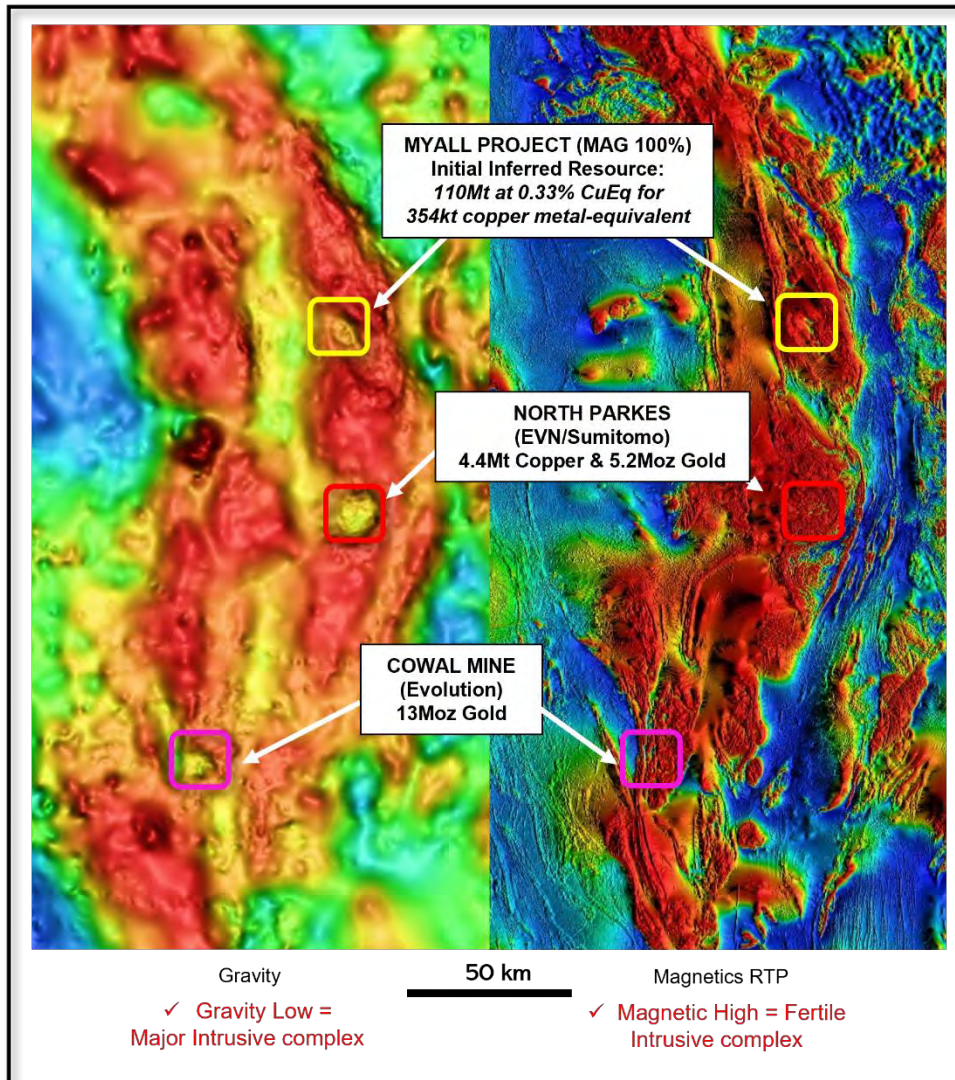


Figure 2. Regional gravity and aeromagnetic images showing similarities between Cowal, Northparkes and Myall.

The first deeper diamond drilling was conducted by Resolute in 1999, completing seven angled aircore-diamond drillholes with the main focus on the Kingswood and Gemini Prospects following up copper anomalies defined by RGC. The Newcrest joint venture continued with systematic aircore grid pattern and deeper diamond drilling. This work included the first deep diamond tail holes to be drilled into what is now the Corvette Prospect, along with several deep holes targeting epithermal gold mineralisation at the Barina and Gemini Prospects. Newcrest's focus turned to epithermal gold mineralisation after results from the Corvette-Kingswood area showed the Kingswood area to be copper-dominant.

Basement Copper and Gold Anomalies

Air core holes (with some diamond tails) have been used extensively over the project area to identify anomalies due to the depth of cover. This drilling has defined coherent, kilometre-scale basement copper anomalies with thresholds ranging from 500 ppm to 1,000 ppm Cu. Highest copper grades are generally seen immediately below the transported cover, with supergene mineralisation including native copper and occasional chalcocite being common. Higher tenor copper anomalies are notable in the Corvette-Kingswood region, with coherent zones of >2,000 ppm Cu straddling the eastern and western margins of the Corvette Monzodiorite over a north-south strike length of greater than 2,000 m.

Gold anomalies in the air core drilling are highly variable and are much harder to correlate with large-scale bedrock mineralisation. Many higher-order gold anomalies have been targeted by previous explorers with variable results. Gold anomalies tend to be more significant when coincident with anomalous copper.

Data and sample preservation

Drilling to date at Myall has included 763 drill holes for 110,000 m, including about around 25,000 m of diamond core. This has resulted in an extensive assay database including 35,000 analyses, with two thirds being multi-element data. Almost all the drill core and chips collected by RGC, Resolute, Newcrest, Clancy Exploration and Gold Fields Australasia have been photographed and maintained by Magmatic Resource, with re-examination of this drilling greatly assisting in the continuing development of the current geological models for the region.

Corvette Discovery (2022)

During the 2022-2023 period, Magmatic discovered extensive Cu-Au mineralisation at Corvette while conducting follow up diamond drilling to Newcrest hole ACDNM090, which had previously intersected *77 m at 0.55 % Cu, 0.15 g/t Au and 102 ppm Mo*. Drilling was oriented from west to east, effectively forming a scissor hole to ACDNM090 and targeting an assumed vertically-orientated mineralised system. This initial Magmatic hole (22MYDD415) intersected multiple zones of strong chalcopyrite ± magnetite bearing breccia zones. As drilling progressed north and south, additional strong mineralisation was intersected, with these zones appearing to terminate in a massive monzodiorite intrusive. This monzodiorite had previously been interpreted as late stage, potentially stopping out mineralisation.

Some of the more significant mineralised intersections encountered during the 2022-23 period included:

- 22MYDD415 722.5 m at 0.25 % Cu, 0.07 g/t Au & 14 ppm Mo from 134.5 m
including 111 m at 0.55 % Cu, 0.10 g/t Au & 5 ppm Mo from 499 m
- 22MYDD417 466.6 m at 0.30 % Cu, 0.07 g/t Au & 12ppm Mo from 134.4 m
including 117 m at 0.55 % Cu, 0.12 g/t Au & 33 ppm Mo from 137 m
- 22MYDD422 875.2 m at 0.21 % Cu, 0.04 g/t Au & 6 ppm Mo from 146.8 m
including 241.0 m at 0.45 % Cu, 0.11 g/t Au & 7 ppm Mo from 261 m

These intersections commenced from the base of transported cover.

GEOLOGY

Cover Sequence

The NIC is covered by the southern extremities of the Great Artesian Basin over the entire Myall Project, with cover thickness varying from 100-140 m in the west to 40-60 m in the east. The cover consists of clays, silts, sands and gravels with minor carbonaceous layers. The cover sequence can cause complications with RC drilling which are overcome using mud-rotary pre-collars and diamond tails as the preferred drilling method.

Narromine Igneous Complex

The Myall Project is hosted within the NIC located in the northern portion of the Junee-Narromine Volcanic Belt within the Macquarie Arc. The NIC consists of the basal Narromine Volcanics, the batholith- to laccolith- shaped diorite-gabbro suite, monzodiorite to quartz-monzodiorite and tonalite intrusions, and rare late mineralised quartz-feldspar porphyry intrusions. The monzodiorite intrusion history is complex and work to further understand the geology in this area is ongoing. Late stage unaltered porphyritic andesitic and basaltic dykes also cut the sequence.

Lithology names vary with authors and Magmatic are using the names and descriptions from Joel Fitzherbert petrographical reports (2022) with variations.

Rock types

Narromine Volcanics

In the Kingswood-Corvette area, the earliest units are the Narromine Volcanics, which are poorly exposed and mostly occur at Kingswood and Corvette as fragments in breccias, and possibly as larger blocks, assumed to have been brought upwards during brecciation events. The volcanics are mostly andesites with stout plagioclase phenocrysts (1-2 mm) (Figure 3A and 3B).

Diorite to gabbro

This extensive unit varies in composition from monzodiorite to monzogabbro to monzonite and is characterised by its coarse grain size (up to 3 mm) and uniform texture. The example shown in Figure 3C is a hornblende diorite with interlocking plagioclase, hornblende and minor interstitial quartz.

Quartz-monzodiorite (“Corvette Monzodiorite”)

The quartz monzodiorite unit (“Corvette Monzodiorite”) is an extensive unit which has been traced over 2 km in a generally north-south trend, ranging between 200-400 m wide, and believed to be dipping at 60° to 70° to the east (Figures 5 to 8). It is a distinct unit with characteristic 2-3 mm acicular hornblende and irregular 20-700 mm rounded mafic xenoliths. The intrusion of this unit appears to be consistent with development of an adjacent breccia “damage” zone which may have provided fluid conduits for later mineralised porphyry intrusions and related fluid flow (Figure 3D).

Quartz monzodiorite porphyry (“crowded porphyry”)

This porphyritic unit comprises 80% euhedral plagioclase in a quartz-feldspar matrix, is more sporadically located and has not been consistently logged. This unit hosts rare, rounded quartz phenocrysts 1-2 mm in diameter (Figure 3E). This unit is also referred to as tonalite (e.g. Dobbin, 2022)

Quartz monzodiorite

Rare quartz monzodiorite (similar to the crowded porphyry above) intruding breccias have been identified which appear closely related to late mineralising events (Figure 3F). Other quartz-feldspar porphyries with rare, rounded quartz phenocrysts have been identified which appear related to mineralisation.

Late basalt dykes

Late, mostly unaltered fine-grained mafic dykes are fairly common, ranging from a few metres to tens of metres thick and tend to cross-cut all other lithologies.

Breccias and Mineralisation

The dominant mineralisation style encountered to date is hosted in hydrothermal breccias. These zones are characterised by angular, jigsaw to polymict breccias. Breccia infill variably comprises chalcopyrite, magnetite, carbonates, quartz and lesser anhydrite/gypsum. Away from the breccia zones mineralisation is characterised by sheeted to braided chalcopyrite-pyrite veins, with disseminated chalcopyrite giving way to a distal pyrite halo. Occasional bornite and molybdenite also occur in these zones.

Vein types observed include early magnetite veins (M-veins), dominated by sheet-like to networks of 1-10 mm magnetite veins, mm-cm chalcopyrite-pyrite veins, as well as chalcopyrite-epidote-quartz-pyrite C-type veins and centre-line quartz-chalcopyrite veins. Mineralisation examples are shown in Figures 4A to 4F.

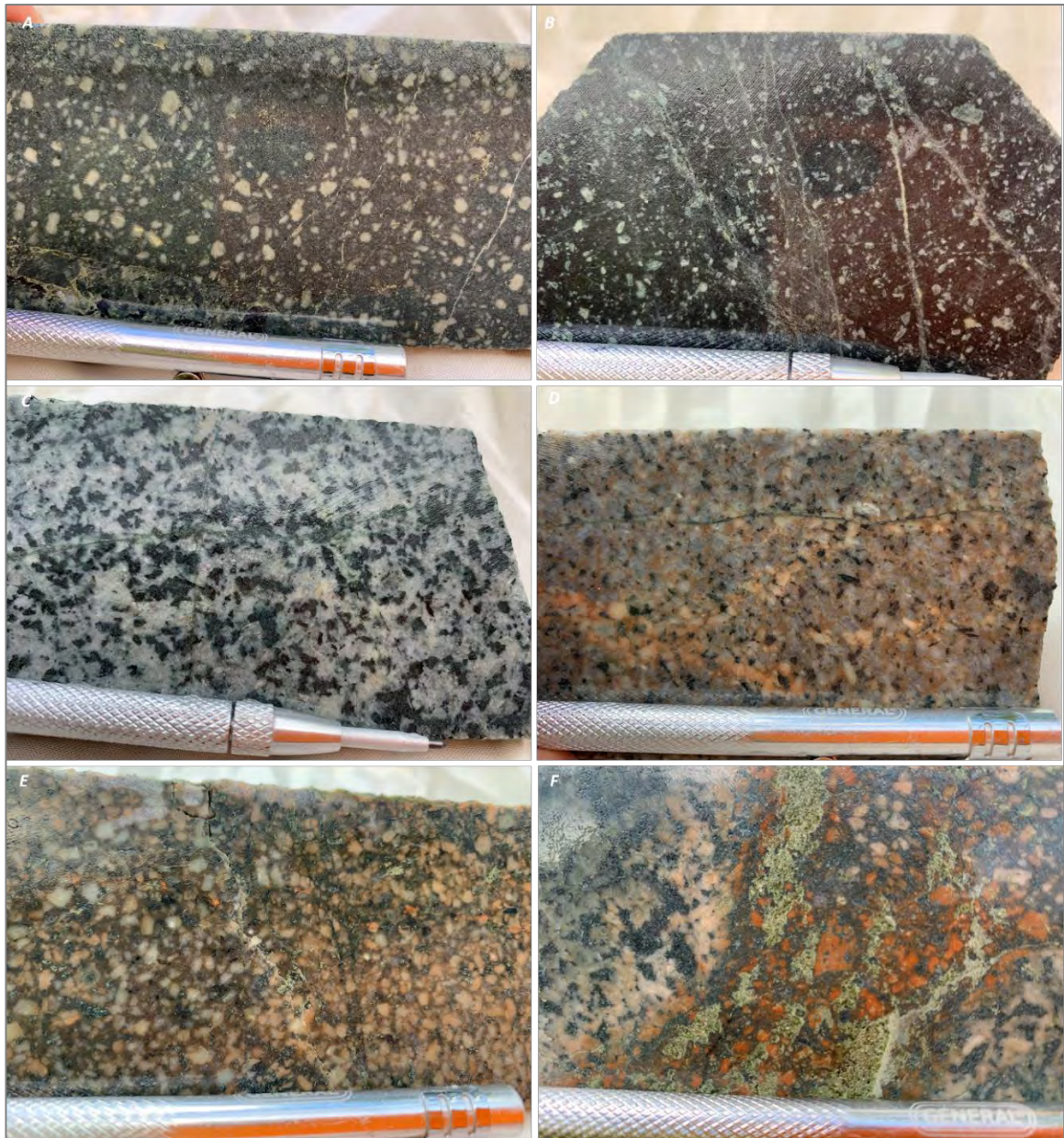


Figure 3. Images from Joel Fitzherbert petrography report. A) and B) porphyritic andesite; C) diorite; D) Corvette Monzodiorite; E) crowded quartz monzodiorite; and F) mineralised quartz monzodiorite breccia fill within brecciated diorite.



Figure 4. Typical mineralisation styles at Corvette. A) brecciated andesite displaying chalcopyrite / pyrite infill associated with chlorite and sericite alteration; B) polymict andesite/ diorite breccia with chalcopyrite infill; C) magnetite-chalcopyrite cemented polymict breccia; D) rare quartz-carbonate vein with chalcopyrite inclusions to 10mm; E) disseminated chalcopyrite/pyrite in magnetite-epidote-chlorite altered diorite; F) strongly epidote-altered brecciated diorite with chalcopyrite infill and patchy K-feldspar alteration.

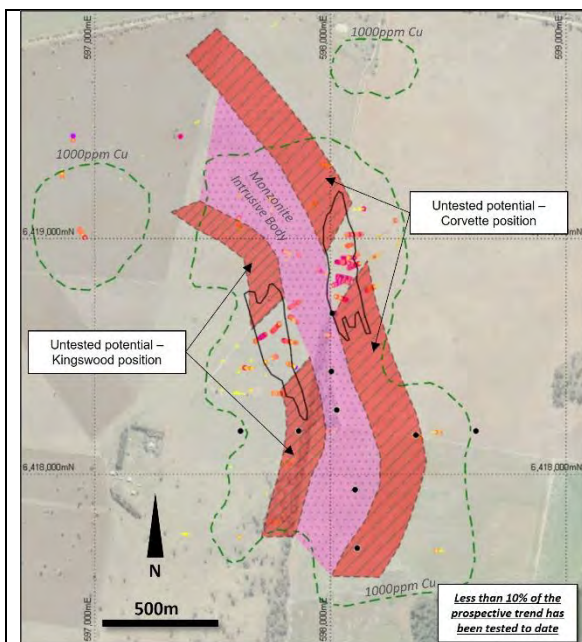


Figure 5. Corvette and Kingswood MRE located adjacent to the Corvette Monzodiorite and untested positions both north and south. Drilling shown is top 150m below the base of cover. Plan on satellite. Black dots are the initial nine RGC ACD holes

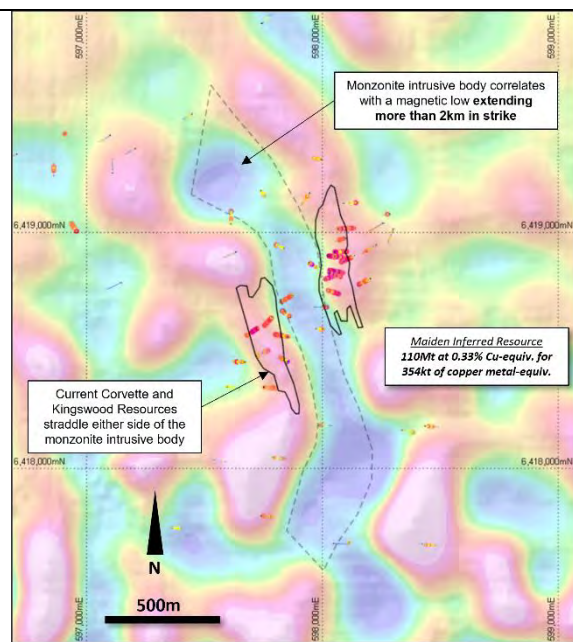


Figure 6. Same plan and drilling on MVI magnetics. Clear magnetic image of the Corvette Monzodiorite extensions north and south and substantiated with sparse previous drill positions.

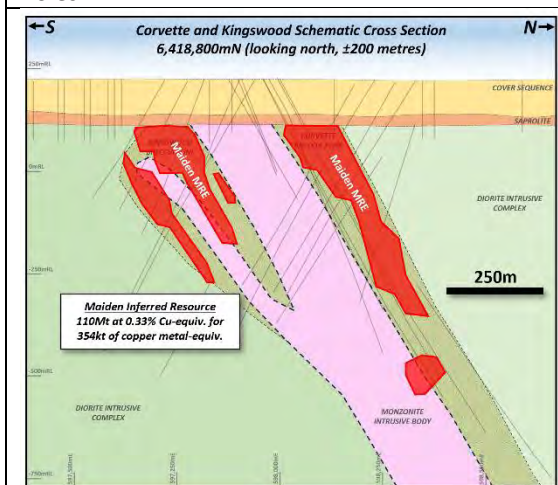


Figure 7. 400m cross-section through Corvette (RHS) and Kingswood (LHS) showing MRE sitting in the hanging wall and the footwall to the Corvette Monzodiorite.

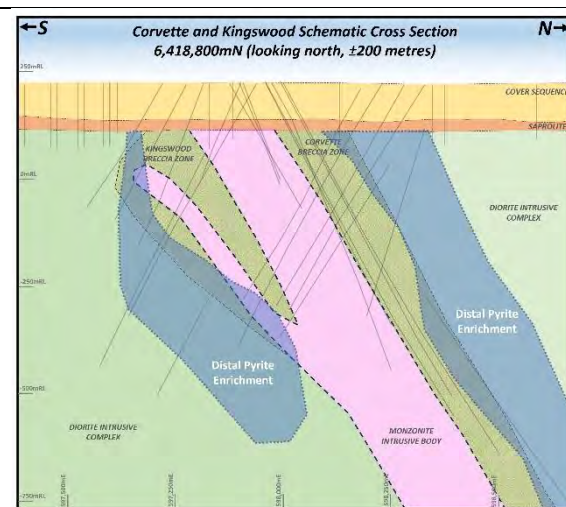


Figure 8. Same cross-section showing the distal calculated pyrite enrichment zones to both Kingswood and Corvette mineralisation.

DEVELOPMENT OF NEW GEOLOGICAL MODEL

Previous explorers at Myall have used various porphyry models to target mineralisation. Comparisons have been made to the pipe-like geometry of the Northparkes Cu-Au deposits, Cowal dispersed vein gold deposits, or the Cadia Au-Cu systems. Magmatic initially adopted the sub-vertical Northparkes ‘pencil porphyry’ model.

Reprocessing and re-interpretation of the aeromagnetic data following the Corvette discovery indicated a NNW strike to the mineralisation with suggestion of an easterly dip. During resource model estimation in 2023, modelling of the variography for copper also suggested the mineralisation had a dominant orientation striking NNW with dip moderately to the east. This contrasted somewhat with structural data collected from the drilling that indicated a NNE strike and sub-vertical orientation.

Subsequent geological modelling of the monzodiorite unit (Corvette Monzodiorite) incorporating the new drilling at Corvette confirmed this NNE orientation, suggesting that monzodiorite formed the footwall to mineralisation rather than stopping the mineralisation out. Reinterpretation of the Kingswood mineralisation using the same orientation suggested it was hosted in an equivalent position in the footwall of the monzonite. The latter interpretation for Kingswood remains to be fully tested due to lack of available data in the down dip position.

Cross-sectional interpretation combined with lithogeochemical data suggest this model is also consistent with drilling data over a strike exceeding two kilometres.

CONCLUSIONS AND EXPLORATION IMPLICATIONS

The ongoing efforts at the Myall Copper-Gold Project have underscored the significant value of persistence and detailed geological investigation in exploring undercover in the region. The reinterpretation of the Corvette Monzodiorite's orientation and timing has been pivotal in understanding the controls on mineralisation. Future exploration efforts will focus on testing the revised geological model, with a particular focus on the untested lower contact of the monzonite and areas to the south of Corvette. This exploration strategy has the potential to significantly increase the existing resource and potentially uncover previously unknown mineralised zones.

These results also have the potential to contribute to an understanding of the geological framework in the broader region and may enhance exploration success rates for other ventures.

ACKNOWLEDGMENTS

The authors acknowledge the Magmatic Board and JV partners FMG Resources Pty Ltd for permission to publish data from the project.

REFERENCES

- DOBBIN F. H. 2022. Geology and genesis of the Kingswood porphyry Cu-Au prospect, NSW, A research thesis submitted in partial fulfilment of the requirements for the degree of Bachelor of Science with Honours, University of Tasmania (unpubl.)
- FITZHERBERT J. 2022. Petrographic report for samples taken from drillcore 22MYDD415 and 22MYDD414, Corvette Prospect, Myall Project NSW (unpubl.)

PLATE TECTONICS OF THE NEW ENGLAND OROGEN AND ITS MINERAL DEPOSITS

Gideon Rosenbaum

School of the Environment, the University of Queensland

Key Words: New England Orogen, ore deposits, subduction, oroclinal, tectonics.

INTRODUCTION

The New England Orogen (NEO), which occupies the easternmost portion of the Tasmanides, has commonly been described as an Andean-type orogenic system (Day et al., 1978; McPhie, 1987). However, unlike the Andes, the NEO does not host major porphyry fertile systems. Sporadic mineral deposits include porphyry, epithermal, and orogenic gold, but the relationship of these mineralised zones with plate tectonics is relatively poorly understood. Plate tectonic reconstructions are rudimentary and contain many unresolved problems, whose answers could help understanding the spatio-temporal distribution of mineral systems in the NEO.

The aim of this contribution is to provide an overview of the plate tectonic history of the NEO and to discuss the geodynamic context of mineral deposits. There are aspects in the plate tectonic history of the NEO that are well constrained; I will discuss these topics first, followed by a discussion on more contentious issues that warrant further research. Some of these research topics are crucial for constraining plate tectonic reconstructions that may explain occurrences of known mineral deposits and potential exploration targets.

PLATE TECTONICS OF THE NEW ENGLAND OROGEN

Several aspects in the plate tectonic history of the NEO are supported by robust constraints. First, there is strong evidence that from the Late Devonian to the end of the Carboniferous, a west-dipping (present coordinates) subduction zone produced continental arc magmatism in the NEO and a broad forearc region comprising an accretionary complex and a forearc basin (Murray et al., 1987). Second, there is widespread evidence that during the early Permian, the NEO was predominantly under the influence of backarc extension (Holcombe et al., 1997). This is indicated by the development of sedimentary basins (Korsch et al., 2009; Shaanan et al., 2015), and thermal anomalies that produced high-temperature metamorphic complexes (e.g., Craven et al., 2012) and crustal melting (S-type granitoids). The transition from an arc/forearc environment in the Carboniferous to a backarc setting in the Early Permian implies oceanward retreat of the subduction zone. Third, the presence of voluminous arc-related plutonic and volcanic rocks, dated from the Middle Permian to Late Triassic (270–220 Ma), indicates that during this period, the NEO was again positioned in an arc setting. The change from a backarc setting in the Early Permian to an arc setting in the Middle Permian implies a switch from trench retreat to advance. This change was accompanied by the onset of the Hunter-Bowen orogeny, at ~270 Ma (Campbell et al.,

2022). Hunter-Bowen deformation was episodic and involved three main pulses of deformation and magmatism (at ~265 Ma, ~250 Ma, and 235–230 Ma) intermitted by phases of tectonic relaxation (Babaahmadi et al., 2015; Hoy and Rosenbaum, 2017).

In detail, the “simple” plate tectonic configuration described above is more complicated and many outstanding questions remain unresolved. For example, there are two major issues in the geology of the NEO that are still not fully reconciled by plate tectonic reconstructions. The first problem relates to the structure of the Late Devonian – Carboniferous forearc region. While typical forearc basins are deposited unconformably on top of accretionary wedges, the forearc basin units in the NEO are juxtaposed tectonically against accretionary complex units. The former forearc system, therefore, must have been restructured sometime after the Carboniferous. Moreover, exposed along the tectonic contacts that separate forearc basin and accretionary complex units (Yarrol, Peel, and Manning faults) are relics of older “Tasmanides” components, including Cambrian (or possibly even Neoproterozoic) ophiolitic assemblages (Aitchison et al., 1992; Bruce et al., 2000), blocks of blueschist and eclogite metamorphosed during the Ordovician (Tamblyn et al., 2020), and Devonian arc terranes whose geochemical signatures are consistent with an island arc origin (Offler and Murray, 2011; Rosenbaum et al., 2021). The interpretation of these tectonic units is crucial for plate tectonic reconstructions, because (1) the older rocks provide a window into the earlier (pre-Devonian) history of the NEO; and (2) the occurrence of these rocks in association with orogen-scale tectonic contacts implies a post-Carboniferous plate tectonic configuration that cannot be easily reconciled with a “simple” Andean-type continental margin. It is possible that the belt of ophiolitic relics, tentatively referred to as the Eastern Australian Ophiolitic Belt, represents remnants of an oceanic domain that once separated different components of the NEO. However, further work is needed to test this hypothesis. Current and future research can also address the questions whether high-pressure rocks in the NEO represent subduction processes associated with the closure of this ocean, and whether this process could have led to the accretion of Devonian island-arc terranes.

The second problem in plate tectonic reconstructions is the difficulty to explain the origin of multiple bends and curvatures (oroclines) that characterise the structural grain of the NEO. The southern part of the orogen is particularly contorted, forming an “ear-shaped” pattern (Rosenbaum, 2012), but orogen-scale map-view bending is also recognised in the northern NEO. Outcomes from our previous research suggest that the curvatures reflect plate boundary migration, predominantly associated with trench retreat (Rosenbaum et al., 2012). The timing of orocline formation was likely during the Early Permian. The geodynamic setting of the NEO during the Early Permian might have been analogous to the post-Miocene geodynamics in eastern Indonesia or western Mediterranean, where high rates of trench retreat (up to 100 km/Myr!) resulted in the development of incipient oceanic crust in the backarc region (Rosenbaum and Lister, 2004).

MINERAL DEPOSITS IN THE NEW ENGLAND OROGEN

The geodynamic context of mineral deposits in the NEO can be classified into four main groups: (1) deposits associated with the Eastern Australian Ophiolitic Belt; (2) arc-related Devonian–Carboniferous deposits; (3) extension-related Early Permian deposits; and (4) deposits associated with Late Permian to Triassic continental-arc magmatism and the contemporaneous Hunter-Bowen orogeny. By far, the largest number of ore deposits in the NEO belong to the last group.

Ultramafic rocks of the Eastern Australian Ophiolitic Belt host chromite and nickel mineral deposits. They are mainly concentrated in the Marlborough area (where ultramafic exposures are widespread), but there are also deposits in other ultramafic massifs, such as in the areas of Kilkivan (SE Queensland) and Baryulgil (NE New South Wales). In the southern NEO, along the Great Serpentine Belt (Peel Fault), there are also gold deposits in quartz and/or calcite veins (Ashley, 1997).

Devonian–Carboniferous subduction-related units in the NEO do not host significant mineralised systems. The only major ore deposit associated with the Devonian–Carboniferous arc is the Mount Morgan gold-copper orebody, which is a volcanogenic massive sulfide (VMS) deposit that may have formed in an oceanic arc during the Middle Devonian (Murray and Blake, 2005). There are other deposits hosted in rocks of the Early–Middle Devonian oceanic arc in Queensland (Calliope terrane), such as the Struck Oil and Kroombit copper deposits, but their formation was likely associated with fluids derived from Early Triassic intrusions (Murray, 1986). In New South Wales, the Cangai copper deposit is hosted in the Devonian island-arc(?) related Willowie Creek beds (Silverwood terrane), but it is debated whether mineralisation was linked to Devonian volcanism (Murray, 1988) or younger (Triassic?) granitic fluids (Barnes, 2010). From the Late Devonian and throughout the Carboniferous, the NEO was positioned in a supra-subduction continental margin, but there is little evidence that this “Andean-type” tectonic environment involved major mineralisation events. Known deposits include the epithermal Zelma gold deposit within the Carboniferous volcanic arc (Murray, 1986) and few, mainly orogenic gold deposits, within the accretionary complex (Dalmorton, Coramba-Orara, Mount Taylor, Agricola). The absence of major ore deposits in this long-lived (~70 Myr) Andean-type tectonic setting may either reflect a barren arc or a lack of exposure due to burial (in the southern NEO) and erosion (in the northern NEO).

Early Permian mineralisation in the NEO was tectonically associated with extensional processes. The eastern Gondwanan margin was subjected to trench retreat, giving rise to the development of widespread backarc extensional basins and elevated thermal gradients. Mineralised zones associated with this tectonic environment include epithermal gold deposits (e.g., Cracow, Mount Carlton, Mount Mackenzie) and VMS deposits (Mount Chalmers, Silver Slur, Rookwood, Foresthome).

Arc magmatism during the Late Permian to Triassic was responsible for the vast majority of ore deposits in the NEO (Murray, 1986). Intrusion-related ore deposits include porphyry copper (e.g., Coalstoun, Chinamans Creek, Kiwi Carpet) and molybdenum (e.g., Anduramba, Whitewash) deposits, and numerous gold, tin and tungsten deposits in the southern NEO (Ford et al., 2019). Examples of skarn deposits in the northern NEO are Ban Ban (zinc-copper-lead-silver-gold), Many Peaks (copper-gold), and Kroombit

(copper-zinc). Orogenic gold deposits include the Gympie orebody (and other deposits in the Gympie goldfield) (Cranfield et al., 1997). Arc modulation and cyclicity during the Middle Permian to Late Triassic Hunter-Bowen orogeny may have played a role in controlling the spatio-temporal distribution of ore deposits, with mineralised events occurring mainly during the end of magmatic cycles (~250 Ma and ~230 Ma).

CONCLUDING REMARKS

Three major aspects in the plate tectonic history of eastern Australia have apparently contributed to the origin and spatial-temporal distribution of mineral deposits in the NEO. First, the spatial distribution of ultramafic rocks in the NEO, involving a contorted belt that stretches for ~1500 km from Port Macquarie in New South Wales to Marlborough and Percy Islands in Queensland, raises the possibility that these, potentially ophiolitic rocks, represent an ancient ocean that now forms a tectonic suture. Future research on the nature of this ocean — its size, age, position relative to the continent, and final demise that produced the limited present-day exposures of the ophiolitic belt — may provide crucial information on the origin and location of nickel and chromium deposits (as well as gold, cobalt, scandium and PGE). Second, Early Permian, extension-related, deposits formed in the NEO during a period that was ultimately controlled by trench retreat and oroclinal bending. Reconstructing the complex geodynamic and kinematic interactions associated with the development of these oroclines could help contextualising the prospectivity associated with this mineralisation phase. Third, the identification of numerous mineral deposits within the Late Permian to Triassic arc in NEO warrants further research on arc modulation, episodicity, bending, and segmentation, with the aim of establishing whether clusters of ore deposits are potentially linked to “anomalous” subduction processes (e.g., Rosenbaum et al., 2005; Ward et al., 2024). In this respect, a high-resolution reconstruction of the Permian–Triassic convergent plate boundary in the NEO could potentially offer a tangible tool for future discoveries of mineral deposits, for example, within arc segments that are currently concealed by the sedimentary cover.

REFERENCES

- AITCHISON, J.C., IRELAND, T.R., BLAKE, M.C., FLOOD, P.G., 1992. 530 Ma zircon age for ophiolite from the New England orogen: Oldest rocks known from eastern Australia. *Geology* 20, 125-128.
- ASHLEY, P., 1997. Silica-carbonate alteration zones and gold mineralisation in the Great Serpentine Belt, New England orogen, New South Wales, *Tectonics and Metallogensis of the New England Orogen*. Geological Society of Australia Special Publication, pp. 212-225.
- BABAAHMADI, A., ROSENBAUM, G., ESTERLE, J., 2015. Alternating episodes of extension and contraction during the Triassic: Evidence from Mesozoic sedimentary basins in eastern Australia. *Aust. J. Earth Sci.* 62, 563-579.
- BARNES, R.G., 2010. Exploration and opportunities in the New England Orogen, NSW, in: Buckman, S., Blevin, P.L. (Eds.), *New England Orogen 2010*, The University of New England, Armidale, Australia, pp. 28-30.

- BRUCE, M.C., NIU, Y., HARBORT, T.A., HOLCOMBE, R.J., 2000. Petrological, geochemical and geochronological evidence for a Neoproterozoic ocean basin recorded in the Marlborough terrane of the northern New England Fold Belt. *Aust. J. Earth Sci.* 47, 1053-1064.
- CAMPBELL, M.J., HOY, D., ROSENBAUM, G., FIELDING, C., ALLEN, C.M., 2022. The onset of Gondwanide Orogeny in Eastern Australia: Insight from the provenance of syn-orogenic strata in the New England Orogen (Australia). *Tectonics* 41, e2021TC006940.
- CRANFIELD, L.C., SHORTEN, G., SCOTT, M., BARKER, R.M., 1997. Geology and mineralisation of the Gympie Province, in: Ashley, P.M., Flood, P.G. (Eds.), *Tectonics and metallogenesis of the New England Orogen*. Geological Society of Australia Special Publication, pp. 128-147.
- CRAVEN, S.J., DACZKO, N.R., HALPIN, J.A., 2012. Thermal gradient and timing of high-T-low-P metamorphism in the Wongwibinda Metamorphic Complex, southern New England Orogen, Australia. *J. Met. Geol.* 30, 3-20.
- DAY, R.W., MURRAY, C.G., WHITAKER, W.G., 1978. The eastern part of the Tasman Orogenic Zone. *Tectonophysics* 48, 327-364.
- FORD, A., PETERS, K.J., PARTINGTON, G.A., BLEVIN, P.L., DOWNES, P.M., FITZHERBERT, J.A., GREENFIELD, J.E., 2019. Translating expressions of intrusion-related mineral systems into mappable spatial proxies for mineral potential mapping: Case studies from the Southern New England Orogen, Australia. *Ore Geology Reviews* 111, 102943.
- HOLCOMBE, R.J., STEPHENS, C.J., FIELDING, C.R., GUST, D., LITTLE, T.A., SLIWA, R., MCPHIE, J., EWART, A., 1997. Tectonic evolution of the northern New England Fold Belt: Carboniferous to Early Permian transition from active accretion to extension, in: Ashley, P.M., Flood, P.G. (Eds.), *Tectonics and metallogenesis of the New England Orogen*. Geological Society of Australia Special Publication, pp. 66-79.
- HOY, D., ROSENBAUM, G., 2017. Episodic behavior of Gondwanide deformation in eastern Australia: Insights from the Gympie Terrane. *Tectonics* 36, 1497-1520.
- KORSCH, R.J., TOTTERDELL, J.M., CATHRO, D.L., NICOLL, M.G., 2009. Early Permian East Australian Rift System. *Aust. J. Earth Sci.* 56, 381-400.
- MCPHIE, J., 1987. Andean analogue for Late Carboniferous volcanic arc and arc flank environments of the western New England Orogen, New South Wales, Australia. *Tectonophysics* 138, 269-288.
- MURRAY, C.G., 1986. Metallogeny and tectonic development of the Tasman Fold Belt System in Queensland. *Ore Geology Reviews* 1, 315-400.
- MURRAY, C.G., 1988. Tectonic evolution and metallogenesis of the New England Orogen, in: Kleeman, J.D. (Ed.), *New England Orogen-tectonics and metallogenesis*, University of New England, Armidale, Australia, pp. 204-210.
- MURRAY, C.G., Blake, P.R., 2005. Geochemical discrimination of tectonic setting for Devonian basalts of the Yarrol Province of the New England Orogen, central coastal Queensland: An empirical approach. *Aust. J. Earth Sci.* 52, 993-1034.
- MURRAY, C.G., Fergusson, C.L., Flood, P.G., Whitaker, W.G., Korsch, R.J., 1987. Plate tectonic model for the Carboniferous evolution of the New England Fold Belt (Australia). *Aust. J. Earth Sci.* 34, 213-236.
- OFFLER, R., MURRAY, C., 2011. Devonian volcanics in the New England Orogen: tectonic setting and polarity. *Gond. Res.* 19, 706-715.
- ROSENBAUM, G., 2012. Oroclines of the southern New England Orogen, eastern Australia. *Episodes* 35, 187-194.

ROSENBAUM, G., GILES, D., SAXON, M., BETTS, P.G., WEINBERG, R., DUBOZ, C., 2005. Subduction of the Nazca Ridge and the Inca Plateau: insights into the formation of ore deposits in Peru. *Earth Planet. Sci. Lett.* 239, 18-32.

ROSENBAUM, G., LI, P., RUBATTO, D., 2012. The contorted New England Orogen (eastern Australia): new evidence from U-Pb geochronology of Early Permian granitoids. *Tectonics* 31, TC1006, doi:10.1029/2011TC002960.

ROSENBAUM, G., ROGERS, A., GÜRER, D., ANDJIĆ, G., ALLEN, C.M., 2021. Origin of the intra-oceanic Silverwood Block (New England Orogen, Australia): evidence from radiolarian biostratigraphy and detrital zircon petrochronology. *Tectonics* 40, e2021TC006920.

SHAANAN, U., ROSENBAUM, G., WORMALD, R., 2015. Provenance of the Nambucca Block (eastern Australia) and implications for the early Permian tectonics of eastern Gondwana. *Geol. Soc. Am. Bull.* 127, 1052-1063.

TAMBLYN, R., HAND, M., KELSEY, D., ANCKIEWICZ, R., OCH, D., 2020. Subduction and accumulation of lawsonite eclogite and garnet blueschist in eastern Australia. *J. Met. Geol.* 38, 157-182.

WARD, J.F., ROSENBAUM, G., UBIDE, T., SANDIFORD, M., 2024. Slab segmentation, anomalous arc volcanism, and giant porphyry copper deposits in Indonesia. *Earth Planet. Sci. Lett.* 626, 118532.

GENESIS OF THE RAVENSWOOD GOLD DEPOSIT

Hugo Serra¹ & Steve Harper² (revised by Dr. Gregg Morrison²)

¹ James Cook University, Queensland

² Ravenswood Gold

Keywords: Ravenswood, gold, mineral deposit genesis

INTRODUCTION

The Ravenswood Gold Mine is situated approximately 130km south of Townsville in northeast Queensland. Reports of artisanal and small-scale gold mining within the Ravenswood district date back as far as 150 years ago. Large-scale, open pit mining at the Ravenswood mine has operated continuously since 1987, targeting mostly low-grade, high-tonnage mineralisation. The Ravenswood deposits contain combined reserves and resources of more than 8 Moz of gold, positioning Ravenswood as Queensland's premier gold mining operation.

As highlighted by Morrison et al. (2014), the Ravenswood deposit is part of a larger group of Intrusion Related Gold Systems (IRGS) located in northeast Queensland. The NQ IRGS province includes multimillion-ounce deposits such as Kidston (5.1 Moz), Mount Leyshon (3.5 Moz), Mount Wright (1.0 Moz), and other numerous systems accounting for a gold endowment of over 20 Moz in the region, which may be set in comparison with the world-class Yukon-Alaska region.

Despite the regional significance of the Ravenswood Gold Mine, several aspects of the deposit's genesis remain unconstrained. Such aspects include the implication of a single versus multistage deformation in link with mono or multiphase mineralising event, the origin of the hydrothermal fluid source and the nature of the mineralisation in the context of an intrusion-related gold deposit mineral system or porphyry mineral system. This collaborative research project between Ravenswood Gold Pty Ltd and James Cook University aims to address a thorough structural, geochemical and geochronological analysis at both the mine and batholith scale in order to test, enhance, and refine existing models, as well as to define new interpretations of the largest gold operation in Queensland. The outcomes of this research will potentially provide a greatly improved understanding of the deposit genesis, and better exploration tools for resource growth and future greenfield discoveries in the district.

GEOLOGICAL CONTEXT

Regional geology

During the Neoproterozoic-Palaeozoic, eastern Australia was positioned along the northeastern margin of the Gondwana supercontinent. Coeval convergence with differing vergences along the eastern, southern, and western margins of Gondwana was accommodated by the Terra Australis subduction system (Edgar et al., 2022; Aitchison & Buckman, 2012). The long-lived evolution of this subduction system, and growth of the eastern Australian continent, has been recorded within the Tasmanides orogenic system. The Tasmanides consist of tectonic domains expressing the succession of five subduction-related orogens younging west to east (Rosenbaum, 2018). In the northern segment, the evolution of the Tasman Orogenic Zone is recorded by the Thomson, the

Mossman and the New England orogens (Edgar et al., 2022; Jessop et al., 2019; Rosenbaum, 2018; Champion, 2016; Withnall & Henderson, 2012). Its evolution started with a tectonic switch at ~510Ma from a Neoproterozoic passive margin to a Cambrian active margin along the eastern Gondwana margin (Henderson et al., 2020, and references therein), followed by a syn-subduction extensional far-field tectonic response driven by slab retreat with coeval intracontinental basin infill and granitic plutonism during the Cambro-Ordovician.

The Charters Towers Province is part of the northern extent of the Thomson Orogen and is in tectonic contact to the north with the Broken River Province (southernmost extent of the Mossman Orogen) along the Clarke River Fault. This major structure has been interpreted as an Early Palaeozoic continental suture zone between the Thomson and Mossman orogens (Edgar et al., 2023; Edgar et al. 2022; Dirks et al., 2021). To the south and west, the Charters Towers Province is constrained by both the Late Devonian to Early Carboniferous Drummond basin and the intracratonic Permian Galilee basin. Finally, to the east, the Charters Towers Province is in contact with the Connors Subprovince, a subset of the New England Orogen.

The development of the New England Orogen has been initiated with a Silurian-Devonian ocean-ocean collision with westward obduction (Blake, 2013; Offler & Murray, 2011), followed by a west dipping subduction zone with continental arc and intracontinental basin infill (Drummond basin) during the Devonian-Carboniferous period (Champion 2016; Glen, 2013; Champion et al., 2009; Davis & Henderson 1996; Leitch, 1975). From the Late Carboniferous until the Mid-Permian, protracted thermal relaxation associated with subduction rollback led to crustal thinning and subsidence affecting the forearc basin, the accretionary wedge and the continent along eastern Australia (Rosenbaum et al., 2012; Korsch et al., 2009).

The Hunter-Bowen compression phase began from ~265 Ma by advance of the subduction zone towards the continent forming the Late Permian-Mid Triassic Hunter-Bowen continental arc (Jessop et al., 2019), followed by extension during the Triassic (Champion, 2016). Widespread intrusive bodies progressively younging eastward were emplaced throughout the Tasmanides during the Late Carboniferous to mid-Permian period. While the tectonic regime associated with the Middle Carboniferous to Early Triassic magmatism of the Kennedy Igneous Association is not fully understood, it is generally interpreted as corresponding to a relatively stable arc and back-arc setting (Champion & Bultitude, 2013, 2003; Hutton et al., 1997). Although the debate persists, this interpretation aligns with observations from the New England Orogen (Van Noord, 1999). Supporting evidence includes similar magmatic ages between the Kennedy Igneous Association and the northern New England Orogen (Champion et al., 2016; Champion & Bultitude, 2013; Purdy et al., 2013).

Local Geology

The Mount Windsor Subprovince of the Charters Towers Province consists in a main sub-greenschist to greenschist facies metamorphic belt running east-west assigned to the Seventy Mile Range Group. The sequence is made up of pelagic sediments and marine volcanic formations dated from Late Cambrian to Early Ordovician (Fergusson & Henderson, 2013). The formation of the belt is associated with the Early Palaeozoic Thomson Orogen-facing subduction and relates to the development of the intracontinental back-arc basin at about 480 Ma (Edgar et al., 2023).

The basement has been intruded to the north by the Ravenswood Batholith which predominates in the eastern half of the Charters Towers Province. The batholith formed

through three distinct periods of magmatism and experienced a series of deformation events starting with the emplacement of the Macrossan Igneous Association during the Early to Mid-Ordovician. In the area, the intrusive complex is composed mainly of I-type granite and mafic intrusions (Withnall & Cranfield, 2013). From Standing (2006), the deformation assigned to the Macrossan Igneous Association developed cleavage and folding at the margins of neighbouring calc-alkaline plutons. The diapir-like ascent is interpreted as the main driver of the local stress fields. Moreover, this deformation accounts for the major east-west Alex Hill Shear Zone exhibiting vertical mylonite and stretching lineation between Pocket Dam and Mingela plutons.

After the termination of the active plate margin at around 430 Ma, the region underwent a major sinistral transcurrent deformation associated with a northwest-trending compressive regime and coincides with the onset of the Benambran Orogeny (Korsch et al., 2012, Henderson et al., 2011, Glen et al., 2007). As mentioned by Glen et al. (2007), the inferred deformation implied transfer or lateral ramp faulting systems initiated by differential tectonic inversion in response to the accretion of the intra-oceanic Macquarie Arc onto the eastern Gondwanan plate.

The timeframe between the Silurian to Early Devonian characterises the calc-alkaline intrusive activity of the Pama Igneous Association (Withnall et al. 2002), which hosts the Ravenswood gold deposit within the Late Silurian-Early Devonian Jessop Creek Tonalite Complex. Concurrent with the magmatic activity, this period saw brittle-ductile structures forming in conjunction with northeast-southwest shortening. Kreuzer (2005, 2006) interprets these brittle-ductile structures as part of the inferred D4 regional event responsible for developing orogenic gold mineralisation in the Charters Towers Goldfield. The major Plumwood-Connolly Fault strikes southwest-northeast across the southeastern margin of the Ravenswood Batholith and has offset the Seventy Mile Range Group in an apparent dextral strike-slip. According to Hutton & Rienks (1997), its activity is coincident with the Pama Igneous Association magmatism.

As per Standing (2006), subsequent rapid uplift of the thickened crust exposed the Charters Towers deposits at the surface within a short timeframe before deposition of the Collopy Formation between the Late Devonian to Early Carboniferous to unconformably overlie the Ravenswood Batholith. Following this uplift, Standing (2006) interprets a northwest-southeast regional shortening, triggering high-angle sinistral offsets of the north-south trending Jessop's Creek Fault and dextral transcurrent shearing along the Plumwood-Connolly Fault with sets of late brittle kinks and faults.

Ultimately, the tectonic switch that occurred during the Late Carboniferous to Early Permian period is described by Standing (2006) as an overall east-west directed compression that has reactivated and offset the preexisting structures with the development of extension veins and moderately dipping thrusts. This event is interpreted as coeval with the Kennedy Igneous Association magmatism. However, as explained in the previous section, it is important to emphasise that the tectonic regime related to this magmatism is not fully understood. The Kennedy Igneous Association of the Late Carboniferous to Early Permian period consists mainly of felsic I-type granites and minor mafic igneous activity (Hutton et al. 1997) manifesting as intrusions, sub-volcanic complexes and volcano-sedimentary formations. Throughout the batholith, these units account for ~6% of its volume (Clark & Dickson, 1996) and are especially more concentrated in the east and southeast.

As highlighted by Champion & Heinemann (1994), the Kennedy Igneous Association magmatism is extensively mineralised, with related deposits predominantly linked to I-type granites. Quoted from Beams & Dronseika (1995): "All the significant gold

occurrences in northeast Queensland are associated with Permo-Carboniferous subvolcanic complex with dykes, plugs, vein stocks and breccias of rhyolitic to trachytic composition, their spatial distribution forms either distinct camp clusters or are localised in, or adjacent to, a regional scale lineament." Several northwest and northeast-trending discrete intrusive corridors with ductile-brittle faulting have been identified (Kreuzer et al., 2007). A notable example is the prominent northeast-trending Mount Leyshon Corridor, which extends from the Mount Leyshon gold mine (located ~75 km west of Ravenswood) through the Tuckers Igneous Complex (Wormald, 2017; Morrison 1988).

RAVENSWOOD MINERAL SYSTEM

Host rock

Dated at around 420 Ma (Lisowiec & Morrison, 2017; Hutton et al., 1994), the Jessop Creek Tonalite Complex principally consists of medium-grained tonalite and encloses small sub-rounded gabbro bodies. The complex grades in composition from mafic to felsic away from the gabbro (Malagun, 1985, Talbot, 1982). As interpreted by Talbot (1982), the mafic bodies are considered as remnants of the roof chamber with stoped mafic xenoliths incorporated into the main tonalite phase. From the same study, the petrographic zonation shows a systematic concentric pattern from medium-grained gabbro, through hornblende diorite, hornblende tonalite, hornblende-biotite tonalite to granodiorite. The Jessop Creek Tonalite is crosscut by felsic dykes (aplite, microgranite and pegmatite). One undeformed pegmatite dyke, situated in the Sarsfield Pit and lying in a shallow-dipping structure, has been dated at 411.1 ± 5.9 Ma based on SHRIMP U-Pb dating on zircon (Morrison, 1996; unpublished report), interpreted as the latest stage of crystallisation of the intrusive complex. Lastly, sporadic andesite dyke swarms intrude along some of the major pre-existing structures reactivated during the mineralising event (Lisowiec & Morrison, 2017), the age of emplacement remains undetermined.

Deposit architecture

The mineralisation at Ravenswood is structurally controlled and all the known mineralisation styles are related with open space infill. The mineralised structures include features such as extension-breccia vein shoots (e.g. Sunset, General Grant, Duke of Edinburgh faults), stockwork-breccia developed within reactivated structures such as Area 4 Fault (Sarsfield pit) and Buck Reef Fault (being the dominant deposit feature), and sets of tension vein arrays encountered in all pits and making up the bulk of the mineralisation.

Based on the structural analysis conducted by Orefind (2017), the most up-to-date understanding of the Ravenswood gold mineralisation system is supported by considering a single strain pattern. This model is characterised by a 3D orthorhombic fault system with four sets of normal faults accommodating a three-dimensional strain. The associated first-order 3D strain pattern suggests a horizontal north-south shortening, an intermediate strain axis moderately plunging to the east consistent with the easterly plunge of the district-scale grade distribution, and an extension axis moderately plunging to the southwest in agreement with the thrust kinematics of the Keel Fault Zone interpreted by Standing (2006), but inconsistent with its dextral movement deduced from the same study. The inferred model unifies all the varying grade distributions and vein patterns that are observed at Ravenswood.

Three categories of vein intersections have been distinguished depending on their gold endowment which is relative to fluid decompression, itself proportional to the amount of structural dilatation. Ranked from the highest gold endowment to the least endowed vein

population, category A encompasses the Sunset-Grant-Duke set of veins with an intersection plunge to the northeast, these major structures underwent the most dilatation and intersect at a high angle to the intensely mineralised Buck Reef Fault. This latter pre-existing structure is inferred to have acted as a transfer plane with dextral strike-slip motion during mineralisation, enabling the development of the different vein sets of category A to form independently of one another. However, the geometric and overprinting relationships between the Buck Reef fault and these structures have not been established in the structural analysis carried out by Orefind (2017). Category B defines the Nolan's vein set with an intersection plunge to the southeast (Area 4 & Nolans faults). Finally, category C manifests the set of veins seen in the pit walls, they have developed away from the main mineralisation as populations of conjugate faults, shears and veins with an overall sub-horizontal north-south trend. The intersection lines between the mineralised structures of category C have been interpreted to represent local mineralisation continuities and be the second-order product of through-going master structures in relation to local strain accommodation. Formed nearly perpendicular to the east-west striking intermediate strain axis, interpreted impermeable faults appear to bound high-grade and low-grade zones. In all pits, early-formed structures typically manifest as steeply dipping east-west and north-south oriented chlorite \pm carbonate joints or narrow planar faults. These pre-mineralisation features have likely influenced the orientation of subsequent structures. Steep post-mineralisation faults (shear veins or cataclasite) are common and have developed preferentially using the orientation of the pre-mineralisation structures, some can be seen displacing mineralised structures.

Mineralisation features

This section draws primarily from the most recent compilation in Monograph 32: Australian Ore Deposits, authored by Lisowiec & Morrison (2017). The mineralised fluids have been deposited within the Early Devonian to Late Silurian Jessop Creek Tonalite complex as vein networks/stockworks within reactivated preexisting steep structures and conjugate quartz-sulphide vein arrays (as described above: Deposit architecture). The subvertical reactivated structures, such as Buck Reef Fault and Area 4 Fault, exhibit extensive brecciation due to the ongoing tectonic activity and are most mineralised where intersected by moderate to shallow-dipping structures with associated quartz sulphides.

These faults typically display chlorite-biotite alteration, overprinted by bucky quartz and pyrrhotite. Biotitic alteration is predominating in Sarsfield when chloritic alteration primes elsewhere. Ore mineralisation within the fault manifests as breccia infill with a mineral assemblage characterised by early pyrrhotite with pyrite \pm marcasite-sphalerite-chalcopryrite. In the surrounding rock, wide and intense chlorite-biotite alteration halos have developed along the selvages of these structures. Mineralised quartz-sulphide veins ranging from moderate to shallow dipping (e.g. Sunset, General Grant, Duke of Edinburgh, Keel Faults as well as all the second-order tension vein arrays) have developed in the vicinity of the reactivated structures and may locally overprint them.

In all pits, three significant tension vein types are observed, which have developed narrow to pluri-decimetric chlorite-sericite or sericite-carbonate alteration along the vein selvages with variable alteration intensity from intense to moderate, while the unaltered host rock is weakly to very weakly chlorite-sericitised.

These vein types encompass pyrite-dominant vein sets with minor to no quartz, quartz-dominant veins with pyrite \pm sphalerite-pyrrhotite-chalcopryrite, the latter one being the most abundant vein set and represents the bulk of the gold endowment. The carbonate vein sets with minor quartz-pyrite-sphalerite-chalcopryrite-arsenopyrite-galena define the

latest stage of the paragenetic sequence and can present occasionally fragments of earlier veins within, synonym of reactivation of earlier structures.

Gold typically occurs as fine free electrum grains Au-Ag (75% Au) near the sulphides (notably galena and chalcopyrite). Locally gold has precipitated in association with native bismuth and pilsenite (Bi_4Te_3) (Lisitsin et al., 2024).

The analysis of ore stage fluid inclusions from Sarsfield and Buck Reef deposits conducted by Bertelli et al. (2009) indicates temperatures for ore deposition between 200-300°C at Buck Reef West, and 300-400°C at Sarsfield. Salinities for the fluid inclusions from the different deposits are similar and mostly between 8 and 12 wt% NaCl equivalent. From the same study, stable isotope data on sulphides ($\delta^{34}\text{S}$) are consistent with a magmatic source for the ore forming fluids at Ravenswood. According to Ar-Ar dating on biotite and sericite, and K-Ar on sericite (Perkins & Kennedy, 1998; Morrison, 1996 unpublished report; Bassotti, 2002), the alteration ages (and the associated gold mineralisation timing) span from 329 ± 0.7 Ma to 296 ± 2 Ma, with a notable age concentration at 310 Ma.

Deposit style

The Ravenswood deposit exhibits several attributes consistent with the Intrusion Related Gold Systems deposit style, these distinctive characteristics include:

- 1) The analyses conducted by Bertelli et al. (2009) on sulphide stable isotopes in Sarsfield and Buck Reef are consistent with a magmatic source provenance for the ore forming fluids. The current mineralisation model at Ravenswood (Morrison et al., 2014) suggests a source for the hydrothermal fluids related to a deep intrusion, implying vein networks acting as pathways, facilitating gold deposition away from the pluton at the intersection with structures. The paleo-depth of emplacement is inferred as mesozonal, approximately 4 km deep within the porphyry level. Though being interpreted so far as intrusive-driven, the source of these hydrothermal fluids is not recognised yet.
- 2) The overall geochemical pattern describes a textbook concentric metal zoning showing a classical mushroom shape centred on the feeder (Morrison et al., 2015). The feature reflects the evolution from a hot core centred on Area 4 Fault (Sarsfield pit) towards the cooler periphery. The zoning up and out from the source is: Cu-Te → Cu-Au-Te → Au-Zn-Bi → Au-As-Pb → Ag-As-Sb, the highest gold concentration being situated in the Zn-Pb zone and the adjacent Cu zone in the shallow and central part of the system. The interpreted zoning is consistent with the analysis of ore stage fluid inclusions from Bertelli et al. (2009), indicating temperatures for ore deposition between 300-400°C at Sarsfield and 200-300°C at Buck Reef West, and the concentric alteration zones from biotite and K-feldspar, through phyllic to argillic outward (Switzer, 2000).
- 3) The ages of alteration and gold mineralisation at Ravenswood are directly related to the Kennedy Igneous Association. These ages are synchronous with the timing of emplacement, alteration and mineralisation of well-recognised Permo-Carboniferous intrusion-related gold systems, such as the Mount Wright volcanic-breccia complex (located ~10 km northwest of Ravenswood) and the porphyry-breccia complex of Mount Leyshon (situated ~75 km west from the deposit) (Dean & Carr 1988; Perkins & Kennedy, 1998; Murgulov et al. 2008).
- 4) As mentioned by (Lisitsin et al., 2024), the ore geochemistry at Ravenswood shows similar multi-element signatures with Mount Leyshon, both deposits have a strong Au-Bi-Te metal association.

SCOPE OF THE CURRENT PHD RESEARCH PROJECT

The research project will be conducted by Hugo Serra, PhD candidate at James Cook University (JCU) based in Townsville. The primary supervisors are Dr. Ioan Sanislav (Researcher-Lecturer at JCU and Director of the Economic Geology Research Centre - EGRU) and Dr. Daniel Wiemer (Researcher-Lecturer at JCU). Steve Harper (Exploration Manager at Ravenswood Gold) is designated as the secondary advisor, and Dr. Brett Davis (Principal Structural Geologist at Olinda Gold Structural Geology Consulting) as the external advisor. This new collaborative research project between Ravenswood Gold and James Cook University aims to address a thorough structural, geochemical and geochronological analysis at the mine and batholith scale to test, enhance, and refine the existing models, as well as to define new interpretations of the largest gold deposit in Queensland. Spanning regional to mine-scale perspectives, the present review synthesizes the current state-of-the-art understanding of the Ravenswood Gold deposit. While thorough within the given constraints, the analysis has allowed the identification of key areas where additional research will likely provide an improved understanding of the deposit genesis that may have unprecedented impact and implications for resource growth and future greenfield discoveries in the district. Several aspects of the deposit remain unconstrained, they include the implication of a single versus multistage deformation in link with one or several mineralising event(s), the origin of the hydrothermal fluid source and the nature of the mineralisation in the context of an IRGS or porphyry mineral system. Here are the proposed outlines for the PhD subject focussed on the Ravenswood Gold deposit and the near-mine brownfield environment, it must be noted here that this list is an early non-exhaustive draw where chronological ranking will be modified.

1) Geochronology of the key lithologies and thermochronology using apatite fission track

As described by Malagun (1985) and Talbot (1982), the Jessop Creek Tonalite Complex presents a systematic concentric inward zoning, from felsic lithologies at the rim towards mafic at the centre. This pattern is anomalous as according to the process of crystal fractionation, mafic crystals precipitate first and deposit on the edge of the magmatic chamber, leading towards a the most felsic magma, in this case, the granodiorite. As a hypothesis, this might indicate that the Jessop Creek Complex has potentially experienced multiple phases of magma input during its emplacement, resulting in the formation of rheological boundaries due to quenching at the contact of the different magmatic phases. Hence it is likely these boundaries may have created inherited weaknesses within the complex influencing its architecture and orientating preferentially subsequent dykes and structures. To date, a unique pegmatite dyke has been dated, though the results remain unpublished (Morrison, 1996 unpublished report). Furthermore, following recent communications (Morrison, pers. comm., 2024), the emplacement of cross-cutting andesite dykes is potentially the driver of the mineralising event and may be directly linked to the magmatism associated with the Kennedy Igneous Association. Consequently, to improve the understanding of the deposit genesis, precise age dating of the key lithologies using Sensitive High-Resolution Ion Microprobe (SHRIMP) U-Pb analysis on zircons appears necessary. This geochronological approach, combined with the establishment of the deposit paragenesis (see sections below) would elucidate the temporal relationships between various igneous events and their link with the mineralisation.

Although the tectonic regime associated with the Middle Carboniferous to Early Triassic magmatism of the Kennedy Igneous Association is not fully understood, it is generally interpreted as corresponding to a relatively stable arc and back-arc setting. The

thermochronology method using apatite fission tracks may give an insight about the average cooling age and exhumation rate since crystallisation of the different igneous associations (Pama and Kennedy). This analysis may potentially help towards the understanding of how, within the same timeframe, at a distance of 10 km apart and at a similar current elevation, has an inferred mesozonal deposit (Ravenswood at ~4km deep) developed near an epizonal deposit (Mount Wright ~1km deep).

2) Geochemistry of the key lithologies

Short Wave Infrared Spectroscopy (SWIR) and electron microprobe analysis conducted by Lisowiec et al. (2008) on the Ravenswood Gold deposit indicate a higher Fe+Mg contents in phengite and chlorite in the immediate vicinity of mineralised veins. Beyond this spectral analysis, no other publication or internal report have been found so far mentioning the use of the available geochemical data to segregate the geochemical signature of each lithology to map the units downhole. Following up with the above section, it would be interesting to characterise each lithological signature using loGAS and map the units in three dimensions. Considering a detailed downhole litho-geochemical analysis may induce new interpretative perspectives linking the lithologies, their geochemical signatures, the potential rheological boundaries and the structure geometries.

3) Test/enhancement of the structural model: single vs multiphase deformation

The primary goal of the structural analysis is the establishment of the full paragenesis of the system, allowing the differentiation between the inherited structures from the Late Silurian – Early Devonian period and the ones developed syn-mineralisation during the Permo-Carboniferous epoch (including the subsequent reactivation of preexisting structures). The pegmatite dyke dated as Late Silurian is undeformed and lies in a shallow-dipping structure (Morrison, pers. Comm., 2024), which suggests a temporal constraint on the deposit's architectural inheritance prior to 411 Ma and likely coeval timing with the regional D4 event (Kreuzer, 2005, 2006). Regarding the structures highlighted as ore controlling by Orefind (2017) and considered as the result of a single strain system, these structures may potentially represent the reactivation of syn-Kennedy Igneous Association tectonics of the architecture developed in the late Silurian – Early Devonian. The methodology to answer this main enquiry in order to establish the full paragenesis of the system are as follows:

- A) As Buck Reef pit has undergone significant development since the Orefind (2017) analysis, pit mapping of Buck Reef is key, with a particular focus on the geometric and overprinting relationships between Buck Reef Fault and the mineralised structures. In addition to surface mapping, interpretative extrapolation downhole by core analysis will provide the Buck Reef structural understanding to the greatest extent.
- B) The comprehensive pit mapping conducted at Sarsfield by Orefind (2017) provides a solid foundation for the structural analysis and can be completed with additional analysis. However, the Sarsfield pit is currently filled with Mount Wright tailings and plans to remove them are not expected to be achieved for at least 2-3 years. These current circumstances preclude additional pit mapping analysis beyond what has already been accomplished. Despite these constraints, the potential integration of the existing data from Orefind (2017), plans on additional pit mapping, along with the structural interpretation conducted by Clarke (2003) and the structural analysis on drilling cores will greatly enhance the structural model at Sarsfield.
- C) Structural analysis of the bornite vein sets using geometric and overprinting

relationships to incorporate them within the overall structural model.

4) Use of alteration minerals to trace the fluid source (IRGS versus Porphyry model)

Recent discoveries at Ravenswood may challenge the prevailing Intrusion-Related Gold System (IRGS) model. The recent identification of bornite-bearing veins at depth between Buck Reef and Sarsfield pits suggests potentially a more complex mineralisation system. According to (Morrison, pers. Comm., 2024), bornite, though uncommon, is recognised in certain vein sets associated with chalcopyrite-pyrite-pyrrhotite ± arsenopyrite. These veins exhibit chlorite-sericitic alteration selvages overprinting the more pervasive biotite-magnetite alteration, localised by shear zones and andesite dykes. Morrison (2016) proposes that the presence of a Cu-Te core indicates a mafic intrusion, specifically andesite dykes, as the primary driver of mineralisation.

This hypothesis is supported by several factors: the overall alteration halo, metal zoning pattern, magmatic isotope signatures suggesting a more reduced environment than an oxidised felsic intrusion, and the extensive biotite alteration in Buck Reef that extends into the mafic host rocks. A potential source for this mineralisation could be a diorite intrusion responsible for the formation of the andesite dyke swarms. To further investigate this hypothesis, detailed geochemical analysis and dating of these dykes are crucial (as outlined in sections 1 & 2). Geochemical analysis should include Ti/Li ratios, which can provide valuable insights into fluid evolution and ore-forming processes. In igneous systems, Ti tends to be enriched in mafic rocks and depleted in felsic rocks, while Li often increases with magmatic differentiation. The Ti/Li ratio typically decreases as fluids evolve from magmatic to hydrothermal conditions, potentially revealing trends related to magmatic evolution. Currently, a collaborative study with Jonghyun Lee, a PhD student at James Cook University, is underway. Jonghyun's research focuses on the magmatic activity associated with the Kennedy Igneous Association and its relationship with the mineral occurrences throughout northeast Queensland, including the Ravenswood district. This study will involve field sampling, laboratory analyses (including major and trace element geochemistry and age dating), modelling of magmatic processes, and the development of a metallogenic framework. A key aspect of this research will be examining the potential adakitic signature of some intrusives, characterised by high Sr/Y ratios indicative of an enriched mantle source. These signatures have the potential to be compared with the geochemistry of the hydrothermal veins to further elucidate the genetic relationships between magmatism, hydrothermal fluids and mineralisation in the Ravenswood area.

Once the full paragenesis is established, hydrothermal minerals will be used as tools to hopefully discriminate the source of hydrothermal fluids- e.g. back-arc magmatism (IRGS), gold-fertile arc magma, mantle delamination (adakitic porphyry signature) or overprint of mineralisation styles. Minerals that will be investigated include:

- a) Hydrothermal monazite and xenotime chemistry as genetic discriminators for intrusion-related and orogenic gold deposits. (e.g. <https://doi.org/10.1007/s00126-023-01240-5>)
- b) Chlorite geochemistry as vectoring tool for detecting porphyry ore deposits (e.g. <https://doi.org/10.1016/j.gexplo.2015.01.005>)
- c) White mica chemistry: trace element signatures of phengite reflect the composition of the fluids from which it precipitated, potentially allowing it to fingerprint fluid sources and track fluid evolution.

5) Single vs multistage mineralising event

The impressive gold endowment at Ravenswood Gold Mine exceeds 8 Moz Au, more than twice that of Mount Leyshon (the district's second-largest deposit). This substantial gold concentration may be linked with the frequent association of overprinting mineralising events in the formation of world-class deposits.

A Late Silurian (424 Ma) Re-Os age was obtained from molybdenite, both sampled from the Sarsfield pit in a shear vein containing quartz-molybdenite-pyrite-chalcopyrite. Notably, this age predates the Permo-Carboniferous hydrothermal system and aligns instead with the relationship between the felsic fractionated phases of the Jessop Creek Complex and the molybdenite-bearing buck and coarse comb quartz veins (Morrison, pers. comm., 2016). Ore stage fluid inclusion analysis by (Bertelli et al., 2009) indicates ore deposition temperatures between 300-400°C at Sarsfield and is interpreted to relate to the Permo-Carboniferous event. Both studies might suggest a distinct mineralising event, as the preservation of the Silurian molybdenite age implies that the Permo-Carboniferous event did not reach temperatures sufficient to reset the molybdenite system, given its closure temperature of approximately 550°C. Such observation highlights a potential multi-phase nature of mineralisation at Ravenswood, hence further analysis on Re-Os age dating on molybdenite must be considered, especially if the paragenesis observations link gold and molybdenite.

According to the recommendations from Scott Halley (pers Comms, 2006) to investigate gold precipitation mechanisms, gold is typically soluble as bisulfide complex in relatively oxidised and neutral pH fluids, and precipitates when the system becomes reduced and acidic. An interest exists in looking for paragenetically early pyrite associated with gold in Sarsfield (characterising the core of the system). By preparing polished thin sections and etching them, internal zoning within the pyrite grains can potentially be observed. If such zoning is present, submitting these samples for sulfur isotope analyses of the pyrite cores and rims could provide evidence of changes in fluid chemistry over time, particularly shifts in redox conditions. By reconstructing the evolution of the mineralising fluids and their specific conditions leading to gold deposition, it may have the potential to highlight different mineralising phases.

6) Extrapolation into near-mine brownfield environment

According to (Morrison, pers. Comm., 2024), part of the relationship to Mount Wright is in the mafic intrusion occurrences from Totley through Drabble and Mount Wellington area. Mapping and sampling of those locations is proposed to unravel this link. At a larger scale, additional field mapping/sampling and new geophysical self-interpretation might also develop the intricate link between the intrusion input (if discovered) and the deformation.

REFERENCES

- AITCHISON, J. C., AND BUCKMAN, S., 2012. Accordion vs. quantum tectonics: Insights into continental growth processes from the Palaeozoic of eastern Gondwana: *Gondwana Research*, v. 22, no. 2, p. 674-680.
- BASSOTTI, M., 1998. A possible genetic association between the granophyric microgranites of Charters Towers and the local gold mineralisation. BSc (Hons), James Cook University, EGRU.
- BEAMS, S.D. & DRONSEIKA, E.V., 1995. Mineral Deposits of Northeast Queensland: Geology and Geochemistry (Edited S.D. Beams), pp.137-153. EGRU Contribution 52, James Cook University, 17th International Geochemical Exploration Symposium.

- BERTELLI, M., WILLIAMS, P.J., BAKER, T., LISOWEIC, N., AND BOYCE, A., 2009. Nature and origin of ore-forming fluids in the Ravenswood gold system, north Queensland: evidence from fluid inclusions and stable isotopes. In: Proceedings of the 10th Biennial Meeting of the SGA 2009 (1) pp. 344-346. From: 10th Biennial Meeting of the SGA 2009, 17-20 August 2009, Townsville, QLD, Australia.
- BLAKE, P. R. 2013. New England Orogen – Calliope Province. In P. A. Jell (Ed.), *Geology of Queensland* (pp. 311–317). Brisbane Qld: Geological Survey of Queensland.
- CHAMPION, D. C. 2016. Geodynamic synthesis of the Phanerozoic of eastern Australia. Second edition. *Geoscience Australia Record* 2016/07, 58–82.
- CHAMPION, D.C. & BULTITUDE, R.J., 2013. Chapter 6 Kennedy Igneous Association. In: Jell, P.A. (Editor): *Geology of Queensland*. Geological Survey of Queensland, Brisbane, 473–513.
- CHAMPION, D. C., KOSITCIN, N., HUSTON, D. L., MATHEWS, E., & BROWN, C., 2009. Geodynamic synthesis of the Phanerozoic of eastern Australia and implications for metallogeny. *Geoscience Australia Record* 2009/18, 259.
- CHAMPION, D.C. & BULTITUDE, R.J. 2003. Granites of north Queensland. In: Blevin, P., Jones, M. and Chappell, B. (eds) *Magmas to Mineralisation: The Ishihara Symposium*. *Geoscience Australia Record* 2003/14, 19-23.
- CHAMPION, D.C. AND HEINEMANN, M.A., 1994. *Igneous rocks of northern Queensland: 1:500 000 map and explanatory notes*. Australian geological Survey Organisation, Record 1994/11.
- CLARKE, G. W., 2003. Review of structural mapping results for the Sarsfield open-cut pit, Ravenswood, PhD thesis.
- COLLINS, W. J., 2002. Nature of extensional accretionary orogens: *Tectonics*, v. 21, no. 4, p. 1-12.
- DAVIS B. K., COWAN, E. J., 2017. Structural geological review and deposit architecture, Ravenswood Gold project, North Queensland, Confidential report for Resolute Mining Ltd
- DAVIS B. K., HENDERSON R. A., 1996. Rift-phase extensional fabrics of the back-arc Drummond Basin, eastern Australia. *Basin Res.* 8:371–81
- DIRKS, H. N., SANISLAV, I. V., & ABU SHARIB, A. S. A. A. 2021. Continuous convergence along the paleo-Pacific margin of Australia during the early Palaeozoic: Insights from the Running River Metamorphics, NE Queensland. *Lithos*, 398–399, 106343.
- DE CARITAT P, BRAUN J. 1992. Cyclic development of sedimentary basins at convergent plate margins. 1. Structural and tectono-thermal evolution of some Gondwana basins of eastern Australia. *J. Geodyn.* 16:241–82
- EDGAR, A., SANISLAV, I., AND DIRKS, P., 2023. The origin of mafic–ultramafic rocks and felsic plutons along the Clarke River suture zone: implications for porphyry exploration in the northern Tasmanides: *Australian Journal of Earth Sciences*, v. 70, no. 8, p. 1123-1138.
- EDGAR, A., SANISLAV, I. V., DIRKS, P. H., AND SPANDLER, C., 2022. Metamorphic diamond from the northeastern margin of Gondwana: Paradigm shifting implications for one of Earth’s largest orogens: *Science Advances*, v. 8, no. 27, p. eabo2811.
- EVANS PR, ROBERTS J., 1980. Evolution of central eastern Australia during the late Palaeozoic and early Mesozoic. *J. Geol. Soc. Aust.* 26:325–40
- FERGUSON, C. L., AND HENDERSON, R. A., 2015. Early Palaeozoic continental growth in the Tasmanides of northeast Gondwana and its implications for Rodinia assembly and rifting: *Gondwana Research*, v. 28, p. 933-953.

- FERGUSON, C.F. & HENDERSON, R.A., 2013. Chapter 3 Thomson Orogen. In: Jell, P.A. (Editor): *Geology of Queensland*. Geological Survey of Queensland, Brisbane, 113–224.
- FERGUSON, C. L., HENDERSON, R. A., WITHNALL, I. W., FANNING, C. M., PHILLIPS, D. AND LEWTHWAITE, K. J. 2007. Structural, metamorphic, and geochronological constraints on alternating compression and extension in the Early Palaeozoic Gondwanan Pacific margin, northeastern Australia, *Tectonics* 26.
- GLEN, R. A., 2013. Refining accretionary orogen models for the Tasmanides of eastern Australia: *Australian Journal of Earth Sciences*, v. 60, no. 3, p. 315-370.
- GLEN, R. A., S. MEFFRE & R. J. SCOTT, 2007. Benambran Orogeny in the Eastern Lachlan Orogen, Australia, *Australian Journal of Earth Sciences*, 54:2-3, 385-415, DOI: 10.1080/08120090601147019
- HENDERSON, R. A., FERGUSON, C. L., AND WITHNALL, I. W., 2020. Coeval basin formation, plutonism and metamorphism in the Northern Tasmanides: extensional Cambro-Ordovician tectonism of the Charters Towers Province: *Australian Journal of Earth Sciences*, v. 67, no. 5, p. 663-680.
- HENDERSON, R. A., INNES, B. M., FERGUSON, C. L., CRAWFORD, A. J., AND WITHNALL, I. W., 2011. Collisional accretion of a Late Ordovician oceanic island arc, northern Tasman Orogenic Zone, Australia: *Australian Journal of Earth Sciences*, v. 58, no. 1, p. 1-19.
- HUTTON, L. J., DRAPER, J.J., RIENKS, I.P., WITHNALL, I.W. AND KNUTSON, J. 1997. Charters Towers region. In: Bain, J.H.C. and Draper, J.J (eds). *North Queensland Geology*. AGSO Bulletin 240 and *Queensland Geology* 9, 165–224.
- HUTTON, L.J., RIENKS, I.P., 1997: *Geology of the Ravenswood Batholith*. *Queensland Geology*, 8, 60pp
- JESSOP, KIM & DACZKO, NATHAN & PIAZOLO, S., 2019. Tectonic cycles of the New England Orogen, eastern Australia: A Review. *Australian Journal of Earth Sciences*. 66. 1-38.
- KEMP, A., HAWKESWORTH, C., COLLINS, W., GRAY, C., AND BLEVIN, P., 2009. Isotopic evidence for rapid continental growth in an extensional accretionary orogen: The Tasmanides, eastern Australia: *Earth and Planetary Science Letters*, v. 284, no. 3-4, p. 455-466.
- KORSCH, R. J., HUSTON, D. L., HENDERSON, R. A., BLEWETT, R. S., WITHNALL, I. W., FERGUSON, C. L., COLLINS, W. J., SAYGIN, E., KOSITCIN, N., MEIXNER, A. J., CHOPPING, R., HENSON, P. A., CHAMPION, D. C., HUTTON, L. J., WORMALD, R., HOLZSCHUH, J. & COSTELLOE, R. D., 2012. Crustal architecture and geodynamics of North Queensland, Australia: insights from deep seismic reflection profiling. *Tectonophysics*, 572-573 (N/A), 76-99.
- KORSCH, R. J., ADAMS, C. J., BLACK, L. P., FOSTER, D. A., FRASER, G. L., MURRAY, C. G., ... GRIFFIN, W. L., 2009. Geochronology and provenance of the Late Palaeozoic accretionary wedge and Gympie Terrane, New England Orogen, eastern Australia. *Australian Journal of Earth Sciences*, 56(5), 655–685.
- KREUZER, O. P. 2006: Textures, paragenesis and wallrock alteration of lode gold deposits in the Charters Towers region, North Queensland: implications for the conditions of ore formation. *Mineralium Deposita*, 40, 639-663.
- KREUZER, O. P. 2005: Intrusion-hosted mineralisation in the Charters Towers Goldfield, North Queensland: new isotopic and fluid inclusion constraints on the timing and origin of the auriferous veins. *Economic Geology*, 100, 1583-1603.
- LEITCH EC. 1975. Plate tectonic interpretation of the Palaeozoic history of the New

England Fold Belt. *Geol. Soc. Am. Bull.* 86:141–44

LISITSIN, V., DHNARAM, C., VON GNIELINSKI, F., TAPU, A., 2024. Signatures of Carboniferous to Permian intrusion-related Au and Sn-W deposits in NE QLD, Mineral Systems of NE QLD - EGRU conference, Charters Towers

LISOWIEC, N. AND MORRISON, G., 2017. Ravenswood and Mount Wright gold deposits: in Phillips, G.N., (Ed.), 2017 Australian Ore Deposits, The Australasian Institute of Mining and Metallurgy, Mono 32, pp. 705-710.

LISOWIEC, N., HALLEY, S. H., AND RYAN, L., 2008. Spectral characteristics of the Ravenswood Gold Deposit, North Queensland, and its application to near-mine and regional exploration, in Proceedings PACRIM Congress 2008, pp 201-205 (The Australasian Institute of Mining and Metallurgy: Melbourne).

MORRISON, G.W, NICHOLLS, A & LISOWIEC, N., 2015: Towards a genetic model for the Ravenswood Deposits. Presentation at Project Annual meeting May, 2015.

MORRISON, G., LISITSIN, V., AND DHNARAM, C., 2014. Intrusion-Related Gold Systems of North Queensland, Digging Deeper 12 Symposium Geol. Surv Qld.

MORRISON, G. W., 1988. Palaeozoic Gold Deposits of northeast Queensland. Bicentennial Gold 88 Geological Society of Australia Extended Abstracts 22, pp. 91-101.

OFFLER, R., & MURRAY, C., 2011. Devonian volcanics in the New England Orogen: Tectonic setting and polarity. *Gondwana Research*, 19(3), 706–715.

PERKINS C, KENNEDY AK, 1998. Permo-carboniferous gold epoch of northeast Queensland. *Aust J Earth Sci* 45:185–200.

PURDY, D.J., CARR, P.A. AND BROWN, D.D., 2013: A review of the geology, mineralisation and geothermal energy potential of the Thomson Orogen in Queensland. *Queensland Geological Record* 2013/01.

ROSENBAUM, G., 2018. The Tasmanides: Phanerozoic Tectonic Evolution of Eastern Australia. *Annual Review of Earth and Planetary Sciences*, 46(1), 291–325.

ROSENBAUM, G., 2012. Oroclines of the southern New England Orogen, eastern Australia. *Episodes-Newsmagazine of the International Union of Geological Sciences*, 35(1), 187.

STANDING, J, 2006. Tectonic setting and evolution of the eastern half of the Ravenswood Batholith from traverse mapping, Ravenswood region, NE Queensland. Jigsaw Geoscience report for Resolute Mining.

SWITZER, C.K., 2000: Comments on the Geochemical Evolution, Alteration and Structural Setting of Gold Mineralisation at Ravenswood, northeast Queensland. M.Sc. thesis James Cook University of north Queensland, 128p.

VAN NOORD, K.A.A. 1999. Basin development, geological evolution and tectonic setting of the Silverwood Group. In: Flood, P.G (editor). *New England Orogen. Regional Geology, Tectonics and Metallogensis*, pp 163-180. University of New England, Armidale.

WITHNALL, I. W., & CRANFIELD, L. C., 2013. Geological framework. In P. Jell (Ed.), *The geology of Queensland* (pp. 13–34). Queensland Government.

WORMALD, P. J., 2017. Mount Leyshon gold deposit: in Phillips, G.N., (Ed.), 2017 Australian Ore Deposits, The Australasian Institute of Mining and Metallurgy, Mono 32, pp. 697-704.

EXPLORATION POTENTIAL FOR PERALKALINE REE DEPOSITS IN CENTRAL WESTERN NEW SOUTH WALES

Brenainn Simpson

Geological Survey of New South Wales

Key words: Lachlan Orogen, Hunter-Bowen Orogeny, peralkaline, post collisional, volcanism, rare earth elements (REE), high-field strength elements (HFSE), critical minerals.

INTRODUCTION

Peralkaline magmas, defined as having an excess of alkali metals (Na+K) relative to Al, have the potential for concentrating rare earth elements (REE) along with other high-field strength elements (HFSE) such as Zr, Hf, Nb, and Ta which are critical resources for the green economy transition (Goodenough et al. 2018). Typically, these magmas are the products of low degree partial melting of metasomatically enriched subcontinental lithospheric mantle (SCLM) due to plume activity or continental extension associated with failed rifts or orogenic collapse (Figure 1).

Prospective igneous rocks can be identified by a) abundance of Na and K relative to Al; the occurrence of Na-rich indicator minerals e.g., aegirine, arfvedsonite, or sodalite; c) enrichment in HFSE measurable on pXRF e.g., Zr; d) ore minerals including zirconosilicates (zircon, baddeleyite, or eudialyte), phosphates (apatite, monazite, xenotime), and oxides (niobite or pyrochlore). Other geochemical criteria include evidence of extensive fractional crystallisation (strong depletion in Ti, Ca, Mg, enrichment in Fe, Mn, and pronounced negative Eu anomalies), high Ga/Al ratio, and enrichment in halogens (Cl, F). Prospective rocks can be distinguished from other high-K rocks using radiometric geophysical data by the enrichment of actinides (Th, U) relative to K.

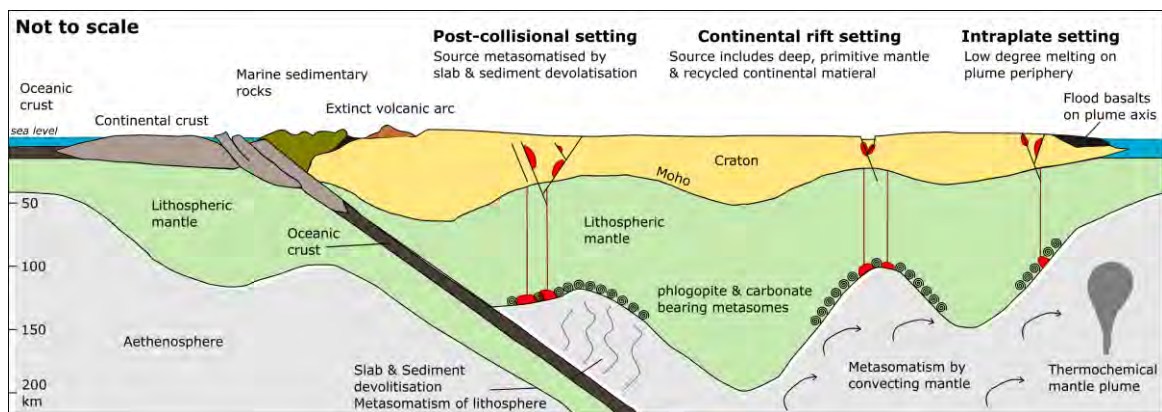


Figure 37. Geodynamic endmembers associated with peralkaline magmatism after Beard et al. 2023.

PERALKALINE ROCKS IN NSW

A-type peralkaline granites and volcanics occur in the Lachlan Orogen (LAO) from the Devonian to the Cenozoic. Notable examples include the Narraburra Granite (~360 Ma), and the newly defined Benolong Volcanic Suite associated with the K-feldspar+aegirine+eudialyte phyric Toongi trachyte which forms the core the Dubbo Zirconia Project (Figure 2). The magmatic age of the Mesozoic volcanics in central NSW is currently underestimated by K-Ar and fission track techniques. New U-Pb (apatite,

zircon) and Ar-Ar (K-feldspar) geochronology presented here constrains the timing of peralkaline volcanism in central NSW to the Late Triassic (~215 Ma). In both cases, this magmatism is associated with post-collisional relaxation attributed to the Tabberabberan and Hunter-Bowen Orogeny (HBO) respectively. The LAO is a fertile terrane for REE and HFSE enriched peralkaline magmatic rocks due to repetitive subduction related metasomatic enrichment of the SCLM since the Cambrian as an oceanic island arc terrane which ultimately accreted onto Gondwana in the Silurian. Subsequent orogenesis and the accretion of New England (NEO) provide both a mechanism for low degree melting post-collision (Goodenough 2021) and a crustal scale suture exploited by ascending magmas (Spandler and Morris 2016).

Benlong Volcanic Suite

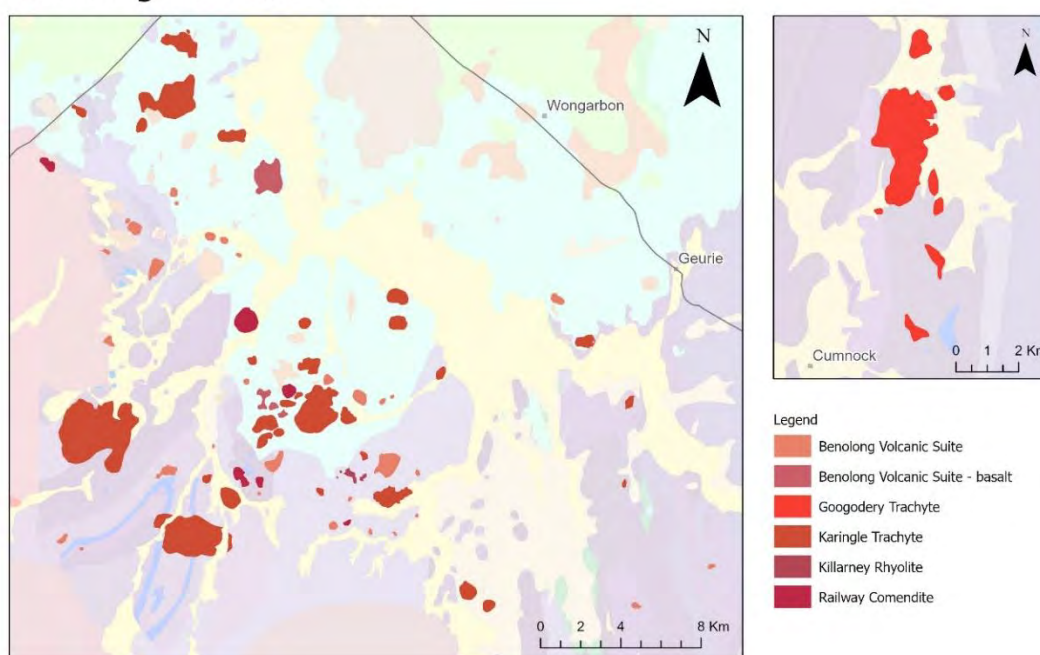


Figure 38. Extant of the Benlong Volcanic Suite (Simpson and Fitzherbert 2023) as included in version 2.4 of the Seamless Geology of NSW (Colquhoun et al. 2024). The volcanic suite is defined by voluminous trachyte flows, plugs, and subvolcanic intrusions, alongside rarer comendite, rhyolite, and poorly preserved basalt.

Post HBO extension in the NEO is recorded by a N-S belt of low volume A-type granites between 235-210 Ma (Li et al. 2011) and is now revealed to be temporal equivalents with A-type peralkaline volcanism in the LAO. In addition to the ~215 Ma Benlong Volcanic Suite, ungrouped peralkaline volcanics described by Meakin and Morgan (1999) occur to the east of Mudgee. An existing U-Pb zircon SHRIMP 231.1 ± 2.5 Ma age for a phonolite 11km N of Lue (Black 1998) indicates that these rocks align with the post-HBO window and are likely an older component of the same peralkaline magmatic event that produced the Toongi Trachyte, occurring further east due to change in subduction angle during slab roll back. Investigations into other Mesozoic volcanics described as peralkaline (e.g., the Bulga Complex Bean 1974) are ongoing. These results demonstrate the mineral system which produced the Toongi deposit is more widespread than previously thought.

REFERENCES

- BEAN, J.M. 1974. The geology and petrology of the Mullaley area of New South Wales. *Journal of the Geological Society of Australia* **21**, 63–72.
- BEARD, C.D., GOODENOUGH, K.M., BORST, A.M., WALL, F., SIEGFRIED, P.R., DEADY, E.A., POHL, C., HUTCHISON, W., FINCH, A.A., WALTER, B.F., ET AL. 2023. Alkaline-Silicate REE-HFSE Systems. *Economic Geology* **118**, 177–208.
- BLACK LP (1998) SHRIMP zircon U/Pb isotopic age dating of samples from the Dubbo 1:250 000 Sheet area, batch 2, Geological Survey of New South Wales.
- COLQUHOUN, G.P., HUGHES, K.S., DEYSSING, L., BALLARD, J.C., FOLKES, C.B., PHILLIPS, G., TROEDSON, A.L., AND FITZHERBERT, J.A. 2004. New South Wales Seamless Geology dataset, version 2.4 [Digital Dataset] (Geological Survey of New South Wales), Maitland.
- GOODENOUGH, K.M., WALL, F., AND MERRIMAN, D. 2018. The Rare Earth Elements: Demand, Global Resources, and Challenges for Resourcing Future Generations. *Natural Resources Research* **27**, 201–216.
- GOODENOUGH, K.M., DEADY, E.A., BEARD, C.D., BROOM-FENDLEY, S., ELLIOTT, H.A.L., VAN DEN BERG, F., AND ÖZTÜRK, H. 2021. Carbonatites and Alkaline Igneous Rocks in Post-Collisional Settings: Storehouses of Rare Earth Elements. *Journal of Earth Science* **32**, 1332–1358.
- LI, P.-F., ROSENBAUM, G., AND RUBATTO, D. 2012. Triassic asymmetric subduction rollback in the southern New England Orogen (eastern Australia): the end of the Hunter-Bowen Orogeny. *Australian Journal of Earth Sciences* **59**, 965–981.
- MEAKIN, N.S., MORGAN, E.J. (COMPILERS) 1999. Dubbo 1:250 000 Geological Sheet SI/55-4, 2nd Edition. (Sydney: Geological Survey of New South Wales).
- SIMPSON, B.P., AND FITZHERBERT, J.A. 2023. Petrographic character of variably peralkaline Mesozoic volcanics, Dubbo 1:250000 Geological sheet SI/55-4 (Maitland: Geological Survey of New South Wales).
- SPANDLER, C., AND MORRIS, C. 2016. Geology and genesis of the Toongi rare metal (Zr, Hf, Nb, Ta, Y and REE) deposit, NSW, Australia, and implications for rare metal mineralization in peralkaline igneous rocks. *Contributions to Mineralogy and Petrology* **171**, 104.

THE BAULOORA EPITHERMAL PROJECT, NSW: AN EARLY DEVONIAN EPITHERMAL AU-AG-PB-ZN SYSTEM

Thomas Wall¹, Chris Byrne¹, Ava Stevens²

¹Legacy Minerals Pty Ltd.

²Newmont Corporation Ltd.

Keywords: Bauloora, epithermal, Devonian, epithermal veining

INTRODUCTION

The Bauloora epithermal system occurs in the exploration licence EL 8994. It is located near the township of Cootamundra, NSW, and is hosted within the Early Devonian Cowcumbala Rhyolite. The mapped epithermal style quartz veins and anomalous epithermal pathfinder element surface geochemistry define the system's extent. Mineralisation exhibits characteristics of both low-sulphidation epithermal (LSE) and intermediate sulphidation epithermal (ISE) styles.

The Bauloora Project has a history of small-scale mining at the Mt Felstead Mine, also known as the Bauloora Mine. Very little has been published on the mineralisation in the Bauloora area and its relation to the local geology and regional tectonic evolution, with the most comprehensive description of the area completed by Downes *et al.* (2004).

Exploration by Legacy Minerals Holdings Ltd (LGM or the Company) resulted in the discovery of a large gold and silver-bearing LSE-ISE vein field. Recent work with Earn-in partner Newmont Corporation (Newmont) has extended the known vein field and greatly increased the understanding of the project.

HISTORY

The Bauloora district has been intermittently explored for over 50 years, initially focussed on VHMS mineralisation after the discovery of the Woodlawn deposit and then primarily as a gold project since the mid-1980s when it was recognised that the project area hosts a significant amount of epithermal style veins. Crustiform-colloform banded quartz veins are widely distributed; however, detailed exploration has been limited to areas where higher grades of gold, often with base metals, are known. Historical exploration activities have included: (i) surface geological mapping, (ii) geophysical surveys including airborne magnetics and dipole-dipole induced polarisation (DDIP), (iii) rotary air blast (RAB) and air core (AC) drilling, and; (iv) reverse circulation (RC) and diamond core drilling (DD).

The Mt Felstead Mine has been the focus of this testing due to its historical production of high-grade mineralisation (face samples up to 1,021.5 g/t Ag, 7.2 g/t Au, 22.2% Pb+Zn and 2.5% Cu). It is the only substantial workings in the region and is located on the southwestern edge of the known Bauloora vein field. An estimated 6,000 tonnes of ore was extracted sporadically between 1903 to 1957. Ground geophysics and drilling by multiple companies tested the depth extensions beneath the historical workings but only to relatively shallow depths and with only a limited number of diamond-cored holes. Though small surficial prospecting has occurred on some vein outcrops, no other significant workings outside of Mt Felstead are known in the area.

Exploration by Teck Exploration Ltd. in the early 1970s assessed the wider project area for potential volcanic-hosted massive sulphide (VHMS) mineralisation, in particular at the Bauloora East prospect, where four drill holes were completed.

In the 1980s, the project was held by BP Minerals Ltd, managed by Mineral Management and Securities Pty Ltd. followed by the Shell Company of Australia Ltd.

During this time, the most extensive and intensive programs were completed. Stream sediment sampling identified a 24 km² area of anomalous gold. The area included the Mt Felstead mine; however, the most anomalous catchment was east of the historic mine. Geological mapping using a grid-based approach identified epithermal quartz veins over wide areas. Despite mapping a wide distribution of quartz veins, most subcrop and float trains were not sampled. Five air-core drill holes at the Gravel Scrapes prospect and five at the Breccia Sinter prospect returned anomalous gold grades. However, the peak intercept of 20 meters at 0.44 g/t Au from 2 meters from PDHB6 was lower than hoped for, and the ground was relinquished.

North Limited explored the ground from the early to mid-1990s, completing airborne magnetic surveys, soil sampling and rock chip sampling. RAB and RC drilling at Breccia Sinter to follow up on the large gold in soil anomaly; however, no economic intersections were achieved, and the licence was relinquished.

The last major program of work was completed by Robust Operations Pty Ltd who held the project between 2005 and 2014. During this time, the focus was on potential depth and strike extensions to the Mt Felstead Mine. Reconnaissance rock chipping of veins at the Mee Mar prospect returned encouraging assays. Follow-up RC drilling for a total of four holes at the Mee Mar prospect returned a peak gold result of 3 m at 1.13 g/t Au including 15.8 g/t Ag; 3.64% Pb and 3.55% Zn, yet the project was not considered a priority and was eventually relinquished.

While previous explorers recognised the epithermal setting and concluded that the vein-system had potential for concealed bonanza gold development, historic exploration programs remained focused in discrete areas with little systematic testing of the full extent of the vein field.

Legacy Minerals focussed on the acquisition of data sets that would provide a more systematic assessment of the potential of the known vein field and a more comprehensive target ranking criteria. In particular, the focus was on understanding the level of the system based on quartz textural observations, and through understanding geochemical variation between different veins and within vein trends.

The following data sets were acquired by LGM: (i) high density rock chip sampling of mapped vein occurrences, (ii) grid-based soil sampling, (iii) gradient array IP, (iv) ground magnetics, (v) dipole-dipole IP, and (vi) advanced spaceborne thermal emission and reflection radiometer (ASTER) interpretation. A total of 10 RC holes and 10 DD were drilled by the company. Drilling resulted in new mineralised epithermal vein trends and extensions to previously known vein trends being defined, including:

Mt Felstead

- BM007: 9m at 2.0g/t Au, 28.4g/t Ag, 0.2% Cu and 9.9% Zn+Pb from 145m.
- BM008: 3m at 1.65g/t Au, 152.8g/t Ag, 0.35% Cu and 6.9% Pb+Zn from 149m.

Blue Cap

- MM008: 13m at 1.66g/t Au, 6.68g/t Ag, 0.14% Cu and 4.23% Pb+Zn from 57m.

Mee Mar

- MM002: 3.8m at 0.93g/t Au, 6.60g/t Ag, 0.28% Cu and 4.17% Pb+Zn from 179.6m.
- MM004: 9m at 0.16g/t Au, 5.0g/t Ag, 0.07%Cu and 1.75% Pb+Zn from 79m.

An earn-in agreement was reached with Newmont Exploration in April 2023 on the Bauloora Project. Since that time, the following data sets have been acquired:

- (i) Airborne magnetics and radiometrics,
- (ii) Geological mapping,
- (iii) Ground gravity,
- (iv) Surface geochemistry including BLEG, soil sampling and rock chip sampling,
- (v) Audio-magnetotellurics (AMT).

A total of 11 diamond drillholes have been completed, resulting in the identification of new mineralised epithermal vein trends.

GEOLOGICAL SETTING

The exploration licence is dominated by Early Devonian Cootamundra Group subaerial felsic volcanic rocks with lesser nearshore and shallow marine sedimentary rocks. Downes *et al.* (2004) describe this volcanism as appearing to have been related to renewed activity along the pre-existing siliceous magmatic/volcanic rises. In addition, several I-type intrusions were emplaced within the volcanic package; the relationship between this intrusive activity and the felsic volcanism is unknown.

Underlying the Cootamundra Group is the Frampton Volcanics, which is characterised by bimodal subaerial and submarine volcanic infill of the Early Silurian Tumut Trough. The origin and geological history of the Tumut Trough is poorly understood. Basden *et al.* (1990) suggested that the basin formed by rifting beginning in the Early Silurian. Other workers suggest a range of tectonic settings, including an intracratonic rift, a back-arc basin, a pull-apart basin, a fore-arc basin (and subsequent collision with a continental margin), a suspect terrane or a para-autochthonous tectonic model (Warren *et al.* 1995).

For reasons not yet clear, the significant deformation of the Tabberabberan Orogeny that took place in the Middle Devonian did not greatly affect the Bauloora Project area and the rocks and mineralisation are not strongly deformed.

Sedimentation in the Late Devonian formed the Hervey Group, which bounds the eastern and northeastern extents of the epithermal vein field. It is hypothesised that the Hervey Group's deposition has contributed to preserving the Bauloora epithermal system.

The Late Devonian to Early Carboniferous Kanimblan Orogeny appears to have resulted in broad folding across the project area. At the project level, this deformation appears to have gently folded the Hervey and Cootamundra Group.

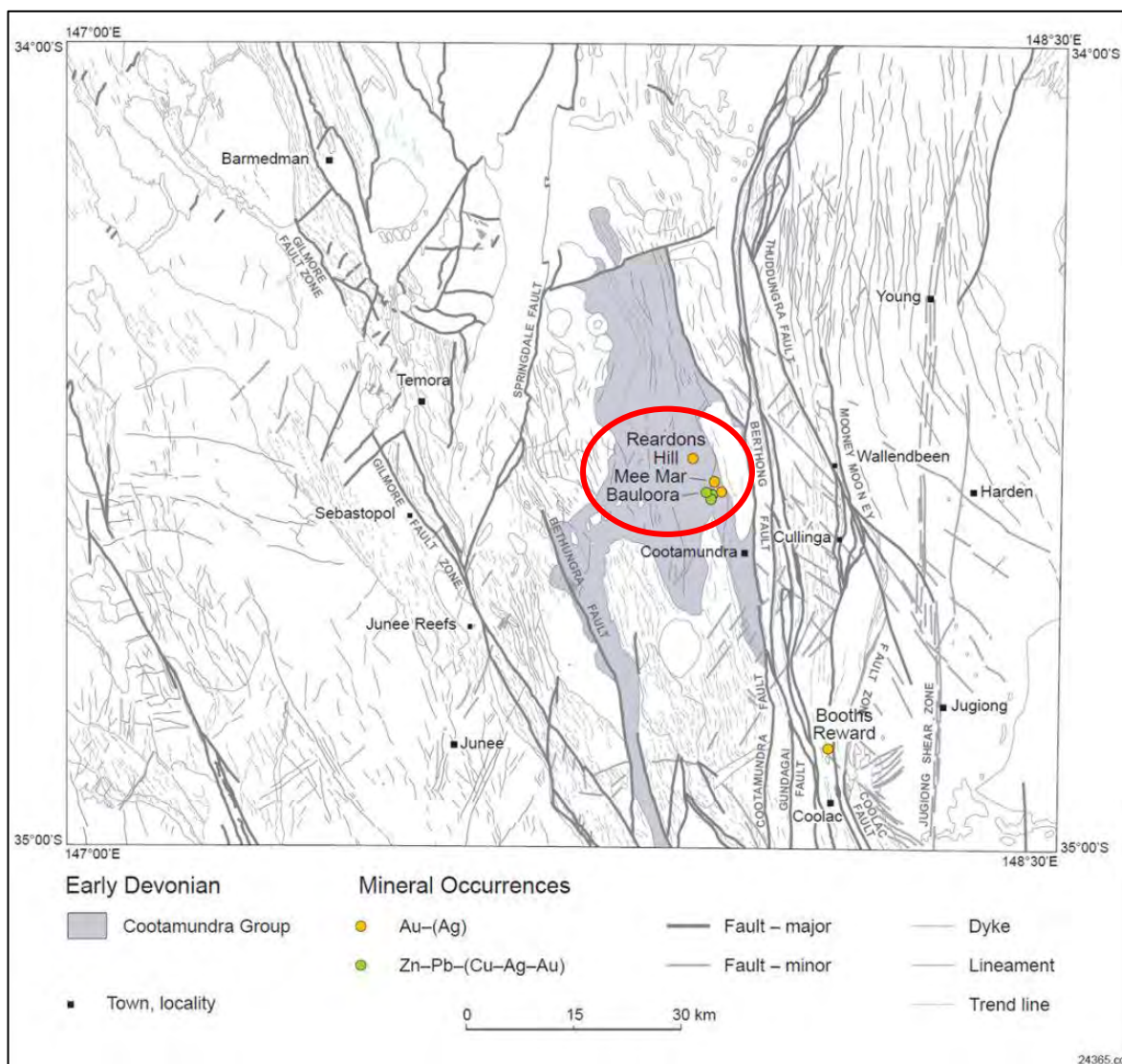


Figure 39. Cootamundra 1: 250,000 Early Devonian mineral deposits – Downes et al (2004).

LOCAL GEOLOGY

The Bauloora exploration area is dominated by the Cootamundra Formation, a felsic volcanic unit. The volcanics include bedded flow units and fragmental volcanics and it is proposed flow domes are present. The dome volcanics are described in a number of petrology samples described by mineral exploration companies over the last 50 years and support the emergent, to perhaps shallow marine, environment. The volcanic history may include a phase of extrusive and intrusive andesitic activity due to the recognition of intermediate to mafic clasts within the Deep Gully Creek Conglomerate.

Acidic dome volcanism and the relatively complete preservation of the volcanic system are supported by the presence of fracture filling of fine-grained milled volcanic powder, which is thought to represent 'tuffsite'. Tuffsite is a fracture filling of rock powder 'fluidised' in a shallow fumarolic environment. The relatively complete preservation of the volcanic system is also supported by the presence of sinter and sinter-related lithologies.

Younging directions, bedding orientations and regional scale map patterns indicate that the Bauloora project is positioned on the eastern limb of a broad wavelength anticline

that plunges gently to the north (4° - 18°). Across the Bauloora vein field, the identified lithologies dip gently to moderately to the east.

Six broad stratigraphic packages are identified and are found to young from east to west. From youngest to oldest, these are:

1. Late Devonian Mandagery sandstone (Hervey Group). The Mandagery Sandstone is >140 m thick and consists of quartz-lithic sandstone and conglomerate, interbedded with shale. Conglomerate fragments are subangular to rounded and include cherts, siltstones and, in some cases epithermal textured quartz veins.
2. Early Devonian upper dacite (Cowcumbala Rhyolite) - ~280 m thick, quartz-feldspar phyric dacite with occasional flow banding.
3. Early Devonian Deep Gully Creek Conglomerate: ~110 m thick and an intermediate character that includes pebble conglomerates, sandstones and siltstones. The conglomerates occur in lenses and contain rounded fragments of andesite, quartzite, jasper, chert and banded acid tuff as well as juvenile dacitic clasts interpreted as volcanic “bombs” into a shallow marine environment.
4. Early Devonian lower dacite (Cowcumbala Rhyolite) - ~300 m thick, quartz-feldspar phyric dacite.
5. Early Devonian dacite volcanoclastic (Cowcumbala Rhyolite) - <500 m thick, dacite unit as above, with frequent very fine-grained felsic intrusions and brecciation that may represent mud-dykes through the sequence. Lenses of siltstone and mudstone are also recognised.
6. Early Devonian lower conglomerate (Bethungra Formation) - >110 m thick, matrix-supported, conglomeratic sandstone and immature polymictic sandstone. Conglomerate clasts are sub-angular cobbles of dacite and rhyolite.
7. The Early Silurian Yeo Yeo Rhyodacite Member of the Frampton Volcanics is the lowermost unit present in the project area.

Epithermal veins are hosted in the Early Devonian Cowcumbala Rhyolite lithologies and do not extend into the Late Devonian Mandagery sandstone. The age of the epithermal veins is interpreted to be synchronous with the development of the Cowcumbala volcanic system. The colloform veins display low-temperature quartz textures, and sinter-like material has been recognised in petrology. It is, therefore, reasonable to assume limited erosion of the epithermal system and has high preservation potential. The descriptions from the petrographic examinations include suggestions of flow banding, quartz recrystallisation from earlier chalcedony and recognition of groundmass textures suggestive of high-level emplacement.

MINERALISATION

There are at least two varieties of epithermal mineralisation that are often found together at Bauloora;

- Crustiform-colloform banded epithermal quartz or quartz-adularia veining; and,
- Carbonate-base metal veining and brecciation.

Both have their local variants that include:

- planar fault/fracture-controlled veins.
- splays and other complications.

- breccias with fragments of quartz, silicified wall rock and mineralised vein material cemented by later mineralised vein fill.
- stockwork veining with vein networks filling fracture wall rock at various scales.

The vein paragenesis observed as comparable to the generalised paragenetic sequence for intermediate sulphidation systems shown by Leach and Corbett (1994; Figure 2).

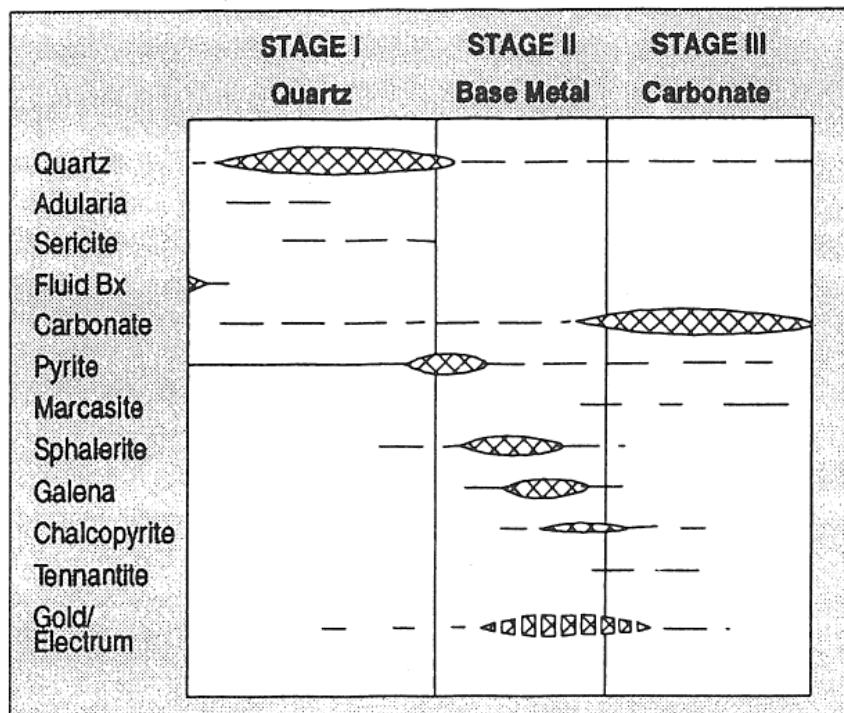


Figure 2. Generalised paragenetic sequence for intermediate sulphidation systems (Leach & Corbett 1994).

Sphalerite is commonly iron poor, ranging from yellow through to pale white-green. It has been observed as a more iron rich red sphalerite at the Mt Felstead Mine.

Based on the presence of quartz textures, mineralisation found to date has formed at relatively shallow crustal levels and appears to be typical of LSE-ISE systems formed from near-neutral, moderate- to high-temperature fluids with at least a portion of the fluids being derived from a magmatic source. Ornate crystalline adularia has been observed throughout and occurs in the colloform-crustiform banded veins. The banded quartz veins and sinter-related lithology at Bauloora are typical of low-temperature epithermal-style vein systems. Re-brecciation and veining occurred following ore deposition in localised areas where base metal-rich veins have an intermediate epithermal geochemical affinity.

Sulphur isotope data for ten sulphide analyses from the Bauloora mine range from -2.4 to 4.3 $\delta^{34}\text{S}$ per mil (average -0.7 $\delta^{34}\text{S}$ per mil). The results suggest that the ore-forming fluids were reduced and that sulphur was derived from a magmatic reservoir, either as a direct magmatic contribution or indirectly through the dissolution and recycling of sulphur from the host-rock sequence.

MINERALISATION SETTING

Sulphur isotope data referenced by Downes et al. (2004) from the Bauloora Mine suggests the fluid that led to mineralisation is of magmatic origin and consistent with a volcanic environment where degassing of shallow magmas is occurring beneath active

volcanic domes. Downes et al. (2004) also noted that Carr et al. (1995) used lead isotope data from the Bauloora deposit to date the mineralisation at 385 Ma, falling within the Devonian granite field. These data support a setting above a slightly reduced magmatic centre consistent with NSW Devonian granites where subaerial to shallow marine effusive volcanism occurred. It is likely that the development of the volcanic package has generated the heat required to promote fluid circulation, leading to hydrothermal alteration and extensive epithermal veins.

It is considered that epithermal mineralisation is closely associated with the same volcanic event based on quartz textural observations within unlithified sediments, burial of sinter-related lithology, and phreatomagmatic brecciation. It is interpreted that the base metal mineralisation developed in a high-level setting proximal to a periodic magmatic volatile source, domes and their roots. The colloform quartz veins are distal mineralisation developed as part of the same system. It is suggested that the base metal events are related to short-duration events involving brecciation, perhaps shallow subdomal explosive events. Capital Mining 1990 – reported Billiton study – Honours thesis by Chris Kreagh veins with 17.8 % NaCl and temperatures of deposition 179-245 °C.

STRUCTURE

Given the prevalence of east-dipping bedding planes and the broad normal grading/ eastward younging of sedimentary packages, it is interpreted that the Bauloora project is located within the east-dipping limb of a broad wavelength, northerly trending anticline.

The geological fabric of the Bauloora area is dominantly north-south and this is apparent in the arrangement of mineralisation. The geophysical data products strongly reinforce a north-south grain.

The regional outcrop patterns/ map interpretation of Warren et al. (1995) infers that older stratigraphy of the Frampton Volcanics outcrop within the core of anticlines that are located to the south and south-west of the Bauloora Project, thus suggesting a regional northerly plunge. Furthermore, this interpretation regarding the plunge of the Bauloora anticline agrees with the previously described quartz facies distribution and geochemical patterns.

Veins and vein breccias vary from cm-scale up to an estimated 8 m true width, and these structures can be strike extensive (up to 2 km). Significant late-stage chalcedonic vein overprinting earlier LSE and ISE indicates the system experienced at least one significant period of collapse and overprinting possibly due to significant exhumation during volcanic activity or substantial tectonic extensional activity resulting in pressure and temperature drops.

Mineralisation is controlled by north-south orientated faulting due to east-west extension. It is thought extension from the Cootamundra Fault in the east resulted in the formation of a graben that was infilled with the Cootamundra Volcanics and eventually overlain by the Hervey Group. Cross faults appear to trend dominantly NE.

ALTERATION

The main observed alteration characteristics are as follows:

- Hematite alteration: widespread and can be pervasive and strong, commonly <50m from vein structures. This may suggest an oxidised magmatic fluid influence or oxidised descending meteoric waters through the volcanics. Hypogene hematite is frequently observed within the vein breccias.
- Distal chlorite alteration: typically patchy or selective in altering volcanic fabrics such as flow bands.
- Illite alteration: common as pervasive alteration proximal to vein zones.

GEOCHEMISTRY

Geochemical surveys consisting of soil sampling and high-density rock chip sampling have been completed across the epithermal vein field. The soil program was completed across 13km² of the project on a 50m x 100m grid with localised areas infilled to 25m x 50m. Samples taken were residual soils collected from the B soil horizon at depths between 0.1m and 0.4m. Rock chip sampling aimed to directly assist in defining precious metal bearing locations within veins, log quartz textures to provide evidence of preservation level, and provide pathfinder element analysis to both assist with vectoring towards precious metals and implications to level of the epithermal system.

The Bauloora epithermal system is represented by a large area of strong epithermal and possible IRG pathfinder anomalism (Au-Ag-Sb-As-Pb-Cu-Zn-Hg-Bi-Mo-W). At the prospect level epithermal veins are broadly recognised in association with Sb-As-Hg (Au-Ag), Pb-Zn (+/- Bi-Cu), and Mo-Bi-W. The rock chip sampling adjacent to many of these geochemical anomalies includes strong gold anomalism (up to 55.5g/t Au) and silver (up to 904g/t Ag) with quartz vein textures consistent with low-intermediate sulphidation epithermal style mineralisation.

CONCLUSION

Bauloora hosts an extensive epithermal vein system. A working hypothesis envisages an evolving sub-aerial volcanic system developing towards dacitic (to rhyolitic) dome volcanism with hydrothermal cell (s) associated with these domes. The base metal mineralisation is proposed to be localised by the domes with epithermal veins developing in a more distal setting above or adjacent. The presence of two separate but closely temporally and spatially related systems remains an alternate possibility. The two styles of mineralisation have their own characteristics in terms of vein morphology and geochemical character, and each has its own specific geophysical characteristics.

In volcanic systems elsewhere, dome development is typically located along important faults and associated fractures representing planes of weakness. Banded veins develop during protracted periods of extension where groundwater circulation continues and provides the potential for sustained repeated mineral deposition. Local complications and periodic readjustments accommodating accumulating or changing stress trigger episodic mineralisation and if over-pressuring occurs brecciation. Related triggers at depth, closer to the location(s) of magmatic input, allow metal influx to 'mineralise' the geothermal circulation system. At Bauloora, many of these characteristics of epithermal systems are present.

Epithermal vein systems in preserved volcanic terrain require testing to depth as the mineralisation is strongly vertically zoned. The vein textures at Bauloora suggest

volcanic preservation with only modest erosion. The low-temperature nature of the mineralising environment is supported by the discovery of abundant chalcedonic veining and exposed sinter-related lithology at the Breccia Sinter prospect. The low-temperature environment and the extensive distribution of colloform banded material across the surface, provide significant scope for discovering concealed mineralisation. The district shares many of the key aspects with world-class epithermal gold systems where persistent drilling in those districts has resulted in the discovery of high-grade multi-million-ounce deposits.

ACKNOWLEDGEMENTS

The authors would like to especially acknowledge and thank their families for their support during work on the project. Furthermore, acknowledgement is made to all the Legacy Minerals team who have been a part of the exploration effort to date (Oliver O'Sullivan, Joeseoph Wall, Niclas Thiele, James Egan, Paul Flitcroft and Chris Byrne), Newmont's Generative exploration team (Ava Stevens, Mike Harris, John Greenfield, Craig Miller and Pip Sivwright), Rod Davies, David Burt and Michael Rennison of Cobre Nuevo Consulting Pty Ltd., Doug Menzies of Geolnsite Pty Ltd., and Gregg Morrison of Klondike Exploration Services Pty Ltd.

REFERENCES

- BASDEN, H., ADRIAN, J., CLIFT, D. S. L., AND WINCHESTER, R. E. 1978. Geology of the Cootamundra 1:100,000 Sheet 8528. Geological Survey of New South Wales, Sydney, 276.
- BOWMAN, H., 1975. Forbes Anticlinorial Zone. pp. 196-214 In Markham N. & Basden H. eds. The mineral deposits of New South Wales. Department of Mines, Geological Survey of New South Wales, Sydney, 682 pp.
- CLIFT, D., 1973. Mining History of the Cootamundra 1:100,000 Sheet, Geological Survey of New South Wales – Department of Mineral Resources.
- COBRE NUEVO CONSULTING, 2022. R. Davies. Review of strategy, geological model and targeting. Internal report.
- COBRE NUEVO CONSULTING, 2022. R. Davies and D. Burt. Technical Report on the Mineral Exploration Potential of the Bauloora Area (EL8994), New South Wales. Internal report.
- DOWNES, P., M., MCVILLY, R. AND RAPHAEL, N., M., 2004. Mineral deposits and models, Cootamundra 1:250 000 map sheet area. Geological Survey of New South Wales, Quarterly Notes 116, 1-38.
- LEACH, T. M. AND CORBETT, G. J. 1994. Porphyry-related carbonate-base metal gold systems in the southwest Pacific: characteristics. AusIMM Proceedings of the PNG Geology, Exploration and Mining Conference 1994, Lae. Rogerson, R. (Ed.), 84-91.

PURSUIT OF IOCG SYSTEMS IN WESTERN TASMANIA

Sean Westbrook

CopperCorp Resources Inc.

Key Words: IOCG, western Tasmania, Tyennan mineral systems

INTRODUCTION TO IOCG DEPOSITS

Iron oxide copper-gold (IOCG) type deposits are among the most significant and economically valuable mineral resources in the world. They are renowned not only for their potential to host large tonnage and high-grade Cu-Au orebodies but also for their potential to yield significant amounts of additional strategic and critical metals such as iron, cobalt, uranium, and rare earth elements.

Typical characteristics of IOCG deposits include: (1) Fe-Cu-Au-Co-U-REE-Ba-F element associations, (2) high Fe-S ratio manifested by magnetite- and/or hematite-rich (typically 15-40 wt.% Fe) host rocks of the ores, (3) extensive, commonly spatially and temporally zoned iron oxide and alkali Fe-Na-Ca-K metasomatism in and around the deposits, (4) highly saline aqueous \pm carbonic fluids related to alteration and mineralisation, and (5) spatial correlation with crustal-scale fault and shear zones. Host rock sequence, f_{O_2} , f_{S_2} and depth as well as temperature of the mineralisation events vary extensively between the known deposits causing considerable diversity in their characteristics.

All IOCG deposits commonly share spatial and sometimes genetic associations with other mineralisation and deposit types including magnetite dominant iron oxide-apatite (IOA), pyrite-pyrrhotite dominant iron sulphide copper-gold (ISCG) deposits, and other affiliated deposits. A continuum between IOCG and porphyry-epithermal systems has been postulated in some belts, and IOCG systems with epithermal style alteration caps have been identified worldwide (Corriveau et al, 2022). The common shared connection between these relatively diverse deposit types in the same metallogenic belts is their occurrence in large regional-scale hydrothermal iron oxide and alkali-calcic (magnetite-hematite and sodic-calcic-potassic) alteration systems (Corriveau et al, 2022), collectively referred to as iron oxide-alkali-(calcic) altered (IOAA) systems (Porter, 2010; Corriveau et al, 2022).

IOCG deposits are characterised by the large to giant size of the most significant deposits (typically in the order to 100's to 1000's Mt), although smaller examples are also common. Cu and Au grades are commonly in the range of 0.5-1.5 wt.% Cu, 0.2-1.0g.t Au, although higher grade deposits (>1.5 wt.% Cu, >1g/t Au) are known. In addition to the Fe-Cu-Au association, the deposits typically display at least elevated values, if not ore grades, of Ag, Ba, Bi, Co, F, Mo, P, Se, Te, U and REE. Less commonly, the deposits are enriched in As, B, Ni, Sn, W, or Zn. They occur in a wide range of host rocks, among which bimodal basaltic-andesitic and felsic volcanics sequence, and meta-sedimentary and meta-igneous rock associations are particularly prominent. Temporal, and sometimes spatial, association with large intrusive granitoid complexes is evident in most IOAA systems containing IOCG deposits.

IOCG POTENTIAL IN TASMANIA

The exploration potential for iron oxide copper-gold (IOCG) deposits in western Tasmania has, until recently, been largely unrecognised. However, compelling indications, including favourable tectonic settings, regional-scale iron oxide and alkali-calcic alteration (IOAA), crustal- to local-scale structural pathways, I-type magnetite

series igneous associations, and extensive occurrences of magnetite-apatite (e.g. the Savage River magnetite mine - 498 Mt @ 46% DTR magnetite) and magnetite-hematite-Cu-Au associations (e.g. the Prince Lyell orebody - 114Mt @ 1.2% Cu and 0.3g/t Au) with variable Ag, Co and REE mineral associations suggest a compelling opportunity for the discovery of IOCG type deposits in the region. These mineral systems in western Tasmania were active during the Early-Middle Cambrian (520-500 Ma) Tyennan Orogeny involving a major arc-continental collision and subduction event (Crawford & Berry, 1992; Gray et al., 2024) which resulted in the establishment of the large-scale structural framework of present-day western Tasmania and represents one of the most important metallogenic episodes of the region. The Tyennan Orogeny of Tasmania is broadly time equivalent with the Delamerian Orogeny of mainland Australia.

EXPLORATION ON COPPERCORP'S AMC AND SKYLINE PROJECTS

CopperCorp Resources Inc (CopperCorp) is currently exploring two district-scale geological belts prospective for IOCG systems in western Tasmania – the Arthur Metamorphic Complex belt (AMC Project) and the Mount Read Volcanics belt (Skyline Project). Re-interpretation of historical studies and recent exploration results have been combined with recent advances in the understanding of IOCG systems to provide new insights into the district- and deposit-scale controls to interpreted IOCG-IOAA type systems in western Tasmania. This has contributed significantly towards the development of new district-scale exploration models and exploration targeting criteria for the region.

The 110km long by up to 10km wide Arthur Lineament comprises a high-strain metamorphic structural deformation zone that is host to widespread iron oxide-alkali alteration and mineralisation indicative of a large IOAA type system. The poorly explored belt hosts the large Kiruna-style IOA type magnetite-apatite deposits of the Savage River mine (Bottrill and Taheri, 2007), the emerging IOCG type Alpine copper prospect (e.g. AP035: 23.0m @ 1.14% Cu within 92.0m @ 0.5% Cu), and hundreds of magnetite, copper and gold mineral occurrences, historical small-scale prospects and mine workings. CopperCorp has identified 23 Cu-Au exploration target areas within the belt.

At the Skyline Project, CopperCorp is targeting a district-scale magmatic-hydrothermal IOCG system related to the emplacement of granitoid and porphyry intrusives along the eastern margin of the Mount Read Volcanics (MRV) belt. The regional tectonic setting, host rock sequences, and styles of IOCG style mineralisation of the MRV belt can be broadly compared with the Andean Coastal Cordillera IOCG belt which hosts numerous large IOCG deposits such as Candelaria (470Mt @ 0.95% Cu, 0.22g/t Au). Alteration studies (Large et al., 1996; Corbett, 2002; Wyman, 2000; Denwer, 2018) show that key alteration facies associated with Cu-Au mineralisation in the MRV belt are zoned from deep level cores of K-feldspar-magnetite-biotite-tourmaline and chlorite-sericite (phengite)-magnetite-pyrite dominant assemblages with IOCG type affinity, upwards and outwards to high-sulphidation style sericite (muscovite)-silica-pyrite-pyrophyllite-hematite-barite alteration, and then to shallowest upper advanced argillic pyrophyllite-silica-alunite dominant alteration. Post-mineralisation deformation and erosion means that different levels of the original system are now preserved/exposed at current surface throughout the district. Our current thinking is that the alteration zones formed as vertically extensive, structurally controlled magmatic-hydrothermal discharge zones, possibly extending up to 3-4km above the source granitoid intrusives. Pipe-like zones of massive to stockwork and disseminated magnetite-apatite with or without Cu-Au, REE, and/or Au-Co mineralisation occur throughout these extensive discharge zones but appear to be best developed within the deeper level iron oxide-alkali alteration facies.

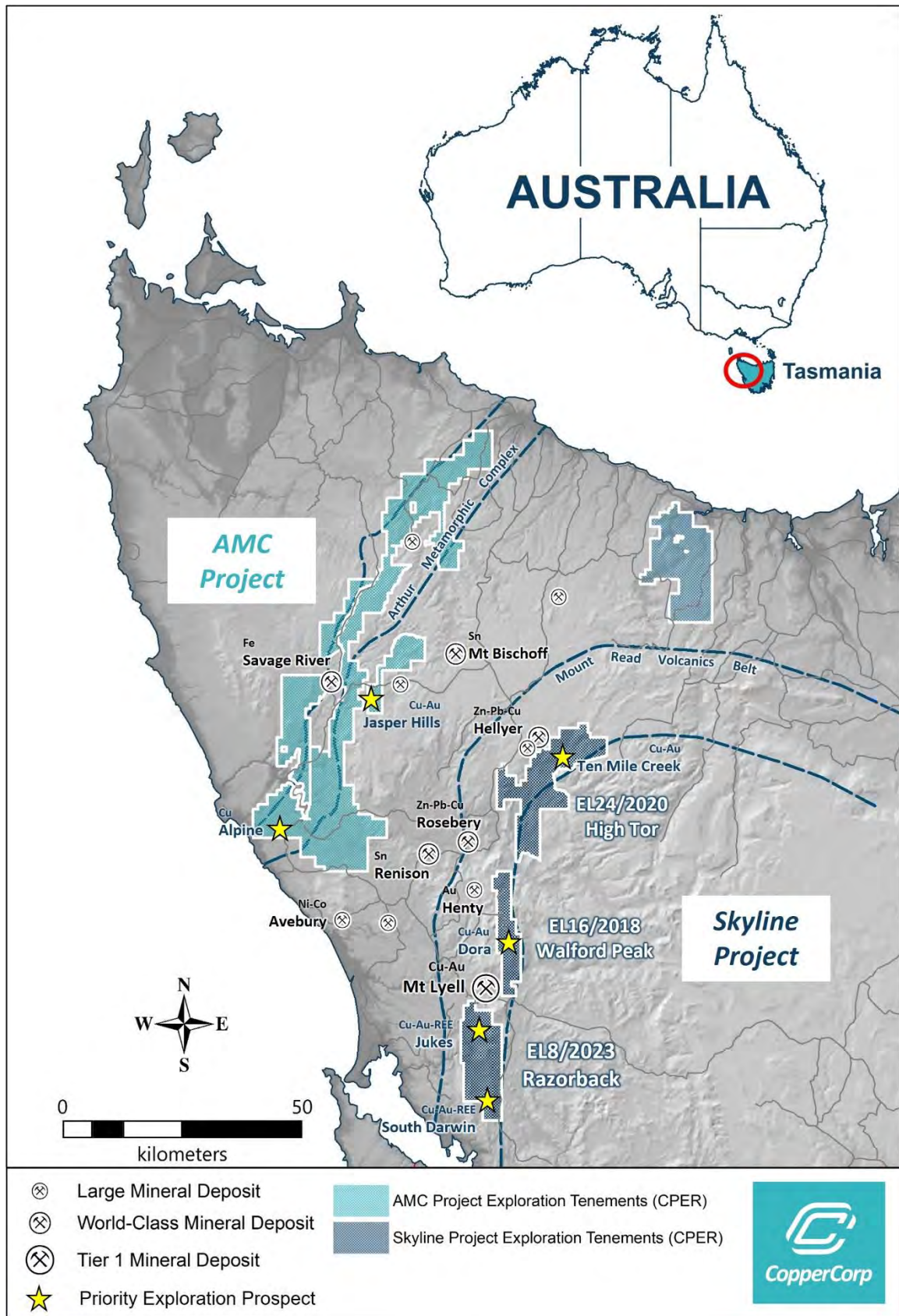


Figure 1. Location plan showing the project areas in western Tasmania.

REFERENCES

- BOTTRILL, R.S. AND TAHERI, J., 2007. Petrology of the host rocks, including mineralisation and adjacent rock sequences, from the Savage River mine. *Tasmanian Geological Survey Record* 2007/05.
- CORBETT, K. D., 2001. New mapping and interpretations of the Mount Lyell mining district: A large hybrid Cu–Au system with an exhalative Pb–Zn top. *Economic Geology*, 96, 1089–1122.
- CORRIVEAU, L., MUMIN, A.H., AND POTTER, E.G., 2022. Mineral systems with iron oxide copper-gold (Ag-Bi-Co-U-REE) and affiliated deposits: introduction and overview. *In: Corriveau, L., Potter, E.G. and Mumin, A.H., eds., Mineral systems with iron oxide copper-gold (IOCG) and affiliated deposits: Geological Association of Canada, Special Paper 52, p. 1-26.*
- CRAWFORD, A. J., & BERRY, R. F., 1992. Tectonic implications of Late Proterozoic–Early Palaeozoic igneous rock associations in western Tasmania. *Tectonophysics*, 214(1-4), 37–56.
- DAVID ROSS GRAY, M. J. VICARY & A. W. MCNEILL., 2024. The Tasmanian Tyennan Domain—a structural synthesis and review with tectonic and dynamic implications for continental margin subduction and exhumation, *Australian Journal of Earth Sciences*, 71:2, 153-210
- DENWER, K.P., 2018. Alteration and mineral zonation at the Mt Lyell copper–gold deposit, Tasmania, *Australian Journal of Earth Sciences*, 65:6, 787-807.
- LARGE, R. R., DOYLE, M., RAYMOND, O., COOKE, D., JONES, A., & HEASMAN, L., 1996. Evaluation of the role of Cambrian granite in the genesis of world-class VHMS deposits in Tasmania. *Ore Geology Reviews*, 10, 215–230.
- PORTER, T.M., 2010. Current understanding of iron oxide associated alkali altered mineralised systems. Part 1 - An overview. *In: Porter, T.M., ed., Hydrothermal iron oxide copper-gold and related deposits: a global perspective, v. 3: PGC Publishing, Adelaide, p. 5-32.*
- WYMAN, W.F., 2000. Cambrian Granite-Related Hydrothermal Alteration and Cu-Au Mineralisation in the Southern Mt Read Volcanics, Western Tasmania, Australia. Unpubl. PhD Theses, University of Tasmania.